21st

Annual Conference on Mass Spectrometry and Allied Topics

May 20-25, 1973
San Francisco, California

Twenty-First Annual Conference on Mass Spectrometry and Allied Topics

May 20-25, 1973
San Francisco, California

Arranged by the
American Society for Mass Spectrometry

Table of Contents

Introduction

This volume is a collection of papers presented at the Twenty-First Annual Conference on Mass Spectrometry and Allied Topics, held in San Francisco, California, May 20-25,1973. It is intended that this volume be distributed only to members of ASMS, and registrants of the Conference, and therefore should not be considered as a publication.

It is suggested that any future reference to individual reports be cited in the form: author(s), presented at the Twenty-First Annual Conference on Mass Spectrometry and Allied Topics, San Francisco, California, May 20-25, 1973.

ASMS

The American Society for Mass Spectrometry thanks the following companies and their representatives for their generous support in the sponsorship of the 1973 ASMS meeting:

AEI Scientific Apparatus, Inc. 500 Executive Blvd. Elmsford, N.Y. 10523 Tel: (914) 592-4620	Gerald L. Kearns
Avco Electronics Div. Avco Corporation 10700 East Independence St. Tulsa, OK. 74115 Tel: (918) 437-1778	L. A. Payne Charles Law
Bendix Scientific Inst. & Equipment Div. Bendix Corp. 1775 Mt. Read Blvd. Rochester, N.Y. 14603 Tel: (716) 458-2550	Donald C. Damoth
Cameca Instruments, Inc. 101 Executive Blvd. Elmsford, N.Y. 10523 Tel: (914) 592-4714	Warren Singer Robert Lewis
Digital Equipment Corp. 146 Main Street Maynard, MA 01754 Tel: (617) 897-5111	Dell Glover
E.I. DuPont de Nemours & Co. 1500 S. Shamrock Avenue Monrovia, CA 91016 Tel: (213) 357-2111	U. McCleary, Jr. D. E. Neil
Dynaspec, Inc. 2634 Bayshore Frontage Road Mountain View, CA 94040 Tel: (415) 961-2653	Robert B. Wilcox
Extranuclear Laboratories, Inc. P.O. Box 11512 Pittsburgh, PA 15238 Tel: (782-3884	Michael McKeown Philip Irving
Finnigan Corp. 595 North Pastoria Avenue Sunnyvale, CA 94086 Tel: (408) 732-0940	T. Z. Chu Mike Story
Hewlett Packard Scientific Instruments Div. 1601 California Avenue Palo Alton, CA 94304 Tel: (415) 493-1311	D. B. Harrington
JEOL Inc. 235 Birchwood Ave. Cranford, N.J. 07016	Jack Doherty Harry Fukino
LKB Instruments, Inc. 12221 Parklawn Drive Rockville, MD 20852 Tel: (301) 881-2510	Terry O'Donovan
3M Company 3M Center St. Paul, MN 55101 Tel: (612) 733-1110	Robert F. Goff A. K. Lockhard

Nuclide Corp. 642 East College Avenue State College, PA 16801 Tel: (814) 238-0541	Leonard F. Herzog Gil Brezler
Perkin-Elmer Corp. 761 Main Avenue Norwalk,CT 06852 Tel: ((203) 762-4008	A. Struck J. Hannon
Process Analyzers, Inc. 5440 Alder Houston, TX 77036 Tel: (713) 664-8151	Rodney W. Supple
Scientific Instruments Accessories 1106 High Road Austin, TX 78746 Tel: (512) 327-0570	F. C. Maseles
Scientific Research Instruments 6707 Whitestone Road Baltimore, MD 21207 Tel: (301) 944-4020	Alfred Yergey David Beggs
Spectrometer Data Systems, Inc. 5801 Christie Avenue Emeryville, CA 94168 Tel: (415) 658-5095	Donald E. Hagge
Systems Industries 535 DelRey Sunnyvale, CA 94086 Tel: (408) 732-1650	Nevil Crook
Vacumetrics, Inc. 241 Crescent Street Waltham, MA 02154 Tel: (617) 899-3706	Thomas Shannon John J. Hoppe
Varian MAT 611 Hansen Way Palo Alto, CA 94303 Tel: (415) 493-4000	Don Hatler Helmut Raddatz
Uthe Technology International 320 Soquel Way Sunnyvale, CA 94086 Tel: (408) 738-3301	George Bunyard

F. E. SAALFELD
Secretary

*Plenary Lecture

*Plenary Lecture

LIGHT EMISSIONS FROM LOW-ENERGY ION-NEUTRAL COLLISIONS

B.M. Hughes, E.G. Jones, C.D. Miller and T.O. Tiernan
Aerospace Research Laboratories, Chemistry Research Laboratory
Wright-Patterson Air Force Base, Ohio 45433

Optical emissions from ion-neutral collisions have been reported by Lipeles et al.[1] and Dworetsky et al.[2], who studied reactions of He^+ ions with the rare gases. More recently low energy He^+/metal atom interactions have been observed to produce excited metal ions which decay radiatively,[3] suggesting that such processes may be important as a pumping mechanism for ultraviolet lasers. The present paper is an initial description of experiments utilizing a new apparatus designed and constructed in our laboratory for the investigation of optical emissions from very low energy, (as low as leV), ion-neutral collisions. The accessible translational energy range of the apparatus in its present configuration is about 1 to 170eV, (lab).

Figure 1 shows a diagram of the apparatus. The incident ion beam is produced by a conventional electron impact source and mass analyzed by a 90° magnetic sector. The ions are accelerated to 170eV on leaving the source, pass through the sector, and are then decelerated to the desired terminal ion velocity. The mass and energy resolved beam is then focused into a collision chamber. The exit slit of this chamber is located at the focal point of a concave grating housed in a 1-meter VUV monochromator, and serves as the monochromator entrance slit. For the experiments described herein, a 1 mm wide slit was used, which results in an optical resolution of 16Å in the second order of a 600 l/mm ruled grating. Data on Lyman-α emissions were obtained using an EMR-542F photomultiplier with LiF windows. Lyman-β emissions and other radiation in the wavelength region below 1100 Å were observed using a Channeltron electron multiplier. Photon counting is used to measure the intensities of the emitted radiation.

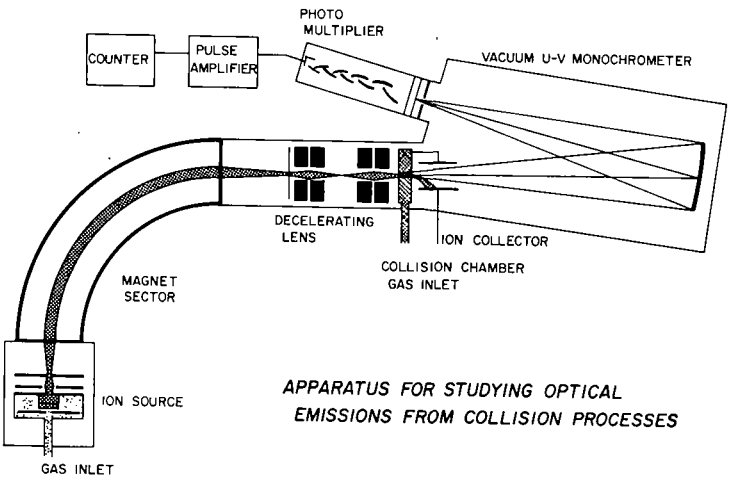

Figure 2 shows a resolved spectrum of the emissions from 100eV He^+ collisions with H_2. The production of excited H atoms (n = 2, 3, 4, 5 and 6) is evident from the corresponding emissions of the Lyman series. Since these emissions are endothermic at low He^+ energies, it was of interest to determine the thresholds for these processes. To accomplish this, the emission at a particular wavelength was monitored continuously while the He^+ translational energy was varied. Figure 3 and 4 show the excitation functions determined for the He^+/H_2 and He^+/D_2 reactions, for Lyman-α and Lyman-β emissions.

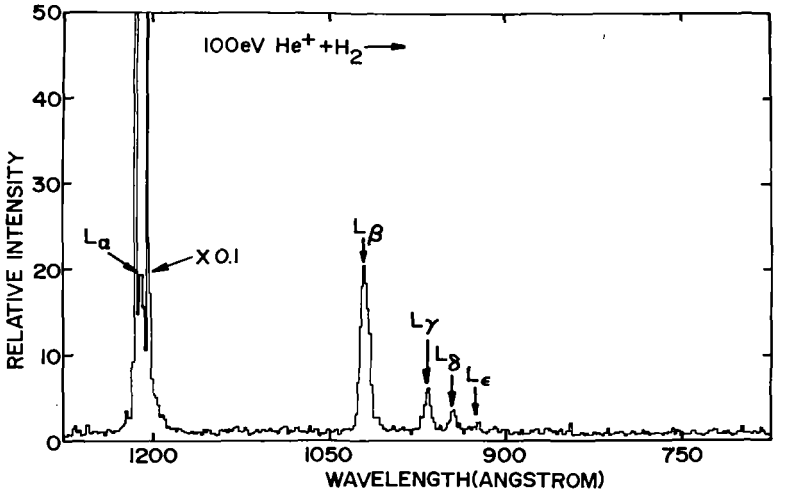

Figure 2. Emissions from Collisions of 100eV He^+ Ions with H_2

Owing to the mass differences in these targets and the light mass reactant ion, there is a substantial difference in the thresholds for the two processes in the laboratory scale. The Lα threshold is at ~ 28eV for He^+/H_2 while it occurs at ~19eV for the He^+/D_2 case. Of course, when the cross sections are plotted as a function of center-of-mass energy, as in Figures 3 and 4, the thresholds are identical, since it is the center-of-mass collision energy which is converted into electronic excitation.

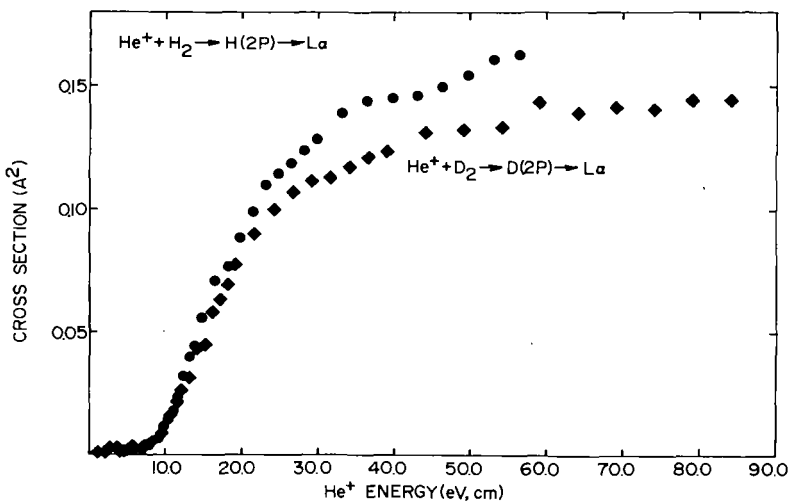

Figure 3. Translational Energy Thresholds for Lyman-α Emissions from He^+/H_2 and He^+/D_2 collisions.

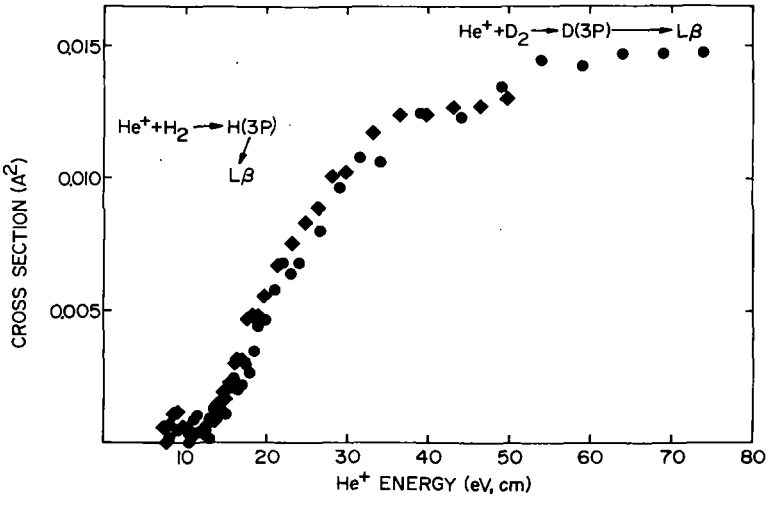

Figure 4. Translational Energy Thresholds for Lyman-β Emissions from He^+/H_2 and He^+/D_2 Collisions

Thresholds similar to those illustrated were also measured for Lα emissions from He^+ collisions with CH_4, H_2O, NH_3, and H_2S. In all these cases, the linearly extrapolated threshold energies are 2-4eV larger than the minimum energies calculated for these transitions from thermochemical data. The maximum cross sections determined for these processes ranged from 0.1 to 0.2 A^2. All cross sections were determined assuming a quantum efficiency of 6% for the photomultiplier, 20% reflectance of the grating and uniformly dispersed light in the collision region. More accurate cross section determinations are in progress.

References

1. M. Lipeles, R. Novick and N. Tolk, Phys. Rev. Letters 15, 815 (1965).

2. S. Dworetsky, R. Novick, W.W. Smith, and N. Tolk, Phys. Rev. Letters 18, 939 (1967).

3. C.E. Webb, A.R. Turner-Smith and J.M. Green, J. Phys. B., Atom. Molec. Phys. 3, L135 (1972).

A more detailed account of this work will be submitted for publication in the Journal of Chemical Physics.

Equilibrium Studies of the Acidity of Molecules in the Gas Phase

Robert T. McIver, Jr.*, Judith A. Scott, and Jeffrey H. Silvers
Department of Chemistry, University of California
Irvine, California 92664

Structure-reactivity relationships are among the most useful concepts used to understand chemical reactions. By knowing the molecular structure of a reactant species, it is often possible to predict the type reactions it will undergo and even how rapid the reactions will be. Correlations of this type have been studied for many years for reactions in solution, but interpretation of the results has been complicated by the large effect of solvation on the reactions.

For this reason we have chosen to study the acidity of molecules in the gas-phase. In the absence of solvation the intrinsic acidity of the molecules can be measured. This approach not only helps to elucidate the factors governing the intrinsic stability of negative ions but also helps us to understand the role of solvent in chemical reactions.

The purpose of this presentation is to demonstrate that chemical equilibria can be studied by Pulsed Ion Cyclotron Resonance techniques and to discuss results obtained recently by our group at U. C., Irvine.

Pulsed ICR experiments have been described previously.[1,2] A "trapped ion analyzer cell" is enclosed in a high vacuum system and placed between the pole caps of a 9" electromagnet. Pulsed ICR is essentially a mass spectrometric technique, so the trapped ion cell simply consists of a filament and grid assembly for producing ionization, and six metal plates suitably biased for trapping the ions. The trapped ion cell serves two functions. First, the combination of the magnetic field and the dc trapping voltages provides very efficient ion trapping. Once formed by a pulse of the electron beam, either positive or negative ions can be trapped with essentially no ion loss for 500 msec at a pressure of 10^{-5} Torr. The trapping efficiency of the cell decreases gradually after 500 msec, and measureable ion signals have been obtained after trapping times of up to 10 sec. The second function of the trapped ion cell is mass analysis. After reacting for a given period of time, a marginal oscillator is pulsed on to mass analyze the ions in the cell.[3] No ion extraction is required; the reaction region serves also as the mass analysis region. The marginal oscillator is turned off while the ions are reacting chemically, so thermal energy ion-molecule reactions can be studied. Mass analysis of the ions requires about 4 msec, a time much shorter than the reaction period of 500 msec. Mass discrimination is not a problem with this technique. The marginal oscillator responds linearly to all ions in the entire reaction volume, regardless of chemical composition or mass.

This technique can be used to study gas-phase equilibria of the type

$$A^- + BH \rightleftharpoons B^- + AH \qquad (1)$$

where AH and BH are Brönsted acids, and A^- and B^- are the corresponding conjugate bases.[4,5] Equilibrium constants for reactions of this type are a quantitative measure of the intrinsic relative acidity of AH and BH. As an example, in a mixture of NF_3, H_2S, and HCN, impact by thermal energy electrons produces F^- initially.[5] The F^-

then abstracts a proton from H_2S and HCN to give SH^- and CN^-. The Pulsed ICR can be used to monitor the concentration of each of these ionic species as a function of reaction time. At a total pressure of 2×10^{-6} Torr, the concentrations of CN^- and SH^- are observed to reach constant values after about 200 msec. A steady state is obtained with respect to the reaction

$$SH^- + HCN \underset{k_2}{\overset{k_1}{\rightleftharpoons}} CN^- + H_2S \qquad (2)$$

The Pulsed ICR measurements are used to determine the equilibrium concentration of SH^- and CN^-, and an ionization gauge calibrated against a capacitance manometer is used to determine the partial pressures of HCN and H_2S. The equilibrium constant at 298° K is easily evaluated

$$K = \frac{[CN^-]\,[H_2S]}{[SH^-]\,[HCN]} \qquad (3)$$

We find $K = 9.1 \pm 0.6$ for this reaction.[5]

The Pulsed ICR time plots show clearly that a steady state situation is reached. The central question, however, is whether this corresponds to a true equilibrium. In particular, one should be concerned whether excited ions are present and whether the rates of the forward and reverse reactions are rapid compared to the total trapping time. McIver and Eyler have performed several tests on this system.[5] Varying the ratio of the neutral reactants and varying the total pressure produce a constant value for K in eq. 3. Double resonance ejection can be used to measure k_1 and k_2 for reaction 2, and it is found that $K = k_1/k_2 = 8.9 \pm 0.5$. This kinetic method of measuring K is in good agreement with the value 9.1 obtained from eq. 3. The proton transfer reactions are very rapid compared to the total ion trapping time. Other means have been used to generate the negative ions: direct electron impact on H_2S and proton abstraction by CH_3O^-. Both processes would be expected to generate reactants initially with different states of internal excitation, but closely similar values of K are obtained. These reactions are rapid and well-behaved in terms of all the tests employed. We believe that the steady state does correspond to an equilibrium situation.

Figure 1 shows our data for the relative acidity of alcohols and acetylenes. The more acidic species are shown at the bottom of the figure, and the numbers represent ΔG^0_{298} values measured for each pair of Brönsted acids. The effect of the alkyl groups on the acidity of these molecules was first reported by Brauman and Blair.[6,7] Our equilibrium experiments provide the actual values of ΔG^0 so that the magnitude of the effects can be evaluated quantitatively. Space does not permit a full interpretation of these trends. It is interesting, however, to point out how multiple overlaps serve as an additional test of the equilibrium hypothesis. For example, direct measurement between CH_3OH and C_2H_5OH gives $\Delta G^0 = 1.9$ kcal/mole. This is to be compared with the cycle CH_3OH to $CH_3C{\equiv}CH$, $CH_3C{\equiv}CH$ to $CH_3CH_2CH_2C{\equiv}CH$, and $CH_3CH_2CH_2C{\equiv}CH$ to C_2H_5OH which sums to $0.1 + 1.2 + 0.5 = 1.8$ kcal/mole.

FIGURE I: RELATIVE ACIDITY OF ALCOHOLS AND ACETYLENES

IN THE GAS PHASE

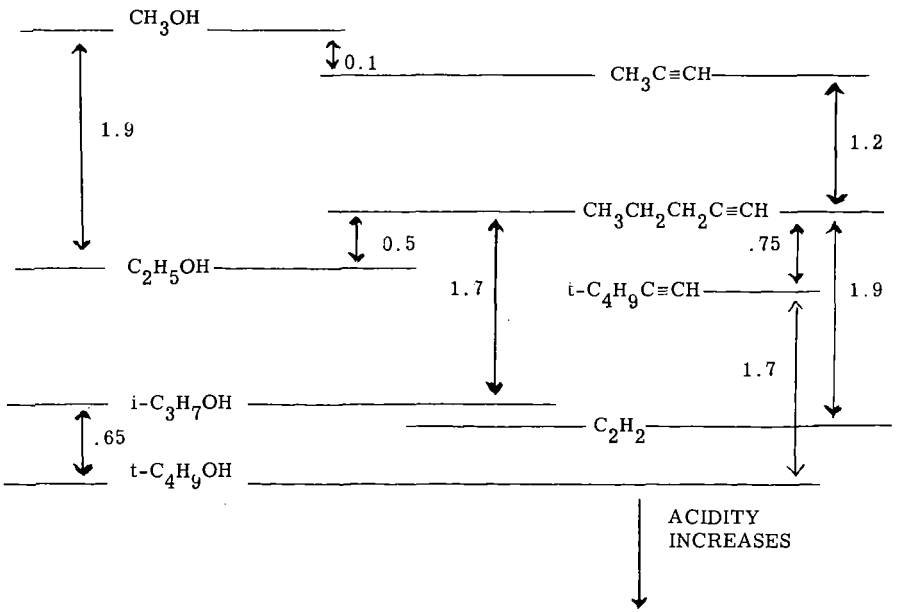

References:

1. R. T. McIver, Jr., Rev. Sci. Instrum., 41, 555 (1970).
2. R. T. McIver, Jr. and R. C. Dunbar, Int. J. Mass Spectrom. and Ion Phys., 7, 471 (1971).
3. R. T. McIver, Jr., Rev. Sci. Instrum., in press.
4. M. T. Bowers, D. H. Aue, H. M. Webb, and R. T. McIver, Jr., J. Amer. Chem. Soc., 93, 4314 (1971).
5. R. T. McIver, Jr. and J. R. Eyler, J. Amer. Chem. Soc., 93, 6334 (1971).
6. J. I. Brauman and L. K. Blair, J. Amer. Chem. Soc., 92, 5968 (1970).
7. J. I. Brauman and L. K. Blair, J. Amer. Chem. Soc., 90, 5636 (1968).

THE RELATIVE PROTON AFFINITIES OF H_2S AND CH_3OH

L.Y. Wei and L.I. Bone

Department of Chemistry
East Texas State University
Commerce, Texas 75428

Recently we[1] have measured the relative proton affinities of H_2S and H_2O using the East Texas State Photoionization Mass Spectrometer. Since there was still disparity in the measured values for the absolute proton affinities of these two compounds, we have measured the relative proton affinities of H_2S and CH_3OH in order to better establish the absolute value of all three compounds.

Mixtures of CH_3OH and H_2S are photoionized at 10.63 eV in the source of a quadrupole mass spectrometer. H_2S^+ which is the only ion produced reacts with H_2S and CH_3OH to produce H_3S^+ and $CH_3OH_2^+$ respectively. Further reactions of these ions lead to the equilibrium of interest.

$$H_3S^+ + CH_3OH \rightleftharpoons H_2S + CH_3OH_2^+$$

Although equilibrium can not be established at the pressures, or within the time scale of our instrument, the equilibrium constant has been calculated by a method involving steady state kinetics.

The equilibrium constant is measured at a series of temperatures and a van't Hoff plot is constructed. We obtain $\Delta H^\circ = -5.8 \pm 0.3$ kcal/mole and $\Delta S^\circ = 4.3 \pm 0.2$ e.u. for the equilibrium as written. Comparison with other literature values suggest that the best values for the proton affinities are: H_2O = 167 kcal/mole, H_2S = 170 kcal/mole, and CH_3OH = 173 kcal/mole.

Funded by the Robert A. Welch Foundation

1. J.M. Hopkins and L.I. Bone, J. Chem. Phys., 58, 1473, (1973)

Effect of Reaction Exothermicity on Proton Transfer Reaction Rates

B. H. Solka and A. G. Harrison, Department of Chemistry, University of Toronto, Toronto, Ontario M5S 1A1.

The rates of proton transfer from protonated methyl mercaptan to a series of substrates have been measured using the trapped-ion technique developed in this laboratory.[1]

In pure CH_3SH, at electron energies where the molecular ion is the only primary ion, reaction of CD_3SH^+ produces $CD_3SH_2^+$ and CD_3SHD^+ in a 23:1 ratio. The $CD_3SH_2^+$ secondary ion undergoes no significant net reaction in CD_3SH, but the CD_3SHD^+ reacts according to

(1) $CD_3SHD^+ + CD_3SH \longrightarrow CD_3SH_2^+ + CD_3SD$

The rate coefficient for this "symmetrical" proton transfer is taken as representative of that of a thermoneutral process. This reaction can be made effectively exothermic by increasing the internal energy in the reactant ion and the effect this has on the rate coefficient is seen in Table I. Here the internal energy of the reactant has presumably been

Table I

Rate Coefficients for

$MeSHD^+ + MeSH \longrightarrow MeSH_2^+ + MeSD$

Preparation of $MeSHD^+$	-ΔH production (kcal $mole^{-1}$)	k x 10^9 (cm^3 $mole^{-1}$ sec^{-1})*
$CD_3SH^+ + CD_3SH \longrightarrow CD_3SHD^+$	-8(?)	0.25 ± 0.03
CD_3SH^+, CD_2SH^+, CD_3S^+ + $CD_3SH \longrightarrow CD_3SHD^+$	-8 to 16	0.58 ± 0.06
$CD_5^+ + CH_3SH \longrightarrow CH_3SHD^+$	62	0.88 ± 0.1

*Observed rate coefficient has been multiplied by two for comparison with data in Table II. This assumes no H/D isotope effect.

successively increased by preparing it in three ways: from M^+ at low electron energy, from the more exothermic D^+ transfer from primary fragment ions at higher electron energies, and from deuteron transfer from CD_5^+ in mixtures of CD_4 and CH_3SH. The rate of proton transfer from $MeSHD^+$ is significantly increased (Table I) as the internal energy increases.

To place this effect on a more quantitative basis, we have measured the rates for proton transfer to the series of molecules listed in Table II, where -ΔH for the reaction is set by the difference in proton affinity between MeSH and M. The experiments were done using from 3:1 to 10:1 MeSH: Additive mixtures at total ion source concentrations on

the order of 1 x 10^{13} molecules cm^{-3}.

Table II

Rate Coefficients for Proton Transfer

$MeSH_2^+ + M \longrightarrow MH^+ + MeSH$

M	μ(Debye)	k x 10^9 cm^3 $mole^{-1}$ sec^{-1} exp.	calc.*	$k_{exp.}/k_{calc.}$	$-\Delta H$ (kcal $mole^{-1}$)
CD_2SH	1.52	0.25 ± 0.03	1.97	0.13	∿ 0
CH_3CHO	2.69	0.73 ± 0.09	2.70	0.27	1
CH_3CH_2CHO	2.52	0.56 ± 0.03	2.52	0.22	3
CH_3OCH_3	1.30	1.24 ± 0.10	1.86	0.67	6
CH_3SCH_3	1.50	1.74 ± 0.05	2.02	0.86	14
$(CH_3)_2C=O$	2.88	2.30 ± 0.21	2.70	0.85	18

* "locked'in" dipole for 0.4eV (Lab) ions[1]

The rate coefficients for these processes increase markedly as the exothermicity increases. To normalize the data for comparison we also tabulate the experimental rates relative to the calculated collision rate, using the completely locked-in dipole collision rate expression to represent the maximum collision rate. It is seen that collisions have an increasingly better chance of leading to reaction as the exothermicity increases. This trend is plotted in Fig. 1, where two additional points (squares) are included for reaction (1) showing the effect of preparing the reactant ion via more exothermic reactions.

Normalizing this data to the locked dipole collision rate may not be strictly valid because of evidence[2] that dipole orientation may not occur, but the same trend is observed if we consider only ion-induced dipole collision rates.

This behaviour is consistent with a reaction mechanism which proceeds through a proton-bound complex of mercaptan and M which may undergo unimolecular decay to products, where the proton remains associated with M, or decay back to reactants, where the proton remains associated with MeSH. As the overall exothermicity of the reaction increases, decay into the forward channel becomes more probable relative to backward decay.

1. A. A. Herod and A. G. Harrison, Int. J. Mass. Spectrom. Ion Phys. 4, 415 (1970).
2. J. V. Dugan and J. L. Magee, J. Chem. Phys. 47, 3103 (1967); T. Su and M. T. Bowers, J. Amer. Chem. Soc. 95, 1370 (1973).

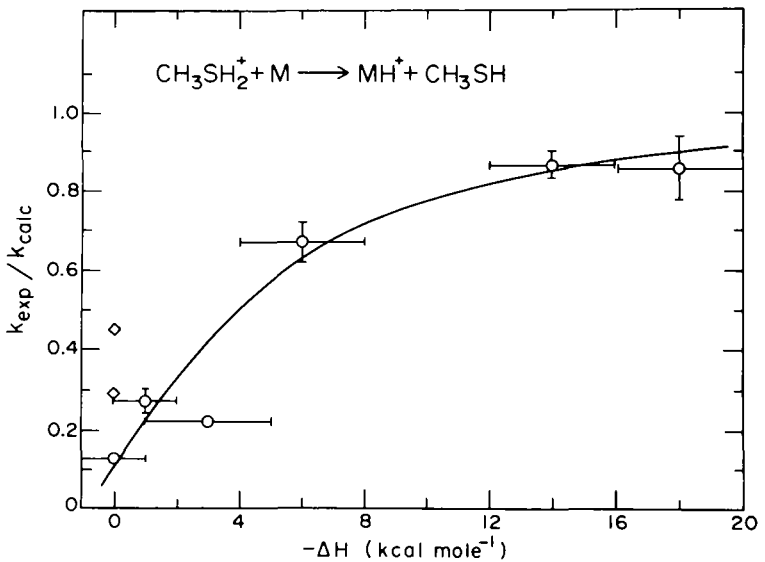

Fig. 1. Reaction Efficiency vs. Reaction Exothermicity

ION-MOLECULE REACTIONS AND VIBRATIONAL DEACTIVATION OF H_2^+ IONS IN MIXTURES OF HYDROGEN AND HELIUM*

by

Lowell P. Theard and Wesley T. Huntress, Jr.
Jet Propulsion Laboratory, Pasadena, California 91103

ABSTRACT

Ion cyclotron resonance techniques have been used to determine the thermal energy rate constants for the ion molecule reactions:

$$(H_2^+)^v + H_2 \xrightarrow{k_1} H_3^+ + H$$

$$(H_2^+)^v + He \xrightarrow{k_2} HeH^+ + H$$

$$\xrightarrow{k_v} (H_2^+)^{v'} + \vec{He}$$

$$He^+ + H_2 \xrightarrow{k_3} HeH^+ + H$$

$$HeH^+ + H_2 \xrightarrow{k_4} H_3^+ + He$$

For a near Franck-Condon distribution of initial vibrational states in H_2^+; $k_1 = 2.08 \pm .03$, $k_2 = 0.13 \pm .01$, $k_3 < .002$, and $k_4 = 1.83 \pm .06 \times 10^{-9}$ cm^3/molecule-sec. Collisional deactivation of vibrationally excited H_2^+ ions appears to occur in non-reactive encounters with He atoms. The rate constant k_v for this process increases with increasing vibrational quantum number and is approximately equal to k_2^v for H_2^+ ions in vibrational state v.

* Submitted for publication to the Journal of Chemical Physics.

THE DETERMINATION OF THE DIFFERENCES IN THE GAS-PHASE ACIDITIES AT 296 K OF NH_3, NH_2CH_3 AND $NH(CH_3)_2$ FROM EQUILIBRIUM MEASUREMENTS

D. K. Bohme, R. S. Hemsworth, G. I. Mackay, and H. I. Schiff
C.R.E.S.S. and Department of Chemistry, York University, Toronto, Canada

The flowing afterglow technique[1] has been employed in a determination of the equilibrium constants at 296 K for the following proton transfer reactions, each of which is written in the direction in which proton transfer occurs preferentially:

$$NH_2^- + H_2 \rightleftarrows H^- + NH_3 \qquad (1)$$

$$NH_2^- + NH_2CH_3 \rightleftarrows {}^-NHCH_3 + NH_3 \qquad (2)$$

$${}^-NHCH_3 + H_2 \rightleftarrows H^- + NH_2CH_3 \qquad (3)$$

$$H^- + NH(CH_3)_2 \rightleftarrows {}^-N(CH_3)_2 + H_2 \qquad (4)$$

The standard free energy changes ΔG°_{298} for these reactions, which can be deduced from the measured equilibrium constants, can provide values for fundamental molecular parameters as follows: For the general reaction

$$A^- + BH \rightleftarrows B^- + AH$$

the standard enthalpy change, ΔH°_{298}, is given by

$$\Delta H^\circ_{298} = EA(A) - EA(B) + D^\circ_0(B\text{-}H) - D^\circ_0(A\text{-}H) + \int_0^{298} \Delta C_p dT$$

where ΔC_p represents the change in heat capacity at constant pressure. Usually the heat capacity term is negligibly small. Also the assumption can often be made that $T\Delta S^\circ << \Delta H^\circ$, where ΔS° represents the standard entropy change. Then

$$\Delta G^\circ_{298} \cong PA(B^-) - PA(A^-)$$

and

$$\Delta G^\circ_{298} \cong EA(A) - EA(B) + D^\circ_0(B\text{-}H) - D^\circ_0(A\text{-}H).$$

Reference to well established values can then yield values for (1) the proton affinity $PA(B^-)$ or $PA(A^-)$ or the gas-phase acidity of BH or AH, and (2) the electron affinity EA(A) or EA(B) or (3) the bond energy $D^\circ_0(B\text{-}H)$ or $D^\circ_0(A\text{-}H)$.

The experimental results for reaction (1) and their analysis have been described in detail elsewhere[2]. The measured value for K = 27 ± 9 at 297° K and corresponds to $\Delta G^\circ_{297} = -1.9 \pm 0.2$ kcal mole^{-1}. A calculation of ΔS°_{298} leads to a value for $\Delta H^\circ_{298} = -3.2 \pm 0.3$ kcal mole^{-1} so that $PA(NH_2^-) = PA(H^-) + 3.2 \pm 0.3$ kcal mole^{-1}. Reference to well established values for EA(H), $EA(NH_2)$ and $D^\circ(H\text{-}H)$ leads to a value for $D^\circ_0(NH_2\text{-}H) = 106.0 \pm 1.1$ kcal mole^{-1} or $D^\circ_{298}(NH_2\text{-}H) = 107.4 \pm 1.1$ kcal mole^{-1}.

The experimental results for reactions (2) to (4) and their analysis will be reported elsewhere as part of a more comprehensive study of the acidities of the simple amines[3]. Preliminary investigations indicate that $\Delta G^\circ_{296} = -0.54$, -1.4 and -5.1 kcal mole^{-1} respectively for reactions (2), (3) and (4). These values yield the proton affinities $PA({}^-NHCH_3) \cong PA(H^-) + 1.4$ kcal mole^{-1} and $PA({}^-N(CH_3)_2) \cong PA(H^-) - 5.1$ kcal mole^{-1}. Reference to the best available values for EA(H), $D^\circ(H\text{-}NHCH_3)$ and $D^\circ(H\text{-}N(CH_3)_2)$ suggests that $EA(CH_3NH) \cong EA((CH_3)_2N) \cong EA(H) = 17.4$ kcal mole^{-1}, within the uncertainties in the bond energies (~4 kcal mole^{-1}).

Finally, the negative-ion chemistry identified in these studies suggests an alternate route for the gas-phase decomposition of the amines in the presence of negative ions. For example, the consecutive reactions

$$H^- + NH_2CH_3 \rightarrow NH_2^- + CH_4 \qquad \Delta G^\circ_{298} = -20 \text{ kcal mole}^{-1}$$

$$NH_2^- + NH_2CH_3 \rightarrow H^- + CH_4 + H_2 + N_2 \qquad \Delta G^\circ_{298} = -19 \text{ kcal mole}^{-1}$$

would provide an anion-catalysed route for the decomposition of monomethylamine at 298° K according to

$$2NH_2CH_3 \rightarrow 2CH_4 + H_2 + N_2 \qquad \Delta G^\circ_{298} = -39 \text{ kcal mole}^{-1}$$

References

1. D. K. Bohme, R. S. Hemsworth, H. W. Rundle and H. I. Schiff, J. Chem. Phys. 58, 3504 (1973).

2. D. K. Bohme, R. S. Hemsworth, H. W. Rundle, J. Chem. Phys., in press.

3. G. I. Mackay, R. S. Hemsworth, H. I. Schiff and D. K. Bohme, J. Amer. Chem. Soc., to be submitted.

Gas Phase Ion Chemistry of the Methyl Phosphines*

R. H. Staley and J. L. Beauchamp
Department of Chemistry
California Institute of Technology
Pasadena, California 91109

Abstract

The gas phase ion chemistry of the methyl phosphines, $(CH_3)_nPH_{3-n}$ (n = 1-3), has been investigated using ion cyclotron resonance spectroscopy. Reaction pathways, product distributions and rate constants have been determined using trapped ion techniques complemented by the more usual method of examining the variation of ion abundance with pressure. Reaction of the parent ion to give protonated parent was observed for methyl and dimethyl phosphine only. In contrast to the methyl amines, formation of proton bound dimers was not observed in the methyl phosphines. However, a condensation reaction of the parent ion and neutral with loss of methyl radical occurs in all three phosphines. Various condensation reactions of the fragment ions with loss of ethylene or other small molecules or radicals were also studied. The gas phase basicities of the methyl phosphines were determined by studying the course of proton-transfer reactions in binary mixtures of methyl phosphines with appropriate molecules. The effect of successive methyl substitution on the basicity of the phosphines was found to be both larger and more additive than for the amines. Possible interpretations of the differences in basicities and gas phase ion chemistry between the methyl phosphines and the methyl amines are discussed.

---

*A more detailed account of this work will be submitted for publication in the Journal of the American Chemical Society.

Formation and Reactions of Bihalide Anions (XHX^-, X = F, Cℓ, Br) by Ion Cyclotron Resonance Spectroscopy*

Michael S. Foster and J. L. Beauchamp
Department of Chemistry
California Institute of Technology
Pasadena, California 91109

Abstract

The techniques of ion cyclotron resonance spectroscopy have been used to examine sequential bimolecular reactions in mixtures of SF_6 with HX which result in formation of bihalide anions of the type FHX^- (X = F, Cℓ, Br). Further reactions of these ions with hydrogen halides gives products with all possible combinations of halogens, $X_1HX_2^-$. The reactions of bihalide anions with organic acids and electron deficient inorganic complexes have been examined and lead, respectively, to the formation of strongly hydrogen bound dimers and Lewis acid-base adducts. Rate constants, limits on bond dissociation energies and the chemical implications of these processes will be discussed.

---

* A more detailed account of this work will be submitted for publication in the Journal of Inorganic Chemistry.

Gas Phase Ion Chemistry of Fluoroalkanes by Ion Cyclotron Resonance Spectroscopy*

J. L. Beauchamp, J. Y. Park, D. P. Ridge,
T. B. McMahon, and R. J. Blint
Department of Chemistry
California Institute of Technology
Pasadena, California 91109

Abstract

The gas phase ion chemistry of the fluoromethanes $CH_{4-n}F_n$ (n = 1-4), fluoroethanes ($C_2H_{6-n}F_n$, n = 1-6), the several isomers of C_3H_7F and C_4H_9F, and a variety of other simple fluorinated hydrocarbons has been examined using the techniques of ion cyclotron resonance spectroscopy. Kinetics of reactions involving parent and fragment ions have been determined over a range of pressure and electron energies using trapped ion techniques. Fragmentation and reaction mechanisms have been examined using deuterium labeled fluoroalkanes. Fluoride and to a lesser extent hydride transfer reactions between substituted carbonium ions are a dominant feature of the observed ion chemistry. A detailed examination of these processes provides information relating to fluorine substituent effects on carbonium ion stabilities and reveals interesting ionic chain reactions. Useful information relevant to the interpretation of the gas phase ion chemistry of fluoroalkanes has been obtained in other experiments, including photoionization mass spectrometry, photoelectron spectroscopy, and high pressure mass spectrometry.

---

* A more detailed account of this work has been submitted to the Journal of the American Chemical Society and is in press.

FORMATION OF $C_7H_7^+$ FROM THE REACTIONS OF $C_3H_5^+$, $C_3H_3^+$, AND CH_3^+ WITH BENZENE

R. P. Clow* and T. O. Tiernan
Aerospace Research Laboratories, Chemistry Research Laboratory
Wright-Patterson Air Force Base, Ohio 45433

The work of Meyerson and coworkers[1] some years ago, focused attention on the tropylium ion, the cyclic $C_7H_7^+$ structure. A more recent ICR study of the chemical ionization reactions of benzene with methane reagent gas, by Clow and Futrell,[2] obtained evidence that $C_3H_5^+$ reacts with benzene to form $C_7H_7^+$. Previous chemical ionization experiments of a similar nature by Munson and Field[3], however, did not reveal this product ion. Nor was it observed in experiments by Bone and Futrell[4], in which low energy $C_3H_5^+$ ions were reacted with benzene in a tandem mass spectrometer. In an effort to obtain further evidence for tropylium ion formation, the present study was undertaken to investigate the reactions of CH_3^+, $C_3H_3^+$ and $C_3H_5^+$ with benzene again using a double mass spectrometer. Experiments with isotopically labelled reagents were accomplished to obtain insight into the reaction mechanisms and structural effects.

As indicated by the data in Table I, the reactions of CH_3^+, $C_3H_3^+$, and $C_3H_5^+$ with benzene do indeed produce $C_7H_7^+$ under single-collision conditions, and the cross sections for these reactions are quite large. The reported cross sections were measured relative to the reaction, $CH_4^+ + CH_4 \rightarrow CH_5^+ + CH_3$, for which the reported cross section[5] at 0.3eV is $63 \times 10^{-16} cm^2$. The large cross sections observed for these reactions are not surprising in view of the fact that all three reactions are clearly exothermic. The calculated exothermicities obtained by using tabulated thermochemical data[6] are also listed in Table I.

Energy dependences of the cross sections of the reactions shown in Table I were also determined and provide some indication that different mechanisms are involved in the three cases. All three processes exhibit their maximum cross sections at 0.3eV and decrease sharply with increasing translational energy. The $C_3H_5^+$ reaction cross section has dropped to 10% of its maximum at 1.0eV ion energy, while the CH_3^+ reaction cross section is about 30% of its maximum at this energy, and the $C_3H_3^+$ cross section is about 40% of its maximum at 1.0eV. The latter reaction reaches a cross section plateau at energies above 4eV.

The sharp energy dependences of these processes at low energies are characteristic of reactions which proceed through a tight collision complex. Moreover, when reactions 1, 2, and 3 are studied using deuterated reagent ions or neutrals, it is evident that a completely randomized intermediate, in which the energy is equally partitioned, is not involved in these interactions. The product distributions shown in Tables II, III, and IV indicate that the observed $C_7X_7^+$, (X = H or D), ions incorporate specifically one, two or three hydrogen (deuterium) species from the reactant ion. In Table II, isotope distributions in the tropylium ion products from the reactions of $C_3H_5^+$ with C_6D_6 and of $C_3D_5^+$ with C_6H_6 are reported. The cross sections of the three isotopic products were observed to exhibit identical energy dependences. These results suggest that a single complex mechanism probably leads to all three product species. If an activated complex is visualized for the $C_3H_5^+/C_6D_6$ reaction, in which two deuterium atoms of the neutral molecule and three hydrogen atoms of the incident ion are completely randomized, (a structure such as I), then purely on the basis of statistics, the distribution as shown in Table II is calculated.

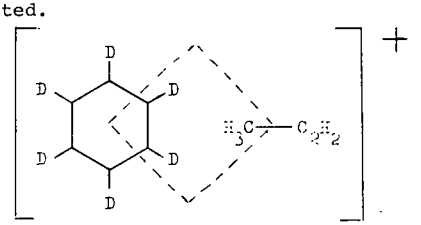

I

As can be seen from the table, there is remarkably good agreement between the experimental product distribution and that calculated in this manner. Similar considerations for the $C_3H_3^+$ reaction with C_6D_6 indicate that good agreement between calculated and observed isotope distributions in the $C_7X_7^+$ product can be achieved if the intermediate is assumed to have a fused ring structure such as II.

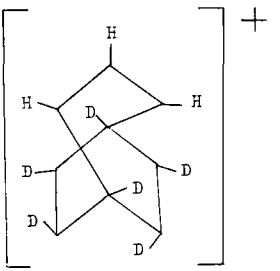

II

In this case three hydrogen atoms and either four or six deuterium (depending on whether just the 7-membered ring species or the complete fused ring system are activated) are considered to participate in the randomization and subsequent elimination process. From Table III, it is seen that the calculated distribution for the (D_4H_3) case agrees much more closely with the measured distribution.

A similar analysis for the CH_3^+ reaction with C_6D_6 forces one to conclude that none of the mechanisms indicated in Table IV yield a calculated distribution which reproduces the experimental results. It is probable therefore, that more than one reaction channel is open in this case. From an energetic standpoint, a multiplicity of reaction channels might be expected for this interaction because the reaction is rather highly exothermic (> 3eV).

A more detailed paper describing these results will be submitted for publication in the International Journal of Mass Spectrometry and Ion Physics.

References

* National Research Council - Air Force Systems Command Postdoctoral Research Associate, 1971-73.

1. H.M. Grubb and S. Meyerson in (F.W. McLafferty, ed.) Mass Spectrometry of Organic Ions, Academic Press, New York, 1963, pp. 516-519 and literature cited therein.

2. R. P. Clow and J. H. Futrell, J. Amer. Chem. Soc. 94, 3748 (1972).

3. M.S.B. Munson and F.H. Field, J. Amer. Chem. Soc. 89, 1047 (1967).

4. L.I. Bone and J.H. Futrell, J. Chem. Phys. 47, 4366 (1967).

5, R.P. Clow and J.H. Futrell, Int. J. Mass Spectrom. Ion Phys. 4, 165 (1970) and references therein.

6. J.L. Franklin, J.G. Dillard, H.M. Rosenstock, J.T. Herron, K. Draxl, and F.H. Field, "Ionization Potentials, Appearance Potentials, and Heats of Formation of Gaseous Positive Ions", U.S. Department of Commerce, NBS, Washington, D.C. 1969.

TABLE I. Cross Section and Heat of Reaction for Tropylium Ion Formation

	Reaction	Cross Section[a] $X10^{16}cm^2$	ΔH_R[b] kcal $mole^{-1}$
1.	$C_3H_5^+ + C_6H_6 \rightarrow C_7H_7^+ + C_2H_4$	48	-15
2.	$C_3H_3^+ + C_6H_6 \rightarrow C_7H_7^+ + C_2H_2$	10	-12
3.	$CH_3^+ + C_6H_6 \rightarrow C_7H_7^+ + H_2$	44	-71

a. Cross sections were measured at 0.3eV, lab energy relative to the methane ion reaction (see text).

b. Thermochemical data from reference (6).

TABLE II. Isotope Distribution of the Tropylium Ion from the Reaction of $C_3H_5^+(C_3D_5^+)$ with C_6D_6 (C_6H_6)

Reaction	Relative Cross Section Experimental	Calculated (D_2H_3)
$C_3H_5^+ + C_6D_6 \rightarrow C_7D_6H^+ + C_2H_4$	2.3	3
$\rightarrow C_7D_5H_2^+ + C_2H_3D$	6.0	6
$\rightarrow C_7D_4H_3^+ + C_2H_2D_2$	1.0	1
$C_3D_5^+ + C_6H_6 \rightarrow C_7H_6D^+ + C_2D_4$	3.4	(H_2D_3) 3
$\rightarrow C_7H_5D_2^+ + C_2D_3H$	6.8	6
$\rightarrow C_7H_4D_3^+ + C_2D_2H_2$	1.0	1

TABLE III. Isotope Distribution of the Tropylium Ion from the Reaction of $C_3H_3^+(C_3D_3^+)$ with C_6D_6 (C_6H_6)

Reaction	Relative Cross Section Experimental	Calculated (D_6H_3)	(D_4H_3)
$C_3H_3^+ + C_6D_6 \rightarrow C_7D_6H^+ + C_2H_2$	1.0	1	1
$\rightarrow C_7D_5H_2^+ + C_2HD$	4.7	6	4
$\rightarrow C_7D_4H_3^+ + C_2D_2$	3.4	5	2
$C_3D_3^+ + C_6H_6 \rightarrow C_7H_6D^+ + C_2D_2$	1.0	(H_6D_3) 1	(H_4D_3) 1
$\rightarrow C_7H_5D_2^+ + C_2HD$	4.3	6	4
$\rightarrow C_7H_4D_3^+ + C_2H_2$	3.4	5	2

TABLE IV. Isotope Distribution of the Tropylium Ion from the Reaction of CH_3^+ (CD_3^+) with C_6D_6 (C_6H_6)

Reaction	Relative Cross Section				
		Calculated			
	Experimental	(D_6H_3)	(D_4H_3)	(D_2H_3)	(ring opening)
$CH_3^+ + C_6D_6 \rightarrow C_7D_6H^+ + H_2$	1.0	1	1	3	3
$\rightarrow C_7D_5H_2^+ + HD$	3.8	6	4	6	0
$\rightarrow C_7D_4H_3^+ + D_2$	1.0	5	2	1	0
		(H_6D_3)	(H_4D_3)	(H_2D_3)	
$CD_3^+ + C_6H_6 \rightarrow C_7H_6D^+ + D_2$	1.0	1	1	3	3
$\rightarrow C_7H_5D_2^+ + HD$	7.0	6	4	6	0
$\rightarrow C_7H_4D_3^+ + H_2$	2.6	5	2	1	0

Trapped Ion Cyclotron Resonance Studies of Fast Electron and Atomic Ion Transfer Processes*

T. E. McMahon, P. G. Miasek and J. L. Beauchamp

Department of Chemistry
California Institute of Technology
Pasadena, California

Abstract

Techniques have recently been developed which permit trapping of ions in the source region of an ion cyclotron resonance cell for times up to several seconds. Detection is effected by drifting ions from the source through the analyzer regions where their power absorption is monitored by the usual marginal oscillator-detector. In addition, a time delayed ion ejection technique has been devised whereby an ionic species may be selectively removed from the source region of the cyclotron resonance cell after a given reaction time by applying a secondary radiofrequency oscillator. These techniques have been used to advantage to investigate the kinetics and thermochemistry of a wide variety of ion-molecule processes. Among these are charge transfer reactions in a number of gases of atmospheric interest, thermoneutral charge exchange and proton transfer reactions in methyl halides, proton transfer in simple hydrides and fluoride transfer in fluorinated hydrocarbons. Equilibria observed in these transfer reactions permit an accurate assessment of relative neutral and ion thermochemical properties such as proton affinities and carbonium ion stabilities.

---

* A more detailed account of this work will be submitted for publication in Chemical Physics Letters.

Dependence of Some Ion-Molecule Reaction Cross Section on Internal Energy of Reactant Ions†. W. A. CHUPKA and M. E. RUSSELL, Argonne National Laboratory, Argonne, Illinois 60439.

Reactant ions have been prepared by photoionization in various vibrational and electronic states and their reactions with neutral molecules studied at kinetic energies varying from thermal to 500 eV. The cross sections for collision-induced dissociation of diatomic and polyatomic ions generally show a strong increase with vibrational and electronic energy. The reactions of O_2^+ ions with H_2 have been studied for both the ground and quartet metastable states of the ion with varying distributions of vibrational energy. The effect of electronic excitation on reaction probability is governed by the properties of the potential surfaces on which reaction occurs and the degree of adiabaticity. The varying effects of electronic excitation on some reactions of rare gas ions will be described and discussed in this framework.

†Work performed under the auspices of the U S. Atomic Energy Commission. To be published in the Journal of Chemical Physics.

IONIC SPECIES OF ORGANIC COMPOUNDS IN PLASMA CHROMATOGRAPHY

F. W. Karasek, D. M. Kane and O. S. Tatone
Department of Chemistry, University of Waterloo
Waterloo, Ontario, Canada

Functioning at atmospheric pressure, the plasma chromatograph first creates both positive and negative ions in a carrier gas using a Ni^{63} source. These reactant ions undergo ion-molecule reactions with trace molecules injected into the carrier gas stream. The resultant ion-molecules are separated in a coupled ion-drift spectrometer to give positive and negative spectra characteristic of the organic molecules involved and the reactant ions generated. Both the instrumentation and the technique have been previously described (1,2,3).

When using a N_2 carrier gas to create reactant ions the negative species are thermal electrons. This allows one to observe both dissociative and associative electron attachment and study these processes over a wide range of compounds and conditions. Using the plasma chromatograph, it has been shown that oxygen will react with electrons to form $(H_2O)_nO_2^-$ species and that this reaction is a function of temperature, fewer product ions being formed at higher temperatures (4). These data confirm the effect of trace air on performance of the gas chromatographic electron capture detector. When electrons react with monohalogenated aromatic compounds, dissociative capture occurs to give only a negative halogen ion (2). With aromatic compounds containing multiple halogen substitution, only the most reactive halogen ion is dissociated. Nitrobenzene forms only a negative molecule ion by associative electron capture, while a halogenated nitrobenzene exhibits both associative and dissociative capture. In a series of isomeric chloronitrobenzenes, the 1,3 isomer forms a stable molecular ion, with very little dissociation, while the other isomers exhibit complete dissociation to the Cl^- and the $C_6H_4NO_2^-$ (5). The negative ion spectra obtained are very simple and characteristic. In many instances they can be related to those obtained in negative ion mass spectrometry.

The positive reactant ion species formed in a N_2 carrier gas are primarily of the type $(H_2O)_nH^+$ and $(H_2O)_nNO^+$. These very reactant particles react with trace molecules to give either protonated molecular ions (2,5) or simple fragmentation patterns quite similar to those found in chemical ionization mass spectrometry. The n-alkane hydrocarbons will give quasi-parent ions, either by proton addition or hydride extraction, along with a number of simple fragments. In many cases there is a close correspondence to the fragment ions and simple patterns exhibited in chemical ionization mass spectrometry using a CH_4 reactant gas (6).

Table I lists the positive and negative ion-molecule products identified with the plasma chromatograph in some of this work.

TABLE I. SOME PROMINENT IONS OBSERVED IN PLASMA CHROMATOGRAPHY

NEGATIVE IONS	POSITIVE IONS	
Cl^-	$(C_6H_6)H^+$	
Br^-	$(C_7H_8)H^+$	
I^-	$(C_6H_5X)H^+$	(X = Cl, Br, I)
$(C_6H_5NO_2)^-$	$(C_6H_4ClNO_2)H^+$	(o-, m-, p-)
$(C_6H_4ClNO_2)^-$	$(C_6H_4BrNO_2)H^+$	(o-, m-, p-)
$(C_6H_4BrNO_2)^-$	$(C_6H_5NO_2)H^+$	
$(C_{12}H_4Cl_6)^-$	$(C_{12}H_4Cl_6)H^+$	
$(C_{12}H_2Cl_8)^-$	$(C_{12}H_2Cl_8)H^+$	
$(C_{12}Cl_{10})^-$	$(C_{12}Cl_{10})H^+$	
$(o\text{-}C_6H_4OHNO_2)^-$	$(o\text{-}C_6H_4OHNO_2)H^+$	

The research for this paper was supported by the Defence Research Board of Canada, Grant Number 9530-116, and the National Research Council of Canada, Grant Number A5433.

REFERENCES

1. F. W. Karasek, Anal. Chem., 43, 1982 (1971).
2. F. W. Karasek and O. S. Tatone, ibid, 44, 1758 (1972).
3. F. W. Karasek and D. M. Kane, J. Chromatogr. Sci., 10, 673 (1972).
4. F. W. Karasek and D. M. Kane, Anal. Chem., 45, 576 (1973).
5. F. W. Karasek, O. S. Tatone and D. M. Kane, Anal. Chem., 45, 1210 (1973).
6. F. W. Karasek, D. Denney and E. DeDecker, Unpublished Work, Waterloo, Ontario.

TEMPERATURE AND PRESSURE STUDIES IN A DRIFT TUBE ION-SOURCE

J. W. Long and J. L. Franklin

Department of Chemistry

Rice University

Houston, Texas 77001

ABSTRACT

The extent of an ion-molecule reaction in conventional mass spectrometer sources modified for high pressure work is limited by the short ion residence time in the source, even at high source pressure. A new source constructed in this laboratory has a reaction pathlength of 5.5 cm. which greatly increases the extent of ion reaction. A low voltage gradient is applied to metal rings inside the source to reduce ion diffusion to the walls, thus allowing studies to pressures greater than 1 torr. The source temperature is thermostatically controlled over the range 100 to 400°K permitting temperature studies. An analysis of temperature and pressure effects on ion-cluster reactions observed in the new source gave thermochemical data on ionic solvation for ammonia and phosphine.

This work will be submitted for publication.

ION CYCLOTRON RESONANCE STUDIES OF MERCURINIUM IONS

R. D. Bach, J. Patane, L. Kevan

Department of Chemistry, Wayne State University

Detroit, Mich.

Mercurinium ions have been postulated as intermediates in the oxymercuration of olefins for many years. Here we report observations of mercurinium ions in the gas phase studied by ion cyclotron resonance mass spectrometry. The electron impact ionization of dimethylmercury with 22 eV electrons produces the following mercury containing ions: Hg^+ 30%, CH_3Hg^+ 40% and $CH_3HgCH_3^+$ 30%. All of these ions appear to react with olefins. The most prominent reaction is the addition of CH_3Hg^+ to ethylene, allene, propylene, 1-butene, cis-2-butene, trans-2- butene and isobutene to form presumedly cyclic mercurnium ions. The symmetrical cyclic structure is supported by extended Hückel molecular orbital calculations. Hg^+ also reacts with the mono-olefins to form cyclic mercurinium ions as indicated by extended Hückel calculations. In contrast, Hg^+ appears to react with allene to give a acyclic resonance stabilized allylic cation. This acyclic structure appears to be more stable than the cyclic mercurinium ion with Hg^+. $CH_3HgCH_3^+$ also appears to add to the above olefins and allene to form a complex with the π-electrons of the double bond. It appears that several interesting aspects of organometallic chemistry can be extended to the gas phase.

SOME RESULTS USING ANALOG INCREMENTAL INTEGRATION FOR SIGNAL ENHANCEMENT

R.P. Page and A.V. Nowak
Atlantic Richfield Company
Harvey Technical Center
Harvey, Illinois 60426

When a high-speed ADC is used with a sample and hold amplifier, a single analog value on a peak envelope is converted to a single digital value. For example in our data system the sample and hold amplifier has an acquisition time of 1 microsecond. If the signal is small and noisy, the single analog value converted may not be representative of the peak envelope. A way to improve this value is to integrate the signal between analog to digital conversions and to convert the integrated signal to a digital value. (Slide 1)

This slide shows a circuit which does this. A switch with current amplification is used to provide fast reset of the integrator. In our system a full 10 v output of the integrator is reset in less than 10 microseconds. This is done while the ADC is holding the digital value for reading by a data channel on an IBM 1800 computer. The integrator and switch are described in detail in a Burr Brown applications manual. (Slide 2)

This slide shows what the input to the ADC looks like with a 50 Hz sine wave input to the integrator and a 2500 pt/sec sampling rate. The integrator gain is 4 and the oscilloscope attenuator was used to keep the signal on the screen. The phase shift observed is due to a 200 Hz, 24 db/octave Bessel function active filter in the electron multiplier amplifier. (Slide 3)

This shows a 50 Hz square wave input under the same conditions. At 10,000 resolution (10% valley definition) with a 6 minute quadratic scan and 2500 pts/sec sampling rate our singlet peaks vary from about 25 to 50 points per peak. One can see about 7 points are required to respond to a step function so that maximum peak broadening due to the 200 Hz filter will be about 7 points. We have found this filtering acceptable and it improves the reliability of detection for small peaks. (Slide 4)

This is a plot of the profile of a doublet at mass 185 with and without the integrator circuit. An integrator gain of 4 was used. This is typical of a number of profiles taken using the repetitive sweep on the peak matching circuit. A 9 point Golay-Savitzky smoothing routine has also been applied to this profile.

We applied this technique first to our CEC 21-110 C spectrometer and now we have just installed a similar circuit on our DuPont 21-490 GC-MS instrument. We also tested this technique on our CEC 21-103 C mass spectrometer which uses a faraday cup and sensitive electrometer rather than an electron multiplier. Here we found the period of the noise observed was about half the period of the peaks and no improvement in signal to noise ratio was obtained. Thus we should add the obvious caution that the period of the noise involved should be short relative to the time available for integration.

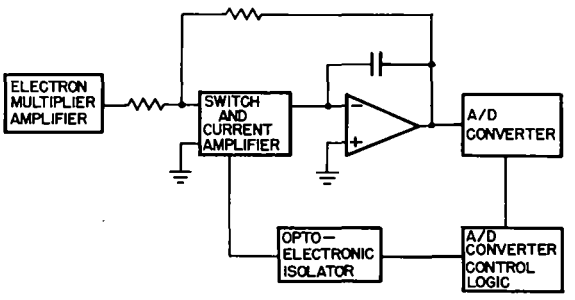

Figure 1 Block Diagram of Integrator

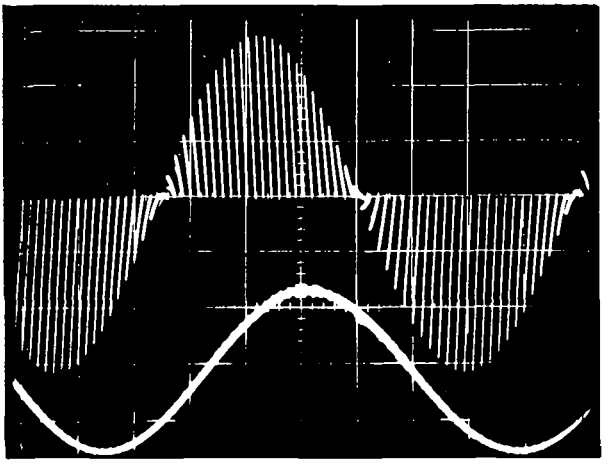

Figure 2 Integrator Output with Sine Wave Pattern

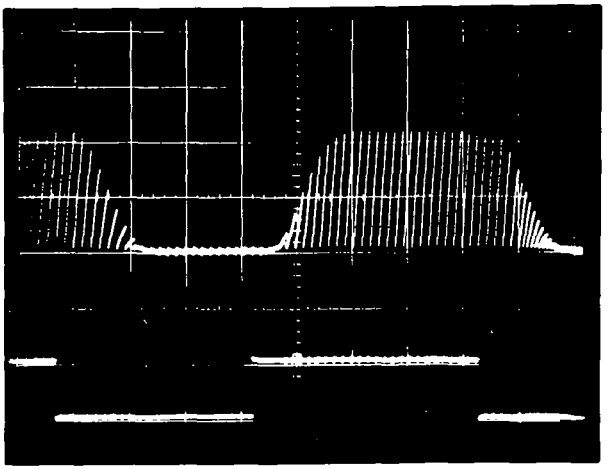

Figure 3 Integrator Output with Square Wave Input.

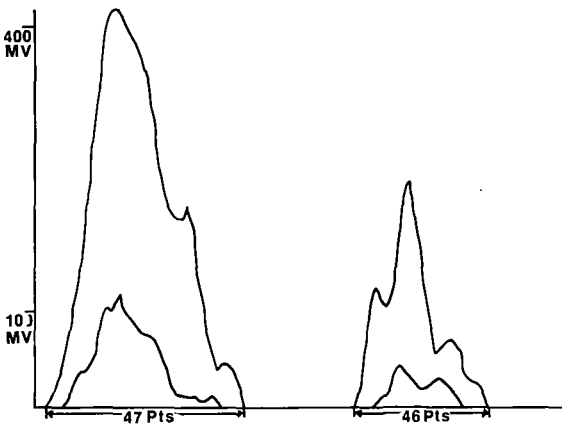

Figure 4 Plot from Digital Data of a Doublet at Mass 185 with and without the Integrator

THE MULTICHANNEL ANALYZER AS A SPECTRA ACCUMULATOR IN SPARK SOURCE MASS SPECTROMETRY

W. W. Harrison, W. A. Mattson, D. L. Donohue, and C. W. Magee

Department of Chemistry
University of Virginia
Charlottesville, Virginia 22901

A 4096 channel analyzer has been interfaced through a V/F converter to a spark source mass spectrometer with electrical detection. The mass spectrum is stored during the scan by using the analyzer in the multiscale mode and selecting a channel dwell time coordinated with mass spectrometer scan time. A digital integrator allows peak areas of any desired isotopes to be compared with an internal standard for quantitative analysis. Repetitive scans may be accumulated in the analyzer, significantly improving the signal-to-background statistics, thus improving a chronic problem associated with spark source spectra. A modified cyclic scan system permits similar accumulation of repetitive scans over a limited mass range for isotope ratio studies. The analyzer-integrator output may be put on-line for data reduction by a time-sharing computer at the University of Virginia.

A paper detailing this study will be submitted to Analytical Chemistry

A COMPUTER-CONTROLLED, ION COUNTING, ISOTOPE RATIO MASS SPECTROMETER

J. M. Hayes and D. A. Schoeller, Department of Chemistry and Geology, Indiana University, Bloomington, Indiana 47401

Stable carbon isotope ratio analysis has been a useful tool in carbon geochemistry (1,2). In addition, stable isotope techniques have been utilized as an alternative to the more dangerous radio-isotope techniques in metabolic studies (3). Carbon isotope ratio measurements have generally been performed using a mass spectrometer with dual Faraday cup collectors and a ratio measurement bridge (4,5). In the differential mode (comparison of a sample and a standard), this instrumentation offers a relative standard deviation of 0.05°/oo on samples of 300 µg C, but only 3°/oo on samples of 10 µg C.

Unfortunately, organic chemical laboratory technology has surpassed these sample levels. In gas-liquid chromatography for example, normal sample loads vary from 0.01 to 1 µg C per single component, at least a factor of ten smaller than that required for analysis with a dual collector instrument.

The limiting factor is the noise inherent in the detector and the ion beam itself. Because of Johnson noise arising in the feedback resistor, currents smaller than 10^{-12} amps cannot be measured by direct electrometric means with the required precision. The use of an electron multiplier instead of a Faraday cup for analog measurements allows reduction of the Johnson noise, but the gain of an electron multiplier is inherently unstable (6); and therefore, measurements with a relative standard deviation of 1°/oo or better are very difficult to obtain.

This paper presents a system for differential measurement of carbon isotope ratios which offers a precision of 1°/oo on 500 ng C. The major factor is the use of an ion counting detection system (7). The effect of noise (including gain instability) arising in the detector is greatly reduced in the mode; in fact, the random fluctuations in the ion beam particle flux are the only non-negligible noise source. Thus, the precision is limited only by the number of ions counting. The number of ions collected from a 500 ng C sample of CO_2 during a 400 second analysis time gives a precision of 1°/oo. Using a 5 µg sample, a precision of 0.3°/oo is obtainable, but a counting time of over an hour is required.

A more detailed discussion of the relationship between the number of CO_2 ions counted and the standard deviation in δ^{13} was presented at the previous ASMS conference.

Experimental

The details of the ion-counting mass spectrometer system have been presented elsewhere (8). Briefly, it is a closed-loop computer-controlled system incorporating a Varian 620i computer which is used to control the accelerating voltage of a Varian MAT CH-7 mass spectrometer and to monitor the output of the ion-counting detection system.

Results and Discussion

To test the instrumentation, a number of analyses were run on a pair of CO_2 samples of known isotopic difference (table 1). The sample size varied from 40 µg to 500 ng C. In all cases, the observed $\delta^{13}C$ and standard deviation were not significantly different from that predicted from ion-counting statistics. For the analysis of samples smaller than 10 µg, it was necessary to dilute the CO_2 with helium by a factor of 100:1 in order to obtain a large enough volume of gas to raise the pressure in the inlet reservoirs to 100 torr, a high pressure being required to assure viscous (non-fractionating) flow though the capillary leaks that carry the sample to the ion source.

It was necessary to correct all data for coincident count losses. This correction is characteristic of particle counting techniques (9). Each ion that strikes the multiplier produces a pulse of finite width. This pulse is further widened by the pulse amplifiers and counter. Any successive pulse that occurs before the first pulse has decayed below the counter threshold will not be recognized as a second event and will therefore be lost.

In order to correct for count loss due to coincidence, it is necessary to measure the dead time, the minimum time-interval allowing resolution of two separate ion pulses. The determination of dead time has proven to be a complex task. Measurements made on isolated system components, such as determination of the amplifier output pulse width, fail because they do not take into account the pulse stretching effects that occur in normal operation. Small pulses arising from such sources as thermionic emission in the electron multiplier or RF pick-up in the transmission lines are not large enough to be counted, but when superimposed on an ion pulse they can increase its width. In addition, the amplifier output pulse width can be a function of the amplitude of the input pulse.

Sample Size μG C	No. Anal.	Avg. $\delta^{13}C$ ‰	S.D. ‰	S.D. mean ‰
40	16	29.6	1.2	0.25
20	5	29.8	1.0	0.45
10	5	29.0	0.8	0.45
0.5	5	29.2	1.2	0.45
	31	29.5	1.1	0.18
	true values	29.5	1.0	

Table 1. Replicate differential analysis of known CO_2 samples

A method of measuring the dead time of the entire system, which takes into account these pulse stretching effects, has been developed by G. Riley (10). Because of the importance of obtaining an accurate measurement of ρ when using an ion-counting system, the method will be discussed in a separate paper (11). In brief, the method consists of measuring the apparent isotope ratio of a compound whose ratio is greater than 10:1 over a range of count rates. Because the count loss for the major isotope will be greater than that for the minor isotope and because count losses will be greater at higher count rates, the apparent ratio will change as a function of count rate. This variation can be utilized to compute the dead time. This method has permitted measurement of the dead time with a relative standard deviation of 5%. The system reported here used a 21 stage Varian electron multiplier, a LeCroy model 234 amplifier, and a Varian model PIC amplifier, peak shaper in series. The dead time of the system was 18 ± 2 n sec. Using this figure it was possible to correct the data for count loss with negligible effect on the precision of the measurement.

1. H. Craig, Geochim. et Cosmochim. Acta, 3, 53 (1953).
2. F. E. Wickman, Geochim. et Cosmochim. Acta, 9, 136 (1956).
3. R.W.E. Watts, J. C. Crawhall, J. Biochem. 73, 277 (1959).
4. A. O. C. Nier, Rev. Sci. Inst. 18, 398 (1947).
5. C. R. McKinney, et al., Rev. Sci. Inst. 21, 724 (1950).
6. C. la Lau, in A. L. Burlingame (ed.) Topics in Organic Mass Spectrometry, Wiley-Interscience, New York, 1970, p. 93.
7. F. A. White and T. L. Collins, Appl. Spec. 8, 17 (1954).
8. D. A. Schoeller, et al., Proc. 20th Ann. Conf. on Mass Spectrometry and Allied Topics, p. 231, American Society for Mass Spectrometry, (1972).
9. R. D. Evans, The Atomic Nucleus, McGraw-Hill, New York, (1955), p. 785.
10. G. H. Riley, J. Sci. Inst. 44, 769 (1967).
11. J. M. Hayes and D. A. Schoeller, To be submitted to Rev. Sci. Inst.

A PROPOSED STANDARDIZATION OF THE MATHEMATICAL METHODS USED IN THE CALCULATIONS AND PRESENTATION OF DATA FROM ISOTOPE DILUTION EXPERIMENTS

John F. Holland, Richard E. Teets, Mark A. Bieber and Charles C. Sweeley

Department of Biochemistry
Michigan State University
East Lansing, Michigan 48823

Stable isotope dilution methods are becoming increasingly popular and currently represent an analytical methodology with great potential in the medical and biochemical fields as well as the traditional industrial and academic areas. Many investigators are presently active in this field as attested by the numerous reports in the literature. However, these publications also reveal the lack of a uniform terminology or a consistent mathematical approach to the processing and reporting of the results of these experiments. This paper presents a review of the basic concepts involved in isotope dilution experiments, defines the most commonly used calculations, and suggests a general approach that may hopefully lead to a consistent terminology and better communication in this field.

Isotope Dilution Method

Fig. 1 illustrates the basic situation in its simplest case where an isotopically labeled compound is added to its non-labeled form producing a mixture. A specific ion is selected as a linear measure for each of the isotopic forms of the compound and these two *m/e* values are then measured in the labeled and the non-labeled forms and in the final mixture. In the mixture, both ions will contain a contribution from each of the two forms. Due to the many variables of mass spectrometric analysis, absolute intensities are not generally accurate enough for reliable quantitative measurements. To minimize the effects of long term variables and greatly enhance the reliability of the method, ratios of the intensities of the two ions are used for the quantitative calculations. Fig. 2 illustrates the composition of the mixture. I_{L_1} and I_{N_1} represent the contributions at one mass from the labeled and the non-labeled forms, and I_{L_2} and I_{N_2} indicate the contributions at the other mass. Since the ratios for the two ions in each isotope will remain constant, mathematical solutions for the intensity of each component in the mixture can be obtained (Fig. 3). The roles of the labeled and non-labeled forms are interchanged when applied to reverse isotope dilution techniques.

The Rittenberg Approach

The Rittenberg procedure has been widely used and when its basic definitions are correctly employed, it presents an exact formula for concentration calculations (2). This method may be classified as Fractional Molecular Excess, and in changing the authors' original terminology, it may be derived in the following way. The classical material balance formula for a two component mixture may be written as:

$$C_n F_n + C_1 F_1 = (C_n + C_f) F_m$$

where C_n = the amount of non-labeled compound
C_1 = the amount of labeled compound
F_n = fraction of the labeled ion in the non-labeled compound

$$F_n = \frac{I_{N_2}}{I_{N_1} + I_{N_2}}$$

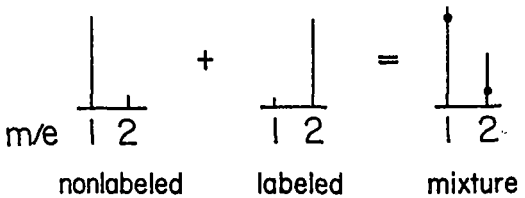

$$R_N = \frac{I_2}{I_1} \qquad R_L = \frac{I_2}{I_1} \qquad R_M = \frac{I_2}{I_1}$$

Figure 1. Isotope Dilution Method

$$I_{M_1} = I_{L_1} + I_{N_1} \qquad I_{M_2} = I_{L_2} + I_{N_2}$$

$$I_{M_1} = I_{L_1} + I_{N_1}$$

$$I_{M_2} = I_{L_1} \cdot R_L + I_{N_1} \cdot R_N$$

Figure 2. Composition of the Mixture

$$I_{L_1} = I_{M_1} \cdot \frac{R_M - R_N}{R_L - R_N} \qquad I_{L_2} = R_L \cdot I_{L_1}$$

$$I_{N_1} = I_{M_1} \cdot \frac{R_L - R_M}{R_L - R_N} \qquad I_{N_2} = R_N \cdot I_{N_1}$$

Figure 3. Solution of Simultaneous Equations

F_1 = fraction of labeled ion in the labeled compound $\quad F_1 = \dfrac{I_{L_2}}{I_{L_1} + I_{L_2}}$

F_m = fraction of the labeled ion in the mixture $\quad F_m = \dfrac{I_{m_2}}{I_{m_1} + I_{m_2}}$

Expanding and converting all fractions into molecular excess above normal:

$$C_n(F_n-F_n) + C_1(F_1-F_n) = C_n(F_m-F_n) + C_1(F_m-F_n)$$

Solving for C_n:

$$C_n = C_1\left(\frac{F_1-F_n}{F_m-F_n} - 1\right)$$

which is the familiar form of the equation.

Several restrictions must be observed whenever this method is applied:

1. The same fragment ion must be used for both molecules.
2. All isotopic, instrumental, or concentration-related variables must either be negligible or the same for each ion.
3. The dimensions used for C_n and C_1 may vary, i.e., weight, moles, equivalents, number of atoms, etc., but must be consistent within any single analysis and should always be clearly defined. The need for molecular weight correction should be observed when mass units are employed (3).
4. The F factors must represent the fraction of the labeled molecules in each form; the labeled, non-labeled, and the mixture.

Atom Percent Excess by Ratios

In considering the enhancement of an ion representing the isotope-labeled species (at mass 2 in Fig. 2), one can define a quantity, δ, that measures the relative extent of this enhancement in the final mixture above that of the non-labeled starting compound.

$$\delta = I_{L_2}/I_{N_2}$$

Substituting the solutions from Fig. 3, δ can be expressed in terms of ratios only:

$$\delta = \frac{R_m-R_n}{R_n} \times \frac{1}{1 - R_m/R_1}$$

Under conditions where $R_m \ll R_1$,

$$\delta \propto \Delta \equiv \frac{R_m-R_n}{R_n}$$

This quantity, Δ, is often used in the calculations for dilution experiments (4) and will be linear with concentration of the labeled species, with the following restrictions:

1, 2, and 3 are the same as in the previous method.

4. There must be a large relative dilution of the labeled form.

It must be noted that Δ is an approximate solution. Whenever the relative dilution is not sufficiently large, as in the case when a pure labeled form cannot be synthesized

or isolated, R_m will not be significantly less than R_1, and the correction factor, $\frac{1}{1 - R_m/R_1}$, should be applied to maintain the linearity of the calculation with the concentration of the labeled species.

Several factors encourage the adoption of a more general formula for future dilution experiments. In many cases, it is not possible to use the same ion fragment to quantitate the different molecular species. This situation may arise as a result of the presence of interfering ions or from the need to utilize an expanded range of concentration. In addition, instrumental performance is continuously improving and more sophisticated data processing is being attained from widespread use of mini-computers. This suggests that many of the variables of the analyses which tend to differentiate between the two designated ions will be identified, measured, and may even be entered in the calculations with a subsequent improvement in the accuracy of the method. A mathematical formulation capable of accommodating these factors as they are delineated should be available and the following is offered as an example of this type of approach.

General Method

All of the above methods assume that measured ion intensities are directly and linearily related to amounts of the molecular isotopic forms from which they arise. This, of course, is fundamental to the analytical capability of the technique. In fact, each of the ions are usually selected to attain this linearity if possible. The quantitative identification in the terms from Fig. 2 may be defined as:

I_{L_2} = the measure of the labeled molecule

I_{N_1} = the measure of the non-labeled molecule

Ideally,

$$I_{L_2} = k_L C_L$$

$$I_{N_1} = k_N C_N$$

and both k_L and k_N are constants.

The ratio of the amounts of the two forms contributing to the mixture may be represented as I_{L_2}/I_{N_1}. Solving for this ratio in terms of measurable quantities:

$$I_{L_2}/I_{N_1} = \frac{R_m - R_n}{1 - R_m/R_1},$$

and substituting for the intensities,

$$\frac{C_L}{C_N} = \frac{k_L}{k_N} \times \frac{(R_m - R_n)}{(1 - R_m/R_1)}.$$

Again, when $k_L = k_N$ and $R_m \ll R_1$, $\frac{C_L}{C_N} = R_m - R_n$.

It is clearly recognized that k_L and k_N are complicated constants, if constants at all, and that they may be further expanded into several factors, some of which will be definable and measurable. In any case, they represent the analytical limitations of the method and will vary with different compounds, different instruments, and different conditions of analysis. This general approach offers a simple formula for calculations involving dilutions and an exact formula for other conditions. It also has the

flexibility to accommodate the new analytical factors as they become identified, measured, and separated from the complex factors, k_L and k_N. This approach will be expanded in greater detail in a future publication being submitted to *Analytical Chemistry*.

This work was supported in part by NIH Grant RR 00480.

References

1. K. Bloch and H. Anker, *Science*, 107:228 (1948).
2. D. Rittenberg and G.L. Foster, *J. Biol. Chem.*, 133:737 (1940).
3. H. Gest, M.P. Kamen, and J.R. Reiner, *Arch. Biochem.*, 12:273 (1947).
4. J.H. Beynon, "Mass Spectrometry and Its Applications to Organic Chemistry", Elsevier, London, 1960, p. 91.

A COMPARATOR-MICRODENSITOMETER-PROGRAMMABLE CALCULATOR SYSTEM FOR PROCESSING HIGH RESOLUTION MASS SPECTROGRAPHIC PLATES

J. H. Weber, D. G. Earnshaw, D.W.K. Severin,[1] and A. W. Decora
U.S. Department of the Interior, Bureau of Mines
Laramie Energy Research Center, Laramie, Wyoming 82070

The hardware system and software package for the semiautomatic acquiring and automatic processing of high-resolution mass spectrographic plates are described. The semiautomatic data acquisition part of the system allows a tenfold time savings as compared to hand-read data acquisition. The processing technique described is particularly adaptable to small laboratories having budgets that preclude access to more sophisticated data processors. Automatic processing of the high-resolution data to yield exact masses, intensity, and the corresponding empirical formulas is accomplished by efficient programming on a small, inexpensive, programmable calculator and related accessories. The system may be expanded as available funds allow to increase the capability of the processing system.

[1]Max Kade Postdoctoral Fellow, 1972-1973.

A DISPLAY-ORIENTED DATA SYSTEM FOR PROGRAMMABLE MULTIPLE ION DETECTION

Donald R. Pelster and J. Throck Watson
Department of Pharmacology, Vanderbilt University
Nashville, Tennessee 37232

Although the technique of multiple ion detection (MID) was developed by Sweeley et al (1) on a magnetic mass spectrometer, operation of this type of instrument has several features which are not optimal for refined MID. Since the magnetic field is too sluggish to be cycled rapidly between discrete levels, the accelerating voltage is attenuated by using a series of voltage divider circuits which are preset for the m/e values of interest. Since a reduction in accelerating voltage also reduces ion abundance, the first commercial versions of MID equipment, such as the LKB AVA unit on our standard LKB-9000, were limited to a 10% reduction in accelerating voltage and thus only a 10% mass range for MID. That is to say, that if m/e 200 happened to be the lowest ion of interest we could only monitor ions up to m/e 220 on that particular run.

The limitation of only 3 ion current channels on the early AVA or MID units is a problem. We have often needed a minimum of 4 ion current channels, 2 for the compound of interest and 2 for the internal standard; this version of MID instrumentation is now commercially available. Of course, the more ions one can monitor, up to a certain point, the greater confidence he will have in his final results. Another feature of our original MID hardware which limited the effectiveness of our MID data system (2) was the use of mechanical relays to switch the accelerating voltage between preset values. Since variable lengths of time up to 100-150 msec were sometimes required for the reed relays to close, much valuable data acquisition time was lost.

To overcome some of these limitations in MID hardware, we have designed a more flexible MID system built around a programmable power supply (3) which is controlled by a PDP-12 computer. The LKB-9000 power supply is adjusted to produce 2500 volts and the programmable power supply is connected in series to supply an additional voltage of from zero to 1000 volts to the ion source. This voltage range between 3500 volts (normal or "Full" voltage) and 2500V corresponds to a mass range of approximately 40% in which up to 12 ions can be monitored.

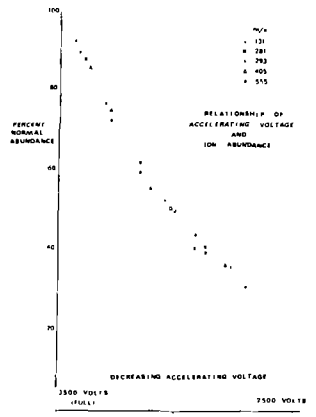

Fig. 1. Attenuation of Ion Abundance with Decreasing Accelerating Voltage expressed as percent of Abundance at full accelerating voltage.

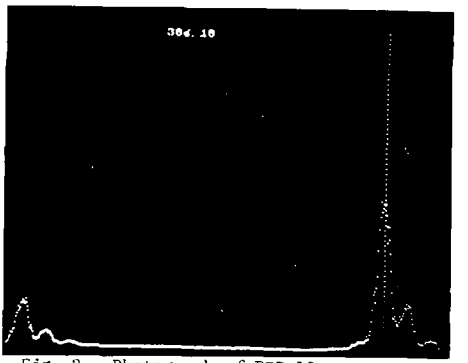

Fig. 2. Photograph of PDP-12 computer CRT showing results of rapid, electrical scan over 1000 volt range for THC-TMS (mol. wt. 386).

The effect of decreased accelerating voltage on ion abundance is shown in Figure 1 which expresses the attenuated abundance of each of 5 ions from perfluoroalkane (PFA) as a percent of their ion abundance at full accelerating voltage. These data indicate that for ions in the m/e range 100 to 600, the ion abundance at 2500 volts will be attenuated to 30% of its abundance value at 3500 volts.

During the "tune up" procedure, the limits of the mass range of interest are verified by acquiring data from a rapid electrical scan of ions of PFA over the 1000 volt range. The operator then enters the m/e values for up to 12 ions of interest. "Fine tuning" of appropriate voltages involves a second, rapid electrical scan of the compound(s) of interest as they emerge from the GLC. An example of the acquired data from such a rapid electrical scan can be seen in Figure 2 which shows the region of the mass spectrum near the molecular ion (386) for the TMS derivative of tetrahydrocannabinol (THC). To "set" the appropriate voltage for this ion, the operator has adjusted a mass/charge cursor (vertical line on CRT) to the center of the peak of interest (note that the value of the mass scale at this selected point is 386.18). The operator then commands the computer, through the teletype (TTY), to store or "set" the corresponding value of accelerating voltage (represented as the abscissa in Fig. 2) for reference purposes of acquiring the ion current profile of m/e 386. This procedure, which provides for human intervention and judgement in an otherwise computer-controlled process, is repeated for the other ions of interest.

The computer then cycles the accelerating voltage between these reference points

and acquires data according to the following protocol. A programmed delay, T_1=2 msec, ensures that the accelerating voltage has stabilized before data acquisition. The analog to digital converter (ADC) of the computer then samples the electron multiplier n times (usually n=100) at T_2=1msec intervals. All these parameters (n, T_1, T_2) are programmable and can be optimized for a given analysis if desired.

A large proportion of MID in our laboratory involves quantitative determination of prostaglandins in biological samples by measuring the ratio of endogenous or unlabelled prostaglandin derivative to that of a deuterium-labelled (d-4) analog used as an internal standard. There are several ion pairs (423, 427*; 494, 498*; 513, 517*; 569, 573*) in the mass spectra of the $PGF_{2\alpha}$-ME-TMS3 derivatives which ordinarily would have to be monitored individually (4) because of hardware limitations in mass range and the number of ions accomodated; thus, measurement of all 4 ion pairs would require 4 experimental "setups" with the previous AVA unit. The programmable MID unit, on the other hand, could monitor all 8 ions (or 4 ion pairs) simultaneously as illustrated by the CRT photograph in Figure 3.

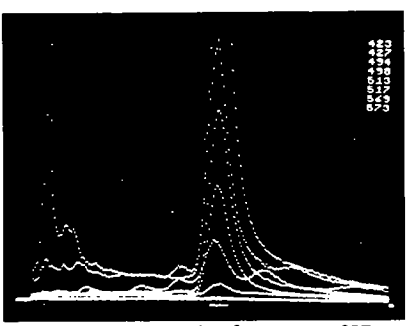

Fig. 3. Photograph of computer CRT showing composite of 4 ion pairs monitored during analysis of urine sample for $PGF_{2\alpha}$-ME-TMS3 containing d-4 internal std.

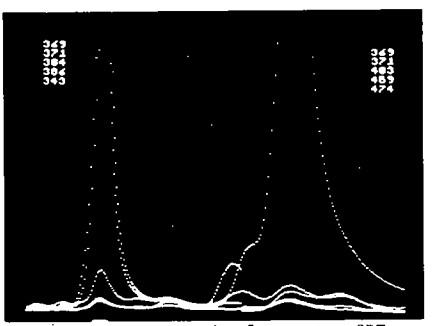

Fig. 4. Photograph of computer CRT showing 2 groups of 5 ions monitored during consecutive periods of the GLC analysis of THC-TMS and 11-OH-THC-TMS.

A composite display such as this is only useful for qualitative purposes; this type of data record would be practically impossible with a mechanical recorder. Selected ion pairs may be examined individually or compared quantitatively with other sub-routines of our MID software (2). Agreement in abundance ratio of the ion pairs in several different segments of the spectrum is used as an index of confidence in the analytical method (4).

Finally, the programmable MID unit provides the opportunity to emphasize detection of different ions during different periods of the GC run. That is, it would be inefficient to dedicate the computer to monitor a given ion current for the whole of a 10

*d-4 prostaglandin $PGF_{2\alpha}$ kindly supplied by the Upjohn Co., Kalamazoo, Michigan.

minute GLC run, if it is known that no compound of interest which produces that ion will emerge from the GLC after the first 3 minutes of the GLC analysis. The results of a more efficient process of data acquisition is illustrated in Figure 4 which shows MID results from analysis of a microsomal incubation of THC. During the first period, 5 ions (369, 371, 384, 386, 343) shown at upper left were chosen for THC-TMS. During the second period, the 5 ions (369, 371, 403, 459, 474) at upper right were chosen to optimize detection of 11-OH-THC-TMS (a metabolite). The discontinuities in ion current profiles in the middle of Figure 4 indicate the change in emphasis of ion-of-interest during the MID run.

This programmable MID system essentially eliminates the mass spec hardware limitations of our display-oriented data system. Twelve or more ion current channels are available without the additional cost of as many individual amplifiers or hardware circuits and the usual time-response problems associated with mechanical devices. This programmable, flexible MID system facilitates optimum acquisition and display of data which are meaningful to the investigator.

REFERENCES

1. C.C. Sweeley, W.H. Elliott, I. Fries, and R. Ryhage, Anal. Chem. 38:1549-53, 1966.
2. J.T. Watson, D.R. Pelster, B.J. Sweetman, J.C. Frolich, and J.A. Oates, Anal. Chem. (in press).
3. for comparable system, see W.F. Holmes et al, these Proceedings; to be published in Anal. Chem., autumn, 1973.
4. B.J. Sweetman, J.T. Watson, K. Carr, J.A. Oates, and J.C. Frolich, Prostaglandins 3:385-387, 1973.

ACKNOWLEDGEMENT

This work was supported by The Research Center for Clinical Pharmacology and Drug Toxicology (NIH-GM-14531). We are grateful to the Upjohn Company for d-4-$PGF_{2\alpha}$.

Diagnostic Codification of Mass Spectral Data

D. H. Robertson and C. Merritt, Jr.
Pioneering Research Laboratory
US Army Natick Laboratories
Natick, Massachusetts 01760

Certainly there is general agreement among mass spectroscopists that the way in which we can render automatic interpretation of mass spectra most infallible is to cause it to accurately emulate the function of a human interpreter. Effecting such emulation continues to be a major problem for two reasons: a) the difficulty of decision about what steps must be emulated and b) the arduous task of programming these steps for use on a system of reasonable size.

There is in addition the matter of computer facility for effecting the acquisition, reduction and search phases involved in mass spectrometery investigations.

Recently there has been considerable attention given to compression of data files by design of special codes that reduce the amount of storage required and speed the search of a library of known compounds for identification of an unknown spectrum.

A useful characteristic of several of these codes is the elimination of peak intensity in the codification scheme; thus, small variations in mass spectral patterns are smoothed when such coding is applied and the effect of small contributions to the spectra from impurities is eliminated; except in the obvious case where the impurity is present in a concentration near that of the compound being identified. Within the framework of such approaches to codification which compress the over-all amount of data, as well as minimizing the effect of impurities and small variations in the production of spectra, one may adopt two general approaches: a) the theoretical modeling approach and 2) the pragmatic application related to the characteristics of mass spectra. The first of these topics is discussed by Dr. Grotch in paper number D-1. This paper will discuss a few aspects of the pragmatic approach; i. e. the approach which takes into consideration such features of mass spectra as diagnostic ions in constructing a codification and search procedure. This approach has been developed with especial consideration for its implementation on a mini-computer system which it is assumed will have a modest amount of core memory, e. g. ca 8K and operate typically in the 16 bit word domain.

The graph depicted in Figure 1 represents the distribution of masses in a library of some 7,000 compounds. The code used for processing this library was the 1 peak/7 amu scheme which was referred to at the 20th Annual Conference on Mass Spectrometry and Allied Topics†, as octal coding. That is, the mass range from 23-364 is divided into groups or (to use Dr. Grotch's terminology) windows of 7 amu each. Coding is effected by assigning to the most intense mass in each group of seven masses a number from one to seven which represents the position of that mass in the group or window. The Y axis represents the per cent of compounds in the library which have a mass in the window as shown on the X axis. A not surprising observation is that the most intense peaks for the majority of compounds lie between 50 and 250 amu. It is in this region that one finds coding of 1 amu/7 an advantage in differentiating among possible compounds. In the higher molecular weight region represented by the trailing edge of the curve, a wider window will be satisfactory, i. e. 1/14 amu or larger.

Intuitively, a practicing mass spectroscopist would feel that starting mass for the groups or windows would have an effect upon the success of the search algorithms in differentiating among spectra, insomuch as there exists a series of ions which are routinely used as diagnostics for specific functional groups.

†American Society for Mass Spectrometry, Dallas, Texas, 4-9 June 1972

TABLE I

NUMBER OF ONES CODED

Starting Mass	Threshold level			
	.01	1.	5	10
20	17.5	13.0	5.9	8.1
21	17.5	13.3	6.3	8.6
22	17.5	13.3	6.4	8.7
23	17.4	12.6	5.8	7.9
24	17.2	12.2	5.7	7.7
25	17.0	12.0	5.5	7.4
26	16.9	12.5	5.9	8.0

The figures in Table I would not support this statement. Thus it is brought to our attention that one needs to consider statistical data in light of the basic character of the discipline producing them.

Since the number of binary bits or "ones" coded in the library represents its information content or entropy, such representation is frequently employed when discussing data compression techniques. Considering a range of starting masses for the first window from 20-26 amu, it can be seen for the intensity found at each transition (i. e. threshold) level the number of "ones" coded remains essentially constant. The information content of the spectrum as an entity remains constant. Such a conclusion is rather obvious. But it also is misleading because it imputes to the code the ability to select the most diagnostic mass in each group of seven when it is actually selecting the most intense mass in each group of seven amus. A look at some statistical values based on the total 6880 compound library illustrates the point as suggested in Table II.

TABLE II

m/e VALUES AT WINDOW BOUNDARY, OCTAL CODE, ONE in 7

50 | 51	211 | 212	225 | 226
253 | 254	281 | 282	309 | 310

Each pair of masses in this figure (selected from the statistical distribution of "ones" when the starting mass is 23) represents respectively the last mass or position 7 in one window and the first or position 1 mass in the next higher adjacent window or group. It can be readily appreciated that if the scale is moved left or right to accommodate any starting mass that any one of these mass values would be moved into the adjacent window where it might or might not be coded as the most intense peak, depending, of course, upon the intensity of the other peaks in the window under consideration. In other words, for this group of adjacent mass pairs or indeed for any adjacent mass pair, a shift of starting mass used in the code will stand a very good chance of eliminating the boundaries which allow each mass to be coded in a separate window. Appearance of adjacent masses in a spectrum is in many instances a highly diagnostic feature. Commonly known examples would be the P and P-1 peaks and the isotope distribution peaks.

TABLE III

COMPARISON OF CODES

CONFUSION	14 AMU	7 AMU	14 AMU + 2
0	64.8	57.6	79.2
1	72.8	74.4	89.6
2	76.8	79.2	94.4
3	82.4	80.8	95.2
4	87.2	83.2	95.2
5	88.0	84.8	95.2

In addition to the question of what starting masses to use in filling the groups or windows, one must address himself to the problem of selecting the codification scheme whereby these selected masses are represented by a binary code within the computer.

In Figure III, we see a comparison of coding schemes, using, from left to right, one peak in 14 amu, one peak in 7 amu and one peak in 14 amu, plus 2 bits for coding intensity. The first scheme requires 64 bits per spectrum, while the remaining two schemes each require 96 bits per spectrum. The term confusion refers to the number of compounds which agree as well or better than the right answer. The values listed under each code are percentages of unique matches for the confusion factors with which they correspond. When one considers the absolute percentages for a single unique identification i. e. for a confusion factor of zero, it is obvious that use of an intensity factor substantially increases the percentage of matches at all confusion levels. However, a comparison of the values for one in 14 amu vs. 1 in 7 amu differs much less and in practical work proves to be less important than the absolute difference in these values might indicate. The following factors have been shown to be important in enforcing this statement: a) Since most mini-systems for laboratory applications use a 16 bit word, a group of seven, each requiring three bits can be very easily coded i. e., 5 groups of 3 bits with one left over as a pointer or indicator. (b) No intensity factor is coded, making possible more rapid on-line acquisition of gas chromatography/mass spectrometry data. c) Working with groups of 7 amu provides twice the opportunity for coding a mass which is diagnostic for a specific functional group, especially in the high density area of the curve which is depicted in Figure 1; that is, in the area of maximum occurrence of unique peaks. In most practical cases the investigator is in possession of some ancillary information about the compound or compounds he expects to identify; so the fact that more than one answer is given by a search algorithm does not necessarily mitigate against its utility.

In terms of practicality, as regards computer power needed to do the job and ease with which the chosen technique provides on-line real-time processing of mass spectral data, it certainly need not be a unique compound. The condition of mass spectral data libraries is such that it would seem unrealistic to hope for a coding and search technique that is always able to abstract the single right answer. There has been, for example in these laboratories, a high degree of success when using the special restricted libraries of compounds expected to appear in particular sample types; these libraries contain spectra coded from the mass spectrometer on which the "unknown" is being run. Therefore greater internal self-consistency of data is achieved. When one goes to larger libraries the spectra in which come from numerous sources, the internal self-consistency factor is reduced, often dramatically.

There exists another case where statistical data creates a problem.

TABLE IV

EFFECT OF THRESHOLD LEVEL

LEVEL	Average Entropy	Average Peaks
0.01	100	82.9
0.10	99.87	74.4
1.00	94.40	40.6
10.00	65.15	10.7

In Table IV there is an example of the potential difficulty in using a generalized calculation (in this case molecular entropy) and interpreting the results on the basis of an average behavior for the library as a whole. At the 1% threshold level, by definition 100% of the possible entropy content is available. As the threshold level is raised, the entropy obviously decreases and with it the information content of the library. These data would suggest that the 10% threshold level is nearly as useful as the 1% level in terms of information content. However, at higher threshold levels one is dealing with more than the fact that overall information content decreases. Again this additional factor depends upon a detailed knowledge of mass spectra. Considering the fact that the molecular weight or parent ion determination is the single most useful piece of information that a mass spectrum can give, it is obvious that compounds which are well known for low-intensity parent ions will not be properly handled, either in a compressed scheme or under conditions where low intensity peaks are omitted from entropy-like calculations.

The basic contention which is maintained about mass spectral data is that it is overdetermined; i.e., there is more information present than is actually needed to uniquely identify a compound if judiciously selected techniques are employed in abstracting the requisite amount of data. A range of approaches has been used to zero in on this elusive irreducible minimum of data required. It is felt that a combination of statistical analysis and thinking like a mass spectroscopist will constitute the most valuable approach; the rate at which work is in progress in this field suggests that a speedy convergence upon the solution will be forthcoming.

One area, however, seems to be sorely neglected, namely that of establishing standard mass spectral data files from which to work. Remarkably little interest has been shown in this area, undoubtedly because so many data libraries already exist. However, attention to standardization of these data as well as new data is certainly well advised.

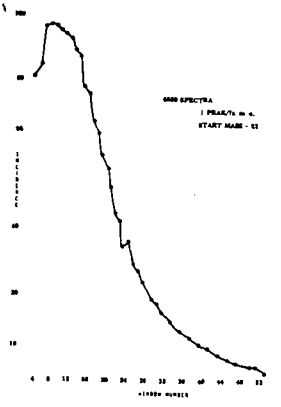

Fig. 1

A MATHEMATICAL THEORY FOR THE FILE SEARCHING OF MASS SPECTRA

Stanley L. Grotch
Jet Propulsion Laboratory
Pasadena, California 91103

INTRODUCTION

In file searching, an unknown spectral code is compared against a larger known file of similarly coded spectra, and those library spectra which "best fit" the unknown code by some criterion are assumed to be the correct answers. Generally, most workers have intuitively developed algorithms for measuring goodness of fit and tested these using a limited number of unknowns.

While this approach is obviously pragmatic, it provides no theoretical framework for understanding the matching in a quantitative manner. With the theory developed here, it becomes possible to compare different matching techniques in terms of their potential efficacy of identification in at least a semi-quantitative manner. The effects of coding errors on identification become clearer, and the outlines of procedures to improve matching algorithms become more apparent.

FILE SEARCHING WITH ONE BIT CODING

One bit coding provides a simple introduction to the proposed theory, and the concepts derived here are readily generalizable to the more complex case. When a binary code is compared against a library using the logical XOR mismatch criterion, a distribution of mismatches is obtained (e.g., the fraction of codes in the library with a given number of mismatches).

The features of this distribution are important in understanding the identification problem, particularly with regard to errors leading to mis-identification. Quantitatively, few codes in the library exist close to any given code, but above a certain threshold of mismatches a very large number of library members arise. If the number of errors between the unknown and its true counterpart in the library lies below this threshold, the unknown code will be correctly identified with little ambiguity. With the theory developed, this threshold can be estimated, without performing the matching, given the unknown code and some simple statistics of the library.

MEAN OF THE MATCHING HISTOGRAM

Let v_i and ℓ_i denote the values encoded in the ith channel for the unknown and a specific library member, respectively. If x_i is the value of the XOR operator in the ith channel:

$$x_i = \ell_i + v_i - 2\ell_i v_i \tag{1}$$

If p_i is the probability that a "1" is coded in channel i for the library, μ is the mean of the XOR distribution for any code:

$$\mu = \Sigma (p_i + v_i - 2p_i v_i) \tag{2}$$

For any library, the p_i are easily obtained in a one-time calculation, and with Eq.2, the mean number of mismatches for any code can be calculated exactly.

APPROXIMATE SHAPE OF THE MATCHING HISTOGRAM

Consider as an "unknown" code, one which contains only "0's" in all channels. When compared with the library, the distribution of XOR found for this code will be identical to the distribution of "1's" coded for the library. If a single channel k in this unknown is changed (0 →1) the mean will change by:

$$\Delta\mu = 1 - 2p_k \tag{3}$$

Assume that as "1's" are added to an all zero unknown to yield the code of interest, that the shape of the all zero histogram remains unchanged, but that its mean shifts according to Eq.3 as each "1" is added. If this assumption holds, all matching distributions for all codes should be the same for a given coding scheme and library when normalized to the same mean value. This common distribution is the known distribution of "1's" coded in the library.

Using 125 different "unknown" binary codes, calculations show that in most cases the matching distribution does, in fact, follow a common curve when normalized in terms of the mean. Using this procedure, the matching distributions for several different encoding schemes with two different libraries also was accurately predicted. It was

found that the lower threshold before confusion in identification occurs could be well predicted for most unknown codes.

GENERALIZATION TO MULTIPLE LEVELS

These results are easily generalized to the case where peak intensities are expressed to more than two levels. It can be shown that if $\bar{\ell}$ and $\overline{\ell^2}$ are the average level and average square level coded in the library, that the mean square disagreement is given by:

$$\mu = \sum_i \left(\overline{\ell^2}_i + v_i^2 - 2 v_i \bar{\ell}_i \right) \qquad (4)$$

By analogy with the binary case, for a least square criterion all unknown codes compared against a given library should yield a universal matching distribution shifted only along the disagreement axis with the mean calculated from Eq. 4. This distribution should be identical to the distribution of levels squared for the library, which is known, a priori. Calculations using two different encoding procedures and 125 unknown codes corroborate this result. Additional calculations show that it is possible to also estimate, a priori, when this procedure is likely to be in error.

CONCLUSIONS

Techniques are developed to predict the matching behavior of unknown codes against a library using a least square difference criterion. The mean square difference is exactly predicted for all codes using simply obtained statistical properties of the library. The matching behavior of many codes is well predicted by a common prediction shifted only in mean value.

The effect of coding errors on spectral mis-identification may be considered in terms of the threshold of the matching histogram. Since this threshold can be approximately predicted, it is possible to determine the magnitude of the error which can be tolerated before mis-identification is likely to occur. The theory should permit a better quantitative assessment of these errors on performance and should suggest methods to better optimize the reliability of these techniques.

* * *

It is planned to publish a more complete version of this work in "Analytical Chemistry."

* * *

This paper presents the results of one phase of research carried out at the Jet Propulsion Laboratory, California Institute of Technology, under Contract No. NAS 7-100, sponsored by the National Aeronautics and Space Administration.

METABOLIC PROFILE ANALYSIS BY GC-MS

S.P. Markey, W.G. Urban, and A.J. Keyser

Department of Pediatrics
University of Colorado Medical Center
Denver, Colorado 80220

The use of small computer data systems for the acquisition and processing of mass spectral data has become commonplace in the last five years. Previously, we described a system based upon a Digital Equipment Corp. PDP 8i for processing data from magnetic deflection mass spectrometers which scan with a decreasing exponential scan rate[1]. The objective in the design and construction of this system was to make it:

1) Useful for the analysis of complex mixtures of organic compounds with gc-ms, mixtures such as those found in physiological fluids.

2) Simplify the reporting of data to either automatic compound identification or plotted mass spectra for permanent storage with a patient's chart.

3) Inexpensive and usable in other laboratories with similar instrumentation, with programs freely available through us or DECUS (DEC Users Society).

The analysis of organic extracts of physiological fluids is of interest in the study of organic causes of mental retardation, the metabolic effects of drugs and diet, and in drug metabolite studies. Most of our efforts are concerned with the analysis of endogenous metabolites in urine and amniotic fluid - the detection of compounds of abnormal concentration (either increased or decreased) due to metabolic problems. A typical silylated extract of the organic acids in urine, in this case a pooled sample from ten newborn infants being formula-fed, yields the gc trace shown in Figure 1. Without difficulty, some 73 peaks can be distinguished using a packed column. Capillary columns are now being used which further resolve this pattern into many additional components.

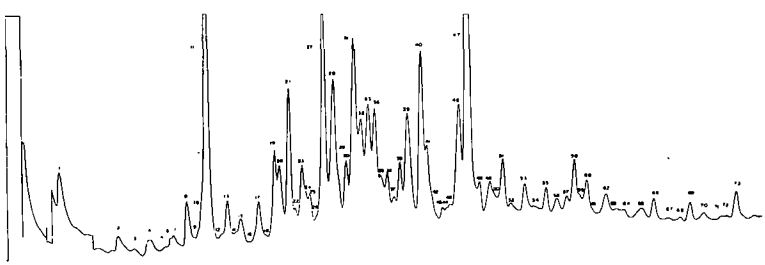

Figure 1. Chromatogram from a pooled urine acid extract from 10 normal infants. Silylated extract chromatographed on a 6' glass column (2mm i.d.) packed with 5% OV-22 on 100-120 mesh Gas Chrom Q. Programmed from 50° - 280°, 2°/min.

Gc-ms analysis of the chromatogram in Figure 1 is not difficult, but the interpretation of the data presents several problems. In order to obtain good mass spectra of major and minor peaks, the sample is re-run several times with different multiplier gains. Spectra, stored on disk or DEC tape, are then available for selective processing. Total ion current plots are conventionally used to select scans and relate them to the gc tracing. Mass chromatograms can be made, and are useful when searching for a specific compound, but are not generally used for interpreting TMS-organic acid extracts. Individual spectra must be selected and compared with standard spectra or manually interpreted. The comparison

of these spectra may be done by one of three options:

1) Manual look-up

2) Off-line computer search...either NIH-type of single spectrum search, or transfer of data to another computer for batch processing or time sharing.

3) On-line, automated library search using the same computer system developed for data acquisition.

The choice of one of these three options will obviously depend upon the requirements of the individual laboratory and the available computer facilities. For the past three years, we have relied upon manual look-up methods. A library of mass spectral data of compounds of physiological interest has been compiled (approximately 300 spectra) and indexed according to peak intensity and molecular weight. The slow printing or plotting of reams of mass spectral data is avoided by rapidly displaying (1200 baud) a tabular listing of a particular spectrum on a display scope. Manual comparison of the display with the indexed library of compounds is rapid and simple. An examination of the compounds in Table I indicates why metabolic profile analysis is a most promising area for biomedical research. In a single analysis, products from the citric acid cycle (such as fumarate, aconitate, citrate), from amino acid catabolism (β-hydroxyisovaleric, β-hydroxy, β-methylgluarate), from sugar metabolism (lactate, tartrate), from lipid metabolism (lactate, β-hydroxybutyrate, adipic), from bacterial sources (hippuric, hydroxybenzoic), from catecholamine metabolism (HVA and VMA), and from drugs (salicyluric) are readily detected and can be quantitated if suitable standards are used. Such gc-ms analyses may be used to give a relative metabolic picture of the state of an individual's health. With the expansion of the library, due to the incorporation of files from other laboratories, an automated library search system would be advantageous. Off-line batch processing of data is not feasible in our environment; single spectrum analysis offers little advantage over manual look-up.

Table I. Peaks Identified in Figure 1.

Peak	Compound	Peak	Compound
1	lactic	25	m-hydroxybenzoic
	glycolic	27	o-hydroxyphenylacetic
2	β-hydroxybutyric	31	aconitic
3	β-hydroxyisovaleric	33	citric
8	benzoic	34	4-hydroxy,3-methoxyphenylacetic
	phosphoric	38	4-hydroxy,3-methoxymandelic
9	fumaric	39	palmitic*
10	urea	40	hippuric
11	succinic	46	stearic*
15	glutaric	47	salicyluric
17	malic	51	C-24 hydrocarbon*
19	adipic	52	m- or p-hydroxyhippuric
20	o-hydroxybenzoic	53	C-25 hydrocarbon*
21	β-hydroxy, β-methylglutaric	55	C-26 hydrocarbon*
23	keto-octanoic (?)	57	C-27 hydrocarbon*
24	β-methyladipic	58	pthalate ester*
		60	C-28 hydrocarbon*

* Compounds observed in procedural blank

The obvious drawback to library searching with a small computer is limited space for spectral storage. Furthermore, if the spectral search time is prohibitively lengthy, data acquisition will be slowed and laboratory productivity will decrease. Finally, programming time and sophistication may be considerable. In spite of these problems, we have designed and partially completed a library search system for a small computer.

In addition to the hardware previously described, a DEC tape unit was required to be added to the system. In fact, the entire system could be operated without disk storage at some sacrifice of speed, so that a complete data acquisition and processing system could be assembled for under $25,000. Unlike magnetic tape, DEC tape restricts record allocation to 128_{10} word blocks rather than allowing variable size pages into which variable length mass spectra could be written. Although not for library search purposes, the system has been expanded to 8 k of core, and current programs are written using this feature.

Previously, the DEC Disk Monitor was used to build the system. However, it cannot be made to control both DEC tape and disk interchangeably as system devices, so all of the data acquisition and processing routines are being converted to work within OS-8, a relatively new monitor developed and fully supported by DEC. The following programs are being written in assembly language for library preparation and search routines:

1) GLIB - generate and edit library (complete)
2) CLIB - compress library data (complete)
3) SLIB - search library (in progress)

Quite obviously, the first requirement is to generate a library of mass spectral data. GLIB has been written for that purpose because a file editor, capable of accessing n records (where n is not limited) of variable length, was not available. Each library sub-set is considered a file. For example, TMS-organic acids may form a single file. The individual spectral records can be added, edited (m/e or intensity changes can be made), or deleted. Accessing of variable length records is possible with the use of MAP blocks into which the starting point of each record is noted. MAP blocks are allocated as needed, and linked by forward pointers. Using GLIB, approximately 730 complete mass spectra can fit onto a single DEC tape, assuming 124 pairs of m/e and intensities/spectrum. Aldermaston format D is used to input data from paper tape. An identification number is assigned to each spectrum, the number of m/e and intensity pairs determined, and the minimum m/e is noted with each record. As experience is obtained, library sub-sets can readily be re-arranged to permit the most rapid identification of commonly encountered compounds.

From the complete mass spectra, a compressed library similar to that described by Grotch[2] is prepared with CLIB. CLIB has been designed such that any number of compression algorithms may be employed. CLIB takes a GLIB generated library tape, opens a new file for compressed format on the disk, and converts each record to compressed form. Currently, the highest peak in a 14 amu window is encoded to four intensity levels (0-3%, 3-30%, 30-80%, 80-100%). Two peaks can thus be stored in a single 12 bit word. The compressed spectra are written as one scan/block or 1460 spectra/tape. It is anticipated that a single library tape will handle all routine work in our laboratory. Most of the library programs that have been discussed in the literature have utilized the Aldermaston library or some fraction of it for testing and determination of the success of a particular algorithm. However, the use of TMS derivatives may lead to a higher success rate for matching if a different compression routine is used. Furthermore, the mixtures of compounds emerging from the gc in a complex mixture, such as that in Figure 1, may require other data to be used in the matching. CLIB can readily be modified to encode mass spectra in a variety of ways (two peaks every 14 amu with or without intensity data, etc.). Once a single successful compressed format has been found, we can compress the data to more than one spectrum per block, and enlarge the library stored on a single tape if desired.

Mass spectra stored on the disk from a gc-ms run can be compared to the library using SLIB. Any or all of the scans in a run can be specified. Each scan will be read off the disk, compressed to the format used for the library, and compared with the library file. The best five fits along with a similarity index factor will then be printed for each scan. No estimate for the time required for a single search can be made at this time.

Although several descriptions of library search routines have been published, this effort represents a departure from the available software. It is a non-commercial data acquisition system for a small computer; it is designed to be versatile and meet the requirements of any laboratory project; and it will be freely available through DECUS or our laboratory. Due to the library construction feature, it will be possible to take a gc-ms run and specify it as the library against which another gc-ms run can be compared. Thus, metabolites or products present in one sample which were not present in the other sample can readily be detected, and those components which are identical can be definitively matched.

Acknowledgement

This work has been supported by NIH Grant HD-04870.

References

1. J. R. Plattner and S. P. Markey. Org. Mass Spectrom., 5:463 (1971)

2. S. L. Grotch. Proceedings of the 20th Annual Conference on Mass Spectrometry and Allied Topics, Dallas, Texas, 1972.

LOGOS II: A LARGE SCALE, REAL-TIME, COMPUTER SYSTEM FOR MASS SPECTROMETRY, INCLUDING LOW AND HIGH RESOLUTION, GC/MS AND SPECTRUM MANAGEMENT APPLICATIONS

A. L. Burlingame, R. W. Olsen and R. V. McPherron
Space Sciences Laboratory
University of California, Berkeley, California 94720

Since our initial report in 1965, extensive studies have been made in the use of small scale computers in mass spectrometry, including our own LOGOS system (1). All of these systems are deficient in their ability to support real-time processing and none at present support multiple on-line mass spectrometers in either batch or GC modes of operation. It is clear that dedicated instruments such as GC/MS and high resolution mass spectrometers, where very large volumes of MS data are commonplace, require and benefit from enhanced computer involvement. This paper describes a large scale computer system for on-line, real-time, multiple instrument mass spectrometry developed in our laboratory. The system is based upon a large XDS Sigma-7 computer, CRT terminals with graphics capability, and a specialized data acquisition interface. The software system is composed of a supervisor program and a collection of processing programs for the specific applications.

A more comprehensive report of this work is being prepared for publication.

1. D. H. Smith, R. W. Olsen, F. C. Walls and A. L. Burlingame, Anal. Chem. 43, 1796 (1971).

EXTENDED AUTOMATION OF A GC/MS DATA SYSTEM BY A NEW COMPOUND IDENTIFICATION PROGRAM.

Fred P. Abramson, Departments of Pathology and Pharmacology, George Washington University School of Medicine, Washington, D.C. 20037

Most library search routines(1) which are employed with gas chromatograph-mass spectrometer(GC/MS) systems have features in common which restrict their use to skilled operators; they give only suggestions as to the identity of the compound which must be further considered by the operator, and the questions of which unknown spectra to search, or whether background of another spectrum should be subtracted cannot be clearly stated in advance of the actual analysis. What this report describes is a new approach to computerized GC/MS which is capable of producing specific chemical identifications from all the data in a chromatogram with no operator judgement required.

This is accomplished by exhaustively searching a limited library of compounds against an entire chromatogram using a routine called Data Limiting Identification(2). In addition to greatly improving the automation capabilities of the GC/MS system, Data Limiting Identification is designed to operate under conditions of substantial interference by overlapping compounds or background as is encountered when trace analyses are performed. The most significant aspect of this routine is that the search is performed in the reverse sense. Rather than selecting a characteristic set of masses and intensities from an unknown spectrum and searching an equivalently reduced library, the reverse search selects a reduced library spectrum, extracts from the unknown spectrum just those intensities corresponding to the library spectrum masses and then compares the intensities. This method of searching has several important advantages over the forward method.

1. Because the basis for the search is the library spectrum whose quality is assured by the way it was generated, it is possible to analyze positive and negative deviations between the unknown and library in substantially different ways. Positive deviations may result from interferences added to the spectrum of a compound and may be allowed up to the point where the spectrum is obscured. A small number of negative deviations are fatal, however, because there is no way that an expected intensity can be dimished. A large number of negative deviations suggests that the base peak selected to normalize this scan is too large and the renormalization routine should be enabled.

2. By sequentially selecting only the intensities in an unknown scan corresponding to each library spectrum, a major amount of coeluting compound overlap and background is ignored. This enables the identification algorithm to operate on merged spectra where the compound of interest produces few, if any, of the significant peaks in any mass range, permitting identification of a compound down to point of obfuscation. The phrase Data Limiting Identification means that the quality of the data, rather than the quality of the algorithm, is to be the limiting factor on the success of the identification.

3. When the ratio of negative to positive deviations is too large, or when too many large negative deviations are encountered a renormalization routine is called up automatically. This temporarily removes the base peak from the library spectrum and renormalizes the remaining unknown peaks before recalculating the deviations. This renormalization may remove up to three library masses for any spectrum-library compound pair in order to reduce isobaric interferences.

4. Because the peaks selected from the unknown spectrum are determined by the library spectrum, flexible identification algorithms may be implemented by the way reference spectra are included in the library. This decision is made by the mass spectroscopist based on his knowledge of which peaks in the spectrum of a compound will permit its identification while excluding erroneous identification of similar materials. On that basis, a compound will be added to the library and its identification from unknown data will be based on this individualized basis. For readily identified compounds, automated library generation is provided based on preset criteria.

Another aspect of the routine which make it different from other search procedures is that quantitative data is collected at the same time as the identification is made. The summed intensities of acceptable masses accumulated for all hits to a particular compound is included in the final report. This substantially improves the utility of a search method by providing a compound specific peak integral which is not complicated by valley or peak shape criteria.

This entire project was undertaken with analyses of such limited classes of compounds in mind as; abused drugs(3), steroids(4), amino acids(5), prostaglandins, selected drugs and their metabolites and chlorinated pesticides(6). With the 8K core size available(7), each library is restricted to 100 compounds and to 10 peaks/spectrum. Each of the categories appears well served by a 100 compound library and most of the members of each family have reasonably well differentiated spectra, thus allowing identification from a limited number of masses. Library searches of a limited number of compounds which are readily interpreted from one another may realistically produce definitive answers, rather than the five best suggestions as to the identity of a compound. Where only subtle differences in spectra exist between two compounds, either their common ions may be included in a library as a common find, or else this search method will be considered inappropriate to that class of compounds. If a category is larger than the 100 limit, sequential searches can be called up on two or more libraries containing these compounds and the separate reports from each search combined. Each library is to be user generated and analytically specific to the user's problem. This will remove all of the inaccuracies present when commercial libraries containing spectra from numerous laboratories are searched. Only with reference spectra from the same instrument as the unknown can the highest similarities be obtained.

Four separate programs are available in this system. NEWLB generates space on a library tape for inclusion of a new 100 compound library. KEYIN and ADLIB add a new compound to a specified library or replace the spectrum of an already included compound from the teletype or from the data tape respectively. KEYIN is used to create a library spectrum where no compound is available and only a mass spectrum is available from the literature. It is also used where the largest 10 peak criteria in ADLIB will not produce a satisfactorily recognizable spectrum as mentioned in 4 above. The main program, SERCH, searches a specified limited library against a continuous series of scans and reports any hits found, the scan number of the first scan where the hit was made, the best (lowest) dissimilarity index found for that compound, and the sum of the ions corresponding to that compound. When no compound is satisfactorily identified, the report will say NO HITS rather than provide the most similar compounds for suggestions(1). In this way, interpretation of the data is straightforward.

REFERENCE AND NOTES

1. S.R. Heller, Anal. Chemistry 44, 1951 (1972) H.S. Hertz, R.A. Hites and K. Biemann, ibid., 43, 681(1971), S.L. Grotch, ibid., 45, 2(1973) and earlier work cited therein.
2. Full details of the Data Limiting Identification routines will be published elsewhere.
3. B.S. Finkle, D.M. Taylor and E.J. Bonelli, J. Chrom. Sci, 10, 312(1972) N.C. Law, V. Aandahl, H.M. Fales and GWA Milne, Clin. Chim. Acta 32, 221 (1971).
4. P. Toft, B.A. Lodge and M.B. Simard, Can. J. Pharm. Sci. 7, 53(1972); C.J.W. Brooks, A.R. Thawley, P. Rocher, B.S. Middleditch, G.M. Anthony and W.G. Stillwell, J Chrom. Sci. 9, 35(1971).
5. E. Gelpi, W.A. Koenig, J. Gilbert and J. Oro J. Chrom Sci. 7, 604(1969).
6. J.N. Damico, R.P. Barron and J.M. Ruth Org. Mass Spectrum. 1, 331(1968); T.R. Kantner and R.O. Mumma in "Residue Reviews", vol. 16, p. 138, F.A. Gunther, Ed., Springer-Verley, New York, N.Y., 1966.
7. The instrumentation used was a Dupont 21-491 gas chromatograph/mass spectrometer equipped with the 21-094 data system. This data system was expanded by adding an additional 4K core to the Hewlett-Pachard 2100 A computer and a second 7970B digital tape unit.

8. The assistance of Norris Huse and Royce Howard of Dupont Instruments is gratefully acknowledged.

Use of a Matched Filter to Resolve Mass Spectra of Overlapping Gas Chromatographic Peaks. JOCHEN HABER and DONALD J. JENDEN, Depts. Biomathematics and Pharmacology, Health Sciences Computing Facility and School of Medicine, Univ. of Calif., Los Angeles, Calif. 90024

A matched filter derived from a reference chromatogram is used to obtain precise estimates of the relative retention times of the chromatographic peaks at each mass. If a single component is present in the peak, the retention times are uniform; if two overlapping peaks are present, the retention times have a bimodal distribution. The retention times and peak widths serve to classify each represented mass as belonging to one, the other or both mass spectra. It is possible in this way to resolve mixtures of compounds or mixtures of isotopic variants of single compounds differing in retention time by < 1 percent. The technique enhances the signal-to-noise ratio, facilitating the reduction of GC/MS data by locating chromatographic peaks embedded in noise. Representative applications will be presented. This study was supported by USPHS Grant MH 17691 and the Health Sciences Computing Facility, sponsored by NIH Grant RR3.

AN INTERACTIVE DISPLAY ORIENTED DATA SYSTEM FOR GC/MS

H.P. Hotz and Victor L. DaGragnano
Finnigan Corporation, Sunnyvale, California, U.S.A.

The use of small computers to control the data acquisition with gas chromatograph mass spectrometers has become common. However, these systems have been rather inflexible in their handling of data. Data have had to be plotted or listed in order to be interpreted, a process that has required considerable time. We have designed a fully-integrated data system which provides live display of the spectra on an oscilloscope. Since the data displayed are resident in the computer's memory, it is straightforward to provide data manipulation directly. To avoid tedious dialogues via teletype, our computer functions are controlled principally by push buttons. The push buttons are read by the computer, which then executes the desired function. Outputs appear as alphanumerics on the oscilloscope or, optionally, typed on the teletype.

The organization of the data system and its relation to the gas chromatograph/mass spectrometer (GC/MS) is shown in Figure 1. The data system controls a setting of the quadrupole mass spectrometer by means of mass-set voltage produced by a digital to analogue convertor (DAC). Data are acquired by taking the output of the electron multiplier through a preamp and amplifier/integrator to an analogue to digital convertor (ADC). These digitized amplitudes are stored in the computer's memory in the form of counts. Thus a mass spectrum consists of a series of counts for each channel, with each channel representing one atomic mass unit. The integration time is determined by the computer and is timed by the computer's real time clock. Live display of spectra is maintained on the cathode ray tube (CRT) during acquisition. Past spectra and additional programs are stored in the disc memory. Hard copy data output may either be obtained on the teletype or on the digital plotter.

Core memory provides space for 2,048 channels of data. During acquisition, this is divided into two halves, one for the gas chromatogram and one for the mass spectrum. Halves of these regions may be displayed at will and small segments may be chosen to be expanded across the entire CRT screen. Any two sections may be displayed simultaneously. After acquisition, one region of memory may be transferred to or stripped from any other region of memory. Thus, data can be manipulated quite freely and flexibly between the core memory divisions. This flexible handling of data in core memory provides the basis for all data handling in the system.

For data acquisition, one enters the parameters for the sample run in to the system. Since a number of parameters must be entered, and alphanumeric information must be supplied, this is done by a means of a dialogue. Promptings are supplied by alphanumerics on the CRT and responses are provided by the operator on the teletype. An example of the information for a run is shown in Figure 2. In general, the parts of the printing prior to the colon are the parts supplied by the computer and the parts following the colon have to be supplied by the operator. Once entered, the parameters remain in the machine and the operator only has to change the parameters he wishes. Figure 2 is an actual printout by the computer of a set of current parameters for a run. Once the parameters have been entered, the computer will take control of the mass spectrometer and execute sequential mass scans recording the data as obtained. Upon the completion of each mass scan, the data are compacted and stored on the disc. The mass scan is integrated and one channel is added to the gas chromatogram in the appropriate region of core memory. One may select the live display region during acquisition just as at other times. Thus one can watch for a desired feature in a mass spectrum or the development of the gas chromatogram during acquisition. Two buttons are provided to control data acquisition. One is for acquire only and the data are not stored on the disc. One may then change to an acquire and save mode by pushing a second button. Mass spectra will then be saved beginning with the one currently being acquired. The computer will not allow acquisition of data with a file name identical to that of data previously acquired. Thus there is no danger of confusing data in the disc files.

A second data acquisition mode is provided, which we call the mass fragmentography mode. In this mode, complete mass spectra are not acquired, but only mass fragmentograms are obtained. Up to four mass fragmentograms may be obtained simultaneously. Upon conclusion of data acquisition, these data are automatically written on disc for future reference. In this mode, the computer chooses the integration time so that maximum precision of the data is insured.

After data have been acquired, data may be recalled from disc memory to core memory by entering the file name into the acquisition parameters. When data from a

past file are recalled, all of the parameters of that run are restored to core so that they may be read or a similar run may be taken. Gas chromatograms, except mass fragmentograms, are not stored on disc. Recalling a gas chromatogram results in a reconstructed chromatogram. This may be either the full chromatogram as acquired or a limited mass gas chromatogram. The mass limitations are determined by intensifying a range as set by the lever wheel switches. Any mass spectrum of the run may be recalled by pushing the button with the number of that spectrum intensified. If more than one spectrum is intensified, the average of those spectra is obtained.

The ability to intensify is controlled by a push button and two lever wheel switches. One switch controls the start channel and the other the number of channels of span. The span may be in either direction from the start channel. The use of intensified channels provides a means of focussing the computer's attention to particular channels in the data, and this procedure is used very much as a light pen is used in larger interactive data systems. One simple use of these switches is to determine the size of a fragment lost in the mass spectrum. One might start with a certain peak, set the direction of intensification downward, and increment the span until it just reaches the next lower peak. The number of mass units lost from the first peak to get the second would then be one less than the reading on the span lever wheel switch.

We provide three push buttons allowing one to determine the amplitude of either mass spectra mass peaks or gas chromatograph peaks. The first of these is total intensity, which is particularly useful for mass spectra. When this is pushed, the total of the channels intensified is output. The output is either in the form of the absolute counts stored in the data system or it may be converted to read in volts output of the preamplifier, corrected for whatever integration time was used in its acquisition.

The area push button allows a background to be subtracted from the total. Three button pushings are required to obtain this output. On the first and second pushings, background is determined by fitting (least squares fit) to the channels intensified. The peak is then intensified and the button pushed for the third time. The result is then output and consists of the net total above the least squares straight line fit to the background, the calculated number in these peak channels below the least squares line fit line to the background, and a size. The size is the net area multiplied by a factor which is the ratio of a size chosen for a standard peak area to the total counts previously obtained in that standard peak. Thus a normalized, or calibrated answer may be obtained for quantification of the analysis.

The ratio of the totals of any two peaks may be obtained by two pushings of the ratio push button. The first peak is intensified and the button pushed. Then the second peak is intensified and the button pushed again. When the second pushing occurs, the counts in the intensified channels of the second peak are divided by the counts in the intensified channels of the first peak and the ratio output. These may of course be either single channels or mutiple channels in either peak, and it may thus be used either for mass spectra or gas chromatograms.

Data output is provided either on the teletype or on the digital plotter. A labeling provision is provided so that one may input one line of text to be applied to the data output. This line of text, which will appear on the CRT, is put at the top of the listing or plot and is followed by a line of the title of the run. When one of the output buttons is pushed, the data output are those shown on the CRT display. Normalization is provided by normalizing either to the highest channel within the display region, or to the first channel intensified if one is intensified. The teletype output may also be in absolute counts. As an example of the flexibility of output one might go through the following sequence of steps: One might recall a mass spectrum from near the top of a gas chromatogram peak, and save it by transferring it to the GC memory region. One could then recall a mass spectrum from a background region adjacent to the gas chromatogram peak, and subtract this background spectrum from the peak spectrum to obtain a net spectrum. The interesting portion of this mass spectrum could be expanded to fill the full screen and the resulting spectrum plotted. Of course, if the plot does not show what one desired, one would not have to plot it, since one can preview it on CRT. Selected portions of the plot may be multiplied by any desired factor so that small features may be made more visible. The plot will automatically indicate these scale factors when this is done. If one does not wish to wait for the output at the time one sets it up, one may add it to a line-up for delayed output. This is done by pushing the delayed output push button and then indicating the kind of output desired. Later, such as when one is ready to leave for the day, one may instruct the data system to perform all of the delayed outputs. Gas chromatograms may also be plotted. When mass fragmentography is used, the resulting plots are somewhat different. The four mass

fragmentograms are plotted above each other.

Automatic comparison of spectra has come to be a useful function of computers. We provide a library search routine in our data system. The search routine provides for storing multiple libraries of spectrum codes on the disc. The operator may add to or delete from these libraries at will. He may also output or input a library from paper tape so that additional libraries may be exchanged with other users. The search scheme is one in which the mass of the most intense peak in each 14 atomic mass unit range is listed. Fifty-two ranges, beginning with mass 34 are used. A spectrum obtained on the data system may be automatically coded, the code edited, and the code searched against the library codes. The 10 best fits are then output, together with the number of mismatches for each. Provision is made for altering parameters in the search so that missing peaks in the library are, or are not significant and unknown missing peaks in the spectrum are, or are not significant.

In conclusion, let us emphasize that the data system is display oriented. During acquisition, that which is displayed are the input data. On output, what you see is what will be reduced to hard copy. Data manipulation is of the displayed data and other data are called into display for use. The display orientation of the system thus allows significantly more rapid data manipulation and insures that only significant data will be outputed.

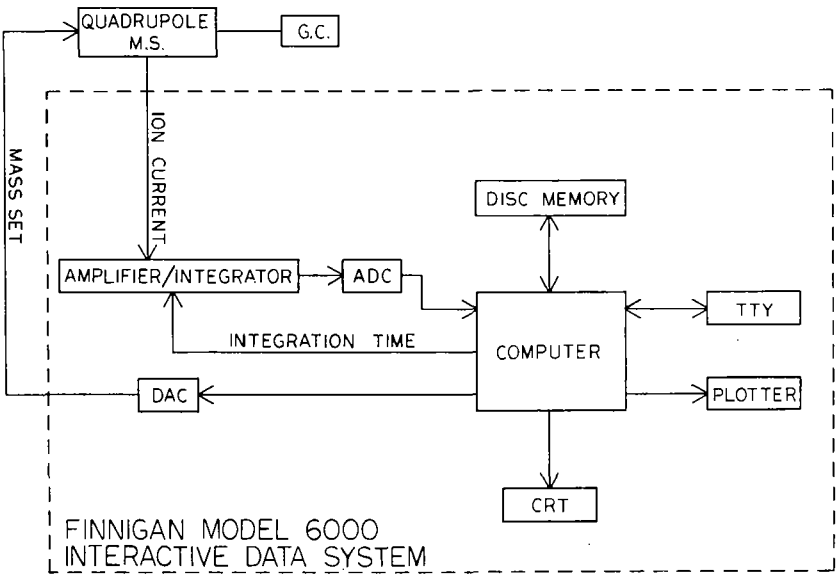

FIGURE 1. BLOCK DIAGRAM OF THE DATA SYSTEM

```
FILE :UNC
TITLE:UNIV. OF NORTH CAROLINA SAMPLE BY GC-EI
MASS RANGE :30-199;200-400
INTEG. TIME:4.8
SECONDS PER SCAN :4
THRESHOLD:1
INST. RANGE SETTING:H
MAX. RUN TIME 66
```

FIGURE 2. EXAMPLE OF RUN PARAMETERS LISTING

APPLICATION OF GC ORIENTED SOFTWARE TO MASS SPECTROMETRIC THERMAL ANALYSIS - EXPERIENCES WITH THE DUPONT 21-094 DATA SYSTEM

David L. Geiger and Gerd A. Kleineberg

Aerospace Medical Research Laboratory
Toxic Hazards Division (THC)
Wright-Patterson Air Force Base, Ohio 45433

INTRODUCTION

The Chemical Hazards Branch of the Aerospace Medical Research Laboratory has been performing mass spectrometric thermal analyses of polymeric and other nonmetallic materials for the past couple of years. The primary purpose for these investigations is to provide the toxicologist with qualitative and quantitative information concerning the thermal decomposition products of materials used in aircraft interior or other closed system construction.

Due to the increased interest in this type of investigation and the resultant increased workload, the necessity arose to incorporate an automated data acquisition and processing system.

INSTRUMENTATION

Figure 1 is a block diagram of the instrumentation presently being used. The thermogravimetric analysis (TGA) instrumentation was existing equipment and has been described elsewhere (1). The mass spectrometer is a DuPont model 21-491B equipped with a capillary inlet. Mass spectral data are acquired and processed using a DuPont 21-094 M.S. Data System with library search capability. The mass spectrometer and data system are standard commercial items with no special modifications or alterations.

TEST METHOD AND RESULTS

Samples weighing between 10 and 20 mg were program heated, in air, to thermal decomposition. By repetitive scanning of the mass spectrometer at the rate of 10 sec/decade, consecutive mass spectral scans from 15 to 617 mass units were obtained throughout the entire temperature program. The data for these scans were acquired and recorded with the DuPont data system.

Figure 2 represents a typical thermogram obtained from a sample of rigid polyurethane foam. The sample was heated to about 750°C during which time 160 mass spectral scans were obtained. From this thermogram one can relate scan number to temperature and points of weight loss of the sample. The various subroutines within the software of the data system were employed in an attempt to identify the components that evolved from the sample during thermal decomposition. The first program normally called up is the "PLOT GC" routine.

Figure 3 represents the data obtained from our rigid foam sample as processed by this program. This is a plot of the normalized total ion current vs scan number. Compare the total ion current that we normally receive with a thermobalance connected to the mass spectrometer, as indicated by the lower curve and the type of similar information that one normally receives when a gas chromatograph is used with the mass spectrometer, represented by the upper curve. In the case of the gas chromatograph, definite peaks were observed, but in the case of the thermogravimetric analyzer (TGA) no definite information could be obtained even in the regions where the sample was losing weight rapidly. Since our samples were analyzed in room air, approximately 99+% of the sample entering the mass spectrometer was air and, therefore, the total ion current obtained for each scan was due primarily to air. Any ions resulting from decomposition products were in trace quantities with respect to the air. The interference due to air could be eliminated by setting the low scan limit at m/e 41; however, in this type of investigation, it is necessary to examine the mass range below m/e 41 for the presence of toxic components such as HCN and NO which occur at m/e 27 and m/e 30, respectively. Since the data presented in Figure 3 provided us with no useful information, the next program called for was the "SIGNFPK" routine.

The significant peak table, as shown in Table I, is a listing of the masses of the significant ions obtained during the course of the entire analysis. This program allows one to ignore up to four masses and in this case, the four most significant ions found in room air were ignored. This listing contains the mass of the ion, the maximum intensity of this ion during any one scan, the number of the scan in which this maximum intensity first occurred and the total number of ions of this mass in all scans.

Inspection of this table indicates that masses, 101, 103, 35, 66, 47, and 105 reached a maximum intensity at about scan 35 and suggests they are ions produced from the same component. In a similar manner, we note that mass 44 reached a maximum intensity in scan 104 and was the base peak in at least this scan. Furthermore, masses 43, 31, 42, 26, 27, 45, 41, 58, 39, 57, 87, 59 and 55 appear to reach a maximum intensity around scan 64. These three scan numbers are in the vicinity of the three distinct weight loss steps observed in the thermogram. A closer look may now be taken at some of these masses to determine the scan number where their maximum intensity occurs and if more than one maximum is present. The program now called for is the "PLOT MC" routine.

Figure 4 is a plot of the relative intensity of the ions with a m/e of 101 versus scan number. This plot clearly indicates that mass 101 reached a maximum intensity at scan number 34 with no other maxima observed. Similar plots of all other ions reaching a maximum in the vicinity of scan 34 as indicated in the significant peak table were nearly identical to the plot for mass 101.

The mass spectrum of scan 34 can now be examined for identification. The program called for is the "PLOT MS" routine. Figure 5 is a bar graph presentation of the mass spectrum for scan 34 which can readily be identified as that of room air. Due to the large quantity of air entering the mass spectrometer, the ratio of peak intensities for mass 28 and 32 are distorted. At this point, one is able to make use of a valuable part of the computer software, i.e., the ability to define background.

Figure 6 is the plotted mass spectrum of scan 34 with scan 2 defined as background. Scan 2 has been subtracted from scan 34 on a raw data basis. The mass spectroscopist is now able to obtain a mass spectrum relatively free of interfering ions and can proceed to identify this spectrum.

An accessory to the DuPont data system is a library containing approximately 7,000 compounds. The software program enables the computer to compare the spectra obtained with the mass spectrometer with those contained in the library. Use of this program is made by calling up the "Search" routine.

The computer print-out of the library search for scan 34 with scan 2 defined as background is shown in Table II. The information contained in this print-out indicates that the spectrum of scan 34 matches a spectrum of trichlorofluoromethane (Freon 11) contained in the library to a goodness of 776, 1000 being a perfect match. We feel certain at this point that Freon 11 was used as the blowing agent in the manufacturing process of the foam.

The same approach can now be used to identify the other components. Recalling from Table I that mass 44 was a significant peak and reached a maximum intensity for the first time at scan 104, one should now look at the mass chromatogram of this ion.

Upon inspection of the plotted mass chromatogram shown in Figure 7, we observe two maxima, one at scan 64 and one at scan 113. The Search routine can now be directly employed for scan 113 without first obtaining a plot of the mass spectrum for this scan.

Table III contains the information obtained from this library search and indicates that our spectrum of scan 113 matches a spectrum for carbon dioxide contained in the library to a goodness of 651. Although this is not a perfect fit, we feel that we have identified the spectrum of scan 113 as that of CO_2. This appears to be reasonable because we were thermally degrading an organic substance in the presence of air. The temperature was about 510°C when scan 113 was recorded and one could expect that carbon dioxide would be formed under these conditions.

Once again, upon inspection of Table I, we can observe that a number of ions appear to reach their first maximum intensity around scan 64. Table IV contains the data obtained from a search of the mass spectrum of scan 64 with scan 2 defined as background and the ions prominent in CO_2 being ignored. The goodness of match is poor because a mixture of several different compounds were being released from the sample at this point and all of them are contained in the spectrum of scan 64 (Figure 8). However, considering that the sample under investigation is a polyether type polyurethane, the information obtained from the search of scan 64 is an indication of the class of compounds that one might expect.

The thermogram of another type of polymeric material is shown in Figure 9 and indicates two distinct steps of weight loss. The maximum of the first derivative of the first portion occurs at scan 114 and that of the second portion at scan 131. Again we inspect a plot of the total ion current versus scan number as shown in Figure 10.

Unlike our previous PLOT GC, we now observe a maximum in the ion current occurring at scan 114, coinciding with the first weight loss as presented in the thermogram. With this information, one may go directly to the Library Search.

The information obtained from the library search of scan 114 is presented in Table V and indicates a match of our spectrum with a spectrum of 1-Pentene in the library to a goodness of 815. One can therefore assume that 1-Pentene was used as a solvent in the production of this polymer and the plotted mass spectrum of scan 114 (Figure 11) confirms the information obtained from the library search.

The significant peaks obtained from all mass spectral scans during the course of thermal analysis of nolymer x are listed in Table VI. The masses from 1-Pentene (42,55,41,70,39,27,29) can be ignored assuming their origin to be only from this component. We can now focus our attention on those masses which appear to reach a maximum in the vicinity of scan 131.

A library search of scan 131, presented in Table VII, defining background as scan 105, indicates a match of our spectrum with that of a phenol spectrum to a goodness of 486. While this is not a particularly good match, consultations with the chemist who snythesized this polymer indicate the match to be correct.

CONCLUSION

The DuPont 21-094 Data System has been an extremely valuable aid in the acquisition and interpretation of mass spectrometric-thermal analysis data. The complete mass spectrometer and data system was in operation after an installation period of three weeks.

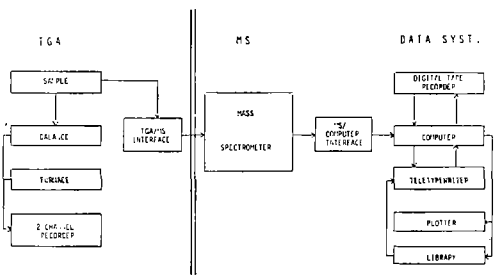

Fig. 1

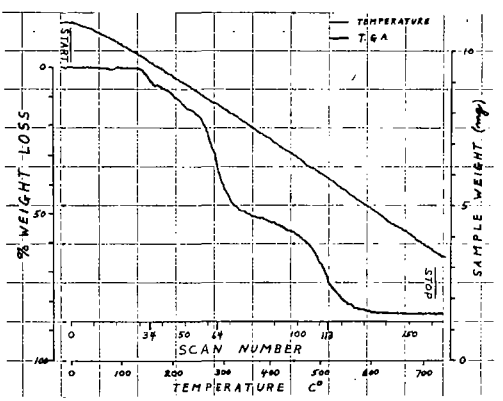

Fig. 2

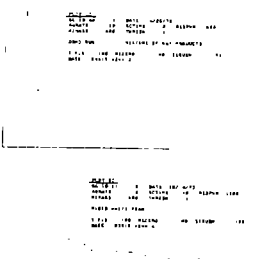

Fig. 3

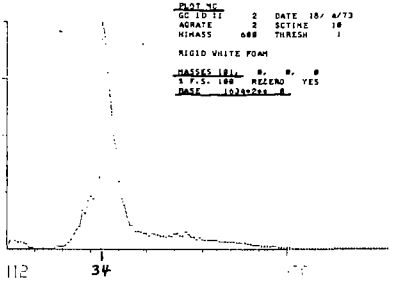

Fig. 4

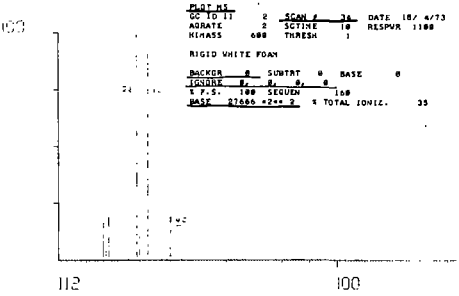

Fig. 5

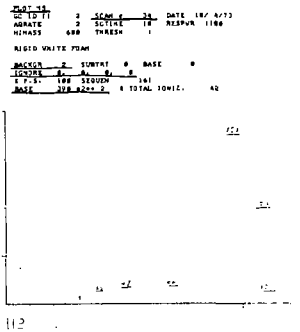

Fig. 6

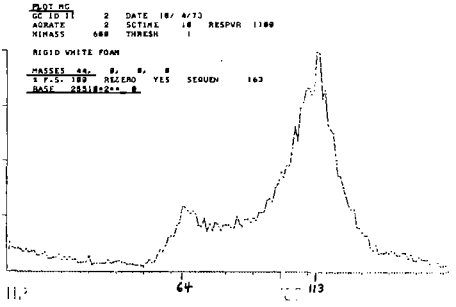

Fig. 7

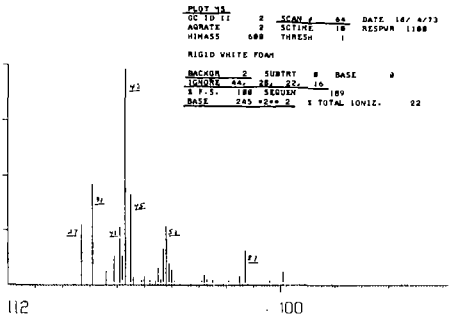

Fig. 8

Table I

SIGVPG
GC ID II 2 DATE 18/ 4/73
AQRATE 2 SCTIME 10
HIMASS 600 THRESH 1

RIGID WHITE FOAM

IGNORE 28, 32, 44, 16
HILOUT 5 SEQU 158

MASS	MAX INTN	FIRST OCCUR	SUM IONS *2** 7
18	1000	1	24158
44	1000	184	9889
69	745	38	17243
17	385	144	5646
20	157	129	2555
38	126	121	1983
33	103	31	1608
34	100	34	1703
101	74	35	187
43	73	64	224
31	64	64	781
85	54	132	876
100	53	35	63
24	36	6	514
37	30	102	332
42	28	64	186
26	27	62	232
27	27	64	144
45	25	62	124
73	21	36	211
36	21	6	268
38	20	137	181
15	19	18	238
19	17	46	236
41	17	64	38
58	15	66	18
22	13	117	61
66	10	34	9
39	9	66	16
47	9	34	8
57	9	64	13
105	9	35	6
87	8	62	7
48	7	2	43
46	7	4	31
49	6	111	14
59	6	63	4
55	5	64	5
75	5	46	4

Table II

LIBRARY SEARCH

GC ID II 2 DATE 18/ 4/73
AQRATE 2 SCTIME 10 RESPWR 1100
HIMASS 600 THRESH 1

RIGID WHITE FOAM

IGNORE 0, 0, 0, 0
SEQUEN 162

INDEX	SCAN	BACKGR	SUBTR	BASE
0	34	2	0	0

LAST INDEX PROCESSED 0
SCAN # 34 BASE 181

GOODNESS	ID. NO.	PAGE	
776	KOD-0030	0680	TRICHLOROFLUOROMETHANE
770	DOW-1146	0680	TRICHLOROFLUOROMETHANE

Table III

LIBRARY SEARCH

GC ID II 2 DATE 18/ 4/73
AQRATE 2 SCTIME 10
HIMASS 600 THRESH 1

RIGID WHITE FOAM

IGNORE 0, 0, 0, 0
SEQUEN 164

INDEX	SCAN	BACKGR	SUBTR	BASE
0	113	2	0	0

LAST INDEX PROCESSED 0
SCAN # 113 BASE 44

GOODNESS	ID. NO.	PAGE	
651	API-1582	0011	CARBON DIOXIDE
520	DOW-0017	0011	CARBON DIOXIDE

Table IV

LIBRARY SEARCH

GC ID II 2 DATE 18/ 4/73
AQRATE 2 SCTIME 10 RESPWR 1100
HIMASS 600 THRESH 1

RIGID WHITE FOAM

IGNORE 44, 28, 16, 22
SEQUEN 200

INDEX	SCAN	BACKGR	SUBTR	BASE
0	64	2	0	0

LAST INDEX PROCESSED 0
SCAN # 64 BASE 43

GOODNESS	ID. NO.	PAGE	
488	DOW-1580	0467	1-PROPOXY-2-PROPANOL
444	API-1120	0840	1,1-DI-N-PROPOXYETHANE

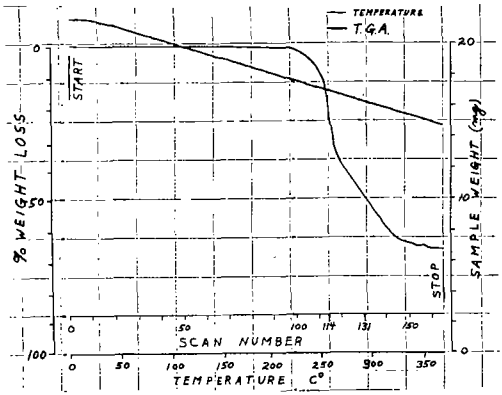

Fig. 9

Table V

LIBRARY SEARCH

GC ID KK 3 DATE 24/ 4/73
AQRATE 2 SCTIME 10
HIMASS 600 THRESH 1

POLYMER X

IGNORE 0, 0, 0, 0
SEQUEN 53
INDEX SCAN BACKGR SUBTR BASE

0 114 20 0 0

LAST INDEX PROCESSED 0
SCAN # 114 BASE 42
GOODNESS ID. NO. PAGE
815 API-0029 0062 1-PENTENE(GAS)
796 API-1652 0061 ETHYLCYCLOPROPANE

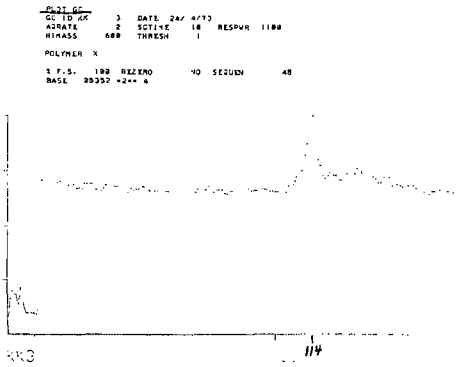

Fig. 10

Table VI

SIGNFPK
GC ID KK 3 DATE 24/ 4/73
AQRATE 2 SCTIME 10
HIMASS 600 THRESH 1

POLYMER X

IGNORE 0, 0, 0, 0
MILOUT 5 SEQU 50

MASS	MAX INTN	FIRST OCCUR	SUM IONS *2** 10
28	1000	1	28156
32	1000	14	18499
42	326	114	384
55	236	114	276
68	209	101	3482
18	176	101	2520
29	165	113	1786
41	152	113	144
70	147	114	165
16	103	18	1948
39	100	114	128
44	82	167	671
27	75	114	77
94	72	131	222
17	42	143	625
28	24	94	331
43	22	113	24
30	21	125	171
53	21	116	15
33	16	12	178
36	14	113	19
26	14	113	11
56	14	114	6
34	13	12	187
65	13	129	22
66	13	138	22
71	11	114	2
69	10	114	6
37	9	114	9
25	8	12	63
31	8	114	44
51	8	113	2
67	8	114	2
54	7	114	2
58	7	114	2
24	5	13	42
75	5	129	5

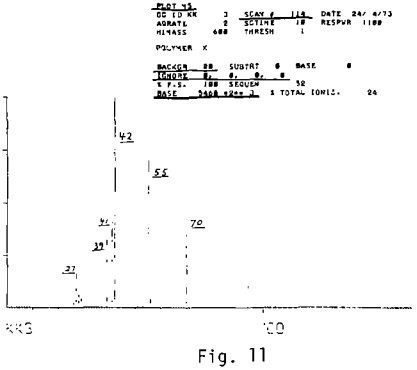

Fig. 11

Table VII

LIBRARY SEARCH

GC ID KK 3 DATE 24/ 4/73
AQRATE 2 SCTIME 10
HIMASS 600 THRESH 1

POLYMER X

IGNORE 0, 0, 0, 0
SEQUEN 61
INDEX SCAN BACKGR SUBTR BASE

0 131 105 0 94

LAST INDEX PROCESSED 0
SCAN # 131 BASE 94
GOODNESS ID. NO. PAGE
486 HUM-0001 0199 PHENOL
456 DOW-0732 0199 PHENOL

REFERENCE

1. G. A. Kleineberg and D. L. Geiger, Thermal Analysis, Proc. 3rd I.C.T.A., pub. Birkhauser Verlag, Basel Switzerland, Vol 1, 325 (1972).

THE PARTITIONING OF EXCESS ENERGY IN DISSOCIATIVE RESONANCE CAPTURE PROCESSES

P. W. Harland and J. L. Franklin
Department of Chemistry
Rice University
Houston, Texas 77001

The translational energies of selected negative ions formed by dissociative resonance capture processes from the polyatomic systems NF_3, BF_3, CF_4, C_2F_6, C_3F_8 and c-C_4F_8 have been measured as functions of excess energy over the resonances. The excess energy in the molecular negative ion intermediate prior to dissociation has been calculated and partitioned into translational, vibrational, and, in some cases, electronic excitation of the dissociation products. The degree of vibrational activation in the intermediate state before dissociation is found to depend on the particular molecule under investigation and to vary from one dissociation channel to another. These observations are discussed in relation to theoretical concepts of dissociative resonance capture and given a qualitative explanation. The measurement of translational energy has led to a more complete interpretation of the states involved in the various processes and in computing ground state thermochemical properties of the decomposition products.

Submitted for publication in J. Chem. Phys.

DISSOCIATIVE ELECTRON ATTACHMENT TO FLUORINE

G. D. Sides and T. O. Tiernan
Aerospace Research Laboratories, Chemistry Research Laboratory
Wright-Patterson Air Force Base, Ohio 45433

Low-energy electrons react with fluorine molecules by dissociative attachment to form an F^- ion and an F atom. This reaction has been studied in the flowing afterglow system shown in Figure 1.

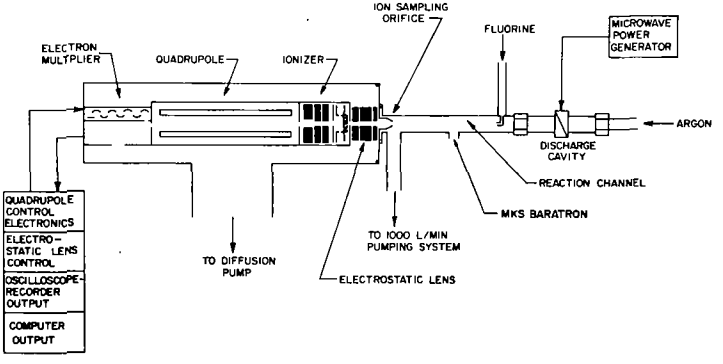

Electrons are produced by a 2450 MHz microwave discharge (approximately 2 watts) in argon buffer gas in a quartz discharge tube. The microwave power supply is coupled to the buffer gas by an Evenson cavity and monitored by a Bendix 120-watt power meter. Buffer gas flows are typically 30 to 40 atm-cc/sec and are monitored by a calibrated rotameter. Electrons produced in the active discharge are rapidly thermalized in the high pressure environment (1 to 4 torr) and flow past the reactant gas injection port where a gas such as fluorine may be introduced into the afterglow.[1] The reactant gas flow is measured by a Hastings-Raydist Model ALL-5 linear mass flowmeter capable of measuring flows over the range 1 to 225 atm-microliters/sec. However, even at fluorine flows of 1 microliter/sec. the dissociative attachment reaction forming F^- ions is so fast that the afterglow is quenched. Therefore, dilute mixtures (0.01 to 0.05%) of fluorine in argon were injected into the afterglow to study the electron-fluorine molecule dissociative attachment reaction. The ions formed are sampled through a 9 mil orifice at the end of a stainless steel cone which is maintained at +4 to +10 volts with respect to ground. The ions are focused by an electrostatic lens into the lens elements of an ionizer. These elements focus the ions into an Extranuclear Model 162-8 voltage-scanned quadrupole mass spectrometer. The ions are then mass resolved by the quadrupole and detected by an electron multiplier. The mass spectrometer is operated in a low-resolution high-transmission mode to eliminate mass discrimination of the ions entering the mass spectrometer. A model 031-2 Extranuclear preamp-electrometer amplifies the resulting signal and provides analog outputs for computer input and X-Y plotter use. The flow tube itself is pumped by a 1000 liter/minute Sargent-Welch Model 1375 rotary pump. The flow tube pressure is measured at the center of the reaction channel by an MKS Baratron capacitance manometer. The system typically operates at flow tube pressures of 1 to 4 torr while maintaining better than 10^{-4} torr in the quadrupole chamber.

During a typical experiment the negative ion current is monitored as a function of reactant gas flow by a Varian X-Y plotter and a Hewlett-Packard 2116C computer system. The data is then stored on punched paper tape for future reduction.

The energy of the electrons in the afterglow was determined by measuring the resulting SF_5^-/SF_6^- ratio when SF_6 is injected into the reaction channel.[1] The electron temperature in this experiment was then estimated to be approximately

500°K from these measurements.

The average value of the binary rate coefficient for the dissociative attachment of electrons to fluorine in an argon buffer was found to be 2.1×10^{-8} cm^3 sec^{-1} over a buffer gas pressure range of 1.5 to 3 torr. This is, however, a preliminary value. The experimental data thus far obtained indicates that metastable-metastable reactions of the type

$$Ar^M + Ar^M \rightarrow Ar^+ + Ar + e$$

may be important downstream sources of electrons in the flowing afterglow.[2] Further investigation of these processes are in progress and should reveal the magnitude of the error introduced by this reaction.

A more detailed account of this work will be submitted for publication in the Journal of Chemical Physics.

References

1. F. C. Fehsenfeld, J. Chem. Phys., 53, 2000 (1970).

2. Phys. Rev., A, 5, 1410 (1972).

COLLISION INDUCED DISSOCIATION REACTIONS OF MOLECULAR NEGATIVE IONS, O_2^-, NO^- AND NO_2^-

R. L. C. Wu* and T. O. Tiernan
Aerospace Research Laboratories, Chemistry Research Laboratory
Wright-Patterson Air Force Base, Ohio 45433

The excitation functions for collision-induced dissociation reactions provides an indication of the efficiency of energy transfer in ion-neutral collisions. In addition, experiments can yield reliable bond dissociation energies, and may also provide useful information about excited states of molecular ions. Although this technique has been employed by several groups[1-4] to obtain such information for positive ions, no data of this kind has yet been reported for negative ions. For this reason, and also to explore further the mechanisms of collisional dissociation processes, a systematic study of the negative molecular ions, O_2^-, NO^-, and NO_2^- was undertaken. In the work reported here, a variety of target gases (Ne, Ar, Kr, Xe, N_2, O_2, NO and CO), were employed and the threshold behavior for the dissociation process is shown to be markedly dependent upon the target species.

The ARL in-line tandem mass spectrometer, which has been previously described[4,5], was utilized in this study. The primary negative ions were formed by electron impact on various gases or on mixtures. The energy spread of the incident ion beam is about ± 0.3 eV (lab.). All cross sections were evaluated relative to the absolute cross section of 63 $(Å)^2$, at 0.3 eV O^- energy, for the O^-/NO_2 charge transfer reaction[6].

The cross sections for the collision-induced dissociation reactions investigated were determined as a function of translational energy for various target molecules. All these reactions exhibit typical endothermic behavior, as illustrated for the O_2^-/X reaction in Figures 1 and 2. Each excitation function is the

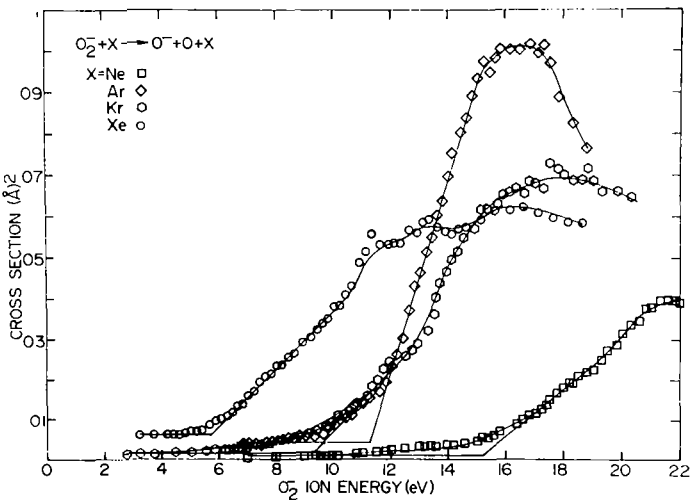

Figure 1. Translational energy dependence of the cross section for the collision induced dissociation reaction of O_2^- with rare gas atomic targets.

averaged representation of many experiments. The cross sections near threshold increase linearly with ion kinetic energy for those reactions in which the target species are molecular. However, the excitation functions for those reactions involving rare gas atomic targets show an exponential increase in the region near threshold and then a sharp linear rise to a maximum. The long tail on these latter reactions cannot be explained satisfactorily either on the basis of vibrational excitation of the reactant ion, O_2^-, or by Doppler broadening[7], which is expected to arise from the thermal motion of the target molecules. Thus, the differences in threshold behavior are presumably caused by the reaction mechanisms prevalent in the two cases.

The observation of two thresholds for the reaction O_2^- with NO suggests that there are two reaction channels. Two possible processes are:

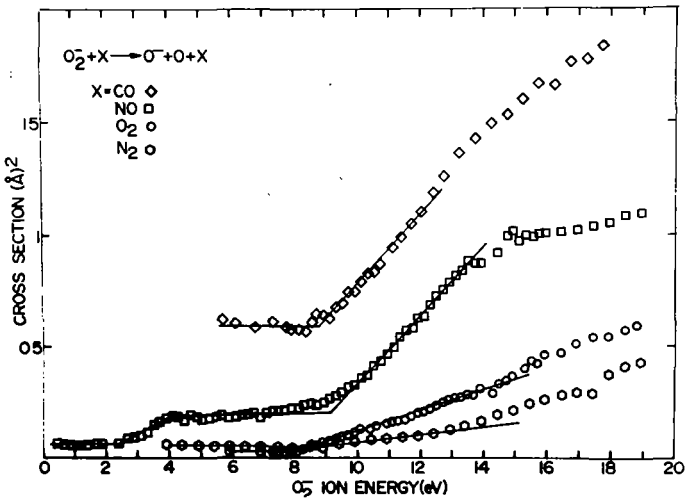

Figure 2. Translational energy dependence of the cross section for the collision induced dissociation reaction of O_2^- with various molecules.

$$O_2^- + NO \rightarrow O^- + NO_2 \quad (1)$$

$$O_2^- + NO \rightarrow O^- + NO + O \quad (2)$$

Reaction (1) would be expected to occur at the lower energy. It is also possible that an intermediate(NO_3^-) species is involved in this interaction. To test this hypothesis, the reaction was studied using $N^{18}O$, and the $^{16}O^-$ and $^{18}O^-$ products were monitored as a function of incident ion energy. The results are shown in Figure 3. Thresholds for these two reactions were found to be the same within the

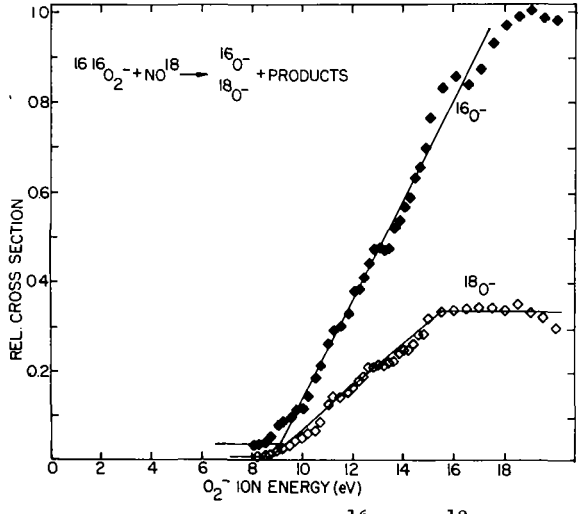

Figure 3. Kinetic energy dependence of the $^{16}O^-$ and $^{18}O^-$ products from the reaction of $^{16,16}O_2^-$ with $N^{18}O$.

experimental error. The cross sections for formation of $^{16}O^-$ were found to be about twice as large as those for $^{18}O^-$ production. From the above data, it seems probable that an intermediate (NO_3^-) collision complex is formed for this reaction. Isotopic scrambling does occur in this reaction complex and the abundance

of the isotopic O^- products is proportional to their statistical representation in the intermediate.

In the case of NO^-/X reactions, linear threshold behavior was observed for those reactions in which the target species are O_2 and NO. The observation of two thresholds for the reaction NO^-/O_2 again leads to the conclusion that two reaction channels are available, probably (3) and (4).

$$NO^- + O_2 \rightarrow O^- + O + NO \quad (3)$$

$$NO^- + O_2 \rightarrow O^- + NO_2 \quad (4)$$

The reaction of $N^{18}O^-$ with $^{16,16}O_2$ was also studied, and here also the reaction thresholds for the processes yielding $^{16}O^-$ and $^{18}O^-$ were found to be the same within the experimental uncertainty. The maximum cross section for $^{16}O^-$ formation was about twice that for $^{18}O^-$ formation. These results again suggest that an intermediate complex (NO_3^-) is formed and that isotopic scrambling occurs as a result of energy randomization. For the reactions of NO_2^-/X, linear threshold behavior was observed for those reactions involving Xe, N_2 and NO as target molecules.

The dissociation energies of the molecular negative ions, O_2^-, NO^- and NO_2^- are given directly by the measured translational energy thresholds if it is assumed that neither the reactants nor the products are in excited states at threshold. The electron affinities of the corresponding neutral molecules were calculated from thermodynamic relations. These results are summarized in Table 1. The only available literature data for the bond dissociation energies of such molecular negative ions is theoretically calculated.[8] The theoretical binding energy of O_2^-, 4.14 eV, given by Zemke, Das and Wahl[8], using the optimized valence configuration method, is in excellent agreement with the present result. The electron affinities of the corresponding molecules evaluated in the present study are also found to be in excellent agreement with the values recently obtained by other techniques; $EA(O_2)$ = 0.43 ± 0.03 eV[9,11]; EA(NO) = 0.024 ± 0.01 eV[10,11] and $EA(NO_2)$ = 2.28 ± 0.1 eV[12].

A more detailed description of this study will be submitted for publication in the Journal of Chemical Physics.

Table 1

Kinetic Energy Thresholds and Thermochemistry of O_2^-, NO^- and NO_2^- Reactions

Reactant Ion	Neutral Target	Measured Threshold,[a] D^o(eV)	Electron Affinity (eV)[b] O_2	NO	NO_2
O_2^-	N_2	4.10(2)	0.47±0.1		
	O_2	4.05(2)	0.42±0.1		
	CO	4.15(2)	0.52±0.1		
	NO	4.30(2)	0.67±0.2		
NO^-	N_2	5.07(3)		0.05±0.2	
	O_2	3.80(5)[c]; 0.55(2)[d]		0.17±0.1[e]; 0.09±0.1[f]	
	CO	5.3(1)		0.28±0.2	
	NO	5.03(3)		0.01±0.1	
	Kr	5.02(3)		0.003±0.1	
	Xe	5.00(3)		-0.02±0.2	
NO_2^-	N_2	4.1(1)			2.46±0.1
	NO	3.9(1)			2.26±0.1
	Kr	4.1(1)			2.46±0.1
	Xe	3.8(1)			2.16±0.1

a. Averaged value of the experiments given in parentheses.

b. $EA(O_2) = D^o(O_2^-) - \Delta H_f^o(O) - \Delta H_f^o(O^-) + \Delta H_f^o(O_2)$

$EA(NO) = D^o(NO^-) - \Delta H_f^o(N) - \Delta H_f^o(O^-) + \Delta H_f^o(NO)$

$EA(NO_2) = D^o(NO_2^-) - \Delta H_f^o(O^-) - \Delta H_f^o(NO) + \Delta H_f^o(NO_2)$

c. ΔH_R^o for the reaction, $NO^- + O_2 \rightarrow O^- + O + NO$

d. ΔH_R^o for the reaction, $NO^- + O_2 \rightarrow O^- + NO_2$

e. $EA(NO) = \Delta H_R^o - \Delta H_f^o(O) - \Delta H_f^o(O^-)$

f. $EA(NO) = \Delta H_R^o - \Delta H_f^o(NO_2) - \Delta H_f^o(O^-) + \Delta H_f^o(NO)$

g. The heat of formation of the following ions and molecules at 298.15°K are taken from Franklin et. al.[13]

$\Delta H_f^o(O) = 2.582$ eV, $\Delta H_f^o(O^-) = 1.053$ eV, $\Delta H_f^o(N) = 4.899$ eV, $\Delta H_f^o(NO) = 0.935$ eV, $\Delta H_f^o(NO_2) = 0.3438$ eV.

References

* Systems Research Laboratories, Dayton, Ohio

1. C. F. Giese and W. B. Maier II, J. Chem. Phys., 39, 197 (1963).

2. D. W. Vance and T. L. Bailey, J. Chem. Phys., 44, 486 (1966).

3. T. F. Moran and J. R. Roberts, J. Chem. Phys., 49, 3411 (1968).

4. T. O. Tiernan and R. E. Marcotte, J. Chem. Phys., 53, 2107 (1970).

5. J. H. Futrell and C. D. Miller, Rev. Sci. Instr., 37, 1521 (1966); B. M. Hughes and T. O. Tiernan, J. Chem. Phys., 55, 3419 (1971).

6. J. L. Paulson, Advan. Chem. Ser. 58, 28 (1966).

7. P. J. Chantry, Bull. Am. Phys. Soc., 16, 212 (1971); J. Chem. Phys., 55, 2746 (1971).

8. W. T. Zemke, G. Das and A. C. Wahl, Chem. Phys. Letters, 14, 310 (1972).

9. R. J. Cellotta, R. A. Bennett, J. L. Hall, M. W. Siegel and J. Levine, Phys. Review A, 6, 631 (1972).

10. M. W. Siegel, R. J. Celotta, J. L. Hall, J. Levine and R. A. Bennett, Phys. Review A, 6, 607 (1972).

11. T. O. Tiernan, B. M. Hughes and C. Lifshitz, J. Chem. Phys., 55, 5692 (1971).

12. B. M. Hughes, C. Lifshitz and T. O. Tiernan, J. Chem. Phys. (in press).

13. J. L. Franklin, J. G. Dillard, H. M. Rosenstock, J. T. Herron, K. Draxl and F. H. Field, U.S. Department of Commerce, National Bureau of Standards (1969).

DETECTION OF ASSOCIATIVE DETACHMENT REACTIONS USING THE SF_6 SCAVENGER TECHNIQUE.

J. C. Haartz*, C. Lifshitz+ and T. O. Tiernan
Aerospace Research Laboratories, Chemistry Research Laboratory
Wright-Patterson AFB, Ohio 45433

Associative detachment reactions of the type:

$$A^- + B \rightarrow AB + e \qquad (1)$$

have been studied previously by flowing afterglow techniques[1-5] and by drift tube methods[6-8]. Since no detectable charged products occur in these reactions, rate coefficients for these reactions were determined either by following the disappearance of the reactant ion or by measurement of the detached electron current. As will be shown in this report, another means of studying these reactions is to employ an electron scavenger such as SF_6 to detect the detached electrons. This technique has been used in other laboratories to detect temporary negative ion resonances for a variety of molecules[9-11]. Since associative detachment reactions are assumed to involve a temporary negative ion state which autodetaches an electron[4], the products should be a vibrationally excited neutral molecule and an electron of thermal or near-thermal energy which can be efficiently scavenged by SF_6. Recent studies by Schulz, et al.[12] have shown that for reaction (1), where B = CO, the energy of the detached electron is typically less than 0.2 eV, for 0^- energies up to 1.5 eV.

The ARL tandem mass spectrometer, which has been described previously,[13,14] was used to study a number of associative detachment processes using the scavenger technique (See Tables I & II). The mass and energy analyzed reactant ion beam is impacted on a mixture of the neutral reactant and the scavenger, SF_6 in the collision chamber, and the ionic products are monitored with the second stage mass spectrometer. A sufficiently high pressure is maintained in the collision chamber to permit the occurrence of reaction (1), followed by attachment to SF_6 of the electron released, which yields the observed product ion, (reaction 2),

$$e^- + SF_6 \rightarrow SF_6^- \qquad (2)$$

A direct reaction of the incident ions with SF_6 was also found to produce SF_6^- and other fragments, (reactions 3a, 3b, 3c).

$$SF_6 + 0^- \rightarrow SF_6^- \qquad (3a)$$

$$SF_6 + 0^- \rightarrow SF_5^- + 0 + F \qquad (3b)$$

$$SF_6 + 0^- \rightarrow F^- + SF_5 + 0 \qquad (3c)$$

However, pressure-dependence studies with mixtures of SF_6 and reactant gases which undergo fast associative detachment reactions showed that at a primary ion translational energy of 0.3 eV and a collision chamber temperature of 30°C, reaction (3a) contributes less than 5% of the observed SF_6^- signal. The SF_5^- and F^- products are formed only by reactions (3b) and (3c).

The dependence of product ion intensity on collision chamber pressure over the range 5μ to 100μ under the above conditions of temperature and primary ion energy was determined for pure SF_6 as well as for all mixtures examined. For pure SF_6, where only reaction (3) occurs, a pseudo-first-order pressure dependence was observed in the low pressure range. At higher collision chamber pressures, scattering and reduced collection efficiency probably contribute to the observed curvature of the pressure plots, (see Figure 1). The same behavior was observed for mixtures of SF_6 and target gases such as He, Ar, 0_2 and CH_4 which do not undergo an associative detachment reaction. For mixtures of SF_6 and molecules which undergo associative detachment reactions (Tables I & II), a pseudo second-order pressure dependence was observed for SF_6^-, (see Figure 2), as expected if SF_6^- is formed via reactions (1) and (2). In those cases where the associative detachment reaction was slow, notably for the interactions of 0^- with C_2H_6 and NO, and of S^- with 0_2, the contribution from the direct reaction (3a) was significant at low pressures, and pseudo-second-order behavior was exhibited over the entire

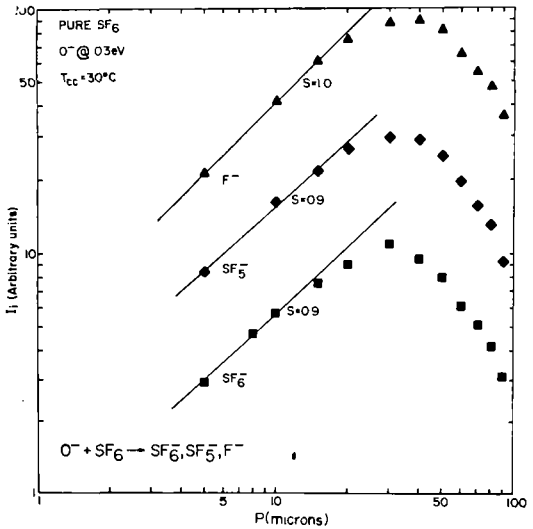

Figure 1. Pressure dependence of product ions for the reaction of O^- with SF_6.

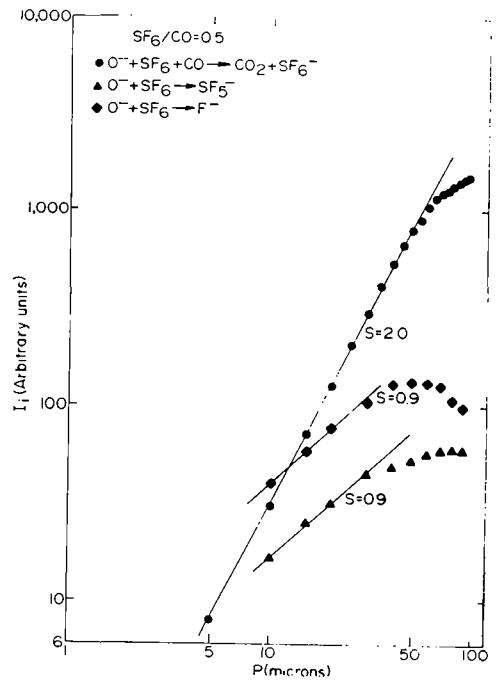

Figure 2. Pressure dependence of product ions for the reactions of O^- with an SF_6/CO mixture.

pressure range only if the contribution from the direct reaction was subtracted. The pressure dependences of SF_5^- and F^- were pseudo-first-order for all of these mixtures (except for F^- produced in the reaction with SO_2). As already noted, this establishes that SF_5^- and F^- are formed only via the direct reactions (3b, 3c) in the mixtures and that these fragments are not formed by dissociative attachment of the electron detached in reaction (1).

Another confirmation of the reaction sequence for these mixtures was obtained from experiments using CO/SF_6 mixtures. The partial pressure of CO was held constant and that of SF_6 varied in a series of experiments, then the partial pressure of SF_6 was held constant while varying that of CO. In each case, the SF_6^- intensity as a function of pressure was shown to be pseudo-first order as expected for the postulated reaction sequence.

Additional products were observed in some of these systems (e.g., OH^- from the reaction of O^- with an H_2/SF_6 mixture; $C_2H_2^-$ from the O^- reaction with the C_2H_4/SF_6 mixture.) In all these cases, with the exception of the SO_2 mixture, the pressure dependences of the intensities of these products were again first order.

The rate coefficient for the reaction

$$O^- + CO \rightarrow CO_2 + e \qquad (4)$$

was determined in drift tube studies[6,8] to be 7×10^{-10} at low O^- translational energies. Since it was shown that the rate is independent of the O^- translational energy at low energies[6], reaction (5) was chosen as a convenient reference for our experiments which were carried out at slightly higher O^- translational energies than is characteristic of flowing afterglow or drift tube measurements. The rate

constants listed in Tables I & II for the associative detachment reactions investigated herein were determined by normalizing the measured relative rates to this absolute rate coefficient of 7×10^{-10} cc/molec sec for reaction (5) at 0.3 eV 0^- laboratory energy.

The cross section for reaction (5) as a function of 0^- energy was obtained as follows. The contribution to the observed SF_6^- signal from the direct reaction, (3a), was determined at each energy point using a 2:1 He/SF_6 mixture and subtracted from the SF_6^- count rate measured for a 2:1 CO/SF_6 mixture at the same energy to give a "corrected" SF_6^- count rate. The absolute cross section for reaction (5) at 0.3 eV 0^- laboratory energy was obtained from the absolute rate constant cited above and the calculated velocity.

$$\sigma(0.3 \text{ eV}) = \frac{k(0.3 \text{ eV})}{v_{0^-}} = \frac{7 \times 10^{-10} \text{ cc/molec sec}}{1.9 \times 10^5 \text{ cm/sec}} = 36.8 \text{ Å}^2$$

Each corrected SF_6^- count rate was then normalized to the value for 0.3eV and the absolute cross section calculated above to obtain the appropriate dependence of the cross section on translational energy. The resultant excitation function (σ vs E) is shown in Figure 3.

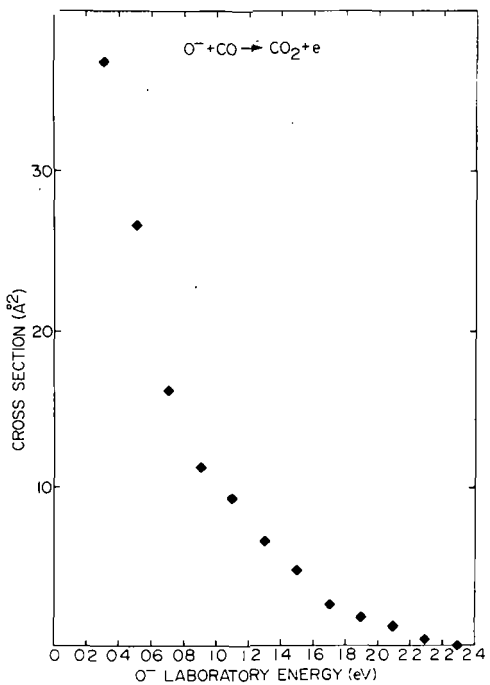

Figure 3.

Dependence of cross section for the associative detachment reaction of 0^- with CO on translational energy.

A more detailed report of this work will be submitted for publication in the Journal of Chemical Physics.

References

* National Research Council-Air Force Systems Command Postdoctoral Research Associate, 1971 - 73.

\+ Visiting Research Scientist (Technology, Inc., Contract F33615-71-C-1463) from the Hebrew University, Jerusalem, Israel.

References

1. F. C. Fehsenfeld, E.E. Ferguson and A.L. Schmeltekopf, J. Chem. Phys. 45, 1844 (1966).

2. F.C. Fehsenfeld and E.E. Ferguson, J. Chem. Phys. 51, 3512 (1969).

3. Ibid., 53, 2614 (1970).

4. E.E. Ferguson, Accts. Chem. Res. 3, 402 (1970).

5. D.K. Bohme and L.B. Young, J. Am. Chem. Soc., 92, 3301 (1970).

6. J.L. Moruzzi, J.W. Ekin, Jr., and A. V. Phelps, J. Chem. Phys. 48, 3070 (1968).

7. D.A. Parkes, J.C.S. Faraday I, 613 (1972).

8. Ibid., 627 (1972).

9. R.K. Curran 38, 780 (1963).

10. R.O'Malley and K. Jennings, Int. J. Mass Spectrom. Ion Phys. 2, App.1,(1969).

11. R.N. Compton, R.H. Huebner, P.W. Reinhardt and L.G. Christophorou, J. Chem. Phys. 48, 901 (1968).

12. J.L. Mauer and G. J. Schulz, Phys. Rev. A 7, 593 (1973).

13. J.H. Futrell and C.D. Miller, Rev. Sci. Instr. 37, 1521 (1966).

14. T.O. Tiernan, B.M. Hughes and C. Lifshitz, J. Chem. Phys. 55, 5692 (1971).

TABLE I

Rate Constants for Associative Detachment Reactions

Reaction	Present Results (at 0.3eV)	$kx10^{10}$ (cc/molecule sec) Flowing Afterglow	Drift Tube
$O^- + CO \rightarrow CO_2 + e$	7.0 *	4.4	7.3,6.5
$O^- + O_2 \rightarrow O_3^+ e$	<0.01	<0.01	---
$O^- + NO \rightarrow NO_2 + e$	1.4	1.6	2.2
$O^- + H_2 \rightarrow H_2O + e$	3.6 ± 0.8	6.0	7.0,7.5
$O^- + D_2 \rightarrow D_2O + e$	4.3	---	4.8
$O^- + SO_2 \rightarrow SO_3 + e$	9.25 ± 0.2	7.0	---
$S^- + O_2 \rightarrow SO_2 + e$	0.07	0.3	---

* Reference Reaction

TABLE II

Rate Constants for Associative Detachment Reactions

Reaction	Present Results (at 0.3eV)	$kx10^{10}$ (cc/molecule sec) Flowing Afterglow	Drift Tube
$O^- + CO \rightarrow CO_2 + e$	7.0 *	4.4	7.3,6.5
$O^- + CH_4 \rightarrow CH_4O + e$	<0.01	---	not obsd.
$O^- + C_2H_6 \rightarrow C_2H_6O + e$	0.21 ± 0.04	not obsd.	---
$O^- + C_2H_4 \rightarrow C_2H_4O + e$	4.7 ± 0.2	7.7	4.0
$O^- + C_3H_6 \rightarrow C_3H_6O + e$	10.9 ± 0.7	not obsd.	---
$O^- + 1\text{-}C_4H_8 \rightarrow 1\text{-}C_4H_8O + e$	18.5 ± 1.3	not obsd.	---
$O^- + 2\text{-}C_4H_8 \rightarrow 2\text{-}C_4H_8O + e$	20.4 ± 1.5	not obsd.	---
$O^- + C_2H_2 \rightarrow C_2H_2O + e$	17.0 ± 0.8	---	13.0
$O^- + CH_3\,\underset{\underset{O}{\|}}{C}CH_3 \rightarrow C_3H_6O_2 + e$	11.4	---	---

* Reference Reaction

NEGATIVE ION FORMATION IN FLAMES CONTAINING: I. CHROMIUM AND POTASSIUM AND II. RHENIUM AND CESIUM*

R.K. Gould and W.J. Miller

AeroChem Research Laboratories, Inc., P.O. Box 12, Princeton, NJ 08540

A specially designed quadrupole mass spectrometer has been used to measure concentrations of negative ions in well-characterized, atmospheric pressure $H_2/O_2/N_2$ flames over a temperature range of 1800 K to 2500 K. The flames are seeded with potassium or cesium salts to provide a source of electrons; the introduction of chromium or rhenium salts leads to formation of the negative ions CrO_2^-, CrO_3^-, $HCrO_3^-$ or ReO_3^- and ReO_4^-, respectively.

Measurements in chromium-containing flames[1] show negative ion concentrations to be directly proportional to the total chromium concentration in the flames. The data is consistent with the establishment of the following scheme of equilibrium reactions:

$$e^- + HCrO_3 = CrO_3^- + H \qquad \Delta H_0^\circ = 125 \pm 40 \text{ kJ mole}^{-1}$$
$$H_2 + CrO_3^- = HCrO_3^- + H \qquad \Delta H_0^\circ = 78 \pm 40 \text{ kJ mole}^{-1}$$
$$H + CrO_3^- = CrO_2^- + OH \qquad \Delta H_0^\circ = 152 \pm 50 \text{ kJ mole}^{-1}$$

Electron affinities inferred from these measurements are: E.A.(CrO_3) = 229 kJ mole^{-1} (2.3 eV) and E.A. ($HCrO_3$) = 390 kJ mole^{-1} (4.05 eV).

Similar measurements in rhenium-containing flames[2] show the negative ion concentrations to be linear in total rhenium. The observations can be explained by assuming that the negative ion chemistry is dominated by the following pair of equilibria:

$$e^- + HReO_4 = ReO_4^- + H \qquad \Delta H_0^\circ = 15 \pm 50 \text{ kJ mole}^{-1}$$
$$H + ReO_4^- = ReO_3^- + OH \qquad \Delta H_0^\circ = 136 \pm 50 \text{ kJ mole}^{-1}$$

These enthalpy changes yield electron affinities of 255 kJ mole^{-1} (2.6 eV) for ReO_3 and 430 kJ mole^{-1} (4.5 eV) for ReO_4.

---

* Work sponsored by the Office of Naval Research under Contract N00014-72-0053.

1. W.J. Miller, J. Chem. Phys. 57, 2354 (1972).

2. R.K. Gould and W.J. Miller, to be submitted to J. Chem. Phys.

ENERGETICS OF FRAGMENTATION OF As_4 GAS*

S. L. Bennett, J. L. Margrave, J. L. Franklin and J. E. Hudson

Department of Chemistry

Rice University

Houston, Texas 77001

As part of a continuing program of investigation of high temperature molecules, the energetics of fragmentation of As_4 gas has been investigated. Negative and positive ions have been studied. Gaseous As_4, generated by heating metallic arsenic contained in a Knudsen cell, was directed into the source of a Bendix Model 14-107 time-of-flight mass spectrometer. The negative ions As^-, As_2^-, and As_3^- were formed by dissociative electron attachment of As_4. Accurate appearance potentials were obtained by mathematical deconvolution of the ionization efficiency curves, and, translational energies have been obtained from ion peak-width measurements obtained throughout the resonance processes. Appearance potentials and translational energies (at threshold) have also been obtained for the positive ions As^+, As_2^+, As_3^+, and As_4^+. From these studies, the heats of formation of the negative and the positive ions, the heat of formation of As_3 gas, the heat of dissociation $D(As_2\text{-}As_2)$, the electron affinities of the neutrals, and the direct measurement of α (the fraction of the oscillators which are effective for the distribution of the excess energy) for the three dissociative resonance capture processes, have all been obtained.

A detailed account is being prepared for publication.

---

*This research is supported by the Office of Naval Research, U. S. Navy, under Contract No. 67-A-0145-0002.

A New Measurement of the SF_6^- Autoionization Lifetime*

R.W. Odom, D.L. Smith and J.H. Futrell

Department of Chemistry
University of Utah
Salt Lake City, Utah 84112

A new technique, which uses an ion cyclotron resonance spectrometer as an ion trap, is used to measure the autoionization process $SF_6^- \xrightarrow{k_a} SF_6 + e$. This measurement is accomplished by using trapping plate ejection of the free electrons in the ICR cell which result from the autoionization of SF_6^-. The experimental procedure is to pulse a beam of low energy electrons "on" for about 50 μsec and at some time after the electron beam is turned "off" but before the charged particles (SF_6^-, SF_5^-, and electrons) reach the total ion current collector, a rf electric field of sufficient amplitude and duration to eject the free electrons from the cell is applied to one of the trapping plates. It is shown that the frequency, amplitude and duration of the rf field has no effect on the heavier ions in the cell, and it is possible to quantitatively remove the free electrons. Since the autoionization process follows first order kinetics, the integrated rate expression is

$$\ln \frac{i}{i^0} = -k_a \tau$$

where i^0 is the SF_6^- current at time $t=0$, i is the ion current at time $t=\tau$ and k_a is the autoionization rate constant. In the present investigation, i^0 is the collected ion current for an electron ejecting rf duration of 5 μsec, and i is the collected current for an rf duration of time τ. A plot of $\ln i/i^0$ versus τ should yield a straight line with a slope equal to $-k_a$. The experimental results show that such a plot has substantial curvature, and this curvature indicates that there is a collection of autoionizing states of the negative ion, and, therefore, a collection of autoionization lifetimes. For example, when the delay time between the electron beam pulse and the electron ejection rf is 400 μsec, the SF_6^- lifetime varies from 0.3 m sec to 2.0 m sec for a variation of τ from 50 μsec to 800 μsec.

---

*To be published in Chemical Physics Letters

Negative Ion Molecule Reactions in Methylfluorosilanes

John G. Dillard
Department of Chemistry
Virginia Polytechnic Institute
and State University
Blacksburg, Va. 24061

ABSTRACT

The reactions of SF_6^- with methylfluorosilanes $(CH_3)_nSiF_{(4-n)}$ have been studied. The dominant reaction process is fluoride ion transfer from SF_6^- to the neutral methylfluorosilane. No charge transfer or atom transfer processes were noted. The reaction cross sections have been studied as a function of ion energy (repeller potential 1.5 - 4.0 V). The reaction cross section decreases with increasing ion energy as expected for exothermic processes. The reaction cross section Q decreases dramatically at repeller voltage 2.0 V proceeding from SiF_4 to $SiMe_4$. Q changes by about 10^2 from SiF_4 to Me_3SiF. The value of Q for the reaction with $SiMe_4$ must be less than about 10^{-8} cm^2/molecule. In addition, no reaction of SF_6^- with SiH_4 was observed at any repeller voltage studied.

The results are consistent with the known fluoride ion acceptor ability of the methylfluorosilanes as determined from fluoride ion exchange with pentacoordinate salts $RSiF_4^-$ in condensed phases. No salts of the type $R_2SiF_3^-$ or $RSiF_4^-$ have been prepared in condensed phases. If the value of Q is taken as a measure of the F^- acceptor ability of methylfluorosilanes, it is expected that the acceptor ability of R_2SiF_2 and $RSiF_4$ is too small to form stable salts.

Submitted to Inorganic Chemistry for publication.

ANIONIC ELIMINATION AND FLUORIDE TRANSFER REACTIONS IN FLUORINATED HYDROCARBON

Douglas P. Ridge, Department of Chemistry, University of Delaware, Newark, Delaware 19711

Examination of available thermodynamic data indicates that in a number of cases reactions of the type

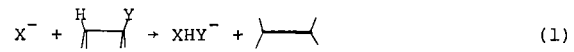

(1)

are rendered exothermic by the formation of the strong hydrogen bond in the species XHY^-. Such base induced eliminations are well known in solution[1]. To determine if such reactions occur in the gas phase, the anionic reactions of a series of alkyl halides have been examined[2]. The studies were carried out with an ion cyclotron resonance spectrometer.

Methoxide anions were generated from methyl nitrite and allowed to react with 2,2,2 trideuteroethylfluoride.

The following reactions were observed:

$$CH_3O^- + CD_3CH_2F \longrightarrow {}^-CD_2CH_2F + CH_3OD \quad (2)$$

$$\longrightarrow CH_3ODF^- + CD_2CH_2 \quad (3)$$

$$\longrightarrow F^- + CH_3OCH_2CD_3 \quad (4)$$

$$\underline{\text{or}}\ CH_3OD + CD_2CH_2$$

$$F^- + CD_3CH_2F \rightarrow FDF^- + CD_2CH_2 \quad (5)$$

$${}^-CD_2CH_2F + CD_3CH_2F \rightarrow CH_2FCD_3F^- + CD_2CH_2 \quad (6)$$

Reactions 2-4 all proceed at approximately the same rate (4×10^{-11} cm^3 $molecule^{-1}$ sec^{-1}). The secondary Reactions 5 and 6 proceed at somewhat higher rates (1.3 and 1.9 $\times 10^{-10}$ cm^3 $molecule^{-1}$ sec^{-1}, respectively). The indicated isotopic products were the only ones observed. The reactions were identified using ion cyclotron double resonance. The kinetics were also consistent with the reactions indicated. Reaction 6 was determined to be a fluoride transfer by examining the reaction in a mixture of CD_3CH_2F and CH_3CH_2F.

Proton transfer, elimination of HF and secondary fluoride transfer in analogy with Reactions 2, 3, and 6 were observed in CH_3CHF_2, CH_3CF_3, CH_2FCHF_2, and CHF_2CHF_2. The elimination in each case involved the formation of CH_3OHF^- and, hence, could be unambigiously identified as an elimination. Only in the case of CH_2FCHF_2 was F^- observed as a primary product. In this case, the F^- went onto form FHF^- in analogy with Reaction 5.

In the series CH_3CH_2F, CH_3CHF_2, and CH_3CF_3, the importance of the elimination process increased with increasing α fluoride substitution. The relative importance of proton transfer decreased with increasing a fluorine substitution. In the ß-substituted fluorethylenes proton transfer and elimination were of approximately equal importance.

The reactions of a number of chloro and bromo ethanes with methoxide anions examined. In each case, the only significant product observed was the halide anion. ß-chloroethanol reacted with methoxide to form CH_3OHCl^-.

Examination of available thermochemical data suggests a partial explanation of the product distributions observed. In each case where halide anion is observed as a product, both the elimination and proton transfer reactions are very exothermic. They are, in fact, sufficiently exothermic that the products could decompose to form methanol, an olefin and halide anion. If such a decomposition is not possible thermodynamically, then the products of elimination and proton transfer are observed. The relative amounts of elimination and proton transfer products formed is determined largely by geometric factors such as the extent of substitution and direction of the dipole moment of the substrate.

Some thermodynamic conclusions of interest can be made from the observations. From the fact that methoxide reacts with CH_3CF_3 to form CH_3OHF^-, it can be concluded that $D(CH_3O^- - HF) > 33$ kcal/mole. From the observed porton transfer reactions and the assumption that all primary C-H bond strengths are 98 kcal/mole, it can be concluded that

EA(CH_2CH_2F, (CH_2CHF_2 or CH_3CF_2), CH_2CF_3, ($CHFCHF_2$ or CH_2FCF_2), CF_2CHF_2) > 1.2 eV.

1. J. F. Bunnett, Surv. Program Chem., 5, 53 (1969)

2. D. P. Ridge and J. L. Beauchamp, to be submitted to J. Amer. Chem. Soc.

Field Desorption Mass Spectrometry.

HANS D. BECKEY, Inst. Phys. Chemie, Univ. Bonn, Germany.

Field Desorption Mass Spectrometry (FD-MS)[1] of large organic molecules is a new branch of Field Ionization (FI)-MS. Theory and techniques are explained . In contrast to other methods of ionization (CI, low voltage EI, FI) the solid organic sample must not be evaporated into the ionization zone. It is deposited directly on the surface of a field anode from a solution. At low temperatures, but with high electric fields applied to the anode, ionized molecules are desorbed from the anode. The heat of ionic desorption in a high field is small. Thus the method is suitable for the study of molecules of biological significance with high polarity and low volatility. Intense M^+ and/or $(M+H)^+$ ions are observed even if they are not clearly detectable with the other modes of ionization. The method stands or falls with the quality of the "activated" field anodes.

"Activation" means formation of a very large number of microneedles on the surface of the field anode. It is the experience of the author's group that tungsten wires of about 10 /mm diameter are most suitable for the FD-technique. The microneedles are formed by high-field pyrolysis of benzonitrile. The length of the needles should be between 20 and 40 /mm. The optimum activation methods for FD-emitters are described in several publications. The apparatus for activation is represented in ref. 2. STEROSCAN micrographs are shown in ref. 3. A detailed description of reproducible production of needles at high temperatures (about 1200°C) is given in ref. 4.

FD of samples deposited on the emitter in the nanogram range are sufficient for taking FD-MS with sensitive photoplates in double focusing machines. The molarity of the samples should be at least 10^{-3} (or perhaps 10^{-4} with mass spectrometers having a higher transmission than those of the author's laboratory (Varian MAT CH_4). The sample is distributed over the microneedles like a cobweb (after evaporation of the solvent).

Normally the anode wire is heated by an electric current in the mA range for field evaporation of samples of low volatility. Recently Winkler [5] found that heating of the sample by IR radiation enhances the intensity of the molecular ion peaks by a factor of about five and reduces the relative intensities of the fragment ions. This effect (which was not observed with all samples) depends on the nature of the substance, the solvent and the structure of the microneedles.
There exists an optimum temperature, T^* , for each substance which yields a maximum M^+ or $(M+H)^+$ and minimum fragment ion currents. If stronger fragment peaks are wanted, the anode wire must be heated to temperatures higher than T^*. This is the case when substances of high molecular weight shall be characterized by their pyrolysis products.
Pyrolysis field desorption mass spectra (Py-FD-MS) of herring DNA have been studied by Schulten et al.[6]. About 5 x 10^{-8} g of the DNA suspended

in acetone were transferred to the high temperature activated 10 /mm tungsten wire. The wire was heated by a slowly increasing dc current. (0 - 80 mA during the exposure time of 6 min). A double focusing mass spectrometer with a photoplate ion detector was used. (Vacuum evaporated AgBr plates). The resolution was about 30.000. The essential bases of DNA, some nucleosides, nucleotides and dinucleotides have been identified (besides a number of phosphate clusters).

The FD mass spectra of certain classes of organic substances have been studied: Nucleosides and nucleotides [7], purine bases [3], amino acids [8], peptides [9], pesticides [10], drug metabolites [11] and substituted sultams [12].

It is also possible to take FD mass spectra of organic salts. The M^+ ions are, of course, unstable, but protonated peaks $(M+H)^+$ are detected. If the salt (sodium acetate, for example) is dissolved in water, strong "cationated" $(M + Na)^+$ peaks are found [3)].

In analogy to the coupling between GLC and MS with EI, CI or FI sources, continuous or discontinous coupling between LLC and FD-MS is an attractive technique. This was pointed out first by Schulten [13], and the first experimental results of this technique have been reported [14]. Further quantitative results are dealt with during the present conference by Habfast and Schulten [15].

In a joint work of three laboratories, the EI, CI, FI and FD mass spectra of a number of substances of biological significance have been compared [16]. (Amino acids, steroids, triglycerides, barbiturates and pesticides). It turned out that these techniques of molecular ionization are complementary, to some extend.

One of the advantages of FD-MS is that one can observe the molecular ions of very small amounts of underivatized oligopeptides, even if they contain amino acid residues of extremely low volatility like arginine or cystine. Winkler, for example, detected the molecular ion peak of the unprotected nonapeptide Arg-Gly_3-Pro-Gly_3-Arg. Although strong sequence peaks are found in the FD mass spectra of numerous oligopeptides at temperatures higher than T^*, a complete sequence determination of a peptide requires measurement of the complementary EI, CI or FI mass spectra. The possibility of obtaining the full sequence information by pyrolysis FD-MS has not yet been fully explored.

References

1. H.D. Beckey, Int.J.Mass Spectrom.Ion Phys. 2,500 (1969)
2. H.D. Beckey, A.Heindrichs, E.Hilt, M.D. Migahed, H.R.Schulten and H.U.Winkler, Messtechnik 78, 196 (1971)
3. H.R.Schulten and H.D.Beckey, Org.Mass Spectrom 6, 885 (1972)
4. H.D.Beckey, E.Hilt and H.R.Schulten, J.Sci Instr. (J.of Phys.E), in press
5. H.U.Winkler, Bonn, personal communication

6. H.R.Schulten, H.D.Beckey, A.J.H.Boerboom and H.L.C.Meuzelaar, Anal.Chem. in press
7. H.R.Schulten and H.D.Beckey, Org.Mass Spectrom., in press
8. H.U.Winkler and H.D.Beckey, Org.Mass Spectrom. 6, 665 (1972)
9. H.U.Winkler and H.D.Beckey, Biophys.Biochem.Res.Comm. 46, 391 (1972)
10. H.R.Schulten and H.D.Beckey, J.Agr.Food Chem. 21, 372 (1973)
11. H.R.Schulten and H.D.Beckey, Twentieth Annual Conf. on Mass Spectrometry and Allied Topics, Dallas (1972)
12. H.R.Schulten, H.D.Beckey, G.Eckard and S.H.Doss, Tetrahedon, in press
13. H.R.Schulten, Research Conference on Pesticide Metabolites - Enzymology, Isolation and Characterization, Fargo,N.D., June 1972
14. H.R.Schulten and H.D.Beckey, First Internatl.Symposium on Column Liquid Chromatography, Interlaken, May 1973
15. K.Habfast and H.R.Schulten, Twenty-First Annual Conference on Mass Spectrometry and Allied Topics, San Francisco (1973) paper H-7
16. H.M.Fales, G.W.A.Milne, J.N.Damico, H.U.Winkler and H.D.Beckey to be published in Anal.Chemistry

PHOTODISSOCIATION OF GASEOUS IONS

Jean DURUP

Laboratoire des Collisions Ioniques*, Université de Paris-Sud

91405 - ORSAY, France.

The present paper will give the main features of the review lecture which the author gave at the Conference. Details will be omitted especially when they may be found in the published literature.

Photodissociation studies on gaseous ions might be considered as complementary to absorption spectroscopy of ions. However, the latter is a very difficult technique and at the present time only about half a dozen of gaseous ions have been studied by absorption spectroscopy [1]. Thus photodissociation spectroscopy, which yields information on the transitions from ground or metastable states to repulsive or predissociated states, may become in the near future the easiest way to study those states of gaseous ions which cannot be observed by emission spectroscopy.

Apart from their fundamental interest, ion photodissociation studies may be important for the understanding of the processes which take place in the ionosphere of the Earth and other planets. For example, martian CO_2^+ ions or terrestrial hydrated H_3O^+ ions might undergo photodissociation by solar light ; this could be an important loss process for these very stable ions.

There has been so far to our knowledge three types of experiments on the photodissociation of gaseous ions.

(i) Measurement of the total photodissociation cross section at variable wavelength in a cross-beam experiment (G.H. Dunn and F. Von Busch, J.I.L.A., Boulder, Colorado).

(ii) Kinetic energy spectra of the fragment ions produced by photodissociation of discrete vibrational levels at fixed wavelength in crossed-beam experiments (N.P.V.B. van Asselt, J. Maas and J. Los, FOM-Instituut, Amsterdam, The Netherlands ; J.-B.Ozenne, Pham D., M. Tadjeddine and J. Durup, Université de Paris-Sud, Orsay, France).

(iii) Photodissociation spectra of ions trapped in an Ion Cyclotron Resonance cell (R.C. Dunbar, J.M. Kramer, E.W. Fu, Case Western Reserve University, Cleveland, Ohio).

These experiments will be reviewed in the indicated order.

Experiments (i) and (ii) were concerned with the photodissociation of H_2^+ through following transition :

(1) $$H_2^+ (1s\sigma_g) \xrightarrow{h\nu} H_2^+ (2p\sigma_u) \rightarrow H^+ + H(1s)$$

In both the Boulder experiment and the Orsay experiment the H_2^+ ions were formed from H_2 molecules by impact of electrons of high enough energy so that all vibrational levels of the ground $1s\sigma_g$ state of H_2^+ were populated, roughly in accordance with Franck-Condon factors. The time of flight of the ions from the ion source to the region where they crossed the photon beam is of course much too short to permit any vibrational

(*) Part of the Laboratoire de Physico-Chimie des Rayonnements, associated to the CNRS.

deactivation, so that the initial population may be considered as preserved when the photoabsorption occurs.

Now the advantage of studying H_2^+ comes from the fact that everything in this ion is known from theory, since it is possible to solve exactly the Schrödinger equations for the electronic wave function. Thus the relevant potential curves (illustrated in fig. 1 of ref.[2]), the energies of the vibrational-rotational levels of the ground state, their vibrational wave functions, and even the electronic dipole transition moment for process (1) as a function of internuclear distance, have been known for many years.

G. Dunn thus calculated theoretically the photodissociation cross section of all vibrational levels of H_2^+ and D_2^+ at any wavelength [3].

Experiment (i).

In experiment (i), by F. von Busch and G. Dunn[2], the total cross section for photodissociation of H_2^+ and D_2^+ was measured between 2472 and 13613 Å on a crossed-bean apparatus which is sketched on fig. 2 of ref.[2].

The H_2^+ ions were formed by ionization of low-pressure H_2 by electrons of 106 to 141 eV ; after mass analysis by a magnet, they crossed the light beam emitted by an arc lamp , monochromatized and focussed. The H^+ secondaries and H_2^+ primaries were separated by a parallel-plate condenser[2].

The cross sections obtained as functions of wave-length were close to, but different by a significant amount from, the cross sections calculated under the assumption of a transition moment for electron impact ionization independent of internuclear distance (i.e., a vibrational population of the $1s\sigma_g$ state of H_2^+ simply derived from Franck-Condon factors for ionization), as shown by figs 6 and 7 of ref.[2]. From these experimental data it was thus possible for F. von Busch and G. Dunn to deduce a law of variation of the relative transition moment for electron impact ionization with respect to internuclear distance ; this law was :

$$(2) \qquad Q_e(r) = 1 + 0.56\,(r - 0.99)^2 \qquad (1 \leqslant r \leqslant 2),$$

the internuclear distance r being in atomic units.

Experiment (ii).

Experiment (ii) was performed under somewhat different conditions in Amsterdam and in Orsay. The first results of the Orsay experiment were published in ref.[4]. The first spectra obtained by J. Los and coll. in Amsterdam [5], and the new, better resolved spectra of J.-B.Ozenne and coll. in Orsay [6] are as yet unpublished and therefore will be reproduced in the present review.

The aim of the experiment is to select the H^+ ions formed from photodissociation, at fixed wavelength, of different vibrational levels of $H_2^+(1s\sigma_g)$. In effect, process (1) will yield H^+ ions with discrete translational energies in the system of the center-of-mass of H_2^+. From the measurement of these energies and of the intensities of the corresponding peaks in the translational energy spectrum of the photo-produced H^+ ions, vibrational populations of the initial H_2^+ ion beam may be inferred.

The relevant transitions an illustrated in fig.1, where the vertical lines represent the transitions which were actually observed in the Amsterdam experiment[5] ($h\nu$ = 2.410 eV) and in the Orsay experiment [6] ($h\nu$ = 1.786 eV). A few loops of the vibrational wave functions of the states involved in the most intense transition of the

Amsterdam spectrum are schematically drawn for illustration of Franck-Condon principle, which allows for significant photodissociation cross sections of several vibrational levels at each wavelength (see e.g. ref.[3]).

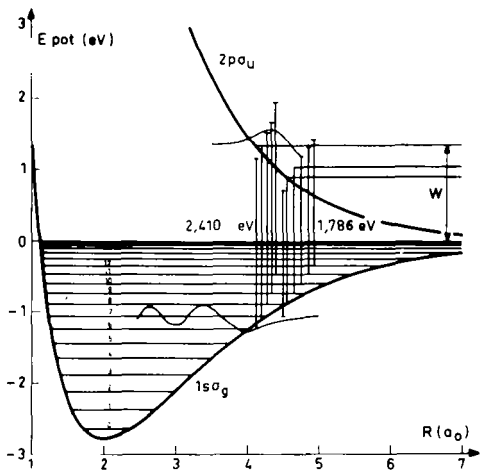

Fig. 1 Scheme of the transitions observed in H_2^+ in the Amsterdam experiment[5] ($h\nu$ = 2.410 eV) and in the Orsay experiment [6] ($h\nu$ = 1.786 eV).

The measurement of the separation energy of the fragments $H^+ + H$ (denoted by W on fig. 1) is achieved with high resolution because of the expansion of the center-of-mass energy scale into the laboratory energy scale, as a result of the law of composition of velocities :

$$T = \frac{1}{2} T_o + (WT_o)^{1/2} \cos\theta + \frac{1}{2} W \quad (3)$$

where T_o is the incident H_2^+ translational energy, T the laboratory energy of the product H^+, W the total translational energy of $H^+ + H$ in the center-of-mass frame, and θ the ejection angle of H^+ (with respect to the incident flight direction) also in the c.o.m. frame.

For example, in the Orsay experiment (T_o = 2000 eV, $h\nu$ = 1.786 eV, θ = 0, the energies T of the H^+ produced from photodissociation of vibrational levels v = 8 and v = 9 (yielding W = 0.891 and 1.047 eV) are 1042.66 and 1046.28 eV, which are easily separated.

But this holds only if θ = 0, i.e. if the collected H^+ are accepted within a very small angle (a few milliradians) well centered about zero deflection.

The experimental set-up in Orsay[6] may be seen on fig.1 of ref.[4]. The H_2^+ ions produced in a Nier-type ion source by 60-eV electrons and accelerated to 2 keV cross the photon beam of a relaxed ruby laser (λ = 6943 Å). Several holes ensure the collimations of the primary and secondary beams ; the H^+ ions are mass and energy - analyzed by a

magnet, detected on an electron multiplier, and counted. To get rid of the background due to collision-induced dissociation of H_2^+ on residual gas molecules, the H^+ ions are counted only during the time of the laser flash (400 μsec.), with a delay of a few μsec to allow for the time of flight of the H^+ ions and to let damp the parasite signals due to the discharge of the capacitors into the flash tube.

The Amsterdam experiment [5] differs mainly in two ways from the Orsay experiment. Firstly the ion source is a duoplasmatron ion source, which yields high H_2^+ intensities but with a vibrational population which is not easy to predict. Secondly the photon beam is emitted by an argon ion laser, with selection of the 5145 Å line. Since this laser is operated continuously, reduction of the background due to collision-induced dissociation had to be achieved by using ultra-high vacuum conditions, with a very strong differential pumping between ion source and interaction region.

Some H^+ kinetic energy spectra obtained in Amsterdam[5] and in the new experiment in Orsay[6] are shown on figs 2 and 3, respectively. Only half of the spectra (either forward or backward ejection of H^+) is shown.

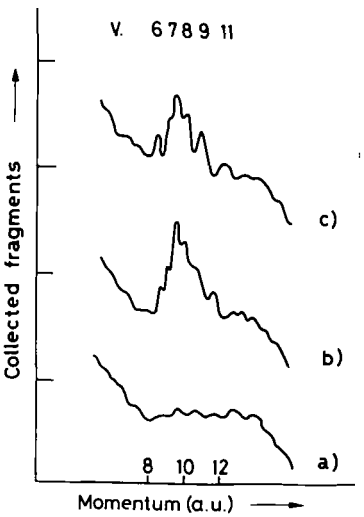

Fig. 2

H^+ momentum spectrum from the Amsterdam experiment [5] :

a) background signal from collision-induced dissociation ;

b) laser-induced spectrum superimposed on background signal ;

c) same as b) except for better resolution.

It is remarkable that the v = 10 level on fig. 2 is absent, as it should be since from Dunn's calculation [3] the predissociation cross section of this level at 5145 Å turns out to be very small, 40 times smaller than that of the neighboring v = 11 level, just by chance.

The spectrum of fig. 3 is decomposed into its components according to an estimate of the shape of the angular acceptance function of the apparatus [6]. It must be emphasized that the energy resolution of the apparatus was good enough for a perfect separation of the individual peaks, but the angular resolution, which was about 5 mrad, although much better than in the preliminary experiment [4], was still insufficient to avoid overlapping of the lines.

The dotted bars on fig. 3 indicate the theoretical positions and intensities of the observed lines. The intensities were calculated from G. Dunn's tables [3] and took into account the variation as $W^{-1/2}$ of the apparatus collection efficiency. The assumed vibrational populations of the incident ions were simply those derived from Franck-Condon principle. We consider the agreement between expected and observed spectra as very satisfactory, and showing that with still some improvement of the angular resolution the experiment may yield quantitative vibrational populations of any H_2^+ beam, for instance extracted from a plasma.

Another kind of information may be obtained from experiment (ii). The spectra of figs 2 and 3 were taken with the light beam polarized in the direction of flight of the ions. In effect, since the $1s\sigma_g \longrightarrow 2p\sigma_u$ transition has its dipole moment parallel to the

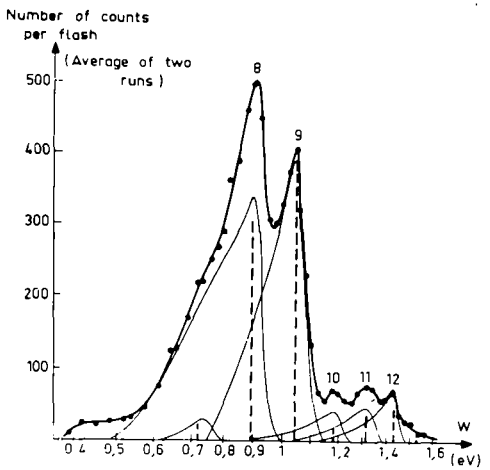

Fig.3

H^+ momentum spectrum from the Orsay experiment [6]

Dots and full line : signal (after background substraction)

Thin line : decomposed spectrum

Dotted line : predicted positions and heights of the peaks.

internuclear axis, and since the dissociation time is very short compared to a rotation period, most ions absorbing the laser photons will then dissociate in a direction with θ close to zero, which favours the success of the experiment. If now the laser beam is polarized in a direction perpendicular to that of the ion beam, most dissociation fragments will be lost. This was done in the Orsay experiment [6] and the spectrum effectively decreased in intensity by a factor 50, and the structure disappeared. Now it is clear that if the H_2^+ ions were produced under such conditions that high rotational states were populated, some molecule ions might absorb a photon polarized at 90° with respect to the ion flight direction, but thereafter rotate while dissociating and thus let the fragments be collected. In other words, comparison of the spectra recorded with the laser beam polarized at either 0° at 90° with respect to the ion beam direction may indicate the presence of ions rotating with a period comparable with the dissociation time.

Now of course experiment (ii) is essentially intended to be applied to other ions than H_2^+. It may yield spectroscopic information on the ground and possibly metastable states of molecular ions, on some dissociative or predissociated states, on the symmetry of optical transitions. This will require the use of other lasers, emitting at shorter wavelengths, since few ions are able to predissociate at the wavelength of the ruby laser and even of the argon ion laser.

Experiment (iii).

The experiment on photodissociation of ions trapped in an Ion Cyclotron Resonance cell has been carried on by R.C. Dunbar and his coworkers since 1970.[7-11].

The possibility to trap ions for times as large as a few seconds allows to observe photodissociation processes even with very low cross sections.

Experiment (iii) was performed with as a light source a 2.5. kW xenon arc with wavelength selection by interference filters [7].

The photodissociation of a primary ion P^+ giving rise to a fragment ion S^+

(4) $$P^+ \xrightarrow{h\nu} S^+$$

is firstly evidenced by the appearance of S^+ in the I.C.R. spectrum when the light beam is turned on.

Next the transition energy is determined by varying the wavelength of the light. Excitation spectra for each photodissociation process are thus obtained [7][11]; from the long wavelength limit the photodissociation threshold is obtained if the initial state is known ; the maximum of the spectrum yields the vertical transition energy.

In cases where different primary ions may give rise to a given secondary ion, double resonance techniques allow for the identification of the parent ion. The experiment consists in the selective ejection of each possible parent ion by heating it with an oscillator tuned on the cyclotron frequency of this particular candidate. When the photo-induced S^+ signal decreases on ejection of a given P^+, the latter is identified as the parent ion [8][9][11].

The polarization of the transition may also be determined , in the same way as in experiment (ii), by varying the direction of polarization of the light, which was done in the Cleveland experiment by the use of a polarizer [10]. Here the method rests upon the fact that the fragment ions usually are ejected with some excess energy. If they fly

along the axis of the ICR cell they will only have to overcome the small potential well (about 0.5 eV) which is used to trap the ions, and then they will escape the detection region and be lost. If on the other hand they are ejected perpendicularly to the axis of the cell they will simply move on large orbits but not be lost.

By this technique R.C. Dunbar and coll.[10] studied the polarization of the transition

(5) $CH_3C\ell^+ \longrightarrow CH_3^+ + C\ell$

A significantly smaller photodissociation signal appeared when the light was polarized in the direction parallel to the axis cell, compared to other directions (see fig. 1 of ref.[10]). This, if one assumes that the $C\ell$ fragment is ejected along the C - $C\ell$ bond, indicates that the transition moment is parallel to this bond, i.e. to the C_3 axis of the molecule. The symmetries and energies of the first levels of $CH_3C\ell$ are known from photoelectron spectroscopy[12] to be ^2E(11.29 eV), $^2A_1$ (14.45 eV), ^2E (15.47 eV). From the observed transition energy he photodissociation might occur as well through the first or the second excited state. But according to the observed polarization the transition should be $^2E \longrightarrow {}^2E$ if the molecule ion retains the C_{3v} symmetry, and $^2E \longrightarrow {}^2A_1$ only if the Jahn-Teller distortion of the ground state is large enough, which is questionable[12]. Thus the assignment of the observed transitions remains somewhat open[10].

Another very important possibility offered by the ICR photodissociation experiment is to answer the question whether the ions arising from isomeric parents have the same geometrical conformation or not. This was tested by R.C. Dunbar and coll.[11] by comparing the photodissociation spectra of such ions. Fig. 4 shows these spectra for $C_7H_8^+$ from toluene, cycloheptatriene and norbornadiene. Similar studies were made for isomers of $C_4H_8^+$, $C_8H_{10}^+$, $C_9H_{12}^+$, $C_{10}H_{14}^+$[11].

The evidence for different geometries of the ions arising from isomeric parents, which is clear from the difference in the spectra on fig.4, seems to the present author to be stronger than evidence obtained from differences in reactivities or in dissociation rates or in fragmentation patterns, which may be due to differences in energy content as well as in geometry. An important additional test used by R.C.Dunbar and coll. consists in cooling down the present ions by letting them collide with molecules of a buffer gas such as methane or ethane, under conditions where a few hundreds of collisions occur during the trapping time of the ions.[9][11] In most cases no alteration of the spectra followed such a cooling of the ions, so that these spectra may be considered as the photodissociation spectra of ground-state isomeric ions.

The observed transition energies for photodissociation of various organic ions were compared with the known energy levels of the involved ions[11], which showed that e.g. for a series of definic cations the photodissociation threshold was slightly above the energy of the first excited state and clearly under the energy of the second excited state. Thus it was shown that the first excited state lead to the observed fragments.

These examples which were picked out of a large amount of data from Prof.Dunbar's laboratory show the various possibilities afforded by the I.C.R. photodissociation technique. The availability of tunable lasers will lead in different laboratories to a large extension of this type of experiment.

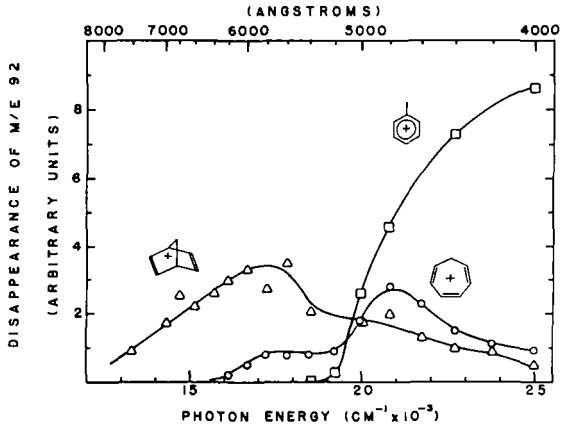

Fig. 4

Photodissociation spectra of $C_7H_8^+$ ions from toluene , cycloheptatriène and norbornadiene (11b).

REFERENCES.

(1) G. Herzberg, Faraday Lecture (30 septembre 1970), 201 - 222 .

(2) F. von Busch and G.H. Dunn, Phys. Rev. A (1972) 5, 1726.

(3) G. Dunn, Phys. Rev. (1968) 172, 1 ; J.I.L.A. Report n° 92 (Jan. 30, 1968).

(4) J.B. Ozenne, Pham D. and J. Durup, Chem. Phys. Lett. (1972) 17, 422.

(5) N.P.F.B. van Asselt, J. Maas and J. Los, unpublished results (courtesy of Prof.Los).

(6) J.-B. Ozenne, Pham D., M. Tadjeddine and J. Durup, to be published.

(7) R.C. Dunbar, J. Amer. Chem. Soc. (1971) 93 , 4354.

(8) J.M. Kramer and J.C. Dunbar, ibid. (1972) 94, 4346.

(9) R.C. Dunbar , ibid.(1973) 95, 472.

(10) R.C. Dunbar and J.M. Kramer, J. Chem. Phys.(1973) 58, 1266.

(11) a) J. Kramer and R.C. Dunbar, ibid. (1973) , in press ; b) R.C. Dunbar and E.W. Fu, J. Amer. Chem. Soc. (1973), in press ; c) R.C. Dunbar, ibid, to be published (courtesy of Prof. R.C. Dunbar).

(12) J.L. Ragle, J.A. Stenhouse, D.C. Frost and C.A. Mc Dowell, J. Chem. Phys. (1970) 53, 178.

INTERNAL EXCITATION IN THE PRODUCTS OF SLOW ION-NEUTRAL COLLISIONS

T. O. Tiernan and B. M. Hughes
Aerospace Research Laboratories, Chemistry Research Laboratory
Wright-Patterson Air Force Base, Ohio 45433

The internal energy distributions of the products formed in ion-neutral collisions are virtually unknown for most such interactions. Owing to the large quantities of energy available from many of these reactions, significant vibrational, rotational and even electronic excitation of the products may occur. If the excited species decay by radiative transitions to lower energy levels then it is often possible to determine their excited states by monitoring the resultant optical emissions. Experiments of this type have been undertaken in several laboratories in recent years, but their application is still rather new. The current status of optical emission studies will be reviewed, and their interpretation in terms of molecular potential curves and collision models will be discussed. An apparatus recently developed for optical excitation experiments at ARL will be briefly described and some preliminary results presented.

Fragmentation Studies using Threshold Electron-Photoion Coincidence Mass Spectrometry*

Roger Stockbauer and Mark G. Inghram
Department of Physics, The University of Chicago
Chicago, Illinois 60637

An experiment is reported which directly determines the kinetics of dissociation of a molecular ion, including the energy release in fragmentation as a function of the internal energy of that ion. The experiment involves photoionization, followed by detection of only those mass analyzed ions which are produced in coincidence with photoelectrons of zero initial kinetic energy. Under these conditions the internal energy of a parent ion is equal to the photon energy minus the adiabatic ionization potential of the molecule. With this technique, in contrast to previously used techniques, the kinetics of dissociation can be studied essentially independent of assumptions concerning variation in cross section above threshold, and autoionization. Fragmentation as a function of internal energy is reported for CH_4^+, CD_4^+, $C_2H_6^+$, and $C_2D_6^+$. The results are compared with previous photoionization, charge exchange and photoelectron-photoion coincidence mass spectrometry, and with fragmentation calculations based on quasiequilibrium theory of unimolecular dissociation.

A detailed account of this work appears in the May 1, 1973 issue of The Journal of Chemical Physics, Volume 58, Page 3800.

*Work supported by the National Science Foundation.

Formation of Ion Pairs by Photodissociation of H_2*

K. E. McCulloh and James A. Walker

Institute for Materials Research
National Bureau of Standards
Washington, D. C. 20234

ABSTRACT

Formation of $H^+ + H^-$ ion pairs has been observed in a narrow wavelength region in the neighborhood of 715 Å. By means of experiments at 110°K and 300°K on para-H_2 as well as the ordinary ortho-para mixture, mutually consistent ion-pair thresholds have been measured for J=0,1, and 2. For the state J=0 the observed threshold is 17.323±0.002 eV. As the data show structure indicating predissociation, this value is an upper bound, from which the lower bound 0.753±0.002 eV is obtained for the electron affinity of the hydrogen atom. This value is in excellent agreement with the theoretical value 0.7542 eV obtained by Pekeris.[1] A paper incorporating these results will be submitted for publication.

* Supported in part by the U.S. Army Research Office-Durham.

1 C. L. Pekeris, Phys. Rev. 126, 1470 (1962).

Observations on Hot Bands in the Molecular and Dissociative Photoionization of Acetylene and the Heat of Formation of the Ethynyl Ion*

Vernon H. Dibeler, James A. Walker, and K. E. McCulloh

Institute for Materials Research
National Bureau of Standards
Washington, D. C. 20234

ABSTRACT

Photoion yield curves in the vicinity of threshold are obtained for the molecular and the ethynyl ions of acetylene and acetylene-d_2 at ion source temperatures of 360, 298, and 130°K. Weak ionization below the adiabatic threshold for $C_2H_2^+$ and $C_2D_2^+$ is ascribed to the ionization of molecules excited by one quantum of the bending vibrations, ν_4 and ν_5. Consideration of selection rules suggests a change in symmetry from the linear ground state molecule to a bent ground state ion. The 0°K curves for C_2H^+ and C_2D^+ are estimated from the observed 130°K data. Satisfactory agreement is obtained when the 298°K data are compared with a curve calculated from the 0°K curve by convolution with vibrational and rotational distributions. The 0°K thresholds corrected for kinetic energy are used to calculate $\Delta Hf^\circ_0(C_2H^+)$ = 17.47±0.01 eV (402.8±0.2 kcal mol^{-1}) and $\Delta Hf^\circ_0(C_2D^+)$ = 17.43±0.02 eV (402.0±0.5 kcal mol^{-1}). The ionization energy of the ethynyl radical is estimated to be 11.96±0.05 eV. Details are recounted in a paper accepted for publication by the Journal of Chemical Physics.

* Supported in part by NASA.

IONIZATION POTENTIALS OF ALKENES AND CARBONYL COMPOUNDS BY PHOTOELECTRON SPECTROSCOPY.

D. GROSJEAN, R. HERNANDEZ, P. MASCLET, G. MOUVIER.

Laboratoire de Physico-Chimie instrumentale, 2, place Jussieu
75005 - PARIS (Tour 44-45, 5e étage).

We have measured by photoelectron spectroscopy the ionization potentials of a large number of alkenes (66, of which 43 are reported for the first time, including 13 tetrasubstituted alkenes) and aliphatic carbonyl compounds (11 aldehydes and 19 ketones).

A complete study of the structural effects of alkyl substitution on the focus of the molecules, $>C=C<$ (1) and $>C=O$ (2) respectively, was undertaken.

It's generally admitted that the first ejected electron of alkenes belongs to the π orbital and that the first ejected electron of carbonyl compounds belongs to the oxygen lone pair orbital (3). Calculations of molecular orbital energies show that the second ejected electron of formaldehyde, and probably of acetone is a π electron of the $>C=O$ bond (4,5).

We have studied the influence of alkyl substitution on the values of the first and second I.P. in these two series. The main effect for the first I.P. of alkenes is the extent of substitution : alkenes are grouped together according to the number of substituents on the double bond, without overlapping between the different groups. Nevertheless, the effect of successive substitution decreases progressively.

The same holds true for the second I.P. of alkenes and for the two first I.P. of carbonyl compounds. Nevertheless there is an overlapping for compounds of different extent of substitution but the first substitution is still more effective than the further.

It seemed reasonable to try to correlate the different ionization potentials with a structural parameter like Taft's σ^*

expressing the inductive effect . For each group of carbonyl compounds, a fair correlation is obtained between the first ionization potential and σ^* (or $\Sigma\sigma^*$, for ketones). It becomes excellent if we limit the population of ketones, for example, to the products having exclusively the substituents : Me, Et, iso-Pr and t-Bu. Compounds with n-Pr , iso-Bu, n-Bu , n-Pent, iso-Amyl and other substituents have lower I.P. with regard to the expected value given by the correlation ; these compounds possess all a γ-hydrogen atom at least ; the difference between the "expected value" and the experimental one depends on the character of the γ- hydrogen and on the number of H atoms.

The specificity and the importance of the position express the existence of "through space" interaction between the oxygen lone-pair electrons and the electrons of the alkyl radical by formation of a six-membered cyclic ion. The ionic state is more stabilized than the molecular state ; accordingly the I.P. is lowered. This can be related to the Mc Lafferty's rearrangement observed in mass spectrometry, whose importance depends in the same way on the degree of substitution of the γ- carbon atom and on the number of γ-hydrogen atoms.

In the case of alkenes the correlation with σ^* is unsatisfactory (except if we consider particular populations like methyl and ethyl tetrasubstituted olefins). The first alkenes'I.P. and the second carbonyl compounds'I.P. don't depend on the inductive effect but on the substituents number of carbon atoms. Alkenes' first I.P. are grouped together according to the total number of carbon atoms. For example, the following compounds $\begin{matrix} R \\ Me \end{matrix}\!\!>\!C = CH_2$ with R = n - Bu, iso - Bu, sec - Bu or t - Bu , have very close I.P: I.P.(t-Bu) $\lesssim$ I.P(sec - Bu) $\lesssim$ I.P. (iso-Bu) $\lesssim$ I.P. (n-bu)). This is due to the molecular ion stabilization by all the σ electrons of the alkyl groups through the C - C and the C - H bonds.

This is similar for the carbonyl compounds' second I.P., but in the case of methylbutyl ketones the I.P. order is not the same

as for alkenes (I.P. (n-Bu) $\lesssim$ I.P. (iso-Bu) $\lesssim$ I.P. (sec.Bu) $\lesssim$ I.P. (t-Bu). This difference may be explained in terms of the " through - space " bond between the oxygen lone-pair electrons and the γ-hydrogen atom, and also from the relative molecular heats of formation.

Nature of ejected electron.

For alkenes, our work confirms the fact than the less bonded electron is a π - electron ; the ion stabilization - and consequently the I.P. - are nevertheless greatly determined by the σ-electrons of the C-C and C-H bonds. The values of the alkenes'second I.P confirm the pronounced interaction between π and σ electrons.

In the case of carbonyl-compounds, the first ejected electron is a non bonding electron from the oxygen atom and the first I.P. is directly influenced by substituents' inductive effect ; for compounds with γ-H atoms , a"through space" interaction lowers the I.P.

It's more difficult to conclude about the nature of the second ejected electron in carbonyl compounds. For formaldehyde, and probably for the lightest compounds, it belongs to the π orbital. But the predominant effect of the main substituent for ketones and the "through space" interaction observed would rather indicate that, for heavier compounds, the second ejected electron belongs to a σ orbital.

REFERENCES

(1)- MASCLET.P., GROSJEAN D., MOUVIER G. and DUBOIS J.E. J. of Electron Spectroscopy and Related Phenomena (in press).

(2)- HERNANDEZ R., MASCLET P., MOUVIER G., to the published.

(3)- TURNER D.W. and al., Molecular Photoelectron Spectroscopy, Wiley- Interscience , London.

(4)- BAKER A.D., BAKER C., BRUNDLE C.R. and TURNER D.W., International J. Mass Spect. Lon. Phys., 1 , 285 (1968).

(5)-NEWTON N.D., BOER F.P. and LIPSCOMB W.N., J. Amer. Chem. Soc., 88 , 2367, (1966).

PHOTON AND ELECTRON FRAGMENTATIONS OF SOME NORMAL KETONES

William L. Stebbings and James W. Taylor

Department of Chemistry
University of Wisconsin
Madison, Wisconsin 53706

The photoionization and electron impact ionization of 2-pentanone, 3-hexanone, 2-octanone, and their deuterium analogs were studied over the energy range 12 to 21 eV. The results from the study show that the energy transfer distribution function necessary to calculate the ion intensities from photon impact can be related to the photoelectron spectrum whereas a function of different shape is required to yield the electron produced ion intensities. Comparison of several rearrangement and cleavage reactions revealed that the low frequency factor/low activation energy and high frequency factor/high activation energy criterion did not fit the calculations. The results of the comparison between the two ionization reagents with labeled ketones suggest that a portion of the fragmentation may occur through different structures or reaction pathways under the two ionization conditions. The material in this paper is being prepared for early submission to *Int. J. Mass Spectrom. and Ion Phys.*

A Study of the Effect of Vibrational Temperature On a Chemical Reaction

J. J. DeCorpo, M. V. McDowell, J. R. Wyatt,
F. E. Saalfeld, R. J. Gordon, and M. C. Lin
Chemistry Division
U.S. Naval Research Laboratory
Washington, D.C. 20375

ABSTRACT

The reaction rates of the hydrogen atom exchange reaction $D + HF \rightleftharpoons H + DF$ have been studied as a function of the vibrational temperature of HF and DF. The apparatus employed in this study, consisting of a HF and DF cw-chemical laser and the appropriate optics which allow the lasing radiation to enter a reaction chamber incorporated into a T.O.F. mass spectrometer is discussed. A rate coefficient of 5.1×10^{10} cc $mole^{-1}$ sec^{-1} has been determined for the background exchange of deuterium with ground state HF. In addition, a temperature dependence study of the ground state reaction yielded a ΔE_a (heat of activation) of 5.4 k cal/mole.

(A detailed manuscript will be submitted to The Journal of Chemical Physics).

INVESTIGATION OF SOLID INORGANIC MATERIALS WITH THE LASER MASS SPECTROMETER

Bruce E. Knox and Edward C. Beahm, Materials Research Laboratory, The Pennsylvania State University, University Park, Pennsylvania 16802

Lasers and mass spectrometers have been coupled for approximately ten years, and a wide variety of systems have been studied. Until recently, no systematic work had been done to elucidate the various factors which determine the vapor species analyzed by the mass spectrometer. This paper is a brief summary of the work done at Penn State to elucidate the spectra-determining factors, namely, vaporization, ionization, and vapor expansion/reaction. Several papers will be submitted for publication in the Journal of Applied Physics and the International Journal of Mass Spectrometry and Ion Physics.

The basic laser mass spectrometer system used in these studies has been described in detail elsewhere (1). The electronic pulse generation circuitry for the time-of-flight mass spectrometer, as well as the various circuits needed for displaying the data, have been completely redesigned so that accurate and precise time measurements can be made for mass identification. The electron (control grid) pulse and the ion drawout pulse are generated and shaped by TTL digital logic integrated circuits. Appropriate delay times between the beginning of the laser pulse and the start of the mass spectrometer cycle are also generated by digital logic, using a highly stable crystal oscillator as a master clock. Time marks and raster generating signals are added to the data trace to make possible accurate time measurements from photographs of oscilloscope traces.

The simplest way to describe the vaporization process for the interaction of a beam of photons from a pulsed laser operated in the normal mode with most solid materials is based on statistical thermodynamics and the assumption of a steady state process. This means that there is a fixed temperature distribution in the solid, and that the vaporizing layer moves into the solid at a constant velocity. The temperature rises quickly and levels off as vaporization becomes important. Obviously, this describes the best case, since solid state lasers do not have uniform outputs but vary rapidly with the lasing action of the rod. Vaporization varies exponentially with temperature; thus, only the highest temperatures are important. In this model, the difference between laser vaporization and other vaporization methods is that a laser supplies much more energy than any other heat source. After heating the solid to the point where vaporization begins, the laser energy is distributed in such a way that those species with the lowest free energy of vaporization will dominate the vapor.

The steady state vaporization rate is given by the following equation:

$$J = \frac{F_a}{\Delta H_v + C\Delta T} \qquad (1)$$

where J is the vaporization rate, F_a is the absorbed laser flux, ΔH_v is the specific heat of vaporization, C is the specific heat capacity of the solid, and ΔT is the temperature change in the solid. Consider the effect of an increase in the absorbed laser flux. Since $C\Delta T$ is usually smaller than ΔH_v, that term cannot account for an increase in the absorbed photon flux. The value of the specific heat of vaporization, ΔH_v, decreases as the vaporizing temperature increases. Thus, once a steady state condition has been attained, changes in absorbed flux will be reflected in changes in the rate of vaporization of the solid.

The steady state model helps to define usable flux densities for the vaporization of solid materials. Generally, flux densities in the range of $10^5 - 10^8$ W/cm^2 will produce stable vaporization conditions in most systems. The lower limit is defined by the maximum rate of removal of heat by thermal conduction in the solid; the upper limit is determined by the attainment of the critical temperature below the surface of the vaporizing layer, resulting in 'explosive' removal of solid material.

Thermal ionization is the only reasonable mechanism for ion formation within normal mode laser systems. The photon flux densities are much too low for multiphoton ionization processes, and the plasmas generated generally are not dense enough for any electron cascade processes. Because of the difficulty of measuring accurate work functions of solid surfaces and ratios of ions, neutrals and electrons in the plasma, neither the Langmuir-Saha nor the Saha equations are very useful in illuminating the ionization process. By using ratios of two different ion intensities in the vapor, a modified equation can be derived from either the Saha or the Langmuir-Saha equation:

$$\ln \frac{I_1^+}{I_2^+} = \frac{11{,}606\ \Delta IP}{T} + \ln\beta\ \frac{C_1}{C_2}\ , \qquad (2)$$

where (I_1^+/I_2^+) is the measured ratio of any two ion intensities, (C_1/C_2) is the concentration ratio of those two species in the solid, ΔIP is the difference in the ionization potentials of species 1 and 2, T is the temperature of the vaporizing surface, and β is a factor which includes the activity coefficients, partial pressures, and electron multiplier response of the two species. (β can be assumed to be equal to 1, if the appropriate ionic species are chosen). Examination of this working equation shows that the ionization potentials completely dominate those factors which determine the observed spectra, if one is working in a region where ions are important constituents of the laser-generated plume. By appropriate doping of a solid with two elements with low but different ionization potentials, the temperature of the vaporizing surface can be estimated from equation (2).

Laser solid interaction produces a dense plasma which expends from the surface at a velocity of 10^4 cm/sec or more. This is not a collision-free beam, since the mean free path of the gas is much smaller than the crater diameter (orifice). Thus, the phenomena which are associated with a high pressure beam are important to any consideration of the beam and the subsequent mass analyses performed. These include rapid cooling, nucleation, and mass separation. Once again, the simplest model of beam formation is sufficient to give an understanding of the important criteria. If one assumes that the beam expands isentropically into a vacuum, the beam is analogous to free jet expansion. The pressure and temperature decrease very rapidly, resulting in the effective quenching of reactions with large positive activation energies. However, recombination, condensation, and ion-molecule reactions have zero or negative temperature coefficients and may be accelerated by large decreases in temperature. This contributes to the explanation of the clusters and other high molecular weight species commonly seen in the spectra recorded with the laser mass spectrometer. The higher the heat of vaporization of a species, the more likely it will undergo nucleation, even if the temperature drops only a few hundred degrees.

Nucleation occurs on cooling in many laser generated plumes. Ion-molecule and chemiionization reactions have larger rate constants than the corresponding neutral reactions; thus these reactions involving ions should be even more readily seen in the laser mass spectrometer. Clustering does seem to dominate; there is little evidence of decomposition, which would indicate that the temperature was not decreasing rapidly. In addition, the pressures in the beams are high enough for three-body reactions to be important. Thus, it is concluded that there is no beam formation from laser vaporization without altering the vapor composition significantly. Furthermore, ion-molecule or chemiionization clustering will obscure even more dominant neutral clustering. Because of the similarities to free jet expansion, one must also be aware of the possibilities of mass separation in the beam.

References

1. Knox, B.E., "Laser Ion Source Analysis of Solids," in Trace Analysis by Mass Spectrometry, A. J. Ahearn, Ed., Academic Press, New York, 1972, Chapt. 14.

THE TOROIDAL ELECTROSTATIC CONDENSER USED AS A MIRROR IN THE MULTIPASSAGE MAGNETIC MASS SPECTROMETER (MMMS)

L. BOLDUC, M. DE CELLES and M. BARIL
Département de Physique,
Université Laval,
Québec, Canada.

It has been shown theoretically by Baril[1] and checked experimentally by Vallerand[2] at Laval University that is possible to obtain an achromatic mass spectrometer by the simple addition of a plane electrostatic mirror to the magnetic prism. In the image plane there is mass dispersion but no first-order broadening due to energy fluctuations from the source.

On the other hand, in order to increase mass resolution, Fortin and Baril[3-4] conceived and developped a multipassage mass spectrometer, in which the ion beam goes through the magnetic analyser repeatedly after being reflected by multielectrode plane mirrors. Figure 1 shows the schematic configuration of the instrument, which has been effectively built-up and successfully tested. The condition of normal entrance here illustrated corresponds to minimum second order aberrations and permits three passages.

However, some difficulties are already met in the situation shown here. First, accurate alignment of the mirror electrodes is critical, in order to maintain the beam intensity to a measurable level. Second, even for perfect alignment, the intensity decreases considerably from one passage to the next as no restoring force is designed to pull the ions back in the plane of the principal ray. Third, the image width at the collector is increased by the energy dispersion of the beam.

To bypass these problems, the idea of using a toroidal condenser concentric to the magnetic element has come up (figure 2). This set-up was seen to open the possibility of obtaining an achromatic image if suitable non-normal entrance conditions could be determined for one passage. Also shown for later reference are the entrance angle β in the magnet, the deflection angle γ and the entrance angle θ in the electrostatic mirror. The dimensionless parameter X is defined for the case of toroidal condensers having $r^{-\alpha}$ potential in their symmetry plane. X is proportional to the ion energy E_T; the value 1/2 corresponds to the energy of a circular trajectory at the entrance of the condenser. To obtain numerical results, it has proved necessary to study first the optical properties of these mirrors(some results are already published[5-6], others will be reported later). Combining these with the well known results of Brown[7] and Enge[8] applied to a circular magnetic prism, one finds it is possible to obtain achromatism for each passage in a certain domain of the variables involved.

Let us see how to proceed in the search for an optimum configuration. For a set of fixed α, X and θ, one looks for the values of β and γ such that point 1 has an achromatic image of unit magnification in 2. Only the values compatible with a positive drift space between magnet and mirror are retained. Among those we then select the conditions for which a particle off the symmetry plane is maintained in the vicinity of it. This is not really anastigmatism but rather the property for the system to confine the vertical motion to the vicinity of the symmetry plane. Other criteria are also considered: sufficient mass separation with regard to the path length, small second-order aberrations and finally the limitations imposed by requiring the system to have an acceptable size.

In all satisfactory cases thus far encountered, the total angle travelled around the origin in one passage turns out to be approximately 280°. The resulting constraints on the physical realization of the system are seen below. Among the various configurations of possible interest, we present here one set of conditions in the case of the spherical condenser, i.e. that of the r^{-1} potential. Figure 3 shows the set. Note that the mass separation is equal to 1.18 R and recall that for a 90° deflection in a prism between two drift spaces the mass separation equals R for symmetrically placed conjugate planes. These conditions permit four passages (the last being incomplete) as indicated in figure 4. The mass separation for the first three is 3 x 1.18R and there is no chromatic aberration. The mass separation for the fourth passage depends on the position of the source and the collector. As presented here, the whole system is not really achromatic, since the aberration produced by the last passage in the magnet

is not corrected by a subsequent electric field. However, slight modifications giving overcorrection at each complete passage are possible and give achromatism for the object and image planes at the source and the collector respectively, once they have been fixed.

Figure 5 illustrates a possible set-up which would permit more than four passages and thus increase the mass separation in proportion, while insuring complete achromatism between source and collector. More work needs yet to be done however before fully optimizing such a system.

References

1. M. Baril, Can. J. Phys. 47, 331 (1969); 48, 2487 (1970).
2. P. Vallerand, Thèse de Maîtrise, Université Laval, Québec (1971).
3. M. Fortin and M. Baril, Rev. Sci. Instrum. 43, 1140 (1972).
4. M. Fortin, Thèse de Maîtrise, Université Laval, Québec (1969).
5. L. Bolduc, M. De Celles and M. Baril, J. Appl. Phys. 43, 1655 (1972).
6. L. Bolduc and M. Baril, J. Appl. Phys. 44, 757 (1973).
7. K.L. Brown, Rev. Sci. Instrum. 35, 481 (1964); 36, 271 (1965).
8. H. Enge, in Focusing of Charged Particles (Academic, New York, 1967), Vol. II.

MULTIPASSAGE MAGNETIC MASS SPECTROMETER (M.M.M.S.)

with multielectrode plane mirrors

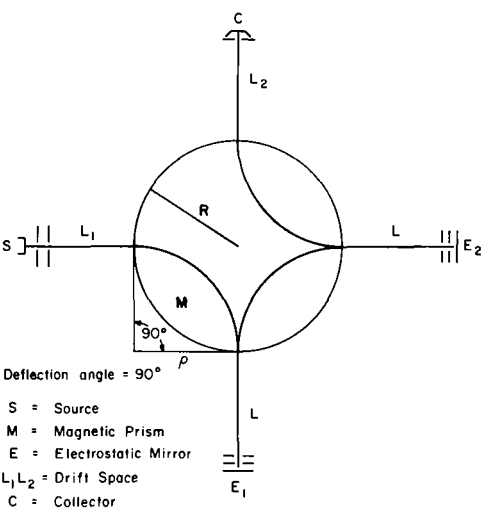

Fig. 1

CONJUGATION, ACHROMATISM AND VERTICAL CONFINEMENT

FOR ONE PASSAGE IN THE MMMS

with spherical mirror

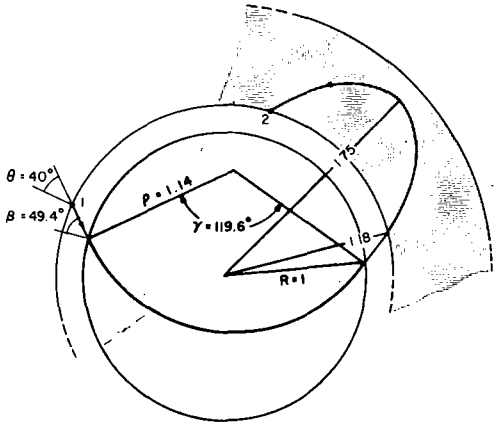

Energy X = 0.4

Total Rotation Angle = 280.6°

a^2 Aberration = 1.42 R

Mass Dispersion = 1.18 R

Fig. 3

CONFIGURATION OF A MMMS

with toroidal mirror

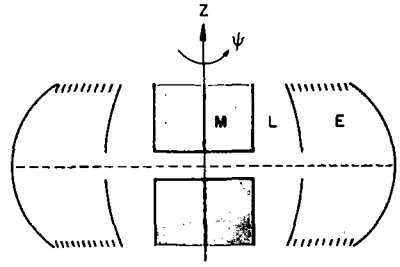

$$X = \frac{E_T}{e(V_2 - V_0)} \frac{1}{a} \left(1 - \frac{R_0^a}{R_2^a}\right)$$

(R^{-a} Potential)

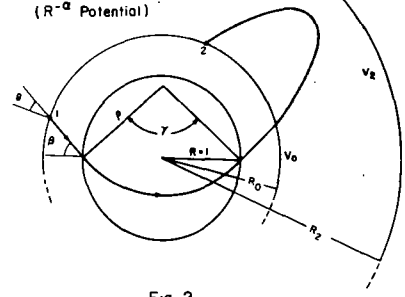

Fig. 2

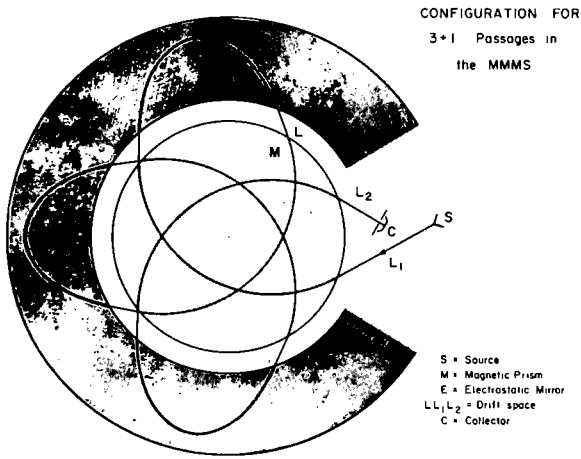

Fig. 4

HIGH - SEPARATION ACHROMATIC MMMS

(A possible configuration)

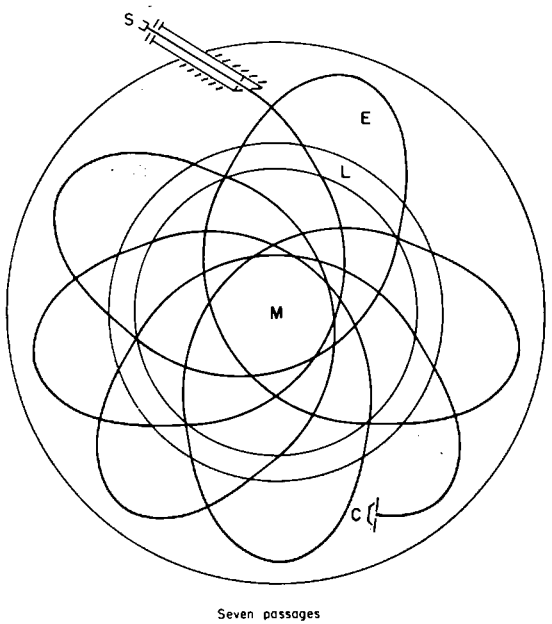

Seven passages

Fig.5

INFINITY ANOMALIES IN TREATMENTS OF CHARGE-EXCHANGE CONTINUA AND METASTABLE-PEAK CONTOURS

J. M. McCREA

P. O. Box 172, Monroeville, Pennsylvania 15146.

Abstract: The author's treatments for the intensity distribution along charge exchange continua in the Mattauch-Herzog and 180° magnetic sector mass spectrometers indicate an infinite intensity if the secondary ions approach the detector in a direction parallel to those of the primary beam. Contour calculations for metastable peaks in a 180° instrument by Hipple, by Coggeshall and by Viney all show a similar effect. These unemphasized infinity anomalies are artifacts of the assumption that the primary beam is a line beam of zero width. A treatment involving an integration over finite slit widths removes the anomalies and gives contours near the maximum intensities in terms of slit widths. The position of the maximum in the contour of a metastable peak is shifted by a small amount corresponding to a fraction of a slit width from that given by the usual formula

$$\text{apparent mass} = (\text{fragment mass})^2 / (\text{initial mass})$$

- - - - - - - - - - -

The three comprehensive studies of the ion optical factors governing the contours of metastable peaks in 180° mass spectrometers by Hipple[1], Coggeshall[2] and Viney[3] were all based on the assumption of a line beam of ions entering the mass spectrometer, and when examined critically the treatments all predict an infinite intensity at the metastable peak position. The author's treatments of charge-exchange continua in the Mattauch-Herzog and 180° instruments are also based on a line beam assumption[4-6], and likewise call for an infinite intensity at maxima in the continua. Since the transitions giving rise to charge-exchange continua and those giving rise to metastable peaks are the same from an ion optical point of view, the author iniated the present studies to consolidate the two cases and to develop a treatment that would not show any infinity anomaly. In order to effect the consolidation of the previous studies of the charge-exchange continua and those for metastable peak contours, it was necessary to replace the previous assumption of equal probability of charge exchange along equal lengths of primary trajectory with the assumption of an exponentially decreasing probability of charge exchange along the trajectory. The new assumption correctly accounts for removal of ions from the primary beam by the charge-exchange process itself, and, although the mechanism is different, its algebraic form corresponds exactly with that required to describe the decomposition of precursor ions in a metastable transition. The simplest case to replace the assumption of a line beam seemed to be the assumption of finite source and collector slit widths with a uniform illumination of the source slit by emergent ions. At first sight it might seem to a casual reader that a treatment based on a uniform band of primary ions surely must have been investigated previously, but there is no report of this having been done. After having carried out the series expansions, series inversions and integrations necessary to obtain an expression for the intensity, the author knows why a treatment involving a uniform band of ions has not yet appeared in the literature, and is certain that if anyone had completed the treatment, the results would have been reported. In view of space limitations, only condensed results will be reported here, and even these will be primarily restricted to the geometrical aspects of the problem such as slit widths. The aspects related to ion lifetimes will be reported at the 6th. International Mass Spectrometry Conference - Edinburgh 1973, and a comprehensive report will subsequently be compiled for journal publication.

In a constant magnetic field free of electric field, the ion speed remains constant and the path is an arc of a circle with its radius proportional to the mass and inversely proportional to the charge. Let r, m, and p respectively be the radius, ion mass and ion charge from the entrance slit to the point of transition, and denote the values after the transition with ' superscripts. Also let m^* be the mass of a singly charged ion that travels a full semicircle of radius r^* without transition and let $F = (m'/p')/(m/p)$. Then $r' = Fr$, and from the usual mass spectrometer equation it can be shown that $r^* = fr$ and $m^* = f^2 m/p$ where $f = (m^* p/m)^{\frac{1}{2}}$. If F is greater than 1, and there is no change in ion mass, the case is that of charge exchange; if the primary ion simply decomposed into a charged and an uncharged fragment, F is less than 1 and a typical metastable transition has occurred.

The cosine law of tirgonometry may be used to determine the relation among F, f, and θ, where θ is the angle through which the primary ion travels before the transition, and the result is

$$\cos\theta = \frac{2f(f-1) - (F-1)}{(2f-1)(F-1)} = \frac{2f(1-f) - (1-F)}{(2f-1)(1-F)} \qquad \text{(Eqn. 1)}$$

This equation is strictly equivalent to Hipple's equation (14)[1] and to Coggeshall's equation (15)[2]; it is not equivalent to Viney's equation (44)[3] because of a typographical omission of a 2 in the latter and an additional typographical error in one of Viney's defining relations. The next step in deve loping the expression for the intensity is to introduce the design radius ℓ, the entrance slit width w and the collector slit width w' and two ratios for convenience in expressing the relationship among them, $s = w/2\ell$ and $\alpha = w'/w$. These quantities, along with a positioning term z that is determined by the relation of r' to ℓ, the design radius, permit a determination of the values of f, and thus of θ, that allow ions originating in a particular portion of the beam to actually pass through the collector slit. Eqn 1. is transformed for this purpose into a power series by division and expansion of the cosine to terms in θ^4, solving as a quadratic in θ^2, taking the square root and expanding as a power series. After integration over the beam width of the primary beam, the intensity is found to be represented to a high degree of approximation by the product of three factors, a constant related to the type of transition, the design radius and the lifetime of the primary ion before transition, a geometrical term involving the positioning term and the slit width ratios s and α, and an exponential term related to the average distance travelled by ions in the beam before transition.

The geometrical term, which is found to converge well for usual values of F, s and α, is given by

$$\sqrt{1+\tfrac{1}{2}z}\Big[(z+s+\alpha s)^{3/2} - (z-s+\alpha s)^{3/2} - (z+s-\alpha s)^{3/2} + (z-s-\alpha s)^{3/2}$$
$$+\Big\{(z+s+\alpha s)^{5/2} - (z-s+\alpha s)^{5/2} - (z+s-\alpha s)^{5/2} + (z-s-\alpha s)^{5/2}\Big\}A(F)$$
$$+\Big\{(z+s+\alpha s)^{7/2} - (z-s+\alpha s)^{7/2} - (z+s-\alpha s)^{7/2} + (z-s-\alpha s)^{7/2}\Big\}B(F)$$
$$+ \text{ terms of order } 9/2,\ 11/2 \text{ and higher}\Big]$$

where $A(F) = (F^2+3F-3)/20(F-1)(2F-1)(1+\frac{1}{2}z)$ and

$$B(F) = (7F^4+90F^3-171F^2+90F-9)/672(F-1)^2(2F-1)^2(1+\tfrac{1}{2}z)^2$$

The geometrical term is independent of F to the order of terms in the square of the slit width ratios, and within this approximation differentiation and equating the result to zero shows that the maximum of of the geometrical term is produced by a z value given by

$$z = s(4\sqrt{1-\alpha+\alpha^2} - 1 - \alpha)/3$$

Since $z = 0$ corresponds to the usual formula $m = m'^2/m$ for the peak of a metastable contour, it is seen that the shift in the maximum possible from the geometric term amounts to a fraction of the average slit width. The effect of the exponential term is to offset some of the possible shift.

The exponential term requires slightly different treatment depending on whether the mass spectrum is scanned by varying the magnetic field or electrically by varying the accelerating voltage. In the former case the primary ion speed remains constant as the scan progresses, and in the latter case it does not. In both cases the primary radius alters and the angle before transition alters. In the case of magnetic scan, the exponent is proportional to $(1+\frac{1}{2}z)\,\bar{\theta}/T$, and in the case of the voltage scan simply proportional to $\bar{\theta}/T$ where T is a half time to transition and $\bar{\theta}$ is an average θ before transition. As a first approximation the θ given by Eqn. 1 may be used for the average, but near z = 0 this approximation is too low and gets worse as s or α is increased. A better approximation can be found by integrating the allowed range of θ values with access to the collector over the width of the beam. T must be found by trial and error to fit the contour of a peak to the calculated contour. This is in fact a major purpose of studying metastable contours in a 180° instrument, as Coggeshall[2] and Viney[3] mentioned. Here the experimenter has a range of measurable T values available, whereas if the metastables are generated in a field free region only upper and lower limits can be put on the lifetime in any one measurement.

A number of calculations have been made for the charge exchange 2+ to 1+ with experimentally practical values of s (0.00005, 0.0005, 0.005) and α (0.4, 0.6, 0.8, 1.0, 1.4, 2.0, 3.0 and 5.0). The geometrical term shows a striking variation in its contribution to peak intensity and peak shape as s is altered, along with a notable shift in the position of the maximum intensity. A variation of s alters the relative width of both source and collector slits simultaneously, and results in an effect on intensity greater that the square of the relative change in widths. The increase of α at constant s has the effect of slowly increasing both peak height and peak width, but there is relatively little shift in the position of the maximum until α is increased over 1.4. The increase of peak height with α is not as rapid as a linear rise with s = 0.0005, because relative values of the intensity divided by α run 1.16, 1.11, 1.06, 1.00, 0.91, 0.81, 0.69 and 0.55 respectively for the selection of α values given at the start of the paragraph.

Although the assumption of a primary ion beam of finite width was used here to replace the assumption of a line beam and avoid infinity anomalies, alternate assumptions can undoubtedly achieve the same effect. One that has been used is the assumption of kinetic energy changes during the transition. Even a slight departure from a perfect 180° eliminates the infinity anomalies, as may be inferred from the author's work for sectors with different angles. From the present work on the effect of finite slit widths on the peak contour, it does seem that slit widths should be considered in experiments relating to ion lifetimes and kinetic energy straggling. In the future it is hoped to compare the effect of primary beam shape on the peak contour by evaluating the case for either a triangular beam or a Gaussian beam and comparing the results with those for the rectangular beam presently evaluated.

Literature Cited

1. J. A. Hipple, Peak Contour and Half-Life of Metastable Ions Appearing in Mass Spectra, Phys. Rev. 71, 594 (1947)

2. Norman D. Coggeshall, Studies of Metastable Ion Transitions with a 180° Mass Spectrometer, J. Chem. Phys. 37, 2167 (1962)

3. B. W. Viney, Determination of Lifetimes of Metastable Ions by Field Ionization Mass Spectrometry, Int. J. Mass Spectrom. Ion Phys. 8, 417 (1972)

4. J. M. McCrea, Intensity Distribution in Charge-Exchange Continua Formed in a Mass Spectrometer, Int. J. Mass Spectrom. Ion Phys. 5, 381 (1970)

5. J. M. McCrea, Intensity Distribution in Charge-Exchange Continua Formed in a 180-Degree, Magnetic Deflection Mass Spectrometer, Int. J. Mass Spectrom. Ion Phys. 9, 167 (1972)

6. J. M. McCrea, Intensity Distribution along Charge-Exchange Continua Formed in Magnetic Sector Mass Spectrometers, Int. J. Mass Spectrom. Ion Phys. 11, (1973)

ISOTOPIC ANALYSIS OF COMPLEX MOLECULES BY MASS SPECTROMETRY: THE FACTOR APPROACH. W. E. BUDDENBAUM and G. D. DAVES, JR., Oregon Graduate Center, Beaverton, OR, 97005.

A new method for isotopic analysis by mass spectrometry is described. This new method which utilizes conventional unit resolution mass spectra is based on the recognition that the factor (roots) of polynomials and the derivatives of polynomials constructed from observed spectral intensities are analytically related to the isotopic content of the ions giving rise to the intensities. The general form of the mass spectral polynomials, the $P^{r}_{M+i}[\lambda]$, is

$$\sum_{j=0}^{i-r} \frac{(i-j)!}{(i-r-j)!} I_{M+j}(-\lambda)^{i-r-j}=0 \qquad (1)$$

where I_{M+j} is the intensity observed at mass M+j, r the order of the derivative and i the order of the polynomial. The origin of Eq 1 is discussed and highlights of its application to some mass spectral data taken from the literature for some ^{13}C-enriched propanes and butanes considered.

This paper has been submitted to the Journal of the American Chemical Society.

THE MECHANISM OF THE ION-MOLECULE REACTION OF o-QUINODIMETHANE RADICAL CATION WITH STYRENE

Michael L. Gross and Ping-Huang Lin
Department of Chemistry
University of Nebraska
Lincoln, Nebraska 68508

The mechanism for the reaction of styrene radical cation with neutral styrene has been recently investigated in our laboratory by ion cyclotron resonance (icr). (1) The reaction procedes through a detectable intermediate possessing the 1-phenyltetralin structure which subsequently loses C_6H_6 by a 1,4 elimination. We now wish to report a study of the ion-molecule reaction of an isomeric C_8H_8 cation, presumably o-quinodimethane, with styrene.

Line ionized styrene, the C_8H_8 ions produced in the fragmentation of o-methylbenzyl alcohol or acetate (equation 1) react with neutral styrene to

(1)

produce a detectable complex in the icr spectrometer which loses C_6H_6 to form an ion at m/e 130 (equation 2).

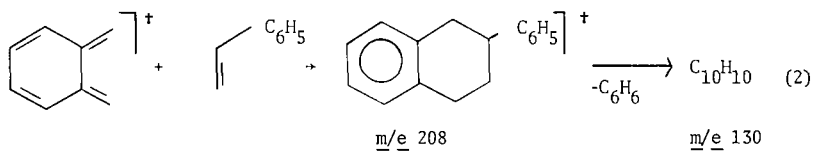

m/e 208 m/e 130 (2)

Evidence supporting the structure of the reactant $C_8H_8^+$ and the intermediate complex include:

(1) The o-quinodimethane radical cation is 15 x more reactive than styrene cation.

(2) The mass spectrum of 2-phenyltetralin shows fragment peaks corresponding to the loss of C_6H_6 (20%, relative abundance) and the retro Diels Adler reaction (base peak).

(3) Extensive deuterium labelling experiments are consistent with hydrogen scrambling in the intermediate involving complete equilibration of the ortho-hychogens on the neutral styrene and the exocyclic hydrogens of the cation. The loss of C_6H_6 is via competitive 1,2 and 1,3 elimin-

ations.

(4) The mass spectrum of 2-phenyltetralin-d_5 (I) shows similar scrambling in both the normal and metastable fragmentations.

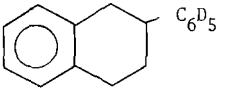

(I)

The work will be submitted for publication to the J. Amer. Chem. Soc.

REFERENCE:

(1) C. L. Wilkins and M. L. Gross, J. Amer. Chem. Soc., 93, 895 (1971).

FIELD IONIZATION KINETIC (FIK) STUDIES OF THE UNIMOLECULAR GAS-PHASE REACTIONS OF BUT-1-ENE

P. J. Derrick,* A. M. Falick and A. L. Burlingame
Space Sciences Laboratory
University of California, Berkeley, California 94720

The capability of field ionization (FI) mass spectrometry to measure the rates of unimolecular gas-phase reactions of organic radical-cations over a time range extending from 10^{-11} to 10^{-5} sec has in the past year begun to make a significant contribution to our understanding of these reactions (1,2).

In an earlier paper (1) we reported on an investigation of the fragmentation and rearrangement induced by FI of cyclohexene. It was proposed that very rapid isomerization via 1,3 allylic rearrangements is induced by both FI and electron impact (EI), such that the H and D atoms in the cyclohexene-3,3,6,6-d_4 species are randomized within 1 x 10^{-9} sec. Individual allylic rearrangements were proposed to occur within times of the order of 10^{-12} to 10^{-11} sec.

In a subsequent study (3) of 2-methyl propene and two deuterated analogs, good support for these proposals was found. The loss of a methyl radical induced by FI of 2-methyl propene, 2-methyl propene-1,1-d_2, and 2-methyl-d_3 propene-3,3,3-d_3 was studied at times from 10^{-11} to 10^{-6} sec. Randomization or "scrambling" of the hydrogens and deuteriums in the deuterated species was observed to begin within 3 x 10^{-11} sec following FI and to be close to completion within 1 x 10^{-9} sec. The randomization could be rationalized as the result of successive isomerizations via 1,3 allylic rearrangement. Further, the occurrence of rapid allylic rearrangements in the branched acyclic 2-methyl propene demonstrates that these rearrangements are not merely a peculiar characteristic of the cyclohexene geometry.

We have now completed a new series of FIK measurements on but-1-ene, but-1-ene-1,1-d_2 and but-1-ene-4,4,4-d_3 undertaken with a view to elucidating the mechanisms and kinetics of the reactions responsible for H/D randomization in this simple straight-chain alkene. These results, although more complex than those in the previous studies, showed that H/D randomization again was complete within a few nanoseconds, but that at least two distinct types of hydrogen (deuterium) transfer reactions were operative.

REFERENCES

1. P. J. Derrick, A. M. Falick and A. L. Burlingame, J. Amer. Chem. Soc. 94. 6794 (1972).
2. P. J. Derrick, A. M. Falick and A. L. Burlingame, ibid. 95, 437 (1973).
3. P. J. Derrick, A. M. Falick and A. L. Burlingame, manuscript in preparation.

* Present address: University College London, Department of Chemistry, 20 Gordon Street, London WC1H OAJ, England.

FIELD IONIZATION MASS SPECTROMETRY OF ORGANIC COMPOUNDS

Gilbert A. St. John and Michael Anbar

Mass Spectrometry Development Group
Stanford Research Institute
Menlo Park, California 94025

Field ionization of organic molecules which produces a fragmentation-free mass spectrum opens up new avenues for analytical applications of mass spectrometry. Within the framework of the Mass Spectrometry Development Program at the Stanford Research Institute, we are pursuing this technique along three avenues. We are developing at present more reproducible and reliable ionization sources. This development is discussed by Aberth in these proceedings.[1] We are applying field ionization to the quantitative determination of the composition of complex mixtures. Because each constitutent in a mixture forms virtually a single peak in the spectrum, a characteristic fingerprint of a mixture can be established faster and in a more meaningful manner than by chromatographic methods. This mode of application is discussed in the paper by Scolnick, et al[2] in these proceedings. The other methodology based on field ionization is the use of multilabeled nonradioactive molecular tracers in biomedical and environmental studies both as tracers and as dilutants in isotope dilution analysis. The latter methodology has been reviewed in a recent paper presented at the Argonne Conference on Stable Isotopes.[3] Both the fingerprint and the molecular tracer methodologies are based on the nonfragmenting nature of field ionization and on the high efficiency and reproducibility of spectra produced by our ionization sources. Because of the newness of field ionization and the difference in configuration of our sources from those of other laboratories, we have determined the field ionization spectra of many organic compounds and thus established the scope and limitations of this mode of ionization. In a number of cases we have carried out measurements on compounds which have been investigated by Beckey and his collaborators[4] in order to determine whether there are differences in the ionization behavior of the two types of sources. In other cases we have added new examples demonstrating the potential usefulness of this method of ionization to biomedical and environmental problems.

By and large it seems that we observe even less fragmentation produced by our source than obtained by Beckey's group in the same and similar compounds. Thus we do not only confirm their results on the efficiency of the method but claim that it is even more effective than could be deduced from the previous findings.

It should be emphasized, however, that field ionization mass spectra are not always fragmentation-free. Obviously, if the ion formed is thermodynamically unstable, it breaks down even if formed at ground state under the mildest conditions. The ionization of neopentane is a good example for such a case. Pure neopentane gives no parent ion whatsoever. If the ion formed is unstable but may revert to a more stable configuration, a significant proportion of excited ions will breakdown instantaneously (within $< 10^{-10}$ sec) on field ionization. The relative yield of these excited ions

which will then break down to give a more stable positively charged fragment is still independent of the voltage gradient at the tips. Examples of such behavior are found in the cases of iso-octane, tert-butanol, and methamphetamine. In the first case we find:

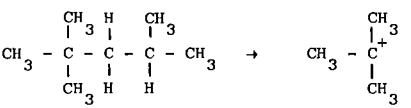

in the second:

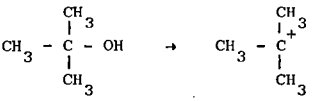

and in the third:

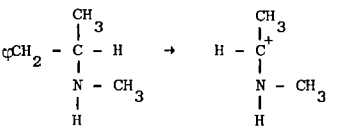

The ratio between the ion beams of masses 114 and 57 in the first case, 74 and 57 in the second, and masses 149 and 58 in the third did not change over a considerable range of tips to grid voltages. However, at higher voltages as in the case of iso-octane, the relative yield of mass 57 started to increase probably due to additional electronic excitations induced in the newly formed ions. In the case of acetic anhydride, we observed voltage dependent fragmentation without a significant voltage independent plateau. In a number of cases, we observed fragmentation which can readily be attributed to thermal decomposition prior to ionization. These cases include guanine, N,N-dimethyl-guanosine, thymine ribose, and possibly d,l-alanine.

The higher regularity of the structure of our ionization source allows a better control of the potential gradient on each of the tips while optimizing the yield. We could induce field ionization fragmentation of many other molecules if we increased the voltage gradient considerably up to the appropriate level. It seems, however, that we manage to reach a plateau of parent ion current before the voltage gradient reaches the level which induces fragmentation.

Figures 1, 2, and 3 show a number of examples of "clean" as well as of spectra contaminated with impurities or with fragments due primarily to thermal decomposition. In Tables 1, 2, and 3 we list examples of compounds we have examined. These demonstrate the broad scope of applications of field ionization.

We have looked into the efficiency of ionization of our source and found it to ionize most compounds tested with an efficiency of 10^{-4} to 5×10^{-3}; that is, we obtain 1 to 50 ions for every 10^4 molecules entering the ionization source. We have also examined the effect of dilution with air on the efficiency of ionization of organic molecules. We diluted toluene with air down to 20 parts per million without any significant loss in ionization efficiency, which was about 10^{-3} in this particular case.

This result shows that air does not interfere with the ionization process of minor constituents even if present in minute quantities. In an analogous experiment toluene was diluted in methanol down to one part per thousand, again without change in the ionization efficiency. A similar result was obtained when methanol was diluted with toluene down to 1:1000. Again the ionization efficiency of methanol did remain constant and equal to that of pure methanol.

Our ionization seems, thus, to be able to ionize minor constituents of a mixture containing dissimilar chemicals without significant changes in the efficiency of ionization. This result suggests that most of the ionization process takes place without chemisorption at the tips. From the practical standpoint, this finding suggests that field ionization may be applied as a quantitative method of analysis of mixtures after initial calibration with known concentrations of the individual constituents.

In another series of experiments we compared the relative ionization efficiencies of organic compounds heavily substituted with deuterium atoms with their normal analogs. These experiments involved the measurement of the relative ion beams of known mixtures of these species. In the cases of d_9-amphetamine, d_{10}-barbital, and d_8-heroin, the ionization efficiency of the polydeuterated compounds was lower by not more than 10%. This small isotope effect on top of the very high yield of the parent ion makes field ionization a method of choice for molecular tracer applications.

REFERENCES:

[1] W. H. Aberth, C. A. Spindt, and R. R. Sperry, 21st Annual Conference on Mass Spectrometry and Allied Topics, San Francisco (May, 1973) p. _____.

[2] M. Scolnick, A. C. Scott, W. H. Aberth, and M. Anbar, 21st Annual Conference on Mass Spectrometry and Allied Topics, San Francisco (May, 1973) p. _____.

[3] M. Anbar, J. H. McReynolds, W. H. Aberth, and G. A. St. John, Proceedings of the Conference on Stable Isotopes in Chemistry, Biology, and Medicine, Argonne, Illinois (May, 1973).

[4] H. D. Beckey, Field Ionization Mass Spectrometry (Pergamon Press, Oxford), 1971.

Acknowledgement: This research has been sponsored in part by a research grant from the National Cancer Institute, National Institutes of Health Grant # CA-13312-01.

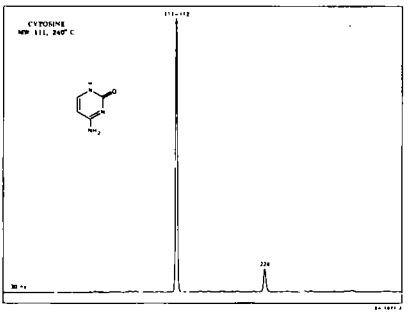
CYTOSINE
MW 111, 240° C
111-112
224

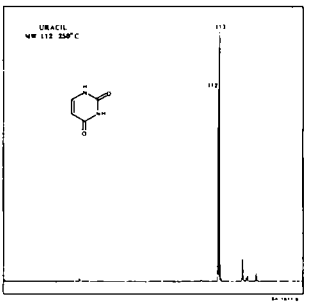
URACIL
MW 112 250°C
113
112

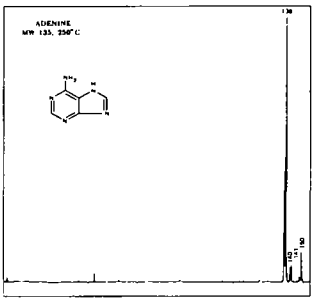
ADENINE
MW 135, 250°C
136
152
151
150

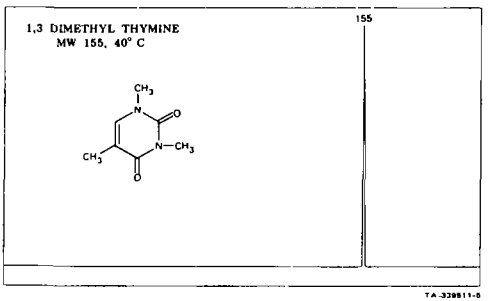
1,3 DIMETHYL THYMINE
MW 155, 40° C
155
CH3
N
O
N—CH3
CH3
O
TA-339811-6

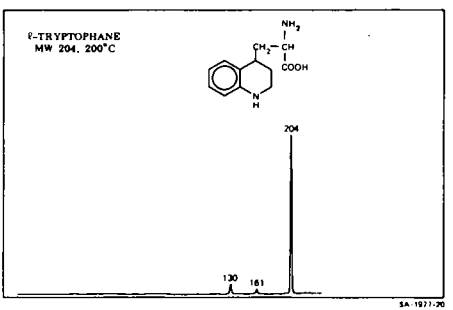
L-TRYPTOPHANE
MW 204, 200°C
NH2
CH2—CH
COOH
N
H
204
130
161
SA-1977-20

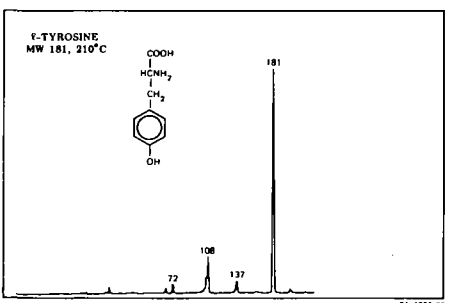
L-TYROSINE
MW 181, 210°C
COOH
HCNH2
CH2
OH
181
108
72
137
SA-1977-22

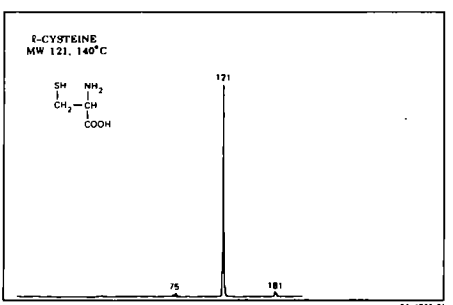
L-CYSTEINE
MW 121, 140°C
SH
NH2
CH2—CH
COOH
121
75
181
SA-1977-21

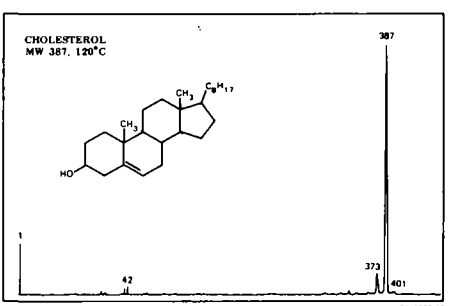
CHOLESTEROL
MW 387, 120°C
387
CH3
C8H17
CH3
HO
373
42
401
SA-1977-19

FIGURE 1

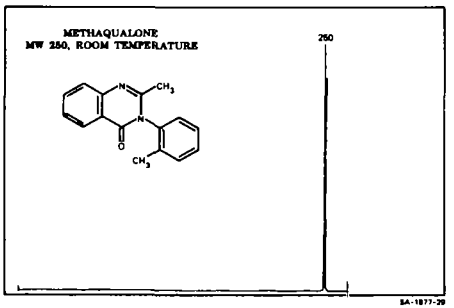
METHAQUALONE
MW 250, ROOM TEMPERATURE
250

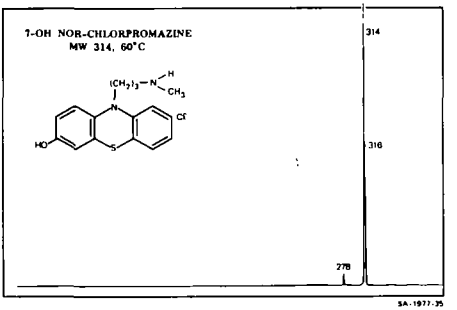
7-OH NOR-CHLORPROMAZINE
MW 314, 60°C
314
316
278

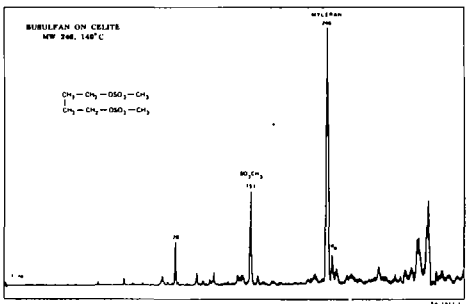
BUSULFAN ON CELITE
MW 246, 140°C

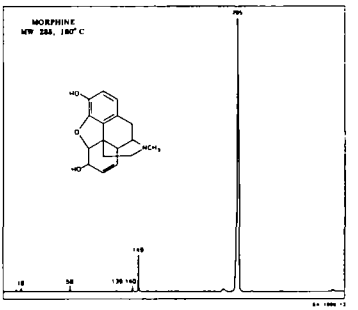
MORPHINE
MW 285, 180°C

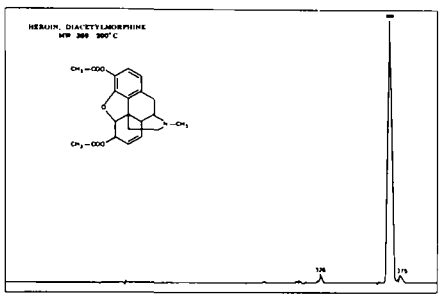
HEROIN, DIACETYLMORPHINE

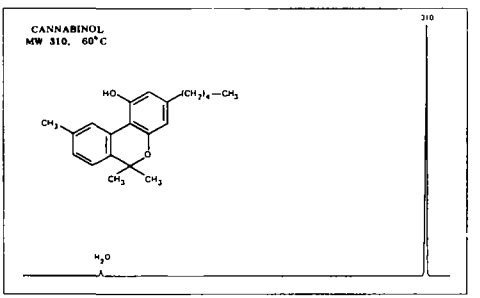
CANNABINOL
MW 310, 60°C
310

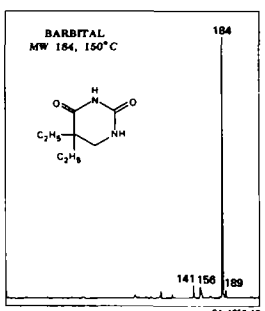
BARBITAL
MW 184, 150°C
184
141
156
189

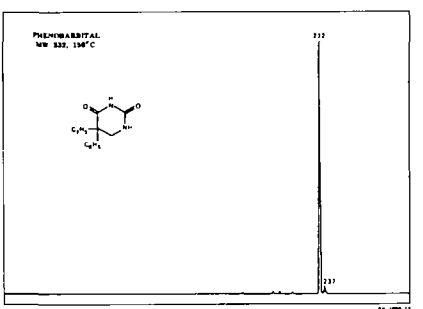
PHENOBARBITAL
MW 232, 150°C

FIGURE 2

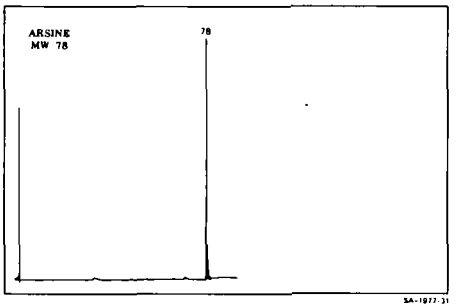
ARSINE
MW 78
78

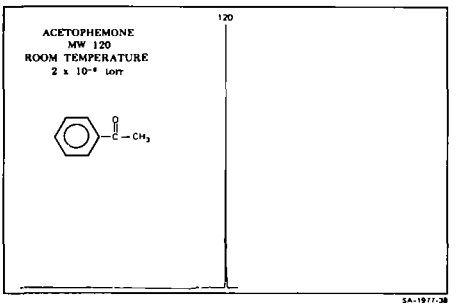
ACETOPHEMONE
MW 120
ROOM TEMPERATURE
2 x 10⁻⁶ torr
120

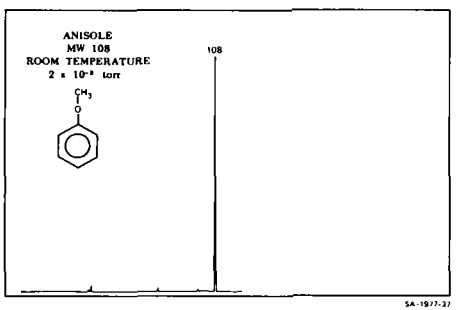
ANISOLE
MW 108
ROOM TEMPERATURE
2 x 10⁻⁶ torr
108

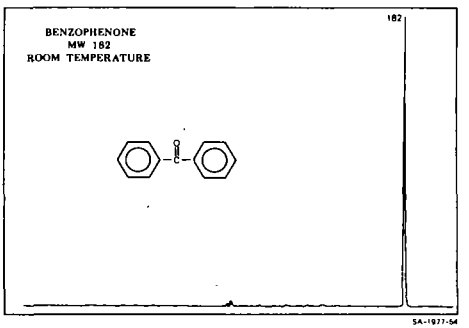
BENZOPHENONE
MW 182
ROOM TEMPERATURE
182

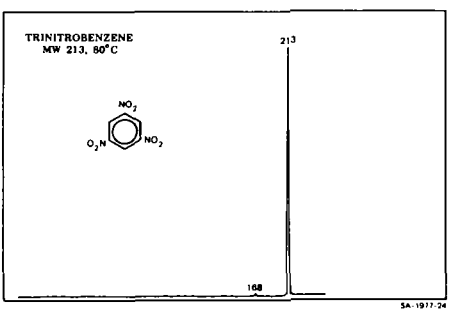
TRINITROBENZENE
MW 213, 80°C
213
168

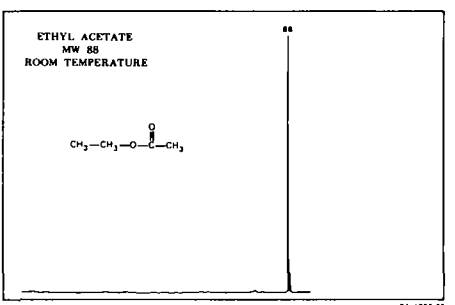
ETHYL ACETATE
MW 88
ROOM TEMPERATURE
88

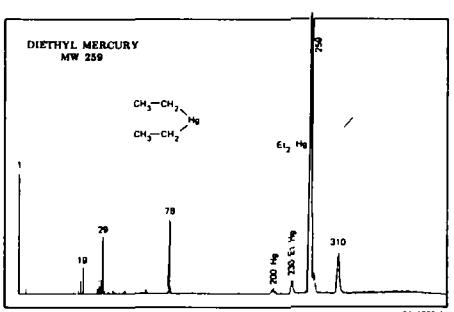
DIETHYL MERCURY
MW 259
250
310
78
29
19
1

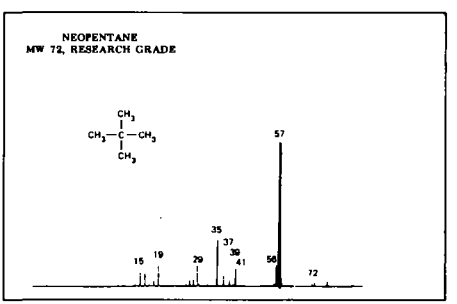
NEOPENTANE
MW 72, RESEARCH GRADE
57
72

FIGURE 3

Table 1

BIOCHEMICAL CONSTITUENTS

	Mol. Wt.	M/e[a]	Remarks
Cytosine	111.1	111[b]	
Uracil	112.09	112[b]	
Thymine	126.11	126[b]	
Adenine	135.14	135[b]	
1,3-Dimethyl Thymine	154.16	154[b]	
Guanine	151.13	151 > 135	Thermal fragmentation
β-Pseudouridine	244.20	244[b]	
N,N-Dimethylguanosine	311.29	179[c]	" ?
Thymine riboside	258.22	258 > 126	" ?
d,l-Alanine	89.09	89 > 45	" ?
l-Tryptophan	204.22	204[b]	
l-Tyrosine	181.19	181[b]	
l-Cysteine	121.16	121[b]	
Cholesterol	386.64	387[b]	

[a] Main isotopic peak

[b] Over 98% of total ion current

[c] Dimethylguanine MW 179.18

Table 2

DRUGS AND NATURAL PRODUCTS

	Mol. Wt.	M/e[a]	Remarks
Methaqualone	250.29	250[b]	
Chlorpromazine	318.88	319[b]	
Busulfan	246.31	246[b]	
Morphine	285.33	285[b]	
Diacetylmorphine	369.40	369[b]	
Methamphetamine	149.22	149 < 56	Unstable ion
Cannabinol	310.42	310[b]	
Tetrahydrocannabinol	314.45	314[b]	
Barbital	184.19	184[b]	
Phenobarbital	232.23	232[b]	
Nicotine	162.23	162[b]	

[a] Main isotopic peak

[b] Over 98% of total ion current

Table 3

MISCELLANEOUS CHEMICALS

	Mol. Wt.	M/e[a]	Remarks
n-Octane	114.22	114[b]	
iso-Octane	114.22	114 > 57	Excited ion
Neopentane	72.15	57	*Unstable ion*
Toluene	91.25	91[b]	
Benzylalcohol	108.13	108[b]	
Benzylchloride	126.58	126[b]	
Bromobenzene	157.02	156,158[b]	
Dibromobenzene	235.92	236[b]	
DDT	354.50	354[b]	
Trinitrobenzene	213.11	213[b]	
4-Heptanol	116.20	116[b]	
Tert-butanol	74.12	74 > 57	Excited ion
Benzophenone	182.21	182[b]	
Anisole	108.13	108[b]	
Acetonitrile	41.05	41[b]	
Acetic anhydride	102.09	42 > 102 > 87 > 69	Unstable ion
Arsine	77.93	78[b]	

[a] Main isotopic peak

[b] Over 98% of total ion current

Field Ionization Mass Spectrometry of Barbiturates

J. B. Callaghan, W. B. Askew, W. E. Mochel

Central Research Department, E. I. du Pont de Nemours & Co., Wilmington, Delaware 19898

From its inception as an analytical technique early this century mass spectrometry has played an increasingly more important role in the determination of molecular structure. Through the years mass spectrometry has undergone many changes, both in application and instrumentation; but today, as in the past, the single most important piece of information to be gotten from it is the molecular weight.

Barbiturates, as a class, are known for producing only low intensity molecular ions by electron ionization. We chose to examine compounds of this class by field ionization because of the current interest in drug identification, and to determine if this technique would be as helpful in determining the molecular weight as Fales, et al[1] had shown chemical ionization to be. The analyses were performed on a DuPont 21-110B mass spectrometer equipped with a dual EI/FI source as described by Chait, et al[2]. The compounds examined were:

Group I	barbital butethal butabarbital amytal pentabarbital
Group II	aprobarbital secobarbital allyl isobutylbarbital
Group III	phenobarbital alphenal mephobarbital allobarbital

The field ion spectra were found to have features which were directly related to the nature of the 5,5-substituents. Compounds having completely saturated substituents (Group I) gave an intense $(M+H)^+$ ion with only a weak M^+. Those compounds having a single site of unsaturation in the 5,5-substituents (Group II) gave the $(M+H)^+$ and M^+ ions at approximately the same high intensity. Where there were multiple sites of unsaturation (Group III) the M^+ is dominant. It appears from this data that those substituents which stabilize the molecular ion give predominantly the M^+. As the degree of unsaturation decreases the less stabilized molecular ion has an increasingly greater tendancy to form the $(M+H)^+$ ion via an ion-molecule reaction on the blade surface. Field ionization mass spectrometry, then, in addition to the molecular weight also gives information on the nature of the 5,5-substituents of barbiturates.

The field ion spectra were calibrated using photoplates by alternating the field ion spectra with EI spectra of PFK. This was achieved by recording the FI spectra with an unexposed band between each exposure. At the end of the day the plate was repositioned, the instrument switched to the EI mode and the EI spectra of PFK recorded between each FI spectrum. This permitted easy assignment of accurate m/e values to the field ions.

Figures: 1 Group I Barbital
Group II Secobarbital
Group III Allobarbital

(1) H. W. Fales, G. W. A. Milne, and T. Axenrod, Anal. Chem. 42, 1432 (1970)

(2) E. M. Chait, T. W. Shannon, W. O. Perry, G. E. VanLear and F. W. McLafferty, J. Mass Spectry. Ion Phys., 2, 141 (1969)

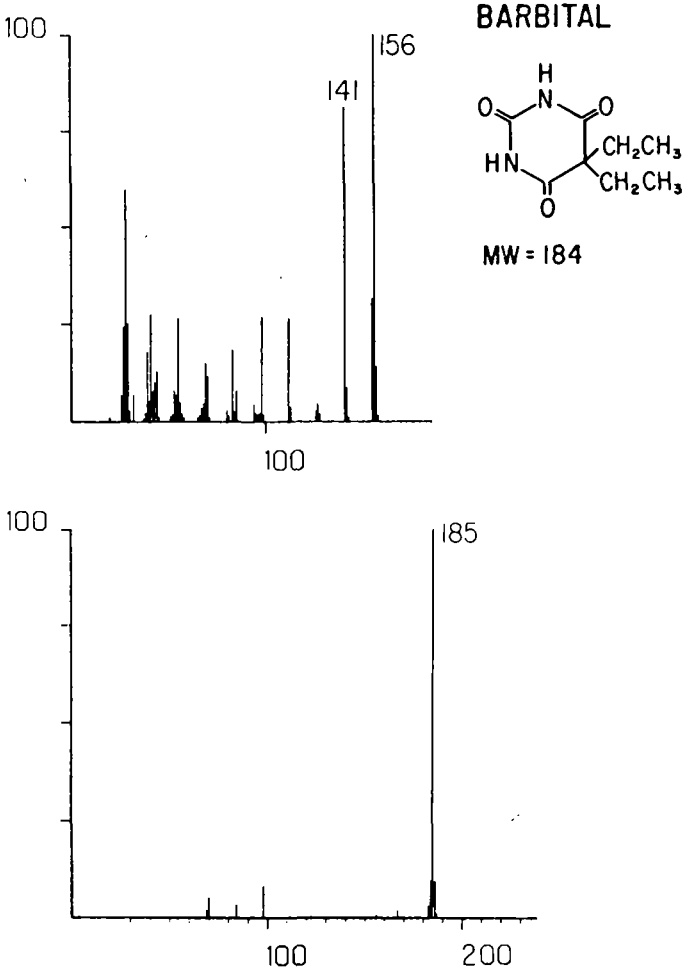

Fig. 1 Group I Barbital

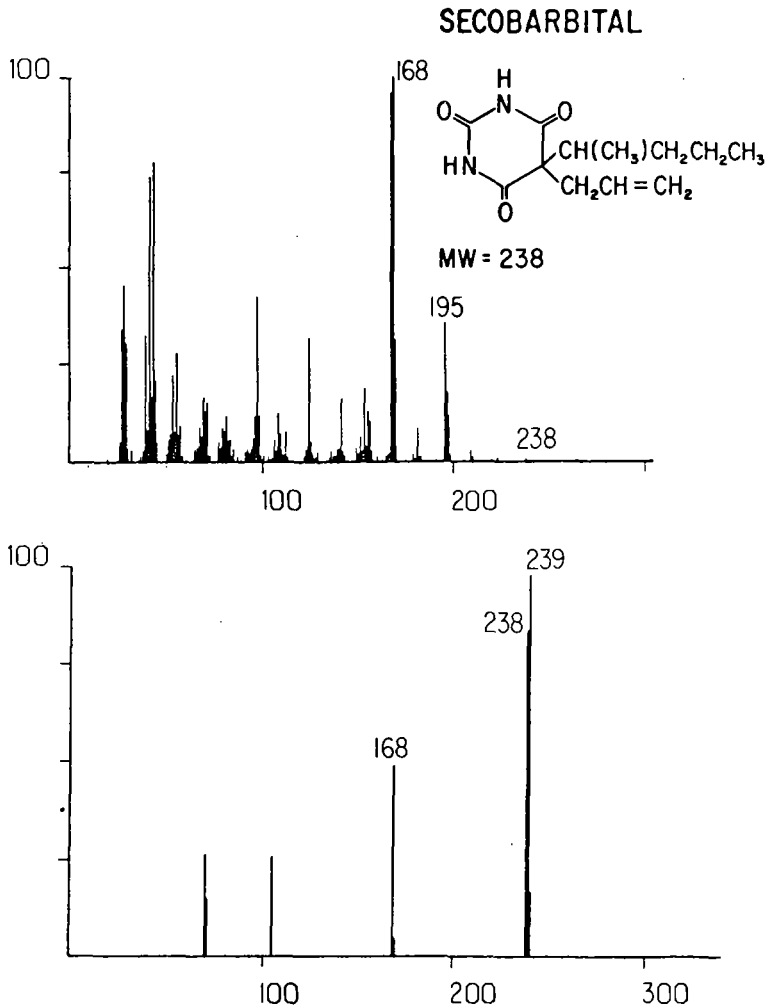

Fig. 2 Group II Secobarbital

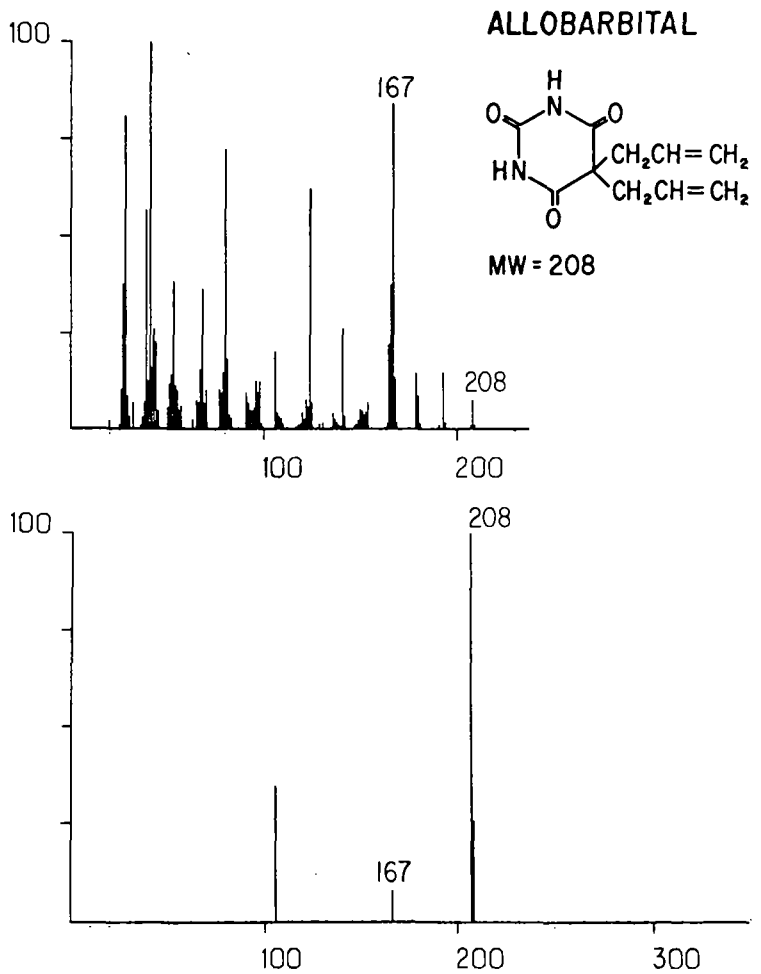

Fig. 3 Group III Allobarbital

FIELD DESORPTION MASS SPECTRA OF ANTIBIOTICS

K. L. Rinehart, Jr., J. C. Cook, Jr.
School of Chemical Sciences
University of Illinois, Urbana, Ill. 61801

K. H. Maurer, U. Rapp
Varian MAT, Bremen, Germany

Antibiotics are often polar, labile, and of high molecular weight.[1] Thus, they constitute an ideal class of compounds for study by field desorption mass spectrometry. We have employed a Varian MAT CH5/DF mass spectrometer to investigate the field desorption spectra of antibiotics of several classes, including erythromycin ($C_{37}H_{67}NO_{13}$, M=733), a basic macrolide; the streptovaricins (e.g., streptovaricin A, $C_{42}H_{53}NO_{16}$, M=827), which are ansamycins; novobiocin ($C_{31}H_{36}N_2O_{11}$, M=612), a complex coumarin; streptolydigin ($C_{32}H_{44}N_2O_9$, M=600), an acyl tetramic acid; the filipins (e.g., filipin III, $C_{35}H_{58}O_{11}$, M=654) and dermostatins (e.g., dermostatin B, $C_{41}H_{66}O_{11}$, M=734), both polyenes; and neomycin ($C_{23}H_{46}N_6O_{13}$, M=614), an aminocyclitol.

All of the antibiotics listed gave intense molecular ions (M) or M+H ions by field desorption mass spectrometry except filipin and dermostatin, for which M-H_2O ions were more prominent. By contrast, only erythromycin and streptovaricin gave molecular ions by electron impact or chemical ionization and these ions were very weak. Thus, field desorption is a technique which is complementary to both electron impact and chemical ionization.

A particularly interesting aspect of the present study was the use of field desorption to estimate the relative amounts of individual components present in mixtures of antibiotics. For example, the streptovaricin (Sv) complex was estimated by field desorption to contain 22% SvA, 11% SvB + SvJ, 44% SvC, 7% SvD + SvF, 2% SvE, and 14% SvG, while chromatographic methods suggest the respective proportions to be 20%, 12%, 41%, 8%, 2%, and 18%. Similarly, field desorption suggests 7% filipin I, 25% filipin II and 68% filipins III + IV, vs. 4%, 25%, and 71% by chromatographic methods. Finally, field desorption suggests 40% dermostatin A and 60% dermostatin B, vs. 43% A and 57% B by other methods.

A complete discussion of these results will be published in the Journal of Antibiotics.

---

[1] K. L. Rinehart, Jr., and G. E. Van Lear, in "Biochemical Applications of Mass Spectrometry," G. R. Waller, ed., John Wiley & Sons, New York, 1972, Chapter 17.

Negative Ion Mass Spectra of Amino Acid Derivatives[1,2]

by

Costello L. Brown* and Frank J. DiSanti

Department of Chemistry
California State University, Los Angeles
Los Angeles, California 90032

A negative ion mass spectrometric study has been carried out on several N-terminal methyl ester derivatives of amino acids. The acetyl, chloroacetyl, dichloroacetyl, trichloroacetyl, trifluoroacetyl and methanesulfonyl derivatives of the methyl esters of several amino acids have been prepared and their negative ion mass spectra have been obtained. The study includes ionization efficiency curves for the P-1 anions of these amino acid derivatives. All spectra were recorded at voltages below 5eV. The relative merits and limitations of these N-terminal groups in negative ion mass spectrometry have been studied in detail.

---

1. This research was supported in part by the Research Corporation, The Cal Tech President's Fund and NASA Contract No. NAS 7-100.

2. The complete paper will be submitted to the J. Amer. Chem. Soc.

MASS SPECTRA OF ORGANOLEAD SUBSTITUTED NITROGEN HETEROCYCLES

M. L. BAZINET and C. MERRITT, JR.
Pioneering Research Laboratory
US Army Natick Laboratories
Natick, Massachusetts 01760
and
R. E. SACHER
US Army Materials Research Center
Watertown, Massachusetts 02172

A limited number of heterocyclic-organolead compounds have been synthesized. Only about a dozen representatives of this class are reported in the literature but an active synthetic program is now in progress in certain laboratories and an increasing number of these compounds are now being prepared. Structural information, especially electron impact fragmentation data is lacking. In this work the mass spectra of some trimethyl and triphenyl lead complexes of pyrole, indole and carbazole have been studied. These lead compounds were analyzed on a Consolidated 21-110 mass spectrometer operated at 70 e. V. Two decoupling methods of observing reaction paths for "metastable" processes were used: By varying the ion accelerating voltage or varying the electric sector voltage. The materials were sampled with the direct solids insertion probe.

Figure 1 shows the generalized formula for the lead-heterocyclic compounds that were analyzed.

Figure 2 illustrates a variable ion accelerator voltage scan of triphenyl lead pyrole, demonstrating the major precursor ions for the lead ion at mass 208. This figure shows three major and two minor precursor ions for the lead daughter ion seen at left hand side of the figure. The three largest peaks to the right of the lead ion peak corresponds to phenyl, diphenyl, and triphenyl lead ions respectively; two other, less abundant ions, are phenyl indole and phenyl lead indole.

Figure 3 shows the ion kinetic energy spectrum of triphenyl lead pyrrole. This method is used mainly as a means of surveying the major metastable processes observed the spectrum. The three metastable processes illustrated here correspond to the fragment losses giving rise to the triphenyl lead ion at mass 439, the lead ion at mass 208, and monophenyl lead at mass 285.

Tabulation of the conventional spectrum, in combination with the metastable ion data from the previous demonstrations provides the information necessary for constructing possible fragmentation pathway diagrams, such as Figure 4. The mass of the principal ion fragments observed in the spectrum, and the ion abundance, are indicated by the numbers shown below the structural representation of each ion. Ion abundance is expressed as the percentage of total ionization. The molecular ion decomposition paths are indicated with arrows. When the pathway is supported by the appearance of a metastable ion, an asterisk is shown besides the arrow. The molecular ion for triphenyl lead pyrrole is observed at mass 505. It is of low intensity;only 0. 6 percent of total ionization. Fragmentation of the rather weak lead-nitrogen bond provides, the phenyl-lead ion series, which finally terminates with the most intense ion in the spectrum, the lead ion itself. Loss of phenyl groups from the molecular ions produces an ion of low intensity at m/e 351. This ion then loses another phenyl group and forms the moderately intense lead pyrrole ion at mass 274. Breaking the weak lead-pyrrole bond provides another path for the formation of the lead ion and another possible path for the formation of the pyrrole ion in addition to direct cleavage from the molecular ion.

Figure 5 illustrates how a kinetic energy spectrum can be useful in tracing the origin of unusual ions in a conventional mass spectrum. This shows an ion kinetic energy spectrum of triphenyl lead indole. The intense ion beam for the parent ion is

seen on the right, and the remainder of the spectrum shows the relative abundances of the ions corresponding to the metastable transitions. These are rather weak except for the peak at mass 90. When the search is made for the precursor ions forming mass 90, by varying the ion accelerating voltage, a very large precursor ion is found 26 mass units higher at mass 116. The transition thus corresponds to the loss of an acetylene neutral to form mass 90.

Figure 6 shows the fragmentation scheme for triphenyl lead indole. The molecular ion at mass 555 has low intensity, as with the triphenyl lead pyrrole complex described previously rupturing the lead-indole bond gives rise to the phenyl lead ion series. The fragments leading to the indolé ion are likewise analogous. The indole ion fragments with loss of acetylene to give a very intense ion at mass 90, as seen from the ion kinetic energy spectrum in Figure 5.

Figure 7 shows the fragmentation pathways for triphenyl lead carbazole ion. Again the ion fragments obtained are quite similar to the other triphenyl lead complexes.

In addition to the triphenyl lead complexes of nitrogen heterocycles studies were made of the behavior of a series of analagous trimethyl lead complexes.

Figure 8 shows the fragmentation scheme for trimethyl lead carbazole. The low intensity parent ion is observed at mass 419. Fragmentation of the trimethyl lead compounds fol lows a fragmentation pathway which is quite similar to the triphenyl compounds. Loss of methyl groups produces low intensity ions at mass 404, and mass 389. Rupturing of the methyl-lead bond in this ion yields a low intensity lead carbazole ion at mass 374 and further fragmentation of the weak lead-nitrogen bond leads to the fórmation of the slightly more abundant carbazolyl ion and the lead ion. Cleavage of the molecular ion at the weak lead-nitrogen bond provides a series of methyl lead ions of relatively great intensity. A comparison of the ions appearing in the spectrum of trimethyl lead pyrrole with trimethyl lead carbazole indicates that the fragmentation pathway is nearly identical with respect to both the nature of the ions formed and their relative intensities. In fact, the similarity is so striking that their spectra are nearly superimposable, except for the weight differences of the carbazole and pyrrole.

The conclusions to be drawn from this study appear perhaps to be rather trivial, since as with the spectra obtained for most organo-metallic compounds, the spectra are both simple and predictable.

In summary, however, a few observations and comparisons can be made. Fragmentation of the parent ion is extensive in all cases. The relative abundance is 1% of total ionization or less. Triphenyl lead derivatives have a more intense molecular ion than trimethyl lead derivatives. This is expected as there is greater resonance in the triphenyl system. The parent ions are approximately the same intensity for the three triphenyl systems.

The lead-phenyl (i. e. lead-carbon) bond is stronger than the lead-nitrogen bond in all cases. Likewise the lead-carbon bond is stronger than the lead-nitrogen bond in the trimethyl heterocyclic systems. This gives rise to the predominant ions in the spectrum, which are the lead aryls or lead alkyls, and the lead ion itself. The lead ion increases in intensity, however, going from pyrrole to indole to carbazole, illustrating the expected stability of the lead-nitrogen bond with the increased resonance of the heterocyclic ring system.

The series of ions arising from cleavage of the lead-nitrogen bonds are much less abundant, but yield ultimately the ions corresponding to the nitrogen heterocyclic forming the complex. These ions and fragments therefrom, though very small, nevertheless are important in identifying the organic moieties present in the complex.

LEAD HETEROCYCLICS

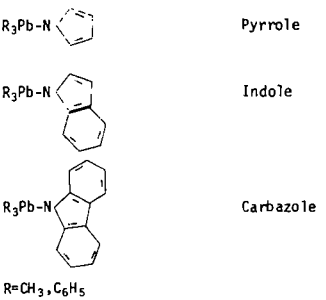

FIGURE 1

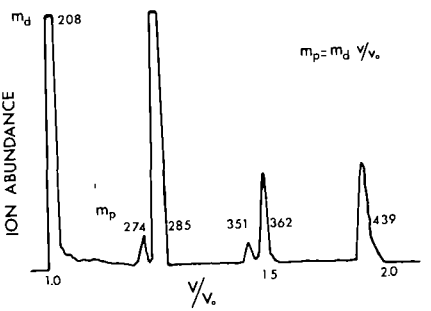

FIGURE 2

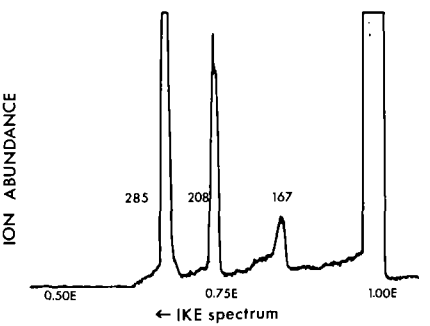

FIGURE 3

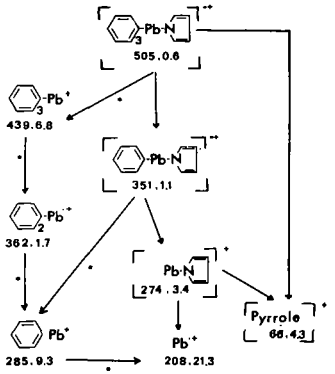

FIGURE 4

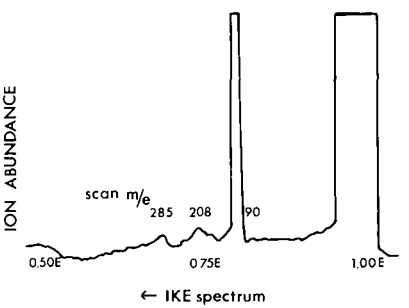

FIGURE 5

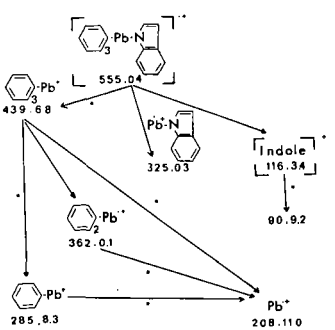

FIGURE 6

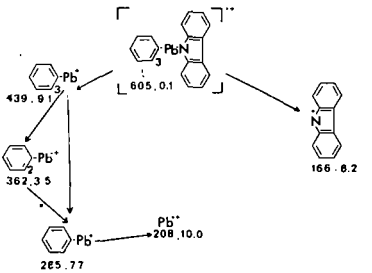

FIGURE 7

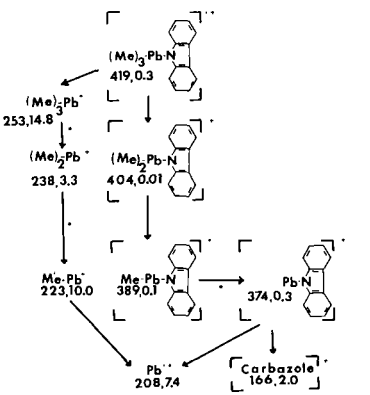

FIGURE 8

The Mass Spectra of some 1-(2-Thienyl)-3-Thiaalkanes and 1-(2-Thienyl)-4-Thiaalkanes.

NORMAN G. FOSTER
Dept. of Chem.
Texas Woman's University
Denton, Texas 76201

The mass spectra of 13 members of these series of two sulfur atom containing compounds are presented. The spectra correspond in part to ions expected from the alkylthiophene series and those typical of the alkylthiaalkanes or alkyl sulfides. The m/e 97 ion is prominent in the spectra of the 3-thiaalkanes but the excess m/e 98 ion peak due to rearrangement is virtually absent. Peaks typical of cleavage beta to both the ring and the alkyl sulfur atom are present indicating some charge competition between two parts of the molecule containing the sulfur atoms. A rearrangement ion at m/e 110 is observed in all 3-thia compounds. In contrast, the most prominent ion present in the 4-thia compounds is a highly unsaturated rearrangement ion of m/e 124. While also present as a major ion, the m/e 97 ion is now accompanied by substantial amounts of the rearrangement ion at m/e 98. Low ionization voltage data is used in conjunction with the fragmentation to support some mechanisms that suggest themselves.

MASS SPECTROMETRY OF ^{14}C-LABELED COMPOUNDS OF HIGH SPECIFIC ACTIVITY

W.J.A. VandenHeuvel, J.L. Smith, H.E. Mertel and R.L. Ellsworth
Merck Sharp & Dohme Research Laboratories, Rahway, N.J. 07065

The mass spectra of ^{14}C-labeled compounds of low specific activity are not discernably different from those of the unlabeled species. At considerably increased levels of radioactivity (e.g., 1-10 mCi/mM) the contribution of the ^{14}C isotope becomes apparent. These and higher specific activity compounds can be employed to study fragmentation patterns and metabolic/biosynthetic pathways in the same way as ^{13}C-labeled compounds. Knoppel and Beyrich (1) collected ions from ^{14}C-labeled benzene on a graphite plate and used autoradiography to ascertain which ions contained the ^{14}C-label. Occolowitz (2) studied ^{14}C as a label with scanning mass spectrometry, and calculated the ^{14}C-compositions of ions. White and coworkers (3) reported on the use of a ^{14}C-label to characterize a fragment ion from the di-trimethylsilyl derivative of adenine. Mass spectrometric techniques have been employed by Chalmers et al. (4) to demonstrate the presence of ^{14}C-label in the catechol moiety of 3-O-^{14}C-methyl-4-hydroxyphenylalanine prepared by incubation of L-dopa with methyl-^{14}C-S-adenosylmethionine in the presence of catechol-O-methyltransferase. Walker et al. (5) used the same methyl donor to demonstrate the enzymatic conversion of N-methyltryptamine to N,N-dimethyltryptamine by indoleamine-N-methyltransferase; the mass spectrum of the in vitro product contained dimethylaminomethylene fragment ions from the side chain at both m/e 58 and 60. The availability of a number of ^{14}C-labeled compounds with a wide range of known specific activities has led us to investigate the determination of specific activities of mass spectrometric techniques.

Several forms of ^{14}C-labeled cambendazole (see below) were investigated including

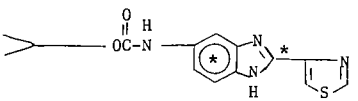

imidazole-C-2-labeled (prepared from glycine-^{14}C-carboxyl) and benzene ring-labeled (prepared from ^{14}C-aniline, itself synthesized from labeled acetylene, allowing for multiple labeling). The specific activities of these compounds were determined by an approach involving calculation of the "Weight Average Molecular Weight" (6) from the molecular ion clusters of the labeled and unlabeled species using the expression

$$\text{Wt Av Ml Wt} = \frac{\Sigma m \times I}{\Sigma I}$$

where m is the m/e value and I is the corresponding ion intensity (average of 2-3 scans with ≈0.6 µg sample) relative to that of the molecular ion. The net label is obtained from these values, and the ^{14}C-content then determined. For example, ring-labeled cambendazole from aniline with a very high specific activity was found to possess a Wt Av Ml Wt of 305.85, compared to 302.25 for the unlabeled drug. The most intense signal in the molecular ion cluster from this labeled cambendazole is M + 4, m/e 306, and ions of this sample containing six atoms of ^{14}C (m/e 314) can be discerned in the spectrum. The net label is thus 3.6. On the average, each molecule of labeled compound is 3.6 mass units heavier than the unlabeled compound, and thus on the average each molecule of labeled drug contains 1.8 atoms of ^{14}C. As the specific activity per atom of pure ^{14}C is 64 mC/mM, the mass spectrometrically determined specific activity of this particular ^{14}C-cambendazole is 115 mC/mM (see Table I). This is the same as the value obtained by liquid scintillation counting. A comparison of mass spectrometric and liquid scintillation counting specific activities for a similarly labeled cambendazole of lower specific activity and for the C-2-labeled cambendazole is also found in Table I.

TABLE I

	Sp. Act., mC/mM	
	MS	LSC
Ring-^{14}C (high)	115	115
Ring-^{14}C (low)	9.2	9.0
C-2-^{14}C	3.4	3.3

Our approach to the mass spectrometric determination of specific activity differs from that of Bowen et al. (7); these authors employ only the intensities of the M, M+2, M+4, etc., ions in their direct calculation.

Another ^{14}C-labeled compound of interest to us was carboxyl-labeled methyl 2-thienylacetate. Rather than calculate the net label, we employed combined GLC-mass spectrometry using the accelerating voltage alternator to give us the M/M+2 intensity ratios for the labeled and unlabeled species. The experimentally determined ratios, 100/38 and 100/5, respectively, led to a ^{14}C-content of 24.5%, or a specific activity of 15.7 mC/mM. LSC gave 16.2 mC/mM.

The mass spectrometric determination of specific activities of ^{14}C-labeled compounds should not be considered just a curiosity or a tour de force. High specific activity compounds are in demand for a variety of reasons, and with the preparation of very small quantities of ^{14}C-labeled compounds there may be too little sample upon which to obtain an accurate weight for LSC measurement. Further, if there is no UV absorption to allow mass determination, this further complicates the conventional measurement of specific activity. Impure samples also present a challenge, one which may be successfully met by a GLC-mass spectrometric approach.

REFERENCES

1. H. Knoppel and W. Beyrich, Tetra. Letters, No. 3, 291 (1968).

2. J. L. Occolowitz, Chem. Commun., 1226 (1968).

3. E. White, V, P. M. Krueger and J. A. McCloskey, J. Org. Chem., 37, 430 (1972).

4. J. P. Chalmers, G. H. Draffan, J. L. Reid, S. S. Thorgeirsson and D. S. Davies, Life Sciences, 10, Part I, 1243 (1971).

5. R. W. Walker, H. S. Ahn, L. R. Mandel and W. J. A. VandenHeuvel, Anal. Biochem., 47, 228 (1972).

6. W. J. A. VandenHeuvel, J. L. Smith, G. Albers-Schonberg, B. Plazonnet and P. Belanger, in Modern Methods of Steroid Analysis, E. Heftmann, Ed., Academic Press, New York, in press.

7. D. H. Bowen, J. MacMillan and J. E. Graebe, Phytochem., 11, 2253 (1972).

This paper will be published in Agr. Food Chem.

PERI-EFFECTS IN THE MASS SPECTRA OF SOME 8-SUBSTITUTED 1-NAPHTHOIC ACIDS AND 1-NAPHTHYLCARBINOLS

Paul H. Chen

Philip Morris Research Center, Richmond, Va. 23261

Donald C. Kleinfelter

Department of Chemistry, University of Tennessee, Knoxville, Tennessee 37916

ABSTRACT

The mass spectra of several 8-substituted 1-naphthoic acids and 1-naphthylcarbinols have been examined to determine if peri interactions are involved in the fragmentation. The substituents at the C_8 position include CH_3O, CH_3, Br, and NO_2. The spectrum of the 8-methoxy acid shows a strong [M-CH_3OH] ion due to peri interaction whereas its isomeric 2-methoxy acid does not. The loss of water in the spectra of the 8-methyl acid and alcohol, and of HBr from the 8-bromo alcohol are indicative of interaction between peri substituents. The expulsion of these neutral molecules from the molecular ion is presumably facilitated by the peri-cyclization to form a stable product. The weak molecular ion and facile loss of the 8-substituent in the spectra of the 8-bromo and 8-nitro acids are interpreted as being due to peri interactions. The presence of [M-H_2O] and [M-OH-OH] ions in the spectrum of the 8-nitro alcohol also indicates the interaction between the peri substituents.

The full paper will be published in a 1973 issue of the Journal of Organic Chemistry.

Mass Spectra and Pyrolysis of Azoles

D.C. DE JONGH, M.L. THOMSON and D.C.K. LIN

Department of Chemistry
University of Montreal
Montreal, Canada.

The electron-impact and chemical-ionization mass spectra of several aromatic azoles which have the general structure 1 (X = S and O; Y = S, O, and NH; R = H and Ph) have been studied and compared with their pyrolysis products. Parallels have been found between pyrolysis and mass spectrometry. For example the molecular ions and (M + H) ions from benzothiazole-2-thione (R = H, X = S, Y = S) lose S. Also, a one-step loss of S_2 is observed in the mass spectrum, a metastable ion being detected in defocussing studies. At 800°, this thione gives a 23% yield of benzothiazole from loss of S and a 13% yield of cyanobenzene from loss of S_2. A number of parallels of this type were discussed in the contributed paper. Some of the work has been published in J. Org. Chem., 38, 1356 (1973) and Can. J. Chem. 51, 0000 (1973).

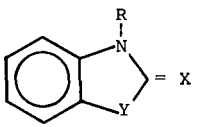

1

Selective Introduction of TMS-d_0 and TMS-d_9 Groups in Hydroxy Steroids. Evidence for Intramolecular Silylation Processes

PAUL VOUROS and D. J. HARVEY

Institute for Lipid Research
Baylor College of Medicine
Houston, Texas 77025

Mixed trimethylsilyl (TMS-$\underline{d}_0$) and perdeuterotrimethylsilyl (TMS-$\underline{d}_9$) derivatives of hydroxy steroids have been prepared, in which the labeled and unlabeled silyl groups occupy specific positions. A typical example of the selective silylation process is shown in Scheme 1. The dihydroxy steroid 17α-methyl-5-androstene-3β, 17β-diol contains an unhindered 3β- and a hindered 17β-tertiary hydroxyl group. Reaction with the relatively weak silylating reagent bis-trimethylsilyl-trifluoroacetamide (BSTFA) under relatively mild conditions as indicated in step I resulted in silylation of the 3β-hydroxyl group. After evaporation of solvent and reagents the partially derivatized

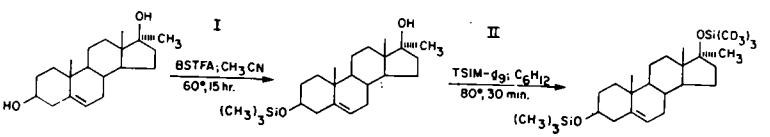

Scheme 1

compound was reacted with labelled trimethylsilylimidazole (TSIM-$\underline{d}_9$; Step II) and the mixed derivative was produced. Such mixed derivatives have been studied by mass spectrometry, and when the silyl groups are widely separated, as in the above diol, the positional identity of the TMS-$\underline{d}_0$ and TMS-$\underline{d}_9$ groups was retained upon electron impact. Thus preparation of these derivatives was helpful in the interpretation of the mass spectra of steroidal TMS ethers.

In cases where the hindered and unhindered hydroxyl groups are in adjacent positions evidence was obtained for the occurrence of intramolecular silylation processes. As an example, consider the selective introduction of TMS-$\underline{d}_0$ and TMS-$\underline{d}_9$ groups in 5-pregnene-3β, 17α, 20α-triol according to the sequence in Scheme 1. Mass spectrometric evidence, based on the well documented cleavage of the 17β-side chain and deuterium and ^{18}O-labeling, support the formation of a mixed TMS-$\underline{d}_0$, TMS-$\underline{d}_9$ derivative as shown in Scheme 2. It is apparent that following silylation of

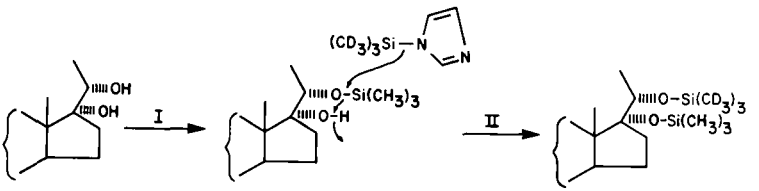

Scheme 2

the unhindered 20α-hydroxyl group, the increased steric hindrance inhibits direct attack of the 17α-OH group by the bulky TSIM-$\underline{d}_9$ molecule and results in an intramolecular completion of the silylation process in Step II. This intramolecular shift is, of course, enhanced by the proximity of the 17α-oxygen atom and the 20α-silicon. This proximity effect also results in electron impact-induced reciprocal exchange of trimethylsilyl groups in the mass spectrum of the mixed TMS-$\underline{d}_0$ and TMS-$\underline{d}_9$ derivative.

Parts of this work have been published in Anal. Chem., 45, 7 (1973).

A MASS SPECTRAL STUDY OF SOME 1- AND 2-SUBSTITUTED ADAMANTANES

Anne Sanderson

International Flavors & Fragrances
Union Beach New Jersey 07735

Published data on the mass spectra of adamantanes have concentrated mainly on the 1-substituted derivatives (1,2,3,4) with the assumption that the adamantanes substituted in the 2-position tend to be more predictable. This assumption is not entirely true and there are some interesting correlations and contrasts between these and the bridgehead isomers.

Because of the rigidity and symmetry of the cage system, adamantane is an extremely stable molecule which is more resistant to fragmentation than most cyclic hydrocarbons, giving rise to a relatively large parent ion. The mass spectra of many 1- and 2-substituted adamantanes show that the preferred route of fragmentation is via simple cleavage leaving the basic adamantane ring system intact. After elimination of a substituent, the resultant adamantyl fragment, m/e 135, can exist as a positively charged tricyclic structure or rearrange to form the structures shown below.

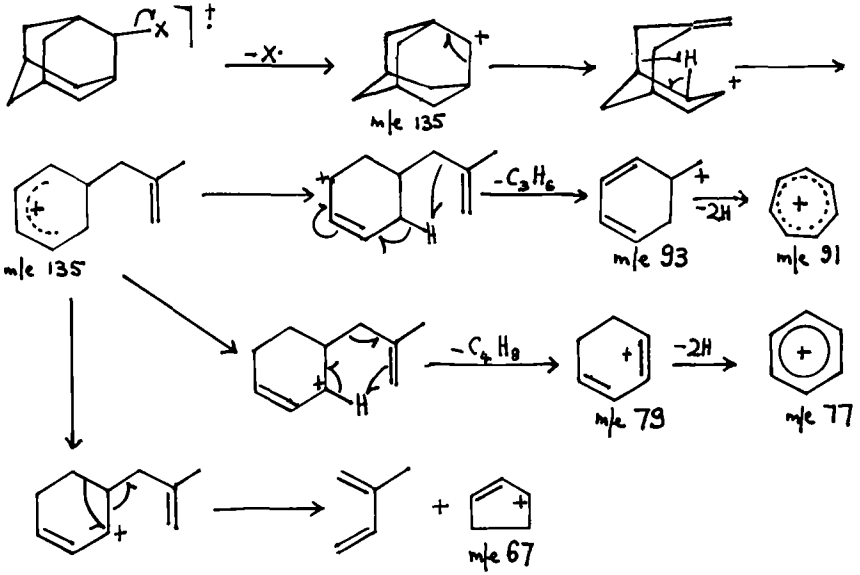

This charged isobutenyl cyclohexene fragment is not as strained as the tricyclic adamantyl ion. The strain will be even more apparent in the adamantyl ion arising from a 1-substituted adamantane, where the charge is at a bridgehead of the tricyclic system. After rearrangement to the substituted cyclohexenyl ring, isopropene is lost to form the more stabilized 4 and 6 π electron systems with m/e 93 and 91, respectively. Metastable peaks for the transition m/e 135 to 93 and 91 are apparent in spectra containing these fragments. Similarly, elimination of isobutene will produce protonized benzene and benzene, 79 & 77. In all the spectra containing a significant m/e 79, a metastable peak at 46.2 was observed, confirming its formation from 135. The formation of m/e 67 is not as easy to explain, although this ion also appears to arise from the cyclohexenyl derivative, as evidenced by a metastable peak at 33.3.

TABLE I

NAME		FRAGMENTATION
2-methyl adamantane	150	135 - 150 - 79 - 41 - 39 - 93
1-methyl adamantane	150	135 - 93 - 150 - 41 - 79 - 39
1-ethyl adamantane	164	135 - 79 - 164 - 93 - 41 - 136
2-adamantanethiol	168	135 - 168 - 93 - 79 - 67 - 91
2-methylthioadamantane	182	135 - 182 - 79 - 93 - 67 - 39
1-acetyl adamantane	178	135 - 79 - 43 - 93 - 41 - 67
2-methylsulfinyl adamantane	198	135 - 67 - 93 - 79 - 81 - 41
2-methylsulfonyl adamantane	214	135 - 67 - 93 - 79 - 136 - 41
di-(2-adamantyl)-disulfide	334	135 - 334 - 67 - 136 - 79 - 335
1,3-dimethyl adamantane	164	149 - 93 - 164 - 107 - 150 - 41
2-bromoadamantane	214	135 - 39 - 79 - 93 - 67 - 41
1-bromoadamantane[1]	214	135 - 93 - 39 - 41 - 79 - 67
2-adamantanethiol	168	135 - 168 - 93 - 79 - 67 - 91
2-adamantanol	152	134 - 92 - 79 - 93 - 80 - 91
1-adamantanol	152	95 - 152 - 94 - 96 - 41 - 109
5,7-dimethyl-1,3-adamantanediol	196	125 - 123 - 196 - 121 - 43 - 55
2-adamantanoic acid	180	134 - 79 - 41 - 39 - 180 - 135
1-adamantanoic acid[1]	180	135 - 79 - 93 - 136 - 107 - 67
2-aminoadamantane	151	151 - 30 - 150 - 134 - 56 - 92
1-aminoadamantane[1]	151	94 - 151 - 95 - 57 - 108 - 77
adamantanone	150	150 - 80 - 79 - 81 - 41 - 78
adamantanethione dimer	332	166 - 332 - 167 - 91 - 45 - 169
adamantanethione trimer	498	166 - 332 - 167 - 91 - 300 - 333
2,2-adamantane dicarboxylic acid	224	180 - 134 - 79 - 135 - 41 - 93
2,2-di(hydroxymethyl) adamantane	196	31 - 148 - 91 - 41 - 165 - 79

[1]Dolejsek, Z., et al. Coll. Czech. Chem. Comm. 31 435 (1966)

Examples of the ions discussed are shown in Table I. 1,3-Dimethyl adamantane is included because it illustrates that the same pathways can be followed when there is more than one substituent on the adamantane ring. With the exception of 1-ethyl adamantane, the spectrum of which was obtained from a GC-MS run on a Hitachi RMU-6E, all the spectra were obtained on an MS-902 and a CEC model 103C.

Compounds with more polar groups substituted in the 1-position of the adamantane ring give a greater number of intra-ring fragments, while those substituted in the 2-position often leave the ring intact, as for example, 2-adamantanethiol cleaves the SH from the ring to form the adamantyl ion at m/e 135.

1- and 2-substituted adamantane derivatives which undergo rearrangement before fragmentation show different pathways. 2-Adamantanol, 2-amino-adamantane and 2-adamantanoic acid are examples of the type of rearrangement for the 2-substituted derivatives. A hydrogen is abstracted from the ring for the elimination of a neutral molecule of water, ammonia and the elements of formic acid, respectively. Bridgehead adamantanes show intra-ring rearrangement with the elimination of C_4H_9, leaving the substituent attached to the charged portion at M - 57. After the loss of the butyl fragment, the 6 π electron system stabilizes the ring and further fragmentation is restricted. This mode of fragmentation shown below, is common to many of the more polar 1-substituted adamantanes. Both 1-aminoadamantane and 1-adamantanol give M - 57 as shown. An exception is 1-adamantanoic acid, which prefers straight cleavage to form a base peak at m/e 135 instead of intra-ring rearrangment with loss of C_4H_9.

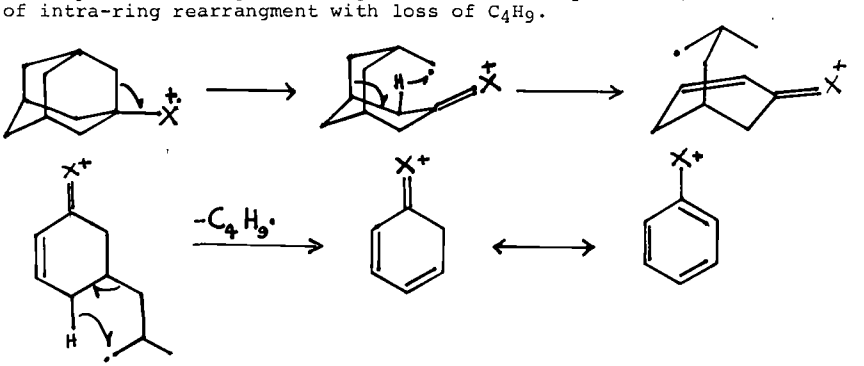

Another interesting example is the adamantane substituted at every bridgehead, 5,7-dimethyl-1,3-adamantanediol. This molecule can either lose a methyl or a hydroxy group with the elimination of a butyl group when it undergoes intra-ring rearrangement. In fact, it does both as there are significant peaks at m/e 125 and 123. Because the oxygen of the hydroxy group will lend more stability to the intermediate and final structures than the methyl group, it would be expected that m/e 125 is more intense than 123. M/e 125 is the base peak in the spectrum of 5,7-dimethyl-1,3-adamantanediol.

The main factor for determining whether the adamantane derivative will undergo simple cleavage or rearrangement followed by fragmentation, appears to be the ability of the substituent to lower the dissociation energy of the bond. Very strong electron-donating groups (hydroxy, amino, etc.), do not appear to lower the dissociation energy and cause rearrangement to be the preferred route before fragmentation. Other groups (such as alkyl, halide, acetyl, etc.) lower the dissociation energy of the bond sufficiently to allow simple cleavage, usually resulting in m/e 135 as the base peak.

An adamantane derivative which appears to have fragmentation rules of its own is adamantanone. Because of the increased rigidity of the molecule as a result of the oxygen double bond on the adamantane ring, the parent ion is even stronger than most substituted adamantanes; in this case it is the base peak of the spectrum. The second most intense peak is m/e 80 and a possible route for this is shown below. As there are no metastable peaks for the loss of the C_3H_7 and CO fragments,

it is assumed that these losses take place simultaneously. Russian

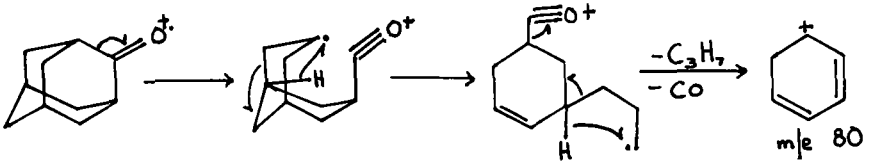

workers claim metastable peaks for the loss of C_3H_7 and C_3H_6 ; however these were not observed in our laboratory. An alternate route to m/e 80 may be via the initial elimination of water. This transition is supported by a metastable peak at m/e 116.2. The cyclohexadiene ion may arise from m/e 132, although there are no metastable peaks to support this transition either. A metastable peak at 78.0 indicates that m/e 79 is formed by hydrogen loss from m/e 80. Similarily, m/e 78 is produced from m/e 79 by hydrogen elimination as supported by a metastable peak at 77.0. No sulfur analog of adamantanone could be obtained, although the dimer and trimer of adamantanethione were analyzed. Both of these show fragmentation forming the adamantanethione ion, in fact m/e 166 is the base peak in both the dimer and trimer. This is analogous to the base peak of adamantanone which is also the parent ion. However, like 2-adamantanethiol and 2-adamantanol, there are no further correlations between the adamantanethione formed and adamantanone.

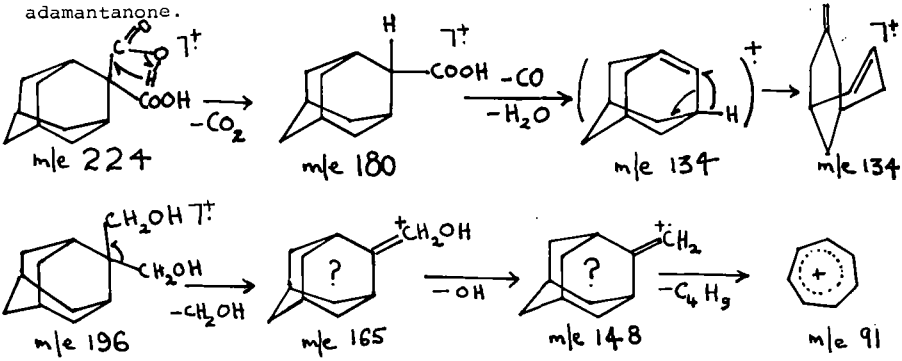

Continuing along similar lines of thought, we would like to discuss some 2,2-disubstituted adamantanes. The above pathways are suggested for the fragmentation of 2,2-adamantane dicarboxylic acid and 2,2-di(hydroxymethyl)adamantane. Fragmentation of the diacid is relatively straightforward, the base peak representing a loss of carbon dioxide to form the monocarboxylic acid ion. After this, elimination of the elements of formic acid occurs as from 2-adamantanoic acid and the 134 ion will be more likely to exist in the form of the second structure rather than the strained tricyclic system. This is the same ion as that formed from 2-adamantanoic acid, the monomer acid. The fragmentation of 2,2-di(hydroxymethyl)adamantane is less obvious, for although the base peak at m/e 31 requires no explanation, the second most intense peak at m/e 148 is interesting. As suggested above, the elimination of the second CH_2OH group with the resultant m/e 135 does not occur probably because the initial loss of 31 produces an intermediate with a double bond to the ring, (or possibly in a ring-expanded rearrangement structure?). M/e 91 is a loss of C_4H_9 from the fragment at m/e 148, via similar pathways as those discussed previously. 2,2-Di(hydroxymethyl)-adamantane and 2,2-adamantane dicarboxylic acid are the only compounds investigated which did not show a molecular ion. Most adamantanes display a distinctive molecular ion because of the rigidity of the adamantane structure and the relative stability of the bond between the substituent and the ring.

To summarize, there appears to be three general methods of fragmentation for adamantane derivatives. Simple cleavage occurs in both 1- and 2-substituted adamantanes. Intra-ring rearrangement with a loss of C_4H_9 is common with some bridgehead compounds, whereas the

2-substituted adamantanes more readily undergo the loss of the substituent with an atom of hydrogen. This loss of HX is easier from the 2-position because of the proximity of the substituent to the hydrogen on the bridgehead of adamantane. Thus, there should be no difficulty distinguishing between polar adamantanes substituted in the 1- and 2-position.

The author would like to thank Mr. W. B. Ahart for obtaining most of the spectra, Mr. H. A. Bondarovich for advice and encouragement and Dr. S. K. Freeman and colleagues for supplying many of the samples.

REFERENCES

1. Dolejsek, Z., et al. Coll. Czech. Chem. Commun. 31 435 (1966)

2. Warren, R. W., et al. Appl. Spectrosc. 22 115 (1968).

3. Chizhov, O.S., et al. Izvestiia Akademii Nauk. SSSR. Seria Khimicheskaia 1972 1028 (1972)

4. Khullar, K. K., et al. J. Org. Chem. 38 1042 (1973)

5. Karpenko, N. F., et al. Izvestiia Akademii Nauk. SSSR. Seria Khimicheskaia 1972 337 (1972)

MASS SPECTROMETRY OF PERMETHYLATED AND PERDEUTERIOMETHYLATED FLAVONOIDS

Permethylation and perdeuteriomethylation of naturally occuring flavonoids by use of NaH, DMF, and CH_3I or CD_3I * yielded derivatives which were readily analyzed by mass spectrometry and combined GC/MS. A great deal of structural information can be obtained from these analyses concerning the flavonoid type and substitution pattern. The mass spectra of a series of flavonoid glycosides yielded information concerning the number and type of sugars present, concerning the position of sugar attachment to the flavonoid skeleton, and concerning the interglycosidic linkages. **

* R. Schmid, Tetrahedron 28:3259(1972)
** This work to be published in Phytochemistry

George Vander Velde
Hugh Waldrum
Ursula Schuecker
Tom J. Mabry
Department of Botany
University of Texas
Austin, Texas 78712

IDENTIFICATION OF N-NITROSO COMPOUNDS BY MASS SPECTROMETRY*

W. Lijinsky, W. T. Rainey and W. H. Christie
Biology and Analytical Chemistry Divisions
Oak Ridge National Laboratory, Oak Ridge, Tennessee 37830

The N-nitroso compounds constitute the most widely acting group of carcinogens we know. Because of this there has been great interest in developing methods for detecting them in the environment. Most of these methods lack specificity and artifactual identifications of nitrosamines have been common. More recently it has been suggested that nitroso compounds can be formed in the gastro-intestinal tract from nitrite and secondary and tertiary amino compounds.

It appears that unequivocal ways of identifying these potent carcinogens are needed, particularly those applicable to small sample sizes. Because we think that mass spectrometry is one of the best ways of achieving this, we have examined the mass spectra, measured under standard conditions, of 96 N-nitroso compounds. We have tried to identify typical features of the mass spectra which would enable us to identify an unknown compound as a nitrosamine and to assign a structure to it.

The first feature of a value is that almost all N-nitroso compounds give a molecular ion. The molecular ions vary enormously in intensity but we found only 4 among the 96 from which we were unable to obtain a molecular ion even with a relatively large sample of the compound.

The second feature was that almost all of the nitroso compounds examined showed an M-30 or M-31 fragment, corresponding with a loss of NO or HNO. All of the nitrosamines, with the exception of perhaps 2 or 3, gave an M-30 or M-31 ion which was a reasonable size relative to the molecular ion. Such a fragment was, however, usually absent from the mass spectra of nitrosamides. Aliphatic nitrosamines gave either an M-30 or M-31 ion, whereas cyclic nitrosamines gave exclusively an M-30 ion.

Aliphatic nitrosamines showed losses of alkyl groups (e.g. ethyl from di-n-propylnitrosamine) and the alkyl ion (e.g. n-butyl) was often prominent in the spectrum.

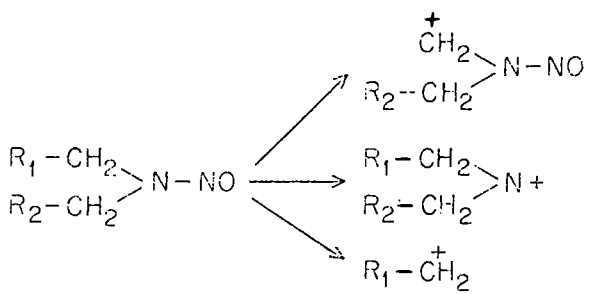

A third feature was a M-17 ion which corresponded with loss of OH and we believe led to formation of a transient cyclic species. It was not due to migration of a proton from a carbon atom alpha to the nitrogen, since nitrosamines labeled with deuterium in the alpha position showed loss of OH, not of OD. The relative intensity of the M-17 ion varied considerably and seemed to increase with increasing chain length from ethyl up, or increasing molecular size in the case of cyclic nitrosamines (Table 1)

Table 1

Nitrosamine	M-17 as % of M
Dimethyl	0
Diethyl	2
Di-n-propyl	12
Di-iso-propyl	0
Di-n-butyl	25
Methylethyl	2
Methyl-n-propyl	31
Methyl-n-butyl	56
Methyl-n-dodecyl	10000
Methylcyclohexyl	17

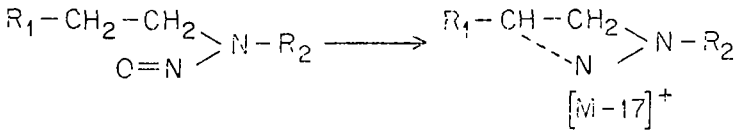

The spectrum of the largest aliphatic nitrosamine we examined, nitroso methyl dodecylamine, shows that the M-17 ion is the base peak of the spectrum (Fig. 1).

Fig. 1. Mass spectrum (70 eV) of N-nitrosomethyl-n-dodecylamine

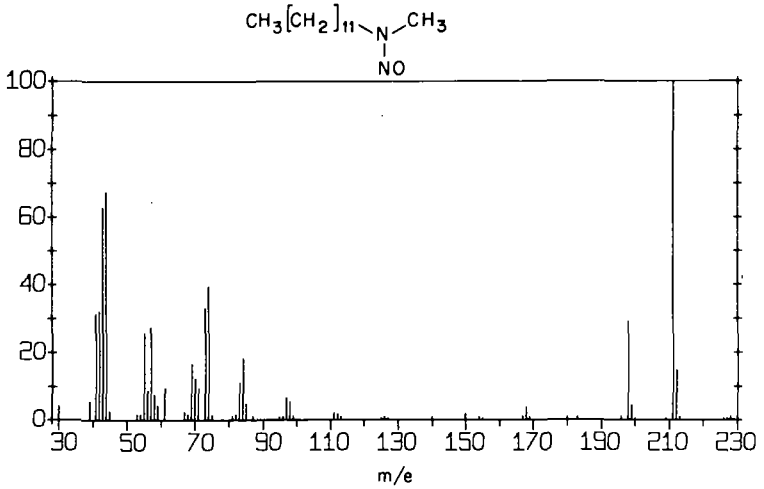

A large number of cyclic nitrosamines were examined and showed characteristics typified by nitroso-2-methylpiperidine, for example loss of NO and loss of the methyl group.

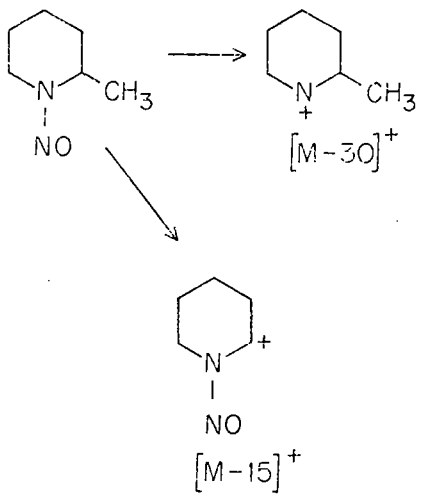

In the spectrum of nitroso-2-methylpiperidine (Fig. 2) we see an M-17 ion indicating loss of OH. The proton was again not from the α-carbon atom since the ion from nitrosoazetidine-2,4-d_4 was M-17.

Fig. 2. Mass spectrum (70 eV) of N-nitroso-2-methylpiperidine

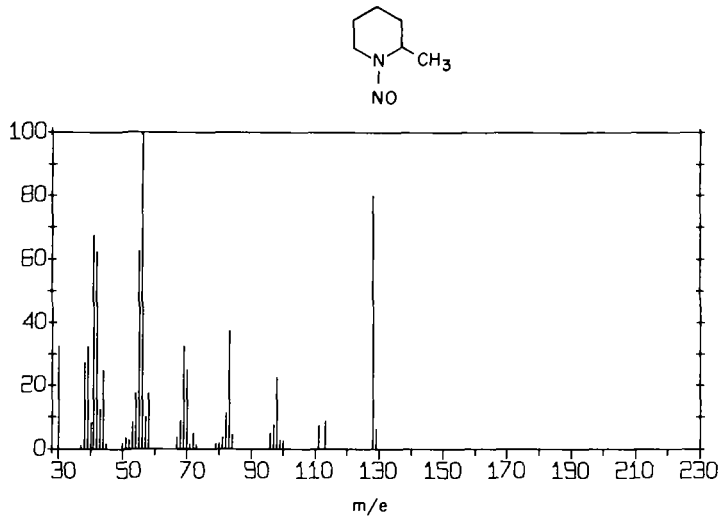

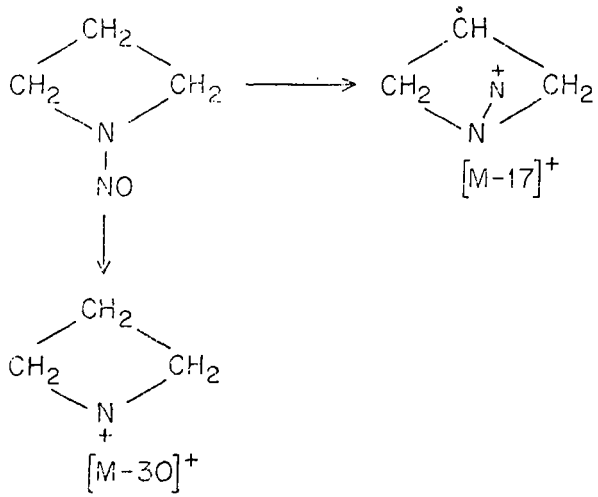

Nitrosomorpholines and nitrosopiperazines did not give an M-17 ion.

Nitrosamino acids, such as nitrosoproline, show an M-45 ion, corresponding to loss of the carboxyl group (COOH), as well as an M-30 ion.

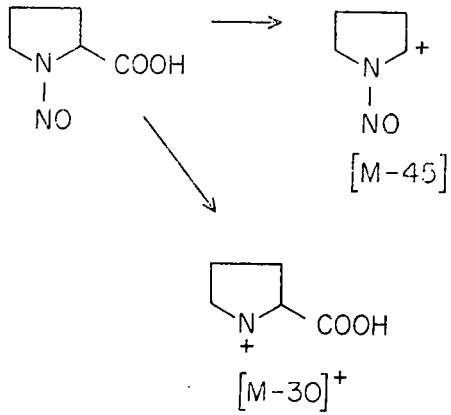

Nitrosamides such as nitrosoethylurea show quite different patterns from nitrosamines. The prominent ions identified by accurate mass measurement include those at m/e 74 and 56. The ion at m/e 44 was N_2O and this ion was not seen in the mass spectrum of any nitrosamine. We cannot explain its formation yet.

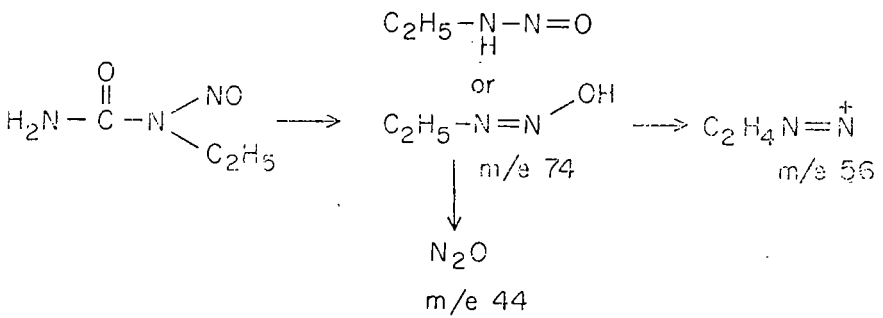

Some similar fragments were seen in the spectra of nitrosoalkyl carbamate esters, but in the case of nitroso ethyl urethane there was an ion at m/e 101 which was not present in the spectrum of nitrosoethylurea.

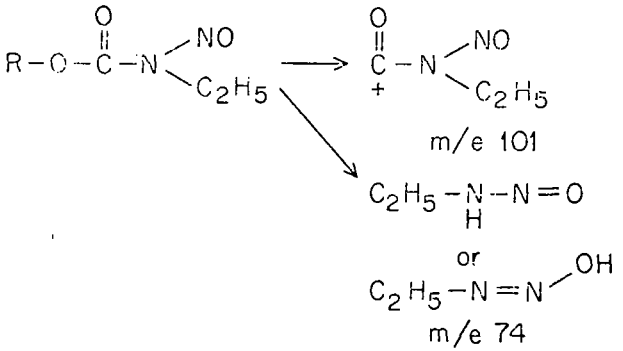

We feel that these (Table 2) and other special features of individual nitroso compounds will enable us to identify almost any N-nitroso compound from its mass spectrum.

Table 2

Mass Spectral Characteristics of 96 N-Nitroso Compounds

4 had no molecular ion
16 had no M-30 or M-31 ion
43 had M-17 ion

*Research jointly sponsored by the National Cancer Institute, and by the U. S. Atomic Energy Commission under contract with the Union Carbide Corporation.

MECHANISMS FOR THE ELIMINATION OF WATER FROM IONIZED ALCOHOLS.

Peter Brown, John J. Mattick, William D. Lucky and Morton E. Munk
Chemistry Department, Arizona State University, Tempe, Arizona 85281.

Although the regiospecificity of the loss of water from several types of ionized alcohol in the gas phase has been determined, very little is known concerning the detailed reaction mechanisms actually involved. At least four mechanisms must be considered, one concerted and three stepwise in nature. A fifth pathway, pyrolytic loss of water followed by ionization of the M-18 species, can contribute perhaps more than is generally realized with alcohols.

In attempts to differentiate between these mechanisms, we have employed stereochemical probes, isotope effects, thermodynamic data and metastable ion studies on a series of structurally different organic substrates.

For example, with the 1,2-diphenylethanol system (at 10 eV), a stereoselectivity of 55:45 for abstraction of the diastereotopic protons on C-2, and an isotope effect $k_H/k_D = 1.87$ have been reported[1]. However, absence of a metastable peak for loss of water, coupled with IP/AP measurements, suggest a thermal component operating in this particular system.

In the expectation of observing higher stereoselectivities, the relatively rigid 1-acenaphthenol system was studied next. In Fig. 1, the diastereomers synthesized and raw M-H_2O/M-HDO data are given, and in Fig. 2 the stereoselectivity (64/36) and isotope effect (1.36) calculated (at 12 eV). In this instance a prominent metastable ion peak is present, and IP/AP data (Fig. 3) demonstrate that direct loss of H_2O as a neutral is a lower energy process than stepwise loss of H· and ·OH radicals.

Also given in Fig. 3 are IP/AP derived data for cyclopentanol, cyclohexanol and isoborneol. These systems are being examined further, due to a surprising report[2] of high stereoselectivity for the exo-3-H ($\sim$ 75/25) for the 1,2-dehydration of both borneol and isoborneol, the explanation given[2] being a two step mechanism where loss of ·OH precedes that of ·H.

These results will eventually be published in Organic Mass Spectrometry.

References:

1. M.E. Munk, C.L. Kulkarni, C.L. Lee and P. Brown, Tet. Letts., 1377 (1970).

2. D.R. Dimmel and J.M. Seipenbusch, J. Amer. Chem. Soc., 94, 6211 (1972).

	$M-H_2O$	$M-HDO$
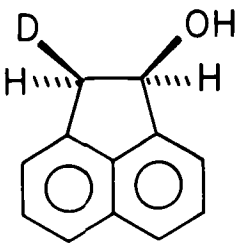	43	57
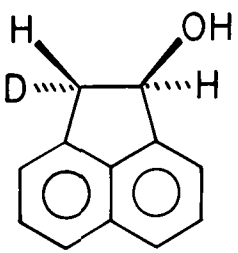	71	29

Stereoselectivity and Isotope Effect

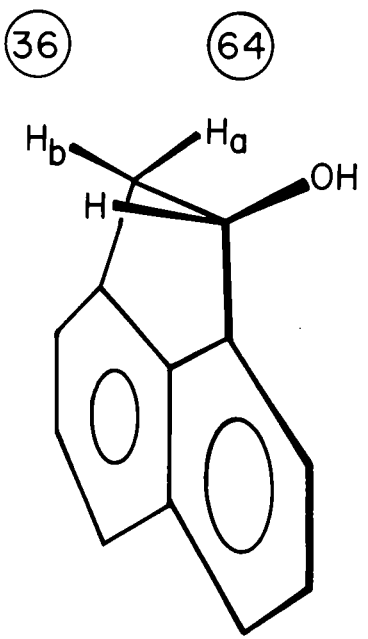

IE (H/D) = 1.36

Energetics of H_2O Elimination

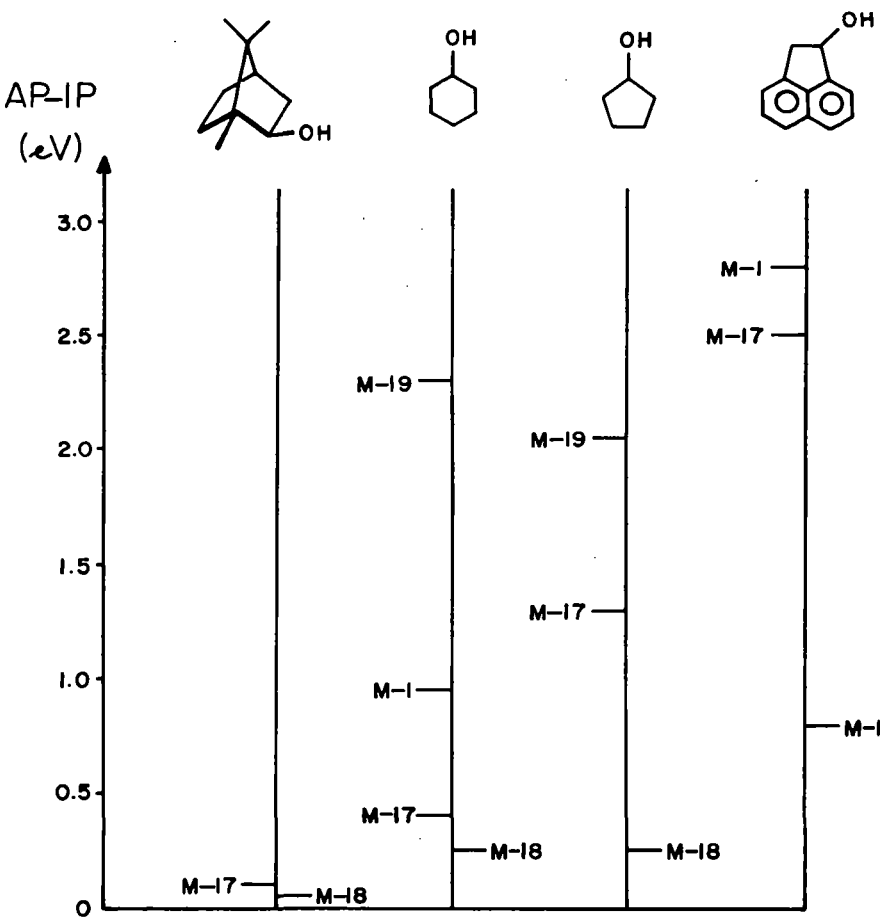

Electron Impact-Induced Elimination of Methylene Imine in Dimethylamino N-Heteroaromatic Systems

D. L. von Minden, J. G. Liehr and J. A. McCloskey

Institute for Lipid Research
Baylor College of Medicine
Houston, Texas 77025

The expulsion of the elements of CH_3N is a common and highly characteristic process in the mass spectra of N-heteroaromatic compounds containing dimethylamino substituents adjacent to the ring nitrogen. This structurally diagnostic fragmentation is especially important in the characterization of purine bases or nucleosides containing methyl- or dimethylamino moieties. Earlier proposed mechanisms depicted an initial methyl migration to the ring nitrogen followed by the loss of methyl nitrene,[1,2] or by rearrangement of a methylamino radical substituent to methylene imine and its subsequent expulsion.[3]

However, partial labeling of the dimethylamino moiety (i.e., CH_3-N-CD_3) revealed a unique rearrangement shown by the loss of CH_2ND and CD_2NH, in contrast to the loss of CD_2ND and CH_2NH predicted by the earlier proposals. The new rearrangement mechanism features formation of the methylene imine unit by hydrogen migration ($M_0 \rightarrow M_1$) and cyclization ($M_1 \rightarrow M_2$), followed by reopening and elimination (M_5 or M'_5).

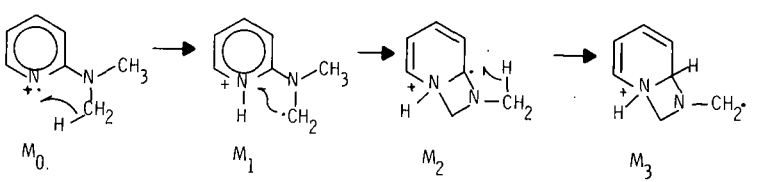

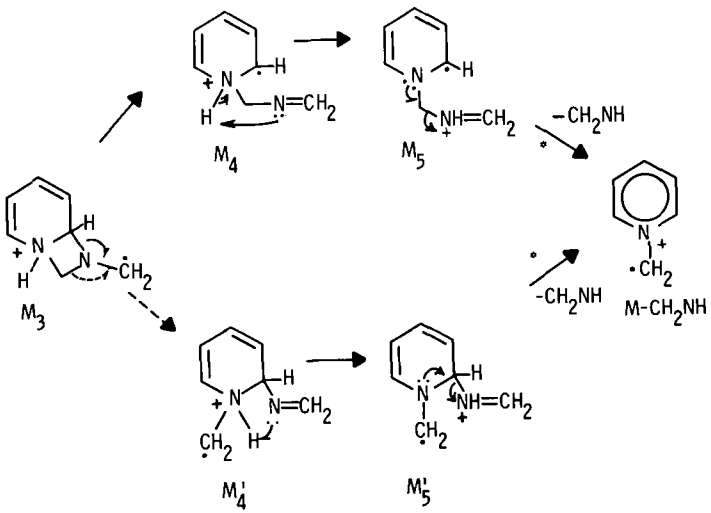

A detailed account of this work will be published elsewhere.

References

1. N. Neuner-Jehle, Tetrahedron Lett., 2047 (1968).

2. C. P. Whittle, ibid., 3689 (1968).

3. Y. Rahamin, J. Sharvit, A. Mandelbaum and M. Sprecher, J. Org. Chem., 32, 3856 (1967).

EQUILIBRIUM STUDIES OF INTRAMOLECULAR AND INTERMOLECULAR STRONG HYDROGEN BONDING

by

Donald H. Aue, Hugh M. Webb and Michael T. Bowers
Department of Chemistry, University of California
Santa Barbara, California, 93106

Intramolecular strong hydrogen bonds have been characterized thermodynamically as a function of ring size by measuring proton affinities of diamines capable of such bonding.[1]

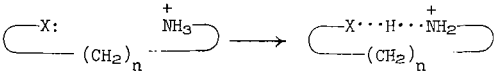

Eqn.1

The effect of formally varying the basic end (-X) of the intramolecular hydrogen bond (Eqn.1) from $-NH_2$ to -OH can be seen in Table I. The heats of ring formation are

TABLE I*

	GB	$-T\Delta S$	PA	$-\Delta H_{\text{ring form}}$
$HO(CH_2)_3NH_2$	221.0	12.6	233.6	10.8
$CH_3(CH_2)_3NH_2$	214.3	8.6	222.8	
$HO(CH_2)_6NH_2$	220.0	15.5	235.5	12.5
$CH_3(CH_2)_6NH_2$	214.6	8.6	223.1	

*All values in kcal/mole

5-6 kcal lower for the amino-alcohols than corresponding diamines[1] suggesting that the strong hydrogen bond energy of an unstrained $-\overset{+}{N}H_2\cdots H\cdots OH-$ bond is ca. 19 kcal/mole compared to ca. 24 kcal/mole for the $-\overset{+}{N}H_2\cdots H\cdots NH_2-$ bond. These values agree well with Kebarle's[2], Table II. This effect appears to be the result of the lower basicity

TABLE II[2,4]

		$-\Delta H$ (kcal/mole)
$NH_4^+ + NH_3$	$\rightleftharpoons H_3N\cdots H\cdots\overset{+}{N}H_3$	24.8
$CH_3NH_3^+ + CH_3NH_2$	$\rightleftharpoons CH_3NH_2\cdots H\cdots\overset{+}{N}H_2CH_3$	21.7
$H_3O^+ + H_2O$	$\rightleftharpoons H_2O\cdots H\cdots\overset{+}{O}H_2$	31.6
$NH_4^+ + H_2O$	$\rightleftharpoons H_3N\cdots H\cdots\overset{+}{O}H_2$	~18

of R-OH relative to $R-NH_2$. The proton affinity of CH_3OH is ca. 40 kcal lower than that of CH_3NH_2, for example.[3]

On the other hand increasing the acidity of the acidic end of the strong hydrogen bond (Eqn.1) from $H_3\overset{+}{N}-R$ to $H_2O\overset{+}{-}R$ while keeping the basic end constant (ROH), leads to an increase in the hydrogen bond strength of ca. 10 kcal/mole in comparing the heats of ring formation of diols, Table III, and amino alcohols with comparable ring strain.

TABLE III*

	GB	$-T\Delta S$	PA	$-\Delta H_{\text{ring form}}$
$HO(CH_2)_4OH$	202 ± 3	14.2	216	26 ± 3
$CH_3(CH_2)_4OH$	182 ± 3	7.8	190	

*All values in kcal/mole

The strain-free $R-OH\cdots H\cdots\overset{+}{H}OR$ hydrogen bond can be estimated[1] from the data in

Table III to be about 30 kcal/mole. This agrees well with Kebarle's[4] value for the $H_2O\cdots H\cdots OH_2^+$ hydrogen bond energy (Table II).

We have found that in mixtures of alkyl amines at high pressures it is possible to collisionally stabilize the proton bound dimer intermediate for proton transfer.[3] Such dimers can be shown to be in equilibrium with each other as illustrated in the following scheme derived from preliminary studies of dimer equilibria. When piperidine, diethylamine, and triethylamine are mixed in the three pairwise combinations, dimer equilibrium constants and ΔG^o's for reactions (1) to (6) are measurable, two for each of the three mixtures. To be sure that equilibrium was

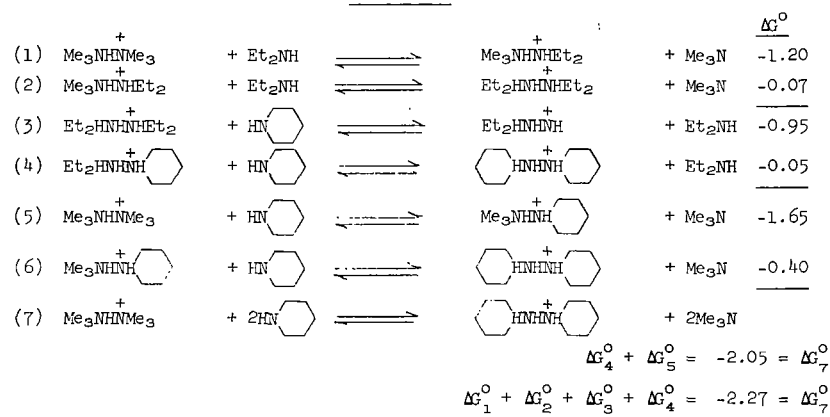

truly established and the ΔG^o's are accurate, the set of six ΔG^o's can be checked for internal consistency by checking ΔG^o_7 for reaction (7) by adding reactions (4) and (5) or reactions (1), (2), (3), and (4) to give reaction (7). The inconsistency in the ΔG^o's is 0.22 kcal/mole, about the same error as we find in PA overlaps. We have measured such dimer equilibria for a number of binary mixtures of amines and have found evidence in these data for steric destabilization of the proton bound dimers of hindered amines. For example, we have found that in a mixture of triethylamine and quinuclidine the hindered triethylamine does not form a dimer with itself but the less hindered bicyclic quinuclidine does. Such steric effects can be studied quantitatively in comparing equilibria (1)-(6) above. The general trend in such equilibria is for the dimers containing the amines of higher proton affinity to be favored, expecially with relatively unhindered primary amines (Table IV). In comparing relative proton

TABLE IV
Relative Affinities for X^+ [a,b]

	$EtNH_3^+$	H^+ (PA)
$EtNH_2$	0	0
n-$PrNH_2$	0.9	1.2
i-$PrNH_2$	1.1	2.2
$(Me)_3N$	> 1.9	8.0

a) All values in kcal/mole.

b) All numbers are relative ΔG's which have been corrected to remove symmetry effects in $T\Delta S$.

affinities with relative alkylammonium ion affinities derived from equilibria (1)-(6), however, differences in the quantitative patterns are evident (Table V). These differences appear to result from steric effects in the proton bound dimers. For

TABLE V
Relative Affinities for X^+ a,b

	H^+	Me_3NH^+	$Et_2NH_2^+$	
Me_3N	0	0	0	0
Et_2NH	1.0	0.8	1.2	1.0
	1.2	1.2	1.7	1.5
	0.1	1.1	-	0.4

a) All values in kcal/mole

b) All numbers are relative ΔG's which have been corrected to remove symmetry effects in $T\Delta S$.

example, the trimethylammonium ion affinity of pyrrolidine is 1.1 kcal/mole greater than trimethylamine, while its proton affinity is only 0.1 kcal/mole greater. Since the alkylammonium ion affinities used are free energies, differences may well result from changes in the entropy term. Note that the trimethylammonium ion affinity of diethylamine is 0.3 kcal/mole less than pyrrolidine while the proton affinity is 0.9 kcal/mole greater, suggesting a loss of internal rotational freedom in diethylamine on dimerization. This hypothesis will be tested by studying the temperature dependence in such equilibria to determine the entropy effect. We will extend these

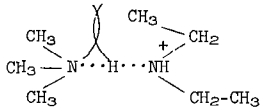

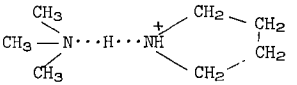

overlapping dimer equilibrium measurements to other hindered and unhindered systems to look for steric effects and other possible effects influencing such equilibria. We have detected trimerization reactions for some amines and plan to study equilibria between trimers as a further step toward understanding the solvation phenomenon.

References

1. D. H. Aue, H. M. Webb and M. T. Bowers, J. Amer. Chem. Soc. 95, 2699 (1973).
2. P. Kebarle, private communication.
3. D. H. Aue, H. M. Webb and M. T. Bowers, J. Amer. Chem. Soc. 94, 4726 (1972), and references therein.
4. A. J. Cunningham, J. D. Payzant and P. Kebarle, J. Amer. Chem. Soc. 94, 7627 (1972).

DYNAMICS OF THE REACTION $Ar^+ + CH_4 \rightarrow ArH^+ + CH_3$

P.M. Hierl, J.R. Wyatt, L.W. Strattan, and S.C. Snyder
Chemistry Department, Kansas University, Lawrence, Kansas 66044

INTRODUCTION

In the past decade molecular beam techniques have provided much valuable information concerning the dynamics of reactive molecular collisions. In particular, accelerated ion beams have been used to elucidate the energy dependence of reaction mechanisms. Considerable attention has been given to simple hydrogen atom transfer reactions between molecular hydrogen and atomic or diatomic ions. We have extended these studies to polyatomic systems and report here the results obtained for the reaction of Ar^+ with CH_4, CH_2D_2, and CD_4.[1]

EXPERIMENTAL

Argon ions, formed by electron impact, are collimated into a monoenergetic beam of variable energy. This beam passes through a collision chamber containing the neutral target gas under single collision conditions. Ions emerging from the collision chamber pass through a narrow detection slit, are energy analyzed by a retarding potential analyzer, and are mass analyzed by a 12" 90° sector instrument. The angular distribution of the reaction product is obtained by rotating the ion gun about the center of the collision chamber. A more detailed description of the instrument is available.[2]

RESULTS AND DISCUSSION

Product angular and velocity distributions were measured at various primary ion energies over the range 0.3-30 eV (cm). The measurements clearly indicate that the hydrogen abstraction reaction is dominated by a direct mechanism over the entire energy range studied, with no evidence for the formation of a long-lived complex. The spectator stripping (SS) model, although providing a first approximation to the reaction dynamics, consistently overestimates the most probable translational energy of the reaction products by about 0.1 eV. By contrast, ArH^+ from reaction of Ar^+ with H_2 possesses greater translational energy than expected on the basis of the SS model. However, the present findings are consistent with the same model previously proposed to explain the Ar^+-H_2 reaction.[3]

By integrating the product laboratory angular distributions, integral reaction cross sections were obtained for the various primary ion energies. Two interesting features were observed:

(1) The reaction cross section passes through a maximum (~ 0.2 Å^2) at 4 eV (cm) and falls rapidly as the collision energy is decreased, appearing to have a threshold at approximately 0.1 eV. This is a most unexpected feature for such an exothermic ($\Delta H \simeq -1.65$ eV) ion-molecule reaction. However, the measured velocity distributions indicate that the most favored reaction channel is one in which the reaction exothermicity appears as internal energy of the products and that the final translational energy is less than the initial translational energy. We attribute this net deceleration to the relatively strong attractive forces between the products of this reaction and hypothesize that the decrease in reaction cross section at low energies is caused by the inability of the products to separate under the influence of the strong attractive forces. The ArH^+ and CH_3 will then undergo secondary encounters of a "clutching" nature and must either reform reactants or follow another reaction channel (such as dissociative charge exchange).

(2) Experiments with CH_4 and CD_4 reveal a large isotope effect favoring abstraction of H over D at high energies. Results obtained with CH_2D_2 show that this isotope effect is intramolecular rather than intermolecular in nature. Similar isotope effects have also been reported for reactions of simple ions with the isotopic variants of molecular hydrogen and have been attributed to the difficulty of stabilizing reaction products formed in high energy collisions.[4] Hot atom studies of the abstraction reaction between energetic tritium atoms and various hydrocarbons[5] have also shown isotope effects that are remarkably similar in magnitude to those observed in the Ar^+-CH_4 system. Theoretical calculations[6] on the T-CH_4 system indicate that this effect is clearly a high energy phenomenon analogous to the present results. It appears, therefore, that such isotope effects might be a common feature of many simple atom-transfer reactions occurring at relatively high energies (> 5 eV).

ACKNOWLEDGEMENTS

Acknowledgement is made to the donors of the Petroleum Research Fund, administered by the American Chemical Society, for partial support of this project. Additional support was provided by the Research Corporation and by the University of Kansas General Research Fund.

REFERENCES

(1) A more detailed account of this work has been submitted to the Journal of Chemical Physics.

(2) P.M. Hierl, L.W. Strattan, and J.R. Wyatt, Int. J. Mass Spectrom. Ion Phys. 10, 385 (1972/73).

(3) P.M. Hierl, Z. Herman, and R. Wolfgang, J. Chem. Phys. 53, 660 (1970).

(4) See, for example, A. Henglein, Adv. Chem. Ser. 58, 63 (1966).

(5) R. Wolfgang, Progr. Reaction Kinetics 3, 97 (1965), and references cited therein.

(6) D. J. Malcolme-Lawes, J. Chem. Phys. 57, 5522 (1972), and references cited therein.

THE RATE OF FORMATION OF Ar_2^+ FROM Ar^+ IN Ar GAS*

W. C. Liu and D. C. Conway

Department of Chemistry

Texas A&M University

College Station, Texas 77843

The rate of the ion molecule reaction

$$Ar^+ (^2P_{3/2}) + 2Ar \xrightarrow{k_1} Ar_2^+ + Ar$$

has been measured in a drift tube ion source from liquid N_2 temperature to 140°C. In general, the reaction has only been studied at reduced pressures P_0 (corrected to 0°C) up to 3 torr, but at room temperature the reaction was studied up to 9 torr. The E/P_0 values used in the drift tube ranged from 1.48 - 4.45 V/cm torr, so the increase in the collision energy in the center-of-mass coordinate system corresponds to a field heating of less than ∿8°C. Ions from the drift tube effused directly into a time-of-flight mass spectrometer where the mass spectrum was determined by ion counting. Differential pumping between the drift tube and the mass spectrometer was not used. Approximate values for the rate constant were first obtained by neglecting all reactions except reaction (1) and analyzing the data with $P_0 \leq 3$ torr. A more accurate value was obtained at room temperature by correcting for the following reactions using the high pressure data:

$$Ar^+ (^2P_{1/2}) + Ar \rightarrow Ar^+ (^2P_{3/2}) + Ar + KE \qquad (2)$$

$$Ar^+ (^2P_{3/2}, {}^2P_{1/2}) + X \rightarrow \text{Impurity ions} \qquad (3)$$

$$Ar_2^+ + X \rightarrow \text{Impurity ions} \qquad (4)$$

After such an analysis it was found that $k_1 = 2.1 \times 10^{-31}$ cc^2/sec.

This research was supported by the Robert A. Welch Foundation.

*A more detailed account of this work will be submitted for publication to the Journal of Chemical Physics.

MASS SPECTROMETRIC STUDIES OF WATER CLUSTERS*

Frank T. Greene, Jacob E. Beachey, and Thomas A. Milne
Midwest Research Institute, Kansas City, Mo. 64110

A combination of mass spectrometry and molecular beam sampling techniques was used to measure the equilibrium concentrations of water clusters. From a determination of these equilibrium cluster concentrations as a function of a temperature heats of formation, and hence hydrogen bond strengths, can be deduced.

The basic apparatus used for most of these studies was a double cell consisting of a thermostated reservoir which determined the water pressure and an independently thermostated upper chamber which determined the water vapor temperature. The water vapor expanded through a small orifice, was chopped by a vibrating reed driven at its resonant frequency, and was collimated into a molecular beam. This molecular beam was passed through a differentially pumped chamber and was then introduced into the ion source of a Nuclide 12-90 HT single focusing mass spectrometer where it was ionized by electron bombardment. Ion counting with synchronous demodulation was used to improve the stability and signal-to-noise ratio and to facilitate the use of the long integration times which were often required.

In order to obtain measurable cluster concentrations it was often necessary to use combinations of pressures and orifice sizes which produced noneffusive flow through the sampling orifice. As a consequence, possible sampling perturbations had to be considered. Mass separation and cluster production during the beam formation process were anticipated and observed under some conditions. In addition, it was found, surprisingly, that for small orifices, thicknesses of the order of the orifice diameter could perturb the dimer concentrations. The extent of ion-molecule reactions was also determined and found to be negligible under sampling conditions of interest.

A reliable value for the heat of dimerization of water of 5.0 kcal per mole was obtained. These two results support a hydrogen bond strength in water of about 5 kcal per mole. In addition to the dimer and trimer data, preliminary concentration measurements were made for several higher clusters. The measured cluster concentrations, which were calculated assuming additive cross sections, are given in Table I.

TABLE I

EQUILIBRIUM MOLE FRACTIONS OF WATER POLYMERS
AT 50 TORR MONOMER PRESSURE AND 40°C

$(H_2O)_2$	$(H_2O)_3$	$(H_2O)_4$	$(H_2O)_5$	$(H_2O)_6$
6.6×10^{-4}	1.9×10^{-6}	3.9×10^{-6}	7.4×10^{-8}	1.2×10^{-6}

*This work was supported by the Chemical Physics Branch, Office of Saline Water

Simple Method for Adiabatically Sampling Reactive Gaseous Systems for Mass Spectrometric Analysis

J. R. Wyatt, J. J. DeCorpo, M. V. McDowell
and F. E. Saalfeld
Chemistry Division
U.S. Naval Research Laboratory
Washington, D.C. 20375

ABSTRACT

An understanding of the nature of the chemical processes occurring in dynamic, reactive, gaseous systems, such as hydrocarbon flames and chemical lasers, requires knowledge of the chemical species that actually exist in these systems. This paper reports the design and use of a flow-type reactor tube which is passed through the ion source of a mass spectrometer permitting the components of a reacting gas phase system to be extracted adiabatically through a 10 μ orifice into the ion source for analysis. The procedure for drilling this orifice with a focussed CO_2 laser is presented, together with data which indicate that the reactive species extracted from a flame zone are representative of those existing within the reactive system.

(Submitted for publication in The Review of Scientific Instruments).

MASS SPECTROMETRIC ION SAMPLING FROM REACTIVE PLASMAS

by

M. J. Vasile & G. Smolinsky
Bell Laboratories
Murray Hill, New Jersey 07974

ABSTRACT

As part of a study to obtain more information on the mechanism by which polymers are formed in gas discharges, an apparatus was constructed to sample ionic and neutral species from 13 MHz discharges in which such polymerization is taking place. The system studied in most detail was a mixture of vinyltrimethylsilane (VTMS, $C_2H_3SiMe_3$) and argon in concentrations from 1 to 13% VTMS. Discharges were set up in a capacitively coupled system which has the capability of sampling different regions of the discharge via movable electrodes. The pressure range examined was 0.1 to 1.0 torr.

Two distinctly different distributions of ionic species were observed when discharge parameters were varied. For example, at pressures less than $\sim$ 0.3 torr the dominant ions consisted of H_2^+, H_3^+, Ar^+, ArH^+, and C_2 fragments. As the pressure was increased above 0.3 torr using a fixed power input, the total number of ions observed decreased sharply. The dominant ions in this mode were silicon containing fragment ions $SiMe_3^+$ and $HSiMe_2^+$. The silicon containing fragment ions observed from the discharge were the same as those found by electron impact on the VTMS molecule, however, the relative intensities of these ions were completely different from those obtained by electron impact. The characteristic ion distribution could also be changed from one regime to another at constant pressure by a change in power input.

Neutral species observed from the discharge also were pressure/power dependent. At low pressures or high input power C_2H_2, C_2H_4, and H_2 were the dominant neutrals. At high pressures or low power the silicon containing neutral fragments were observed in addition to the aforementioned.

Some rather unexpected results were obtained:

1- For discharges with less than 13% VTMS, neutral molecules (i.e. unreacted VTMS) could not be detected. The discharge was found to effect at least 95% of the monomer, in spite of a low steady-state ion/electron concentration.

2- Under conditions where the electrons in the discharge had enough energy to ionize Ar or H_2, and the probability of secondary collision before the ions sampled was low, almost no evidence of primary electron impact products of VTMS was found.

3- A search for associated ions or neutrals under low resolution/high transmission operation of the spectrometer showed these species to be absent.

A more detailed report of these findings has been submitted as a two part paper to the International Journal of Mass Spectrometry and Ion Physics.

AN EXPERIMENTAL INTERNATIONAL CONVERSATIONAL MASS SPECTRAL SEARCH SYSTEM

Stephen R. Heller, Henry M. Fales, G. W. A. Milne, Richard J. Feldmann, National Institutes of Health, Bethesda, Maryland 20014, N. R. Daly, D. C. Maxwell, and A. McCormick, Mass Spectrometry Data Centre, Aldermaston, Reading, U. K.

Abstract

A prototype of an interactive, conversational mass spectral search system, developed at the National Institutes of Health, has been tested since September 1971 and is now being used by more than 200 scientists in the U. S. and Canada. The response has led to management of the system being given to the Mass Spectrometry Data Centre, Aldermaston, England for use by the international mass spectrometry community.

COMPUTER DETECTION OF MS PEAKS BY REAL-TIME CROSS CORRELATION

N. W. Bell
HEWLETT-PACKARD CORP.

The problem is to detect mass "peaks" in an incoming train of digital samples of ion current. When a peak is detected its mass and area should be accurately determined. It is a challenging task because of the wide range of peak areas, the speed requirements, and the noise contamination.

The solution to be described is a computer algorithm that was developed for a digitally-controlled mass filter scanned at 325 AMU per second. (The program can be adapted to a continuous scanning mass filter using a mass marker.) Briefly, the computer examines stored samples of ion current signal and decides if a peak has been scanned. The decision process is based upon a modified cross-correlation technique[1] used in communications and other areas to locate a shape that is similar to a reference shape represented by a number sequence, f_t. A simple reference shape for skewed quadrupole peaks is the sequence of integers 1, 3, 4, 3, 2, 1. This sequence is cross-correlated with the stored samples of ion current signal represented by $g_{t+\tau}$. The discrete cross-correlation function is given in equation (1):

$$C_\tau = \sum_{t=0}^{m-1} f_t \, g_{t+\tau} \tag{1}$$

When the reference peak is 1, 3, 4, 3, 2, 1, C_τ is simply:

$$g_0 + 3g_1 + 4g_2 + 3g_3 + 2g_4 + g_5$$

When the signal sequence matches the reference, the cross-correlation function rises abruptly. Since noise bursts can produce similar rises, mass peaks cannot be detected reliably by simply looking for peaks in the correlation, C_τ. Further, it is not practical to eliminate the noise by thresholding the correlation because shifts in the signal baseline produce large shifts in the correlation. Black[2] proposed a method of suppressing the background by subtracting from each signal sample the average of the stored samples. This method enhances the structure and suppresses the background. The average is defined in equation (2):

$$A_\tau = \frac{1}{m} \sum_{n=\tau}^{\tau+m-1} g_n \tag{2}$$

when m = 6 the average is:

$$(g_0 + g_1 + g_2 + g_3 + g_4 + g_5)/6 .$$

The modified cross-correlation function will be called the detection function because it is used to detect MS peaks. The function is defined in equation (3):

$$D_\tau = \sum_{t=0}^{m-1} f_t(g_{t+\tau} - A_\tau) \qquad (3)$$

If the 1, 3, 4, 3, 2, 1 sequence is used as f_t and if 7/3 is approximated by 2, the detection function becomes simply:

$$-g_0 + g_1 + 2g_2 + g_3 - g_5 \cdot$$

Note the simple integer coefficients.

The detection function rises rapidly when the incoming data train matches the reference peak. There are negative lobes on both sides of the rise due to the subtracted average. Figure 1 shows the detection function for a signal that is equal to the reference peak and for a signal that is 3 times the amplitude of the reference. The maximum of the function coincides with the ion current peak. The signal offset is nearly suppressed so that a threshold may be used to decide when a peak has passed. D_τ and $D_{\tau+1}$, the current and previous values of the detection functions, are sufficient to find the location of the ion peak and to find when the peak has passed.

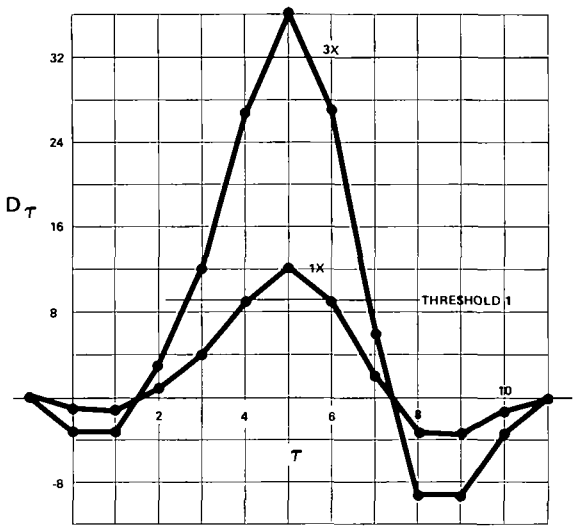

Figure 1. Detection Function

After the detection function has been calculated, we apply the 6 tests shown in Figure 2 to see if a peak is present. Test 1 checks that the previous value of D in box 7 to see if it is below the threshold. If it is we know that the previous peak has been completed, a fact that is remembered. In decision 2 we check that the previous peak has been completed. If so we get to decision 3 to see if D is decreasing. This check

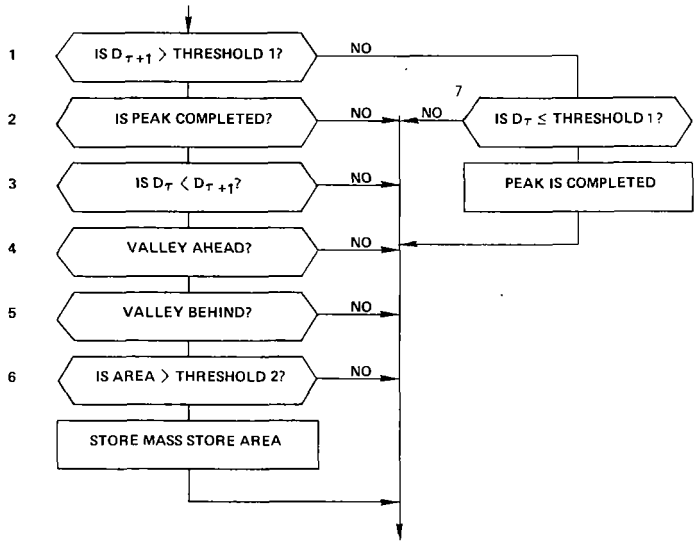

Figure 2. Six Peak Tests

locates the top of the peak. Next we look ahead in the stored samples to see if there is a valley. The test requires that the signal at the tentative peak location be at least twice the value at the valley .5 AMU ahead. Next we apply a similar test to the valley behind the peak. (These tests may eliminate peaks due to multiply charged ions.) If the peak has valleys on both sides we go to decision 6 and check that the area under the peak is greater than a second threshold. This test rejects noise pulses that have less area than a real ion peak. If all 6 tests have been met a peak has been detected. We store the mass and the area of the peak and go on.

In Figure 3 the entire process is shown. The ion current signal is read and stored along with the previous samples. The mass filter is shifted to be ready for the next iteration. (This operation would be omitted with a self-scanned MS.) Next the old detection function is shifted to make room for the new one, D_τ. The new detection function is calculated and the 6 tests of Figure 2 are applied to see if a peak is present. If one is found its mass and area are stored. Next the area under the signal samples is calculated in preparation for the next iteration. The process is repeated until the end of the spectrum is reached. By careful programming and the use of integer arithmetic the loop time was made 308 microseconds with a Hewlett-Packard 2100A Computer. This provides a scan rate of 325 AMU/second with a tenth AMU sampling intervals. A program option provides signal averaging of the ion current with a scan speed reduction proportional to the number of samples taken.

Experience under varied conditions has shown that the algorithm provides better noise immunity, more accurate mass and abundance information, and a wider dynamic range than previously known methods.

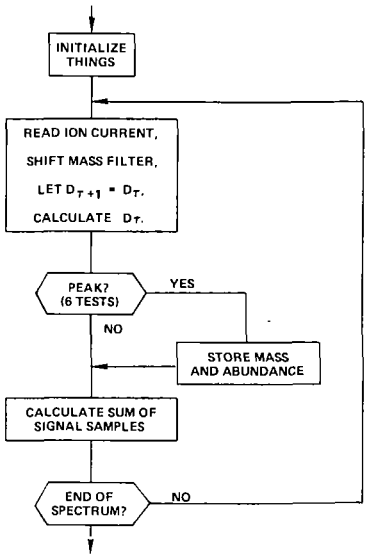

Figure 3. Peak Detection Flow Chart

References

1. J.S. Bendat and A.G. Piersol, Measurement and Analysis of Random Data, Wiley, 1966.

2. W.W. Black, "Application of Correlation Techniques to Isolate Structure In Experimental Data", Nuclear Insts. and Methods, v. 71 (1969), 317-327.

A Self-Training Interpretive and Retrieval System for Unknown Mass Spectra. R. VENKATARAGHAVAN, K.-S. KWOK, G. PESYNA, and F. W. MCLAFFERTY, Dept. of Chem., Cornell Univ., Ithaca, N.Y. 14850.

A self-training system is described for computer interpretation of mass spectra which utilizes directly data of all available reference spectra, and does not require prior spectra/structure correlations of these data either by human or computer effort. Ten different classes of spectral data have been defined for the computer, which are known to have high structural significance, such as characteristic ions, series of ions, and masses of neutrals lost. The computer extracts these data from the unknown mass spectrum and matches them against the corresponding data of 25,000 reference spectra. The Wiswesser Line Notations of the reference compounds of closest match in each data class are examined for common structural features; the reliability of computer identification is generally 95 - 99%. A dedicated PDP 11/45 system will be described which makes possible the real-time application of STIRS. For this the present FORTRAN program requires 10 to 12 minutes for one unknown; a machine-language program in preparation should reduce this time requirement by an order of magnitude.

References:

K.-S. Kwok, R. Venkataraghavan and F. W. McLafferty, J. Amer. Chem. Soc., 95, June (1973).

F. W. McLafferty, M. A. Busch, Kain-Sze Kwok, B. A. Meyer, Gail Pesyna, R. C. Platt, Ikuo Sakai, J. W. Serum, Akira Tatematsu, Rengachari Venkataraghavan, "Mass Spectrometry and NMR Spectroscopy in Pesticide Chemistry," F. J. Biros and R. Haque, Eds., Plenum Press, New York, 1973.

Resolution Enhancement by Iterative and Fourier Techniques

M. F. Zabielski and T. M. McHugh
United Aircraft Research Laboratories, E. Hartford, Conn. 06108

Extended Abstract

THEORY

It is well known that the distribution of energy in a spectrum obtained with a real instrument can vary considerably from the "true" or "ideal" distribution. It is also known[1] that the distortion on the ideal data can be represented by the Fourier convolution integral

$$F(x') = \int_{-\infty}^{\infty} T(x)A(x'-x)dx \qquad F = AT\text{(matrix form)} \qquad (1)$$

where: $F(x')$ represents the actual output of the instrument; $T(x)$ represents the ideal distribution free of the instrument smearing effects; $A(x'-x)$ represents the smearing effects that the instrument introduces on the ideal distribution.

The effective resolution of an instrument can be improved by solving this equation for the ideal distribution, which in matrix form is simply

$$T = A^{-1}F \qquad (2)$$

where $A^{-1} = A^{\dagger}/|A|$ and $A\dagger$ is the adjoint of A. However, in practical cases, as the number of data points used to define A becomes large, $|A| \to 0$, and hence $A^{-1} \to \infty$. For this reason equation (2) is frequently referred to as "ill-conditioned".[2,3]

For the above integral to be a valid representation of instrument behavior, several conditions must be satisfied. First, the instrument must be stable while all data are obtained. Second, within the spectral region under consideration, there must be only one smearing function $A(x)$. Third, the smearing function should have only one maximum and have zeros at its ending points. Finally, the noise content of the data should be low.

Of the many techniques that can be employed to solve equation (1) for the ideal function, Fourier techniques and the modified Gauss-Seidel iteration, which will be described below, can readily be implemented. The works of Rautian[1], Morrison[4], and Dromey and Morrison[5] describe the principles and methods of Fourier deconvolution. The Gauss-Seidel iterative technique is also a well-known mathematical technique[6]; however, application of this technique, like the above Fourier technique, yields oscillatory solutions. However, these oscillatory solutions can be suppressed if this technique is modified as written below

$$t_j^{(i+1)} = ZH(Z)$$

where

$$Z = \alpha\left(Y - t_{j-1}^{(i+1)}\right) + t_{j-1}^{(i+1)}$$

$$Y = \frac{G}{1+Ga_{jj}}\left(f_j - \sum_{n=1}^{j-1} a_{jn}t_n^{(i+1)} - \sum_{n=j+1}^{N} a_{jn}t_n^{(i)}\right)$$

and where f_j is an element of the output matrix, t_j is an element of the ideal matrix, a_{jn} is an element of the apparatus matrix, i designates the iteration number, α and G are constants, and H(Z) is the Heaviside step function. This modified iteration has its origins in the analog work of B.R.F. Kendall,[7] which was extended by him and one of us (M.F.Z.)[8], and also by J. Rarick[9]. The distinctive elements of this iteration are the incorporation of the terms H(Z), G, α. The Heaviside step operator constrains the solution to be positive semi-definite. The term G, which is similar to the gain in the analog work, can be viewed as a relaxation factor. Finally, the term α serves as a filter which suppresses oscillatory solutions resulting from inaccuracies in the data. Typical values of these parameters are G = 10-30 and α = 0.5-0.75. In addition to the standard convergence criterion ($F-AT<\varepsilon$, where ε is an arbitrarily small number), we have also imposed the criterion that after the normalization of $A(x)$, the area under the output function $F(x)$ must equal the area under the ideal function $T(x)$. This criterion arises from a property of the convolution integral[1].

RESULTS

Synthetic problems were generated by the computer through the convolution of Dirac delta functions with Gaussian apparatus functions. Peak height information was carried by multiplying these delta functions by constants of appropriate magnitudes. These problems typically consisted of 50 to 70 data points. Both the Fourier inverse convolver and direct division techniques were employed. For those problems where the spacings

between the delta functions were large relative to the Gaussian σ, solutions based on peak height were obtained to better than 0.05% with execution times of approximately 0.5 sec.* Peak locations were generally within the digitization error. Similar results were obtained with the modified Gauss-Seidel technique after 15 to 20 iterations with execution times of approximately 5 sec. For those cases where the distances between delta functions were small relative to the Gaussian σ, the Fourier solutions were oscillatory. The oscillations in these solutions were then suppressed as much as possible with "windowing" techniques[10,11]. If the remaining small oscillations were ignored, the errors in both peak heights and areas ranged between 5-10%. For the same types of problems, the iterative technique, after 20 iterations, had similar peak height errors of 5-10%; however, the area errors were less than 1%. After 50 iterations, the peak height errors remained essentially unchanged, while the area errors decreased to less than 0.1%.

Spectra from a defocused time-of-flight mass spectrometer were also processed. Peaks in the region from 36 amu to 46 amu were considered. These peaks were due to Ar, CO_2 and fragments of C_4H_{10}. This region was chosen because the instrument function could be obtained from the spectra of pure Ar and pure CO_2. Both graphical and calculational methods were used to obtain this function. The graphical method consisted of plotting the data on a semilog scale and proceeding by trial and error. The calculational method was premised on the convolution property that the functional forms of T and A can be interchanged. If the mass scale of the instrument is defined and if the natural isotopic abundances are assumed to exist at the correct locations on this mass scale, then A(x) can be calculated from F(x). The self-consistency of this method was checked by using the computed A(x) to redetermine the abundances. For all spectra considered, the iterative technique completely resolved all of the peaks in this interval (36-46 amu) including the $C_3H_6^+(42)$ fragment which was barely visible in the leading edge of the $C_3H_7^+(43)$ peak. Quantitative results based on peak areas were accurate to better than 10%. On the other hand, the Fourier methods were unsuccessful in completely separating all of the peaks being considered because of the smoothing that was necessary to suppress oscillatory solutions; however, the $C_3H_6^+$ was made clearly visible from the $C_3H_7^+$. The quantative results based on peak heights were usually accurate to within 25%. Areas were not used because of the remaining overlaps.

SUMMARY

For the data considered, both the Fourier and iterative techniques can yield reasonable peak locations. With regard to execution time, the Fourier techniques are 5-20 times faster; however, the iterative technique requires approximately one-third the core of the Fourier methods. For overlapping peaks of approximately equal magnitude, the Fourier technique can yield quantitative information. For unresolved peaks whose magnitudes vary by more than a factor of 2 to 3, the Fourier methods do not yield quantitative information apparently due to its sensitivity to noise and Gibbs phenomena. The modified Gauss-Seidel iteration, when considering areas, can yield quantitative information in those cases where the Fourier methods are no longer useful. This seems to result from the fact that the iterative method is not subject to Gibbs phenomena.

FUTURE WORK

Further work is planned in the area of smoothing techniques. Additional "window" functions are being investigated for use in the Fourier techniques. Also, multipoint weighting in the iterative method is a planned extension to the two point weighting that has been used. In the real cases considered to date, no attempt has been made to correct the width of the apparatus function over the mass range of interest. This omission is a cause of some of the observed errors. Consequently, the program will eventually incorporate a peak width correction routine.

REFERENCES

1. Rautian, S.G., Soviet Physics (Uspekhi), 1(66), 245 (1958).
2. vonNeumann, J., and Goldstine, H.H., Bull. Amer. Math. Soc., 53, 1021 (1947).
3. Tal, A.A., Univ. of Maryland, Sci. Rpt. 1, WBG-8D, Jan. (1967).
4. Morrison, J.D., J. Chem. Phys., 39, 200 (1963).
5. Dromey, R.G., and Morrison, J.D., Int. J. Mass. Spec. Ion Phys., 6, 253 (1971).
6. Varga, R.S., Matrix Iterative Analysis, Prentice Hall, N.J. (1963).
7. Kendall, B.R.F., Rev. Sci. Instr. 33, 30 (1962).
8. Kendall, B.R.F., and Zabielski, M.F., Fifteenth Annual Conference on Mass Spectrometry and Allied Topic, Denver, Colorado, 1967.
9. Rarick, J.P., M.S. Thesis, Pa. State Univ., 1969; also, Sci. Rpt. No. 344, Ionosphere Res. Lab, Pa. State Univ., November, 1969.
10. Lanczos, C., Discourse on Fourier Series, Oliver and Boyd, London (1966).
11. Gold, E., and Rader, C.M., Digital Processing of Signals, McGraw-Hill, N.Y. (1969).

* PDP-6

ION SPECTRA FROM MASS SPECTRA

Robert W. Kiser and Buddy L. Bruner
Department of Chemistry
University of Kentucky
Lexington, Kentucky 40506

It has become more common in the past decade to identify the composition of ions in a mass spectrum by making precise mass measurements. Earlier and still frequently used approaches employ chemical knowledge and intuition in the identification process; these methods, usually tedious and incomplete, both benefit and suffer due to their inherent subjectivities. This subjective approach remains practical, however, particularly in those installations that do not include high resolution mass spectrometers. The intent of this work was to remove much of the subjectiveness and to increase the thoroughness of mass spectral interpretation in the absence of precise mass measurements. The underlying strategy is to deconvolute the mass spectrum through exploitation of the uniqueness of the isotopic abundance patterns of individual ions.

To minimize subjectivity, all possible atomic combinations of the elements present in the supplied molecular formula are used to generate every possible ionic species. A Diophantine equation is used to obtain all possible isotopic permutations and enable the construction of the fractional abundances for all isotopic components of the ionic species whose masses are within the mass boundaries of the experimental spectrum being considered. The fractional abundances of the isotopic components for each ion are taken as the coefficients of a set of linear non-homogeneous simultaneous equations. The unknowns in these equations are the amounts of the monoisotopic species. The products of the isotopic coefficients for a given mass times the unknown amounts are set equal to the relative abundances for each corresponding mass in the experimentally determined mass spectrum.

The number of equations and the number of ionic species dictate the feasibility of solution. Practical computer considerations currently limit us to a maximum of 150 equations with 90 ionic species. The experimental spectrum is not bound by such artificial restraints; consequently, it is necessary except in cases of the simplest molecules to partition or "block" the complete set of equations and species into smaller subsets. Since most mass spectra consist of relatively discrete groups of peaks, it is possible to block a mass spectrum so that the corresponding sets of equations are (for practical purposes) independent and meet the computational limitations. The blocking and resultant mathematical independence of the blocks essentially is achieved by requiring that the relative abundances of all ions within a block be greater than 0.2%.

With any set of these equations one of three cases will be recognized: the system is (i) overdetermined (and usually inconsistent), (ii) unique, or (iii) underdetermined. Case (ii) is handled directly and solutions obtained through inversion of the coefficient matrix. An overdetermined system (case (i)) is first reduced to the normal equations by requiring that the sum of the squares of the residuals be a minimum and then treated as case (ii). In the event that any solution goes negative in this treatment, the overdetermined equations are solved instead by requiring that the absolute value of the residuals be minimal and equal and that all solutions be positive. The simplex algorithm is employed in the latter instance.

No mathematical solution is possible for an underdetermined system of equations (case (iii).) One is forced, therefore, to reduce the number of ionic species in order to obtain any information from this block. Any such procedure is necessarily subjective and may only be judged on the basis of its performance. First, minimal valence considerations are invoked to delete ionic species that exceed a saturated system by more than one bond. This restriction is not severe and merely removes unlikely species (e.g., CH_6^+; note, however, that CH_5^+ is retained as a distinct possibility). Subsequently, the "central atom" concept may be used (through data entered from a control card); this is based upon nearest

neighbor interactions and prevents consideration of unlikely atomic combinations (e.g., C_3^+ would not be permitted in the mass spectrum of $Cr(CO)_6$, whereas CrC_3^+ would be). Metastable transition data also may be used, if available, to assist in the determination of the daughter ion composition from the determined composition of its precursor. For this reason, the data blocks are treated in order of decreasing M/z. Also, (and usually only as a last resort) use may be made of the "small neutral" concept to select a given species from among several possible; the assumption made is that ionic decompositions tend to proceed *via* the elimination of a neutral fragment which contains relatively few atoms. Although the application of the "small neutral" concept has proven useful and does guarantee the reduction of an underdetermined system, it remains a very subjective approach and the majority of present shortcomings in the treatment are attributable to necessary utilizations of the "small neutral" concept.

The deconvolution schema described was programmed in FORTRAN IV for the IBM 360/65. To maximize computational speed, the program and all storage arrays were maintained incore. The machine-computed ion spectrum was compared with the results of hand computations for each molecule. The "correct" assignments were based in most cases on high resolution mass spectra and were assigned by judicious use of metastable transition information. The final comparisons were quantified by employing a performance index.

The performance index must weigh most heavily the most abundant ions. For this reason, all spectra were subdivided into six "triploids" - those ions with intensities in the range of 30-100% of the base peak (t_1), 10-30% (t_2), 3-10% (t_3), 1-3% (t_4), 0.3-1% (t_5), and 0.1-0.3% (t_6). Since the blocking is accomplished at 0.2%, only few values below 0.1% will be encountered (largely doubly-charge ions), and these are treated as if they belonged to the t_6 triploid. The weighting factor applied to each triploid is the maximum abundance of that triploid, expressed as a fraction. The performance index used is given by

$$P = 100 \cdot \prod_{i=1}^{6} \left[(0.04)^{f_i^e \cdot w_i} \right]$$

where f_i^e is the fraction of ion assignments in error in the *i*th triploid and w_i is the weighting factor for that triploid. The value of 0.04 was chosen so that a completely erroneously determined ion spectrum would have a value of 1.

The thirty compounds listed below were chosen for study; they possess a reasonably wide range of molecular weights, varied functional groups, represent inorganic as well as organic substances, and include a distribution of elements including from one to ten isotopes/element and a range of atoms per molecule. The mass spectra were obtained for most with an Hitachi RMU-7 in our laboratory, although some data were obtained from an A.E.I. MS-9 and a Bendix 12-101. Also included were two spectra taken from the literature (mass spectral compilations) so that our coverage with these limited test data would be as broad as possible. Twenty-two spectra included peaks due to metastable transitions, and six of these spectra were supplied with electrostatic sector voltage variation data.

Methylaziridine
Dimethyl sulfoxide
n-Propyl formate
Cyclohexanone
Ethyl cyanoformate
2,2,4-Trimethylpentane
Dimethylglyoxime
Chloromethyltrimethylsilane
Nitrobenzene
Triethyl phosphate
Bis(cyclopentadienyl)iron
Pentacarbonyliron(0)
Tetraethyl silicate
Hexacarbonylchromium(0)
Bis(cyclopentadienyl)zirconium dichloride
Dibromodichloromethane
Cyclopentadienyltricarbonylmolybdenum monochloride

Trimethyl phosphite	Tris(trifluoromethyl)-s-triazine
Phenyldifluoroborane	Bis(p-chlorophenyl)disulfide
Bromochloromethane	Trifluorophosphinepentacarbonyl-molybdenum(0)
Tetrachloromethane	Hexamethyldistannane
3-Phenylnitropropane	Phosphonitrilic dichloride trimer
Cobalt tricarbonyl nitrosyl	Perfluorobutylfuran
Tetramethylstannane	

The "average" molecule in the above test group of thirty has: 17 atoms, 4 elements, M.W. = 189; its spectrum contains 153 peaks (120 of z = 1, 18 of z = 2, and 15 "metastables"), partitioned into 15 blocks; 45 ionic species are identified (3 in t_1, 5 in t_2, 9 each in t_3, t_4, and t_6, and 10 in t_5); CPU time = 45 seconds; and P = 82.4.

In the treatment of the mass spectra of the above molecules by means of the program developed, it was found that two molecules had to be deleted from further consideration. This was due to the presence of significant impurities that became obvious in the computer analyses - a welcome result of the application of this technique. The performance of the algorithms used in the program, as applied to the twenty-eight remaining molecules is shown in Figure 1. To achieve a performance index of greater than 50, no errors may be encountered in t_1 (on the average); to achieve a performance index greater than 80, no errors may be found in either t_1 or t_2. Since the eight most intense peaks in the mass spectrum will usually occur in t_1 and t_2, the "average" performance index of 82.4 indicates that the schema successfully identifies the major peaks and most of the minor peaks in a diversity of mass spectra (although C,H,N and C,H,O molecules are significantly less susceptible to this treatment at the present).

The overall performance of this approach is superior in scope and in decreased subjectivity as compared to "hand" treatments; however, this success is moderated by the present requirement of a large digital computer. The exhaustive consideration given the experimental data also is much more sensitive to the quality of those data. Small differences in ion abundances may yield misleading analyses, e.g., CHO^+ *vis-a-vis* $C_2H_5^+$. These disadvantages are to be weighed against the ability to rapidly, accurately, and relatively inexpensively process the reduction of large volumes of data. Most molecules of interest may be treated and any available metastable transition data is directly and naturally used to extract the maximum information. The final result is an ion spectrum (see Figure 2; P = 88.1 for trimethyl phosphite), a compact and unique presentation containing more information per datum than the typically tabulated mass spectrum, and which may be operated upon to easily regenerate the mass spectrum.

The authors express their appreciation for the use of the IBM 360/65 system and facilities of the University of Kentucky Computing Center.

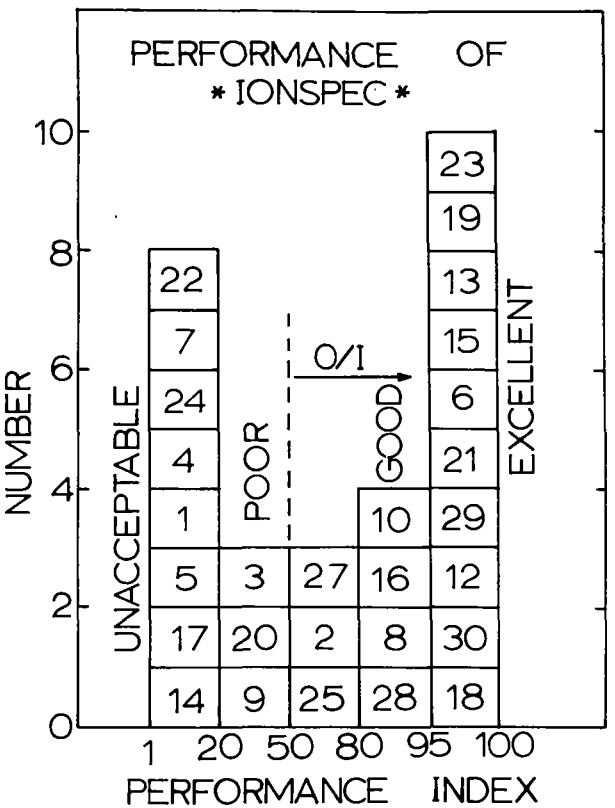

Figure 1. Performance Index of Test Molecules.

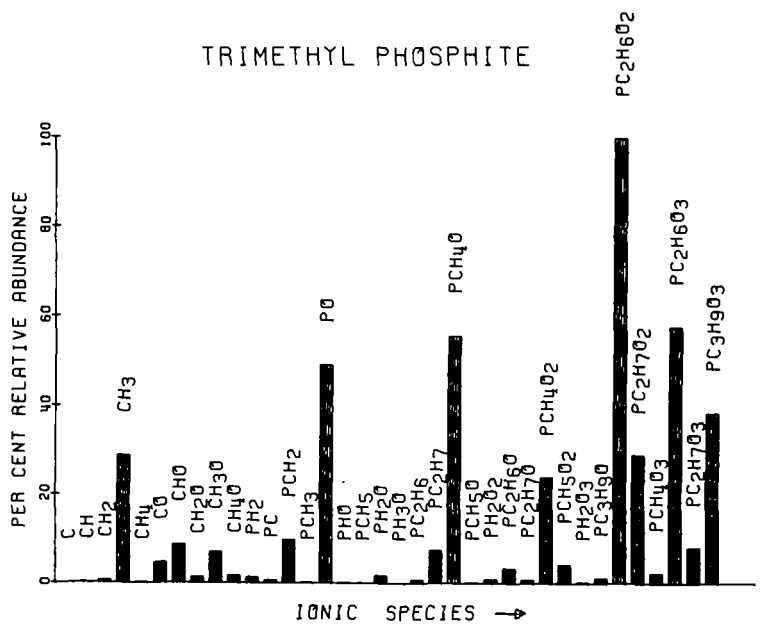

Figure 2. Ion Spectrum of Trimethyl Phosphite.

DATA FROM AND IMPROVEMENTS TO THE DA/CS-III AUTOMATION SYSTEM USED FOR ISOTOPE RATIO MEASUREMENTS BY PEAK STEPPING

At the last ASMS meeting held in Dallas, Texas, Nuclide's Automation Group reported the development of a Data Analysis and Control System used for isotopic ratio determination. Only a limited amount of data was available to report at that time. This paper will review some of the data acquired over the last year using the Nuclide DA/CS-III system. The data presented herewith have been generously provided by groups in the Department of Geology at the Ohio State University, the Department of Geology at the University of North Carolina and the Lunar Receiving Laboratory at the NASA Manned Spacecraft Center in Houston, Texas.

Prior to the introduction of automated systems for isotope ratio measurements, several manual methods were used for those determinations. For example, the spectrum of interest was scanned and each peak had to be "weighted" to compensate for irregular emission. Peak stepping (i.e., varying the MS ion accelerating potential) was introduced later. With the incorporation of magnetic field sensing devices, peak stepping by varying the magnetic field was introduced. Magnetic field sensing devices eliminated the problems associated with the magnet's hysteresis loop. All of these methods had one common disadvantage: the results were obtained only after many hours of tedious labor. In 1968, G. J. Wasserburg reported the development of a system at the California Institute of Technology which used a time-shared computer for computations. The estimated cost of this system was about $500,000. When the cost of minicomputers decreased, it became economical for laboratories to utilize dedicated computer systems. Nuclide began development of the DA/CS-III at that time.

Fig. 1 shows the block diagram of the acquisition system. The computer controls the mass spectrometer's magnetic field with a dual digital-to-analog converter. A dithering technique is employed to obtain peak centering. The voltage calculated to focus the mass spectrometer on the top of a peak is stored in the coarse D-to-A converter while the fine converter is stepped over the peak to the 50 percent peak height points. That procedure permits accurate peak centering.

The 8-channel multiplexer selects the signal to be converted by the 12-bit analog-to-digital converter. The block labeled DCVGA represents an amplifier. DCVGA gain is controlled by the computer. The CPU for this system is a model SPC-12 minicomputer manufactured by General Automation. The SPC-12 has an 8K-word core memory with 8-bit word length.

A standard stepping sequence is called a cycle. Fig. 2 shows a typical cycle. The Xs indicate points in the spectrum at which data are taken by the A-to-D converter. Each cycle is a mirror-image scan. This cycle format allows one to average peaks about a common point in time so that if a sample is decaying rapidly, the isotope abundances measured will not be biased. The average of the two points labeled READ TIME is also printed so that an interpolation back to time zero may be performed.

Fig. 3 shows a typical dialogue sequence between the operator and the data system along with the results of a set of 20 cycles. The program used for this run was specifically written for strontium analyses, where the 87-Sr/86-Sr ratio is normally corrected on the basis of adjusting 86-Sr/88-Sr to 0.1194. Use of the feature which rejects "for cause" one or more cycles of data is also illustrated in Fig. 3. As used at Ohio State, cycles, if rejected, can only be dropped in pairs, corresponding to the highest and lowest values. Notice that the principal effect of dropping ratios is that it increases the precision— the average ratio remains essentially unchanged.

Since last year we have now been able to compare the quality of the data obtained by the DA/CS-III systems with that of other automated systems and traditional mechanical calculation methods. Some 87-Sr/86-Sr ratios reported for sea water samples are plotted in Fig. 4. The samples were taken from such places as the Ross Sea, the Red Sea, and the Black Sea. The location of samples 2, 3 & 4 were not given. Note that each small division on the chart corresponds to a ratio difference of approximately 5 parts in 70,000.

All these investigators adjusted their strontium 87-Sr/86-Sr ratios on the basis of the correction necessary to make the 86/88 ratio equal to 0.1194, but no corrections were made for procedural differences occurring at different laboratories. The lines above and below each ratio in Fig. 4 are the upper and lower limits of the "windows" of values allowed by the reported standard deviation of each analysis. The number below the bottom line is the year the data was reported. Ratio #7 is a result obtained at the Ohio State University by Dr. Gunter Faure using the Nuclide DA/CS-III for a sample collected from the Red Sea. It agrees quite well with the other values. The "drop ratio" feature of the data system was not used in these measurements.

In addition, evidence is now available about the reproducibility achievable using DA/CS-III systems for comparisons of analyses of the same sample by two different laboratories. Fig. 5 shows data taken at the Ohio State University (labeled #1) and at the University of North Carolina (labeled #2). The sample was the Eimer and Amend strontium carbonate interlaboratory standard. At both laboratories the DA/CS-IIIs were interfaced to Nuclide 12-inch, 90-degree, triple-filament thermionic source mass spectrometers. The first data point shows the 87-Sr/86-Sr ratio corrected as previously described; ten sets of 5 cycles per set were used in the calculation of this ratio. Measurements were made using the standard 12-bit analog-to-digital converter shown in Fig. 1. The solid lines above and below the ratio show the standard deviation while the dotted lines above and below the point show the standard deviation of the mean. The generally accepted value for this standard is 0.7080; OSU obtained 0.70801 and UNC obtained 0.70790.

The second data point in Fig. 5 represents data taken and corrected in the same manner as the first except that 18 sets of 5 cycles per set were used. The standard deviations of a single run and the mean are shown as they were for data point #1. Notice that one large block represents a ratio difference of approximately 1 part in 7,000 in the 87-Sr/86-Sr ratio.

A conventional technique for measuring isotopic ratios is to use an integrating digital voltmeter. In order to compare this technique with the analog-to-digital conversion method used in the standard DA/CS-III, we installed a voltage-to-frequency converter followed by a counting circuit in the DA/CS-III system at the University of North Carolina. This arrangement permitted data to be taken in either mode. Integration times were increments of 1 second. This meant that a 3-second peak sampling time would result in the average of three 1-second measurements. This would give all measurements a normalization to 1 second. The voltage-to-frequency converter used gives an output frequency of 100 kHz for a 10-volt input with a linearity of 0.005%. The third data point on the graph shows the ratio calculated for 15 sets of 5 cycles per set using the V-to-F converter. The ratio of 0.70802 agrees well with the accepted value of 0.7080. The precision of the measurement appears to be slightly better than that achieved using the A-to-D converter, however more experiments must be made before accepting that conclusion.

The DA/CS-III system used in the Lunar Receiving Laboratory at the Manned Spacecraft Center in Houston, Texas is interfaced to a Nuclide 6-inch radius, 60-degree deflection SGA type "static" mass spectrometer equipped with a 20-stage electron multiplier. One of the recent analyses reported by the LRL group was the study of Xenon isotopic abundances in a sample from the Allende meteorite. The ratio of the 136-Xe peak (with an ion current of $\sim 1.2 \times 10^{-15}$ ampere) to the 132-Xe peak (with an ion current of $\sim 3.6 \times 10^{-15}$ ampere) was determined using the DA/CS-III with a relative standard deviation of the mean of 0.10% from a "run" consisting of 9 cycles. The sample size was 2.8×10^{-10} cc STP. Determination of the same ratio with a sample size of 2.1×10^{-11} cc STP (which produced an ion current an order of magnitude lower) had a relative standard deviation of the mean of 0.22% for 9 cycles. This level of precision is readily attained automatically with a system such as the DA/CS-III without extraordinary efforts on the part of the operator.

A natural application for DA/CS-III is the determination of uranium and plutonium isotopic composition. The programs required to generate reports of such analyses are more elaborate than those provided with the standard DA/CS-III package. For example, calculation for atom percent and weight percent must be made, stored, and printed. These calculations require more memory for program storage than the standard DA/CS-III programs. The 8-bit, 8K-core memory of the standard minicomputer is already essentially filled with programs and stored data. That fact plus the various advantages offered by a 16-bit machine prompted Nuclide to develop a more powerful system, i.e., the DA/CS-III/U, which uses a General Automation model SPC 16/45 minicomputer. A point-by-point comparison of these two minicomputers is not appropriate for this discussion. One should realize that the SPC 16/45 unit offers more flexibility to the overall system as well as increased memory. The SPC 16/45 is presently being used in two systems designed for uranium/plutonium data handling.

One of those systems is interfaced to two Nuclide 12-inch, 60-degree, thermionic source mass spectrometers. They are controlled alternately. The other DA/CS-III/U is interfaced to a Nuclide 12-inch, 90-degree, thermionic source mass spectrometer.

Another obvious application for the DA/CS-III system is for studies using "multiple mass monitor" or "multiple ion detector" techniques.

The standard DA/CS-III system contains all required hardware for such applications and a CRT presentation module is optionally available. In this type of application peak-switching speed and stability may be limited by the mass spectrometer's electronics. Since it is very difficult to switch the magnetic field rapidly (i.e., in the low millisecond time frame), peak switching is ordinarily accomplished by changing the accelerating potential. The multiple mass monitoring approach can also be used, for example, to measure the variations in the abundances of particular masses as a function of depth as one examines the composition of materials with an ion microanalyzer. In such work, the standard feature in the DA/CS-III system which permits automatic peak centering is especially valuable.

These applications, and others, are readily serviced with the DA/CS-III due to its modular software design. Small subroutines are called by an executive program. This format allows for insertion or deletion of subroutines as needed. The system application can therefore be changed considerably by merely changing the executive program.

In many laboratories the system user is not familiar with assembly language programming. Nor does he have available one who is trained in this area. The question then arises, how can the user make minor changes to his system programs without consulting a programmer? In the next few months Nuclide plans to implement a system using acoustic couplers whereby control of the user's computer – and therefore his mass spectrometer – can be effected using a teletype at the Nuclide plant by means of this telephone hook-up. With this capability, system program modification may be accomplished by Nuclide engineers at the customers convenience simply by placing a telephone call.

Mr. Gilbert L. Brezler
Nuclide Corporation
642 East College Avenue
State College, PA 16801

PUBS 1347-0573

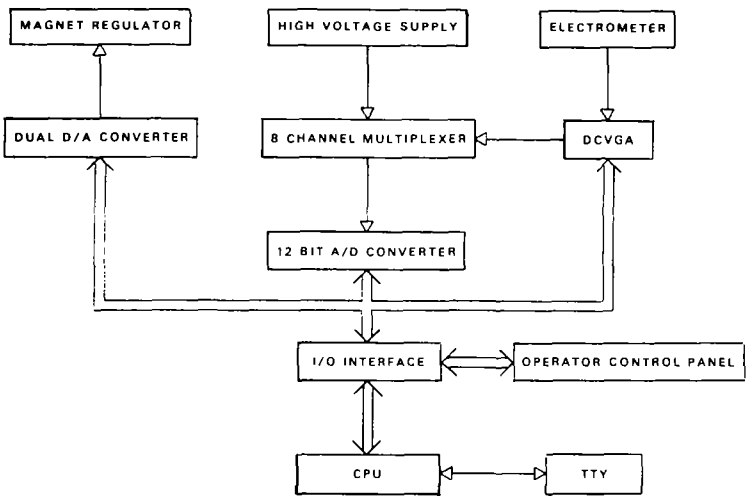

DA/CS-III SYSTEM BLOCK DIAGRAM

Figure 1

DA/CS-III STEPPING SEQUENCE

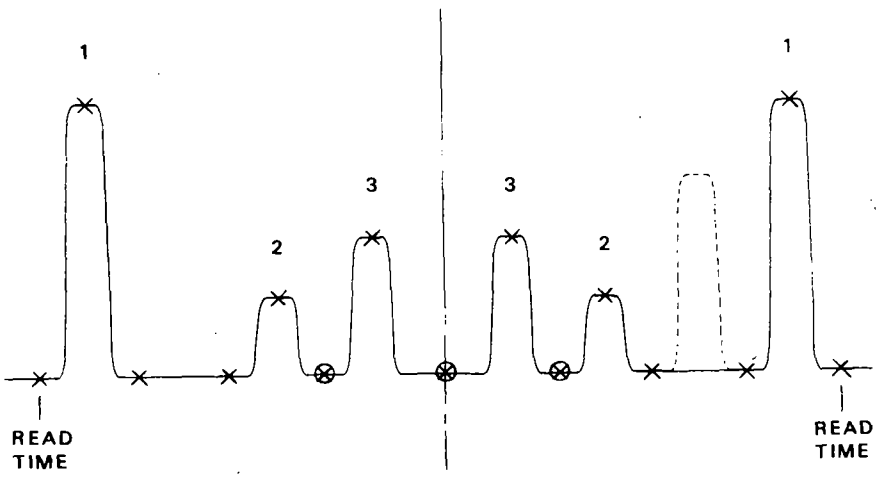

Figure 2

```
1. SAMPLE: O,F,CORE 100-3-3 RED SEA
2. SAMPLE CODE: RUN NO. 31
3. SET NO.: 1
4. DATE: 3/8/73
5. OPERATOR: FAURE
6. INST. CODE: GOLIATH
7. MEASURED MASSES: 89,87,86,85
8. MEASURE 85(Y OR N): N
9. CALIBRATE (Y OR N): N
10.ENTER CONTAM. CONST.: 2.5906
11.ENTER NO. OF CYCLES: 20
12.ENTER PEAK SAMP. TIME(IN SEC.): 2
13.ENTER BASE SAMP. TIME(IN SEC.): 2
14.SELECT MODE (A,S,M): A


SET NO. 0001

TIME CYCLE          87/86          86/88          87/86(CORR.)

0045 0001          0.70907        0.11947        0.70928
0151 0002          0.70957        0.11947        0.70979
0248 0003          0.70796        0.11955        0.70840
0345 0004          0.70820        0.11952        0.70855
0442 0005          0.70822        0.11965        0.70898
0539 0006          0.70880        0.11950        0.70910
0636 0007          0.70761        0.11955        0.70805
0733 0008          0.70852        0.11953        0.70892
0830 0009          0.70928        0.11961        0.70991
0927 0010          0.70811        0.11959        0.70869
1024 0011          0.70832        0.11956        0.70881
1121 0012          0.70791        0.11956        0.70840
1218 0013          0.70869        0.11950        0.70899
1315 0014          0.70928        0.11962        0.70994
1412 0015          0.70907        0.11952        0.70942
1509 0016          0.70846        0.11953        0.70886
1606 0017          0.70841        0.11949        0.70867
1703 0018          0.70755        0.11972        0.70848
1800 0019          0.70787        0.11959        0.70845
1897 0020          0.70889        0.11952        0.70924


RATIO AVG          0.70848        0.11955        0.70893
STD. DEV.           .00057         .00006         .00051

DROP RATIOS?Y
1,7;2,7;3,7;1,14;2,14;3,14

RATIO AVG          0.70849        0.11955        0.70893
STD. DEV.           .00053         .00006         .00044

DROP RATIOS?N
```

Figure 3

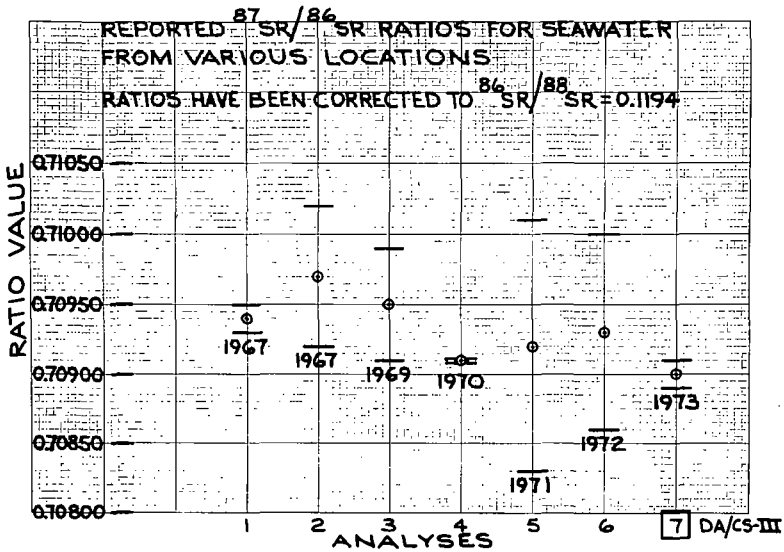
REPORTED $^{87}SR/^{86}SR$ RATIOS FOR SEAWATER FROM VARIOUS LOCATIONS
RATIOS HAVE BEEN CORRECTED TO $^{86}SR/^{88}SR = 0.1194$
RATIO VALUE
0.71050
0.71000
0.70950
0.70900
0.70850
0.70800
1967
1967
1969
1970
1971
1972
1973
1
2
3
4
5
6
7
ANALYSES
DA/CS-III

Figure 4

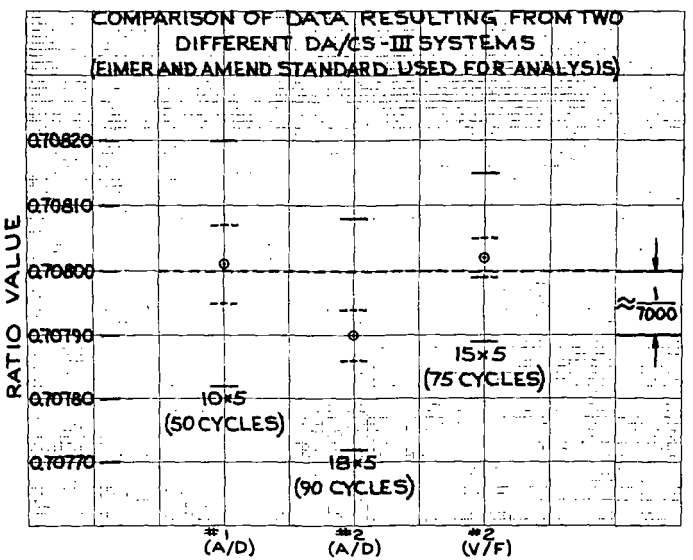
COMPARISON OF DATA RESULTING FROM TWO
DIFFERENT DA/CS-III SYSTEMS
(EIMER AND AMEND STANDARD USED FOR ANALYSIS)
RATIO VALUE
0.70820
0.70810
0.70800
0.70790
0.70780
0.70770
10×5
(50 CYCLES)
18×5
(90 CYCLES)
15×5
(75 CYCLES)
≈1/7000
#1
(A/D)
#2
(A/D)
#2
(V/F)

Figure 5

The Distinction of Isomers with A Chemical Ionization Mass Spectrometer.

EDWARD M. CHAIT, and VICTOR H. ADAMS, Instrument Products Division, E.I. Du Pont de Nemours & Co.(Inc.), Monrovia, California 91016.

One of the problems of mass spectrometry is that conventional electron ionization spectra for isomers are often indistinguishable. This makes the identification of specific isomers of a compound difficult with any degree of certainty since often one must depend on only slight variation of relative abundance to make the distinction. Some progress has been made by adding additional information with the use of ion kinetic energy spectra to obtain distinction of isomers. Chemical ionization solves the problem of differentiating isomers, by exploiting the varying structure of reactivity relationships of reagent gases. When a chemical ionization mass spectrometer is used in the gc/ms mode, it is possible by selection of the reagent gas to actually produce different spectra for different isomers where the conventional electron ionization spectra were identical. An example of this is the analyses of morphine and its isomer, dilaudid. Methane chemical ionization gives different spectra for these compounds which can be rationalized in terms of the keto-enol differences of the two isomers. Several examples will be cited on the application of the chemical ionization technique to the distinction of isomers.

Mechanisms of Fragmentation in Proton-transfer Chemical Ionization. RODGER L. FOLTZ, Battelle-Columbus Laboratories, Columbus, Ohio 43201

Relatively little attention has been devoted so far to the mechanisms by which complex molecules fragment after ionization by proton transfer under chemical ionization conditions. Field, Munson and Becker[1] have proposed a process of random attack followed by localized reaction to rationalize the methane chemical ionization mass spectra (CI-MS) of aliphatic hydrocarbons; whereas the chemical ionization fragmentation of compounds containing nucleophilic centers are generally considered to involve protonation at the nucleophilic center with fragmentation occurring at that location[2].

While the latter mechanistic view permits rationalization of the CI-MS of many compounds, it does not adequately explain some of the prominent fragment ions observed in the CI-MS of polyfunctional molecules such as the macrolide antibiotics[3,4]. Examples of isobutane CI-MS of complex molecules are described as well as the results of a model compound study providing evidence that fragmentation can occur remote from the point of protonation.

This work is being submitted for publication to the J.C.S. Chem. Commun.

1. F. H. Field, M.S.B. Munson, and D. A. Becker, Advances in Chemistry Series, No. 58, American Chemical Society, Washington, D. C. 1966, pp. 167-192.

2. M.S.B. Munson, Anal. Chem., 43, 28A (1971).

3. L. A. Mitscher, H.D.H. Showalter and R. L. Foltz, J.C.S. Chem. Commun., 796 (1972).

4. L. A. Mitscher, H.D.H. Showalter and R. L. Foltz, J. Antibiotics, 26, 55 (1973).

Performance of a Chemical Ionization Source on Both Single and Double Focussing Magnetic Sector Mass Spectrometers.

A.M. Hogg, Department of Chemistry, University of Alberta, Edmonton, Alberta, Canada, T6G 2G2

The earliest work on chemical ionization was done using a single focussing magnetic mass spectrometer (1) and it was reported that at source pressures in excess of 1 Torr no significant loss of resolution was experienced. The compounds studied however were gases or volatile liquids and so no work at high mass was reported.

Later work in other laboratories on high molecular weight compounds was done on modified high resolution double focussing instruments and in this case there was an apparent increase in resolution using the CI source (2) (3).

During the past two years, CI work in this laboratory on high MW compounds has been done using a single focussing instrument (AEI MS12) (4) and while resolution at low mass is very good it drops considerably as mass is increased. Similar problems have been experienced in other laboratories using other sector instruments with different source designs but it has been hard to determine how much is due to source design and how much to analyser geometry. Recently we have modified a double focussing MS9, which is virtually identical to the MS12 except for the addition of an electrostatic sector between the source and the magnetic sector, so that the same CI source and inlet system used on the MS12 can be mounted on it. It has thus been possible to compare directly the performance of the source with both single and double focussing analysers.

Figs. 1 and 2, show the peak shape obtained on the two instruments using identical conditions and a source pressure of 1.3 Torr. The peak at m/e 696 is the $(M + NH_4^+)$ ion from sucrose pentaacetate/NH_3. For comparison a peak of similar mass has been recorded on each instrument using the standard AEI electron impact source.

It can be seen that, while the MS9 is not greatly superior in resolution using EI and wide slits, under CI the low energy tail on the peaks is no longer detectable. Further, the peak on the MS9 is "flat-topped" and the collector slit can be reduced without loss of sensitivity to give a resolution of 3200.

In Fig.3 the resolution of the MS12 is plotted as a function of ionic mass. In attempting to obtain this data it was found that the nature of the ion had an effect on resolution and, for example, a reactant ion did not fall on the same curve as a sample ion. The points used in Fig.3, therefore, are the averages of several experiments using the $(M + NH_4^+)$ ion from the sugars xylose, glucose, 1-6 deoxy glucose triacetate, glucose pentaacetate and sucrose octaacetate. The spectra were recorded at 0.3 Torr source pressure so that unit resolution could be obtained at the highest masses allowing accurate measurement of resolving power. It can be seen from the lower curve that resolution is linearly related to $\sqrt{m/e}$ and thus to the residence time of the ions in the region of intermediate pressure between the source and the analyser entrance slit. This indicates that the major factor contributing to loss of resolution is collisions of the ions with gas molecules probably just beyond the source exit slit but after the ions have gained some kinetic energy from the accelerating field.

It seemed possible that inadequate pumping speed in the source housing was contributing to the problem but it was found that deterioration of resolution was as pronounced with NH_3, which is rapidly pumped by the liquid nitrogen trap on the source pump, as with CH_4 which is only pumped by the diffusion pump. The conductance of the pipe between the trap and the source housing is about 700 l/sec and should not be a limiting factor.

Between the ion exit slit and the source adjustable slit, are beam centering plates and a grounded acceleration plate and together they must restrict local pumping speed. In order to determine the importance of this the 1/4" high adjustable slit/acceleration plate stack was replaced by a 0.030" thick plate with a 0.004" wide fixed slit mounted on it and the original beam centering plates replaced by a pair which were machined away so as to present two narrow strips of metal parallel

to the ion exit slit and only enough of a skeleton of the rest of the plate to permit mounting and jigging. This should result in a considerable increase in local pumping speed but in fact the behaviour of the source was not noticably affected and resolution was not improved.

The only other obvious means of reducing local pressure outside the ion exit slit is to lower the throughput of reactant gas (and hence the source pressure if the dimensions of the slit are not altered) and in Fig.4 the effect of this is shown over a somewhat limited range. It can be seen that at low pressures the resolution of the source exceeds that of the standard EI source (RP $\sim$ 1100) but only at the expense of greatly reduced sensitivity. A thirty fold loss in sensitivity for the addition of ammonium ions is experienced over the range of the plot while maximum sensitivity is not obtained until a source pressure of 0.45 Torr is reached.

It is apparent that a double focussing magnetic sector instrument provides the maximum flexibility for CI work being amply capable of compensating for the energy spread of the ions under the worst case condition of high mass and high reactant gas pressures up to the point where high voltage breakdown occurs.

Single focussing geometry is much less suitable but if source pressures are limited somewhat or the conductance of the ion exit slit reduced, it is still adequate for all but very high molecular weight work. While it is sometimes difficult to determine the optimum pressure of reactant gas required for a CI experiment, particularly when the sample used is solid and its partial pressure cannot be measured, it appears that it is normally closer to 0.5 Torr then to 1.0 Torr, and in fact we are using 0.3 Torr routinely with as much success as we previously had at 1.0 Torr. At this pressure resolution with the MS12 is still 800 at m/e = 700 which is adequate for almost all low resolution work. Closing the slits provides increased resolution and R.P. > 3000 can be obtained at the cost of reduced sensitivity.

References:

1) F.H. Field, Accounts of Chemical Research 1, 42 (1968).

2) D. Beggs, M.L. Vestal, H.M. Fales and G.W.A. Milne, Rev. Sci. Inst, 42 1578 (1971).

3) J. Yinon and H.G. Boettger, Chemical Instrumentation 4, (2), 103 (1972).

4) A.M. Hogg, Anal. Chem. 44, 227 (1972).

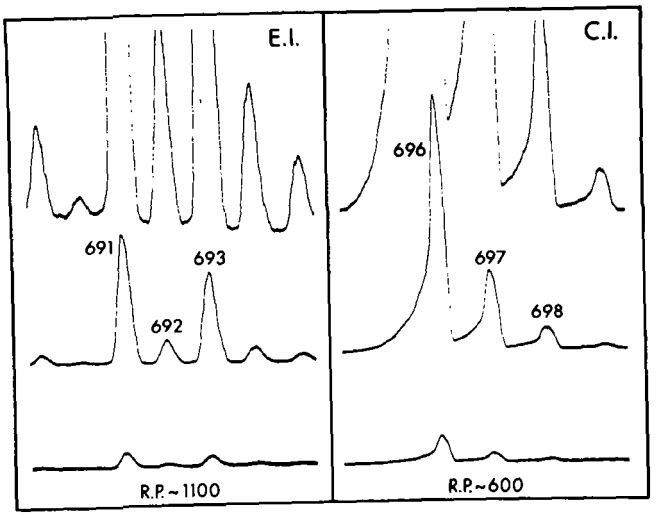

MS12 SPECTRA $W_S = W_C = 0.004"$

FIG. 1

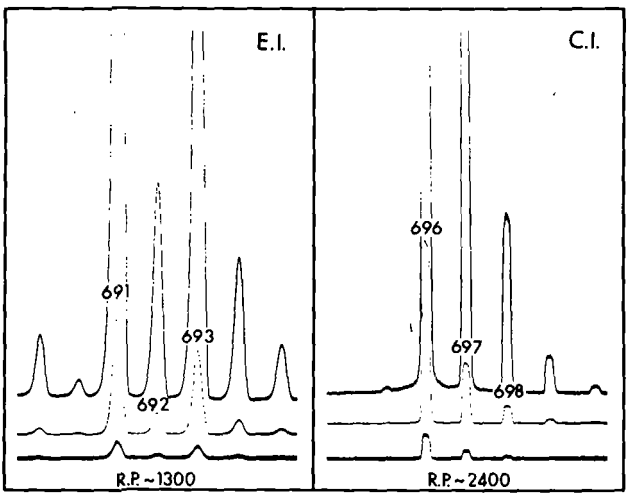

MS9 SPECTRA $W_S = W_C = 0.004"$

FIG. 2

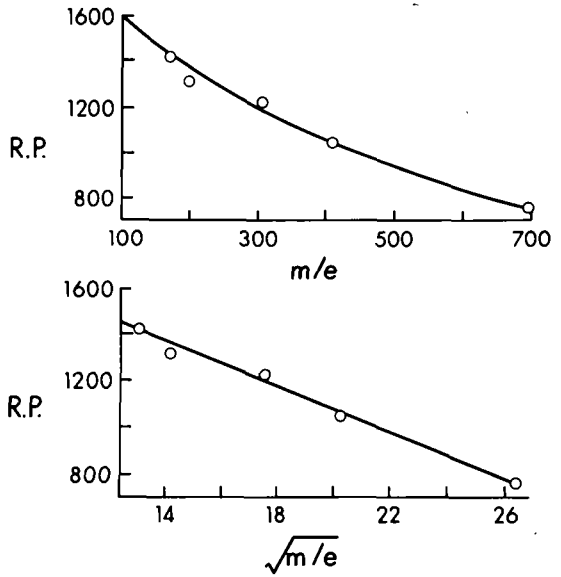
1600
1200
800
R.P.
100
300
500
700
m/e
1600
1200
800
R.P.
14
18
22
26
√m/e

FIG. 3

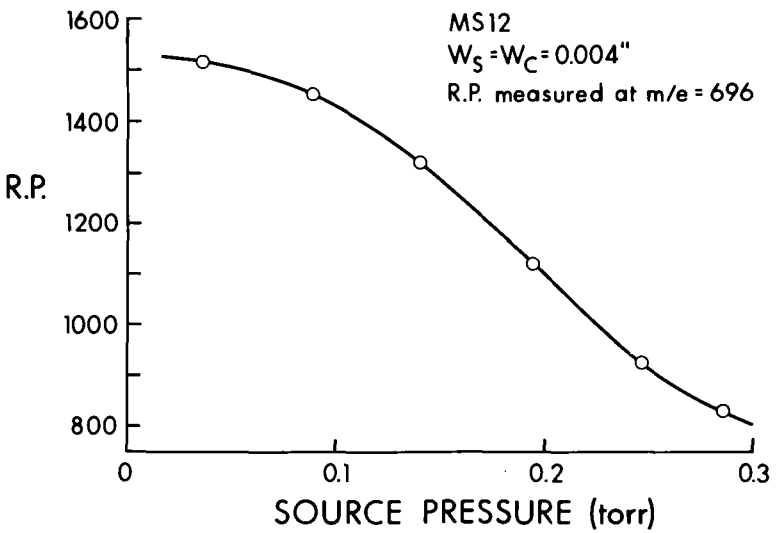
MS12
$W_S = W_C = 0.004"$
R.P. measured at m/e = 696
1600
1400
1200
1000
800
R.P.
0
0.1
0.2
0.3
SOURCE PRESSURE (torr)

FIG. 4

CHEMICAL IONIZATION MASS SPECTRA OF METAL ACETYLACETONATES

TED T. L. CHANG and CHARLES F. KUHLMAN
Wyeth Laboratories Inc., P.O. Box 8299, Philadelphia, Pa. 19101

In relation to the biological and pharmaceutical studies, the behavior of metal acetylacetonates(Me$\underline{acac}$) under the CI condition was investigated. The instrument used was a MS 902 attached with a SRI dual EI/CI source. The reagent gas was isobutane. Metal complexes studied were acetylacetonates of Co(II), Cu(II0, Ni(II), Fe(II), Al(III), Cr(III) and Fe(III).

The divalent metal complexes gave simple spectra as would be expected from a CI spectrum. The M+1 ion was the base peak, excluding the reagent gas peaks. There were very few fragment ions except a weak MH-100 (MH-Hacac) and the M+1 of the dissociated acetylacetone.

The trivalent metal complexes gave more complicated spectra than the divalent metal complexes. The chromic acetylacetonate showed two major peaks, MH and MH-100(MH-Hacac). The MH-100 was the base peak of aluminium acetylacetonate. The MH ion was negligible in the aluminium acetylacetonate spectrum.

The spectrum of ferric acetylacetonate not only showed MH and MH-100 ions, but also an intense MH-99(MH-acac) ion. The loss of acac from the MH is the result of a valency change of metal ion, as shown in the following scheme. This valency change was predominant in the spectrum of Co(III) acetylacetonate. The spectrum of Co(III) acetylacetonate was almost identical to the spectrum of Co(II) acetylacetonate.

$$Me(III)\underline{acac}_3H^+ \longrightarrow (Me(II)\underline{acac}_2H^+)(\underline{acac}\cdot)$$

$$\longrightarrow Me(II)\underline{acac}_2H^+ + \underline{acac}\cdot$$

In all cases polymerized peaks were observed. However, the polymerized peaks were 2M+1-Hacac and 3M+1-Hacac, and not 2M+1 and 3M+1. The relative intensity of these polymerized peaks enhanced considerably when the sample to reagent gas ratio was increased. Formation of these polymerized peaks are proposed as follow.

$$Me\underline{acac}_nH^+ \xrightarrow[Me\underline{acac}_n]{} Me_2\underline{acac}_{(2n-1)}^+ + Hacac$$

$$\downarrow -Hacac$$

$$Me\underline{acac}_{(n-1)}^+ \xrightarrow[Me\underline{acac}_n]{} Me_2\underline{acac}_{(2n-1)}^+ \xrightarrow[Me\underline{acac}_n]{} Me_3\underline{acac}_{(3n-1)}^+$$

A detailed account of this work will be submitted for publication elsewhere.

Skeletal Rearrangement of Allyl Acetates after Protonation by Chemical Ionization

J. G. Liehr and J. A. McCloskey

Institute for Lipid Research and Department of Biochemistry

Baylor College of Medicine

Houston, Texas 77025

In the methane chemical ionization mass spectra of allyl phenylacetate and several of its phenyl substituted analogs, abundant ions have been observed to occur at MH^+-H_2O and MH^+-H_2O-CO. This unusual mode of decomposition, not found in the corresponding electron impact spectra, is rationalized as an intramolecular electrophilic substitution of the phenyl ring by the allyl group prior to final bond ruptures:

Path I

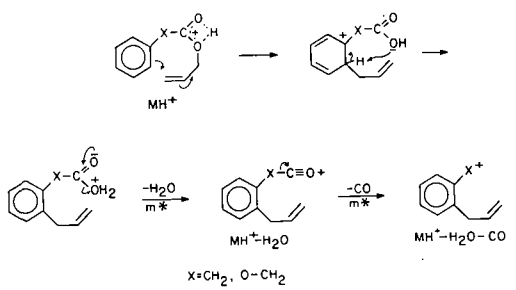

Extensive testing with the help of allyl phenoxyacetate and labeled analogs of both parent compounds revealed two pathways of hydrogen transfer, each traversed with approximately equal probability.

Path II

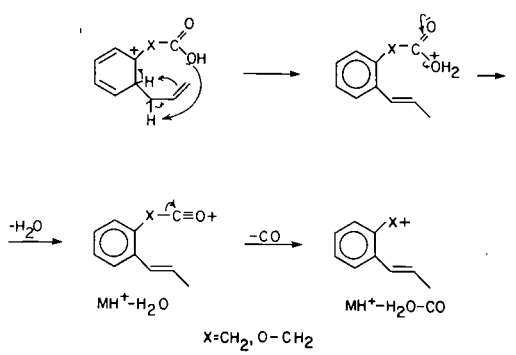

After bond formation between the allyl and the phenyl moieties, rearomatization can be achieved by transfer of the o-proton directly to the carboxyl group (path I), or to the allyl group with proton abstraction from the newly formed benzyl position (path II), thus permitting the release of water and carbon monoxide.

Attempts to influence the relative abundances of product ions by suitable substitution of the phenyl ring were successful. Since a positive charge is developed in the aromatic ring in the intermediate stage, electron withdrawing substituents have been found to restrain the rearrangement. On the other hand, electron enrichment in the ring can lead to an enhancement of the described process.

Details of this study will be published elsewhere.

Gas Phase Exchange Reactions with Tetramethylsilane Under Chemical Ionization Conditions.

T. J Odiorne, D. J. Harvey and Paul Vouros

Institute for Lipid Research
Baylor College of Medicine
Houston, Texas 77025

The electron impact mass spectrometry of trimethylsilyl (TMS) derivatives of organic compounds has produced a vast amount of evidence indicating the high reactivity of alkyl siliconium groups.[1] This has generally been characterized as attack of a positively charged siliconium moiety upon an electronegative site. We decided to utilize this property in a new type of chemical ionization (C.I.) reagent gas system.

Alkyl siliconium ions were generated in the C.I. source of a modified C.E.C. 21-110B mass spectrometer[2] by introduction of tetramethylsilane at pressures of 0.2-0.6 torr. The reagent gas spectrum shown below is typical for the pressure range of 0.2-0.6 torr.

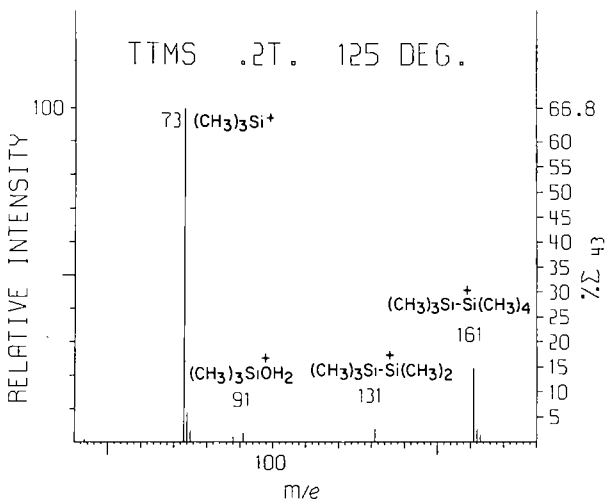

Since a large number of the molecules of biological interest require TMS derivatization before their mass spectrum can be determined, it was necessary to assess the extent of interaction between sample TMS groups and reagent gas ions. This was done by measuring the tetramethylsilane C.I. mass spectra of the perdeutero-TMS derivatives of several alcohols and acids.

The mass spectrum of the TMS-d_9 derivative of tetradecanol is typical of such compounds with the base peak at $[M+73]^+$ (m/e 368; 60 % Σ)and peaks at $[131]^+$ (m/e 426; 7% Σ), $[M+1]^+$ (m/e 296; 9% Σ), $[M+1-19]^+$ or $[M+73-91]^+$, (m/e 277; 10% Σ). However, also of significance are peaks at $[M+73-3]^+$ (m/e 365; 5% Σ), $[M+73-6]^+$ (m/e 362; 1% Σ) and $[M+73-9]^+$ (m/e 359; 6% Σ). These peaks, of course, correspond to methyl exchanges between the sample TMS group and the reagent gas. Similar exchanges for the $[M+1]^+$ ion were also observed at very low intensities. By separate experiments these exchanges were shown to be ionically and not thermally induced.

Explanation of the observed exchange processes requires determination of the origin of the $[M+73]^+$ ion. While a large portion of this ion probably results from the

simple addition of a trimethylsiliconium cation (m/e=73) to the sample molecule, $[M+73]^+$ may also be formed from the unimolecular decomposition of a higher mass adduct ion. Metastable defocussing did confirm the formation of $[M+73]^+$ ions from $[M+131]^+$, $[M+161]^+$ and other similar ions. A reasonable mechanism for the observed exchanges, utilizing the favorable elimination of tetramethylsilane, is shown below.

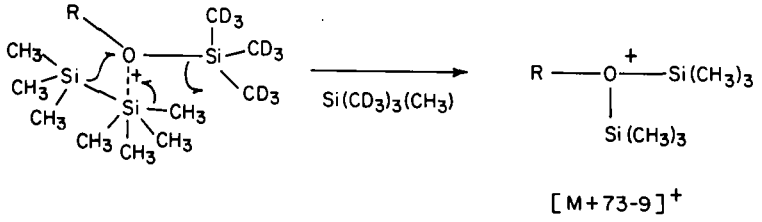

A similar argument utilizing protonated trimethylsilanol would explain the various protonated molecular ion species. The protonated silanol is formed readily from reaction of m/e = 73 (TMS) with residual water in the system. This mechanism was confirmed by saturating the system with D_2O.

Reactivity of trimethylsilyl groups in solution is strongly influenced by steric factors, and therefore we decided to investigate the analogous effects in the gas phase reaction.

C.I. mass spectra in tetramethylsilane were recorded for the TMS derivatives of 1-hexadecanol and 5-hexadecanol. The spectrum of the former was clearly dominated by a peak at $[M+73]^+$ (m/e 387; 80% Σ). The spectrum of the secondary TMS ether contained principal peaks at $[M+1]^+$ (m/e 315; 30% Σ) and $[M+1-90]^+$ (m/e 225; 35% Σ), while [M+73] (m/e 387) had virtually disappeared (1% Σ).

Thus from the work presently completed, tetramethylsilane as a C.I. reagent gas offers spectra of considerable sensitivity and simplicity plus a very strong potential for application in problems involving steric parameters.

References

1. J. Diekman and C. Djerassi, J. Org. Chem., 32, 1005 (1967).

2. I. Djidic, D. M. Desiderio, M. S. Wilson, P. F. Crain, and J. A. McCloskey, Anal. Chem., 43, 1877 (1971).

Chemical Ionization Mass Spectra of Trimethylsilyl Ethers of Biologically Important Compounds

Barbara Jelus and Burnaby Munson
Chemistry Department
University of Delaware
Newark, Delaware 19711

and Catherine Fenselau
Department of Pharmacology and Experimental Therapeutics
Johns Hopkins University School of Medicine
Baltimore, Maryland 21205

Many compounds of biological importance are converted to their trimethylsilyl (TMS) ethers in order to facilitate their separation by gas chromatography. The electron impact spectra, as well as the methane chemical ionization spectra, of the TMS ethers of one such group of compounds, the bile acids, exhibit low intensity or nonexistent molecular ions and very extensive fragmentations.

In order to identify rapidly the TMS ethers of the bile acids, a GC/MS compatible* technique that gives M or M+1 ions and retains the major fragment ions is desired. Use of common GC carrier gases such as N_2, Ar, or He as charge exchange reagents[1] was not satisfactory in that the spectra resembled the EI spectra of the compounds.

The technique of using mixed reagent gases has been discussed previously[2,3]. In this technique, several percent of a second reagent gas is added to the main reagent gas. The majority of the electron ionization is of the main reagent gas and some of these ions react with the second reagent gas. The ionization of the additive (present in trace amounts) is produced by reactions of ions from both reagent gases. The relative amounts of ionization of the additive by the two sets of reagent ions depends on the ratios of the two reagent gases. The addition of 5-10% of many compounds to N_2 drastically changes the distribution of ions from N_2^+ and N_4^+: i-C_4H_{10} gives mostly $C_4H_9^+$; NH_3 gives mostly NH_4^+; tetramethylsilane gives mostly $(CH_3)_3Si^+$; and NO gives mostly NO^+.

Addition of small amounts (up to 15 mole %) of a proton transfer reagent, such as isobutane or ammonia, to the charge exchange gas gave predominately ions that correspond to M+1 - TMSOH and little or no enhancement of M+1 ion intensity. Use of tetramethylsilane, hexamethyldisiloxane, and hexafluoroacetone as additives to the "carrier gas" also gave ions corresponding to M-TMSO and little or no enhancement of molecular ion intensity.

A mixture of nitric oxide with nitrogen (or argon or helium), in which the NO is 2-15 mole % of the mixture, proved to be the reagent system that gave the desired results of enhancement of molecular ion intensity and retention of the major fragment ions. This is shown in Tables I and II which report the partial charge exchange spectra of two bile acid derivatives.

The spectra obtained with He + NO, N_2 + NO, and Ar + NO mixtures were very similar. The abundant ion at m/e = 75 may result from impurities in the probe sample and not from the TMS derivatives. With these mixtures of NO, no deliterions effects were noted on the samples or hot wire filaments although pure NO greatly decreases the lifetime of W or Re filaments. It is projected that the conventional carrier gas will be used in the gas chromatograph and that NO will be added in the low pressure region of the inlet lines to the mass spectrometer. It is hoped that these N_2 + NO, Ar + NO, or He + NO mixtures will prove to be analytically useful for other types of compounds that give low intensity or nonexistent molecular ions in other mass spectrometric techniques.

---

* All work reported was obtained in experiments using direct insertion probe introduction of the TMS ether samples into a high pressure (CI) source of a CEC 21-110B mass spectrometer.

1. N. Einolf and B. Munson, Int. J. Mass Spectrom. Ion Phys., 9, 141 (1972).
2. G. P. Arsenault, J. Amer. Chem. Soc., 94, 8241 (1972).
3. D. F. Hunt and J. F. Ryan III, Anal. Chem., 44, 1306 (1972).

An expanded version of this paper will be submitted to Biochem. Biophys. Res. Comm. for publication.

TABLE I

CE Spectra of the TMS Ether of Methyl Lithocholate

m/e	% I add. N_2	% I add. N_2/7.8 % NO	
463	0.17	2.75	M + H and ^{13}C isotope
462	0.21	5.16	M
447	0.78	1.49	M - 15
373	4.04	7.68	M + 1 - TMSOH
372	2.84	4.26	M - TMSOH
257	0.94	1.85	
230	1.20	0.68	
215	2.68	1.27	
75	6.53	8.22	

TABLE II

CE Spectra of the per-TMS Ether of Methyl Cholate

m/e	% I add. N_2	% I add. N_2/2.5 % NO	
638	--	0.38	M
623	--	0.75	M - 15
566	--	0.72	diether impurity
459	0.66	3.00	
458	0.66	4.98	M - 2TMSOH
369	2.30	5.72	
368	1.40	4.84	M - 3TMSOH
253	2.96	2.94	
75	25.12	24.12	

INDUCED FRAGMENTATION IN CHEMICAL IONIZATION MASS SPECTROMETRY

By Ronald F. Skinner

The fragmentation patterns of many compounds in Chemical Ionization (CI) mass spectrometry have not yet been as well characterized as those which occur in Electron Impact (EI) mass spectrometry. The spectra produced in CI for many compounds differ markedly from their EI spectra and therefore different mechanisms of fragmentation can often be postulated. This paper will deal with the methane-CI spectra of a group of compounds, the cannabinoids. The ion source conditions which affect the degree of their fragmentation will be discussed and postulated fragment structures and routes of fragmentation will be given. It will be shown that ion source conditions can be changed to produce more intense fragments without changing the mode of fragmentation and that the fragments produced are wholely a result of chemical ionization and not the result of mixed EI and CI.

The cannabinoids were chosen for this study because of the general interest in their structures and the fact that their EI spectra have been well characterized making comparison of fragmentation routes possible. The major cannabinoids have three basic ring structures, figure 1, with different R substituents on each ring structure. In the most commonly found compounds R is either a methyl, propyl, or pentyl group. For the purposes of this paper the compounds will be named Cannabidiol-R, e.g. Cannabidiol-propyl, for ring structure 1, tetra-hydrocannabinol-R for ring structure 2 and cannabinol-R for ring structure 3. The fragmentation obtained in methane-CI can be shown to be the result of the particular ring structure and the amount of fragmentation a result of ion source temperature.

The instrument used for this work was a Finnigan Model 1015 quadrupole mass spectrometer equipped with a chemical ionization source. The column used was 5 ft X 2 mm i.d. glass packed with 3% OV-1 on 100/120 mesh Gas Chrom Q with a flow of 20 ml/min CH_4. No separator was used and the entire column effluent was admitted to the source. The column temperature was 220°C. The source temperature was varied to produce the desired degree of fragmentation. The source pressure, electron energy, and beam current were adjusted to give the maximum sensitivity. The source pressure was 1 torr as measured by a thermocouple gauge and the source temperature was determined by an iron-constantan thermocouple mounted on the source.

All of the cannabinoid ring structures were found to give the M+1, M+29, and M+41 mass peaks which are typical of most compounds in methane-CI. They also all show the loss of CH_3 represents the base peak in the EI spectrum. Increasing the ion source temperature was found to increase the amount of fragmentation of the ring structure but did not cause any new fragments to be formed. The fragmentation can be shown to be wholly CI by the lack of m/e 231 in the spectra of compounds with CBD and THC ring

This fragment is the base peak in the CBD EI spectrum.

Table 1 shows the major fragments of the three cannabinoid ring structures and their relative intensities. At a source temperature of 150°C m/e 81 is the base peak in the CBD CI spectrum. When the source heater is turned off and the source is at 100°C, heated only by the filament, m/e 81 is only 10% of the quasi-molecular ion, which is now the base peak. It can also be noted from Table 1 that the relative intensities of the fragments m/e 81 and m/e 135 with respect to the quasi-molecular ion are related to the parent ring structure.

A postulated mechanism for the formation of the m/e 81 fragment from the CBD ring structure is shown in figure 2. This mechanism has not been verified by deuterium labeling but seems plausible when one considers that the reaction is taking place in a gaseous solution of a strong acid. The fragmentation mechanism occurring therefore probably involves proton attack at specific centers rather than single electron transfer and the formation of radical ions. This attack causes re-arrangements and the extent to which these re-arrangements take place is the function of the ion source temperature. Increased ion source temperature makes the ions more prominent and easy to distinguish and thus aids in interpretation.

The postulated fragmentation pattern for the m/e 135 fragment is shown in figure 3 and differs from the previous mechanism in the site of proton attack on the ring. As would be expected, the m/e 81 and m/e 135 fragments are less prominent with the THC ring structure where an additional re-arrangement step would be required and are not present for the CBN ring structure where the molecule is stabilized by its biphenyl structure. Further evidence for this route of fragmentation is the fact that the delta-8-THC which has the double bond in the 8 position does not give the m/e 135 fragment.

The benzyl fragment provides an additional aid to structure determination as its mass is dependent on the mass of the R substituent. A mechanism for the formation of this fragment is given in figure 4. This mechanism involves the transfer of a positive charge in conjunction with a ring contraction. The benzyl ion is also seen with the CBN ring structure and the mechanism for its formation probably involves proton attack at the 9 position on the benzyl ring.

Thus while CI is usually used because of its lack of fragmentation, in this case the few fragments formed can provide as much or more structural information than EI mass spectra.

TABLE 1

PERCENTAGE OF BASE PEAK

SOURCE TEMPERATURE OF 150°C

Fragment	CBD	THC	CBN
m/e 81	100%	33%	---
m/e 135	37%	13%	---
benzyl	44%	15%	4%
M-15	4%	16%	29%
M	60%	100%	100%

FIGURE 1

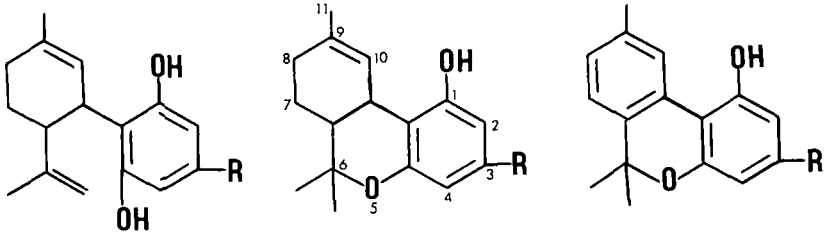

1 2 3

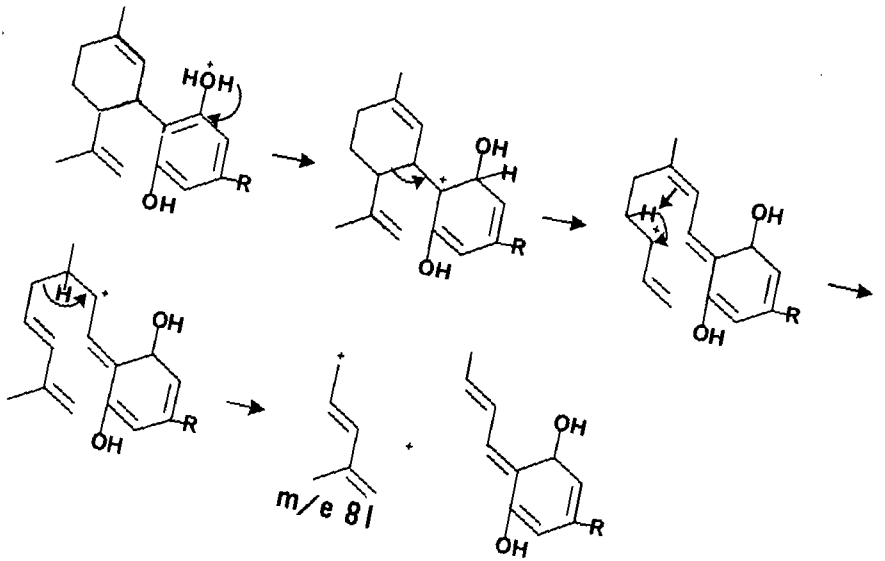

FIGURE 2

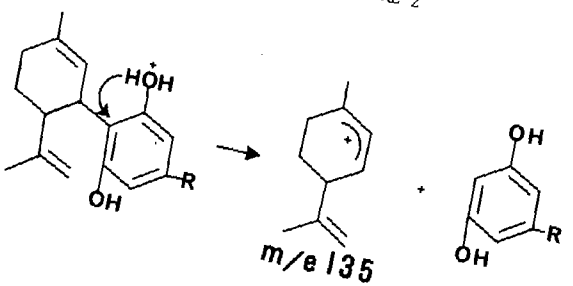

FIGURE 3

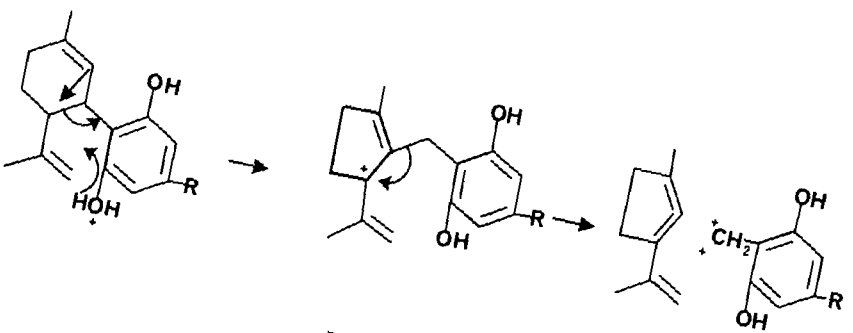

FIGURE 4

USE OF CHEMICAL IONIZATION MASS FRAGMENTOGRAPHY FOR RAPID ANALYSIS OF VARIOUS TYPES OF HYDROCARBONS PRESENT IN A COMPLEX MIXTURE OF BUNKER OIL

James B. Knight

Finnigan Corporation
595 North Pastoria Avenue
Sunnyvale, California 94086

It has recently been shown (1) that some very useful and interesting mass spectra of hydrocarbons can be generated by chemical ionization (CI) mass spectrometry (MS) using methane as the reactant gas. The technique of mass fragmentography (MF) was first reported (2) as a technique mainly suitable for detecting low nanogram or even sub-nanogram quantities of compounds eluting from a GC column. The conventional way of doing MF is to focus the mass spectrometer so that only specific ions usually between 2 and 8 are detected. This technique is very useful when only two or three compounds are being investigated, but not so useful when several hundred components are present as is normally encountered in oils. The first question that usually arises when complex samples of oils are being investigated is what types of compounds are present and secondly what they are.

The information presented here is intended to show how a computerized GC/CI/MS system can be used to first acquire and store complete CI mass spectra of all components eluting from a GC column, then search the acquired data (Figure 1) for specific fragments that are indicative of various compound types. The resulting fingerprints or fragmentograms (Figure 2) show where mass spectra should be taken from to confirm the presence of specific compounds (Figure 3). The time required to acquire the data is dependent on the nature of the sample and the GC parameters used. The time required to do specific ion searches throughout 500 complete spectra taken over a range of 60-400 amu and produce the resulting spectra on a cathode ray tube for quick display and investigation is about four minutes each.

The equipment used for this investigation was a Finnigan Model 1015D quadrupole type mass spectrometer equipped with a chemical ionization source. A Finnigan Model 6000D interactive data system was used to acquire and output the data. The ion source pressure was operated at 1 torr using methane as the reactant gas. The energy of the bombarding electrons was 150 eV. The lens and repeller voltages are adjusted for maximum sensitivity using perflurotributyl amine as a calibration gas. The GC column used was a 5' X 2 mm ID pyrex glass packed with 3% OV-1 on 80/100 mesh Gas Chrom Q. The column was connected directly to the mass spectrometer via a piece of glass lined metal capillary tubing. Methane was used as the carrier gas at a flow rate of approximately 15 cc/min.

It is well known that the relative intensities of parent ions for normal hydrocarbons decreases with increasing carbon numbers when analyzed by electron impact mass spectrometry. When such compounds are investigated by CI mass spectrometry the $(M+1)^+$ ion (quasi-parent ion) usually dominates the spectrum, and the remainder of the spectrum comprises of fragment alkyl ions with different carbon numbers.

Pure samples of these and other hydrocarbons when investigated by CI MS were in good agreement with the results previously published by Field. To summarize a few observations: the methane CI spectra of cycloparaffins differ quite meaningfully from those of alkanes in that prominent $(M+1)^+$ ions are produced in addition to $(M-1)^+$ ions which still are most prominent. In addition to the quasi-parent ion the rest of the CI spectra of cycloparoffins consists of two series of ions, namely, an alkyl series (C_nH_{2n+1}) and alkynyl series (C_nH_{2n-1}).

The straight chain 1-alkenes produce CI spectra that consist almost entirely of two series of ions as do the cycloparoffins, however, the olefins with 16 carbons or less the alkyl ions in each series is of greater intensity than the alkenyl. Also fragmentation at lower m/e values was more intense than for cycloparoffins.

Aromatic hydrocarbons show large M+1 as well as prominent M+29+41 fragments. When alkyl groups are substituted on the ring some fragmentation is observed.

REFERENCES

1. F. H. Field, M. S. B. Munson, and D. A. Becker, Advances in Chemistry Series 58, 167-192, (1966).

2. Hammar, E. G., et al, Analytical Biochemistry 1965, 25:758

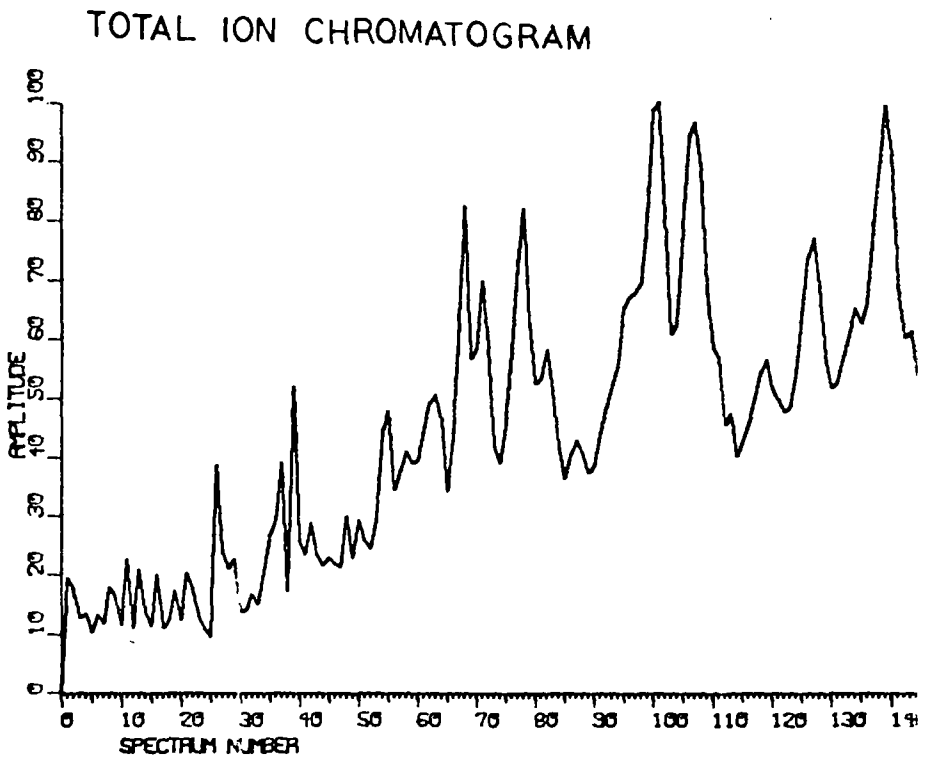
TOTAL ION CHROMATOGRAM
AMPLITUDE
0
10
20
30
40
50
60
70
80
90
100
0
10
20
30
40
50
60
70
80
90
100
110
120
130
SPECTRUM NUMBER

FIGURE 1

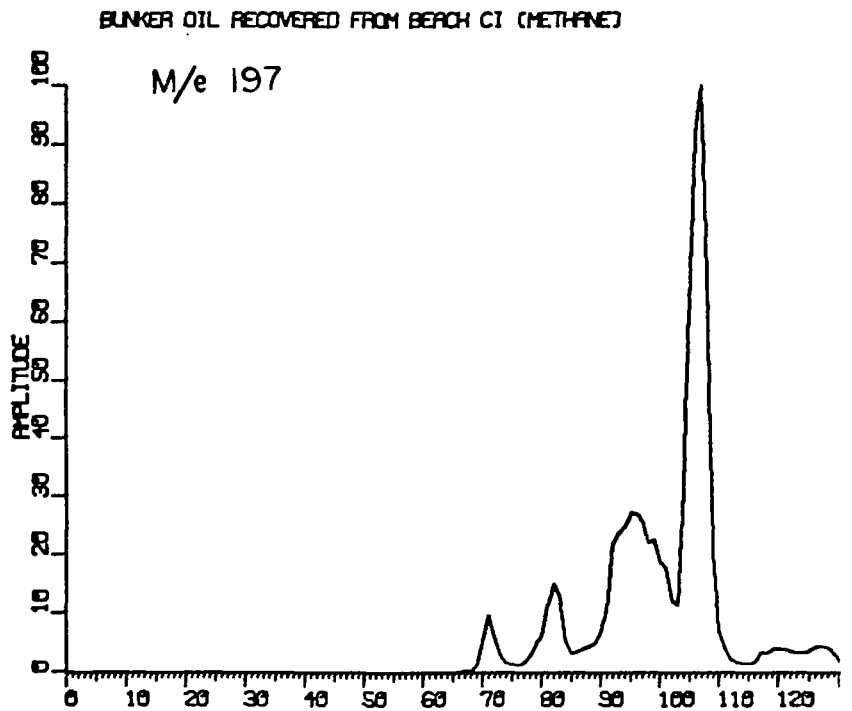

FIGURE 2 SPECIFIC MASS SEARCH

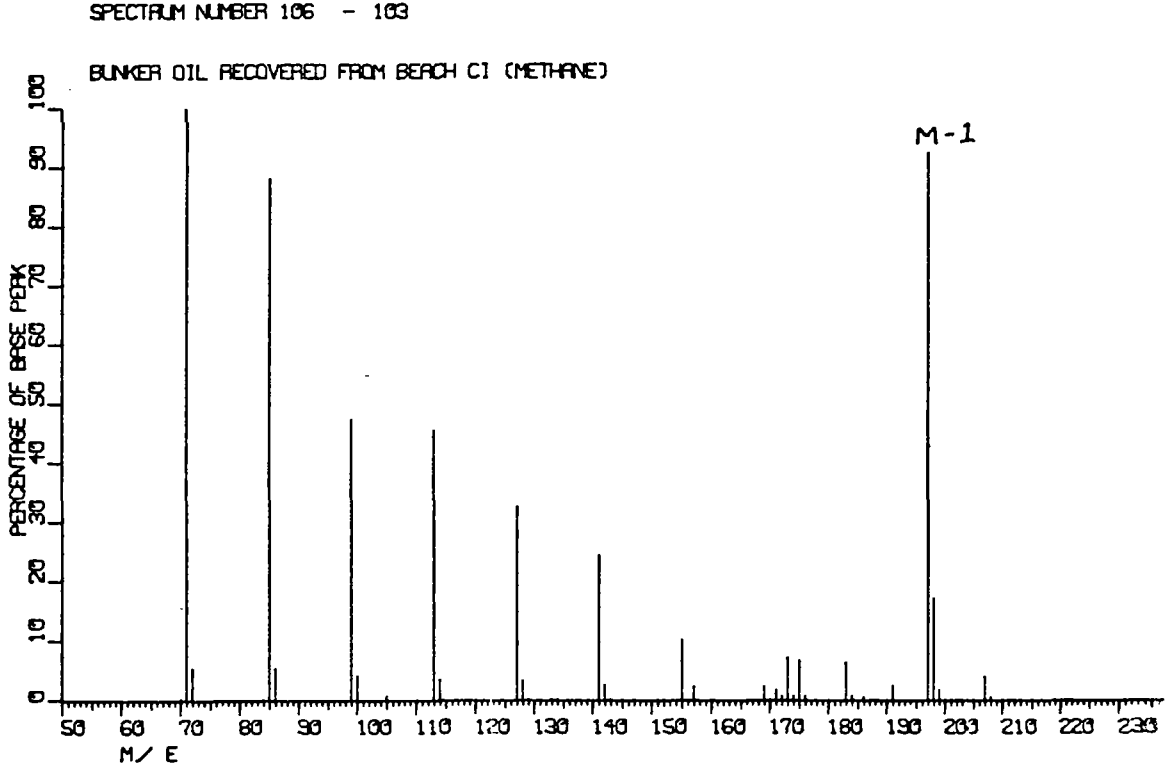

FIGURE 3 CI MASS SPECTRUM OF A C_{14} PARAFFIN

STUDIES IN CHEMICAL IONIZATION MASS SPECTROMETRY

II. POLYFLUORO COMPOUNDS

by

Arun K. Bhattacharya* and Wilbert R. Powell
Air Force Materials Laboratory, TUA
Wright-Patterson Air Force Base, Ohio 45433

and

Jean H. Futrell
Department of Chemistry,
University of Utah, Salt Lake City, Utah 84112

The technique of chemical ionization mass spectrometry is being used now to solve numerous Air Force problems at the Air Force Materials Laboratory, Wright-Patterson Air Force Base, Ohio. Table 1 contains the list of compounds that have been chosen for this communication. The spectra were obtained by a DuPont 21-490 Analytical Mass Spectrometer which has been modified to operate as a chemical ionization instrument.[1] Methane was used as a reagent gas. The repeller voltages were kept near zero and the temperature was about 185°C. The pressure was estimated to be of the order of 0.5 Torr.

Table 1

LIST OF POLYFLUOROBENZENES STUDIED

(I) HEXAFLUOROBENZENE

(II) PENTAFLUOROBENZENE

(III) 1,2,3,4-TETRAFLUOROBENZENE

(IV) 1,2,3,5-TETRAFLUOROBENZENE

(V) 1,2,4,5-TETRAFLUOROBENZENE

(VI) 1,4-DIFLUOROBENZENE

(VII) METHYLPENTAFLUOROBENZENE

(VIII) OCTAFLUOROTOLUENE

* University of Utah, Air Force Contract

The chemical ionization results were compared with the electron impact results obtained earlier.[2] It was noticed that the intensity of the peaks due to the molecular ion are generally higher in CI studies as compared to EI studies, which is quite reasonable and expected (vide Table 3). In the case of the compound (VIII) i.e., methylpentafluorobenzene the difference is quite striking. This points out to a distinctive advantage of CI, if only the identity of these types of compounds are required. As a matter of fact, in more Air Force problems, the need for knowing the molecular weight is maximum. This is the reason why CI studies are now being favored over EI studies in many instances. Tables 2 and 3 give an idea about the intensities of peaks by CI and EI modes.

In most CI spectra the peak due to the protonated molecular ion is the abundant peak in the spectra. The next significant peak is due to the $[M + C_2H_5]^+$ adduct. The peaks due to M^+ are possibly obtained as a result of the charge transfer mechanism. Very few fragmentation peaks are seen. In the case of the compound (VIII) the fragmentation appears to be due to the loss of HF from the protonated molecular ion. Other details will be communicated for publication in "Applied Spectroscopy."

Table 2

[Molecular Ion Peak intensities by CI]

COMPOUND	% TOTAL INTENSITIES OF PEAKS DUE TO MOLECULAR ION BY C. I. MODE			
	M+29	M+2	M+1*	M
I	2.4	3.1	39.1 (100)	29.9
II	2.4	3.3	62.0 (100)	15.1
III	10.9	3.1	49.9 (100)	17.5
IV	9.1	3.8	62.1 (100)	16.1
V	9.2	3.0	49.4 (100)	23.5
VI	8.9	2.5	48.2 (100)	24.1
VII	9.4	4.3	63.4 (100)	10.2
VIII			13.1 (17.2)	

*Value under parentheses is due to the relative intensity values.

Table 3

[Comparative intensities of peaks by CI and EI modes]

COMPOUND	% TOTAL INTENSITIES OF PEAKS DUE TO MOLECULAR ION		% TOTAL INTENSITIES OF PEAKS DUE TO FRAGMENTATION	
	C. I. MODE	E. I. MODE	C. I. MODE	E. I. MODE
I	76.7	46.8	23.3	53.2
II	83.7	25.9	16.3	74.1
III	83.0	74.3	17.0	25.7
IV	92.2	52.6	7.8	47.4
V	85.7	50.0	14.3	50.0
VI	84.6	56.2	15.4	43.8
VII	88.2	9.8	11.8	91.2
VIII	13.1	8.7	86.9	91.3

REFERENCES

1. A. K. Bhattacharya, W. R. Powell and J. H. Futrell, Proceedings of the 20th Annual Meeting of the American Society for Mass Spectrometry and Allied Topics, 322-324, 1972.

2. A. K. Bhattacharya, L. D. Smithson and C. Tamborski, 158th Annual Meeting of the American Chemical Society, Division of Fluorine Chemistry, New York, 1969; Org, Mass Spec., 4, 1-15, 1970

QUANTITATIVE DETERMINATION OF DRUG LEVELS IN PLASMA USING DIRECT INSERTION PROBE CHEMICAL IONIZATION MASS SPECTROMETRY

Robert J. Weinkam and S. B. Matin

School of Pharmacy, University of California
San Francisco, California 94143

The determination of drug levels in blood plasma can contribute to the understanding of their mode of action and clinical effectiveness. In instances where the drug can produce toxic effects, the knowledge of these levels can be used to improve drug therapy. We have utilized chemical ionization mass spectrometry to perform this type of analysis by exploiting the properties of a mild ionizing species. As an ideal these CI spectra of plasma extracts would consist of a single molecular ion (MH^+) for each component. This greatly simplifies the spectra of the complex mixture and provides the basis for the analytical approach. The drug or metabolite present in the plasma extract can be quantitated by comparing its ion current to that of an added internal standard. The lower limit of quantification is determined by the ion current at the respective masses derived from endogenous compounds or by the instrumental sensitivity.

The analytical approach has been applied to the quantification of the oral hypoglycemic sulfonylurea, tolbutamide, and two of its metabolites. The levels of these compounds can be determined from 50 µl of plasma by extraction with ether of pH 5, followed by treatment with diazomethane. The diazomethane quantitatively methylates the sulfonamide nitrogen of tolbutamide and its hydroxymethyl and carboxy metabolites, as well as methylating the carboxy function. Known amounts of the conveniently prepared trideuteriomethyl analog of each compound can be added to the plasma to provide the internal standards. The desired plasma levels can be determined from a single CI (isobutane) scan of this mixture without interference from endogenous materials at levels above 0.5 µg./ml.

This work will be published in Analytical Chemistry.

STUDY OF CARBON GASIFICATION REACTIONS USING A CHEMICAL IONIZATION MASS SPECTROMETER

A. L. Yergey
Scientific Research Instruments Corporation
Baltimore, Maryland 21207

F. W. Lampe
Penn State University
University Park, Pennsylvania 16802

A chemical ionization mass spectrometer especially adapted for use in non-isothermal kinetics experiments was used to determine the composition of the gas flow from a carbon gasification reactor. Use of non-isothermal kinetics to analyze plots of the concentrations of selected components in the gas stream as a function of temperature allows the determination of rate constants and frequency factors for gasification reactions of interest. Of particular interest is the identification of a new low temperature gasification step in the $CO_2 + C = 2CO$ reaction. A reaction mechanism has been determined for this low temperature step through experiments with solid ^{13}C.

A paper describing this work is being prepared for publication.

Coupled Gas-Solid Chromatography Chemical Ionization Mass Spectrometry - A New Analytical Technique

F.D. Hileman, T.A. Elwood, M.L. Vestal, J.H. Futrell

Department of Chemistry
University of Utah
Salt Lake City, Utah 84112

R.E. Sievers
Aerospace Research Laboratories
Wright-Patterson Air Force Base, Ohio 45433

Applications of gas-solid chromatography have been limited by the conflicting requirements of low sampling loading necessary to maintain high column efficiency and relatively low sensitivity of detectors for classes of compounds for which gas-solid chromatography is an especially promising analytical technique. Chemical ionization mass spectrometry is an extremely sensitive analytical technique whose applications in GC/MS work have been limited by column bleed. Thus a chromatograph was directly coupled to a Varian MAT CH-7 mass analyzer modified for chemical ionization[1] which was used as a sensitive, compound-specific detector for gas-solid chromatography.

When using a chemical ionization mass spectrometer, the total ion mode normally used to follow chromatographic peaks is useless. Thus to obtain a GSC/CIMS chromatogram, the spectometer was interfaced to a PDP-11/20 computer system.[2] The spectrometer was then rapidly and repeatedly scanned over a desired mass range throughout the entire chromatographic run. The computer stores the peaks and their intensities for each scan. A plot can then be made of the total ion intensity exclusive of reagent gas peaks to give a reconstructed chromatogram. The spectrum for any desired chromatographic peak can be either plotted or listed.

Application of this system has been in the area of trace metal analysis through the formation of the volatile trifluoroacetylacetonate chelate of the metal of interest. These chelates are then chromatographed on a new in-situ formed polyurethane support[3] using hydrogen as both carrier gas and reagent gas. The advantage of using chemical ionization over electron impact is that little fragmentation of these chelates occurs resulting in improved sensitivity.

Another application involves the analysis of various gases, in particular the concentration of carbon monoxide in nitrogen. This is a difficult analysis for mass spectrometers requiring high

resolution techniques. Using GSC/CIMS, the carbon monoxide and nitrogen were separated on an eight foot molecular sieve 5A column with hydrogen as carrier gas. Monitoring the m/e 29 peak (protonated nitrogen or carbon monoxide) the two gases eluted as two well resolved peaks thus allowing for quantitantion of carbon monoxide in nitrogen.

---

[1] M.L. Vestal, T.A. Elwood, L.H. Wojcik, J.H. Futrell, 20th Annual Conf. on Mass Spectrometry and Allied Topics, ASMA, Dallas, Texas, June 4-9, 1972.

[2] Reference no. 1.

[3] F.D. Hileman, R.E. Sievers, G.G. Hess, W.D. Ross, Analytical Chemistry, 45, 1128 (1973).

IONIC EQUILIBRIA AND PSEUDOEQUILIBRIA IN NEGATIVE CHEMICAL IONIZATION MASS SPECTRA

Ralph C. Dougherty, H.P. Tannenbaum and J. David Roberts

Department of Chemistry, Florida State University, Tallahassee, Florida 32306

This paper is a progress report on our continuing studies of S_N2 reactions in the gas phase.[1] The question of equilibrium and pseudoequilibrium is important to these studies particularly if direct comparison is to be made between the gas phase studies and results obtained in condensed phase. A pseudoequilibrium is a reaction system that gives all the appearances of equilibrium without actually being at equilibrium in a chemical sense.

There are at least three potential sources of pseudoequilibria in a "field free" chemical ionization sources such as the one that we use. If the equilibration half life is of the order of the ion residence time a van't Hoff plot for the equilibrium could be linear but the apparent equilibrium constant would reflect only partial equilibration. Since ion residence time is not appreciably influenced by pressure van't Hoff plots at different pressures could give similar results. This kind of pseudoequilibrium could be detected by relaxation methods.

Reactions that occur through multi-step processes, so that the forward and reverse pathways are different, can give the appearance of equilibrium. For example, Br^- and HBr_2^- appear to be in equilibrium in our studies of alkyl bromide NCI mass spectra. The HBr_2^- is presumably formed by decomposition of the RBr_2^- ions in the source, and it reverts to Br^- by direct decomposition. In our experiments with alkyl bromides the Br^- - HBr_2^- pseudoequilibrium always gave linear van't Hoff plots, and in the cases we have examined, the entropy and enthalpy for the apparent equilibrium between these two ions was independent of the source pressure. Once again the determination of the relaxation spectrum for this series of coupled reactions by the use of analysis of arrival time distributions[2] should provide values for the rate constants for each of the reactions in the system.

A third source of pseudoequilibrium in our NCI source is ions with the same mass but distinct chemical structures. If two different ions are independently in equilibrium with a pair of distinct ions of the same mass the original ions may appear to be in equilibrium with each other. One example of this phenomena was obtained in the NCI spectra of mixed alkyl halides. When the NCI spectrum of mixed methyl chloride and bromide was obtained the chloride and bromide ions appeared to be in equilibrium with each other. The thermochemical data for the exchange process indicated that the reactions were not in equilibrium, presumably because the two distorted structures for the CH_3ClBr^- ion were not in equilibrium with each other. In order to confirm the fact that distinct structures for two RClBr ions would not interfere with the apparent equilibrium between Cl^- and Br^- we examined the apparent equilibrium in mixtures of cyclopropylchloride and bromide. Cyclopropyl halides fail to undergo S_N2 reactions in solution because of the increase in ring strain on going to a penta-coordinate carbon. The van't Hoff plots obtained in this experiment resembled those for the methyl halides in every detail and indicated that the equilibria in the former case were like those shown below.

$$CH_3Cl + Br^- \rightleftharpoons Br\cdots CH_3Cl \quad ; \quad \bar{C}l\cdots CH_3Br \rightleftharpoons CH_3Br + Cl^-$$

We are presently constructing a pulse system for our NCI source so that we can investigate these reactions in detail using relaxation methods.

References

1. R.C. Dougherty, J. Dalton and J.D. Roberts, Org. Mass Spectrom., in press.
2. G.S. Sroka, C. Chang and G.G. Meisels, J. Amer. Chem. Soc., 94, 1052 (1972).

NEGATIVE CHEMICAL IONIZATION MASS SPECTRA OF ARYLDIAZOKETONES AND POLYCHLORINATED BIPHENYLS

Harvey P. Tannenbaum and Ralph C. Dougherty

Department of Chemistry, Florida State University, Tallahassee, Florida 32306

Negative ion beams as intense as positive ion beams can be easily obtained under chemical ionization conditions.[1] For organic compounds capable of forming stable anions, negative chemical ionization (NCI) mass spectrometry is a valuable tool for the study of anion reactivity in the absence of solvation effects. In addition, ion molecule reactions occurring in the chemical ionization source can be a guide to new reactions in solution chemistry.

We have examined several classes of organic compounds, specifically aryl diazoketones and polychlorinated biphenyls (PCB's), which under NCI conditions exhibit intense molecular anions and undergo ion molecule reactions for which the analogous process in solution chemistry would be of considerable interest.

The NCI/isobutane mass spectra of substituted diazoacetophenones ($X\text{-}C_6H_5COCHN_2$) exhibit a high degree of sensitivity toward both the electronic nature of substituents on the phenyl group and the concentration of substrate in the CI source. Table I lists NCI mass spectra for both electron

Table I. NCI/isobutane spectra of substituted diazoacetophenone. Source temperature ~25°, isobutane pressure ~1 torr.

R	$[M-28]^{\cdot}$	$[M-12]^{\cdot}$	$[M-1]^{-}$	$M^{\cdot}$	$[2M-1]^{-}$	$[2M]^{\cdot}$
p-CH_3-	20	-	53	18.3	100	31.4
p-CH_3O-	14	-	47	93.4	38	100
H-	3.8	-	18	1.5	100	5.4
p-CN-	10	100	9	44.1	-	-
p-NO_2-	6.7	41	8	19.3	-	-

donating and withdrawing substituents obtained at approximately equal concentrations of substrate. Loss of nitrogen to give the observed $[M-28]^{-}$ ion presumably occurs by a process analogous to the well known Wolff rearrangement of diazoketones. It is apparent that deprotonated dimer formation was facilitated by the presence of an electron donating substituent while electron withdrawing substituents exhibited primarily molecular anion formation and ions corresponding to the loss of 12 mass units from the molecule anion. The corresponding $[M-12]^{-}$ ion in the spectra of compounds containing electron donating substituents was only observed when the concentration of substrate was significantly less than the amount employed in determining the spectra listed in Table I. At low concentrations of substrate $[M-12]^{-}$ corresponded to the base peak in these NCI mass spectra.

The intense $[M-12]^{\cdot}$ ion is of particular interest in that there are several plausible mechanisms for its formation. One mechanism involves rearrangement and subsequent expulsion of a carbon atom from the molecular anion. Labeling experiments in which the carbonyl carbon and the diazocarbon were enriched with C^{13} indicated that neither of these carbon atoms were lost in formation of the $[M-12]^{-}$ ion. A second mechanism for loss of 12 daltons involves formation of the ketene dimer by decomposition of the diazoketone followed by dimerization and subsequent fragmentation as shown in equation (1).

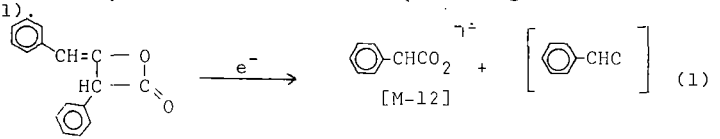

(1)

The NCI/isobutane spectrum of synthetically prepared phenyl ketene dimer failed to exhibit any fragmentation corresponding to the observed $[M-12]^{-\cdot}$ ions from diazoacetophenone. A third mechanism for formation of $[M-12]^{-\cdot}$ involves the addition of oxygen and loss of N_2 from the molecule ion. Examination of the NCI spectrum of diazoacetophenone, under conditions for which $[M-12]^{-\cdot}$, (m/e 134), was the base peak, in the presence of O^{18} enriched water shifted the m/e 134 ion to m/e 136 in an amount corresponding to the percentage of O^{18} in the mixture (equation 2).

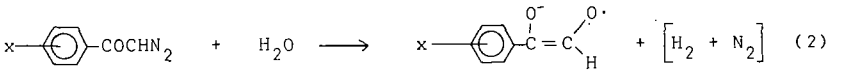

(2)

Another class of compounds for which the NCI mass spectra exhibit unexpected reactions of the molecule anion with impurities in the CI source are the polychlorinated biphenyls. The NCI/methane mass spectra of a mixture of PCB's containing from one to eight chloride atoms exhibited strong ions corresponding to an apparent loss of 19 daltons from the molecule ion. Examination of pure PCB standards indicated that ion molecule reactions of the PCB's with oxygen in the source produced the $[M-19]^-$ anions. Introduction of H_2O^{18} failed to shift the position of the $[M-19]^-$ ions. The formation of $[M-19]^{-\cdot}$ ions was only observed for PCB's containing a minimum of three chlorine atoms suggesting that molecular anion formation and activation toward nucleophitic displacement are necessary requirements in order to observe ion molecule reactions of the type suggested in equation (3).

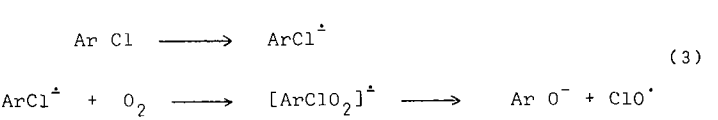

(3)

The NCI mass spectra of 2,4-dinitro-chlorobenzene, 4-nitrochlorobenzene, 4,4'-dichlorobenzophenone and 4-bromobenzophenone also exhibited strong molecule anion formation and varying amounts of $[M-X+O]^{-\cdot}$. In all cases added oxygen (O_2) was observed to completely eliminate the molecule anions with increased formation of $[M-19]^{-\cdot}$. Naphthalene and α bromonaphthelene which did not exhibit significant molecule anions under these NCI conditions did not exhibit ions corresponding to formation of the corresponding phenoxide.

We are presently investigating the solution analogs of these reactions.

References

1. a) R.C. Dougherty, J. Dalton and J.D. Roberts, Org. Mass Spectrom., in press.
   b) H.P. Tannenbaum, J.D. Roberts and R.C. Dougherty, Anal. Chem., in press.

ORIGIN OF LINEAR VAN'T HOFF PLOTS UNDER NON-EQUILIBRIUM CONDITIONS IN CHEMICAL IONIZATION STUDIES OF REVERSIBLE IONIC REACTIONS

G. G. Meisels, G. J. Sroka and R. K. Mitchum
Department of Chemistry
University of Houston
Houston, Texas 77004

ABSTRACT

Arrival time measurements in the water system confirm earlier suggestions that, under typical operating conditions, equilibrium in proton hydration is not achieved in chemical ionization sources. Previous evidence cited to support the establishment of equilibrium, the independence of results of water concentration and the linearity of Van't Hoff Plots, can be understood quantitatively on the basis of a model which recognizes the temperature dependence of ion residence times in the source and derives the apparent equilibrium constant from its operational definition using the kinetics of sequential or of opposing quasi-first order reactions.

I. INTRODUCTION.

The study of ionic equilibria in the gas phase has received considerable attention during the past few years because of its ability to provide heats of reaction of gaseous ions,[1-13] intrinsic acidities and basicities, and a better understanding of the solvation process. One of the systems of greatest interest and fundamental importance is the hydration of the proton.[1,3,5,6,11,12,14] Early investigations based on ion sampling from a field-free source at approximately atmospheric pressure[1] led to heats of hydration which were in reasonable agreement with each other and with theoretical calculations based on ab-initio considerations.[16] However, in a series of extensive investigations using chemical ionization techniques and hydrocarbons as major constituents, under conditions where pressure was on the order of a few torr and small extraction fields were present, a set of heats of reaction was derived which differed sharply from those reported earlier, particularly for the first two hydration steps.[6,11] The discrepancy is that much more perplexing because of independence of water concentration and linearity of Van't Hoff Plots were unquestionable, and these are generally accepted as indicators of achievement of equilibrium.

We report here why these criteria are insufficient evidence for the attainment of equilibrium in chemical ionization sources and present a partial resolution of the discrepancies.

II. EXPERIMENTAL.

Arrival time distributions were determined using a modified Atlas CH-4 mass spectrometer as described previously[17-19] by providing a 0.1 microsecond pulse of electrons which ionizes the gas and gates a time-to-pulse height converter. Ion arrival pulses terminate the converter whose output pulses are sorted on a 400 channel pulse height analyzer, each channel corresponding to an interval of 0.25 μsec. After a few minutes of accumulation, the PHA output is transferred onto paper tape. All data manipulations and calculations are performed on a Univac 1108 computer using the time sharing mode.

III. RESULTS AND DISCUSSION.

Figure 1 shows illustrative arrival time distributions of H_3O^+, $H_5O_2^+$ and $H_7O_3^+$, obtained over various periods and taken directly from the output of the multichannel analyzer. They are shifted slightly to take into account the variation in transit time in the analyzer as a result of the difference in mass, using $t(\text{transit}) = 1.5(m/e)^{1/2}$ μsec.[17] It is apparent that equilibrium is not established over most of the range of times accessible in a typical chemical ionization source since the normalized arrival time distributions would then be identical for the ions shown.[17] Only at times in excess of 0.2 milliseconds does the ratio of the distributions approach constancy (Figure 2).

Arrival time distributions of H_3O^+ are dominated by times of less than approximately 150 microseconds, and those of $H_5O_2^+$ by times less than 200 microseconds; these periods are much shorter than those required for the establishment of equilibrium. In continuous experiments these portions of the distribution dominate the measured ion current; the observed ion current ratio is a time average which can approach the equilibrium value only if the areas under the arrival time distribution curves at times less than those required for the attainment of equilibrium are negligible. Even when

the average residence time is in excess of that required for the attainment of equilibrium, the ion current ratio may include significant time regions where equilibrium is not established.

IV. QUASITHERMODYNAMIC PARAMETERS DERIVED UNDER CONDITIONS OF KINETIC CONTROL.

The earlier work of Cunningham, et.al.,[12] as well as Figure 2 clearly demonstrate that at relatively low temperatures the reaction is far from equilibrium but that relative ion intensities are determined instead by the kinetics of the approach to equilibrium. The reaction sequence representing the first few hydration steps is:

$$MH^+ + H_2O + M \underset{k_{-1}}{\overset{k_1}{\rightleftharpoons}} M + M + H_3O^+ \qquad (1)$$

$$H_3O^+ + H_2O + M \underset{k_{-2}}{\overset{k_2}{\rightleftharpoons}} H_5O_2^+ + M \qquad (2)$$

$$H_5O_2^+ + H_2O + M \underset{k_{-3}}{\overset{k_3}{\rightleftharpoons}} H_7O_3^+ + M \qquad (3)$$

$$H_7O_3^+ + H_2O + M \underset{k_{-4}}{\overset{k_4}{\rightleftharpoons}} H_9O_4^+ + M \qquad (4)$$

In pure water, MH^+ is merely H_3O^+; with methane as the major drift gas, MH^+ is CH_5^+ and yet another reaction step must be added.

$$CH_4^+ + CH_4 \xrightarrow{k_0} CH_5^+ + CH_3 \qquad (5)$$

In addition to reactions 1 - 4, each ion is also lost by diffusion to the walls, by extraction from the source, and by neutralization. As long as the diffusion recombination and coefficients are of similar magnitude for all ions involved, these ion loss processes should affect all ions nearly equally. Differences arise from the kinetic behavior which converts initial ions earlier in time so that the mean time during which each ion exists in the source increases as the number of steps required to produce it increases. For simplicity, we neglect this complication here.

The greatest disparity in reported heats, free energies, and entropies of reaction exists for the second equilibrium, reaction 2. We confine our further considerations to this step.

The operational definition of the equilibrium constant is

$$K_a = [H_5O_2^+]/([H_3O^+]\cdot[H_2O]) \qquad (I)$$

The subscript, a is used to indicate that the quantity calculated via equation (I) is not necessarily the equilibrium constant K but an experimental observable whose relationship to the equilibrium constant is to be established.

The first approach is based on a model in which reactions 1, 2, and 3 proceed only in the forward direction. The additional approximation that reaction 0, the formation of reagent MH^+, occurs instantaneously is supported by simple considerations.[17] The linear first order differential equations describing the time dependent behavior of ion concentrations lead to

$$K_a = \frac{k_2[M]}{e^{-k_1[M][H_2O]} - e^{-k_2[M][H_2O]}} \left\{ \frac{e^{-k_1[M][H_2O]t} - e^{-k_3[M][H_2O]t}}{(k_3-k_1)[M][H_2O]} - \frac{e^{-k_2[M][H_2O]t} - e^{-k_3[M][H_2O]t}}{(k_3-k_2)[M][H_2O]} \right\} \qquad (II)$$

In the limit where all exponents are near zero, one can write

$$\lim_{t\to 0} K_a = (k_2/2)[M]t \qquad (III)$$

This quantity is clearly independent of the concentration of water in the system.

The second explicit solution in closed form is based on the assumption that all steps other than reaction 2 are at equilibrium. The approach to equilibrium of two opposing quasi-first order reactions is given by

$$K_a = K \frac{1 - e^{-(k_2[M][H_2O] + k_{-2}[M])t}}{1 + K[H_2O]e^{-(k_2[M][H_2O] + k_{-2}[M])t}} \qquad (IV)$$

This equation clearly shows that K_a is always less than K unless time approaches infinity. In the limit (i.e., under kinetic control),

$$\lim_{t \to 0} K_a = k_2[M]t \qquad (V)$$

This relationship is again independent of water concentration, and differs from III by a factor of two as a result of the assumption that step 1 is at equilibrium.

Comparison of the preceding equations with experiments can be made by inserting rate constants determined under ideal conditions where all ions are indeed at their equilibrium concentrations, using experimental arrival times. In the absence of arrival time distribution measurements, mean drift times given by drift theory may be employed, since these have been shown to lead to calculated residence times within a factor of two of those experimentally observed.[17-19] The mean residence time $\bar{t}$ is conveniently given by[19]

$$\bar{t} = (z/T)(P/E)\sqrt{\alpha\mu} \times 10^{-2} \text{ sec} \qquad (VI)$$

where z is the drift length in cm, T in °K, the pressure P of [M] in torr and the repeller or extraction field E in V/cm; α and μ are the polarizability and reduced mass in atomic units.

Unfortunately, the rate constants k_1, k_{-1}, k_3, and k_{-3} are not known sufficiently well to evaluate the temperature dependence of K_a through equation II. However, $k_2 = 3.16 \times 10^{-30} e^{4900/RT}$ cm^{6}sec^{-1} and $k_{-2} = 5.19 \times 10^{-6} e^{-26700/RT}$ cm^{3}sec^{-1} are given by Cunningham, et.al.[12] Figure 3 summarizes the calculated quasi-Van't Hoff Plot based on equations IV and VI, these rate constants, a drift length z of 1 cm and a field strength of 1 V/cm at 1 torr methane as the drift gas. It is apparent that results are independent of water concentration and reasonably linear at higher temperatures.

The linearity of Van't Hoff Plots under non-equilibrium conditions can be understood easily by consideration of equations III or V and VI, and by the variation of log T with 1/T. The latter is very nearly a linear function of temperature between 300° to 700°K and over this range, can be represented by log T = 3.147 - 2.22 x 10^2/T with a deviation of less than 0.5%. In the limit of complete control by kinetic parameters, we may therefore write, beginning with V and VI and the ideal gas law:

$$\lim_{t \to 0} \log K_a = -14.175 + \log\left(\frac{A_2\sqrt{\alpha\mu}\, P^2 z}{kE}\right) - \left(\frac{E_2 - 2025}{2.303\ RT}\right) \qquad (VII)$$

where A_2 and E_2 are the preexponential factor and activation energy of reaction 2, respectively. The apparent heat of reaction ΔH_a obtained from a Van't Hoff plot is $E_2 - 2025 = -6.9$ kcal/mole if Kebarle's value[12] for E_2 is employed. A line corresponding to this equation is drawn in Figure 3 and represents the assymptote to the full equation at higher temperatures.

Our calculated value of ΔH_a is in almost exact agreement with $\Delta H_a = 7$ kcal/mole reported by Beggs and Field[6] when they employed methane as the major gas. This agreement is probably fortuitous because we have assumed that drift is entirely dictated by gross drift considerations. Since it is customary to adjust the repeller potential at will, it is well possible that in other investigations a lesser potential was employed where mean residence times are more nearly described by diffusion considerations, thereby possibly changing the functional dependence of mean residence times on temperature and with it the limiting slope of Van't Hoff plots.

V. CONCLUSIONS.

The analysis based on kinetic limitation of reactions presented here demonstrates that independence of pressure and linearity of Van't Hoff plots does not assure the achievement of equilibrium. It leads to a calculated value of the apparent heat of

reaction which depends only on the activation energy of the rate controlling step and the functional form of the temperature dependence of mean residence times. As long as applied fields are sufficient to assure the applicability of VI the resultant ΔH_a will be independent of instrumental parameters, drift lengths, field strengths, etc. and will be approximately 2 kcal/mole less than the activation energy of the limiting step. These factors will, however, affect the intercept of Van't Hoff plots and thereby exercise considerable influence on the apparent values of free energies and entropies of reaction. This is consistent with earlier observations.[6,11]

VI. ACKNOWLEDGEMENTS.

This investigation was supported in part by the Robert A. Welch Foundation, grant number E-210, and in part by the United States Atomic Energy Commission under contract number AT-(40-1)-3606. We are sincerely grateful for this assistance.

LITERATURE CITED.

1. P. Kebarle and E. W. Godbole, J. Chem. Phys. 39, 1131 (1963).
2. P. Kebarle, in "Ion-Molecule Reactions," J. L. Franklin, ed., Plenum Press, New York (1972), Chapter 7.
3. P. Kebarle, S. K. Searles, A. Zolla, J. Scarborough and M. Arshadi, J. Amer. Chem. Soc. 89, 6393 (1967).
4. J. I. Brauman and L. K. Blair, J. Amer. Chem. Soc. 90, 6561 (1968); Ibid., 93, 7139 (1971); Ibid., 93, 4315 (1971).
5. A. Good, D. A. Durden, P. Kebarle, J. Chem. Phys. 52, 212 (1970).
6. D. P. Beggs and F. H. Field, J. Amer. Chem. Soc. 93, 1567 and 1576 (1971).
7. W. G. Henderson, M. Taagepera, D. Holtz, R. T. McIver, Jr., J. L. Beauchamp and R. W. Taft, J. Amer. Chem. Soc. 94, 471 (1972).
8. E. M. Arnett, F. M. Jones, III, M. Taagepera, W. G. Henderson, D. Holtz, J. L. Beauchamp and R. W. Taft, J. Amer. Chem. Soc. 94, 4724 (1972).
9. D. H. Aue, H. M. Webb and M. T. Bowers, J. Amer. Chem. Soc. 94, 4726 (1972).
10. J. P. Briggs, R. Yamdagni and P. Kebarle, J. Amer. Chem. Soc. 94, 5128 (1972).
11. S. L. Bennett and F. H. Field, J. Amer. Chem. Soc. 94, 5186 (1972).
12. A. J. Cunningham, J. D. Payzant and P. Kebarle, J. Amer. Chem. Soc. 94, 7627 (1972).
13. R. Yamdagni and P. Kebarle, J. Amer. Chem. Soc. 95, 4050 (1973).
14. C. E. Young and W. E. Falconer, J. Chem. Phys. 57, 918 (1972).
15. M. DePaz, J. J. Leventhal and L. Friedman, J. Chem. Phys. 51, 3748 (1969).
16. M. D. Newton and S. Ehrenson, J. Amer. Chem. Soc. 93, 4971 (1971).
17. G. J. Sroka, C. Chang and G. G. Meisels, J. Amer. Chem. Soc. 95, 1052 (1972).
18. C. Chang, G. J. Sroka and G. G. Meisels, J. Chem. Phys. 55, 5154 (1971).
19. C. Chang, G. J. Sroka and G. G. Meisels, Int. J. Mass Spectrom. Ion Phys. 11, 367 (1973).

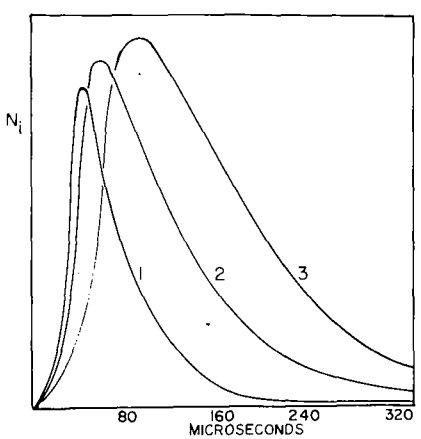

Figure 1. Residence time distributions of H_3O^+, $H_5O_2^+$ and $H_7O_3^+$ (curves 1, 2 and 3) at a field strength of 1 V/cm, 440°K, and 1 torr water.

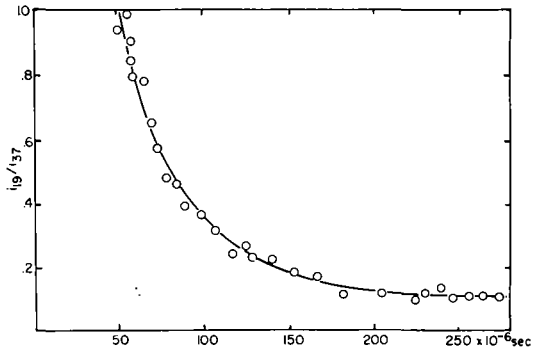

Figure 2. Dependence of Ratio of Ion Currents of H_3O^+ to $H_5O_2^+$ on time.

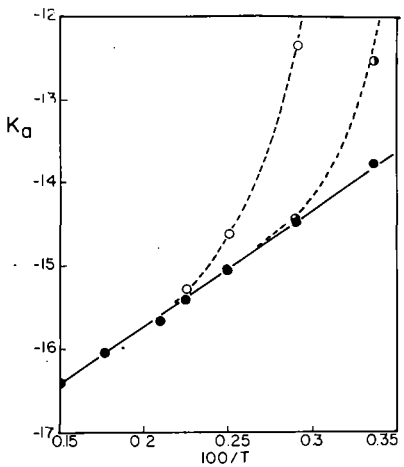

Figure 3. Van't Hoff Plot of quasi-equilibrium constant K_a calculated from equation IV. The slope of the line is that defined by equation V for complete kinetic limitation and no reverse reaction. Solid circles: water pressure 0.001 torr; semi-filled circles: 0.01 torr, open circles: 0.1 torr.

CHEMICAL IONIZATION: RATE EFFECTS ON QUANTITATIVE MEASUREMENTS

G. G. Meisels, R. K. Mitchum and G. J. Sroka
Department of Chemistry
University of Houston
Houston, Texas 77004

ABSTRACT

Rate constants for total ion reactivity have been determined for a series of compounds using the arrival time distribution method and methane as the reagent gas. Reasonable agreement between experimental and theoretical rate constants is obtained.

INTRODUCTION

Little attempt has been made to date to develop chemical ionization mass spectrometry as a quantitative analytical tool; the need for standardization and quantization of this technique is apparent. The determination of reaction rate constants provides one convenient approach to an investigation of anomalies associated with chemical ionization measurements. In this communication we report preliminary results obtained in the investigation of proton transfer rates to highly dissimilar compounds. The well known reagent CH_5^+ was chosen for this study because it undergoes proton transfer readily and suffers no complicating reactions with the parent gas.

One point of departure is a comparison of the proton transfer reaction rates of CH_5^+ with those predicted from theoretical models using both non polar and polar substrates. The microscopic rate constant k may be calculated by four established techniques.[1-4] The rate constant for reaction of an ion with a non polar neutral molecule where the interaction potential results only from ion-induced dipole interactions was developed by Langevin[1a] and further refined by Gioumousis and Stevenson.[1b]

For simple systems agreement with experiment is obtained but for more complex molecular systems serious deviations from theory are found. Moran and Hamill[2a] proposed that the dipole of the neutral molecule aligns itself with the positive ion. Harrison, et.al.[2b] compare experimental rate constants to those predicted by such a "lock-in" mechanism for various systems. The findings indicate that the "lock-in" mechanism may not be an accurate model since the rate constants were found to have little dependence upon ion exit energy for the processes investigated. The "lock-in" model neglects any rotation of the neutral species, however, conservation of angular momentum prevents complete alignment of the dipole. Dugan and Magee[3] evaluated the collision trajectories of an ion and a rotating permanent dipole and indicate that the induced dipole and locked dipole treatments should give only a lower and upper limit for the rate constant for reaction of an ion with a polar molecule. The last and most recent approach[4] is based on an average dipole orientation model (ADO). It assumes that (a) the orientation angle of the dipole with the line of centers of the collision can be treated as an average angle which is a function approach distance, (b) on the average there is no net transfer of angular momentum between the rotating molecule and the system as a whole and (c) the rotor can be treated as a diatomic molecule thus including only two of the three degrees of rotational freedom.

In this summary we provide rate constants for reactions of CH_5^+ with a series of compounds having a wide range of dipole moments. These experimental rate constants are compared to theoretical values based on ion-induced dipole, locked dipole and average dipole orientation models. The effect of both dipole moment and of the average ion energy upon the rate constant is discussed.

EXPERIMENTAL

Instrumentation: the experiments were conducted using a modified Atlas MAT CH-4 mass spectrometer which has been described elsewhere.[5] The gases are introduced into the ion source at a total pressure of 0.6 torr and a temperature of 167±5°C. They are then ionized by a 0.1 μsec pulse of electrons having an energy of 220 eV. Ions are withdrawn after drift over a minimum of 0.7 cm (electron entrance plane to exit slit distance) using drawout potentials of 2-15 V. They are then mass analyzed and detected individually with an electron multiplier. The delays between the electron pulse are sorted on a pulse height analyzer. The output of this analyzer yields an arrival time distribution. The analyzer output was either recorded on an x-y recorder or via an interface to a teletype unit which records the data on paper punch tape. This off-line data acquisition system is coupled via acoustic coupler to a Univac model 1108 computer. The complete numerical analysis was performed in this manner.

The gas introduction system consists of two bakeable 5 liter stainless steel reservoirs. The gas mixtures were prepared by standard techniques and introduced into the ion source via a Granville-Phillips automatic metering valve. The source pressure was measured and controlled directly by a MKS Baratron capacitance manometer.

RESULTS AND DISCUSSION

Recently Meisels, et.al.[5] have developed a technique for the determination of ion molecule reaction rate constants from arrival time distributions. The rate constants in this work were calculated using equations I and II which are derived from a quasi-first order kinetic treatment,[5a]

$$\ln(R^+/R_0^+) = -k_1 t[N] \quad \text{(I)}$$

$$\ln(R_1^+/R_2^+) = \ln(R_{0,1}^+/R_{0,2}^+) - k_2 t[N_1 - N_2] \quad \text{(II)}$$

where R and N are reagent and substrate concentrations respectively. A plot of either $\ln(R^+/R_0^+)$ or $\ln(R_1^+/R_2^+)$ versus t should yield a straight line with a slope corresponding to $-k(N)$ or $-k(N_1-N_2)$ respectively. The concentration of R as a function of residence time is evaluated directly from the arrival time distribution of the reactant ion. In this experimental arrangement the measurable quantity is the arrival time distribution of the reagent ion, namely CH_5^+. Only the consumption of CH_5^+ according to reaction 1 is observed.

$$CH_5^+ + N \xrightarrow{k'_1} CH_4 + NH^+ \quad (1)$$

Further reactions of NH^+ are of no consequence as long as they do not proceed by reaction 2,

$$AH^+ + B \xrightarrow{k'_2} CH_5^+ + C \quad (2)$$

where AH^+ is any ionic species and B is any neutral present. The absence of reaction 2 can be assumed by establishing that the rate constant k'_1 is independent of additive concentration.

The total reaction rate constants of CH_5^+ with four non polar substrates, (n-butane, iso-butane, n-pentane, and n-heptane) are of the same magnitude as those calculated from ion-induced dipole theory[1] (Table I). Although these molecules have no permanent dipole moment they provide a range of polarizabilities from 8.21 to 13.86 $Å^3$. The calculated rate constants should be an upper limit. Serious deviation from these limiting values was not observed and the experimental values obtained are in reasonable agreement with the calculated values. As expected, rate constants increase with increasing polarizability of the substrate. Within the limits of error the experimental rate constant is independent of the average ion energy calculated from the Wannier equation.[6]

The second series of substrates studied covers a range of dipole moments from 0.643 to 3.67 Debye (Table II). Although both the "lock-in" and ADO models may be expressed as a function of the relative ion energy[2a-b,7] only the "lock-in" model will be considered at the present time, providing only an upper limit to that value. The experimental values are bracketed by the limiting values calculated from the ion-induced dipole and locked dipole models. Within the limits of error the experimental rate constants do not significantly vary with average ion energy. However, this is not a sensitive test of theoretical models because the energy dependent upper limit rate constant, established by the "lock-in" model, shows little variation over the range of average ion energies investigated here. The rate constant for proton transfer from CH_5^+ to 1,1-difluoroethylene was previously determined by Bowers, et.al.[8] as 1.27×10^{-9} cc/sec, in good agreement with our average of 1.41×10^{-9} cc/sec. These authors also reported a calculated value of 1.87×10^{-9} cc/sec based on the ADO model and thermal energy distribution. While the average ion energy under our experimental conditions is about 0.1 eV, and since the maximum (locked dipole) rate constant varies only little with energy, it appears that the ADO model overestimates k somewhat.

ACKNOWLEDGEMENTS

This investigation was supported in part by the United States Atomic Energy Commission under Contract No. AT-(40-1)-3606 and in part by the Robert A. Welch Foundation. We are sincerely grateful for this assistance.

LITERATURE CITED

1a. P. Langevin, Ann. Chim. Phys., 5, 245 (1905).
1b. G. Gioumousis and D. P. Stevenson, J. Chem. Phys., 29, 294 (1958).
2a. T. F. Moran, and W. H. Hamill, J. Chem. Phys. 39, 1413 (1903).
2b. S. K. Gupta, E. G. Jones, H. G. Harrison and J. J. Myler, Can. J. Chem. 45, 3107 (1907).
3a. J. V. Dugan, and J. L. Magee, J. Chem. Phys. 47, 3106 (1967).
3b. J. V. Dugan, J. H. Rice and J. L. Magee, Chem. Phys. Letters, 2, 219 (1968).
4a. T. Su and M. T. Bowers, J. Chem. Phys. 58, 0000 (1973).
4b. T. Su and M. T. Bowers, J. Amer. Chem. Soc. 95, 1370 (1973).
5a. G. Sroka, C. Chang and G. G. Meisels, J. Amer. Chem. Soc. 95, 1052 (1972).
5b. C. Chang, G. J. Sroka and G. G. Meisels, J. Chem. Phys. 55, 5154 (1971).
6. C. Chang, G. G. Meisels and J. A. Taylor, Int. J. Mass Spectrom. Ion Phys.; in press.
7. M. T. Bowers and T. Su, private communication.
8. M. T. Bowers and T. Su, J. Chem. Phys. 56, 4711 (1972).

TABLE I. Comparison of Experimental and Calculated Rate Constants[a]

Neutral	α, Å^3	$\bar{E}$[b] eV	Experimental	Langevin
$n\text{-}C_4H_{10}$	8.21	.168	1.56 ± .08	1.85
$iso\text{-}C_4H_{10}$	8.28	.168	1.94 ± .05	1.86
		.084	2.02 ± .06	
$n\text{-}C_5H_{12}$	10.0	.084	2.42	2.00
$n\text{-}C_7H_{16}$	13.86	.168	2.59 ± .18	2.30
		.084	2.68 ± .06	

(a) Ion source pressure and temperature were .6 torr and 433 ± 10°K.
(b) Average ion energy, $\bar{E}$, calculated from the Wannier equation.[6]

TABLE II. Comparison of Experimental and Calculated Rate Constants[a]

Neutral	μ_D[b]	$\bar{E}_1$[c] eV	k, 10^{-9} cc sec^{-1} Experimental	Locked Dipole	Langevin
Trimethylamine	.643	.061	2.17	2.72	1.85
		.075	2.38	2.69	
1,1-Difluoro-ethylene	1.38	.075	1.54 ± .05[d]	3.09	1.31
		.097	1.37 ± .14	3.01	
		.128	1.32 ± .09	2.93	
Methanol	1.70	.075	2.44	3.78	1.27
		.097	2.95 ± .04	3.67	
		.128	2.98 ± .10	3.56	
		.168	3.09 ± .02	3.44	
Acetone	2.88	.061	3.55 ± .13	5.55	1.64
		.075	4.09 ± .24	5.43	
2-Butenal	3.67	.061	5.6	6.69	1.85

(a) Source pressure and temperature .6 torr and 440° ± 5°K.
(b) Dipole moment in Debyes.
(c) Average ion energy calculated from the Wannier equation.[6]
(d) Bowers, et.al.[8] report $k_{exp} = 1.27 \times 10^{-9}$ cc/sec and an ADO calculation resulting in $k_{ADO} = 1.87 \times 10^{-9}$ cc/sec at 300°K.

FIELD DESORPTION APPLICATIONS IN HIGH RESOLUTION MASS SPECTROMETRY OF UNSTABLE ORGANIC COMPOUNDS

by K. H. Maurer and U. Rapp

VARIAN MAT GMBH, Application Laboratory, D - 2800 Bremen, Germany

1. Introduction

Many organic molecules are labile under electron impact conditions and decompose partially or even completely. In the latter case, the molecular ion cannot be detected in the electron impact spectrum. Also in many cases the fragment ions formed don't give informations on the structure and the elemental composition of the molecule. For approximately 10 years, field ionization (FI) has been frequently and successfully applied for such problems and as a further gentle ionization method Chemical Ionization is used since some years.

The above mentioned ionization methods fail, however, in the cases in which the compound decomposition is caused by the energy necessary to bring the compound from the solid phase into the gas phase. Prof. Beckey's introduction (1), about 4 years ago, of a special field desorption technique (FD) has brought a significant breakthrough in this problem. By using this method, the spectra of a number of polar compounds of low volatility have been obtained for the first time without thermal decomposition. A number of papers concerning the method and the application of the FD-technique especially in Biochemistry have been published by the Bonn team (2,3,4). We have presented first results with a new combined electron impact/field ionization and field desorption ion source in 1970 at the International Conference of Mass Spectrometry in Brussels (5). In the meantime we have developed this new ion source further and we have applied it to problems in organic chemistry and in biochemistry.

2. Experimental

We want to report here some FD-results of labile substances mainly of biochemical interest. For the measurements we have used the double focusing mass spectrometer MAT 731 equipped with the combined source and electric and photographic recording systems. The low resolution FD-spectra have been recorded electrically, the high resolution spectra photographically.

The design of the combined ion source is very similar to conventional electron impact ion source, which results in comparable sensitivity in electron impact mode. The pusher plate, which forms the backside of the ionization chamber, is bored through for introduction of the field ion emitter. In its final position, the field ion emitter is located at the place where, under electron impact conditions, ionization normally occurs. The direct insertion probe, therefore, can be used for both electron impact and field ionization measurements.

For the FD-measurements we normally used as field ion emitters tungsten wires between 10 to 30 microns diameter, especially activated in a separate activation device at high wire temperature under 10^{-3} Torr benzonitrile partial pressure. These wires are extremely stable and can be used for many measurements. The position of the wire within the ion source is extraordinarily reproducible and for several FD-analyses there is no need for refocusing the ion source. So the analysis procedure is very easy: One takes the insertion rod system with the wire affixed on the top of the insertion rod and dips the wire into a solution of the compound to be examined. Then the insertion rod system is connected to the lock, the lock volume is pumped down, the wire introduced into the ion source and the system is ready for recording a FD-spectrum. The whole procedure needs about 2 minutes. Depending on the sample one has to choice the wire temperature by different currents and to start the scan depending on the total ion current signal. At the end of a measurement the wire will be heated up to about 1200 ^{0}C for cleaning and is then prepared for a new measurement.

In the most cases to make our life easier we have coupled the MAT 731 with the data system SS 100 for recording of low resolution FD-spectra. A calibration with PFK in the electron impact mode once a day is sufficient to obtain FD-spectra with correct mass numbers. Typical acquisition parameters are: resolution 1000, scan-times between 4 - 10 sec/dec, typical concentrations of the used solutions are 10 - 30 µg / µl corresponding to adsorbed sample amount on the wire of some 100 ng to 1 µg as a maximum.

3. Results and Discussion

In the application of the field desorption technique, the investigation of sugar derivatives with higher molecular weight seemes to be of some interest, especially the glycosides. As a representative, the g-strophanthin which is an important cardiac glycoside containing g-strophanthidin and one L-rhamnose residue is shown in fig. 1. In contrast to the electron impact spectrum, which shows only fragment ions in the low mass range giving little structure information, the FD-spectrum shows a strong molecular ion and some fragment ions mainly in the higher mass range.

One other example is shown in fig. 2. The helveticoside is a glycoside isolated and identified by Reichstein. Brown (6) has confirmed the proposed structure by taking an FI-spectrum. The FD-spectrum is easy to interprete showing only some characteristic fragment ions besides the molecular ion. The fragment ion m/e 131 can be attributed to the sugar-part (a digitoxose-residue) without the binding oxygen. The peak at mass number 403 represents the strophanthidine-moiety containing the binding oxygen. The fragment ion at mass number 358, which has been found by Brown as the base peak in the field ionization spectrum, results possibly from the ion m/e 403 by elimination of water and CO. The fragment at mass number 488 may be formed by loss of water and HCO from the (M + H)-ion.

Since introduction of penicillin to medicine, a great variety of antibiotics has already been developed and used for modern antibacterial chemotherapeutics. The name antibiotic is commonly applied to very complex molecules of different chemical classes such as penicillines, tetracyclines, aminoglycosides, macrolides, polypeptides and others. However, many antibiotic substances of interest give, under electron impact conditions, no or only weak molecular ions. With the FD-technique one obtains very intense molecular ion - groups for some important antibiotics such as neomycin, streptomycin, streptovaricin, filipin and several others as shown by Rinehart and Cook (7). Fig. 3 presents, as an example well known in medicine the antibiotic lincomycin produced by a streptomyces strain. The electron impact spectrum of this substance has been published in the last year (8) and shows a weak molecular ion. The base peak is the fragment ion m/e 126, which has been associated with the pyrolidine-part of the molecule. The three FD-spectra show very clearly the influence of the wire current on the break down pattern. At low temperature only the molecular ion group is observed, then increasing the temperature some fragment ions occur in addition and at least the fragment ions are dominating whereas the molecular ion-groups still present but only with an intensity of a few percent.

For exact mass measurements to determine the elemental composition of molecular ions and fragment ions in FD-spectra the photographic recording is a very useful method. Since only the molecular peak group and some characteristic fragment ions normally occur in the FD-spectrum it is obvious also to use a simple evaluation method. Fig. 4 shows the molecular ion-group of lincomycin at a resolution of about 10.000 and as a reference, the molecular ion-group of the hydrocarbon $C_{28}H_{58}$ in the same trace. We have manually measured the distances of the lines with a precise projector and calculated the lincomycin masses with a table computer using the slope of the PFK trace and the exact mass of the hydrocarbon spike. This simple method results in an accuracy of better than 3 millimass units in this mass range.

In biochemistry and pharmacy the purines and their derivatives as the nucleosides are of great interest, because they are also important components of RNA and DNA or enzymfactors, as of metabolite products. Therefore knowledge of the mass spectra will be useful for definite structure elucidation. Brown and co-workers (9) have published a thorough paper dealing with the electron impact and field ionization of mass spectra of nucleosides. Fig. 5 and Fig. 6 will show two FD-spectra of selected nucleosides. Interpretation of all nucleoside-spectra taken by field ionization and field desorption is very easy. We have chosen the purine containing nucleoside guanosine (Fig. 5). The published electron impact and field ionization spectra do not contain a molecular ion. Two peaks at m/e 265 and 266 are the highest mass numbers found in the field ionization spectrum, corresponding to water elimination, whereas the base peak is represented by the peak at m/e 151. In contrast to this finding, the field desorption spectrum reveals a dominating molecular ion group. Fragmentation occurs in the manner mentioned previously. The sugar moiety appears at m/e 133 and the purine base part plus one hydrogen appears at m/e 151.

Fig. 6 shows the high resolution FD-spectrum of inosine. We have changed the wire temperature during exposition, so that the molecular ion group and the main fragment ion group occur. The sugar moiety also appears at mass number 133 and the purine base part plus one hydrogen at mass number 136.

In the field of drug analysis the identification of several classes of compounds with electron impact mass spectrometry has failed because of absence of the molecular ion. As an example Fig. 7 shows the FD-spectrum of the sympathomimetic agent ephedrine. The pattern is quite simple and informative. The two important fragment ions at mass numbers 58 and 107 result by a benzylic cleavage, one containing the oxygen, the other the nitrogen. The electron impact spectrum published shows also the peak at mass number 58 as base peak but at masses higher than 100 no peak is observed.

Many barbiturates yield similar fragmentation patterns under electron impact lacking a significant molecular ion. Here again field desorption spectra show strong molecular ions. Fig. 8 demonstrates the necessity to have very simple spectra containing the molecular ion for easy identification of components in mixture analysis. We have mixed the four barbiturates barbital, pentobarbital, hexobarbital and heptabarbital. No overlapping of molecular ions and fragment ions takes place in this high resolution FD-spectrum.

The last example to show the capabilities of the field desorption method is the spectrum of cholic acid. Cholic acid is a main occuring bile acid. Djerassi and coworkers present in their book a spectrum of the triple-acetylated cholic acid methyl ester (10). Only a weak M - 60 - peak can be determined. The FD-spectrum (Fig. 9)shows in contrast to this finding, a dominating molecular ion group even from the totally underivatised cholic acid. Only small fragment peaks occur which represent water elimination.

The field desorption and electron impact mass spectrometry are quite supplementary methods. The impact of 70 eV electrons to organic molecules causes a variety of different information concerning the structure, whereas the soft field desorption yields relatively intense molecular ions of very unstable compounds in cases where the electron impact method and even other soft ionization methods like Chemical Ionization and Field Ionization fail. Furthermore with the field desorption technique one can obtain some characteristic fragment ions which deliver additional structure information.

4. References:

1. H. D. Beckey, J. Mass Spectr. Ion Phys. 2, 500 (1969).
2. H. U. Winkler and H. D. Beckey, Biochem. Biophys. Res. Comm. 46, 391 (1972).
3. H. R. Schulten and H. D. Beckey, Org. Mass Spectrom. 6, 885 (1972).
4. H. U. Winkler and H. D. Beckey, Org. Mass Spectrom. 6, 655 (1972)
5. H. D. Beckey, G. Hoffmann, K.H. Maurer and H. U. Winkler, Adv. in Mass Spectrometry, Vol. 5, p. 626, The Institute of Petroleum, London, 1971.
6. P. Brown, F. Bruschweiler, G. R. Pettit and T. Reichstein, Org. Mass Spectrom. 5, 573 (1971).
7. K. L. Rinehart and J. C. Cook, Paper presented at 21st Annual Conference on Mass Spectrometry and Allied Topics, San Francisco, May 1973.
8. F. Kagan and M. F. Grostic, Org. Mass Spectrom. 6, 1217 (1972).
9. P. Brown, G. R. Pettit and R. K. Robins, Org. Mass Spectrom. 2, 521 (1969).
10. H. Budzikiewicz, D. Djerassi and D.H. Williams, Structure Elucidation of Natural Products by Mass Spectrometry, Holden-Day Inc., San Francisco, 1964, p. 101.

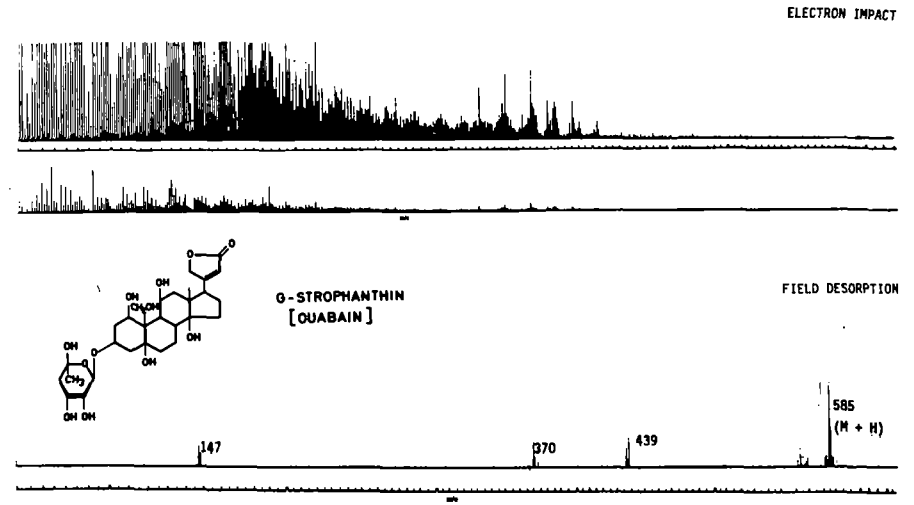

Fig. 1. Electron impact and field desorption mass spectra of g-strophanthin

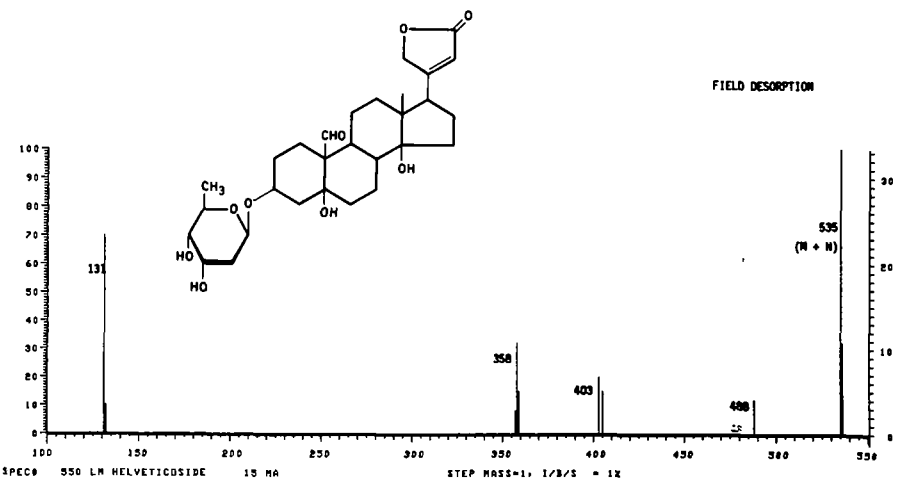

Fig. 2. Field desorption mass spectrum of helveticoside

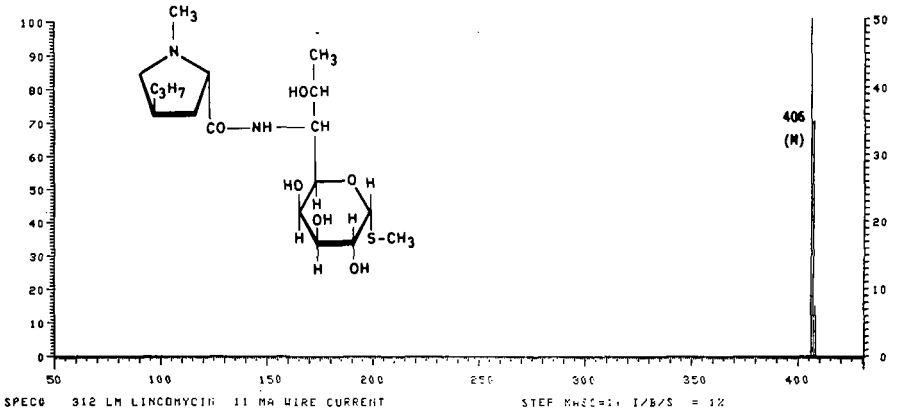

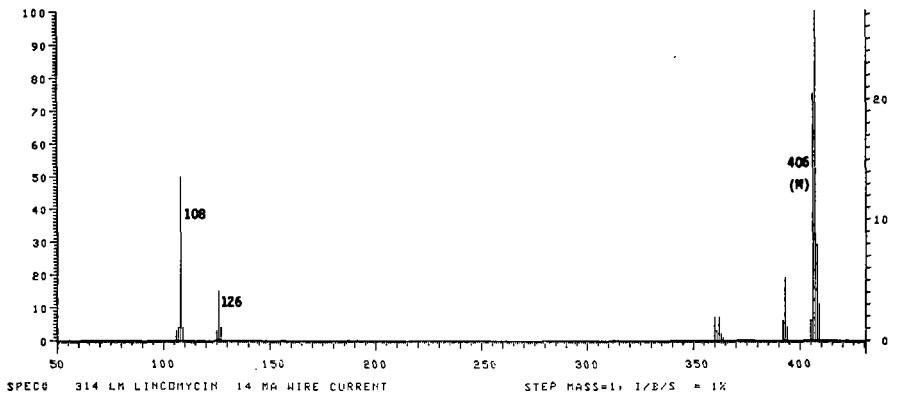

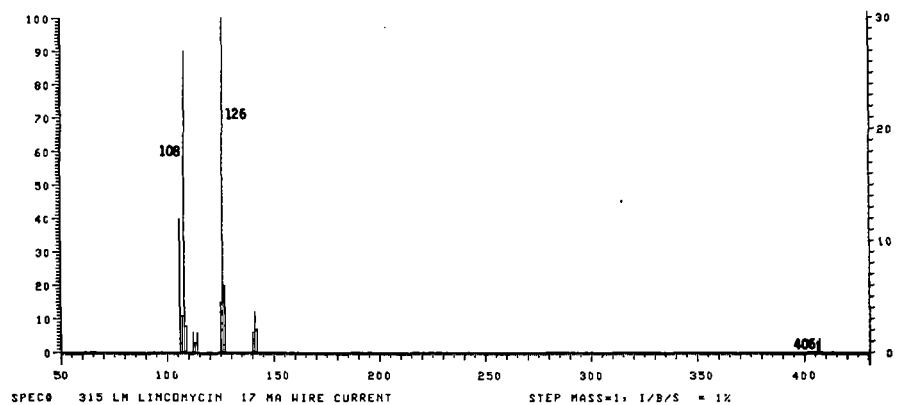

Fig. 3a - c. Field desorption mass spectra of lincomycin at different wire currents

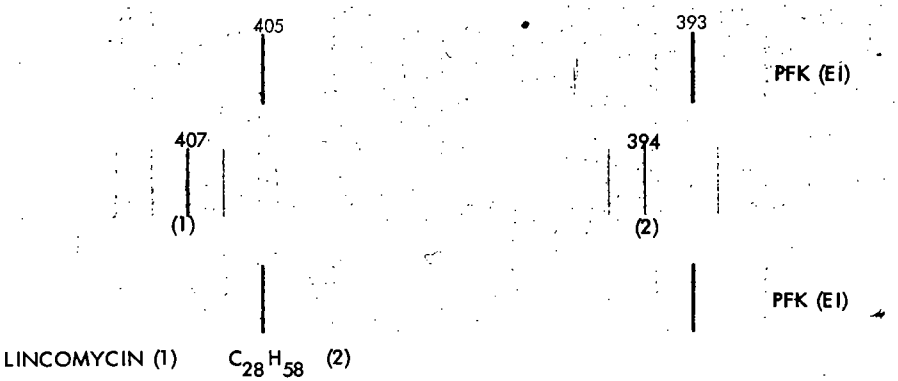

Fig. 4 High resolution field desorption mass spectrum of lincomycin (molecular ion group plus reference)

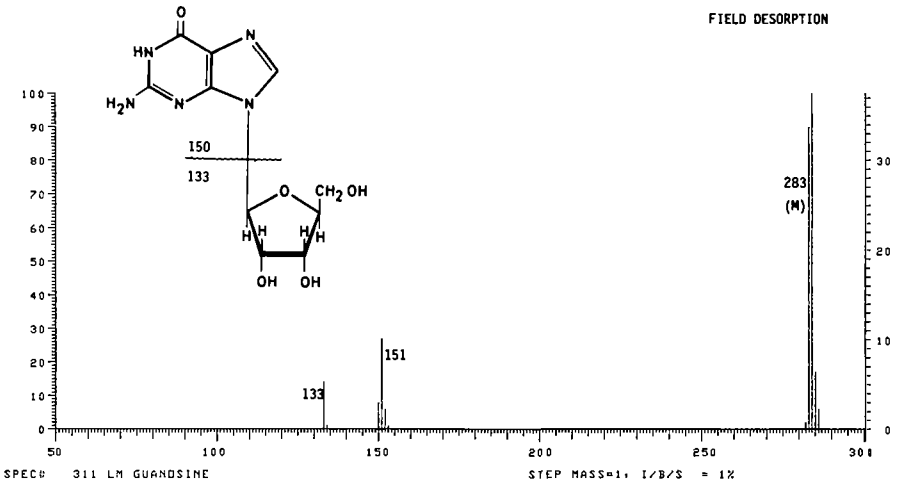

Fig. 5. Field desorption mass spectrum of guanosine

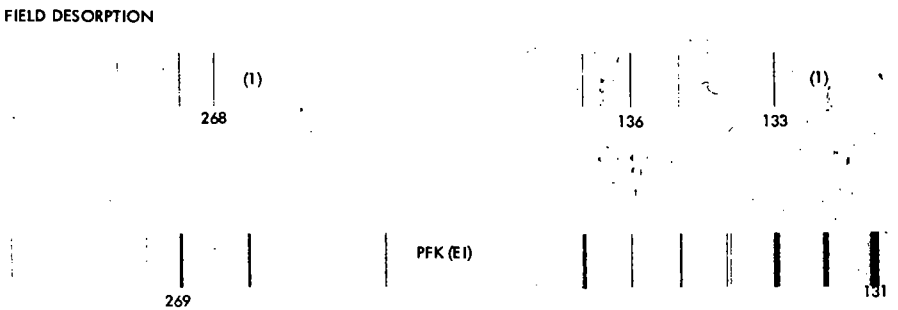

Fig. 6. High resolution field desorption mass spectrum of inosine

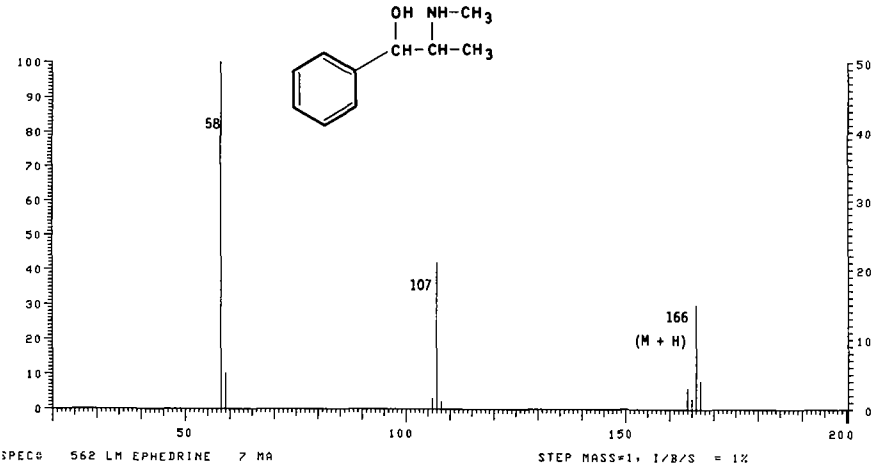

Fig. 7. Field desorption mass spectrum of ephedrine

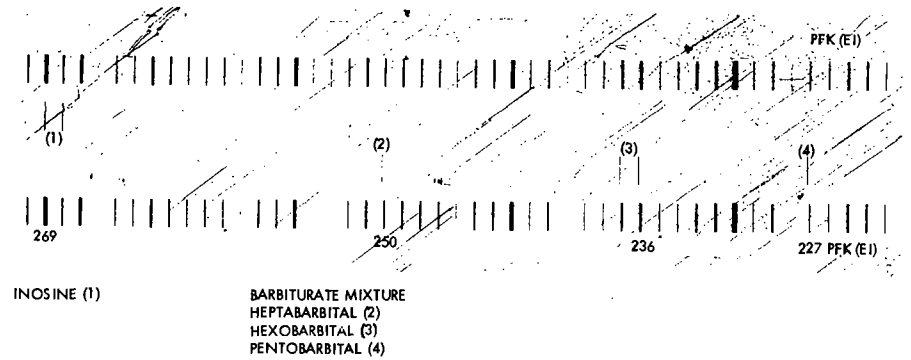

Fig. 8. High resolution field desorption mass spectrum of a barbiturate mixture

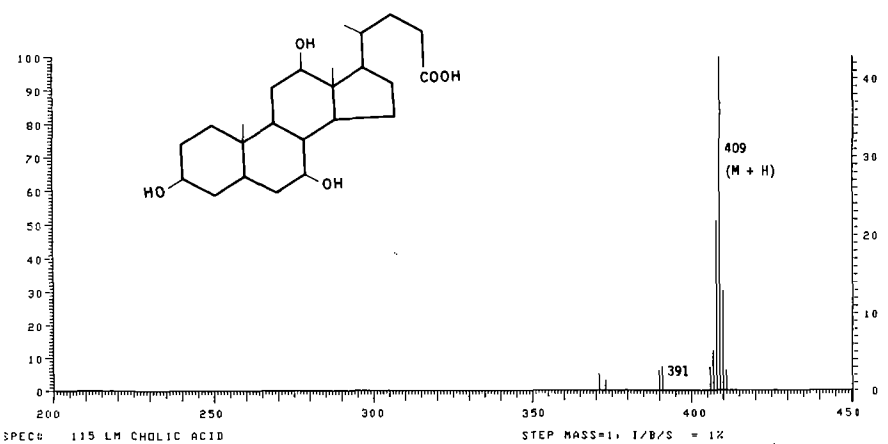

Fig. 9 Field desorption mass spectrum of cholic acid

In Vivo Measurement of Deuterium Labelled Alanine and Glucose Turnover in Plasma.
D.M. Bier, W.R. Sherman, W.H. Holland and D.M. Kipnis, Departments of Medicine and Psychiatry, Washington University School of Medicine, St. Louis, Missouri 63110

We have undertaken to devise micro-techniques using stable isotope labelled metabolites to study gluconeogenesis and glucose utilization in the pediatric age group since failure to maintain normoglycemia is a relatively common problem in childhood and one is reluctant to administer radioactive isotopes to the young child for investigative purposes.

Using the well established priming dose - constant infusion technique, we have made simultaneous measurements of alanine-d_4, alanine-^{14}C and 2,3-^{3}H-alanine turnover in 5 dogs as well as simultaneous determinations of glucose-d_7 and glucose-^{14}C flux in 2 dogs. The radioactive isotopes were infused intravenously in nanomolar quantities while the deuterated metabolites were administered in an amount calculated to enrich the free substrate pool to the 1-2% level.

Plasma samples of 50-500 μl were drawn at appropriate times and subjected to rapid ion exchange chromatography "clean up" procedures - using Dowex 50 in the case of alanine and Dowex-1-formate plus Dowex-50 in the case of glucose. After subsequent silylation (for alanine) or conversion to the dibutaneboronate acetate (for glucose), stable isotope enrichment was determined with a PDP-12 computer controlled variable accelerating voltage system developed in our laboratory (by Dr. W.F. Holmes) for multiple ion monitoring with an LKB-9000 combined gas chromatograph-mass spectrometer. With this system, analytical precision (average coefficient of variation between replicate measurements) has been 1.78% for plasma alanine-d_4 and 1.65% for plasma glucose-d_7 determination.

In the 5 dogs studied by combined radioactive and stable isotopic alanine infusions, the turnover rates (μmoles/kg·min) for plasma alanine-d_4, alanine-^{14}C, and 2,3-^{3}H-alanine ranged from 8.5 - 27.6; 7.0 - 24.7; and 9.5 - 34.5 respectively. Three men, studied with intravenous infusions of alanine-d_4 alone, had a mean alanine turnover rate of 316 μmoles/min, a value almost identical with the average alanine-^{14}C turnover rate found in the only published study of alanine turnover in man determined by isotopic infusion.

Plasma glucose-d_7 turnover rates of 10.2 and 13.9 μmoles/kg·min were virtually identical to the respective glucose-^{14}C turnover rates of 9.8 and 14.2 μmoles/kg·min in the two dogs studied by combined isotopic infusions. Furthermore, changes in steady state conditions produced by injections of insulin or glucagon were monitored equally well with either isotope. A single plasma glucose turnover study was performed in an adult man by continuous intravenous infusion of glucose-d_7 alone. The observed turnover rate of 116 mg/min was within the normal range of glucose turnover in adults determined by glucose-^{14}C infusions or by hepatic vein catheterization studies.

These results demonstrate that stable isotope methods can be applied for the study of new glucose production and glucose utilization in vivo. We have begun to extend these studies to the investigation of hypoglycemic conditions in childhood.

APPLICATION OF GC-MS TO METABOLISM STUDIES OF THE ANTINEOPLASTIC AGENT HEXAMETHYLMELAMINE*

By

Bruce M. Johnson, John F. Worzalla, and George T. Bryan†

Division of Clinical Oncology
Center for Health Sciences
University of Wisconsin
Madison, Wis. 53706

Hexamethylmelamine is an experimental antitumor drug currently undergoing clinical trials. The antitumor activity appears to be greatest against lung, ovarian, cervical, and breast cancer. The structure of hexamethylmelamine (HMM) is similar to that of triethylenemelamine (TEM). TEM is also an antitumor agent and is classified as a biological alkylating agent. Although HMM has not generally been classified as an alkylating agent, there are some clinical reports referring to it as such because of its spectrum of clinical activity and toxicity.

Early studies on the metabolism of these drugs showed that HMM is N-demethylated largely to N^2,N^4-dimethylmelamine and monomethylmelamine (1,2), whereas TEM is recovered largely as cyanuric acid (3). Thus, each behaves quite differently in biological systems. The alkylating property of TEM is generally attributed to the aziridine moiety. In the case of HMM, however, the active form of the drug could be any one of the demethylated metabolites. Thus, it becomes important to determine the detailed metabolic pathway. Early studies of HMM metabolism used ion exchange chromatography to isolate the group of methylmelamines and melamine from urine. The compounds were eluted from Dowex 50 using 6.2 N HCl. However, neither gradient elution ion exchange nor thin layer chromatography was capable of separating all of the isomers. Since a rapid and sensitive technique which could give quantitative results was required, a gas chromatographic method was tried. In 1968, Chang, DeMilo, Woods, and Bořkovec reported (4) the separation of the trimethyl- and tetramethylmelamine isomers by gas chromatography using a DEGS column. After several modifications, we found that all nine methyl melamine isomers and melamine could be separated as the underivatized compounds as shown in Figure 1. This separation of 2 micrograms of each isomer was carried out using a 2 foot by 4 mm ID column packed with 15% DEGS on 60/80 mesh Chromosorb W. Some unusual conditions were used in order to maintain sensitivity for the lower homologs. First, the column was conditioned for several days at 230°C, 30°C above the recommended 200°C maximum. Second, an alkali flame detector was employed using a rubidium sulfate-cesium chloride pellet on the flame jet tip. This enhanced the sensitivity towards monomethylmelamine and melamine and reduced the effect of column bleed. The separation is carried out by programming from 180°C to 250°C at 8°/min with a nitrogen carrier flow of 120 ml/min. With this technique, the detection limit for melamine is about 100 nanograms.

The mass spectrometric fragmentations of these compounds was investigated using synthesized samples of each of the isomers. Mass spectra were recorded at 70 eV with a Hewlett-Packard Model 5930A mass spectrometer using direct insertion and a source temperature of 200°C. The data for the more important analytical fragments are shown in Table 1. The values for percent ionization are for single spectra and subject to relative uncertainties of about 20%. In each case, within experimental variation, the molecular ion gives the base peak. There appears to be increased stabilization of the molecular ion in the fully methylated HMM. On the other end, monomethylmelamine and melamine indicate that the s-triazine ring is quite resistant to fragmentation, typical of aromatic systems in general. The peak found at M-15 for loss of a methyl group is seen to be significant only for those compounds having a dimethylamino substituent.

The next largest loss would be expected to involve the methylamino group. In all cases the major fragmentation is loss of 29 amu, with a very weak loss of 30 amu. Thus, one hydrogen is transferred to the ring and the departing fragment has the formula CH_3N. This can be accounted for by transferring a methyl hydrogen to a ring nitrogen to form an imine. Deuterium labelling on the amino nitrogens in N^2,N^4,N^6-trimethylmelamine, N^2,N^4-dimethylmelamine, and monomethylmelamine shows that it is only the methyl hydrogen which is rearranged (SCHEME I). This satisfactorily explains the methylamino group, but there is also an unusually large peak for loss of 29 from the dimethylamino group. A mechanistic study of the loss of methylene imine from the dimethylamino group in several N-heteroaromatic systems was reported at this meeting, paper I-11. Their results indicate that the reaction is more complicated than a simple methyl migration. However, in our study, deuterium labelling of N^2,N^2-dimethylmelamine indicates that there is no involvement of any amino hydrogens in the methylene imine loss. A dilemma arises, however, when the ion intensities for the tetramethyl- and trimethylmelamine isomers are

compared. These values give no straightforward indication of which substituent is responsible for the product ion at M-29. By using deuterium labelled N^2,N^2,N^4-trimethylmelamine, the relative contributions of these processes can be distinguished. The peak at M-29 results from a cleavage of the dimethylamino group, whereas, cleavage of the methylamino group yields an M-30 (SCHEME 2). The peak ratio, at 70 eV, indicates that the fragmentation of the dimethylamino group is about 3.4 times more favorable than the methylamino loss.

SCHEME 1

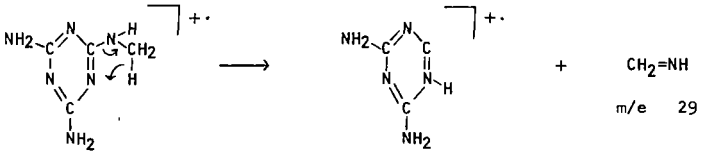

SCHEME 2

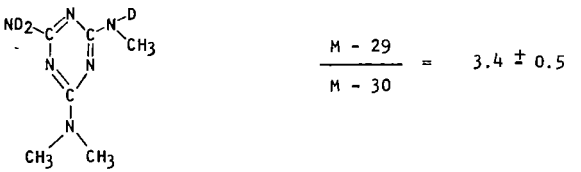

The next major ion to be observed appears as loss of 43 amu. This fragmentation corresponds to the dimethylamino analog of the 29 amu loss of methylene imine from the methylamino group. As can be seen from the intensities in Table 1, this cleavage (SCHEME 3) is indicative of a dimethylamino substituent and is diagnostic for N^2,N^2,N^4-trimethylmelamine and N^2,N^2-dimethylmelamine. In monomethylmelamine and melamine the loss of 43 is most likely the result of a ring cleavage involving an imine hydrogen (SCHEME 4).

SCHEME 3

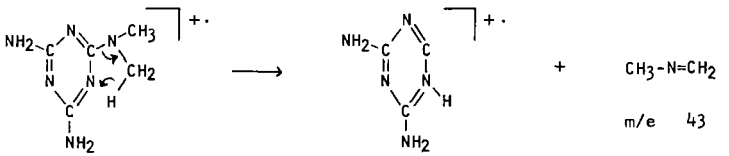

SCHEME 4

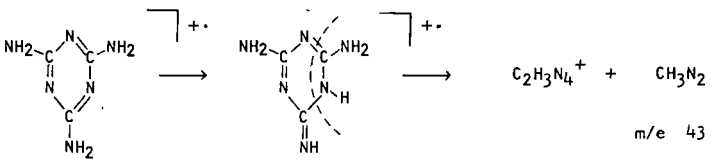

Those peaks at low mass which have relatively large differences for the isomeric pairs having the same molecular weight are shown in Table 2. As can be seen, each pair has several masses at which intensity differences are sufficient to allow unambiguous identification. Thus, mass spectrometric confirmation of metabolite identity can be accommodated for all of the possible N-demethylation products of HMM.

This technique can be applied to urinary excretion studies as follows. A 24 hour urine specimen collected after i.p. injection of 10 mg of HMM into a 200 g. rat is treated as shown in Figure 2. The acidified urine is eluted from ion exchange columns to remove most of the excess ionic materials, followed by concentration to a small volume. At this level of concentration, a one microliter injection provides for detection of any metabolite corresponding to greater than 0.5% of the administered dose.

A typical chromatogram of treated rat urine is shown in Figure 3. The identity of each of the metabolites was confirmed by mass spectrometry. The major metabolites are N^2,N^4,N^6-trimethylmelamine, N^2,N^4-dimethylmelamine, and monomethylmelamine. From these data we can deduce that the N-demethylation is directed primarily at the dimethylamino group. This is then followed by a slower N-demethylation of the methylamino group.

ACKNOWLEDGEMENT

*Supported in part by Grant No. CA-13290 from the National Cancer Institute, USPHS.

†Career Development Awardee of the National Cancer Institute (1-K4-CA-08245).

REFERENCES

1. Worzalla, J. F., G. Ramirez, S. Mackman and G. T. Bryan, Metabolism of ^{14}C-Methyl-Hexamethylmelamine (NSC-13875) in Rats and Man. Proc. Am. Assoc. Cancer Res., 12: 3, 1971.

2. Worzalla, J. F., B. D. Kaiman, B. M. Johnson, R. O. Johnson, and G. T. Bryan, Metabolism of Ring-^{14}C-Hexamethylmelamine (NSC-13875, HMM) in Rats. Proc. Am. Assoc. Cancer Res., 14: 25, 1973.

3. Nadkarni, M. V., E. I. Goldenthal, and P. K. Smith, The Distribution of Radioactivity Following Administration of Triethylenimino-s-Triazine-C^{14} in Tumor-Bearing and Control Mice. Cancer Res., 14: 559-562, 1954.

4. Chang, S. C., A. B. DeMilo, C. W. Woods, and A. B. Borkovec, Metabolism of C^{14}-Labeled Hemel in Male House Flies. J. Econ. Entomol., 61: 1357-1365, 1968.

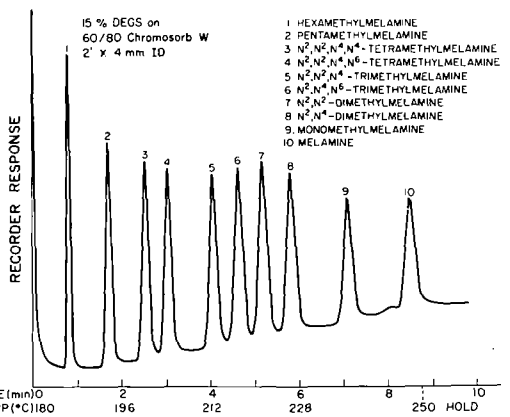

FIGURE 1. Chromatogram of 2 μg. of each of the methylmelamines and melamine.

TABLE 1. IMPORTANT HIGH MASS FRAGMENTS OF THE METHYLMELAMINES AND MELAMINE.

melamine	M	M - 15	M - 29	M - 43
Hexamethyl	17.4	14.3	3.9	5.2
Pentamethyl	8.2	6.8	2.7	3.9
N^2,N^2,N^4,N^4-Tetramethyl	9.1	6.5	3.2	3.1
N^2,N^2,N^4,N^6-Tetramethyl	7.9	4.0	2.7	3.0
N^2,N^2,N^4-Trimethyl	9.8	4.0	3.8	3.8
N^2,N^4,N^6-Trimethyl	12.2	0.19	8.1	0.27
N^2,N^2-Dimethyl	10.6	4.8	5.4	5.4
N^2,N^4-Dimethyl	13.9	0.14	8.4	0.58
Monomethyl	24.2	0.10	14.9	2.4
Melamine	52.8	0.09	0.08	4.3

TABLE 2. LOW MASS PEAKS SHOWING ISOMERIC DIFFERENCES IN INTENSITY

methylmelamines	m/e									
	44	56	57	69	70	71	72	82	83	98
N^2,N^2,N^4,N^4-tetra-			1.3		1.4			1.5		
N^2,N^2,N^4,N^6-tetra-			8.5		0.15			6.1		
N^2,N^2,N^4-tri-	4.0					2.8	2.4			
N^2,N^4,N^6-tri-	0.54					0.31	0.26			
N^2,N^2-di-	5.7	0.34	0.31	8.9				0.34	0.61	0.33
N^2,N^4-di-	0.72	2.5	7.2	2.1				3.2	4.3	2.9

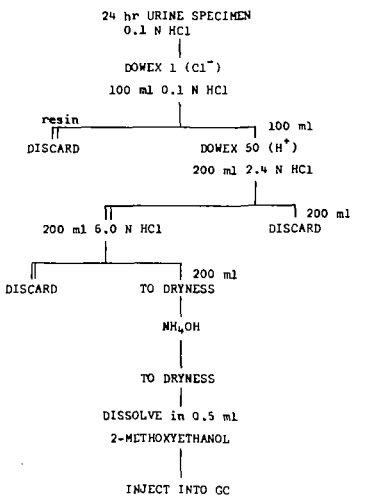

FIGURE 2. Scheme for urine preparation for analysis by gas chromatography.

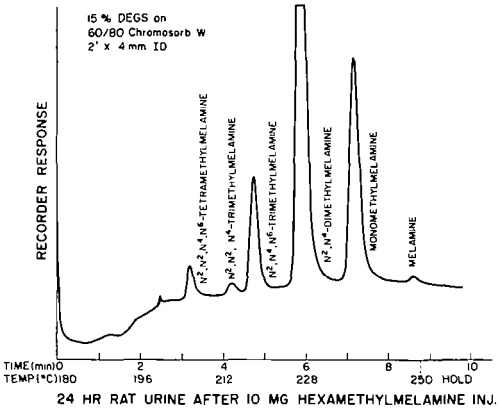

FIGURE 3. Chromatogram of HMM metabolites in rat urine

GC-MS APPLICATIONS TO THE BIOCHEMISTRY OF SCHIZOPHRENIA

N. Narasimhachari

Thudichum Psychiatric Research Laboratory
Galesburg State Research Hospital
Galesburg, Illinois 61401

During the past decade two theories of the biochemical etiology of schizophrenia have evolved. Both involve abnormal transmethylation. One postulates the synthesis of the well-known psychotogenic dimethylated tryptamines, N:N-dimethyltryptamine (DMT), bufotenin and 5-methoxy-N:N-dimethyltryptamine (5-MeODMT), by the N-methylation of the normal metabolites, tryptamine and 5-hydroxytryptamine (5-HT). The biosynthetic pathway for the production of these compounds is shown in Scheme I. All of the enzymes required for these transformations have been identified and the key enzyme for N-methylation, indolethylamine-N-methyltransferase (INMT), which was first reported by Axelrod[1], has since been found in the brain[2,3,4,5], blood[6] and lung[7] of humans and in the tissues of several infrahuman species.

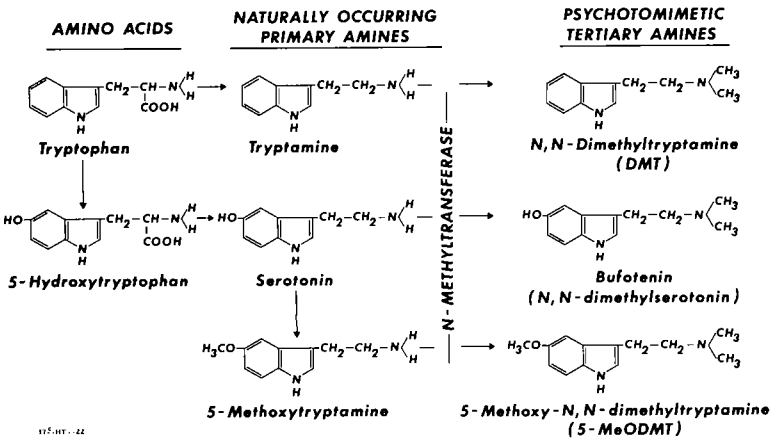

Scheme I. Indoleamine methylation

The second hypothesis deals with the O-methylation of the natural metabolite, dopamine, to 3:4-dimethoxyphenylethylamine (DMPEA), which is structurally similar to the naturally occurring hallucinogen, mescaline[8]. The possible biosynthetic pathway to DMPEA is shown in Scheme II. The presence of the enzyme, catechol-O-methyltransferase, and of enzyme systems capable of monomethylating dopamine is well established. However, the evidence for an enzyme producing the dimethylated compound is not conclusive.

In our continuing efforts to provide conclusive and unequivocal evidence for the presence of these metabolites in urine samples from both schizophrenics and normals, we

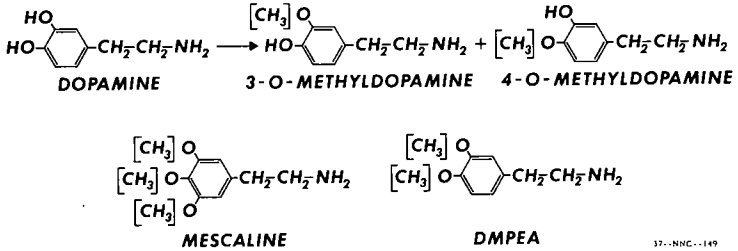

Scheme II. Catecholamine methylation

have investigated the application of GC-MS techniques for the identification of both the indoleamines and the catecholamines.

By a procedure of quantitative derivatization, the dimethylated tryptamines were converted to their trimethylsilyl (TMS) derivatives and their gas-chromatographic and mass spectral data were reported[9]. Similarly, procedures for the GC separation and GC-MS identification of several phenylethylamines, amphetamines and tryptamines as their isothiocyanate (NCS) derivatives were described[10,11].

Using these specific GC-MS methods, we have recently identified bufotenin in the urine samples of two schizophrenic patients and of two children with a diagnosis of early infantile autism[12]. DMT was also identified in the urine samples of two schizophrenic patients and was quantitated by the single ion monitoring technique (in preparation).

We also examined urine samples from schizophrenic subjects and normals for DMPEA. The NCS fraction from the urine extracts was tested for DMPEA-NCS by a sensitive TLC method[13], as well as by GC and GC-MS methods[14]. Since tea had been reported as being a source of DMPEA in the urine[15], some of the normal volunteers were given large quantities to drink. Furthermore, some of the subjects were on an MAO inhibitor and the amine concentrations in their urine were elevated. However, in no case so far have we been able to identify DMPEA in the urine. The results of this study have recently been reported[14].

In our studies on abnormal methylation, we also used specific GC-MS methods to examine the activity, kinetics and inhibition of indole-*N*-methyltransferase and catechol-*O*-methyltransferase.

For indole-*N*-methyltransferase, N-methyltryptamine (NMT) was used as the substrate and the product, DMT, was separated from NMT on an OV-225 column. The GC peak was used to quantitate DMT after its identity and homogeneity as wholly DMT had been confirmed by its mass spectrum. This method was used to screen blood samples for the enzyme activity (in preparation).

For catechol-*O*-methyltransferase activity dopamine, dopamine-NCS, 3:4-dihydroxyphenylacetic acid and its ethyl ester were used as substrate. GC-MS was used to identify

and quantitate the product and to determine the ratio of meta/para-O-methylation[16].

The details of these simple, but specific, nonradiometric methods, which are now in routine use in our laboratories, are being prepared for publication.

References

1. J. Axelrod, Science, 134, 343 (1961).
2. M. Morgan and A. J. Mandell, Science, 165, 492 (1969).
3. A. J. Mandell and M. Morgan, Nature, 230, 85 (1971).
4. J. M. Saavedra and J. Axelrod, Science, 175, 1365 (1972).
5. J. M. Saavedra, J. T. Coyle and J. Axelrod, J. Neurochem., 20, 743 (1973).
6. N. Narasimhachari, J. Plaut and H. E. Himwich, Life Sci., 11 (Part II), 221 (1972).
7. L. R. Mandel, H. S. Ahn, W. J. A. VandenHeuvel and R. W. Walker, Biochem. Pharmacol., 21, 1197 (1972).
8. A. J. Friedhoff and E. Van Winkle, Nature, 194, 897 (1962).
9. N. Narasimhachari, J. Spaide and B. Heller, J. Chromatogr. Sci., 9, 502 (1971).
10. N. Narasimhachari and P. Vouros, Anal. Biochem., 45, 154 (1972).
11. N. Narasimhachari and P. Vouros, J. Chromatogr., 70, 135 (1972).
12. N. Narasimhachari and H. E. Himwich, Life Sci., 12 (Part II), 475 (1973).
13. N. Narasimhachari, J. Plaut and K. Y. Leiner, J. Chromatogr., 64, 341 (1972).
14. N. Narasimhachari, J. Plaut and H. E. Himwich, J. Psychiat. Res., 9, 325 (1972).
15. J. R. Stabenau, C. R. Creveling and J. Daly, Am. J. Psychiat., 127, 611 (1970).
16. R.-L. Lin and N. Narasimhachari, Anal. Biochem., (in press).

QUANTIFICATION WITH STABLE ISOTOPES OF DRUGS AND DRUG METABOLITES BY GC-MS-COM PROCEDURES

W. G. Stillwell, M. G. Horning, and R. N. Stillwell
Institute for Lipid Research
Baylor College of Medicine
Houston, Texas 77025

Quantification of drugs and drug metabolites in human plasma, breast milk and amniotic fluid samples was carried out by single and multiple ion monitoring using the mass spectrometer as the detector. Two GC-MS-computer systems were employed in this work. An LKB-9000 GC-mass spectrometer was interfaced to a PDP 12 computer which was used to drive the accelerating voltage across the m/e values to be measured and determine the electron multiplier output at the corresponding peak maximum. The other system was a quadrupole mass spectrometer operating in chemical ionization mode (methane) and driven by a PDP 8/I computer. Both computers provided both graphic and numerical peak area measurements.

These techniques have been used to measure several barbiturates, anticonvulsant drugs, and steroids in sub-microgram quantities in biological extracts. Internal standards labeled with stable isotopes are preferred for quantitative analysis by selective ion detection. Diphenylhydantoin-2, 4, 5-^{13}C has been used to quantify diphenylhydantoin, and pentobarbital-2, 4(6), 5-^{13}C has been used to quantify amobarbital, secobarbital, caffeine, Demerol, and phenobarbital in 50-100 μl samples of plasma and breast milk. With these analytical procedures it is now possible to measure plasma concentrations of diphenylhydantoin and the barbiturates in newborn infants where sample size is limited. The availability of ^{13}C-labeled drugs which can be used as internal standards greatly improves the accuracy of measurements made at the picogram and nanogram level.

This work was supported by Grant GM-16216 of the National Institute of General Medical Sciences.

A detailed report of this study will appear: M. G. Horning, J. Nowlin, K. Lertratanangkoon, R. N. Stillwell, W. G. Stillwell, and R. M. Hill, Clin. Chem. (In press).

Liquid Chromatography-Mass Spectrometry: Coupling of a Liquid Chromatograph to a Mass Spectrometer. ROBERT E. LOVINS, STEPHEN ELLIS, GARY TOLBERT and CHARLES McKINNEY, Dept. of Biochemistry, University of Georgia, Athens, Ga.

An interface permitting the coupling of a liquid chromatograph to a mass spectrometer has been developed. The interface has been designed to accept the effluent peak directly from a liquid chromatograph, remove the solute from the mobile phase by either flash evaporation or selective adsorption on a high capacity adsorbent and automatically introduce the sample into the mass spectrometer ion source for analysis. The heart of the interface consists of a motor driven hollow probe with a tip containing a high capacity heat stable adsorbent and a small motor driven high vacuum bellows value which isolates the probe from the mass spectrometer ion source. The operation of the interface is accomplished by solenoid valves and has been designed to work semiautomatically. The application of mass spectrometry to the analysis of a number of mixtures separated on the liquid chromatograph and isolated and analyzed using the interfaced system will be discussed.

To be published in Anal. Chem.

Gas Phase Ammonolysis in Chemical Ionization Mass Spectrometry

Klaus D. Haegele and Dominic M. Desiderio

Institute for Lipid Research and Department of Biochemistry

Baylor College of Medicine

Houston, Texas 77025

The macrolide antibiotic antimycin A has found use in fish management and as a specific inhibitor of certain enzyme mechanisms in the electron transport system. The structure is shown below (I) (1-3).

By using several simple derivatives of the complex (II-V) and applying low resolution MS (LKB 9000) and high resolution MS (CEC 21-110B) we were able to propose a fragmentation pathway. Major fragments occur by McLafferty rearrangements (4).

To establish the molecular ion region it was necessary to run chemical ionization MS with ammonia as a reagent gas. Both $(M+1)^+$ and $(M+18)^+$ ions were observed for the homologous series in the Figure. EI accurate mass measurements of the fragments which contain either R_3 or R_4 helped us to semiquantify the results and to detect 23 components in the antimycin A complex. By comparison of the EI and CI spectra, some of the newly observed ions in CI show shifts of 17 mass units. At a pressure of 1 torr NH_3 in the source at 500°K we have 50 μmol NH_3. A total amount of 10 μmol of sample is supplied to that source over a period of 100-300 seconds. This means that there is always an excess of several hundred fold of ammonia over sample. Therefore gas phase ammonolysis of the base sensitive lactone, ester and amide bonds can easily occur. The amides formed are then protonated by the NH_4^+ species. Thus the "fragments" seen in the CI spectrum are actually protonated molecular ions. Another advantage of the CI/ammonia spectra is that the intensity of some of the ions which showed a rather low intensity in the EI spectrum is greatly enhanced.

Another example for this reaction was demonstrated by the dipeptide N-acetyl-prolyl-tryptophan-methyl ester. Ammonolysis of the peptide bond is shown by the occurrence of an ion at m/e 157 corresponding to N-acetyl-prolyl-amide. By using ND_3 as a reagent gas, this ion is observed at m/e 160; the deaminated tryptophan-methyl ester is observed at m/e 202. The peaks due to the ammonolysis products are less intense as compared to the peaks obtained from the gas phase ammonolysis pro-

ducts of antimycin A because of the higher stability of the peptide bond to ammonia.

In summary, the procedures outlined offer advantages in investigating mixtures and/or compounds with ammonia labile bonds.

Acknowledgement. This work was supported by NIH 69-2161 and the Robert A. Welch Foundation (Q-125).

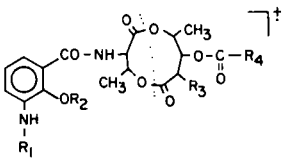

	R_1	R_2	
I	CHO	H	R_3 = CH_3-C_6H_{13}, C_8H_{17} (15)
II	CHO	CH_3	
III	H	H	
IV	CH_3CO	H	R_4 = CH_3, C_3H_7-C_5H_{11}
V	CD_3CO	H	

References

1. B. R. Dunshee, C. Leben, G. W. Keitt and F. M. Strong. J. Amer. Chem. Soc., 71, 2436-2437 (1949).

2. A. J. Birch, D. W. Cameron, Y. Harada and R. W. Rickards. J. Chem. Soc., (1961), 889-895.

3. E. E. Van Tamelen, J. P. Dickie, M. E. Loomans, R. S. Dewey and F. M. Strong. J. Amer. Chem. Soc., 83, 1639-1646 (1961).

4. K. D. Haegele and D. M. Desiderio. J. Antibiotics, 26, 215-222 (1973).

^{18}O Probe into the Mechanisms of Action Of Aldolase Enzymes

E. J. Heron and R. M. Caprioli
Dept. of Chemistry, Purdue University
West Lafayette, Indiana 47907

Enzymes which catalyze the aldol cleavage/condensation of various keto compounds are generally categorized as either Class I or Class II aldolases on the basis of their metal requirement for enzymatic activity, as well as other properties.[1] Class I aldolases do not require divalent metal cations for activity and their mechanism is thought to proceed through Schiff base intermediates. The evidence for such intermediates includes the isolation of reduced Schiff base derivatives of the enzyme-substrate complexes.[2] Class II aldolases, on the other hand, require divalent metal ions for activity and may effect catalysis via a metal chelate rather than a Schiff base intermediate. Although attempts to isolate reduced Schiff base intermediates for these enzymes have been unsuccessful, there is a lack of direct evidence concerning the mechanism of the Class II aldolases.

The reaction mechanisms of fructose 1,6-diphosphate (FDP) aldolases were investigated using a combination of stable isotope labeling and mass spectrometry. The fate of the keto oxygen atom of FDP in the enzymatic reaction was determined using ^{18}O as a tracer. The abundance of ^{18}O in the (2-^{18}O)FDP was determined by rapid hydrolysis to fructose with acid phosphatase, followed by esterification with trifluoracetic anhydride and direct mass spectrometric analysis. The ion at $(M-127)^+$ due to the loss of a terminal $CF_3COOCH_2^{\cdot}$ group was used for these measurements. These experiments showed that the (2-^{18}O)FDP was in isotopic equilibrium with the 47 atom % excess $H_2{}^{18}O$ after 20 hrs. of exchange at room temperature.

The (2-^{18}O)FDP was cleaved to dihydroxyacetone phosphate (DHAP) and D-glyceraldehyde 3-phosphate with aldolases isolated from both rabbit muscle (Class I) and yeast (Class II). The rapid nonenzymatic exchange of the keto oxygen of DHAP[3] made ^{18}O analysis of this compound difficult. To eliminate this exchange, NADH and α-glycerophosphate dehydrogenase were added to the reaction mixture in order to rapidly reduce the keto group of DHAP to the nonexchangeable hydroxyl group of glycerol 1-phosphate. The position and abundance of the ^{18}O label in the L-glycerol 1-phosphate formed in the reaction were determined by direct mass spectrometric analysis of the dimethyl ester, bis-trimethylsilyl ether derivative.[4] Although a molecular ion was not present in the mass spectrum of this derivative, the ion at $(M-15)^+$ was found to be suitable for isotopic abundance measurements. The (2-^{18}O) and (3-^{18}O) analogs of glycerol 1-phosphate

were prepared and used to confirm the absence or presence of these oxygen atoms in various ions. The ion at m/e 299 was shown to arise from $(M-15)^+$ by loss of CH_2O from the C-3 position. Thus, these ions were used to determine the position of the label within the molecule. In order to avoid unlabeled glycerol 1-phosphate arising from the enzmyatic conversion of D-glyceraldhyde 3-phosphate to DHAP catalyzed by triosephosphate isomerase, residual amounts of this enzyme were inactivated with chloroacetol phosphate.[5]

The results presented in Table I show that cleavage of (2-^{18}O)FDP by rabbit muscle aldolase, the prototype of the Class I enzymes, resulted in complete loss of the label. Since the keto oxygen would be lost to the solvent when the Schiff base is formed, this result is clearly consistent with the proposed mechanism for the Class I aldolases. On the other hand, a significant amount of isotope was retained in the yeast aldolase reaction, the prototype of the metal-requiring aldolases. Thus, regardless of the mechanism, the keto oxygen of FDP does not suffer an obligatory loss in the reaction. Since the formation of a metal chelate intermediate does not require that the keto oxygen be lost, this result is consistent with the mechanism proposed for the Class II aldolases.

Table I. Aldolase Catalyzed Cleavage of (2-^{18}O)FDP

Enzyme	Dehydrogenase: aldolase ratio	atom % excess ^{18}O in glycerol 1-phosphate[a]
Rabbit Muscle FDP-Aldolase	4:1	0.0
	40:1	0.2
Yeast FDP-Aldolase	2:1	17.7
	5:1	27.7
	10:1	26.2

[a] The (2-^{18}O)FDP contained 46.5% excess ^{18}O.

The ratio of aldolase to dehydrogenase was varied in order to maximize the retention of label by minimizing the lifetime of free DHAP. Under these conditions, the maximum amount of isotope retained was approximately 60%. Possible reasons for this loss of ^{18}O are: (i) reoxidation of glycerol 1-phosphate to DHAP followed by exchange, (ii) exchange of DHAP prior to reduction, and (iii) nonobligatory enzyme-catalyzed exchange of FDP and/or DHAP. Control experiments indicate that (i) cannot account for all the loss of label observed. Experiments to further characterize this effect are currently in progress.

The results obtained for the prototypes of the two classes of aldolase are consistent with the proposed mechanisms and give direct evidence which can be used to unambiguously classify various other aldolases. The techniques described here are now being used to investigate aldolases whose chemical and physical properties do not clearly place them in either category.

Acknowledgements: The authors wish to thank Dr. R. L. VanEtten for the wheat germ acid phosphatase. One of the authors (E.J.H.) is a National Institutes of Health Trainee, Grant No. 5T01 GM 1195, and thanks NIH for support.

References

1. W. J. Rutter, Federation Proc. 23, 1248 (1964).
2. B. L. Horecker, S. Pontremoli, C. Ricci, and T. Cheng, Proc. Natl. Acad. Sci. U.S. 47, 1949 (1961).
3. P. Model, L. Ponticorvo, and D. Rittenberg, Biochemistry 7, 1339 (1968).
4. R. M. Caprioli and E. J. Heron, Biochim. Biophys. Acta 296, 321 (1973).
5. F. C. Hartman, Methods in Enzymology 25 Part B, 661 (1972).

Chemical Ionization Mass Spectrometry of Nucleosides

Martha S. Wilson and James A. McCloskey

Institute for Lipid Research and Department of Biochemistry
Baylor College of Medicine
Houston, Texas 77025

The identification of nucleosides by electron ionization mass spectrometry is limited in some instances by a low abundance of the molecular ion (M). The molecular weight can be established clearly by means of chemical ionization mass spectrometry (CIMS) resulting in a large abundance of MH^+, sometimes formed at the expense of structurally diagnostic fragment ions. A variety of reagent gases has been investigated, including methane, isobutane, ammonia and mono-, di- and trimethylamines. In each case, the principal ions correspond to base + $2H^+$, MH^+ and nucleoside-reagent gas complexes. The extent of fragmentation is a function of the reagent gas basicity and ranges from considerable fragmentation with methane to very little with trimethylamine. Fragment ion identities and fragmentation mechanisms have been ascertained by means of high resolution CIMS, metastable ion defocussing and the use of ammonia-^{15}N, methane-d_4 and isobutane-d_{10} as reagent gases.

The use of reagent gases covering a wide range of proton affinities from methane to trimethylamine allows an estimation of the gas phase proton affinities of the nucleosides, based on the occurrence of appropriate proton transfer reactions. The order of gas phase basicities was found to be: adenosine, cytidine, guanosine > trimethylamine > methylamine > uridine, thymidine. Purine and pyrimidine bases follow a similar order but with generally lower absolute values.

Ribosomal RNA and several oligonucleotides obtained from transfer RNA and containing modified bases have been degraded enzymatically to nucleosides, permethylated, and the components identified by CIMS.

This approach is potentially attractive because by suitable choice of reagent gas, (1) nearly all of the ion current from each component of the mixture can be channeled into several diagnostic ions, and (2) response from impurities having low proton affinities can be minimized.

Details of this study will be published elsewhere.

Mass Spectra of Prostaglandin Derivatives

Brian S. Middleditch and Dominic M. Desiderio

Institute for Lipid Research and Department of Biochemistry

Baylor College of Medicine

Houston, Texas 77025

In the course of a detailed examination of the mass spectra of trimethylsilyl (TMS) derivatives of prostaglandins, we have found multiple origins for the ions of m/e 173 and m/e 199. These ions were hitherto thought to be characteristic of the C-13/20 chain of TMS derivatives of prostaglandins.

This work was aided by high-resolution mass spectrometry and deuterium labelling. Complete low- and high-resolution spectra were obtained for TMS and methyl oxime (MO) and ethyl oxime (EO)-TMS derivatives of each of the primary prostaglandins and several synthetic prostaglandin analogs. d_9-TMS derivatives were prepared using d_{18}-BSA. Selectively labelled TMS ester d_9-TMS ether derivatives were made from the per-d_9-TMS derivatives by exchange of the more labile ester TMS group during gas chromatography.

The "conventional" ions of m/e 199 and 173 were formed from the TMS derivative of prostaglandin A_1. High-resolution mass measurements showed that these ions had elemental compositions $C_{11}H_{23}OSi$ and $C_9H_{21}OSi$, respectively. The selective d_9-TMS labelling data confirmed that each of these ions contained an ether TMS group. Direct cleavage of the C-12/13 and C-14/15 bonds is unlikely, since they are adjacent to the C-13/14 double bond. An alternative mechanism for the formation of these ions is shown in Scheme 1.

The ion of m/e 199 was absent from spectra of TMS derivatives of prostaglandins of the B series since their formation would have involved cleavage of the C-12/13 bond which is between the conjugated C-8/12 and C-13/14 double bonds. The ion of m/e 173 was also present only in low abundance in most of the spectra, perhaps supporting the route of formation of these ions shown in Scheme 1.

The high-resolution spectrum of the TMS derivative of prostaglandin E_1 showed that the ions of m/e 199 and 173 were both doublets, with additional components of elemental composition $C_{10}H_{19}O_2Si$ and $C_8H_{17}O_2Si$, respectively. Selective d_9-TMS labelling showed that the former contained an ether TMS group, whereas the latter

contained an ester TMS group. Their formation may be rationalised as in Schemes 2 and 3.

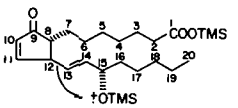

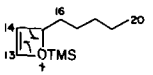

m/e 199: $C_{11}H_{23}OSi$ (ether TMS)

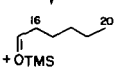

m/e 173: $C_9H_{21}OSi$ (ether TMS)

Scheme 1

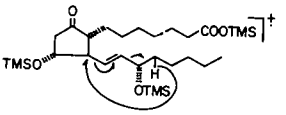

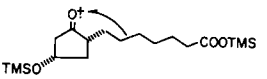

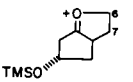

m/e 199: $C_{10}H_{19}O_2Si$ (ether TMS)

Scheme 2

Each of the additional ions of m/e 199 and 173 in the spectrum of the TMS derivative of prostaglandin E_1 was formed by cleavage of the C-5/6 bond. Since this is a double bond in prostaglandin E_2, such ions would not have been expected in the spectrum of its TMS derivative. In fact, the ion of m/e 173 was a singlet. The ion of m/e 199, however, was a doublet with the additional component again having elemental

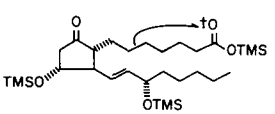

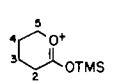

m/e 173: $C_8H_{17}O_2Si$ (ester TMS)

Scheme 3

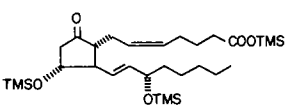

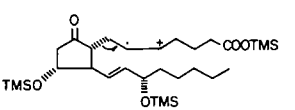

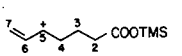

m/e 199: $C_{10}H_{19}O_2Si$ (ester TMS)

Scheme 4

composition $C_{10}H_{19}O_2Si$. Selective $\underline{d}_9$-TMS labelling showed that this additional component contained an ester TMS group. The spectrum of the 3,3,4,4-$\underline{d}_4$ analog confirmed that this component was probably formed as in Scheme 4.

The additional fragmentations were confirmed by examination of spectra of ω-nor, ω-homo, and ω-dihomo analogs.

The prostaglandins were gifts from the Upjohn Company, Ono Pharmaceutical Company, Unilever, and I.C.I. High resolution mass spectra were obtained by Pam Crain. This work was supported by grants from the National Institutes of General Medical Science (GM-13901) and the Robert A. Welch Foundation (Q-125).

McLAFFERTY REARRANGEMENT IN PROSTAGLANDIN MOLECULES

L. Baczynskyj
Research Laboratories
The Upjohn Company
Kalamazoo, Michigan 49006

Prostaglandins are polyfunctional molecules containing double bonds, acid, hydroxyl and keto functions. The presence of these functionalities on a hydrocarbon skeleton, containing a cyclopentane ring, directs the fragmentation of these molecules. The competition of the various functions for the positive charge is illustrated by considering the mass spectra of $PGF_{2\alpha}$ (I), PGE_2 (II), PGA_2 (III) and PGB_2 (IV) methyl esters:

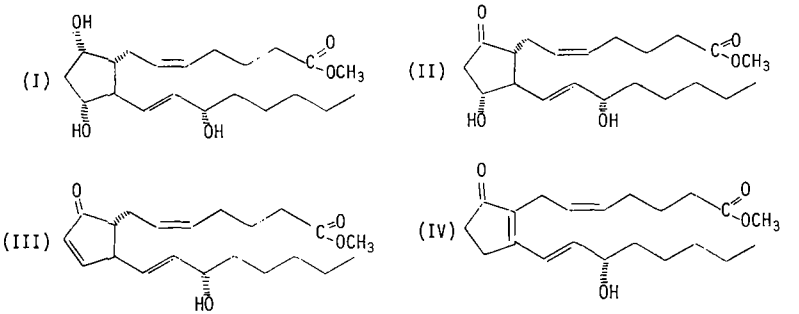

In the case of the methyl ester of $PGF_{2\alpha}$ (I), the positive charge is mainly captured by the hydroxyl function, especially the allylic alcohol at C_{15}, which leads to dehydration and cleavage of the cyclopentane ring (1). The McLafferty rearrangement of the methyl ester function--a very important process in the mass spectra of methyl esters of fatty acids (2)--is minor in this case, as shown by the low intensity of the m/e 74 ion.

The mass spectrum of the methyl ester of PGE_2 (II) shows a very intense ion at m/e 208. This results from the dehydration of the molecular ion and loss of the top side chain with hydrogen transfer to the keto function:

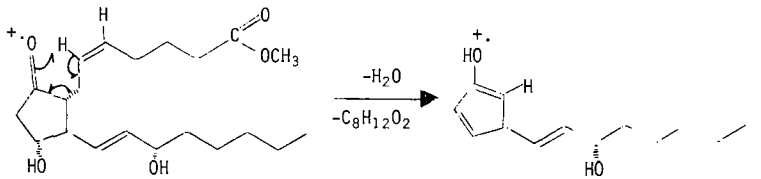

$C_{21}H_{34}O_5$:M.W. 366 m/e 208

The competitive rearrangement due to the methyl ester function is weak, as witnessed by the low intensity of the m/e 74 ion.

The most intense ion in the mass spectrum of PGA_2 methyl ester (III) occurs at m/e 190. High resolution data have shown that this ion is mainly due to the loss of water and of the top side chain with hydrogen rearrangement, in the same manner as for PGE_2 (II). The intensity of the ion at m/e 74 is practically nil, which indicates that in this instance the ester function does not compete with the keto function at 9 for the positive charge.

The methyl ester of PGB_2 (IV) is isomeric with that of PGA_2 (III) except for the position of the double bond in the cyclopentane ring. However, the mass spectrum of (IV) is radically different from that of (III). The McLafferty rearrangement of the ester and keto functions are completely suppressed. Instead, losses of $C_6H_{11}O$ and CH with subsequent losses of methanol are the dominating processes:
OH

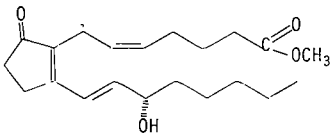

$C_{21}H_{32}O_4$:M.W. 348

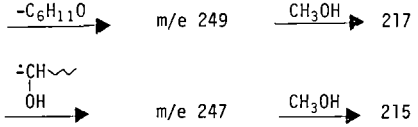

Finally, in the mass spectrum of 11,15 diTMS ether methyl ester of PGE_2, there is no apparent McLafferty rearrangement due to the keto or ester functions. Instead, losses of C_5H_{11}, HOTMS, (C_5H_{11} + HOTMS) and (C_5H_{11} + O=C-CH_2CH·) account for the major fragment ions in the spectrum.
OTMS

These results are easily rationalized by the charge localization concept. The capacity of localizing the positive charge by the various functionalities discussed here is:

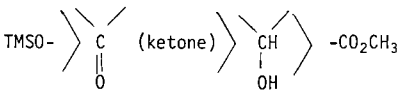

This is in agreement with the classification proposed by G. Spiteller *et al.* (3).

The apparent discrepancy between the fragmentations of PGA and PGB compounds can be explained by the following considerations:

1. On the basis of Dreiding models the closest distance between the carbonyl at position 9 and the hydrogen at position 6 is 1.5 Å for PGA compounds and 1.9 Å for PGB compounds.

2. The McLafferty rearrangement in the PGB series would lead to an ion having an allene structure in a cyclopentane ring:

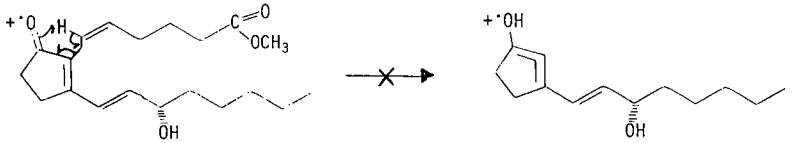

Energetically this is a very unfavorable situation, indeed.

3. In the PGB case, the positive charge, originally located on the oxygen at the 9 position, is probably delocalized over the conjugated system comprising carbons 9, 8, 12, 13 and 14.

References

1. L. Baczynskyj, E. W. Yankee and R. J. Wnuk, 20th Annual Conference on Mass Spectrometry and Allied Topics, Dallas, Texas; June 4-9, 1972.

2. G. Odham and E. Stenhagen in "Biochem. Appl. of Mass Spectrometry", G. R. Waller ed., p. 211.

3. G. Remberg, E. Remberg, M. Spiteller-Friedmann and G. Spiteller, Org. Mass. Spetr., 1, 87 (1968).

ASSAY FOR LOW LEVELS OF GUANETHIDINE IN BIOLOGICAL FLUIDS BY QUANTITATIVE GAS LIQUID CHROMATOGRAPHY-MASS SPECTROMETRY

Fred C. Falkner, Jurgen H. Hengstmann,
J.A. Oates, and J. Throck Watson
Department of Pharmacology, Vanderbilt University
Nashville, Tennessee 37232

Guanethidine (1a) is widely used today as a chemical agent to control hypertension; however, there is considerable variability among individuals in the proper therapeutic dose. In a study of factors which influence this variability, a GLC method utilizing flame ionization detection was developed to monitor guanethidine concentrations to levels of 100 ng/ml of urine. The adaptation of the method to multiple ion detection (MID) extended the sensitivity to 1 ng/ml of plasma or urine.

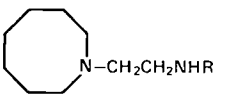

1

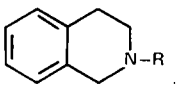

2

1a – 2a; R = $C(NH)NH_2$
1b – 2b; R = $COCF_3$

Briefly, the method involves addition of debrisoquin (2a) as an internal standard and preliminary extraction with diethyl ether or toluene to remove many potentially interfering amines. The sample is then adjusted to pH 13.5 to permit extraction of guanethidine into chloroform followed by its back-extraction into acid. The quanido group is removed by hydrolysis under strongly alkaline conditions. The resulting amine is isolated by extraction into cyclohexane and converted to its trifluoroacetyl (TFA) derivative for GLC analysis on 3% Poly I-110 (Applied Science).

The mass spectrum of the TFA derivative of the amine resulting from hydrolysis of guanethidine, N-(2-trifluoroacetamidoethyl)octahydroazocine (1b), showed a facile alpha cleavage at the site of the tertiary nitrogen to yield an abundant ion at m/e 126 (41% TIC). There were no other ions above mass 70 with a relative abundance greater than 5%. Other derivatives, namely, the perfluoropropionyl, heptafluorobutyryl, and 2,4-dinitrophenyl, gave mass spectra which also showed the overwhelming predominance of the ion at m/e 126 and, hence, had no analytical advantages over the TFA derivative. Because the tertiary amine strongly directed fragmentation to form the ion of mass 126, only single ion detection for guanethidine was possible.

Although debrisoquin is chemically dissimilar to guanethidine, it proved to be suitable as an internal standard. The TFA derivative of its hydrolysis product, 2-trifluoroacetyl-1,2,3,4-tetrahydroisoquinoline (2b), had excellent chromatographic

properties. Its retention time, as well as that of 1b was less than 3 minutes under the GLC conditions employed. These short retention times permitted analysis of 25 samples per day assuming 3 injections per sample.

Importantly, 2b also had several ions capable of being monitored within a 10% mass range of m/e 126, a range to which our LKB 9000 mass spectrometer was restricted at that time. The ability to monitor two ions, in this case m/e 116 and 117, had two advantages. First, any co-chromatographing impurity with ions at either 116 or 117 could be detected by a change in the peak ratio of 0.70 (116/117). Secondly, two calibration curves could be prepared, one using the ratio 126/116 and the other 126/117. If for some reason interference occurred on one of the internal standard ion profiles, the other could be used to calculate a ratio and, hence, the concentration of guanethidine. The collection, reduction, and processing of the data was done by means of a display-oriented computer system described by Watson, et al. (1).

A calibration curve for guanethidine in plasma with debrisoquin as internal standard was linear from 1 to 100 ng/ml and the correlation coefficient was 0.99. The results for urine were similar and showed a correlation coefficient of 0.98. The slopes for the plasma and urine curves were comparable (0.044 vs. 0.052), indicating the consistency of extraction from either medium. An absolute recovery of 48% was obtained for plasma in the range of 2-60 ng/ml.

The relative standard deviation of the ratios of the areas of the ion profiles was determined to be 4.2% by 10 consecutive GLC-MID analyses of a patient plasma sample. The precision of the entire GLC-MID method was obtained by analyzing nine plasma samples each with a concentration of 20 ng/ml. A mean value of 21.8 ng/ml was obtained with a relative standard deviation of 8.6%.

This work has been submitted for publication in Analytical Chemistry and was supported by the Research Center for Clinical Pharmacology and Drug Toxicology (GM-15431).

REFERENCES

1. J. Throck Watson, D.R. Pelster, B.J. Sweetman, J.C. Frolich, and J.A. Oates, Anal. Chem., in press.

Cytotoxic Action of Cyclophosphamide. M. L. Thomson, M. Colvin and C. Fenselau, Depts. of Oncology and Pharmacology, The Johns Hopkins University School of Medicine, Baltimore Maryland 21205

Studies concerning the metabolism of cyclophosphamide (1) were presented. The antitumor and immunosuppressive drug 1 is activated *in vitro* by metabolism in the liver. We have incubated 1 labeled with ^{14}C with mouse liver microsomes and with a nonbiological oxidation system.[1] After preliminary preparation, the biologically active samples were analyzed using mass spectrometric techniques. The mass spectra of some of the metabolites formed, and especially the new cytotoxic metabolite N,N bis(2-chloroethyl) phosphorodiamidic acid (2) were presented and discussed. It was emphasized that conventional mass spectra and GC/MS spectra of cyclophosphamide derivatives are different. This difference is due to a thermal loss of HCl in the GC before the samples enters the mass spectrometer.

In conclusion, a general scheme for the metabolism of 1 was presented and discussed with respect to the new metabolite 2.

Some of this abstract was recently published[2] and the remainder will be submitted for publication at the appropriate time.

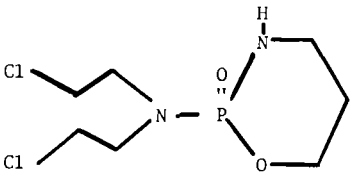

1

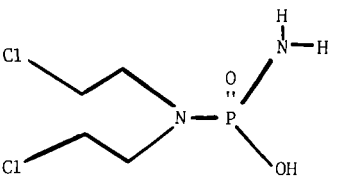

2

1. R. A. Alarcon, Nature New Biology, 233, 250 (1971).
2. M. Colvin, C. Padgett and C. Fenselau, Cancer Research, 33, 915 (1973).

GAS CHROMATOGRAPHY-MASS SPECTROMETRY OF BORONATED-SILYLATED POLYOLS AND AMINES

V. N. Reinhold and K. Biemann
Biology Section, Arthur D. Little, Inc.
and
Dept. of Chemistry, Massachusetts Institute of Technology
Cambridge, Massachusetts.

Trimethylsilyl derivatives of carbohydrates as well as their reduced peracetates have been widely used for gas chromatographic separation of mono- and oligosaccharides and their mass spectra have been investigated for the purpose of characterization of these substances. While both types of derivatives give good mass spectra, they do not lend themselves well to the differentiation of stereoisomers. Furthermore, the mass spectra of polytrimethylsilyl derivatives are generally dominated by fragments containing relatively few carbon atoms of the parent sugar with the greater portion of the fragment mass derived from the silyl groups, thus reducing the value of the spectra for the differentiation of similar compounds. For example, these latter limitations make it difficult or impossible to assign structures for the mass spectra obtained from the common hexoses, mannose, galactose, or glucose, or even the sequence of a simple disaccharide of their composition.

Earlier work of Kuivila (1), Ferrier (2), and Brooks (3) had shown the usefulness of aryl and alkyl boronic acids in esterifying hydroxyl and amino groups and we have introduced the methyl analog, the lowest alkyl boronic acid, for this work.

Figure 1 compares the mass spectra of methyl-α-D-mannopyranoside derivatized with TMS, phenyl-, butyl-, and methyl boronic acid. The major features of this comparison are the decrease in derivative weight, the observation of greater stability in higher mass fragments and, thirdly, the markedly simple mass spectra. The major ion fragments of the boronate derivatives are the 5-membered dioxaborolane and 6-membered dioxaborane rings, which would indicate α-cleavage exocyclic to each of the rings and considerable ability of these cyclic structures to change stabilization.

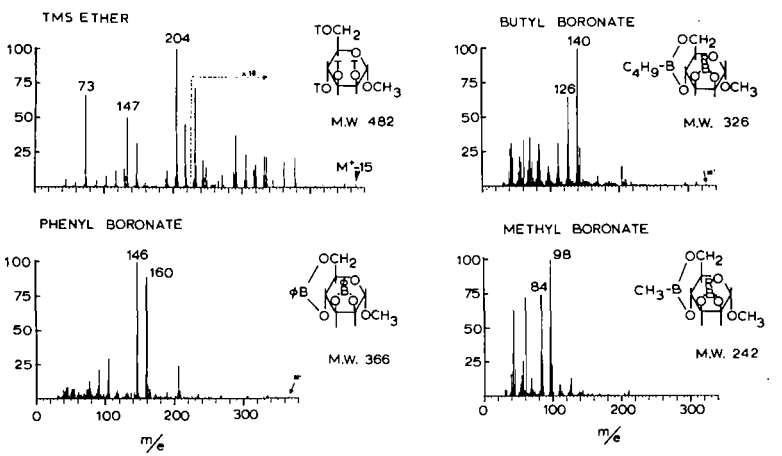

FIGURE 1

With sample molecules possessing additional hydroxyl groups not structurally suited for cyclic boronation, an additional step of silylation (as presented in Figure 2 for mannose, galactose, and glucose) has resulted in a single derivative in each case with excellent glc properties.

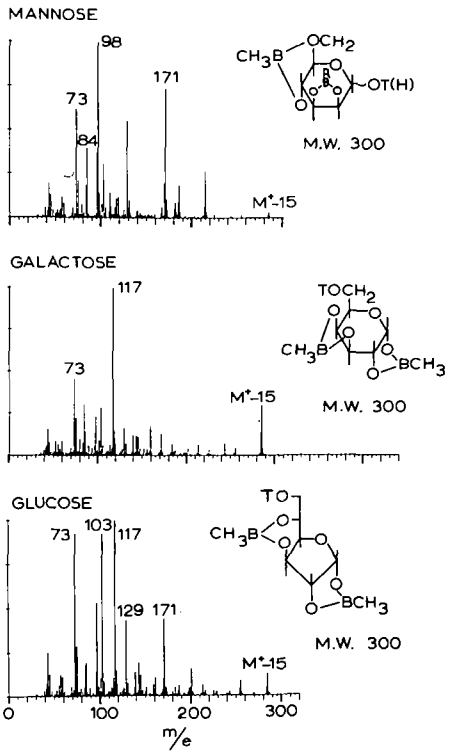

FIGURE 2

The combination of derivative molecular weight and specific ion fragments of constitutional isomers provides an approach to conformational analysis of carbohydrate oligomers, and this approach has been used to sequence a number of disaccharides by direct reading of their mass spectra.

An example of this approach is shown in the mass spectra of the disaccharide, mannopyranose $\xrightarrow{1\text{-}3}$2-acetamido-2-deoxyglucopyranose, shown in Figure 3. Probable structures of selected fragments are shown in Figure 4 and, with their consideration, allow an unambiguous interpretation of the parent molecule.

(1) H. G. Kuivila, A.H. Keough, and E.J. Soboczenski. *J. Org. Chem.*, *19* (1954) 780.

(2) R. J. Ferrier. *J. Chem. Soc.*, (1961) 2325.

(3) C. J. W. Brooks and J. Watson. *J. Chem. Comm.*, (1967) 952.

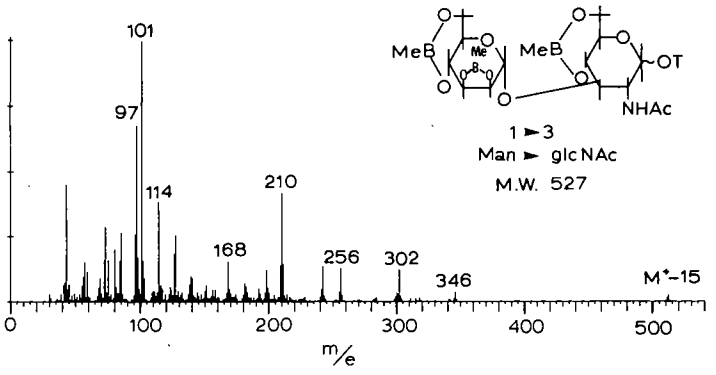

FIGURE 3

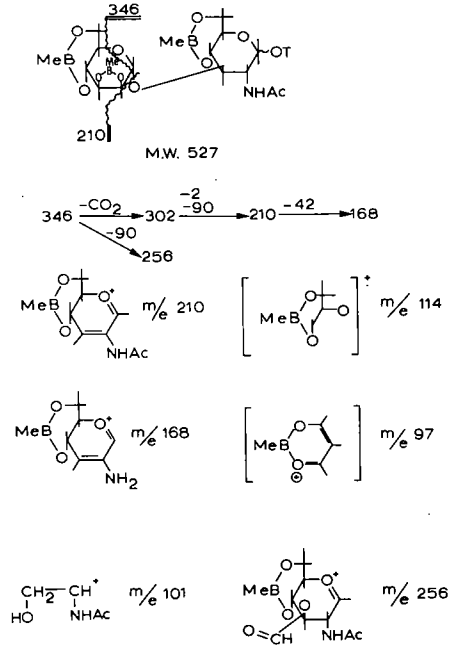

FIGURE 4

FEMTOMOLE LEVEL OF ANALYSIS OF BIOGENIC AMINES AND AMINO ACIDS USING FUNCTIONAL GROUP MASS SPECTROMETRY

F.P. Abramson-Departments of Pathology and Pharmacology, George Washington University School of Medicine, Washington, D.C. 20037, and

M.W. McCaman and R.E. McCaman-Division of Neurosciences, City of Hope National Medical Center, Duarte, California 91010

Although many methods have been described for the determination of biogenic amines and amino acids, few are adaptable to the picomole (10^{-12} moles) level of analysis, a level of sensitivity which is required for the quantitation of these amines in individual neurons of marine molluscs (1, 2). Thin layer chromatography of 14C-dansyl derivatives has been used to determine amines and amino acids in neurons of Helix pomatia(3). Specific fluorimetric methods which have been successfully adapted to the picomole level in nervous tissues include 5-hydroxytryptamine(5-HT) and dopamine(DA), gamma-aminobutyric acid (GABA), glutamate and peptides (1, 4-7). Gas chromatographic (GC) techniques have also been applied to the study of mixtures of volatile derivatives of amines and amino acids. By combining GC with mass spectrometry (GC-MS), increased sensitivity and specificity (by the detection of specific mass fragments) can be obtained. Hammar et al. (8) have demonstrated that such a system is capable of detecting femtomole (10^{-15} mole) levels of certain substances. Recently the determination of catechol and indole amines by mass fragmentography has been described (9-11). These authors have been able to measure these compounds at the picomole level in sample of nervous tissue less than 1 mg.

In this paper we will describe a procedure for the simultaneous determination of 13 amines and omega-amino acids (including DA, 5-HT, glycine and GABA) which can be performed on crude tissue extracts. The ion fragmentation patterns of the trimethylsilyl (TMS) derivatives of this series of compounds show a high abundance of a common fragment at m/e 174. Using a GC system to resolve the individual components of the mixture, the ion fragments at m/e 174 are detected by the mass spectrometer. Similarly, the ion fragments common to alpha-amino acids or to 5-hydroxyindole compounds can be detected at specific mass settings (m/e 218 and 290, respectively). This technique is referred to as "functional group mass spectrometry." Because of the inherent sensitivity of the mass spectrometer when used to detect only a single mass, as little as 10-50 femtomoles of each component can be analyzed. In this paper we describe the mass spectral and chromatographic data on which the procedure is based.

(PUBLICATION IN ANALYTICAL BIOCHEMISTRY IS PLANNED.)

* These studies were supported by grants from the United States Public Health Service (NS8864 and NS9939) and the National Science Foundation (GB-35417x)

REFERENCES

1. McCaman, M.W., Weinreich, D. and McCaman, R.E. (1973) Brain Res. 53, 129.

2. Weinreich, D., McCaman, M.W., McCaman, R.E. and Vaugh, J. (1973) J. Neurochem. 20,969.

3. Osborne, N.N. (1972) Intern. J. Neurosci. 3, 215.

4. Osborne, N.N. (1972) Experientia 27, 1502.

5. Otsuka, M., Kravitz, E.A. and Potter, D.D. (1967) J. Neurophysiol. 30,755.

6. Hirsch, J A. and Robins, E. (1962) J. Neurochem. 9,63.

7. Udenfriend, S., Stein, S., Bohlen, P., Dairman, W., Leimburger, W. and Weigele, M. (1972) Science 178, 871.

8. Hammar, C., Holmstedt, B. and Ryhage, R. (1968) Anal. Biochem. 25, 532

9. Koslow, S.H., Cattabeni, F. and Costa, E. (1972) Science 176, 177.

10. Cattabeni, F., Koslow, S.H. and Costa, E. (1972) Science 178, 166.

11. Karoum, F., Cattabeni, F., Costa, E., Ruthven, C.R.J. and Sandler, M. (1972) Anal. Biochem. 47, 550.

ANALYSIS OF MIXTURES OF OLIGOPEPTIDE DERIVATIVES BY MICRODISTILLATION IN A MASS SPECTROMETER

Ronald D. Grigsby and Eric J. Norman

Department of Biochemistry and Biophysics
Texas A&M University
College Station, Texas 77843

Mixtures of oligopeptide derivatives can be subjected to molecular distillation conditions in a mass spectrometer by introducing the sample with a direct-inlet probe[1,2]. By recording spectra as an increasing function of temperature, the data can be plotted to give elimination curves analogous to those obtained by macro-scale molecular distillation. Mathematical analysis of the data gives relative intensities for the major peaks in the spectra of the individual components as well as the amounts of the components present.

The technique was illustrated with results from a five component mixture consisting of the N-acetyl-O-butyl derivatives of Ala-Ala, Val-Leu, Leu-Try, Met-Leu-Gly, and Leu-Try-Leu. The minimum temperature separation between any two components was 11°K for Ac-Ala-Ala-Bu and Ac-Val-Leu-Bu. This was sufficient, however, to permit calculation of a number of peak intensities in the spectra of both components. Greater temperature differences (51°K for Ac-Met-Leu-Gly-Bu and Ac-Leu-Try-Leu-Bu) separated the other components of the mixture.

Good agreement was obtained between the relative intensities calculated for each of the five components and those of the standard compounds run under the usual isothermal conditions. Sufficient structural information was thus resolved to allow identification of all components present.

A specially designed glass probe was used to introduce the samples into the mass spectrometer. Specifications include a temperature range of less than -100°C to greater than +400°C and a programming rate (nonlinear) of greater than 10°/sec. Typically, 30-35 sec. are required to raise the temperature from ambient to +400°C. The temperature measurement error is estimated to be ±1°C when the probe is calibrated over any 50° span and ±5°C over the entire 500° range. The probe is designed to be used with a CEC 21-110 B mass spectrometer, but with minor modifications it should be usable with other instruments as well.

A more detailed account of this work has been submitted for publication in Biochemical and Biophysical Research Communications.

1. R. D. Grigsby, R. H. Cole, W. G. Fox, and G. M. Gable, Eighteenth Annual Conference on Mass Spectrometry and Allied Topics, San Francisco, California, June, 1970, Paper No. K8.

2. R. D. Grigsby, C. O. Hansen, D. G. Mannering, W. G. Fox, and R. H. Cole, Anal. Chem. 43, 1135 (1971).

POLYPEPTIDE SEQUENCING USING ENZYMATIC AND GC/MS TECHNIQUES

R. M. Caprioli, W. E. Seifert, Jr., and D. E. Sutherland
Department of Chemistry, Purdue University
West Lafayette, Indiana 47907

A new method of sequencing polypeptides has been investigated in which the polypeptide is enzymatically hydrolyzed to dipeptides by the action of dipeptidylaminopeptidase I and the products identified by gas chromatography/mass spectrometry. A typical analysis would therefore first involve hydrolysis of the polypeptide, acylation and esterification of the dipeptides, and separation and identification of the derivatized dipeptides. Since this only gives the sequence of the individual dipeptides and not the order of the dipeptides, a second sample of the polypeptide whose N-terminal amino acid has been removed by the Edman technique would be hydrolyzed and analyzed as above. The sequence of the original polypeptide could then be deduced from this overlapping set of data.

The derivatives used were the N-perflouropropionyl methyl esters. These were prepared by treatment of the dipeptide with thionyl chloride in methanol followed by treatment with perflouropropionic anhydride. The derivatives were then dissolved in dry dioxane for injection into the gas chromatograph. Gas chromatographic analyses were accomplished using a 2mm (ID) x 2m glass column packed with 1% Dexsil 300. On-column injection was used with an injector temperature of 250°. GC/MS analysis was performed under the same conditions using a Varian-Mat CH 7 GC/MS.

The mass spectra of the perflouropropionyl dipeptide methyl esters are easily interpretable, generally giving intense molecular ions and other ions at (M-15), (M-31) and (M-59) due to the loss of a methyl, methoxyl and carbomethoxy group, respectively. A major fragmentation of the molecular ion occurs between the alpha carbon of the N-terminal amino acid and the carbonyl carbon of the peptide bond. This ion together with the molecular ion is usually sufficient to identify the dipeptide. Many other ions are also formed which are derived from both ends of the molecule, giving diagnostic ions with which to sequence the dipeptide.

The sequence technique was illustrated with S-carboxymethylated insulin A chain, a polypeptide containing 21 amino acids of known sequence. Both the complete chain and the des N-terminal amino acid chain were hydrolyzed and analyzed as above. Each of the 10 possible dipeptides from both peptide chains were identified and the original sequence generated by computer analysis of the overlapping dipeptide data. Sequence ambiguities were eliminated by a time-course analysis in which the order that some of the dipeptides appeared on hydrolysis of insulin A chain by dipeptidylaminopeptidase I.

Although problems concerning enzyme specificity still remain, this sequencing technique promises to become a primary method for the sequence determination of amino acids in polypeptides.

A more detailed report of the work described here will appear in Biochemical and Biophysical Research Communications.

Acknowledgement: The authors wish to thank Mr. J. Carter Cook of the Mass Spectrometry Center, University of Illinois, for his aid and the Use of the GC/MS.

PROTEIN SEQUENCING BY COMPUTER-ASSISTED GAS CHROMATOGRAPHY-MASS SPECTROMETRY

H. Nau, J.A. Kelley*, H.-J. Förster#, J.E. Biller, T.R. Smith and K. Biemann

Department of Chemistry
Massachusetts Institute of Technology
Cambridge, Massachusetts 02139

Over the past few years we have developed a new technique for the efficient determination of the amino acid sequence of polypeptides by mass spectrometry for the purpose of determining the primary structure of proteins (1). The general approach involves specific cleavage of the protein by either chemical or enzymatic methods into a set of primary degradation peptides, which are then separated and isolated. The amino acid sequence of these polypeptides has to be determined, but the unambiguous reassembly of the primary structure of the protein usually requires a second degradation of another aliquot of the protein, again the isolation and sequencing of the primary degradation peptides. Thus, the elucidation of the sequence of a single protein requires the determination of the sequences of a number of polypeptides, and our approach is aimed to accomplish this efficiently and reliably.

We wish to present here the determination of the amino acid sequence of a cyanogen bromide fragment derived from the C-terminus of rabbit skeletal muscle actin. This polypeptide contained 20, primarily trifunctional amino acid residues including arginine, histidine and tryptophan (2). An aliquot of the peptide, 0.75 μmoles, was hydrolyzed with 6 N HCl at 110° for 20 minutes. The resulting mixture of oligopeptides was transformed to the corresponding mixture of O-trimethylsilylated polyamino alcohols (1,3) by esterification, acetylation, $LiAlD_4$-reduction and selective O-trimethylsilylation. A 10% aliquot of the resulting mixture was injected into the gas chromatograph which is directly coupled to a low resolution mass spectrometer via a fritted glass tube separator. All data, which have been accumulated by the computer during the GC-MS experiment (4,5), are readily available on microfilm (6) and also remain permanently stored on magnetic tape for further computer-assisted interpretation.

The total ionization plot of this experiment is shown in Figure 1a with the identified oligopeptides assigned to the corresponding gas chromatographic fractions. The identification of these peptides as O-trimethylsilylated polyamino alcohols relied on three sets of data which were generated by the computer in the course of the GC-MS experiment: (a) mass spectra; 320 spectra were taken in this experiment (Figure 1a); (b) mass chromatograms of all ions and (c) retention indices. As an example, the identification of two peptide derivatives, which emerged incompletely separated in a single gas chromatographic fraction around scan 157, shall be discussed.

The mass spectrum taken at the maximum of this peak (Figure 2) is easily interpreted as that of the derivative of Tyr-Asp. O-trimethylsilylated polyamino alcohols in general produce simple and predictable mass spectra (1). Their backbones consist of repetitive ethylene diamine units containing carbon-carbon bonds which, upon electron impact, are readily cleaved to form stabilized immonium ions (1,3). Cleavage of the carbon-carbon bond of the ethylene diamine unit in the derivative of Tyr-Asp thus produces two ions, one (m/e 238) indicating the N-terminal residue Tyr, and the other (m/e 268) the C-terminal residue Asp. The assignment of Tyr-Asp is confirmed by the M-15 ion (m/e 491) as well as an ion formed by elimination of the tyrosine side chain from the molecular ion (m/e 327).

Mass chromatograms (7), which are plots of the intensity of ions versus time, are used to rapidly locate any peptide derivative in the gas chromatogram. For example, the mass chromatogram of m/e 238

---

* Present address: Division of Biochemistry, WRAIR, WRAMC, Wash.,D.C.

Present address: C.H. Boehringer, Ingelheim/Rh., W. Germany.

(indicating N-terminal Tyr, see Figure 2), plotted in Figure 1b below the corresponding total ionization plot (Figure 1a), indicates, in addition to the just discussed derivative of Tyr-Asp, also those of tyrosine itself (scan 78), Tyr-Asp-Glu (scan 218) and Tyr-Asp-Glu-Ala (scan 247). Similarly, the mass chromatogram of ion m/e 114 (Figure 1c) (a substituted piperidinium ion formed by an elimination process involving the side chain of lysine; this ion indicates lysine in any position in the molecule) shows that a number of lysine-containing peptide derivatives are present. The maximum of this plot around scan 160 indicates that a lysine-containing peptide derivative has emerged in the tail of the fraction which has already been assigned to Tyr-Asp (Figure 2). Figure 3 illustrates this in more detail. The mass chromatogram of the ions m/e 238 (left) and m/e 114 (middle) are plotted (dashed lines in Figure 3) over the pertinent portion of the total ionization curve (solid lines). On the right both mass chromatograms have been overplotted to show that they can be used effectively to resolve a gas chromatographic fraction which contains incompletely separated compounds. The peptide derivative emerging in the tail of this peak has been identified as Ile-Thr-Lys by inspection of mass chromatograms of other sequence-determining ions.

Retention indices were used as a final check of the results since it was found that they may be predicted by simply adding the increments determined for the individual amino acid residues. These predicted values usually agree within $\pm$ 20 index units with the experimentally determined ones. Using our standard gas chromatographic conditions, we are able to chromatograph peptide derivatives with retention indices up to 4000. Larger peptide derivatives as well as those containing histidine are presently identified by fractional vaporization of an aliquot of the derivatized sample mixture directly into the ion source of the mass spectrometer.

Arginine-containing peptide derivatives can be handled by our technique without an additional derivatization step. The guanidino group of arginine is reduced by $LiAlD_4$ to a methyl amino group (with concomitant formation of two minor side products) and the resulting N-methyl ornithine derivatives have, like the analogously structured lysine-containing peptide derivatives, good gas chromatographic and mass spectrometric properties. Indeed, the dipeptide derivative of Arg-Lys was identified in the experiment discussed in this paper (scan 137 in Figure 1a).

The simple arithmetic involved in the prediction of the mass spectra of these peptide derivatives as well as their retention indices allow the automation of the identification and computer programs, which have been written for this purpose, are in routine use. The last step of the analysis, the reassembly of the sequence of the original polypeptide, can also be accomplished automatically. Using as input the N-terminal residue (which was identified to be tryptophan by a conventional experiment) as well as all oligopeptides which have been identified in the experiment discussed above (see Figure 1a), three sequences were reassembled by the computer (Figure 4), but only one, indicated by an asterisk, is in agreement with the known amino acid composition (2). The output shows that one overlap (that of His-Arg) is missing, but the program assembles a second partial sequence from the remaining peptides. Thus, GC-MS-Computer analysis of a single derivatized hydrolysis mixture allowed the reassembly of the sequence:

Trp-Ile-Thr-Lys-Glu-Glu-Tyr-Asp-Glu-Ala-Gly-Pro-Ser-Ile-Val-His-Arg-
Lys-Aec-Phe.

The position of the single glutamine, which rapidly hydrolyzed to glutamic acid under the conditions of the acid hydrolysis, was identified by a conventional experiment which involved cleavage of another sample of the polypeptide by trypsin. The resulting peptide mixture was shown to contain a peptide with glutamine at the N-terminus which, taking into account the specificity of trypsin, must correspond to residue 5. The sequence above has been found to agree with that independently deduced by conventional techniques (8).

The use of dipeptidyl aminopeptidase I (DAP I) for the enzymatic degradation of polypeptides had been suggested as a novel sequencing method (9). Since this enzyme sequentially removes dipeptides from the N-terminus of a polypeptide, it produces a mixture of peptides which, after derivatization, is particularly well suited for gas chromatography-mass spectrometry and this approach has been extensively explored (1,10). However, DAP I is blocked by a basic amino acid residue in the original or newly formed N-terminal position and does not cleave any peptide bonds involving proline. This limitation has hitherto limited the general application of this enzyme.

The following example should illustrate that this limitation may, at least in part, be overcome and useful sequence information can be obtained even for the portion of the polypeptide molecule following a proline residue. The eicosapeptide (0.75 μmoles), the sequence of which has been determined by the experiment described above, was exhaustively digested by DAP I and the expected five dipeptides were identified by a GC-MS-Computer experiment (Figure 5). A second DAP I digest was then prepared, subjected to a one-step Edman degradation and again digested with DAP I. Two 'post-proline' dipeptides could now be identified in the derivatized digest in addition to the expected derivatives of some amino acids (Figure 5).

We thank Dr. M. Elzinga, Boston Biomedical Research Institute, Boston, Mass. for the donation of the cyanogen bromide fragment of actin and the National Institutes of Health for support (Grant Nos. GM 05472 and GM 01523).

REFERENCES

1. For a preliminary report, see H.-J. Förster, J.A. Kelley, H. Nau and K. Biemann in "Chemistry and Biology of Peptides", J. Meienhofer, Ed., Ann Arbor Science Publishers, Ann Arbor 1972, pp. 679-686. Detailed publications which will include a discussion of all experimental aspects, are to be submitted to Biochemistry, J. Amer. Chem. Soc., and Anal. Chem.
2. M. Elzinga, Biochemistry 9, 1365 (1970).
3. K. Biemann, F. Gapp and J. Seibl, J. Amer. Chem. Soc. 81, 2274 (1959).
4. R.A. Hites and K. Biemann, Anal. Chem. 40, 1217 (1968).
5. J.E. Biller, Ph.D. Thesis, Mass. Inst. of Tech., June 1972.
6. J.E. Biller, H.S. Hertz and K. Biemann, Proceedings of the 19th Annual Conference on Mass Spectrometry and Allied Topics, Atlanta, Georgia, 1971, p. 85.
7. R.A. Hites and K. Biemann, Anal. Chem. 42, 855 (1970).
8. M. Elzinga and J.H. Collins in "The Mechanism of Muscle Contraction", Cold Spring Harbor Symposium on Quantitative Biology, Vol. XXXVII, Cold Spring Harbor Lab., New York, 1973, pp. 1-7.
9. For a recent review see: J.K. McDonald, P.X. Callahan and S. Ellis in "Methods in Enzymology", Vol. XXV, C.H.W. Hirs and S.N. Timasheff, Ed., Academic Press, New York, 1972, pp. 272-281.
10. Yu.A. Ovchinnikov and A.A. Kiryuskin, FEBS Letters, 21, 300 (1972).

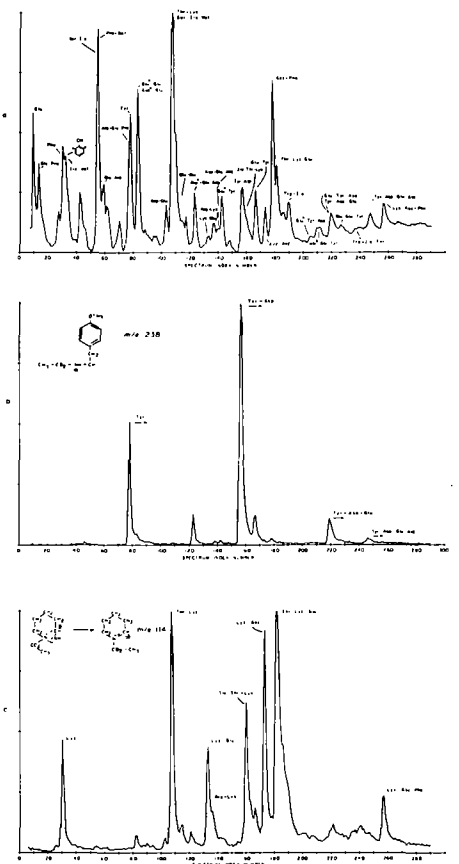

Figure 1.

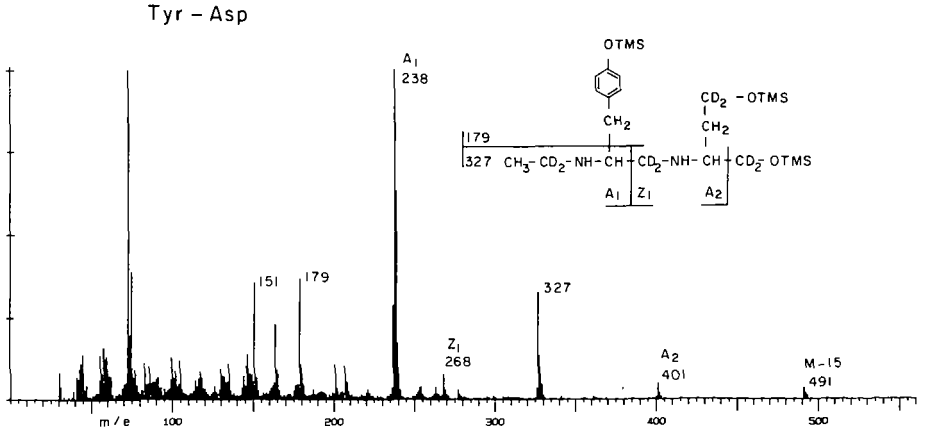

Figure 2. Mass spectrum of the O-trimethylsilylated polyamino alcohol corresponding to Tyr-Asp.

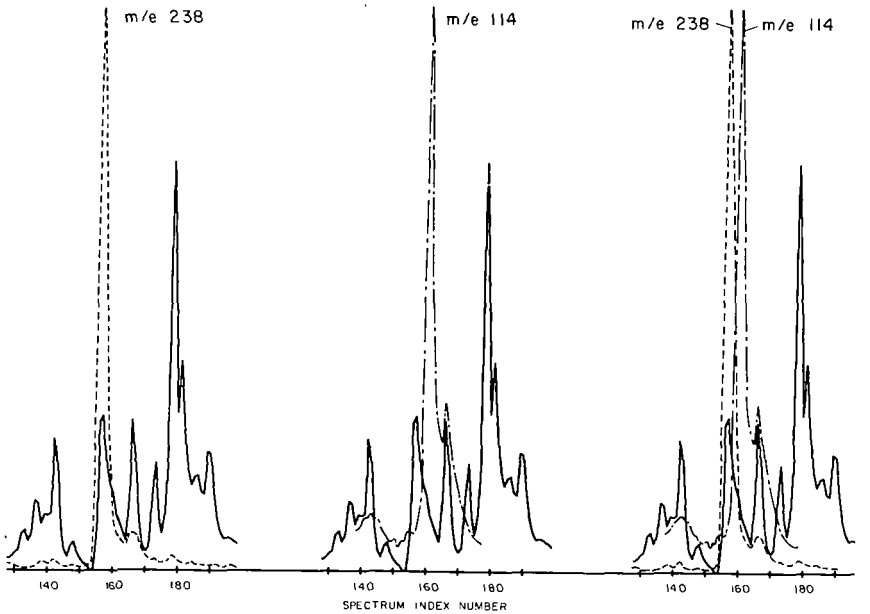

Figure 3. Overplot of a portion (scan 130-195) of the total ionization curve (the complete total ionization plot is shown in Figure 1a) and mass chromatograms of ions m/e 238 (left), m/e 114 (middle) as well as both ions (right).

INPUT

Identified Oligopeptides

GLY-PRO, ILE-VAL, SER-ILE, PRO-SER, GLU-ALA, ALA-GLY-PRO,
ASP-GLU, THR-LYS, SER-ILE-VAL, GLU-GLU, LYS-GLU, ARG-LYS,
ASP-GLU-ALA, TYR-ASP, ILE-THR-LYS, GLU-TYR, LYS-AEC, AEC-PHE,
THR-LYS-GLU, TRP-ILE, GLU-TYR-ASP, TYR-ASP-GLU, GLU-GLU-TYR,
TRP-ILE-THR, TYR-ASP-GLU-ALA, LYS-AEC-PHE, SER-ILE-VAL-HIS

Amino Acid Composition

PRO	SER	GLY	ASP	GLU	TYR	PHE	AEC	TRP	ILE	LYS	THR	ALA	VAL	ARG	HIS
1	1	1	1	3	1	1	1	1	2	2	1	1	1	1	1

RESULTS

Summary

TRP-ILE-THR-LYS-AEC-PHE

TRP-ILE-THR-LYS-GLU-TYR-ASP-GLU-ALA-GLY-PRO-SER-ILE-VAL-HIS

* TRP-ILE-THR-LYS-GLU-GLU-TYR-ASP-GLU-ALA-GLY-PRO-SER-ILE-VAL-HIS ...
ARG-LYS-AEC-PHE

Figure 4. Summary of the input and output of the computer program showing the reassembly of the original structure of the eicosapeptide from fragments which have been identified by the GC-MS-Computer experiment shown in Figure 1a.

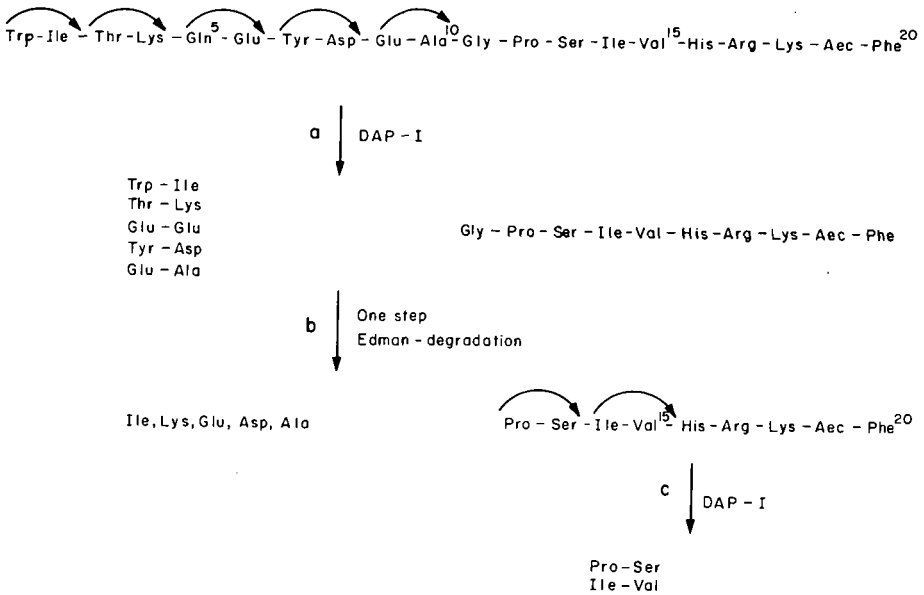

Figure 5. Schematic representation of the results obtained by DAP I digestion of the C-terminal cyanogen bromide fragment of actin (a) and of the further DAP I digestion (c) of the thus generated mixture after a one-step Edman-degradation (b).

CHEMICAL IONIZATION MASS SPECTROMETRY. XXII. DIPEPTIDES

D.V. Bowen and F.H. Field. The Rockefeller University, New York, N.Y. 10021

The iso-butane chemical ionization spectra of 25 dipeptides have been obtained. The major peaks for most peptides correspond to $(M+1)^+$, $(M+1-18)^+$, $(M+1-46)^+$ and sequence ions. The sequence ions most commonly observed are an N-imine ion, and N-amide ion, and an ion with the mass (C-amino acid + 1).

Groups of isobaric peptides have been examined. The i-C_4H_{10} mass spectra can be used to distinguished between order isomers (e.g. Leu-Gly and Gly-Leu). Isomers of Ile/Leu (e.g. Ile-Gly and Leu-Gly) could not be distinguished by this method.

Isobaric peptides such as Gly-Gly and Asp-Ala could be distinguished by i-C_4H_{10} CIMS. Although these acidic peptides showed strong peaks at $(M+1-18)^+$ and $(M+1-36)^+$, and often did not have an observable $(M+1)^+$ ion, their CI spectra could be used for identification and sequencing.

Since the CI spectrum of every peptide showed at least one sequence ion, and most showed two or three, this method gives redundant (hence reliable) sequence information. The results obtained indicate that i-C_4H_{10} CIMS may be able to identify unambiguously more than 75% of the common dipeptides. The milder protonation in i-C_4H_{10} may also be useful in sequencing longer peptides.

This work will be submitted to the International Journal of Peptide and Protein Research.

Analysis of Glucuronides by Multiple Single Ion Detection. Stephen Billets and Catherine Fenselau, Department of Pharmacology, The Johns Hopkins University School of Medicine, Baltimore, Maryland 21205.

We have reported in the literature[1] our study of the mass spectral fragmentation patterns of a wide variety of derivatized glucuronides. A number of characteristic fragment ions were identified which can be divided into a few general categories. One such category is the molecular ion set, which includes ions characteristic of poly(trimethylsilyl) derivatives and can be used to determine molecular weights. A second group of ions are those resulting from fragmentation of the derivatized sugar acid, which may be considered characteristic of glucuronides as a class. A third set of ions provide information about the type of conjugation (aliphatic or aromatic) as well as the structure of the aglycons.

Based on this analysis of the general mass spectral characteristics of glucuronides, we have developed a method to search for unknown glucuronides in urine extracts. Our approach uses multiple single ion detection (MSID) to locate and identify these conjugates in a gas chromatographic effluent, and does not require synthetic standards.

The MSID data used in this research were obtained from a Dupont 21-,91 instrument. This system has the capability to simultaneously monitor four distinct ions, each on its own individually attenuatable recorder channel, over a mass range of 60% above the mass of the lightest ion chosen.

Initial isolation of our samples from urine was carried out on a column of Amberlite XAD-2 polymer, which acts as a hydrophobic adsorbent. The derivatization scheme involved diazomethane esterification of carboxylic groups, followed by trimethylsilylation of hydroxyl and other functional groups. The urine extracts thus derivatized were purified and analyzed on the combined gas chromatograph mass spectrometer, using a 3% OV-101 glass column, with temperature programming to 300° C.

The results of two studies were presented. The first involved identification of the phenolic glucuronide conjugate of morphine from the urine of rabbits receiving the drug. Class characteristic ions[1] of masses 217, 317 and 406 were monitored through the gas chromatographic effluent, and a number of likely glucuronides were identified. On subsequent passes a number of other ions were monitored, predicted on the basis[1] of our earlier study. These included masses 340 (M-427), 429 (M-334), and 658 (M-105). This latter ion is from the molecular ion set.

Coincident formation of all of these ions occurred at only one point in the chromatogram and material eluting from the chromatograph at this point was thus identified as a glucuronide conjugate of morphine. The conjugate was assigned as the phenolic ether, based on the relative ratios[1] of the intensities of the M-334 and M-423 peaks. This conjugate is well known to occur as a major metabolite of morphine.

A similar search was made for glucuronide conjugates of metabolites of methadone extracted from urine of an overdose patient. In this case metabolites were known to be conjugated,[2] but the nature of the conjugates (glucuronide or sulfate) had not been proven. Ions of masses 317 and 407, characteristic of glucuronides in general,[1] were monitored through a gas chromatographic effluent and a number of possible glucuronides were identified.

Ions were monitored from several theoretical molecular ion sets, calculated on the basis of the reported[2] metabolism of the aglycon. At one point in the chromatogram, ions from one molecular ion set [mass 580 (M-105)] were found to occur in coincidence with the glucuronide class ions and also with predicted fragmentation ions, e.g. mass 351 (M-334). The conjugated metabolite which best fits the data is monohydroxylated 2-ethyl-5-methyl-3,3-diphenyl-1-pyrroline, a reported[2] metabolite of methadone.

On the basis of the fragmentation pattern we were unable to fix the point of glucuronic acid conjugation in the phenyl ring but an analysis of our data indicates that conjugation indeed occurs through the aromatic system.

A detailed report of this study will be published elsewhere.

[1] S. Billets, P. S. Lietman and C. Fenselau. J. Med. Chem. 16, 30, 1973.

[2] H. R. Sullivan, S. L. Due and R. E. McMahon. J. Amer. Chem. Soc. 94, 4050, 1972.

IDENTIFICATION AND QUANTITATION OF TETRAHYDROPAPAVEROLINE IN RAT BRAIN

S. Algeri, K. M. Baker, A. Frigerio and A. J. Turner
Istituto di Ricerche Farmacologiche "Mario Negri",
Via Eritrea 62, 20157 Milan, ITALY

Dopamine (3,4-dihydroxyphenylethylamine) can condense with its immediate metabolite, 3,4-dihydroxyphenylacetaldehyde, to form the tetrahydroisoquinoline alkaloid tetrahydropapaveroline (THP). This reaction has been shown to occur in liver and brain homogenates incubated with dopamine[1,2] and in vivo in liver and kidney[3] after i.v. injection of dopamine - ^{14}C. Previous measurements of THP have relied upon thin-layer chromatography and gas chromatography for its identification and quantitation.[1,2]

This compound has not previously been shown to occur in vivo in brain. However, since THP has been implicated in the process of alcohol addiction[4] and in the effects of l-DOPA therapy in Parkinson's disease,[5] it is important to have a method sufficiently sensitive to measure this compound in nervous tissue.

We have developed a more reliable method in our laboratory which involves forming the trifluoroacetate of the THP after extraction from brain and subjecting the derivative to gas chromatography-mass spectrometry (GC-MS).

For GC-MS, a 1 m glass column packed with 1% OV-17 on Gas Chrom Q was used, operating at a temperature of 205°C with a Helium flow rate of 20 ml/min.

The mass spectrum of the THP-penta-trifluoroacetate gives a small molecular ion at m/e = 767 and a very prominent ion at m/e = 452 suitable for quantitation by mass fragmentography. The minimum detectable amount of THP by this method is about 50 pg (7×10^{-14} moles) and above these levels the response is linear with respect to the amount injected into the gas chromatograph.

Using the method described above we have examined the formation of THP both in vitro and in vivo in rat brain. For in vitro experiments rat brainstems were homogenized with 0.1 M sodium phosphate buffer, pH 7.4 to give a 10% homogenate. 0.25 ml of homogenate was incubated with 5 mM l-DOPA or dopamine for 30 minutes at 37°C in a total volume of 1 ml. Control incubations were carried out with boiled homogenates or with homogenates that had been pre-incubated for 20 minutes with 0.4 mM Pargyline (a monoamine oxidase inhibitor).

The reaction was terminated by the addition of perchloric acid to a final concentration of 0.4 M and denatured protein was removed by centrifugation. 1 M KOH was added to the supernatant to precipitate $KClO_4$ at pH 3.5 and then catechols were adsorbed on alumina at pH 8.3. The alumina was washed twice with water and then THP was eluted with 2 x 2 ml 1 M acetic acid. The eluate was lyophilized and the freeze-dried powder was reacted with a mixture of trifluoroacetic anhydride and ethyl acetate (1:3) at 60°C for 3 hours in a closed tube. The derivative was then analyzed by GC-MS. Sufficient THP was formed in these experiments to obtain a complete mass spectrum of the product which was identical to that of the standard compound. No significant THP formation was observed in control incubations.

For in vivo experiments, rats were supplied with DOPA alone, ethanol alone or DOPA + ethanol by oral route for a period of eight days. At the end of this period the rats were killed, the brains removed, frozen on dry-ice and stored at -20°C until the extraction was carried out. Each brain was homogenized in 4 ml ice-cold 0.4 M $HClO_4$ containing 0.1% ascorbic acid and E.D.T.A. The homogenate was centrifuged and the precipitate was rehomogenized with a further 4 ml $HClO_4$ and re-centrifuged. The THP was then isolated from the combined supernatant fractions as described above.

In these in vivo experiments using the present method, THP could not be detected in the brains of untreated rats or of rats treated with ethanol alone. Mass fragmentography of the derivatized brain extracts, from rats treated with l-DOPA or with l-DOPA in combination with ethanol, showed that in the former case THP was present at levels of 1-10 ng/g brain, while in the latter case the concentration was found to be in the range 15-25 ng/g brain.

Although only nanogram quantities of THP could be detected in our in vivo experiments, these results may not represent the total formation of tetrahydroisoquinoline alkaloids from dopamine. THP, when formed, may be rapidly metabolized, e.g. by methylation of the hydroxyl groups or of the amino group, or by oxidation and rearrangement to a morphine-type compound. Our results show that the involvement of THP or related compounds in the mechanisms of alcohol addiction or in the effects of l-DOPA in Parkinson's disease is not an unreasonable assumption.

Acknowledgement

A.J.T. was supported by a fellowship from the Royal Society, and K.M.B. by the Wellcome Trust.

References

1. Holtz, P., Stock, K. and Westermann, E. (1964) Nature 203, 656.

2. Walsh, M. J., Davis, V. E. and Yamanaka, Y. (1970) J. Pharmacol. Exp. Therap. 174, 388.

3. Halushka, P. V. and Hoffmann, P. C. (1968) Biochem. Pharmacol. 17, 1873.

4. Davis, V. E. and Walsh, M. J. (1970) Science 167, 1005.

5. Sourkes, T. L. (1971) Nature 229, 413.

The work presented here has been submitted to Science for publication.

EVALUATION OF MASS CHROMATOGRAPHY AND MULTIPLE ION DETECTION TECHNIQUES FOR ESTIMATION OF STABLE ISOTOPIC ABUNDANCE BY COMBINED GAS CHROMATOGRAPHY-MASS SPECTROMETRY

Charles C. Sweeley, Norman D. Young, Richard E. Teets, Mark A. Bieber and John F. Holland

Department of Biochemistry
Michigan State University
East Lansing, Michigan 48823

Several approaches can be utilized for the selection of ions in the measurement of stable isotopic abundance by GC-MS. One method involves cyclic scanning of magnetic field strength (1) or accelerating voltage (2) over a limited mass range containing the ions of interest. Similarly, repetitive magnetic scanning over a wide mass range can be used to produce mass chromatograms (3). Another technique employs repetitive sequential switching of the accelerating voltage (4, 5) or quadrupole voltage (6) to a series of values which bring into focus only the ions of interest during elution of a peak from the gas chromatograph (AVA, mass fragmentography). Recently minicomputers have been used for the selection of specific ions for mass fragmentography and have also enabled the investigator to automate the method in terms of acquisition and reduction of data (7, 8). We have undertaken to evaluate the relative sensitivities, extent of errors, and precision of these various methods, and this report is a preliminary summary of the results we have obtained to date.

The experiments were carried out with the LKB 9000 equipped with the standard AVA accessory and a PDP-8/I (8K core memory), using a low voltage offset ($\pm$ 15 volts) to the accelerating voltage supply to permit computer-controlled focusing during analysis with the AVA device (7). In this process, data were observed in real time on a Tektronix Model 4002A display terminal which incorporated autoranging as concentration increased and decreased to permit simultaneous observation of concentration differences up to about 1000-fold. The use of two AVA channels independently measuring the minor isotopic species improved the accuracy of the method somewhat for that ion.

Computer-controlled AVA analyses were made of the relative proportions of various isotopic species for the molecular ion (*m/e* 270, 271, and 272) for methyl palmitate (Fig. 1). The determinations were made at mid-range of the multiplier gain with about 500 ng of sample injected. Under these conditions, the relative precision was observed to be near 1% and the accuracy of the average was 0.4% for P_{M+1} and 0.8% for P_{M+2}.

For AVA analyses, stability of the ion optics is probably less important than difficulties in the selection of baseline for either peak height or peak area computations by the computer, especially with samples in the submicrogram range. The error inherent in determination of the baseline parameters can be sizeable when areas are calculated for broad flat peaks; with peak height, however, the error is of a smaller magnitude and the precision consequently is greater than that observed with areas. The error with either method becomes large when the isotopic dilution is higher than 1:100. It should also be noted that an error can be introduced in peak height calculations when there is a chromatographic isotope effect. The blank values for pure labeled and unlabeled forms in such cases should be measured at the apex of the peak for the ion representing the opposite form. These values may be considerably less depending on the magnitude of the isotope effect.

Repetitive scanning at high scan rates over a broad mass range enables the use of

mass chromatography to calculate isotopic abundance. Fig. 2 shows total ion intensity and mass chromatograms for M, M+1, and M+2 ions of methyl palmitate, obtained with a sample containing a mixture of methyl esters from $C_{10:0}$ to $C_{24:0}$. The mass chromatograms are normalized to *m/e* 270 to show the actual areas that were observed on the display terminal for the isotopic cluster. The scans were taken at approximately 5 sec intervals in this experiment. Computer integration between limits selected by the investigator gave data which were used to determine ratios. The relative error of this method was obtained for a series of mass chromatography runs of various methyl esters over a period of several months. As summarized in Table 1, the error was considerably larger with substances of very short retention time, illustrating the importance of sampling frequency. With longer retention times, when progressively more data sets per eluting compound were obtained, the accuracy was improved. The reproducibility of these results (Table 1) did not compare well with those observed with the AVA technique.

Table 1

ERRORS IN ACCURACY AND RELATIVE PRECISION OF ISOTOPE RATIO DETERMINATION BY MASS CHROMATOGRAPHY

Methyl Ester	Mol. Wt.	Accuracy (%)*		Relative Precision in Measurement (%)	
		P_{M+1}	P_{M+2}	P_{M+1}	P_{M+2}
14:0	242	15.6	9.9	29.8	23.8
16:0	270	0.9	17.5	18.4	19.8
18:0	298	1.0	13.8	13.4	11.6
20:0	326	3.4	3.6	12.6	5.1

* % difference of the averaged and predicted values.

A more direct comparison of AVA and mass chromatography is presented in Table 2. Injections of about 900 ng of a mixture of the trimethylsilyl methyl esters of prostaglandin $PGF_{2\alpha}$ and 3,3,4,4-[$^2H_4$]$PGF_{2\alpha}$ in various proportions were made and the intensities of *m/e* 423 and *m/e* 427, fragment ions from the loss of the C_5 side chain and trimethylsilanol, were monitored by computer-controlled AVA and mass chromatography. The reproducibility of the blank value (ratio of *m/e* 423 to *m/e* 427 in pure d_4 form) was less precise with mass chromatography than with AVA and was much higher in absolute value. The precision was improved at higher amounts of the protium species in mass chromatography, however, and compared favorably with the results obtained by the AVA technique at levels of about 10 parts per thousand and higher. The relative error in the measurements by mass chromatography was considerably larger than that observed by AVA. The AVA data, on the other hand, compare favorably with those calculated from oscillographic recordings of the intensities of these ions, taken at very low scan speed on the apex of the gas chromatographic peak (Table 2, Manual).

Baczynskyj *et al.* (1) made use of the relatively higher accuracy that can be achieved at low scan speeds with repetitive scanning of a limited mass range to determine relative abundance of the protium and d_4 forms of $PGF_{2\alpha}$ over a range from 1 to 20 parts per thousand of the protium form, and reported a precision of 2-10% depending on the sample size.

Table 2

COMPARISON OF COMPUTER-CONTROLLED AVA, MASS CHROMATOGRAPHY AND MANUAL MEASUREMENT OF ISOTOPE RATIO

Calc. Ratio (H/D) parts per thousand	AVA				Manual	Rep. Scans			
	Observed	n	Std. Dev.	(%)		Observed	n	Std. Dev.	(%)
0.0	13.2	8	0.12	(1.0)	(8.9)	25.9	4	3.4	(13.0)
4.2	4.4	4	0.20	(1.4)	2.2	4.1	2	1.1	(3.6)
8.4	8.3	4	0.42	(2.2)	7.4	12.4	2	1.4	(3.7)
16.7	16.8	4	0.21	(0.8)	15.1	23.7	2	0.5	(1.0)

Conditions: 6' 1% SE-30 at 225°; multiplier gain X8; 900 ng of ME-TMS derivative of $PGF_{2\alpha}$; analysis of *m/e* 423 (protium) and *m/e* 427 (d_4 form); 70 eV; rep. scans were at 6 sec intervals. Observed values with mixtures are corrected for blank.

A recent paper by Middleditch and Desiderio (9) shows a curve for the sensitivity that can be achieved by single ion monitoring. The lower limit of sensitivity for an ion at *m/e* 217 from 5α-cholestane was 30 pg, although they found increasing uncertainty in results with sample size under about 100 pg; this is typical of what most investigators have been able to achieve with electron impact ionization and magnetic deflection instruments. The lower level depends on the intensity of the ion selected, the adsorption behavior of the compound on the gas chromatography column, and a variety of instrumental conditions. These workers maintained that under ideal and equivalent conditions, the same peak intensities were observed by single ion monitoring and repetitive scanning but admitted that single ion monitoring is capable of a much higher ultimate sensitivity because of minimized statistical variations that can be obtained when the detector is monitoring only one or a small number of ions.

In conclusion, we have shown in preliminary results that the precision and accuracy of the AVA technique are superior to those observed with mass chromatography, especially with sample sizes of less than 1 μg or with isotope ratios in the range of 1:100 and lower. Obviously, techniques such as ion counting should be explored to improve the performance of peak switching techniques, and several papers at this meeting have dealt with this possibility. Secondly, it is desirable to improve the versatility of the method with wide range bipolar power supplies enabling computer selection and control of accelerating voltage for sequential sampling of up to 10 ions (10). Other approaches involving quadrupole mass spectrometry (6) and multichannel analyzers for data acquisition in the AVA technique (11) show promise and determination of isotopic abundance in a combustion product, i.e., CO_2 for ^{13}C, is also of great potential (12).

Exploration of mass chromatography should not be discontinued because of the advantage it offers of obtaining isotope abundance of any compounds in a mixture in a single analysis by GC-MS. It is hoped that the accuracy and precision of high speed repetitive scanning can therefore be improved.

This work was supported in part by NIH Grant RR 00480.

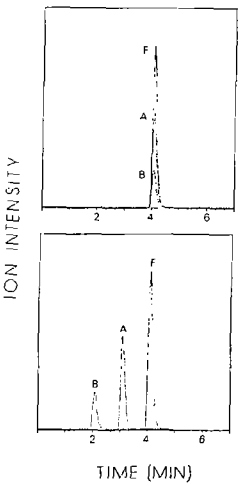

Figure 1. Specific molecular ion intensity chromatograms of methyl palmitate. The proportions of M (*m/e* 270), M+1 (*m/e* 271), and M+2 (*m/e* 272) are indicated by the plots of *m/e* 270 on channel F at 1X, *m/e* 271 on channel A at 3X, and *m/e* 272 on channel B at 10X. The lower curve has an offset time axis.

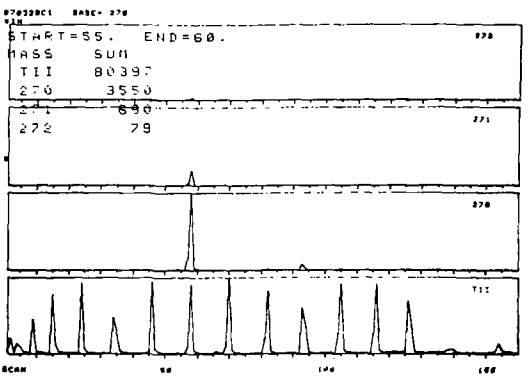

Figure 2. Total ion intensity (TII) of a mixture of fatty acid methyl esters and mass chromatograms of molecular ion, M+1, and M+2 for methyl palmitate.

The ions have been normalized to *m/e* 270 and the integration limits are shown.

References

1. L. Baczynskyj, D.J. Duchamp, J.F. Zieserl, and U. Axen, *Anal. Chem.*, 45:479 (1973).
2. B.H. Albrecht, J.R. Plattner, D. Hagerman, S. Markey, and R.C. Murphy, ASMS 20th Annual Conference, Dallas, 1972.
3. R.A. Hites and K. Biemann, *Anal. Chem.*, 42:855 (1970).
4. C.C. Sweeley, W.H. Elliott, I. Fries, and R. Ryhage, *Anal. Chem.*, 38:1549 (1966).
5. C.G. Hammar and R. Hessling, *Anal. Chem.*, 43:298 (1971).
6. J.M. Strong and A.J. Atkinson, *Anal. Chem.*, 44:2287 (1972).
7. J.F. Holland, C.C. Sweeley, R.E. Thrush, R.E. Teets, and M.A. Bieber, *Anal. Chem.*, 45:308 (1973).
8. A.E. Gordon and A. Frigerio, *J. Chromat.*, 73:401 (1972).
9. B.S. Middleditch and D.M. Desiderio, *Anal. Chem.*, 45:806 (1973).
10. W.F. Holmes, W.H. Holland, B.L. Shore, D.M. Bier, and W.R. Sherman, *Anal. Chem.*, in press.
11. P.D. Klein, J.R. Haumann, and W.J. Eisler, *Anal. Chem.*, 44:490 (1972).
12. D.A. Schoeller, J.M. Hayes, C.A. MacPherson, R.F. Blakely, and W.G. Meinschein, ASMS 20th Annual Conference, Dallas, 1972.

THE USE OF MACRORETICULAR RESINS IN THE ANALYSIS OF WATER FOR TRACE ORGANIC CONTAMINANTS

Gregor A. Junk and H. J. Svec

Ames Laboratory-USAEC and Department of Chemistry
Iowa State University, Ames, Iowa 50010

I'll begin by thanking Dr. Levins for inviting me to share our experience in the use of resins for trace analyses and by acknowledging the efforts of several colleagues----all of whom have contributed to the results which I will discuss this morning.

Before introducing the analytical procedure, I will briefly review those resins which we have found to be most useful in pollution analyses. This review will include the visual appearance, the chemical composition, the physical properties and the sorption mechanism.

Slide 1 is a magnified photograph of a mixture of two macroreticular resins. The large opaque spheres are XAD-2 porous polymer beads. The smaller translucent spheres are XAD-4 beads. The change from opaque to translucent is due to the Rayleigh scattering of light by the different sized pores. Although the visual appearance is dramatically different, these two resins have identical chemical compositions and this is shown on slide 2.

Pictured here are four styrene molecules and one divinyl-benzene cross-link as a small section of the total polymer. I do not mean to imply here a 4 to 1 ratio. The actual ratio of styrene to divinylbenzene is known only by the Rohm and Haas suppliers.

I have included on slide 3 only three of the many resins which are commercially available.[1-3] These three appear to have the best application to water and air pollution studies. The chemically identical XAD-2 and 4 are low polarity polymers which differ only in their surface area and average pore size. In this regard, most of the test results for XAD-2 which I refer to later on---these results may also be applied to XAD-4. The only difference is in the higher adsorption capacity of XAD-4 due to its higher surface area. Very little of this area, by the way, is peripheral. For a 60 mesh bead of XAD-4, the external area is less than 10^{-6}% of the total surface available for adsorption. XAD-7 is an acrylic ester polymer of medium polarity which we have found useful for some analysis. However, the utility of this resin is not as great as the non-polar styrene-divinylbenzene polymers.

The exact mechanisms involved in the extraction of organic solutes from water solutions are quite complex. I have attempted to depict on slide 4 a simple model for explaining the adsorption. This figure represents a cross-section of one of the internal pores of an XAD-2 bead. When the water solution passes through the pores of the resin the organic solutes will partition themselves in such a manner that they will be where they "like", that is on the resin as shown by the model rather than in the water. This "likes sorb likes" principle is similar to the "likes dissolve likes" partitioning in solvent extraction. However an additional factor complicates this correlation. The sorption principle must be coupled with another concept commonly referred to as the "iceberg effect". This effect was first proposed in 1945 by Frank and Evans.[4] Briefly it suggests that a non-polar organic molecule in the highly polar water solvent system remains in solution because of the orientation of many layers of H_2O molecules around the organic molecule. This tendency for water to become more crystalline when it orientates itself around the organic, was termed by Frank and Evans, the "iceberg effect". The important physical concept here is that this ordering of the water molecules leads to a significant decrease in the entropy of the water system. When the organic molecules are sorbed by the resin the icebergs are partially dispersed as shown by the model and the entropy of the water system greatly increases. Fundamental thermodynamics principles suggest that a large positive entropy change is usually accompanied by a negative free energy change. The adsorption process is

therefore favorable and spontaneous. This rather simple model allows one to readily visualize and to fundamentally accept the observed effective removal of non-polar organics from water solutions by columns packed with the XAD-2 resin.

The analytical procedure employed to achieve the quantification and the identification of organics in water is more interesting than the results obtained from the use of this procedure for natural or true water samples. For this reason, I will dwell much longer on the discussion of this procedure and later on will pass rather quickly through the discussion of some analyses of natural waters.

On slide 5 is the outline of the analytical method which we employ for trace amounts of organic compounds. This involves sampling the contaminated water either as 1 to 4 liter snatch sample or in a dynamic sampling mode for 100 to 500 sample volumes. The organics are extracted from the water by passage through a column containing two grams of XAD-2 resin. The sorbed organics are then removed by eluting the column with an appropriate solvent. The eluate is then pre-concentrated and an aliquot of this pre-concentrate is separated by gas chromatography. This GC step also provides the information necessary for quantification. Our most useful identification procedure is combined GC-MS analyses. This qualifies this talk for inclusion at a mass spectrometry meeting. Confirmations for the GC-MS identifications are provided by relative GC retention volumes and UV, IR and/or NMR analyses of fraction collected components.

It may be helpful to reconsider this entire outline for a few minutes. Naturally sampling is the essential cornerstone upon which the rest of the analytical scheme depends for its success. This basic principle requires no additional comment. Aside from sampling, when the rest of the outline is considered, a satisfactory procedure is projected only if the XAD-2 resin is near 100% effective in extracting all organics from the water sample and an eluting agent capable of removing near 100% of all the sorbed components is employed. Then, provided no material is lost during pre-concentration and the contaminants are volatile enough to be gas chromatographed, a technique which is accurate for organics in water is available. Now adequate documentation already exists for steps 4 through 7. The losses due to pre-concentration are predictable and easily confirmed by direct experimentation. Components which are not volatile enough to be gas chromatographed are obviously not detected by our analytical scheme but these too are predictable and easily confirmed. The powerful identification potential of GC-MS, IR, UV and NMR are not seriously questioned by anyone. However, very little is known about the combined extraction and elution efficiency of macroreticular resins, and the success of this scheme is vitally dependent upon these parameters. Consequently, I will for the next four slides emphasize this feature of our research efforts.

Listed on slide 6 are some early results which show the combined extraction and elution efficiencies for 18 compounds used to spike pure water at the 10 to 50 ppm level. To avoid a megabit slide I have combined and averaged the results for individual compounds which fall into various functional group classifications. The % recoveries, you will note, are quite acceptable. These limited data suggested to us very early that the XAD-2 method may be universal for all non-ionic and slightly soluble organics. If we ignore the acids this appears to be a valid deduction, at least at the ppm level as shown here for phenols, amines, aromatics, alcohols, esters and ketones.

Some later results are listed on slide 7 for additional compounds but this time the tests were at the 10 ppb level. Again, the combined extraction and elution values are quite good. Now, the detection method used to obtain these values and those shown on the previous slide--this method was not the same detection scheme which we employ for natural water samples. Here we used UV analyses with refractive index measurements for those compounds which did not exhibit a strong UV absorbance. This procedure tests only the extraction and elution efficiency. In our most recent tests we handled the spiked water in a manner exactly identical to that used for natural water samples where we use a gas chromatographic detection scheme. By doing this we get an accurate estimation

of the validity of the entire analytical procedure. The data from these tests, using the GC detection scheme, are listed on slide 8.

The summarized results for water spiked at the 10 ppb level are again grouped according to compound type. If one momentarily ignores the acid and alkyl benzene data, these results are highly favorable since we have proven here 70% or higher recoveries for eight classes of compounds with 5 to 10 compounds per class. In addition to this, the 14 miscellaneous compounds yielded an average of 76% recovery. These compounds included alkanes, phosphates, styrenes, sulfides and others. We have found similar high efficiency for all other organics which we have tested excepting of course those which are highly ionic. Thus the acids tested here yielded low efficiency values since ionic forms of these acids passed through the resin unhindered by surface adsorption. To improve the efficiency for these low molecular weight acids we add 5 milliliters of concentrated HCl to one liter of spiked water prior to passage through the XAD-2 column. Then the efficiency is greatly enhanced from the average of 7% recovery, and I can now include the number which was not available at the time this slide was made---the efficiency improves from 7% to over 90% for the acids. Naturally, if one resorts to this acidification for natural water samples, the efficiency for certain basic contaminants will greatly decrease.

Now for the alkylbenzenes. The low average % recovery for alkylbenzenes is somewhat disturbing mainly because it is unexpected. At this time, the low value is not completely explainable. For the other classes of compounds which have less than 100% recovery, we can significantly improve the values here, that is we can get near 100% recovery by careful adjustment of the pH, by careful attention to the flow rate through the column, and by the use of proper salting our procedures. However we prefer to test our method for practical routine usefulness where the contaminants, for example in a natural water sample, are unknown. Thus extensive tests of conditions for individual compounds are not warranted unless of course a high interest exists for specific contaminants. Then, conditions can be adjusted to optimize recoveries for the compounds of interest.

Before leaving this slide and proceeding to the summary of the recovery tests I should mention that these efficiency values were obtained in three ways. First, with water spiked with single contaminants. Second, with water spiked with multiple contaminants from a single homologous series of compounds. Lastly, with water spiked with selective contaminants from each compound class. From inspection of these data we can report that there are no synergetic effects when water containing a wide variety of compound types is passed through an XAD-2 column.

Slide 9 shows the summary of our recovery tests. The second and third columns show the comparative efficiency at two different contamination levels, covering a range of 1000 in concentration, for those individual compounds and those compound classes for which we have accumulated data. It is encouraging to note that the quantitative efficiencies are almost identical as one goes from the ppm to the ppb level. Also shown by inspection of the last two columns is the comparison of the recoveries as tested directly and when the spiked water is carried through the entire analytical scheme. This entire procedure includes pre-concentration, storage, several transfers, and the eventual gas chromatography. Slightly lower recoveries are obtained when the samples are carried through the entire scheme but the results are still quite satisfactory. We feel certain that the concentration can be extended further to the ppt level or even lower for most all organics. This has already been done for pesticides[5] as I will show later on, but for now the primary current interest seems to be in the ppm to ppb level. At these levels we have here the documented evidence of reliability.

Why does the XAD-2 method fail to achieve 100% recoveries in all cases? The answer to this question is related to three factors. Firstly, this technique is relatively new and therefore subject to some natural evolution to the eventual ideal usage. Secondly, for our tests, a variety of personnel from the undergraduates to Ph.D.'s conducted various phases of the lab work. Lastly, as I stated earlier, no attempt was made to select the data for optimum conditions for each class of compounds tested. However, we have eliminated some suspects from the list of

candidates which could cause something less than 100% recoveries. The probable losses during pre-concentration have been checked and found to be negligible. The elution procedure has also been extensively tested and these results are shown on slide 10. Rohm and Haas recommends the use of methanol for regenerating the resin and methanol as an eluant. We have tested 103 compounds with methanol and diethyl ether eluants. The level for these tests was 40 micrograms of solute sorbed on a column containing two grams of the XAD-2 resin. In every case, ether was a more effective eluant than methanol. On the average it is almost twice as effective in stripping the sorbed components from the resin. Because of this better performance of ether we use it to elute the columns. Ether is also more advantageous for the pre-concentration and gas chromatography steps in our procedure. As you may have already noted, seven milliliters are sufficient for complete elution of all the compounds tested. Yet some pre-concentration is almost always necessary to detect low levels of contamination so we recommend a safety factor and suggest the use of 20 milliliters of ether for eluting two grams of resin.

Although I'm hesitant to even introduce this subject, I will offer a brief comparison of the XAD-2 method to solvent extraction and to charcoal adsorption. The XAD-2 method is similar to solvent extraction but it is easier to employ. Emulsification is never a problem and smaller amounts of solvent are required. Additionally the XAD-2 technique is easily capable of sampling large volumes of water in either the snatch or dynamic mode. Compared to charcoal, XAD-2 is not as effective a sorbing agent but it is much easier to remove the sorbed components from XAD-2 without causing any chemical transformations. Indeed, the same resin may be employed for successive samples without using any rigorous clean-up or pre-treatment techniques. I intend to offer only one direct comparative result, and this comparison only because it may be of interest to those of you doing pesticide analyses. The amount of the pesticide, dieldrin, in surface waters is regularly tested. We have monitored one river in central Iowa for the past year using EPA recommended solvent extraction technique and the XAD-2 method. The results on slide 11 are representative of the usual comparison. In every case, and we have made this comparison for 20 different river water samples, the XAD-2 procedure yielded a higher value than the solvent extraction technique. Now, I well realize that direct comparisons such as these are not always valid due to subtleties peculiar to each technique. However these results at least suggest that the XAD-2 method is competitive in relation to the current accepted methodology.

Some discussion of natural water samples are now in order. On slide 12 is shown a summary of the data for 24 water samples taken from cities located in the Midwest. The raw waters were either surface or well waters depending on the locality. The treated waters were the waters as they left the municipal water plants for distribution to the public. The mean or more properly this is the median value and the average levels of contamination in micrograms per liter of water are listed along with the upper and lower limits of the values from which this average was calculated. The range in the level of total contamination is rather wide going from a high of 79 micrograms to a low of 20 nanograms per liter of water. One observation about these particular waters is most interesting. For some cities which have deep wells as a source of their potable water, the water as it is pumped from the wells contains a lower level of organic contamination than does this same water after plant treatment. The source of this contamination, added somewhere in the treatment process, may well be the transfer lines used in the water plant operations.

The most common contaminants in these waters are alkylbenzenes, herbicides, pesticides, polyaromatics, plasticizers and common industrial solvents. To some extent, the amount of contamination and the identity of the individual contaminants reflect man's influence on the environment in the Midwest and as such this influence is different from that which one would expect to find in the more populated Northeast or here in the far West. To illustrate this influence, I'll cite two specific pollution problems. First, huge amounts of herbicide, mainly atrazine, are used in the Midwest to control weeds on farm land. The source of the herbicide pollution of our surface and well waters is therefore obvious and rather easily traced. This is not always the case.

A more difficult to trace problem is the coal tar product contamination in the Ames, Iowa well water. The source of this pollution was finally traced to man's activity prior to the year 1935. At that time, the residues from a coal gas plant were periodically discarded into pits located at the end of what was then Main Street. Unfortunately several wells were subsequently drilled in this general vicinity and an underground leaching and transport mechanism has been polluting the water with coal tar products for the past 38 years. Today, the citizens of Ames are still paying the price for this seemingly harmless past activity.

I'll quickly change the pace now to air pollution since I promised to include our preliminary studies in the area. Atmospheric sampling may best be introduced by recalling the explanation of why XAD-2 is effective in removing organics from water solutions. The "likes sorb likes" principle also applies for atmospheric samples. Although there is no entropy advantage, the XAD-2 resin is still a very effective sorbing agent for organics in air.

I'll ignore the sampling procedure and devices which we employ and go directly to some results. Our most infamous air pollution sample to date is peculiar to farm areas. I refer to it as our HHA extract. This HHA label may sound too esoteric but I assure you---this designation is much more appropriate than some used by our people when I decide to work with the extract obtained from sampling the atmosphere in hog houses. My family knows and I suspect even my neighbors are aware when I've spent the day with HHA. For those of you who question this description---take the family for a drive on a hot summer evening, down-wind from a farmer spreading nature's nutrients. You'll shudder. Your wife will complain. The children will close the windows. It won't help. The odor is penetratingly distinct or da stink is penetrating. Both descriptions are accurate--- Take your choice.

About seventy compounds have been identified from the hog house aroma extract and these are partially summarized on slide 13. Most of these have little or no correlation with the odor. However, we can produce a synthetic blend of aliphatic acids, alkylpyrazines, diacetal and hexanal which has a familiar putrid smell which always leads to one common question--"Where are the hogs?"

Our immediate concern with swine extract samples is due to air quality problems near confined feeding areas. A secondary aim of this research is an attempt to correlate metabolic disorders with the composition of urine and feces. Some veterinarians claim we are working on the wrong end of the swine. The M.D.'s disagree and suggest that, near the rear is where chemists belong. We're not sure which advice to accept but I'm inclined to agree that the swine and human metabolic processes are remarkably similar---so I'll continue to feel my way through huge piles of manure--manure data. As a concluding thought, that last statement may be in bad smell so I'll continue with one final explanation.

The abstract of this talk states that I will discuss our use of video tape recording of GC-MS data and our use of XAD-4 in a simple fraction collector for gas chromatography. I have chosen to delete these discussions because this research will soon appear in the literature.

References

1. E. F. Meitzner and J. A. Oline, Union of South Africa Pat. Appl. 59/2393.

2. R. Kunin, E. F. Meitzner and N. Bortnick, J. Am. Chem. Soc., 84, 305 (1962).

3. K. A. Kun and R. Kunin, J. Polymer Sci., 6, 2689 (1968).

4. H. S. Frank and M. W. Evans, J. Chem. Phys., 13, 507 (1945).

5. G. R. Harvey and W. G. Steinhauer, Technical Report #CQ 16020, WHOI-72-86, Woods Hole Oceanographic Institution, Woods Hole, Massachusetts 02543.

Acknowledgments

The efforts of Drs. H. Svec, V. Calder, J. Fritz, D. Witiak and E. Hammond were vital to the success of the research reported here. The help of J. Richard, M. Arguello, R. Vick, R. Willis, J. Witiak and M. Avery are also acknowledged.

This research was generously supported by the Institute for Atomic Research, Iowa State University and grants from the National Science Foundation, the Iowa State Water Resources Research Institute and the City of Ames, Iowa.

SLIDE 1

XAD-2 STRUCTURE (ALSO XAD-4)

SLIDE 2

Properties of XAD-2, XAD-4, XAD-7 Porous Polymers

Name	Functionality	Polarity	Surface Area $m^2/gram$	Average Pore Diameter in Å
XAD-2	Styrene-DVB	Low	300	90
XAD-4	Styrene-DVB	Low	784	50
XAD-7	Acrylate	Med	450	90

SLIDE 3

EXTRACTION MODEL FOR ORGANICS FROM H_2O SOLUTION

SLIDE 4

Analytical Scheme

1. Sampling
2. Extraction
3. Elution
4. Pre-concentration
5. Separation
6. Quantification
7. Identification

SLIDE 5

Combined Extraction, Elution, Pre-concentration and Transfer Efficiency of XAD-2 Method at the PPB Level.

Compound Type	No. Tested	Average % Recovery
Polyaromatics	10	94
Aldehydes & Ketones	6	91
Ethers	5	88
Esters	8	80
Alcohols	5	80
Nitrogen Compounds	7	78
Aromatic halides	6	70
Alkylbenzenes	10	49
Acids(unbuffered)	5	7
Acids (buffered)		

SLIDE 8

Extraction and Elution Efficiency (XAD-2)

PPM Level

Compounds Tested	Ave % Recovery
7 phenols	89
4 acids	29
2 amines	99
2 aromatics	100
n-hexanol	85
ethyl butyrate	98
methylisobutyl ketone	100

SLIDE 6

Comparative Efficiency of XAD-2 at Different Concentration Levels and Detection Techniques

Compound or Compound Type	Extraction +Elution ppm	Extraction +Elution ppb	Total Analytical Scheme (GC) ppb
polyaromatics	100	105	94
alcohols	85	~	80
ketones	100	102	93
esters	100	104	79
naphthalene	97	100	100
acetophenone	100	110	96
dibutylphthalate	~	104	72

SLIDE 9

Extraction and Elution Efficiency (XAD-2)

PPB Level

Compounds Tested	Ave % Recovery
4 amines	49
3 aromatics	102
2 phenols	24
acetophenone	108
dibutylphthalate	104
benzothiazole	108

SLIDE 7

Organic Contamination in Water Supplies Using
Dynamic Sampling and the XAD-2 Method

Water Supplies	Parts per 10^9 by Wt. (µg/l)			
	Mean	Average	Upper Limit	Lower Limit
24 Raw + Treated	0.40	5.16	79	0.02
12 Raw	1.43	10.30	79	0.02
12 Treated	0.30	0.42	2	0.49

SLIDE 12

Some Components Present in HHA Extract

alkyl benzenes	hexanal
cresols	diacetal
benzoic acid	alkylpyrazines
aliphatic acids	phenols

SLIDE 13

Elution Efficiency of Methanol and Ether for
Organics Sorbed on XAD-2

Compound Type	No. Tested	Milliliters	
		MeOH	Et_2O
Acids	17	5.9	4.0
Alcohols	8	6.0	5.9
Aldehydes	3	10.0	6.5
Alkanes	5	5.0	6.0
Amines	5	10.2	6.3
Aromatics	19	22.0	7.1
Esters	12	6.3	5.5
Ethers	3	7.3	5.3
Halides	11	8.9	5.5
Ketones	8	15.1	6.0
Sulfur Compds.	12	9.9	5.1
	Total=103	Ave.=9.7	Ave.=5.7

SLIDE 10

Dieldrin in River Water

Method	Sample Size	Parts per 10^{12} by Wt. nanograms per liter
Solvent Extraction	4 liters	3.5
XAD-2	4 liters	4.4

SLIDE 11

Application of Gas Chromatograph-Quadrupole Mass Spectrometry-Computer System to the Analysis of Environmental Samples

BY R. C. Lao, H. Oja, R. S. Thomas and J. L. Monkman

Chemistry Division, Technology Development Branch, Air Pollution Control Directorate, Department of the Environment, Ottawa, Canada.

A computerized GC/quadrupole MS/ data processor system is ideal for routine identification and measurement of pollutants in environmental samples. It is a relatively inexpensive, simple and fast system. Although it has only moderate resolution, it is sufficient for identification and measurement purposes. Because of the large number of compounds found in air samples, a GC alone, having only retention time and detector response information to go by, cannot provide a complete unambiguous analysis. Furthermore, standardization of GC methods is limited by the lack of standard reference compounds. A MS, used as a GC detector, is able to overcome these difficulties and unmistakeably identify components by means of their unique mass spectra.

Because of the great amount of data obtained from each GC run, a computer data system is almost obligatory. The computer is used for two main purposes. It controls the MS scan and data acquisition, and it provides fast, accurate output of the final results in the form of tables, or plots of chromatograms and spectra.

The system used in this work is a combination of a Finnigan GC(9500) - quadrupole MS(1015D)-computer (System 150). Three samples were analyzed on the GC/MS/computer system. Sample No. 1 was the aromatic fraction of the extract from an industrial air sample. Sample No. 2 was a complete urban downtown air sample extract, while sample No. 3 originated from the sludge from an industrial waste dumping site. Qualitative identification was done on all three samples. The results for sample No. 1 agreed well with those obtained using a Perkin-Elmer 990 GC, Hitachi RMU-6L magnetic scanning MS, and Perkin-Elmer PEP-1 data processor combination. The second and third samples were more difficult to analyze since they were raw samples but recourse was had to computer programs for limited mass searching and background subtraction.

This paper represents the first time that a GC/quadrupole MS/computer system has been used for the determination of air contaminants. The success of this experiment justifies the sue of a system of this kind for the routine analysis of environmental samples.

A more detailed account of the above work will be submitted for publication in The Science of the Total Environment.

A GC/MS STUDY OF ORGANIC COMPOUNDS ABSORBED ON PARTICULATE MATTER EMITTED IN DIESEL EXHAUST

F. W. Karasek and R. J. Smythe, Department of Chemistry
University of Waterloo, Waterloo, Ontario, Canada

INTRODUCTION

The present study is a portion of a larger investigation into the identification of organic materials emitted from a diesel engine (1,2). The compounds were recovered from aqueous solutions obtained by condensing at zero degrees centigrade the exhaust from a 1972 Mercedes-Benz passenger car and from the particulate matter emitted by the test vehicle. Preliminary analysis of the oxygenated species extracted from the aqueous condensates compared favorably with that reported by investigators examining diesel exhaust odors (3).

The analysis of particulate matter produced by internal combustion engines has not received the attention that gaseous by-products have since the link was established between auto emissions and smog (4). The effects of temperature on the size distribution of exhausted particulate matter have been examined by Springer and Sampson (5). Hangerbrauck et al. have investigated the polynuclear aromatic hydrocarbon content of the particulates exhausted from eight spark ignition automobiles and four light trucks (6). Little work, however, has been done on the identification of the organic compounds found on, or adsorbed onto, the particulates.

EXPERIMENTAL

Exhausted particulate matter from a diesel engine was collected by either of two techniques. For one method pads of glass wool filtering fiber (Pyrex Filtering Fiber #3950) approximately 1/8 inch thick were used to accumulate diesel particulates. The damp pads were removed from the sampler, air dried for a day at room temperature and extracted for 24 hours with chloroform in a soxhlet extractor.

A second sample collection technique used a 0°C condensation which generated a dilute heterogeneous mixture of aqueous organics and particulates. The particulates were recovered by gravity filtration, air dried for a day and soxhlet extracted as noted above.

The test vehicle was a 1972 Mercedes-Benz diesel passenger car. All exhaust sampling experiments were done with the engine throttle set to produce a fast idle. Fuels were obtained from local retail distributors.

The dilute chloroform extracts of the particulate matter were allowed to evaporate at room temperature to approximately 5 ml. and were examined on 500 foot X 0.03 inch high resolution large bore open tubular columns. The column chromatographic technique used to provide a preliminary separation of the organic extract was a slight modification of an earlier technique reported by Sawicki et al. (7). The relative composition of the individual column chromatographed fractions was determined from area measurements of the chromatogram made with an Infotronics CRS-208 digital integrator.

Mass spectra for the separated components were obtained by scanning from high to low masses. A typical scan from approximately 450 to 28 AMU required 15 seconds. The reverse scan was always initiated as the solute maxima passed through the ion source, a procedure which ensured a maximum possible intensity for the parent peak. The mass spectra were compared with currently available compendiums to establish solute identities.

Mass spectra obtained from the GC/MS analyses of the column chromatography fractions were counted by hand and the peak heights measured. The spectrum was then coded into punch cards and processed on a batch processing system. Spectra were corrected for background, normalized and displayed in tabular form followed by a normalized bar graph representation of the mass spectral data. The data was processed in blocks consisting of a single GC/MS experiment which entailed up to thirty spectra.

RESULTS AND DISCUSSION

Table I lists the observations made for an exhaust condensation experiment. Three quantitatively documented condensation samplings of 27, 18 and 12 kiloliters of exhaust were used in conjunction with three qualitative dry particulate collections to provide

samples for the development of the analytical methodology presented here.

The components listed in Table II were identified from the fractions generated by the column chromatography of four particulate extracts obtained from both dry and condensation type particulate collection.

The particulates from diesel ignition are thought to be formed under engine load by the pyrolysis of the core of the fuel spray plume. The pyrolysis converts some of the heavy hydrocarbon molecules to carbon through the simultaneous formation of acetylene and hydrogen. Unburnt high molecular weight hydrocarbons are also deposited on the walls of the cylinder where they are subsequently pyrolyzed to form soot particulates (8).

In view of previous theories one is able to visualize the formation of soot particles which encapsulate the relatively abundant unburnt high molecular weight portions of the diesel fuel, PNA produced as by-products of carbonization and any oxygenates generated by the free radical flame propagation. In numerous smaller experiments no obvious difference between particulate extracts obtained from wet or dry collection techniques has been observed (1,2).

SUMMARY

A GC/MS analytical system comprised on a Perkin-Elmer 900 Gas Chromatograph interfaced to a Hitachi RMU-6E mass spectrometer is used to analyze the organic materials extracted from diesel exhaust particulates. The diesel particulates are recovered from aqueous solutions generated through total condensation of exhaust and also from direct sampling.

The organic materials extracted from the diesel particulates are subject to column chromatography which yields four or more fractions. The isolated fractions are further separated on high resolution (500 foot X 0.03 inch I.D.) large bore open tubular columns or on high temperature (200 foot X 0.03 inch I.D.) SCOT columns.

Low resolution mass spectral analysis of the gas chromatographic effluent has led to the identification of 31 hydrocarbons and 6 oxygenates and the probable identification of 23 additional hydrocarbons and 8 oxygenates. The compounds identified are shown to originate from both the high molecular weight portions of the fuel and from the combustion process itself. The identification of PNA and oxygenated analogs in the particulate matter is demonstrated.

CREDIT

The research for this paper was supported by the Air Management Branch of the Ontario Ministry of the Environment.

REFERENCES

1. Smythe, R. J., Ph.D. Thesis, University of Waterloo, Waterloo, Ontario, April 1973.
2. Gilroy, K. M., M.Sc. Thesis, University of Waterloo, Waterloo, Ontario, April 1973.
3. Little, Arthur D., "Chemical Identification of the Odor Components in Diesel Engine Exhaust", Final Report (Years 1 and 2) to Coordinating Research Council and National Air Pollution Control Administration, U.S. Public Health Service and Department of Health Education and Welfare, July, 1970, C.R.C. Project: Cape-7-68 (1-69). HEW Contract No. CPA 22-69-63, Acorn Park, Cambridge, Mass., 02140.
4. Mader, P. P., Gliksman, J., Eye, M. and Chambers, L. A., Industrial and Engineering Chemistry, 50, 1173 (1958).
5. Sampson, R. E. and Springer, G. S., Environ. Sci. and Tech., 7, 55 (1973).
6. Hangerbrauck, R. P., Lauch, R. P. and Meeker, J. E., Amer. Ind. Hyg. Assoc. Journ., 27, 47 (1966).
7. Sawicki, E., Elbert, W., Stanley, T. W., Hauser, T. R., and Fox, F. T., Anal. Chem., 32, 810 (1960).
8. Patterson, D. J. and Henein, H. A., "Emissions from Combustion Engines and their Control", Ann Arbor Science Publishers Inc., P.O. Box 1425, Ann Arbor, Mich., 48106 (1972).

TABLE I. EXPERIMENTAL OBSERVATIONS FROM A REPRESENTATIVE EXHAUST CONDENSATION EXPERIMENT

1.Total running time of experiment.....	21 hours, 20 minutes
2.Total volume of #1 Texaco diesel oil burned.....	12.2 gal
3.Total exhaust passed through condensers.....	667.6 ft^3(18,893 liters)
4.Total volume of liquid condensate collected.....	1430 ml
5.Weight of carbon particulates (dry, minus organic material)	3.169 gm
6.Weight of material extracted from particulates.....	0.8948 gm
7.Average gas velocity.....	31.34 ft^3/hour

TABLE II. COMPOUNDS EXTRACTED FROM DIESEL ENGINE PARTICULATE MATTER

A. IDENTITY BASED UPON A COMPARISON WITH PUBLISHED SPECTRA

1. n-tetradecane
2. n-pentadecane
3. n-hexadecane
4. n-heptadecane
5. n-octadecane
6. n-nonadecane
7. n-eicosane
8. n-heneicosane
9. n-docosane
10. methyl decane
11. methyl undecane
12. 2-methyl pentadecane
13. ethyl tridecane
14. 1-tetradecene
15. 1-heptadecene
16. decahydronaphthalene
17. acenaphthylene
18. acenaphthene
19. biphenyl
20. methyl naphthalene
21. 1-ethyl naphthalene
22. 2-isopropyl naphthalene
23. trimethyl naphthalenes
24. butyl or tetra methyl naphthalenes
25. ethyl fluorene
26. dimethyl fluorenes
27. trimethyl fluorenes
28. 1,2-dihydrotrimethylnaphthalenes
29. dimethyltetrahydronaphthalenes
30. 4,5-dimethyl perhydrophenanthrene
31. dimethylphenanthrene
32. o, m, & p-phenyl phenols
33. 2,6-ditertiarybutyl-4-methyl phenol
34. methoxy phenanthrene
35. anthraquinone

B. STRUCTURES BASED UPON COMPARISON OF OBSERVED SPECTRA WITH AVAILABLE PUBLISHED SPECTRA FOR SIMILAR COMPOUNDS OR ISOMERS

1. methyl decane
2. C_7H_{34}
3. dodecyl cyclohexane
4. long chain methyl ketone $C_{18}H_{18}O$
5. dinaphthyl alkane M/e = 324
6. undecyl naphthalene
7. tetrahydrophenanthrene
8. dimethyl tetrahydronaphthalenes
9. dimethyl perhydrophenanthrene
10. C_7H_{13} substituted chrysene
11. C_9H_{13} substituted chrysene
12. naphthalene
13. binaphthyl
14. methyl fluorene
15. perhydrophenanthrene
16. octahydro phenanthrene
17. trinaphthene benzene
18. diphenyl acenaphthalene
19. dimethyl cyclopentacenaphthylenes
20. iso-amyl substituted fluorene
21. aromatic M/e = 134
22. aromatic M/e = 148
23. aromatic M/e = 148
24. aromatic M/e = 148
25. fluorenone
26. methoxy biphenols
27. ethyl naphthoate
28. 1-acetyl naphthalene
29. phenyl pyrocatechol

Microsimulation Air Pollution Studies by Pyrolysis/GC/MS

CHARLES MERRITT, JR.
US Army Natick Laboratories
Natick, Massachusetts 01760

Some of the worst pollution problems in the United States arise from the manufacture of munitions. In the past year or two, in consonance with the general concern for ecology throughout the country, the Army has become greatly involved in efforts to effect abatement of whatever pollution it may produce.

One of the main themes that has been used in studies of pollution abatement is the use of pyrolysis/gas chromatography/mass spectrometry as a microsimulation technique. In general, the rationale is to try to demonstrate in the laboratory how various pollution abatement problems can be approached by simulation of various processes using pyrolysis/gc/ms.

The basic problem in munitions manufacture is water pollution - large quantities of nitro compounds in dilute concentrations are discharged as water waste. Although there are many studies in progress to treat the problem as water pollution - e. g. by studies of the biodegradation of the nitro compounds- the problem can be regarded as an air pollution problem when the compounds are isolated and concentrated, and the residues incinerated. Studies of conditions for thermally degrading these materials without causing pollution can be simulated and evaluated by combined pyrolysis/gas chromatography and mass spectrometry.

Figure 1 shows a schematic diagram of the combined pyrolysis/gc/ms analysis system. The system is designed to provide the means for carrying out a wide variety of pyrolysis studies using various types of pyrolyzers and under varying conditions of time, temperature, atmospheric environment, and physical state of the sample. The pyrolysis products are separated by the gas chromatograph and the individual components identified by mass spectrometry.

The chromatographic column chamber is fitted with a subambient temperature programmer controller so that the pyrolysis products may be collected on the cold column to achieve efficient narrow band elution behavior as the components are subsequently eluted. A separate cold trap fitted with an adsorbent such as Porapak Q between the pyrolyzer and the column has been used on occasion to eliminate some of the water formed upon pyrolysis by venting the gas stream during collection and thus allowing the organic components to be trapped while the water is vented. The present analysis system uses a time-of-flight mass spectrometer- and with this configuration, it is usually unnecessary to remove the water from the gc eluate, since it can be gated out of the total ion current output which serves as the chromatographic record. The output features of the time-of-flight mass spectrometer also allows us to gate out other unwanted contributions to the chromatographic record, such as that due to carbon dioxide, or other gross diluents present in the effluent due to pyrolysis, or perhaps the carrier gas employed.

In addition to the total ion current monitor of the mass spectrometer, which provides the principle quantitative output for the system, the gas chromatograph is also provided with a flame ionization detector for auxiliary monitoring when the gas stream is being vented. In addition to the usual analog recording the output of the total ion current monitor of the mass spectrometer is fed to a digital integrator which provides a teletype printout of the gc data, or a paper tape output which can subsequently be processed by a computer. A variety of output presentations are also available for the mass spectrum output. This is displayed on an oscilloscope, recorded on an oscillograph, or digitized on-line by means of a small laboratory computer.

There are several inlet ports to the chromatographic column chamber which may accommodate several columns. Switching from one column to another - or contriving special arrangements - is merely a matter of interchanging the column fittings. Since the mass spectrometer is designed with a high capacity vacuum system, either 1/8" packed columns or open tubular columns may be used without a separator. This is

particularly advantageous when using some other gas than helium as a carrier. Usually .02 x 100 ft. SCOT columns/or .03 x 500 ft. wall coated open tubular columns are used for the gc separations. Flow rates to the mass spectrometer are usually from 5 to 15 ml/min., depending on the type of column being used.

This analysis system is capable of employing most of the usual pyrolysis devices that are available, but most of the recent work has been accomplished using the capabilities of the Chemical Data Systems Pyrochrom analyzer and the Chemical Data Systems Microreactor system as inlets. Solids pyrolysis may be accomplished in bulk in a boat-type pyrolyzer or with a CDS pyroprobe in which the sample may be pyrolyzed as a film on a ribbon, or as a core in a coil heater.

The pyrolysis products may be swept directly onto the chromatography column, or if desired, trapped and subsequently pyrolyzed in the gas phase in the non catalytic-thermolytic reactor of the pyrochrom unit. Gaseous samples may be injected directly into the vapor phase pyrolyzer - or eluates from a gas chromatograph may be trapped and analyzed by the vapor phase pyrolyzer. The thermolytic products from the vapor phase pyrolyzer may be analyzed by the combined gc/ms system, or the small molecule analysis technique may be used.

In any of the pyrolysis modes, the atmospheric environment in which the pyrolysis occurs can be controlled by selection of an appropriate carrier gas - or by mixing various gases to produce a particular environment, e.g., a mixture of He w/20% O_2 to simulate air.

The system is fitted with vents and injection ports (for example, as indicated by the wide arrows) so that test gases, or samples, may be injected at any point in the system that may be required.

Most of the work undertaken thus far in studies of pollution abatement has been somewhat preliminary. Nevertheless, the results suggest that some very useful insights into processes that may be adapted for pollution control. One of the main problems of concern is disposal of munition wastes and this in turn leads to a consideration of incineration processes. It is simple enough to solve the water pollution problem by separating the contaminants from the water by absorption or extraction, or any other suitable process. The problem remains, however, of how to dispose of the separated concentrate, and the usual approach is to convert the water pollution problem to an air pollution problem by burning it. Since munitions are generally nitro compounds of some type- simple combustion, or even the thermolytic degradation in inert atmospheres, yields oxides of nitrogen which are undesirable gases to evolve into the atmosphere. Consideration of the problem led to the idea that pyrolysis in a reducing atmosphere might yield more innocuous products and it certainly seemed desirable to study these reactions on a microgram scale in a pyrolysis/gs/ms apparatus where the explosion hazards are minimized, and the reaction products readily determined.

TABLE I

PYROLYSIS PRODUCTS OF NITROCELLULOSE

	He	H_2	CO	O_2
CO	✓	✓		
CO_2	✓	✓	✓	✓
NO	✓	✓	✓	
NO_2				✓
CH≡ CH		✓		
Cyclopropane		✓	✓	
CH_3OH		✓		
CH_3CHO			✓	
HCN		✓		
CH_3CN			✓	

Table I shows the results of an attempt to achieve reductive pyrolysis of nitrocellulose in certain controlled atmosphere environments. The results were disappointing in the sense that no dramatic differences were observed when the material was pyrolyzed in different atmospheres. Although it appears a number of products, such as acetylene, cyclopropane, methanol, acetaldehyde and so forth were obtained by pyrolysis in

H_2 or CO, as compared to He, the amounts of these components were quite small. The most significant difference appeared to be that although NO_2 is formed in O_2 - only NO is obtained in a reducing or inert atmosphere.

Table II shows the results of similar studies with TNT. Again, there are no striking differences, except no NO_2 is produced in the H_2 atmosphere, but NO is the principle oxide of nitrogen formed in either case.

TABLE II

PYROLYSIS PRODUCTS OF TNT

	He	H_2
CO	✓	✓
CO_2	✓	✓
NO	✓	✓
NO_2	✓	
$CH{\equiv}CH$	✓	✓
CH_4		✓
$CH_3C{=}CH$	✓	✓
HCN	✓	✓

Studies on other substances, such as various polymer materials have been somewhat more informative.

The pyrolysis behavior of polyethylene may be summarized by the following equation:

$$(-CH_2-CH_2-)_n \xrightarrow{\Delta} \begin{matrix} CH_4,\ C_2H_6,\ C_3H_8\text{----} \\ C_2H_4,\ C_3H_6,\ C_4H_8\text{ ----} \end{matrix}$$

In general, depending on the temperature and rate of heat input, a series of homologous alkanes and alkenes will be obtained where the products are predominately alkenes and where the smaller molecules will be more abundant, as the rate and temperature increases , - e.g., in a carbon arc or solar furnace the yield will be nearly exclusively ethylene. If the reaction is carried out in hydrogen, one may expect to decrease the ratio of alkene to alkane.

TABLE III

ENVIRONMENT	$\Delta C_6/nC_6$
Helium	95/5
Hydrogen	80/20
Hydrogen + Catalyst	50/50

Table III shows the change in alkene to alkane content of the pyrolysis products obtained in a hydrogen environment compared to helium. Since the yield of lower molecular weight hydrocarbons (i.e., C_2 and C_3 hydrocarbons) was about the same for the pyrolysis conditions employed in this study, (i.e., ~800°C. in 3 sec.) - the ratio of hexene-1 to n-hexane has been used as a hydrogenation index - in the hydrogen environment alone, only a four-fold increase in hexane formation was observed. Realizing that pyrolysis is primarily an intramolecular process, and that the probability is low for collision processes to occur between the carrier and the pyrolysis products in the usual mode of conducting a pyrolysis experiment, it was decided to see if interaction could be enhanced by a catalyst. At the bottom of the table, the yield of hexane is seen to be increased 10-fold when using Pt black as a catalyst mixed with the polymer.

Similar experiments have been performed using a styrene/ divinylbenzene copolymer. A small, but noticeable increase in ethylbenzene vis a vis styrene is observed for pyrolyses performed in H_2 compared to He. - When Pt black is mixed with the polymer, substantially greater amounts of ethylbenzene, as well as other saturated alkylbenzenes are formed upon pyrolyzing in H_2. These experiments are quite preliminary and there are many aspects yet to be studied, but it appears that controlled atmosphere pyrolysis may provide many possibilities for controlling the product yield in a variety of pyrolysis processes.

The two products of thermal decomposition of explosives that are most noxious as gases

evolved to the atmosphere are carbon monoxide and oxides of nitrogen. It has recently occurred to us that these might be converted, by utilizing a reactor in the exhaust stack. A copper/copper oxide system seemed ideal for this purpose. The pyrolysis gases containing NO and CO are passed through Cu where the oxides of N reduced to N_2 and then thru CuO where CO is oxidized to CO_2 - both the effluent gases are now innocuous. By utilizing the multiport inlet system the pyrolysis products -(e. g. , of nitrocellulose in a boat type pyrolyzer) are led through the reactor, and back to the gc column/or directly to the mass spectrometer. In this study, since we are concerned primarily with the conversion of NO to N_2 and CO to CO_2, no gc separation is required and we can monitor the process by ms alone as seen in Figure 2.

The reduction of nitrogen oxides is seen on the right. Both NO and NO_2 have predominant mass 30 peaks so it is easy to follow the reaction by monitoring the change in intensity of the peak in the mass spectrum. The rightmost curves show the relative total ion current - and the mass 30 peak for the NO in a sample - before being reduced. The decrease in the 30 peak on the adjacent pair of curves indicates the reduction when the NO is passed through the reactor.

In a similar manner the oxidation of CO is depicted on the left. Since the spectra for both CO, and N_2, as well as CO_2 all contain a 28 peak, the only way the reaction could be monitored at low resolution is obviously by observing the appearance of mass 44 due to CO_2 in the reactor effluent. Comparison of the intensity of the mass 44 peak demonstrates the oxidation of CO as it passes through the reactor.

The experiment described here is a rather simplified version of a study that requires considerably more detailed experiments to elucidate the stoichiometry and kinetics of these reactions in relation to an actual incineration process. However, the system has great potential (probably as a mixed bed catalysis process) because the reactor can be self regenerated and because the process can be easily monitored by ms analysis. Although this study has only just been initiated, it illustrates the simplicity by which this type of combined analysis system can be used to simulate and study a potential process.

Microsimulation has proven particularly useful in studies of TNT waste water. TNT is soluble in water at about 100 ppm. It is not particularly toxic at that concentration level, but when it gets into the river, it undergoes a photochemical reaction that produces a compound that turns the water pink. TNT can readily be absorbed on charcoal, however, and absorption columns to clean up the plant effluent may be easily used. The problem is what to do with the charcoal after it has become saturated with TNT. In the past, the TNT charcoal mix has simply been burned, and in addition to the pollution hazard, it is expensive because it consumes the activated charcoal. The plant engineers would like to recover the charcoal.

In the studies of TNT pyrolysis behavior, TNT was found to be thermally very stable. This led to consideration of charcoal regeneration by heating. Although TNT is readily detonated by mechanical shock, it can be heated on the solids pyrolyzer to about 700-800°C without apparent decomposition. This was a little misleading because it was found later that actually it was distilling from the wire before it reached its decomposition temperature.

In the vapor phase pyrolyzer after distilling it from the wire at 250°, no decomposition of TNT was observed up to ca. 450°C. At 500°C, in the vapor phase pyrolyzer, the gc eluate shows the presence of unreacted TNT plus several decomposition products, such as NO, CO_2, HCN, ØH, $ØCH_3$ and $ØNO_2$. At 600°C, in the vapor phase pyrolyzer, there was no TNT in the gc eluate, but various pyrolysis products were present in abundance.

These experiments lead to the conclusion that TNT could indeed be distilled from the charcoal. The results are depicted in Figure 3. The top curve on the graph shows a trace of what, in effect, is the summation of a series of pyrolyses performed at increasing temperatures at fixed time intervals. The actual output is the total ion current due to pyrolysis products (in this case reacted TNT). It is, in effect, a distillation curve for the TNT on the pyrolyzer probe and confirms the vapor phase

pyrolysis data in that no breakdown products are observed until the temperature is well above 600-700°C.

The lower curve shows that no volatile compounds are produced when heating charcoal alone up to 1000°C. In the center an unexpected, but very gratifying result is observed. Where absorbed on charcoal, the TNT is totally decomposed to CO_2 and N_2. Up to ca. 400°C there is no reaction, but above this temperature rapid heating yields only CO_2 + N_2, both innocuous gases - and a regenerated charcoal.

It has been very comforting to be able to study these reactions with less than milligram amounts of TNT.

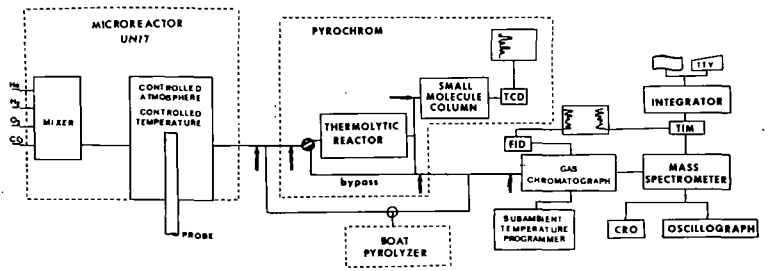

FIGURE 1

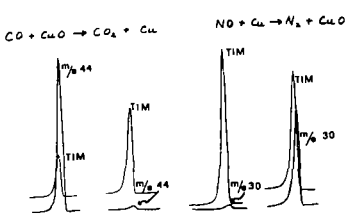

FIGURE 2

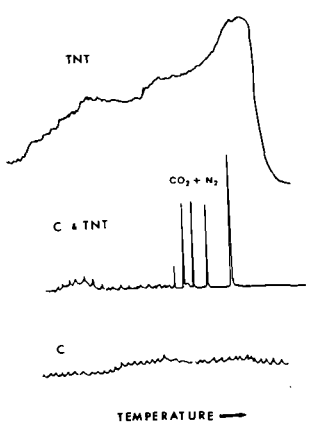

FIGURE 3

ENVIRONMENTAL ASPECTS OF CHEMICAL IONIZATION MASS SPECTROMETRY

G.P. Arsenault

Department of Chemistry
Massachusetts Institute of Technology
Cambridge, Massachusetts 02139

Chemical ionization (1) requires the presence in the ion source of a reactant gas at a pressure of about 1 torr. The use of air or water as reactant gases has been under investigation in this laboratory. The intended purpose of this investigation is to find out the extent to which air or water may be used as reactant gases for the analysis of impurities present in air or water samples, and to develop techniques for introducing these samples in the high pressure ion source. The experimental work was performed with a modified QUAD 300 mass spectrometer (Electronic Associates, Incorporated) described earlier (2).

A distinction will be made here between gases which, under the conditions of our experiments, react mainly via electron transfer reactions, the charge-exchange reactant gases, and those which undergo mainly proton or hydride transfer reactions, the chemical ionization reactant gases. Air samples are made up largely of charge-exchange reactant gases such as nitrogen, oxygen and argon, but also contain a trace of water which is a chemical ionization reactant gas. Water samples contain small amounts of dissolved gases such as oxygen and are therefore also made up of mixtures of both chemical ionization and charge-exchange reactant gases. Thus, it is appropriate to discuss here briefly the properties of mixed charge-exchange-chemical ionization reactant gases in high pressure mass spectrometry.

A simple mixture, as well as an appropriate one to consider in the light of the forthcoming discussion, consists of helium and water. This mixture was used earlier to introduce and illustrate the concept of mixed charge-exchange-chemical ionization reactant gases in high pressure mass spectrometry (3). The reactant ions for a reactant gas mixture consisting of 87% helium and 13% water (by volume) are H_3O^+ (m/e 19), $(H_2O)_2H^+$ (m/e 37) and $(H_2O)_3H^+$ (m/e 55) at a source temperature of 200°C and a pressure of 0.5 Torr. The absence of helium ions among the reactant ions is particularly striking since the bulk of the reactant gas mixture is made up of helium gas. Helium ions are absent because:

1. Primary ionization is by electron impact and the ionization cross-section of water is about 8 times larger than that of helium. The net result is that there is a greater probability of ionizing a water molecule than a helium atom even though there are about seven times more helium atoms present than water molecules.

2. The recombination energy of $He^{+\cdot}$ (24.6 eV) is much greater than the ionization potential (I.P.) of water (12.6 eV) so that $He^{+\cdot}$ formed by primary ionization can charge transfer to neutral water molecules. The net, ultimate result of this charge transfer reaction is the formation of $H_2O^{+\cdot}$ (4). The recombination energy of $H_2O^{+\cdot}$ being 12.4 eV, the reverse charge-exchange reaction with helium atoms (I.P. = 24.6 eV) cannot take place.

3. The proton affinity of water is much larger than the proton affinity of helium so that H_3O^+ cannot protonate neutral helium atoms.

Two separate techniques have been used for the analysis of air samples in the high pressure ion source and were described briefly previously (5). The first technique is a direct one in that air is sampled continuously by means of an atmospheric probe. To suppress the effect of varying amounts of water in air samples from day to day, water is deliberately leaked continuously into the high pressure ion source at the same time as the air so as to make up about 15% of the total reactant gas volume. The reactant ions in these experiments are H_3O^+ (m/e 19), NO^+ (m/e 30), O_2^+ (m/e 32) and $(H_2O)_2H^+$ (m/e 37), and the contaminants in the air are ionized by these species. Recombination energies, ionization potentials and proton affinities are the physical properties which need to be considered to explain the make-up of the air-water reactant ions. NO^+ is the result of a chemical reaction taking place in

the high pressure ion source (6). The second technique is an indirect one in that the air sample is injected into a helium stream to which water is continuously added prior to the entry of the stream in the high pressure ion source. A gas chromatographic column need not be used but can be used with this technique. An example of the results obtained with this technique for automobile exhaust analysis without gas chromatographic separation was reported earlier (5).

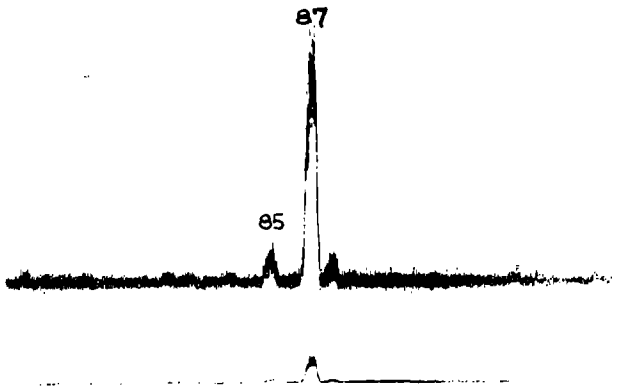

Figure 1. Oscillographic recording of portion of the chemical ionization mass spectrum of a water sample, containing 0.4 ppm of 2-pentanone, vacuum distilled directly into the high pressure ion source; m/e 85 and 87 correspond to the $(M-1)^+$ and $(M+1)^+$ of 2-pentanone.

The analysis of organic impurities in water samples present a formidable problem. For example, 1 ppm of 2-pentanone in water equals 5 ug of 2-pentanone in 5 ml. water. This amount of water expands to 16,200 l. under ion source temperature and pressure conditions. It is nevertheless possible to analyze for volatiles in water samples. Two techniques have been used which in effect involve concentrating the volatiles in the vapor phase at the time the analysis is in progress. The first technique consists in vacuum distilling the water sample directly into the high pressure ion source. This technique was used with a sample containing 0.4 ppm of 2-pentanone in water, and the results are shown in Figure 1. The second technique consists in passing helium through the water sample and admitting about 20% of the resulting gas stream to the high pressure ion source. This second technique shows promise of being suitable for the analysis of ppb volatile impurities in water samples.

Acknowledgement: The author is indebted to Professor K. Biemann for his continuing and enthusiastic support, and to the National Institutes of Health for financial support (Grant RR 00317 from the Biotechnology Resources Branch, Division of Research Resources).

REFERENCES

1. M.S.B. Munson and F.H. Field, J. Amer. Chem. Soc. 88, 2621 (1966).
2. G.P. Arsenault, J.J. Dolhun and K. Biemann, Anal. Chem. 43, 1720 (1971).
3. G.P. Arsenault, J. Amer. Chem. Soc. 94, 8241 (1972).
4. H. Sjögren, Arkiv Fysik, 33, 597 (1967).
5. G.P. Arsenault and J.J. Dolhun, 20th Annual Conference on Mass Spectrometry, Dallas, Texas, June 1972, p. 253.
6. R.F. Potter, J. Chem. Phys. 23, 2462 (1955).

P-6. Application of Field Desorption Mass Spectromentry (FD-MS) to Environmental Research.

H.-R. Schulten and H.D. Beckey
Inst. Phys. Chemie, The University of Bonn, West Germany

The enhanced molecular intensities displayed in FD mass spectra together with the small sample consumption of the method seem to offer advantages for the identification and characterization of highly polar compounds.

The reproducible and fast preparation of high temperature activated emitters (see paper PL-2, ref. 2,3,4 and paper U-1) has turned by now into a routine procedure. Since combined EI/FD instruments are commercially available and a number of potential applications of FD-MS have been demonstrated for different classes of compounds (see paper PL-2, ref. 3,7,8,9,10,11,12 and papers H-6, H-7, N-2) investigations in the field of metabolism studies appear promising.

Both drugs (1) and environmental chemicals have in common that their metabolism produces mostly minute amounts of highly polar substances. An important analytical aim of FD-MS is the fast and direct detection of these compounds in biological samples, avoiding derivatization, GC-coupling and preferably using only crude prepurifications of the extracts. In this respect the suitability of the technique in the identification of thermally unstable compounds (no evaporation) in extracts from living cell material has been shown (1),(2).

The first steps towards investigations of environmental chemicals encountered chlorinated pesticidal compounds and their metabolites and/or non-metabolic decomposition products (3),(4),(5).

The fact that free acids (acetic, sulphonic, phosphoric) and organic as well as inorganic salts (acetate (6), phosphates (7),(8)) yield protonated or cationated ions with FD-MS widens the scope of mass spectroscopic analysis. Moreover, a newly developed technique, Pyrolysis Field Desorption Mass Spectrometry (Py-FD-MS), seems to be a useful tool for research on polymers (8).

At the time of writing investigations are under way to support the potential of FD-MS in soil and marine pollution problems.

(1) H.-R. Schulten and H.D. Beckey, 20th Annual Conference On Mass Spectrometry And Allied Topics, June 4-9, 1972, Dallas, Texas.
(2) H.-R. Schulten et al., Anal. Biochem., in preparation.
(3) H.-R. Schulten and H.D. Beckey, Research Conference on Pesticide Metabolites - Enzymology, Isolation and Characterization, Fargo, N.D., June 20, 1972.
(4) H.-R. Schulten and H.D. Beckey, J. Agr. Food Chem., 21, 372 (1973).
(5) H.-R. Schulten, H. Prinz, H.D. Beckey, W. Tomberg, W. Klein und F. Korte, Chemosphere 2, 23 (1973).
(6) H.-R. Schulten and H.D. Beckey, Org. Mass Spectrom., 6, 885 (1972).
(7) H.-R. Schulten and H.D. Beckey, Org. Mass Spectrom., 7, 853 (1973).
(8) H.-R. Schulten, H.D. Beckey, A.J.H. Boerboom and H.L.C. Meuzelaar, Anal. Chem. in print.

SURFACE IONIZATION OF ORGANIC COMPOUNDS ON RHENIUM

W.D. Davis
General Electric Corporate Research and Development
Schenectady, New York 12301

Surface ionization of organic compounds has been observed for many years but few serious studies have been made, the most extensive being that by Zandberg and co-workers using oxidized W.[1,2,3]

In this investigation, mass spectrometer measurements were made of the ionization of trace amounts of organic compounds in air on contacting the surface of a Re ribbon at 800-1000°C. Oxygen adsorbed on the Re surface increases its work function to 7.0-7.5 eV. In many cases, the ion yields were higher than those usually obtained from electron impact and the spectra were less complex. As a general rule, the ionization efficiency increased with increasing molecular weight.

Three ion sources were used, the main difference between them being the manner in which an integral electron impact ion source for measuring the partial pressure of the organic compound was incorporated into the structure. The ionizer was a flat Re ribbon either 1.6 or 3.2 mm wide and .013 mm thick. The length varied from 10 to 20 mm. Resistance heating was used. The mass analyzers were either 2" or 3" radius 90° magnetic sector types with electron multiplier detectors. The overall ion transmission was 1% and 4% respectively. The pressure of air was 1-4 x 10^{-5} Torr. The ion source for the 3" analyzer used a sampling system that admitted aerosol particles as well as gaseous species (see paper Q9).

Of the five aromatic hydrocarbons studied, only benzene did not produce significant ionization. Toluene, mesitylene and dimethylnaphthalene produced approximately 0.0006, 0.10 and 1.0 amperes of ion current at the ribbon surface per torr of hydrocarbon partial pressure or an estimated ion yield of .01, 1 and 13% respectively. In each case, over 90% of the ions were in the M-1 peak corresponding to the loss of 1 hydrogen atom. This is illustrated for dimethylnaphthalene in Fig. 1. The small peak at mass 141 is probably due to the loss of a methyl group from the parent molecule. The peak at mass 169 could be due to oxidation of a methyl group to $-CO^+$ and that at 183 to further oxidation of the second methyl group to -CHO. Pyrene produced the molecular ion with an ion yield of at least 0.5% (Re oxide ions interfered with the electron impact measurement).

Both ethyl and t-butyl alcohol gave predominantly the M-17 peak corresponding to loss of OH. This is probably to be expected because of the strong attraction of the oxygen atom to the Re surface. The ionization efficiency for t-butyl alcohol was .02% with about 94% of the ions at mass 57. Figure 2 compares the spectrum using surface ionization with that reported for electron impact. The typically simpler spectra obtained using surface ionization is probably due to the smaller amount of energy available for fragmentation and ionization.

Using W instead of Re, aniline gave an ion yield of 2 x 10^{-4} A/Torr cm^2. The molecular ion was 97% of the total ions. Zandberg[3] obtained essentially the same result (3 x 10^{-4} A/Torr cm^2). The ion yield for t-butyl alcohol on W was identical to that for aniline and increased by a factor of 30 for Re. This indicates that the ionization efficiency of aniline on Re would also be ∿.02%.

The spectrum of nicotine on Re is shown in Fig. 3. It is similar to that for electron impact except for relative intensities. The ionization efficiency is 20%, the highest value obtained in this study.

In contrast to the other compounds studied, both camphor and cinchonine gave a number of large peaks rather than only 1 or 2. For camphor, the largest peak, mass 119, constituted only 16% of the total ions. The total ionization efficiency was 0.4%. For cinchonine, mass 134 was 43% of the total ions and the total ionization efficiency was 5%. The results for cinchonine were determined by analyzing a solution of this alkaloid and $CsNO_3$ (∿1 ppm each) by the method described in paper Q9 and comparing the relative yields of organic ions and Cs^+ (100% ionization).

Measurements of low concentrations of organic compounds in air were limited primarily by background ions produced by alkali metal impurities in the Re or on nearby surfaces and more importantly, by organic impurities in the vacuum system. The normal components of air were not ionized

because of their high ionization potential. The use of zone-refined Re reduced the Na and K ions to a level at which they caused little if any interference except at their respective mass positions. This is usually not serious because few organic ions are formed in this region of the spectrum. No Rb was detected but Cs was comparable to Na and K because $CsNO_3$ was used to activate the electron multiplier. For a well baked Hg pumped sytem, the main organic peaks were masses 58, 81, 91 and 105 at about 10^{-17}A output ion current. The general background was 1 or 2 decades below this level. This level of background should allow one to detect about 1 part of an efficiently ionized compound in about 10^{12} parts of air. For example, the mass 155 peak of dimethylnaphthalene at a concentration of 10^{-11} was about 20X above the background at this mass position.

Examination of filtered laboratory air did not reveal any clear cut evidence of gaseous organic compounds present but with the particulate sampling system, large amounts of organic compounds were found. A typical spectrum is shown in Fig. 4, both with filtered air to show the background and with unfiltered air. The vacuum system for particulates uses an oil diffusion pump and the background is higher than with the Hg pumped system. The clearly identifiable inorganic peaks are Li^+, Na^+, K^+ and Pb^+ with mass 133 being partially due to Cs^+. Unfortunately, the multitude of peaks, the limited resolution of the spectrometer and the lack of reference spectra do not allow an unambiguous interpretation of the results. The mass 84 and 161 peaks, however, are probably due to nicotine at about the 2 ppb level. A lighted cigarette in the room produces about the same general organic spectrum but at about an order of magnitude higher level. The measured nicotine concentration of about 20 ppb agrees approximately with the expected level.

In summary, these results indicate that surface ionization on Re can be a very useful technique for measuring small amounts of many organic compounds in air, especially in aerosols. Besides studies of atmospheric pollution, the method might be useful in other fields of organic mass spectrometry such as GCMS or the analysis of sub-picogram solid samples by using a separate supply of oxggen for ionizing purposes. The discovery of even higher work function surfaces should greatly increase its applicability.

---

1. E.Y. Zandberg, U.K. Rasulev and B.N. Shustrov, Dokl. Akad. Nauk SSR, 172, 885 (1967).
2. E.Y. Zandberg and U.K. Rasulev, Soviet Phys.-Doklady 13, 35 (1968).
3. E.Y. Zandberg and U.K. Rasulev, Soviet Phys.-Tech. Phys. 13, 1450 (1969).

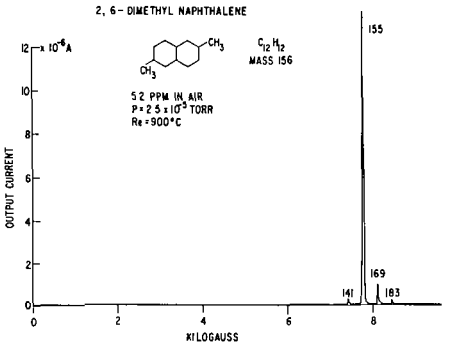

Fig. 1 - Mass Spectrum of 5 ppm Dimethylnaphthalene in Air

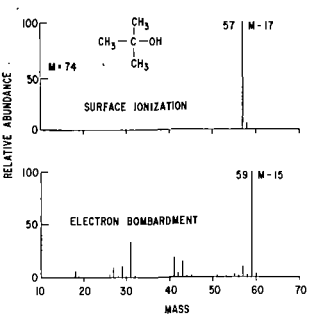

Fig. 2 - Comparison of Surface Ionization and Electron Bombardment Using t-butyl Alcohol

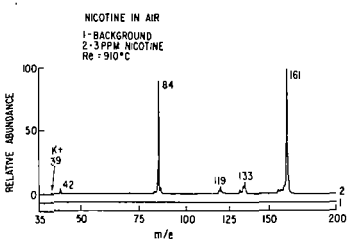

Fig. 3 - Mass Spectrum of 3 ppm Nicotine in Air and Air Alone

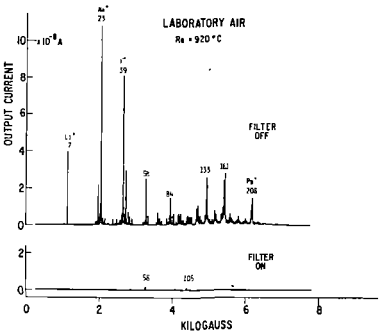

Fig. 4 - Direct Analysis of Air Particulates. Spectrum with Filter on Shows Background

THE ION KINETIC ENERGY SPECTRA OF CHLORINATED DIBENZO-p-DIOXINS

S. Safe, O. Hutzinger, W. D. Jamieson
Atlantic Regional Laboratory, National Research Council of Canada, Halifax, Nova Scotia
and
A. E. Pohland
Biochemistry Branch, Food and Drug Administration, Washington, D. C. (A.E.P.)

Recent work has shown that ion kinetic energy (IKE) spectroscopy is useful in distinguishing between isomeric polychlorinated biphenyls (1), chlorobenzenes (1), and DDT's (2). In addition this technique delineates the ionic decomposition reactions occurring in the first field-free region of the mass spectrometer and the results often complement the metastable-derived reactions. The electron impact-induced fragmentation of dibenzo-p-dioxin and some chlorinated dibenzo-p-dioxins have been reported (3, 4, 5). Since the chlorinated dibenzo-p-dioxins have been shown to be highly toxic environmental pollutants we have therefore examined both the ion kinetic energy (IKE) and mass spectra of a number of these compounds. In all cases the spectrum of each isomer was unique thus providing a characteristic fingerprint spectrum of the compound. In addition the results showed that for a series of mono-, di- and tetrachlorinated dibenzo-p-dioxin isomers there was incomplete substituent (i.e. chlorine) randomization in the decomposing molecular ions. For some of the IKE peaks the identification of the daughter ion peaks present was readily effected using photoplate techniques.

REFERENCES

1. S. Safe, O. Hutzinger, W. D. Jamieson and M. Cook. Org. Mass Spectrom. 7, 169 (1973).
2. S. Safe, O. Hutzinger and W. D. Jamieson. Org. Mass Spectrom. 7, 217 (1973).
3. B. Pring and N. E. St. Jernstrom. Acta Chem. Scand. 22, 549 (1968).
4. E. N. Givens, L. Alexakos and P. B. Venuto. Tetrahedron 25, 2407 (1969).
5. N. P. Buu-Hoi, G. Saint-Ruf and M. Mangane. J. Heterocyclic Chem. 9, 691 (1972).

To be published in Analytical Chemistry

AEROSOL BEAM SPECTROMETRY

Barton Dahneke

Radiation Biology and Biophysics

University of Rochester, Rochester, N. Y. 14642

Aerosol beams, generated by expansion of particle-laden gas through a nozzle into a vacuum chamber where the gas is removed by pumping and the particulates form a beam, are especially well suited for the detection and measurement of small airborne particles for several reasons. First, the particles are confined to a narrow, well defined beam with velocity of the order of 300 m/sec. Second, the small particles are isolated from surrounding gas molecules so that sensitive measurements are not obscured by the gas molecules. Third, the particles can be automatically detected and measured individually in real time rather than being collected over a period of time and analyzed en masse later (present collection techniques lose important volatile fractions, apparently more so than in aerosol beams).

Several aerosol beam techniques have been developed by the author over the past several years. These include aerosol beam focusing[1] and two types of aerosol beam spectrometry[1,2]. The author has also presented evidence[3,4] that evaporation of small droplets in aerosol beams is not significant because of substantial cooling of the particles in the free jet and in initial stages of evaporation. In addition, W. D. Davis has developed a technique, described in this conference, for measuring the composition of individual particles.

Aerosol beam spectrometry thus appears to be a powerful tool for measuring airborne particles, including moist atmospheric particulates. Using both a size measuring technique and a method for measuring composition of the individual particles (such as described by W. D. Davis in this conference) is appears possible to provide, for the first time, sufficiently detailed measurements of individual airborne particles to identify their origins and toxicity.

References:

1. Dahneke, B. and Flachsbart, H., Aerosol Science 3,345 (1972).
2. Dahneke, B., Nature (in press).
3. Dahneke, B., Aerosol Science 4,147 (1973).
4. Dahneke, B., Flachsbart, H., Mönig, F. J., Schwarzer, N. 8th International Symposium on Rarefied Gas Dynamics (in press).

A COMPUTER CONTROLLED QUADRUPOLE MASS SPECTROMETER METHOD FOR POLYCHLORINATED BIPHENYLS IN ENVIRONMENTAL SAMPLES

L.E. HARRIS, J.W. EICHELBERGER AND W.L. BUDDE

U.S. Environmental Protection Agency
National Environmental Research Center
Analytical Quality Control Laboratory
Cincinnati, OH 45268

The polychlorinated biphenyls (PCB's) are widely discussed environmental contaminants which have been observed in air, water, sediment, and food chain samples. Qualitative and quantitative analyses of these mixtures of mono to perchloro position isomers are complicated by the large number of possible individual isomers and by the physical and chemical similarity of this set of compounds to the chlorinated hydrocarbon pesticides, e.g., DDT, DDE, lindane, dieldrin. A suitable analytical method should combine high sensitivity with high qualitative information content in the response in order to obviate the need for elaborate separations and cleanup.

All reported analytical procedures for PCB's employ some type of separation of isomers and closely related compounds. Since most of these compounds are mildly polar non-ionic organic compounds, they are amenable to gas chromatography which has been employed widely. Several standard detectors respond to these compounds at environmentally significant levels and the selective electron capture detector is capable of detecting these compounds well into the subnanogram level. However, it is now widely recognized that the qualitative information content in these detector responses is small and inadequate for analyses of mixtures of PCB's, chlorinated hydrocarbon pesticides, and other organic environmental pollutants.

The application of a mass spectrometer as a chromatographic detector generates the necessary qualitative information but with a substantial loss in sensitivity - perhaps a factor 10^3 - 10^5. A conventional mass spectrometer, which focuses on the detector each sequential ion in the required mass range of about 50 - 500 amu, spends only a very small fraction of the total scan time focusing ions of significant information content. Perhaps for as much as 95-99% of the total scan time the spectrometer is not focusing ions on the collector or is focusing ions which do not contain relevant information. During these periods significant information containing ions are being continuously generated in the ion source and literally discarded with the resultant wasted sensitivity. This occurs whether the spectrometer is operated in a continuously rescanning mode or not.

Substantial gains in sensitivity have been reported where it was possible to rapidly switch focusing between several ions of known significance to the problem. This was accomplished with a magnetic deflection instrument by a device which quickly

modified the accelerating potential; however, the technique was limited to a maximum of three ions separated by a factor of ten percent in mass.

The development of the digital computer controlled quadrupole mass spectrometer opened the possibility of extensive use of program controlled data acquisition with sampling of specific ions, sequences of ions, and varying dwell times on each. Data acquisition from subsets of the ions used in conventional operations should enhance sensitivity without significant loss of information content. This technique is not the same as the "mass chromatogram" concept which used conventional data acquisition, with the wasted ions, but displayed the change in abundance of selected ions under program control to facilitate interpretation.

The application of subset data acquisition techniques to the problem of analyses of PCB's is attractive because of the possibility of gaining needed sensitivity without sacrificing too much of the qualitative information content inherent in a complete mass spectrum. A major problem was to define which of the many ions from the large number of isomers it was most advantageous to utilize in the method.

Several sets of candidate masses were evaluated using PCB's mixed with certain pesticides which are likely to be in a solvent extract of an environmental sample. The method was also tested with a contaminated sediment sample from an Ohio lake.

The full presentation will be submitted to Analytical Chemistry.

DETERMINATION OF TRACE QUANTITIES OF CHLOROPHENOXY-TYPE HERBICIDES AND RELATED CHLORINATED RESIDUES IN SOIL USING GC-MS TECHNIQUES

M.L. Taylor*, R.L.C. Wu*, C.E. Hill, Jr.* E.L. Arnold+,
B.M. Hughes, and T.O. Tiernan
Aerospace Research Laboratories, Chemistry Research Laboratory
Wright-Patterson Air Force Base
Ohio 45433

Methods have been developed for the determination of 2,4-dichlorophenoxyacetic acid, (2,4-D), and 2,4,5-trichlorophenoxyacetic acid (2,4,5-T), and selected esters of these compounds in soil using GC-MS techniques. The compounds of interest are listed in Table 1 along with the base peak in the mass spectrum of each of the compounds.

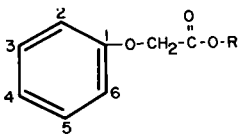

R	COMPOUND (ABBREVIATION)	RING HALOGENS	BASE PEAK (AMU)
H	2,4-DICHLOROPHENOXYACETIC ACID (2,4-D)	2,4-DICHLORO	162*
CH_3	(METHYL 2,4-D)	2,4-DICHLORO	234
H	2,4,5-TRICHLOROPHENOXYACETIC ACID (2,4,5-T)	2,4,5-TRICHLORO	196**
CH_3	(METHYL 2,4,5-T)	2,4,5-TRICHLORO	45
$n\text{-}C_4H_9$	(BUTYL 2,4-D)	2,4-DICHLORO	57
$n\text{-}C_4H_9$	(BUTYL 2,4,5-T)	2,4,5-TRICHLORO	57

* FROM SPECTRUM #8689, MASS SPECTRAL SEARCH SYSTEM, DIVISION OF COMPUTER RESEARCH AND TECHNOLOGY, NIH, BETHESDA, MD.

** FROM SPECTRUM #8773, IBID.

Table I. Herbicide Constituents and Derivatives Determined in This Study

A simple procedure for extraction of the herbicide esters from the soil and simultaneous conversion of 2,4-D and 2,4,5-T to the corresponding methyl esters, which are also extracted, is outlined below.

1. Weigh 10g. of soil and place in a glass stoppered flask.
2. Add 10 ml. of chloroform and 10 ml. of methanol containing 0.1% sulfuric acid.
3. Pulverize soil with glass stirring rod.
4. Let mixture stand for 30 min. at room temperature, swirling every 10 min.
5. Withdraw 3 ml. of extract and place in polyethylene snap cap vial containing anhydrous Na_2SO_4.
6. Inject 1-30 microliter aliquots of the dried extract into the gas chromatograph.

Analysis of the soil extracts was accomplished using a modified DuPont 21-491 mass spectrometer coupled through a Loenco Model 160 gas chromatograph[1,2]. Conditions for the gas chromatographic separation of the herbicide components were as follows:

Column: 6' glass coil packed with 10% SE 30 on chromosorb W

Temperatures: Column, 192°; injection port, 210°, separator, 220°.

Carrier gas: Helium at flow rate 45 cc/min.

Mass chromatograms were obtained by tuning the mass spectrometer to the appropriate mass (the base peak in all cases except methyl 2,4,5-T where m/e 233 was used), utilizing an appropriate standard to calibrate the mass scale (Refer to Table I for the base peaks). The electron multiplier signals are fed to a Datex Electronic Integrator (model DIR-1), and to a 1 millivolt strip chart recorder. A typical mass chromatogram is illustrated in Figure 1.

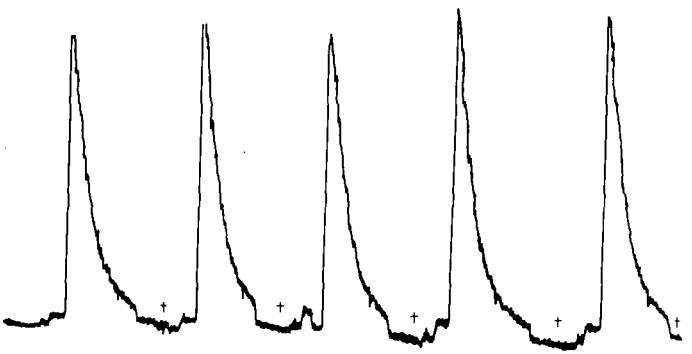

M/e 57

MASS CHROMATOGRAMS FROM FIVE 10ul INJECTIONS OF STANDARD SOLUTION OF N-BUTYL 2,4-D IN CHLOROFORM
% SD = 3.0
† = DISCONTINUITIES IN BASELINE DUE TO OPENING & CLOSING OF VALVE.

Figure 1.

This was obtained by injecting 10 microliters of a chloroform solution of butyl 2,4-D (434 microgram/ml.). Figure 2 shows the mass chromatograms obtained by monitoring m/e 57, when 10 microliter aliquits are injected of an extract from soil prepared to contain 180 micrograms/gram soil of both butyl 2,4-D and butyl 2,4,5-T.

In a similar experiment, 2,4-D was added to soil and Figure 3 shows the mass chromatograms obtained upon replicate injections of the extract.

The methodology described here has been applied to the determination of the herbicide components in several hundred soil samples. In these determinations, previously untreated soil is spiked with herbicide in amounts approximating that found in the soil under analysis, and these doped samples are utilized as standards. This obviates the need for corrections owing to unknown efficiency factors in the overall extraction and esterification processes. The lower limit of detectability for each of the herbicides using this procedure is on the order of 10μg/g soil. Further enhancement of sensitivity by concentration of the soil extracts, by utilizing a smaller extraction volume, or by extracting larger soil samples has not been extensively investigated as yet, but should be feasible.

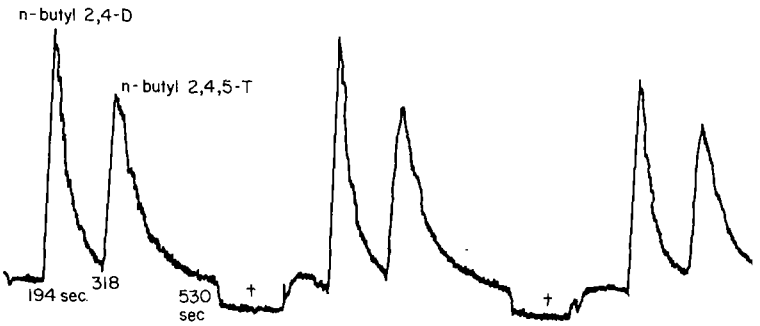

M/e = 57

MASS CHROMATOGRAMS OBTAINED IN REPLICATE ANALYSES OF SO SOIL PREPARED TO CONTAIN 180 ug/g EACH OF N-BUTYL 2,4-D AND N-BUTYL 2,4,5-T.
† = DISCONTINUITIES IN BASELINE DUE TO OPENING & CLOSING OF VALVE.

Figure 2.

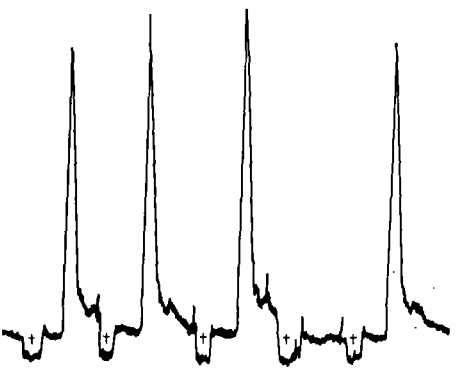

M/e 234

REPLICATE DETERMINATIONS OF THE METHYL ESTER OF 2,4-D IN EXTRACT OF SOIL SAMPLE
SOIL PREPARED TO CONTAIN 423 ug/g of 2,4-D
† = DISCONTINUITIES IN BASELINE DUE TO OPENING & CLOSING OF VALVE.

Figure 3.

References

* Systems Research Laboratories, Dayton, Ohio

+ U.S. Air Force Academy (DFLS), Colorado

1. W.R. Wolf, M.L. Taylor, B.M. Hughes, T.O. Tiernan, and R.E. Sievers, Anal. Chem. 44, 616 (1972).

2. M.L. Taylor, B.M. Hughes, W.R. Wolf, R.E. Sievers, and T.O. Tiernan: 21st Annual Conference on Mass Spectrometry and Allied Topics, Dallas, Texas, 1972.

Acknowledgements

We wish to thank C.D. Miller for technical advice and assistance. Certain of the standard pesticides were obtained from the Pesticide Reference Standard Section, Environmental Protection Agency, Washington, D.C.

A more detailed account of this work will be submitted for publication in Analytical Chemistry.

DETERMINATION OF FRAGMENTATION MECHANISMS OF PESTICIDES BY METASTABLE DEFOCUSSING AND DIRECT ANALYSIS OF DAUGHTER IONS. J. F. Ryan III and F. J. Biros, U. S. Environmental Protection Agency, Primate & Pesticides Effects Laboratory, P.O. Box 490, Perrine, Florida. 33157.

Metastable transitions have proven very useful in aiding the organic chemist in a complete interpretation of a given mass spectrum. Traditionally, metastable ions arising from precursors of a given fragment ion have been identified by scanning the accelerating voltage upward while maintaining electrostatic analyzer (ESA) voltage and magnet current at fixed values[1]. Recently another method of observing metastable transitions has become available. This technique, called direct analysis of daughter ions (DADI)[2,3], requires that the two ion focussing fields be reversed from a normal configuration, i.e., the ESA must follow the magnetic analyzer. This arrangement allows only magnetically selected ions of a particular m/e value to enter a second field-free region between the magnet and ESA sections. Unimolecular decompositions which occur in this region are observed by scanning the ESA to lower voltages while potentiometrically recording the electron multiplier output. We have examined the primary and metastable spectra of a number of pesticides using the DADI technique, and have found them very useful in determining fragmentation mechanisms of these compounds. To illustrate the technique, the mass spectrum of coumaphos, shown in Figure 1, features an intense molecular ion at m/e 362 and as well as an $(M-28)^+$ ion at m/e 334. DADI spectra of these two primary ions are shown in Figure 2. The M^+ ion (m/e 362) directly fragments to produce at least five daughter ions while m/e 334 produces four. Figure 3 shows the specific decompositions which may be inferred from the data in Figures 1 and 2. High resolution mass measurements were performed to verify empirical formulas of product and precursor ions. Abate, Guthion and dicapthon, members of the organophosphate class of pesticides similar to coumaphos, have also been examined[4]. In the latter two examples, DADI spectra could not be observed for the molecular ions since mass spectra of these compounds exhibited no molecular ion. However, accelerating voltage scans of selected fragment ions produced peaks corresponding to decompositions of molecular ion species. Thus, even though molecular ion decompositions cannot be studied using the DADI technique, it is still possible to obtain information which can determine parent-daughter ion relationships through a combination of DADI and conventional metastable defocussing techniques.

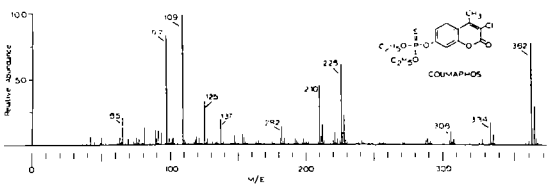

Figure 1. Low resolution mass spectrum of coumaphos.

REFERENCES

1. J. H. Beynon, J. W. Amy, and W. E. Baitinger, Nature, 204, 67 (1964).

2. J. H. Beynon and R. G. Cooks, Res./Dev., 22, 26 (1971).

3. K. H. Maurer, C. Brunnee, G. Kappus, K. Habfast, U. Schroder, and P. Schultz, Abstracts of Nineteenth Annual Conference on Mass Spectrometry and Allied Topics, Atlanta, Ga., May 1971, K9.

4. F. J. Biros and J. F. Ryan, 165th National Meeting of the American Chemical Society, Dallas, Texas, April 1973, Pest. 081.

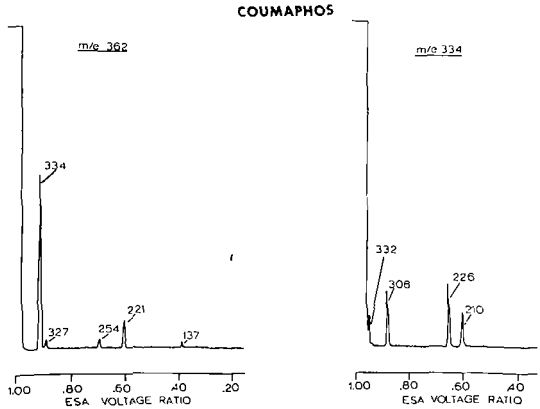

Figure 2. DADI metastable defocussed spectra of molecular (m/e 362) and M-28 (m/e 334) ions of coumaphos.

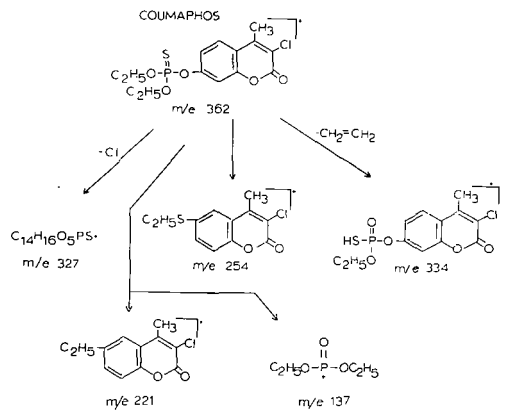

Figure 3. Proposed decompositions of the molecular ion of coumaphos based on interpretation of DADI spectra.

Detection and Confirmation of Trace Amounts of Nitrosamines in Meats by Gas Chromatography -- High Resolution Mass Spectrometry. C. J. DOOLEY, S. F. OSMAN, G. P. MARTIN, and W. FIDDLER, Eastern Regional Research Center, Agricultural Research Service, U. S. Department of Agriculture, Philadelphia, Pennsylvania 19118.

A gas chromatography-high resolution mass spectrometer system is used to detect and confirm the presence of trace amounts of N,N-dimethylnitrosamine, N,N-diethylnitrosamine, and N-nitrosopyrrolidine in meats. Detection and confirmation of as little as 10 ng of these nitrosamines injected on column with a 1:1 splitter can be accomplished even when they are in the presence of large amounts of extraneous materials. High resolution mass spectral data may not in itself provide absolute confirmation of the various nitrosamines. Supplementary data, such as gas chromatographic retention times, may be necessary to insure positive confirmation. The pitfalls that can occur when relying solely on high resolution data will be discussed.

CONTINUOUS MASS SPECTROMETRIC ANALYSIS OF PARTICULATES AND OTHER IMPURITIES IN AIR AND WATER USING SURFACE IONIZATION

W.D. Davis

General Electric Corporate Research and Development
Schenectady, New York 12301

A study was made of surface ionization as a means of analyzing particles in the air on a continuous real-time basis. The sampling system and ion source are shown in Fig. 1. The air sample is pumped down a 1.6mm inside diameter stainless steel tube at about 24 cm^3/sec by a mechanical vacuum pump and impinges on a .05-.07 mm diameter orifice. About one particle in 500 passes through the orifice into the mass spectrometer ion source chamber and hits a Re ribbon (3 mm x 20 mm) heated to 700-1700°C. The ions produced as a particle evaporates from the surface are withdrawn by an electric field in the usual manner, focused and analyzed by a 3" radius 90° magnetic sector with an electron multiplier detector. The pressure of air in the ion source is 1-4 x 10^{-5} Torr.

The ratio of ions to neutral species appears to follow the Saha-Langmuir equation. The higher the pressure of air and the lower the temperature, the greater the amount of O_2 adsorbed on the ribbon and the higher the work function of the surface. With Re, the work function increases from 5.4 eV at 2500°K to a maximum of 7-7.5 eV at 1100°K. However, the rate of emission of ions from the surface decreases with decreasing temperature so that usually a compromise between efficiency of ionization and rate of ion emission must be made. The common components of air (N_2, O_2, H_2O, Ar, CO_2, etc.) have very high ionization potentials, are not ionized and therefore do not cause any interference with the desired signals. At high temperatures, most of the background problems are caused by metallic impurities in the ribbon (primarily Na and K) and evaporation from nearby electrodes and at low temperatures, by easily ionized organic compounds present in the vacuum system. (See paper Q1)

At sufficiently high temperatures, each particle produces a short burst of ions. By counting the bursts, the number of particles per cm^3 can be measured. The number of ions per burst is a measure of the amount of that element per particle. If the particles had a constant composition, this would give the size distribution of the particles. Calibration tests were made with particles of $CsNO_3$, $SrCO_3$, Cr_2O_3, Pb_3O_4, and CuO. The size of the particles was estimated from Stoke's law for the rate of settling in air and was typically in the range 0.3 to 1.3 μm. Reasonably good agreement was usually obtained between the estimated size and that calculated from the Saha-Langmuir equation and the measured transmission of the analyzer (4%). The minimum amount of element in a particle that can be detected is shown in Table 1 for some representative elements. In all cases, the limitation is due to background ions arriving at the detector. Na, K, Rb, and Cs containing particles give results similar to Li with the minimum amount being about 1000 atoms. Particles of MoO , $NiSO_4$, MgO, and $BiCo_3$ of less than 1 μm diameter were easily observed but GeO, WO_3, Sb_2O_3, CdO, and Zn were not detected indicating the cut off limit on ionization potential is about 8 eV.

TABLE 1 - Minimum Detectable Single Particles

	Ionization Potential, eV	Re T°C	Percent Ionized	10^3 Atoms	Diameter, Microns
Li_2O	5.4	830	100	0.8	.003
$SrCO_3$	5.7	1730	50	10	.01
UO_2	6.1	1070	50	1.3	.006
Cr_2O_3	6.8	1500	0.5	300	.02
Pb_3O_4	7.4	910	3	200	.02
CuO	7.7	1130	.02	7000	.06

If analysis of single particles is not desired, one can lower the temperature of the ribbon slightly and from the steady state ion current, calculate the average concentration in the air. Table 2 shows some results using this technique. The background levels were determined by inserting a filter on the inlet to the sampling system so that essentially all the particles were removed from the air. The ambient levels measured in the laboratory (last column) were taken at random and do not necessarily represent comparative concentrations.

TABLE 2 - Air Analysis Using Average Ion Current

Element	IP eV	Re T°C	Percent Ionized	Background Level, ng/m^3	Laboratory Air, ng/m^3
Cs	3.9	600	100	.002	2
Rb	4.2	600	100	.0008	.05
K	4.3	600	100	.0004	.5-200
Na	5.1	600	100	.0004	.4-40
Li	5.4	840	100	.0001	.1-6
Sr	5.7	1500	100	.02	10
U	6.1	1070	50	.003	<.003-.7
Cr	6.8	1130	50	.005	.05
Pb	7.4	910	3	.6	60-600
Cu	7.7	1000	.33	.3	<.3-5

A "practical" use of this technique is illustrated in Fig. 2. The level of Pb inside a fourth floor laboratory was monitored during the time interval when two groups of employees quit work at 4:30 pm and 5:00 pm respectively. The short duration increase in Pb concentration caused by the employees' automobiles is clearly indicated.

For some elements like Pb or U, even lower concentrations can be measured by turning off or reducing the current to the ionizing ribbon, collecting particles on the cooler surface for about a minute and then rapidly reheating the ribbon to obtain a burst of metal ions. About 1 or 2 orders of magnitude gain in signal to noise level can be obtained by this technique, probably because interfering organic compounds are too volatile to be adsorbed. U, for example, can be detected at about 0.2 pg/m^3 for a one minute collection period at 600°C.

The apparatus can also be adapted to the analysis of water by forming a finely divided mist of water droplets, drying the droplets with additional air and injecting the resulting particles into the sampling system. A convenient method for forming droplets is to pass air through a fine fritted disk moistened with the water solution. Using this method, the detection limit for the alkali metals is about 10^{-13} g/cm^3 and for U and Pb, 10^{-12} and 10^{-9} g/cm^3 respectively. Preliminary results indicate, however, that for low Re temperatures, deposition of Ca from natural waters reduces the ionization efficiency for high ionization potential elements.

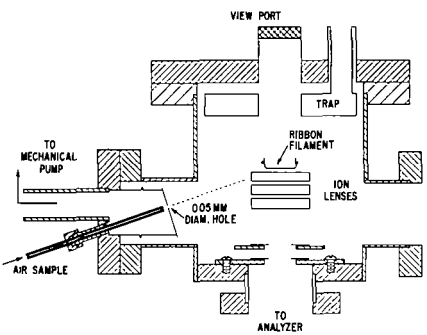

FIG. 1
Ion Source and
Sampling System

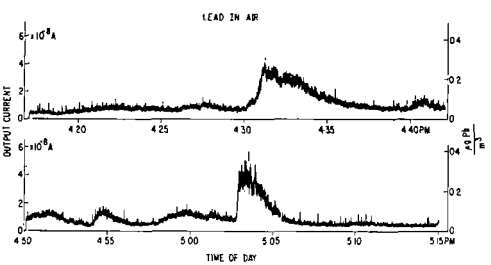

FIG. 2
Continuous Recording of Lead
Levels in Laboratory Air
Showing Effect of Automobiles

OIL SPILL IDENTIFICATION BY FIELD IONIZATION FINGERPRINTING TECHNIQUE*

M. Scolnick, A. C. Scott, W. H. Aberth, and M. Anbar

Mass Spectrometry Development Group
Stanford Research Institute
Menlo Park, California 94025

Oil pollution of oceans, coastlines, and rivers is becoming an increasingly serious threat to our environment. A major obstacle to reducing oil pollution is our inability to identify the source of pollution: the polluter. Without accepted methods of identification, legislation for penalizing oil polluters cannot be enforced. Very often the polluter is unidentified because methods of determining the origin of oil slicks have not been sufficiently developed. If, for example, more than one tanker has passed through an area in which an oil slick is sighted, there is at present no established method of proving which tanker was responsible.

The problem of identifying oil slicks has been discussed at some length in a report by Melpar.[1] The report states that there are two general approaches to oil identification: active tagging (the license plate approach) and passive tagging (the fingerprint approach). The simplest methodology for the fingerprint approach is to assess the chemical composition of the petroleum. Natural oil is a very complex mixture of compounds, and it may be assumed that if the relative concentrations of a sufficiently large number of constituents were determined, these could characterize the sample.

The "fingerprint" methodology requires simultaneous quantitative assessment of a large number of chemical constitutents. There is no doubt that different oil fields, and in fact different oil wells, differ in their hydrocarbon composition to a measurable extent. Moreover, each shipment, consisting of a mixture of different proportions originating from different oil wells, is likely to have its characteristic composition. The key to a successful "fingerprint" approach is the availability of a fast and precise method than can produce enough data to overcome any ambiguity in the identification.

Classical extraction and gas chromatographic techniques for obtaining chemical fingerprints of oil[2,3] are elaborate and require several days of work by qualified analytical chemists to obtain a composition spectrum of certain components of a given sample. Such a lengthy and costly method does not lend itself to building up a large enough data bank of composition spectra of petroleum. Moreover, the precision obtained by even the best examples of the method is not sufficient for legal purposes. The variation in measured abundance readily allows distinction between oil from Kuwait and from Venezuela,[2] but the variation in the measured abundance in different n-paraffins of the same shipment,[2] although strongly indicative, would hardly stand as identical in a court of law.

The complex mixture of organic compounds that constitutes natural oil consists primarily of hydrocarbon: paraffinic, olefinic, cycloaliphatic, and aromatic. In other words, we have compounds of homologous series like C_2H_{n+2}, C_nH_{2n}, and C_nH_{2n-2}. Although numerous isomers have the same C_nH_m composition, the molcular weight spectrum of crude oil shows molecules at practically each mass number between 16 (CH_4) and 3000.

The abundance of different masses in this spectrum is, however, very different for different oils. The wide distribution in abundances in a single homologous series--the n-paraffin has been demonstrated.[2] Similar differences will be observed for any other homologous series. Paraffinic-rich oils will have higher abundance of the C_nH_{2n+2} masses, whereas aromatic-rich oils will show relatively higher abundance of the corresponding $C_nH_{n\pm\ell}$ masses. The abundance of the different masses of weathered oil will also depend on the relative vapor pressures of the individual constituents. Thus, if we measure the same sample following partial evaporation of the more volatile constituents, we will get different patterns of molecular weight distribution, all characteristic of the given oil.

Because of the constituents of lower molecular weight are more likely to evaporate or to be leached out by sea water before being picked up for testing, we prefer to use a given mass range starting, for example, with C_{15} hydrocarbons. The amount of information available in a molecular weight abundance spectrum of, say, 400 mass numbers

between mass 150 and 550 following one partial distillation is enormous. We would have virtually hundreds of variables, which if determined with sufficient precision (say of 2%) will characterize the tested compound to a degree higher than a human fingerprint. If we had only as few as 10 different levels of abundance for each mass peak of 300 variables, we would have virtually 10^{300} different possible combinations of oil composition.

The key to the determination of a molecular weight spectrum of a mixture by mass spectrometry is the availability of an ionization source that ionizes organic molecules without fragmentation. Any excessive fragmentation would make it impossible to identify any particular constituent of the complex mixture, thus making it difficult to distinguish between significant chemical variations in the composition of the samples and trivial artifacts or instrumental fluctuations. In other words, an appreciable degree of fragmentation makes it virtually impossible to prove the identity of two samples of the same origin if one of them underwent even a slight change in composition due to evaporation or weathering.

Nonfragmenting field ionization mass spectrometry[4] has been recently developed into a highly sensitive and reproducible method of ionization applicable to routine analytical mass spectrometry.[5] This was made possible by the specialized technology developed at SRI for manufacturing highly uniform arrays of thousands of microscopic cones deposited on porous substrates.[6] This arrangement, which allows an extremely efficient feed of the gaseous sample to the regions of ultrahigh potential gradients, results in an ionization efficiency that matches or exceeds the ionization efficiency of other methods of ionization.

The multipoint field ionization source mounted on a grid (Figure 1) allows the ionization of materials with vapor pressures lower than 10^{-8} torr. Using this source, it is possible to obtain unfragmented ion spectra of hydrocarbons with molecular weights in the range of 200 to 3500 by heating the sample to merely 350°C. This achievement is made possible by the high ionization efficiency of our source, which requires a minimum of vapor pressure to yield a sizable ion beam. Preliminary experiments indicate a sensitivity threshold of less than 10^{-12} torr. This means that the new multipoint field ionization sources have an unprecedented detection sensitivity. This high sensitivity is critical for monitoring extremely low concentrations of products derived from the photochemical oxidation of oil.

Nonfragmented mass spectra of three different samples of petroleum are shown in Figures 2 through 4. These are, however, single slow mass scans and do not give a quantitative picture of the composition of the oil. Quantitative mass spectrometric "fingerprints" can be achieved only if the total sample is introduced into the ionization chamber and the total mass spectrum is scanned repeatedly at a rate much faster than the change in composition of the evaporating sample. The multiscans must then be integrated into a composite total mass spectrum, which is a true and quantitative representation of the composition of the complex sample. There is no other way to obtain a meaningful and reproducible mass spectrum of a complex mixture.

A unique type of field ionization mass spectrometer has been developed which can obtain reproducible "fingerprint" mass spectra of oil samples. The apparatus is shown schematically in Figure 5. The oil sample in the form of a viscous fluid inside a glass capillary is inserted into the back of the multipoint field ionization source[6] through a ball valve vacuum lock. The source may then be heated from ambient temperature to about 350°C in order to vaporize the sample through the grids of the source. After a pre-specified temperature is reached, the heating power is adjusted to keep the temperature constant and the run is continued until no more volatile material reaches the points. At this point, the total ion current is less than 100 c/sec.

The sample ions are extracted from the source and focused by means of a set of electrodes attached to the source and an Einzel lens positioned about 60 cm from the source. The ion beam then undergoes mass separation by means of a Colutron[7] E x B ion velocity filter.[8] This filter has a 60 cm long mass separating region. Its design is based on that of the Wien filter but with electrostatic and magnetic shims that can trim the E and B fields and eliminate the strong focusing characteristics of the device.[9] The velocity filter is operated with a constant magnetic field and mass scanning is accomplished by varying the electrostatic cross field. A pair of deflection plates

situated immediately after the velocity selector (see Figure 5) provides for positioning the ion beam either on the entrance aperture of the multiplier detector or on the surface of an image intensifier. The image intensifier device consists of two 3.5 cm diameter series connected microchannel electron multiplier plates[10] backed by a fluorescent screen that is visible through a viewing port. A single ion impinging on the front surface of the image intensifier will produce about 10^8 electrons at the output of the second microchannel plate. This current is accelerated by about 1700 volts to the fluorescent screen. Single ion impingements are thus made visible by this device which serves as an invaluable means for optimizing the ion beam optics and beam finding. The mass selected ion beam is detected through a 1 x 3 mm slit by a Bendix 4700 continuous dynode electron multiplier coupled with an SSR model 1120 amplifier/discriminator.

A mass scan covering a range of over 1000 mass units can be completed in less than one second. Repetitive mass scans are performed by supplying the amplified ramp voltage of an Exact Model 126 sweep generator to the electrostatic deflecting plates of the Colutron filter. The mass range covered is obtained by adjusting the ramp voltage amplitude and dc offset. A pulse synchronized to the ramp voltage triggers a Model ND 2400 Nuclear Data 4096 channel multichannel analyzer which operates in the multichannel scaling mode of data acquisition and which obtains its pulsed signal input from the amplifier/discriminator unit. This arrangement permits the storage of signals from a particular mass into a corresponding channel during repetitive mass scanning. The mass resolution of the system is determined by the ion beam optics, the stability of electronics, and the number of storage channels in the multichannel analyzer per mass unit. Present resolution is limited by electronic stability and is in the range of 300 to 1000 depending on the mass number.

Figures 6 through 9 are examples of integrated mass spectra. Figure 6 shows the mass spectra of a "brand X" #6 oil, illustrating the reproducibility of the method. Figure 7 is the spectrum of a pentane extract of the same oil. Figure 8 is the mass spectrum of a "brand Y" #6 fuel oil. These examples demonstrate the potential usefulness of this fingerprint procedure for the identification of oil spills. At present we are collecting fingerprint mass spectra of a large variety of crude oils and fuel oils to determine the scope and limitations of our methodology. In the long run it will be necessary to process the mass spectra information, available in digital form as it comes out from the multiscaler, by a computer. It will be relatively easy to process the data in a form that will allow us to determine similarities between a given spectrum of a new sample and the spectra of hundreds of thousands of oil samples stored in a data bank. The computer program will have to be capable of distinction between trivial differences between samples due to processing or instrumental artifacts and real differences due to composition of the sample.

We are also applying the same instrumentation for the determination of time of exposure of oil to the marine environment. The simplest approach--the changes in the overall mass spectrum of the sample--although demonstrable after lengthy exposure (see Figure 9) is not sensitive enough for determining the exposure duration in the range of 1 to 14 days, which is the most interesting range from the operational standpoint. A more sophisticated methodology based on the photochemical formation of hydroxyolefin has been developed.[11] The space constraints of this paper do not allow an appropriate description of this methodology, and it will be published elsewhere.

*Sponsored by the U. S. Coast Guard under Contract #DOT-CG-22996-A.

REFERENCES:

[1] Melpar, Inc., "Oil Tagging System Study," Water Pollution Control Research Series, DAST 11 15080 DJQ, October, 1969.

[2] J. V. Brunnock, D. F. Duckworth, and G. G. Stephens, J. Inst. Pet. 54, 310 (1968).

[3] S. A. Berridge, R. A. Dean, R. G. Fallows, and R. Rish, J. Inst. Pet., 54, 300 (1968).

[4] H. D. Beckey, Field Ionization Mass Spectrometry (Pergamon Press, Oxford) 1971.

[5] G. A. St. John and M. Anbar, 21st Annual Conference on Mass Spectrometry and Allied Topics, San Francisco (May, 1973). p. _____.

[6] W. Aberth, C. A. Spindt, and R. R. Sperry, ibid. p. _____.

[7] Colutron velocity filter Model 300-6, Colutron Corp. P. O. Box 1288, Boulder, Colo. 80302.

[8] L. Wahlin, Nucl. Instr. Meth. 27, 55 (1964).

[9] R. L. Seliger, 11th Symposium on Electron Ion and Laser Beam Technology, Boulder, Colorado, San Francisco Press, Inc. (1971). p. 183.

[10] Microchannel plates manufactured by Varian, Palo Alto Tube Divisions, Palo Alto, California 94303.

[11] M. Anbar, A. C. Scott, and M. Scolnick, to be published.

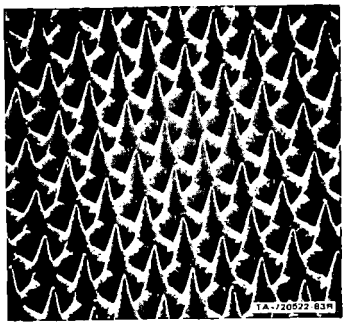

FIGURE 1 SCANNING ELECTRON MICROGRAPH OF MULTIPOINT FIELD IONIZING SOURCE

Gold pyramids are mounted on a gold screen 25 microns apart and are 25 microns tall.

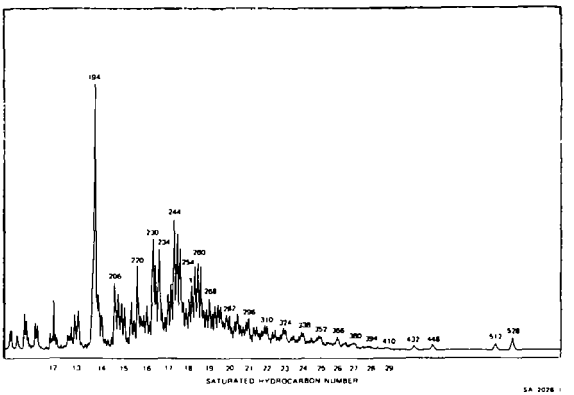

FIGURE 2 MIXED FUEL—100°C AFTER 150°C VACUUM DISTILLATION

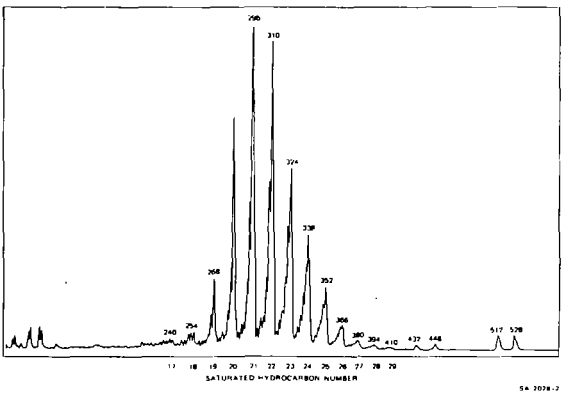

FIGURE 3 CRUDE OIL—100°C AFTER 150°C VACUUM DISTILLATION

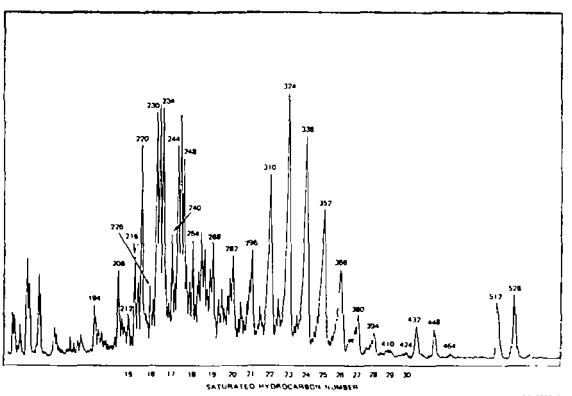

FIGURE 4 FUEL OIL NO 6—100°C AFTER 150° VACUUM DISTILLATIONS

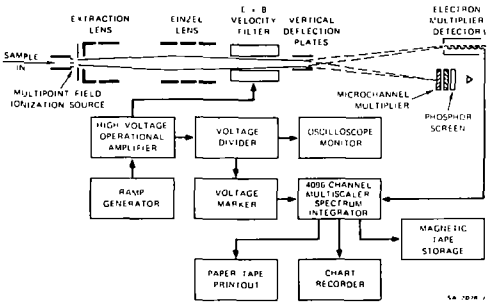

FIGURE 5 SCHEMATIC OF FIELD IONIZATION FINGERPRINT APPARATUS

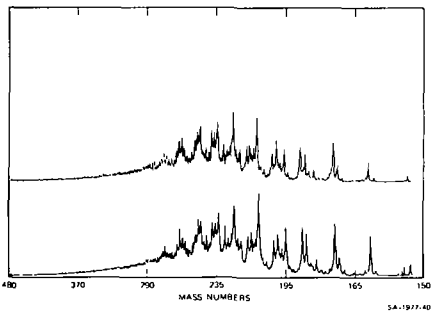

FIGURE 6 TWO "FINGERPRINTS" OF NUMBER 6 FUEL OIL, VACUUM DISTILLED, MID-CUT

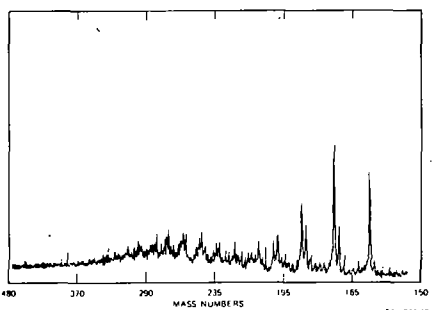

FIGURE 7 NUMBER 6 FUEL OIL, PENTANE EXTRACT

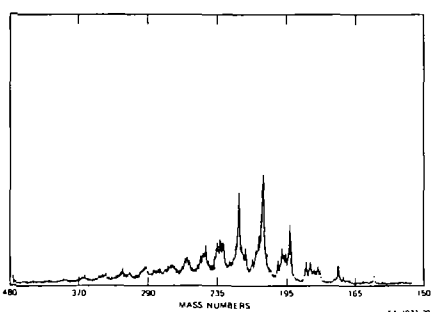

FIGURE 8 NUMBER 6 FUEL OIL, VACUUM DISTILLED, MID-CUT

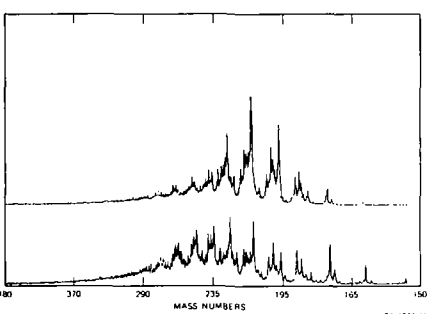

FIGURE 9 NUMBER 6 FUEL OIL, OUTDOOR WEATHERED (UPPER TRACE), *UNWEATHERED (LOWER TRACE)*

MEASUREMENT OF THE MASS SPECTROMETER EFFICIENCY IN THE ISOTOPIC ANALYSIS OF VERY SMALL PLUTONIUM SAMPLES*

Riley D. Carver and R. Jene Dupzyk

Lawrence Livermore Laboratory
Livermore, California 94550

Because of increasing interest in the analysis of very small amounts of plutonium (10^{-13}g or .016 d/m) in environmental samples, our laboratory has developed the capability to measure isotopic abundances at these levels. The instrument has a double filament surface ionization source; tandem magnets with 60° sectors of 34 cm radius; and computer-controlled data acquisition, fast magnetic sweep, and on-line data reduction. While the source is not of the Stevens type, it is valve-isolated from the analyzer portion, and with the fast pumping provided, working pressures of 10^{-7} torr can be achieved within 15 minutes. Pressures of 10^{-9} torr are attainable within two hours. All plutonium samples are traced with 350 pg of ^{242}Pu for isotope dilution normalization.

One of the early experiments was progressive dilution of a plutonium chloride solution to determine how small a sample we actually could analyze. The total Pu found in each analysis along with the 240/239 isotope ratios measured are summarized in Table I. At about sample #0 the results start to degenerate; we consider this to be the smallest sample (about .006 d/m, 30fg) which our laboratory can routinely analyze.

Because these samples were prepared by direct dilution, there remained some question about possible chemical losses and effects. A plutonium solution was analyzed two times: once with ^{242}Pu tracer added before chemistry, and once with the tracer added after chemistry. Conventional nitrate anion exchange was used. The results in Table II show that there was high chemical yield with no particular loss in accuracy.

Real environmental samples have also been analyzed.(1) Mostly these are soil, but others such as plant and animal tissue, water, air filters, etc., have also been run. Table III shows the results for a series of soil samples sent to us from various parts of the country. General chemical separation had already been performed, and alpha counting had been done. We added ^{242}Pu tracer and did an additional nitrate anion exchange to further purify the sample. Previous work(2) has shown that atmospheric fall-out plutonium has a much higher mass 240 content than does the typical plutonium from production reactors such as those at Hanford and Savannah River. The measurement of the 240/239 ratio then is a good method for differentiating between the inescapable fall-out of nuclear test debris from the stratosphere and other sources of plutonium such as accidental spills from plutonium handling facilities.

Other work(3) has indicated that chemical processing strongly degrades mass spectrometer efficiency. Our efficiency measurements for comparable types of samples are shown in Table IV. The efficiencies are the summed counts collected for a given mass, divided by the number of atoms of that mass present in the original sample (as measured by isotope dilution), and then multiplied by 100.

The chemistry seems to improve the efficiency in most cases. The lower efficiencies were for samples on plates. When a sample is on a plate, it is stripped with HNO_3 + HF, and the fluoride may interfere in some unknown manner with chemical yield or ionization efficiency.

In summary, samples as small as .006 d/m $^{239+240}$Pu (30 fg) can be isotopically and quantitatively analyzed. The extensive chemical purifications required are a factor, but do not cause large losses or insurmountable difficulties.

---

*This work was performed under the auspices of the U.S. Atomic Energy Commission.

1. R. J. Dupzyk, et al., Argonne National Laboratory Report 8014, pp. 32-33, October, 1972.
2. P. W. Krey and B. T. Krajewski, Health and Safety Laboratory Report 249, pp. I67-I94, April, 1972.
3. F. M. Rourke and J. L. Mewherter, 20th Annual Conference on Mass Spectrometry and Allied Topics, Paper L-2, June 4-9, 1972, Dallas, Texas.

TABLE I

Diluted Plutonium Chloride Tracer

No.	Gross dpm 239+240 by Mass Spectroscopy	240/239 (atomic) by Mass Spectroscopy
9	63.9 ± 0.13	0.063
8	19.0 ± 0.05	0.063
7	6.2 ± 0.02	0.063
6	1.9 ± 0.01	0.064
5	0.61 ± 0.005	0.064
4	0.20 ± 0.004	0.065
3	0.062 ± 0.002	0.068
2	0.021 ± 0.0009	0.066
1	0.0068 ± 0.0003	0.071
0	0.0020 ± 0.0002	0.082
-1	0.00070 ± 0.00009	0.110

TABLE II

Standard Pu Sample UK-131 (1.5 pg)

	Accepted	Before Chemistry	After Chemistry
240/239 (atomic)	0.216	0.215 ± 0.004	0.214 ± 0.004
isotope dilution assay	-	0.30 d/m	0.27 d/m

Chemical yield 90%

TABLE III

Environmental Plutonium in Soil

Location	240/239	Sample Size $^{239+240}Pu$
California	0.165 ± 0.001	3.9 d/m
Utah	0.117 ± 0.005	18.5 d/m
Colorado	0.149 ± 0.004	0.290d/m
Nebraska	0.149 ± 0.004	0.048d/m
New York	0.175 ± 0.007	27.7 d/m

TABLE IV

Mass Spectrometer Efficiency

Without Chemistry

$^{239+240}Pu$ (pg)*	Counts/pg	% Efficiency
0.125	1.2×10^6	0.049

With Chemistry

$^{239+240}Pu$ (pg)*	Type of Chemistry	Counts/pg	% Efficiency
0.040	anion exchange	3.1×10^6	0.125
0.230	vial strip + anion exchange	3.6×10^6	0.144
1	vial strip + anion exchange	5.2×10^6	0.210
20	Pt plate strip +	0.9×10^6	0.036
0.750	Fe plate strip + anion exchange	1.0×10^6	0.042

*plus 350 pg ^{242}Pu tracer

Thermochemical and Kinetic Information from Metastable Decomposition of Ions

C. E. Klots, Health Physics Division, Oak Ridge National Laboratory, Oak Ridge, TN 37830

The transition state formulation of the quasi-equilibrium theory of unimolecular decompositions can be used to calculate rate constants. It is, however, quite mute on the question of the distribution of any excess energy among the several degrees-of-freedom of the reaction products. A reformulation of quasi-equilibrium theory, presented earlier[1], is cast directly in terms of the final states, and so can be used to discuss the distribution of excess energy. When supplemented with Langevin cross-sections for the recombination process, very simple results are obtained. The distribution of excess energy is found to be governed by a well-defined temperature. In particular, a simple expression relating kinetic energy release with kinetic shifts is obtained. Existing data suggest, nevertheless, that the effective number of internal degrees-of-freedom for energy disposal is often greater than the physical number, a result incompatible with all existing theory. A formal reconciliation, drawing upon ideas from the mainstream of chemical kinetics, can be constructed[2].

---

[1] C. E. Klots, J. Phys. Chem. 75, 1526 (1971).

[2] C. E. Klots, J. Chem. Phys. 58, 5364 (1973).

A NEW METHOD FOR THE DETERMINATION OF DOUBLE AND TRIPLE IONIZATION POTENTIALS OF ORGANIC IONS

R.G. Cooks, T. Ast, and J.H. Beynon
Purdue University
Department of Chemistry
W. Lafayette, Indiana 47907

This paper will appear (1973) in Int. J. Mass Spectrom. Ion Phys.

ABSTRACT

Ion-molecule reactions at high kinetic energy provide a rich potential source of thermochemical data. Charge stripping of singly charged ions (m^+) with a target molecule (N); i.e. the 10/20 reaction type

$$m^+ + N \rightarrow m^{2+} + N + e \qquad (1)$$

can be readily studied in a double focusing mass spectrometer modified to allow accurate determinations of ion kinetic energies. The kinetic energy of the product ion m^{2+} is less than that of the reactant ion m^+ and the energy loss, Q', can be measured accurate to better than 0·5eV. Experiments of this type on rare gas ions provide information on the population of long-lived excited states in the ion beam. Organic ions generally give a single energy loss peak the width of which, at half height, is typically 3eV compared to a main beam width of 1·5eV. By carrying out successive energy and mass analysis on the products of reaction (1) it is possible to study these ions without interference from other processes except for the symmetrical fragmentation reaction

$$m^+ \rightarrow \underline{m}^+ + \underline{m} \qquad (2)$$
$$\quad\ 2 \quad\ 2$$

It is always possible to study the signal due to the ^{13}C isotope of m^+ to avoid this ambiguity. In addition, the peak due to fragmentation is always broadened by kinetic energy release.

The magnitude of the energy loss accompanying reaction (1) for polyatomic ions gives directly the difference between the single and double ionization potentials of the compound, m. Knowing the single IP, the double IP can therefore be determined. This method gives results which agree well with the few available literature values of double IP's. It has the advantage that it may be applied to any ion, molecular or fragment, that the difficulties associated with interpreting ionization efficiency curves are avoided, and that measurements can be made very quickly. The determination of Q' suggests itself as a method of characterizing the structures of ions which are stable to unimolecular fragmentation.

The same general technique can be applied to the determination of triple ionization potentials based upon the kinetic energy loss accompanying the reaction

$$m^{2+} + N \rightarrow m^{3+} + N + e \qquad (3)$$

KINETICS OF UNIMOLECULAR IONIC REACTIONS
KINETIC ENERGY RELEASE IN METASTABLE ION DECOMPOSITION

By

K.C. Kim, T.W. Keough, J.H. Beynon and R.G. Cooks

Purdue University
Department of Chemistry
West Lafayette, Indiana 47907

This paper has been submitted to J. Amer. Chem. Soc. for publication.

PROCEDURE

Ion kinetic energy distributions were measured using a modified RMH-2 double focusing mass spectrometer[1] and a reversed sector mass-analyzed ion kinetic energy spectrometer (MIKES).[2] Fragmentations occurring in the first field free region of the RMH-2 were monitored by the accelerating voltage (HV) scan technique using a narrow (~0.1mm) energy resolving B-slit. An average kinetic energy release, to a first approximation, was calculated from metastable peak widths at half height.[3] Correction for the kinetic energy distribution in a beam of stable ions was made by subtraction of the main beam width measured at the appropriate ion accelerating voltage. Ion life times were varied between 4 and 15μsec by varying the ion accelerating voltage between 250V and 8kV. An average ion life time was calculated as the time required to reach the middle of the field free region assuming a 1μsec source residence time. Measurements at low ion accelerating voltage were made using the same procedure routinely employed for measurements at high voltage. The source conditions were focused for maximum height of the metastable peak at each value of ion accelerating voltage. All reactions studied were unimolecular with no contributions from collision induced decompositions. Analyzer pressures were approximately 10^{-7} torr. All results given represent the averages of multiple scans taken over a period of several months.

RESULTS

The kinetic energy release for the HCN loss from excited benzonitrile was measured as a function of ion life time in the range of 4-15μsec. The average kinetic energy release at 4μsec was 24 meV and the variation of the kinetic energy release over the above range was shown to be less than 5 meV. The unimolecular decomposition of benzene by the $H^{\cdot}$ loss channel was accompanied with 65 meV kinetic energy release and the variation in T was almost negligible within the experimental uncertainties. For the isomeric $C_4H_7Cl^{+\cdot}$ ion, an average of ~580 meV was released as kinetic energy and the variation of T over the ion life time 10μsec was approximately 15 meV. Both 1,4-dichlorobutane and chlorocyclobutane were used as the precursor compounds. The average kinetic energy release for the chlorocyclobutane precursor was higher by about

28 meV but the variation in T was nearly identical for both cases. For benzonitrile, using the experimental k(ε) curve reported by Ottinger et al,[4] one expects 2-3 times larger statistical kinetic energy release and at least 1-2 order of magnitude larger variation in the T value over the ion life times employed in this work. These acute discrepancies can not be reconciled by the statistical theory. However our present experimental results are in a reasonable agreement with the calculated results when angular momentum states of the reacting species are explicitly accounted for.[5] The results on both benzene and isomeric $C_4H_7Cl^{+\cdot}$ ion are in good agreement with RRKM predictions and are consistent with the statistical partitioning of the excess energy above the potential barrier among all active molecular configurations.

CONCLUSIONS

Translational energy release during unimolecular fragmentations of excited ions can be utilized to experimentally characterize the energy dependence of rate constants. The average ion life time, hence the rate constants of the unimolecular reactions, can be varied over a useful range of 4-15μsec by the technique of variation of ion accelerating voltage. Studies of neutral species by other methods such as chemical activation suffer from limitations regarding the degree of excitation. The accuracy of the measurements of the kinetic energy release by ion kinetic energy spectrometry makes this method a convenient way of studying ion kinetics for a variety of unimolecular reactions. These features and some correlations between the statistical theory and the experimental results are illustrated using the reactions of benzene (loss of H· from $C_6H_6^{+\cdot}$), benzonitrile (loss of HCN from C_7H_5N) and $C_4H_7Cl^{+\cdot}$ ions (loss of HCl).

REFERENCES

1. (a) J. H. Beynon, W. E. Baitinger, J. W. Amy and T. Komatsu, Int. J. Mass Spectrom. Ion Phys., 3 47 (1969).

   (b) T. Ast, J. H. Beynon and R. G. Cooks, J. Amer. Chem. Soc., 94, 6611 (1972).

2. J. H. Beynon, R. G. Cooks, J. W. Amy, W. E. Baitinger and T. Ridley, Anal. Chem., in press.

3. (a) J. H. Beynon, R. M. Caprioli, W. E. Baitinger and J. W. Amy, Org. Mass Spectrom. 3 661 (1970).

   (b) J. H. Beynon, A. E. Fontaine and G. R. Lester, Int. J. Mass Spectrom. Ion Phys., 8 341 (1972).

4. (a) B. Andlauer and Ch. Ottinger, J. Chem. Phys., 55 1471 (1971).

   (b) B. Andlauer and Ch. Ottinger, Z. Naturforsch. 27a, 293 (1973).

5. D. L. Bunker, J. Chem. Phys., 57 332 (1972).

MASS SPECTROMETRIC SAMPLING OF A HOLLOW CATHODE DISCHARGE

W. W. Harrison and C. W. Magee

Department of Chemistry
University of Virginia
Charlottesville, Virginia 22901

Demountable hollow cathode tubes have been used in our laboratories for several years in trace element studies involving optical spectroscopy. Thin films deposited on the cathode surface are sputtered and excited for analysis. A similar unit has been interfaced into a source of an MS-702 mass spectrometer to investigate ion formation in the hollow cathode discharge. Argon and helium are used as flow gases at about one torr in the tube; a DC power supply provides the breakdown potential. A high speed pumping system consisting of a 1200 l/second diffusion pump and large backing pump maintains a source pressure of about 10^{-5} torr. Ions are extracted from an anode exit slit with a 10KV accelerating potential. Sensitivity to sub-ppm levels in stainless steel samples has been shown. A high intensity, stable ion beam is observed.

A paper detailing this study will be submitted to Analytical Chemistry

A Beam Study of the $O^+ + H_2, HD, D_2$ Systems from 3 to 50 eV Relative Energy*.

Keith T. Gillen, Bruce H. Mahan, and John S. Winn

Department of Chemistry and Lawrence Berkeley Laboratory

University of California, Berkeley, California 94720

The reaction $O^+ + H_2 \rightarrow OH^+ + H$ and its isotopic variants proceed to ground state ($^3\Sigma^-$) OH^+ by direct mechanisms (rather than through long-lived complexes) at center-of-mass (c.m.) energies as low as 3 eV. An intense spectator stripping (SS) peak is the dominant feature of the c.m. velocity vector contour maps of product intensity. As the collision energy is increased, OH^+ formed by SS has progressively more internal excitation; when the energy of O^+ relative to the abstracted atom exceeds 4.5 eV, $OH^+(^3\Sigma^-)$ cannot be formed by SS and a forward-scattered ridge (of diminished intensity) is attributed to excited OH^+ (probably $^1\Delta$). At this critical energy, the intense forward peak shifts to larger angles with the $OH^+(^3\Sigma^-)$ being stabilized through interaction with the third atom. At higher c.m. energies (12-50 eV), stabilization becomes increasingly more difficult and reactive product gradually decreases in intensity. Simultaneously, the dissociative channels ($O^+ + H_2 \rightarrow O^+ + H + H$) become important and the O^+ scattering patterns at high energies imply a single proton knock-out process for large-angle dissociative scattering.

*Work supported by U.S.A.E.C.

A full account of this work will be published in the Journal of Chemical Physics, and Chemical Physics Letters.

Studies of Ion Beam Energies

by

R.I. Reed and (Miss) M.E.S.F. Silva

Chemistry Department, University of Glasgow, Glasgow G12 8QQ, Scotland

The studies were conducted with an energy spectrometer. This was constructed by adding an electrostatic sector to an AEI MS2 mass spectrometer (No.11 in the series). This sector, which followed the magnetic sector was of 60° of arc and curved in the direction of the other sector. The exit slit of this was the entry slit of the electrostatic sector the exit slit of which was 0.002" (0.0508 mm). Correction was made for the fringing field. A stability of one part per thousand was required which demanded a reconstruction of the electronic circuits. The collector was a channeltron[1] working in the continuous mode. Similar instruments have appeared in the literature[2] or in a commercial form.[3] Several compounds were examined. Atmospheric nitrogen was found to yield two energetic ions in addition to the usual ion at m/e = 14. Following the analysis of Hierl and Franklin[4] these have been assigned as follows:-

$N_2^+ (D:{}^2\pi_g) \rightarrow N^+ ({}^3P) + N.({}^4S^o)$ for the ion with thermal energy only, and

$N_2^+ (C:{}^2\Sigma_u^+) \rightarrow N^+ ({}^3P) + N.({}^2D)$ accompanied by one electron volt of kinetic energy. The third peak will originate from $N_2^{2+}({}^3\Sigma_u^+)$.[5] The $N_2^+ \rightarrow N^+$ was also detected as a metastable.[6] Methane[7] was examined and all the previously identified metastables confirmed. Additionally a metastable m/e = 15.1 was detected which may be $^{13}CH_4^{+\cdot} \rightarrow {}^{13}CH_3^+ + H.$, $^{12}CH_5^+ \rightarrow {}^{12}CH_4^+ + H.$, or some artifact from the pump oil. In a similar way methanol was examined and all the most intense metastables confirmed.[8] Energetic hydroxyl ions were also detected from methanol.[9]

To be published in International Journal of Mass Spectrometry and Ion Physics.

References

1. Mullard, "Channel Electron Multiplier", Type B419 AL
2. F.A. White, F.M. Rourke and J.C. Sheffield, Appl. Spect., 12, 46, 1958; U. Löhle and Ch. Ottinger, 17th Ann. Conf. Mass Spec., Dallas, 1969; No.29; T. Wachs, P.F. Bente III and F.W. McLafferty, Int. J. Mass Spec. and Ion Phys., 9, 33, 1972
3. K. Maurer, C. Brunee, G. Rappus, K. Habfast, U. Schröder and R. Schulze, 19th Ann. Conf. Mass Spec., Atlanta 1971; No.K9
4. P.M. Hierl and J.L. Franklin, J. Chem. Phys., 47, 3154, 1967

5. K.E. McCulloh, personal communication

6. H.Wankenne and J. Momigny, Chem. Phys. Letter, 4, 132, 1969; A.S. Newton and A.F. Sciamanna, J. Chem. Phys., 50, 4868, 1969

7. C.E. Melton and H.M. Rosenstock, J. Chem. Phys., 26, 568, 1957; V.H. Dibeler and H.M. Rosenstock, J. Chem. Phys., 39, 1326, 1963;Ch.Öttinger, Z.Naturforsch, 20a, 1232, 1965

8. C. Lifshitz, M. Shapiro and R. Sternberg, Israel J. of Chem., 7, 391, 1969; J.H. Beynon, A.E. Fontaine and G.R. Lester, Int. J. of Mass Spec. and Ion Phys., 1, 1, 1968

9. T. Tsuchiya, Bull. Chem. Soc. Japan, 37, 1308, 1964

Mobility Spectra of Some Electrohydrodynamically Atomized Solutions of Macromolecules. J. Gieniec, R. P. Blickensderfer, D. Teer and M. Dole, Dept. of Chem., Baylor University, Waco, Texas, 76703.

Supersonic beams of gas phase macroions have been produced by an electrospray technique in conjunction with a nozzle-skimmer system and energy analyzed using a repeller-grid-Faraday cage analyzer-detector. Fractionated samples of polystyrene of 51,000 amu gave indications of macroions of unit charge and containing one or more intact molecules. Results with polystyrene of 411,000 amu could be interpreted on the basis of 2 to 5 charges on a single macromolecule. However, these latter results can also be interpreted as degradation of the molecule with the resulting fragments being singly charged. To resolve this dilemma, an ion-drift spectrometer has been used to obtain electrical mobility spectra of the electrosprayed polymer solutions. The electrical mobility data yields $M\alpha/z$ (α lying between 1/3 and 2/3) while the repeller-grid data yields M/z. Therefore, the two sets of data should yield M and z independently.

FIELD IONIZATION KINETIC (FIK) STUDIES OF UNIMOLECULAR DECOMPOSITION WITH A DOUBLE FOCUSING MASS SPECTROMETER

A. M. Falick, P. J. Derrick* and A. L. Burlingame
Space Sciences Laboratory
University of California, Berkeley, California 94720

It was first demonstrated by Beckey as early as 1961 (1) that a field ionization ion source could be used to measure ion decomposition rates at very short times. Since that time, several studies of ion decomposition kinetics have been published, both by Beckey (2) and others (3-6), and it has been demonstrated that such field ionization kinetic measurements can be extremely valuable in the determination of gas phase ion decomposition kinetics and pathways. The technique offers the unique advantage of permitting the measurement of the rates of gas phase unimolecular decompositions of ions occurring at times between 10^{-12} and 10^{-5} sec after ionization (2). An additional feature is that the primary ionization process produces ions of low internal energy (2), which tends to enhance the more interesting rearrangement processes relative to direct cleavages.

Most of the field ionization kinetic (FIK) work which has been published or presented up to this time has been done with single focusing mass spectrometers, with the exception of the studies from our laboratory (5,6) and the work of Chait and Kitson (3). In our work we have used a double focusing mass analyzer, which can have advantages in some cases. The purpose of this paper is to describe the method which we use, and then to very briefly present some recent results.

The basic method, which is common to both types of mass analyzers, depends upon the very large gradient of the electrostatic field in front of the FI emitter. Parent ions formed at or very near the emitter surface are rapidly accelerated away from the emitter. If they are decomposing during this acceleration, the resultant fragment ions produced along the way will have a range of translational energies when they finally leave the ion source. If the potential distribution and the parent ion trajectories in the emitter region are known (7), then an analysis of the fragment ion translational energy distribution can yield a curve of parent ion decomposition rate as a function of time. When a single focusing mass analyzer is used, the fragment ion energy distribution appears as a more or less extensive broadening of the normal fragment ion peak towards lower masses; the broadened portions of these peaks have been termed "fast metastables" (2).

Under normal conditions, energy deficient fragment ions will not be detected at all when a double focusing mass analyzer is used, because the electrostatic sector (ESA) acts as an energy filter. However, they can be detected by increasing the emitter voltage (8) so as to supply enough additional translational energy to the fragment ions so that they will be transmitted normally. This method produces a curve of fragment ion current vs. emitter voltage which can be converted to a curve of decomposition rate vs. time for fragment ions of any selected mass. The advantage of using a double focusing analyzer lies in the fact that each curve produced is for an ion of a specific nominal mass and is completely independent of ions of nearby masses. In contrast, when a single focusing mass analyzer is used, all of the kinetic information (in the form of broadened peaks)

* Present address: University College London, Department of Chemistry, 20 Gordon Street, London WC1H 0AJ, England.

is superimposed on the normal FI mass spectrum. When two or more competing decomposition pathways produce fragment ions differing in mass by only one or two units, the resulting adjacent broadened peaks can overlap and interfere. Such a situation can arise, for example, in studies of isotopically labeled molecules (see, for example, Ref. 5).

The technique of increasing the blade voltage which we use has two important advantages over the complementary method of reducing the ESA voltage. First, all of those ions which are actually transmitted through the instrument and detected when using this method must always have essentially the same kinetic energy as normally accelerated ions. Therefore there should be no energy discrimination effects in the analyzer. Secondly, the fact that all of the detected ions have the same energy means that the mass scale remains constant at all times.

The specific instrument which we have used for our FIK studies is a modified CEC 21-110 equipped with a blade-type FI source (7). Fig. 1 shows the four regions in the

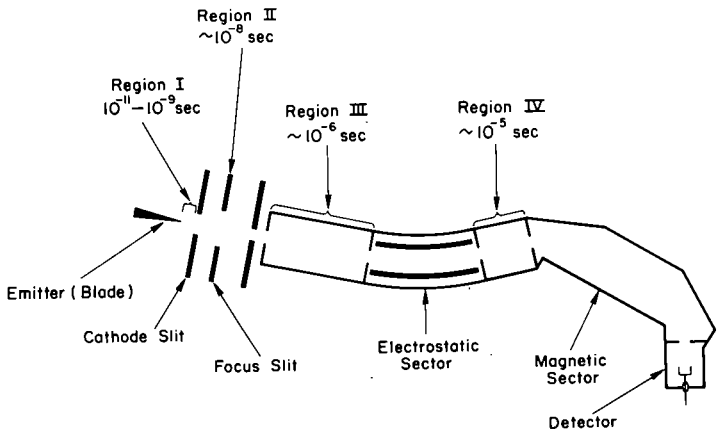

Fig. 1. Schematic diagram of double focusing (Mattauch-Herzog) mass spectrometer showing regions in which gas phase ion decompositions can be measured.

mass spectrometer in which gas phase ion decompositions can be detected. The technique described above pertains to region I, the space between the blade and the cathode. Region II is the small potential plateau (actually a saddle point) between the focus plates. Regions III and IV are the first and second field free regions. Decompositions in the first field free region can be detected by means of the usual defocusing techniques used in electron impact mass spectrometers (9,10). Decompositions in the second field free region (Region IV) are seen as normal metastable peaks in the normal FI mass spectrum. It is important to note that data from Region I form a continuous curve, whereas the data from Regions II-IV provide only one point per region on the curve of decomposition rate vs. time.

Calculations (7) of ion trajectories show that for the case of a singly charged ion of mass 100 decomposing to a fragment ion of mass 50, only those fragments produced at times less than about 10^{-11} sec appear in the normal FI mass spectrum. This includes the ions produced by all of the surface and high-field processes (2) which are peculiar

to FI. Ions which decompose after 10^{-11} sec or so have fallen far enough down the potential curve away from the blade so that their daughter ions will not be detected in the normal spectrum because they will not be transmitted by the ESA. Conversely, when the blade potential is increased sufficiently so that these daughter ions will be detected, the normal spectrum is completely suppressed, and only ions arising from gas phase processes in relatively low field areas will be detected.

Some recent results of ours on isobutane demonstrate the capabilities and potential of the method. In the FI spectrum of isobutane, the molecular ion is the base peak and the most important fragment ions are 57, 43 and 42. Only one normal metastable ion is observed, that for the 58 → 42 transition. The low energy electron impact spectrum is quite similar except that both the molecular ion and the metastable are much weaker. Fig. 2 shows the ion current vs. blade voltage curves for the four important ions. The

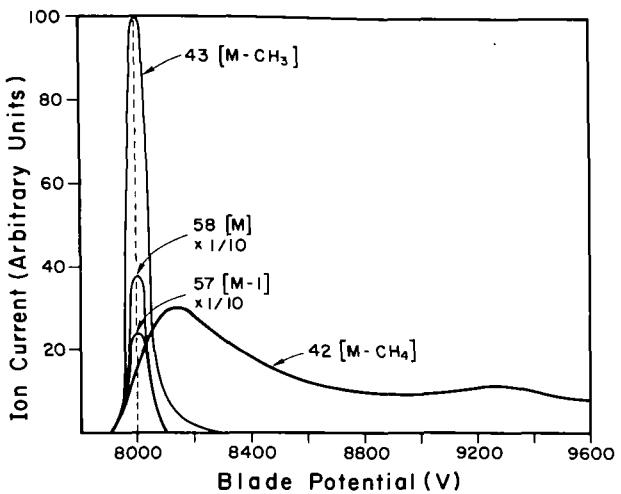

Fig. 2. Ion current vs. blade voltage curves for parent and fragment ions from isobutane.

m/e 58 ions, of course, must be formed at or extremely close to the blade surface, and the shape of the curve for this ion reflects this fact. The m/e 57 curve has the same shape, suggesting that its formation also occurs on or very near the surface. Once the blade potential is increased above about 8100 V, the fragment ions observed must be due to low field gas phase unimolecular decompositions. Portions of the curves for both m/e 42 and 43 fall into this category. The small peak in the m/e 42 curve at about 9300 V represents decompositions occurring in region II. Fig. 3 presents the data for m/e 42 and 43 converted to ion current vs. time. These data only go up to 10^{-9} sec, but the region II, III and IV data (up to 10^{-5} sec) all show the presence of m/e 42, but not m/e 43.

From these results we infer that the loss of methane is a low activation energy, low frequency factor process, as compared to the loss of methyl. Thus the most energetic parent ions can react rapidly to lose methyl, while the less energetic ions must take the slower, lower activation energy path to lose methane.

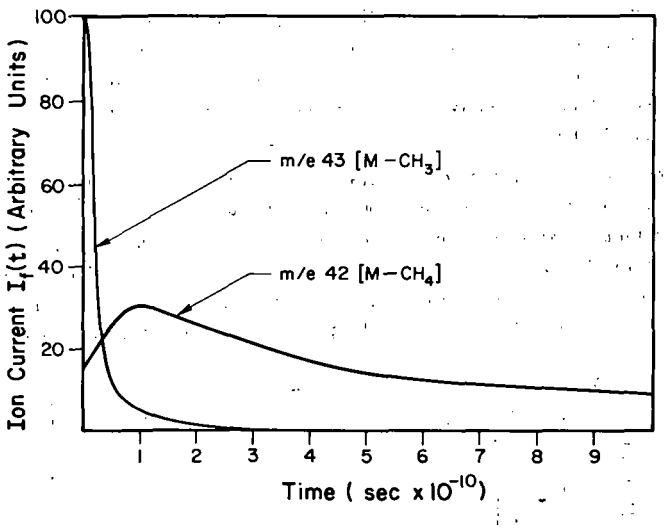

Fig. 3. Curve of ion current vs. time for m/e 42 and 43 ions from isobutane.

Similar experiments were performed on two deuterated analogs of isobutane, $(CD_3)_3CH$ and $(CH_3)_3CD$. The results showed that the loss of methyl was preceded by some 1,2 H/D exchange, but that the loss of methane was not. The results are particularly interesting because they imply that only the more energetic parent ions, those which lose methyl, have enough energy to induce 1,2 H/D exchange. This conclusion is in contrast to results observed with ketones (11) and unsaturated hydrocarbons (5), and suggests that the H/D exchange process which operates in alkanes may be of a different character than that which is operative for other classes of compounds. Further work on this problem is in progress.

REFERENCES

1. H. D. Beckey, Z. Naturforsch. 16a, 505 (1961).
2. H. D. Beckey, Field Ionization Mass Spectrometry, Pergamon Press, New York, 1971, and references cited therein.
3. E. M. Chait and F. G. Kitson, Org. Mass Spectrom. 3, 533 (1970).
4. P. J. Derrick and A. J. B. Robertson, Proc. Roy. Soc. London A 324, 491 (1971).
5. P. J. Derrick, A. M. Falick and A. L. Burlingame, J. Amer. Chem. Soc. 94, 6794 (1972).
6. P. J. Derrick, A. M. Falick and A. L. Burlingame, ibid. 95, 437 (1973).
7. J.-P. Pfeifer, A. M. Falick and A. L. Burlingame, Int. J. Mass Spectrom. Ion. Phys., in press.
8. P. Schultze, W. J. Richter and A. L. Burlingame, 17th Ann. Conf. Mass Spectrom. and Allied Topics, Dallas, 1969, Paper No. 168.
9. P. Schultze and A. L. Burlingame, J. Chem. Phys. 49, 4870 (1968).
10. L. P. Hills and J. H. Futrell, Org. Mass Spectrom. 5, 1019 (1971).
11. P. J. Derrick, A. M. Falick, S. Lewis and A. L. Burlingame, ibid., in press.

Collisional Activation Spectra. P. F. BENTE, III, K. LEVSEN, T. WACHS, J. WINKLER, and F. W. MCLAFFERTY, Dept. of Chem., Cornell Univ., Ithaca, N.Y. 14850.

Collision of an ion passing through a field-free drift region of a mass spectrometer with an atom or molecule can convert part of the ion's translational energy into internal energy. If this energy is sufficient to cause decomposition of the ion, the products can be measured with the same methods used for products from unimolecular metastable ion decompositions. The observed decompositions are similar to those found in electron-impact mass spectra; however, the relative abundances of product ions from higher energy processes are independent of the original internal energy of the decomposing ion. This makes CA spectra uniquely useful for ion structure characterization, as will be illustrated by a variety of examples. Operation of a reversed-geometry double-focusing mass spectrometer under computer feedback control allows automatic collection of CA spectral data for each peak in the mass spectrum.

This work is reported in detail in the following papers:

1. F. W. McLafferty, P. F. Bente, III, R. Kornfeld, S.-C. Tsai, and I. Howe, J. Amer. Chem. Soc., 95, 2120 (1973).

2. F. W. McLafferty, R. Kornfeld, W. F. Haddon, I. Sakai, K. Levsen, P. F. Bente, III, S.-C. Tsai, and H. D. R. Schuddemage, J. Amer. Chem. Soc., June (1973).

3. F. W. McLafferty and I. Sakai, Org. Mass Spectrom., accepted.

4. K. Levsen, H.-K. Wipf, and F. W. McLafferty, Org. Mass Spectrom., accepted.

5. T. Wachs, P. F. Bente, III, and F. W. McLafferty, Int. J. Mass Spectrom. Ion Phys., 9, 333 (1972).

INTERNAL ENERGY DISTRIBUTIONS AND THE FRAGMENTATION OF GASEOUS ORGANIC IONS. DISSOCIATION OF IONS PRODUCED BY ELECTRON IMPACT ON 1-(4-METHOXYPHENYL)-2-PHENYLETHANE-1,2-DIONE.

S. E. Scheppele, R. K. Mitchum, and J. H. Draeger
Department of Chemistry, Oklahoma State University
Stillwater, Oklahoma, 74074

K. F. Kinneberg
Department of Biochemistry, Oklahoma State University
Stillwater, Oklahoma, 74074

G. G. Meisels and R. H. Emmel
Department of Chemistry, University of Houston
Houston, Texas, 77002

Cleavage of the C-1--C-2 bond in the molecular ion of 1-(4-methoxyphenyl)-2-phenylethane-1,2-dione (I), *m/e* 240, produces either the benzoyl ion, *m/e* 105, or the 4-methoxybenzoyl ion, *m/e* 135. The principal pathways for fragmentation of these ions are as follows: loss of CO from *m/e* 105 forming the *m/e* 77 ion, and loss of H_2CO from *m/e* 135 forming the ion of mass 107, which then fragments with loss of CO producing the 77 ion. Since these ions account for *ca* 87 and 99 percent of the total ion abundance in the 70 and 20 eV mass spectra, respectively, other fragmentation reactions having higher energy requirements were not investigated.

The fragmentation mechanism has been investigated by determining internal energy distribution functions. The standard deviations associated with the experimental dI/dE data have been computed from the shot noise associated with the ion beam. These standard deviations were used to compute standard deviations in the second deviative (SDIE) curves obtained by numerical differentiation of the first deviative curves.

The appearance potentials are consistent with the formation of the benzoyl and 4-methoxybenzoyl radicals accompanying the production of the 135 and 105 ions respectively.

Calculation of the variation in the ratio of rate constants (RR) for formation of *m/e* 105 and *m/e* 135 requires knowledge of the relative contributions of CO loss from *m/e* 105 and *m/e* 107 to the area under the SDIE curve for *m/e* 77. Study of 1-(4-methoxyphenyl)-2-(phenyl-$\underline{d}_5$)ethane-1,2-dione (II) avoids this problem because the C_6D_5CO and C_6D_5 ions have *m/e* values of 110 and 82 respectively. Preliminary data on II indicate that RR increases in a smooth fashion with increasing internal energy of the molecular ion up to at least 6 eV of internal energy.

Based upon the preliminary data for II, the agreement between the 70 eV ion intensities and those calculated from the energy deposition functions is excellent for *m/e* 245 (molecular), 135, and 77; the agreement is reasonable for *m/e* 110 and poor for *m/e* 82. These results and those for I suggest that linear or essentially linear threshold laws obtain except for the C_6H_5 ion formed from the benzoyl ion.

A paper will be submitted for publication in *J. Amer. Chem. Soc.*

Modern Magnetic Mass Spectrometer Design

CHARLES W. HULL, Du Pont Instruments, Monrovia, Calif., 91016

New techniques for the design and construction of magnetic mass spectrometers have been developed over the last few years. The early problems associated with calculating ion trajectories in fringing fields have been overcome with extensive mathematical treatment. The now classical second order aberration theory has been largely replaced with more accurate and useful digital computer ray tracing techniques. Finally, it is now possible to make small, high flux density magnetic fields whose flux distribution is independent of flux density. The fortunate coincidence of these three developments has allowed us to produce high performance magnetic mass spectrometers which are lower cost and smaller than their predecessors. This has extended their adaptability and usefulness to the chemical laboratory.

A New Analytical Mass Spectrometer with an Atmospheric Pressure Ion Source

D. I. Carroll, I. Dzidic, R. N. Stillwell, M. G. Horning and E. C. Horning

Institute for Lipid Research
Baylor College of Medicine
Houston, Texas 77025

INTRODUCTION

During the last year at Baylor College of Medicine we have developed and are currently testing a new type of analytical mass spectrometer using an atmospheric pressure ion source. A description of the ion molecule reactions occurring in such a high pressure ion source, and the results of our preliminary study have recently been published (1). In this presentation, details of the instrumentation and the calculation of expected minimum detection limits will be described along with several examples of experimental results.

Apparatus. A drawing of the inlet system and source is shown in Figure 1.

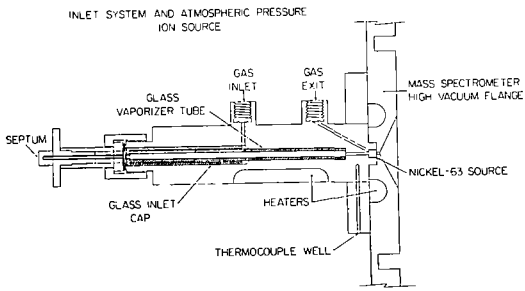

Figure 1

This source differs appreciably from the one described previously in that no provision is made for ion drift fields. This results in a large reduction in clearing time and a great increase in sensitivity. The instrument is separated into two pressure regions. The inlet system and source are at atmospheric pressure. Biologic and reference samples are injected, in common organic solvents such as benzene or dichloromethane, into the glass vaporizer section. This portion of the source is entirely similar to a standard GC inlet system. The sample and solvent vapor then enter the ionization source. Ionization of the solvent vapor and sample are achieved using a nickel 63 beta source of 0.75 mC activity. This source is approximately one-twentieth of the activity of a standard electron capture source. A sample of the resulting ions and neutral molecules in the source is conducted into the mass spectrometer region by a 25 micron pinhole aperture. The ions are then focussed into the quadrupole rod structure by a series of ion lenses. The ions are detected by a Bendix Spiraltron electron multiplier and counted using pulse counting techniques. A conventional EI source is incorporated into the lens structure for calibration purposes. Data acquisition and display is accomplished using a PDP-8E mini-computer.

The source cavity dimensions shown in Figure 1 are 1/8 inch diameter by 1/8 inch deep giving a total active volume of 25 μl. An insulating cover surrounds the inlet system and flanges to maintain thermal stability. Nitrogen gas at a flow of 10 cc/min is used as the carrier gas. The inlet and source temperature is maintained at 200°C.

Source Calculations. The ion density in the source is given by:

$$\frac{dN}{dt} = -K_1 N_0^2 + K_2 P \qquad (1)$$

where N_0 is the total ion density, K_1 the recombination rate constant, and K_2P the ion production rate in the source. Typically, for ion-electron, or for ion-ion dissociative recombination, the recombination rate constant, K_1, will be 10^{-6} cm^3 sec^{-1} ion^{-1}. The ion production rate, K_2P, was derived from the measured saturation current of the source, 1.4×10^{-10} amperes, and the source volume of 25×10^{-3} cm^3, as 3.5×10^{10} ions $cm^{-3} sec^{-1}$. Solving equation one for the steady state value of N_0 yields 1.9×10^8 ions cm^{-3} as the calculated ion density in the source. This calculated value agrees well with values derived experimentally, using the aperture conductance and the measured saturation current at the first ion lens in the mass spectrometer.

The lower detection limit, and sensitivity of the source is determined primarily by the ion lifetimes in the source. Typical values for conventional CI sources are on the order of 10-30 μseconds.

The ion lifetimes in this source are determined mainly by recombination. Under these conditions the ion lifetimes are inversely proportional to the product of the ion density and the recombination rate constant:

$$T = \frac{1}{K_1 N}$$

Using the previously calculated values of N and K_1 the ion lifetimes in this source are found to be about 5 milliseconds. Notice that the ion lifetimes are inversely proportional to the ion density in the source. Thus increasing the ion densities will actually decrease the source sensitivity. The ion densities used in this source appear to be the best compromise between signal level and sensitivity.

Lower Detection Limits. The equation determining the source response under these conditions is:

$$\frac{dN_s}{dt} = -K_1 N_s N_0 + K_3 N S$$

The loss term is the product of the recombination rate constant, K_1, the total ion density, N_0, and the sample ion density N_s. The production rate is the product of the production rate constant K_3, the reactant ion density N and the sample molecular density S. The total ion density is here assumed equal to the sum of the sample ion density, N_s, and the reactant ion density N. The production rate constant is taken as 10^{-10} $cm^3 sec^{-1}$ $molecule^{-1}$ which is typical for charge transfer and proton transfer reactions. The sample molecular density of 4.8×10^9 cm^{-3} pgm^{-1} assumes that the sample material of molecular weight 124 is diluted by 1 cm^3 of sample vapor resulting from the vaporization and heating of a typical 2 μl injection volume. Under these conditions, the ratio of the sample ion density to the total ion density will be:

$$\frac{Ns}{N0} = \frac{K_3 S}{K_1 N_0 + K_3 S} = 2.5 \times 10^{-3}$$

Since the measured total ion current at the detector is 10^6 cps this indicated that a one picogram injection should give a 2500 cps signal. The actual experimental results, for single ion monitoring, are shown in Figure 2. In this example, the material is 2,6-dimethyl-γ-pyrone with a molecular weight of 124. The full scale count range is 10^3 cps. Thus a 1.2 picogram injection gives a nearly full scale response which is in very good agreement with the calculation. As shown, an injection of 150 femtograms is easily detectable. Other tests indicate that the response is linear to about 1 nanogram. Injection of as little as 30 femtograms give easily detectable signals, but the response is not linear at these low levels.

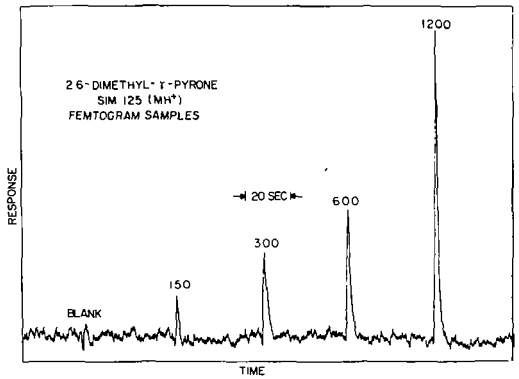

Figure 2

Biologic Samples. Scanned results with biologic samples are shown in Figures 3 and 4. In Figure 3 a urinary extract was made of ammonium carbonate saturated urine from a cigarette smoker taking the drug ethambutol therapeutically using benzene as the solvent. No derivatization or concentration was used. One microliter of the extract was injected to obtain this positive ion profile. The ion at mass 156 is a dimer ion due to the benzene solvent. The ion peaks at 162 and 163 are due to charge transfer (M^+) and proton transfer (MH^+) to nicotine. The ion peaks at 194 and 195 are due to charge and proton transfer to caffeine. The peak at mass 205 is due to proton transfer to the drug ethambutol. Based upon work with reference samples, the nicotine peaks represent an injection of approximately 1 nanogram.

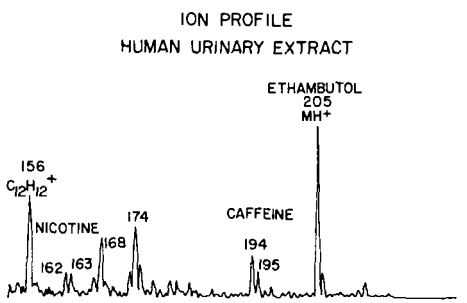

Figure 3

An example of a negative ion profile is shown in Figure 4. In this case a dichloromethane extract of 200 µl of plasma from a patient taking the anticonvulsant drugs phenobarbital and diphenylhydantoin was used. ^{13}C-diphenylhydantoin was added to the plasma prior to extraction as a standard. Again no derivatization or concentration was used and 1 µl of the extract, representing 20 nanoliters of original plasma was injected. The ions Cl^- and $Cl^-(CH_2Cl_2)$ are due to the solvent. The ion at 231 is due to proton abstraction of phenobarbital. The ions at 251 and 254 are due to proton abstraction of diphenylhydantoin and the ^{13}C standard. The ^{13}C peak at 254 represents 480 picograms of injected standard.

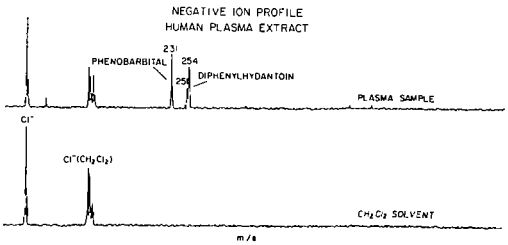

Figure 4

As illustrated by these few examples, the atmospheric pressure ion source mass spectrometer shows promise as a highly sensitive and useful tool in biologic studies. At this point a gas chromatograph is not used at the inlet which results in a great increase in operational speed. At a later date we plan to couple this source with a high resolution capillary column. The low flow rate requirements, lack of separator, and small active volume appear to make this source ideal for such an application.

References

1. E. C. Horning, M. G. Horning, D. I. Carroll, I. Dzidic and R. N. Stillwell, Anal. Chem., 45, 936 (1973).

THE DESIGN AND PERFORMANCE OF A VERSATILE, NEW, ULTRA-HIGH RESOLUTION MASS SPECTROMETER.

Authors : S. Evans, R. Graham.

AEI Scientific Apparatus Ltd, Manchester, England.

Introduction.

The techniques of high resolution mass spectrometry and accurate mass measurement have now become well established. For many applications a dynamic resolution of 10,000 is adequate; however, there is an increasing requirement for resolution in excess of 100,000. Sulphur containing compounds found in petroleum fractions can give rise to C_3 - SH_4 doublets requiring a resolution of 70,000 at m/e 200 to resolve. Similarly, C_{13} - CH and H_2 - D doublets at m/e 200 require a resolution of 45,000 and 130,000 respectively. Improvements in ion optics over the past decade have now made it possible to design an instrument, the AEI MS5074, to fulfil these requirements.

Basic Design and Performance.

Modified Nier-Johnson geometry (fig. 1) similar to that of the AEI MS9, but with an improved electrostatic analyser, has been used for the new instrument. Two hexapole lenses [1], one situated between the e.s.a. and magnet, and the other between the magnet and collector, are used to correct for image curvature effects and rotational misalignment of the image and collector defining slit. These lenses improve sensitivity, particularly at high resolution, thereby making it possible to carry out magnetic scans over wide mass ranges at resolutions up to 40,000. An electrostatic lens situated between the source and electrostatic analyser provides fine electrical control of the final image position. By varying the lens voltage as the magnet is scanned, optimum conditions can be maintained over the mass range covered.

The performance specification of the instrument is summarised in the table below.

Table 1.

1. Static Resolution : 150,000 on 10% valley definition.

2. Dynamic Performance :

Resolution.	Scan Rate (s/decade).	Sample Flow Rate (ng/s).
1,000	3*	0.3
3,000	3	1
10,000	10	1
30,000	100	10

3. Mass Measurement (Peak Matching)

Mass Difference	Mass Measurement Accuracy (ppm R.M.S.)
5%	0.3
10%	1.0
100%	5.0

* maximum scan rate 1.7 s/decade.

The sample flow rates quoted are based on obtaining a 20 to 1 intensity range with a signal to noise ratio of 10 to 1 on the smallest peak, over a mass range from m/e 600 to m/e 60.

The mass measurement accuracy using peak matching, specified as 0.3 ppm r.m.s. for 5% mass differences, results from the improved ion optical design of the instrument together with highly stable electronics and the use of a 7 digit, 0.1 ppm voltage divider. To obtain this accuracy using visual matching, it is necessary to operate at a resolution of 50,000, which is now practical due to the increased sensitivity at this resolution resulting from the use of hexapole lenses. The results of a typical experiment, using C_4Cl_6 as the "unknown" sample, are given in table 2. The four runs were carried out over a total period of 2 days, and it is apparent that the r.m.s. accuracy is well within the 0.3 ppm specified.

Table 2.

Peak Matching Accuracy. The conditions were : Sample C_4Cl_6, resolution 50,000 reference compound perfluorotributylamine.

Composition.	True Mass.	Corrected Errors (ppm)				Mean Error (ppm)	Mean Corrected Mass.
		Run 1	Run 2	Run 3	Run 4		
$C_4{}^{35}Cl_5$	222.844265	0.21	0.27	0.45	-0.1	0. 21	222.84422
$C_4{}^{35}Cl_4{}^{37}Cl$	224.841316	0.54	-0.24	-0.11	-0.06	0.03	224.84131
$C_4{}^{35}Cl_3{}^{37}Cl_2$	226.8383661	0.07	0.20	0.46	0.5	0.31	226.8383
$C_4{}^{35}Cl_2{}^{37}Cl_3$	228.8354164	0.27	0.19	1.00	-0.04	0.36	228.83533
$C_4{}^{35}Cl\ {}^{37}Cl_4$	230.8324667	-0.33		0.39	0.08	0.05	230.83246

R.M.S. (of mean) ± 0.23 ppm.

To achieve resolution and mass measurement accuracies of this order it has been necessary to design a suitably rigid structure for the basic frame. As a result of trial experiments, the basic frame is constructed from 12" x 8" box section girders, free from resonances in the critical range for floor-borne vibrations of 10-15Hz, which can be supported directly on isolating mounts where floor vibration levels are high. Rotary pumps are mounted remote from this main frame to eliminate induced vibrations.

The ultimate resolution is also critically dependent on the precision and control of the collector defining slit. Here, this slit uses parallel action swinging arms which require a greater linear movement of the actuator for small openings than for larger openings.

In addition to diffusion pumps using polyphenyl ether, together with peltier baffles, a 25 l/s ion pump is positioned near the collector to reduce collision scattering of the ion beam and hence improve peak profiles.

A Daly metastable detector [2] is used as the standard detector, giving very stable high gain and low noise in addition to its facilities for examining metastable peaks. The layout of the instrument has been designed for maximum operator convenience by arranging all the major functional tube unit controls, with one or two minor exceptions, within easy reach of an operator seated at the control console. A desk top is positioned under the source, on which a variety of inlet systems can be mounted, grouped conveniently around the source and fully integrated with the instrument. A gas chromatograph interface, consisting of a separator and its associated valves and pumping lines within a simple oven, mounts directly to one of the source inlet ports. A gas chromatograph mounted on the desk top mates directly with this interface.

Scanning and Display Facilities

(i) Display

The built-in oscilloscope display unit can be used for peak matching, spectrum display, setting resolution both statically and dynamically, and checking ion beam beam stability.

When displaying magnet scans the oscilloscope time base is proportional to the square of the magnet current, thus providing a linear mass display across the oscilloscope screen. The same signal can be used to drive the UV recorder if linear mass chart display is required. Limited portions of the magnet scan can be displayed on the screen, minimum mass display being 20 a.m.u. per sweep. This facility enables the presence of a sample in the source to be observed before recording the spectra. For example if it is intended to introduce cholesterol, the magnet could be set to scan repetitively between mass 500 and mass 50, with the spectrum display starting at mass 400 and ending at mass 380. Observation of the intensity of the parent peak of cholesterol at mass 386 is then quite simple and when the desired intensity is reached, the entire spectrum can be readily recorded using any of the output facilities Automatic single peak triggering is also provided to enable dynamic resolution to be checked at several points in a scan.

The maximum scan in the peak switching mode corresponds to a mass range of 40,000 ppm. This corresponds to a 10 mass unit display at mass 250 which, in conjunction with a reference compound such as p.f.k. enables unknown peaks to be identified very rapidly. Once an unknown peak has been identified, it can be moved to the centre of the screen using the magnet controls and then expanded using the peak switch controls to display a single peak only. The instrument can also be tuned in this way to an expected mass, for example when looking for the characteristic peak of a particular drug metabolite. As the oscilloscope sweep is calibrated directly in ppm, it can be used for the measurement of resolution or for estimating mass.

(ii) Matrix Control

The number of parameters to be set up on an instrument of this type is necessarily large, and for research applications, it is desirable that all its operating parameters should be under manual control. Conversely, once a particular set of parameters has been determined for a specified application, it is equally desirable that the number of manual adjustments be reduced to a minimum. To satisfy these conflicting requirements, a programme switch has been included. With this switch in position 0, all parameters are under manual control. When in one of the remaining 10 positions, the manual control of 14 parameters is overridden by a matrix, which preselects these functions. Thus most of the conditions required for a particular mode of operation can be re-obtained at any time by operation of a single switch.

(iii) Data Processing

Outputs suitable for direct connection on line to a computer, and in logarithmic form for connection to an analogue tape recorder, together with all the necessary control signals, are provided by the built-in computer interface.

Metastable Scanning.

In addition to all the conventional features of a high resolution instrument, comprehensive metastable scanning facilities are included. Metastable transitions can be observed in all three field-free regions F1, F2 and F3 (fig. 2) using 5 distinct forms of scan. Two of these use facilities of the Daly metastable detector (2) to examine transitions occurring in regions F2 and F3.

Fig. 3 shows parts of 2 successive 3 second/decade magnetic scans of a mixture of Methyl Hexyl Ketone and perfluorotributylamine with the detector in normal and metastable modes, which illustrate the type of information which can be obtained. The sample parent peak at m/e 128 is of similar height to the m/e 131 peak from perfluorotributylamine in the normal scan, but in the metastable scan, the m/e 128 is considerably larger than m/e 131. This indicates that the m/e 128 peak is decomposing in region F3, the metastable component being obscured in the normal spectrum. At m/e 100, a broad metastable is revealed in the metastable scan, which arises from the same reaction occurring in region F2, and identifies a loss of CH_3

from m/e 128 to give m/e 113. The m/e 113 peak itself can be seen to be decomposing further in region F3.

By tuning the instrument to m/e 113 and then using an energy rejection scan, the reaction occurring could be identified.

Reactions in region F1 can be studied in three ways: (i) The electrostatic analyser voltage can be scanned, with the accelerating voltage V_a constant, to produce an Initial Kinetic Energy (IKE) spectrum. (ii) The accelerating voltage V_a can be scanned with the e.s.a. voltage constant to produce a Barber-Elliott precursor spectrum for a daughter ion. (iii) The accelerating voltage V_a can be scanned at the same time as the e.s.a. voltage kV_a such that V_a^2 is proportional to kV_a. This is a new form of scan which produces a daughter ion spectrum from a precursor ion, over a mass range of 2:1.

Sequential decompositions can be studied by using two of these modes consecutively. Thus by tuning the instrument, at low accelerating voltage, to a peak m_2 and then using the accelerating voltage scan, a spectrum is produced showing the precursor ions m_{11}, m_{12}, etc, of the peak m_2. A combined scan (V_a^2 proportional to kV_a) from the same peak m_2 will produce a spectrum of the daughter ions m_{31}, m_{32}, etc. formed from m_2.

References.

(1) A.J.H. Boerboom. Int. J. Mass Spectrom. Ion Phys., 8 (1972) 475-492.

(2) N.R. Daly, A. McCormack, R.E. Powell, R. Hayes. Int. J. Mass Spectrom. Ion Phys., 11 (1973) 255-276.

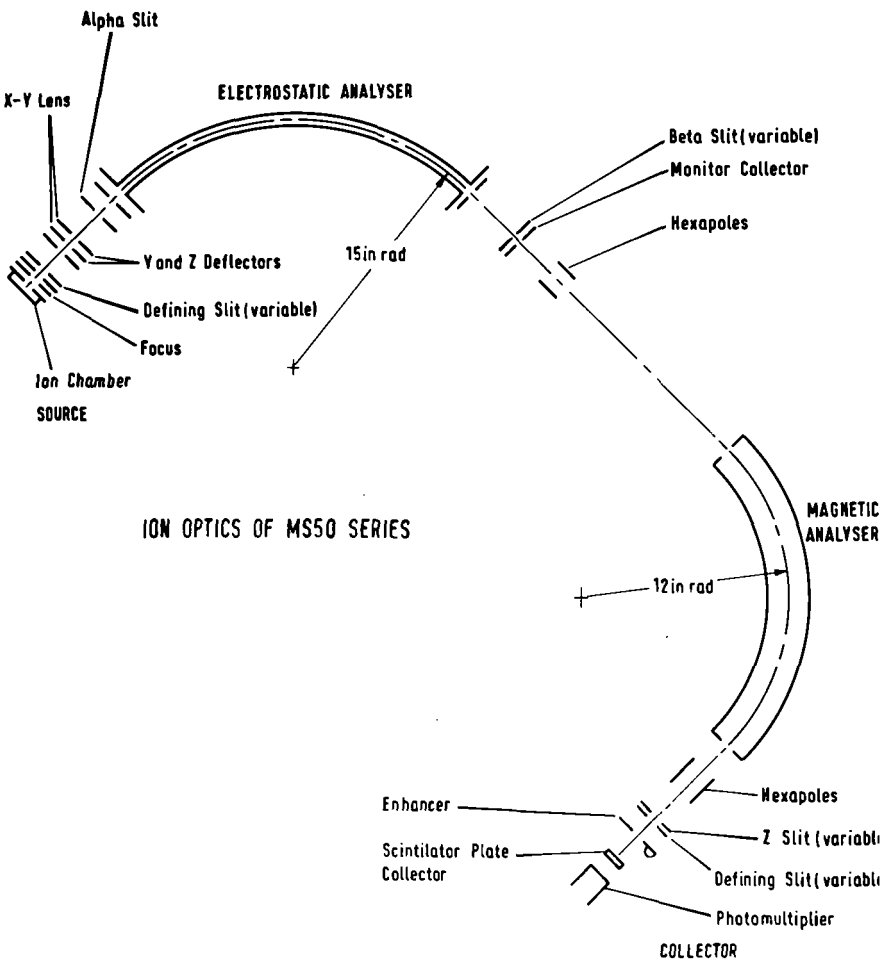
Alpha Slit
X-Y Lens
ELECTROSTATIC ANALYSER
Beta Slit(variable)
Monitor Collector
Hexapoles
Y and Z Deflectors
15in rad
Defining Slit(variable)
Focus
Ion Chamber
SOURCE
ION OPTICS OF MS50 SERIES
MAGNETIC
ANALYSER
12in rad
Enhancer
Hexapoles
Scintilator Plate
Collector
Z Slit (variabl
Defining Slit(variabl
Photomultiplier
COLLECTOR

Fig. 1.

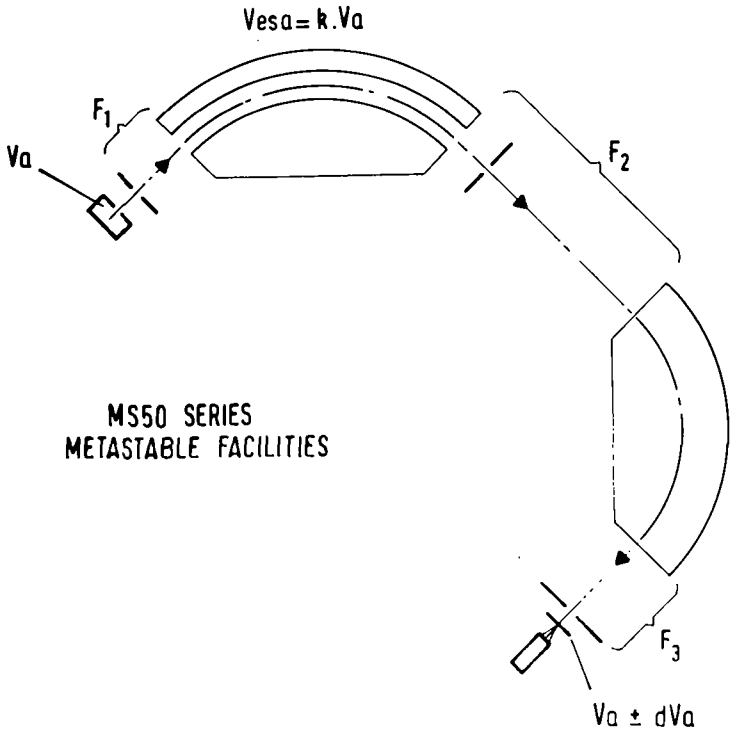

Mode 1 Va_{Scan} → F_1 → M_1 spectra from M_2

Mode 2 $Vesa_{Scan}$ → F_1 → I.K.E. spectra

Mode 3 $Va/Vesa_{Scan}$ → F_1 → M_2 spectra from M_1

Mode 4 V_{Scint} → F_2 F_3 → M_2 spectra from M_1

M^* enhancement

Fig. 2.

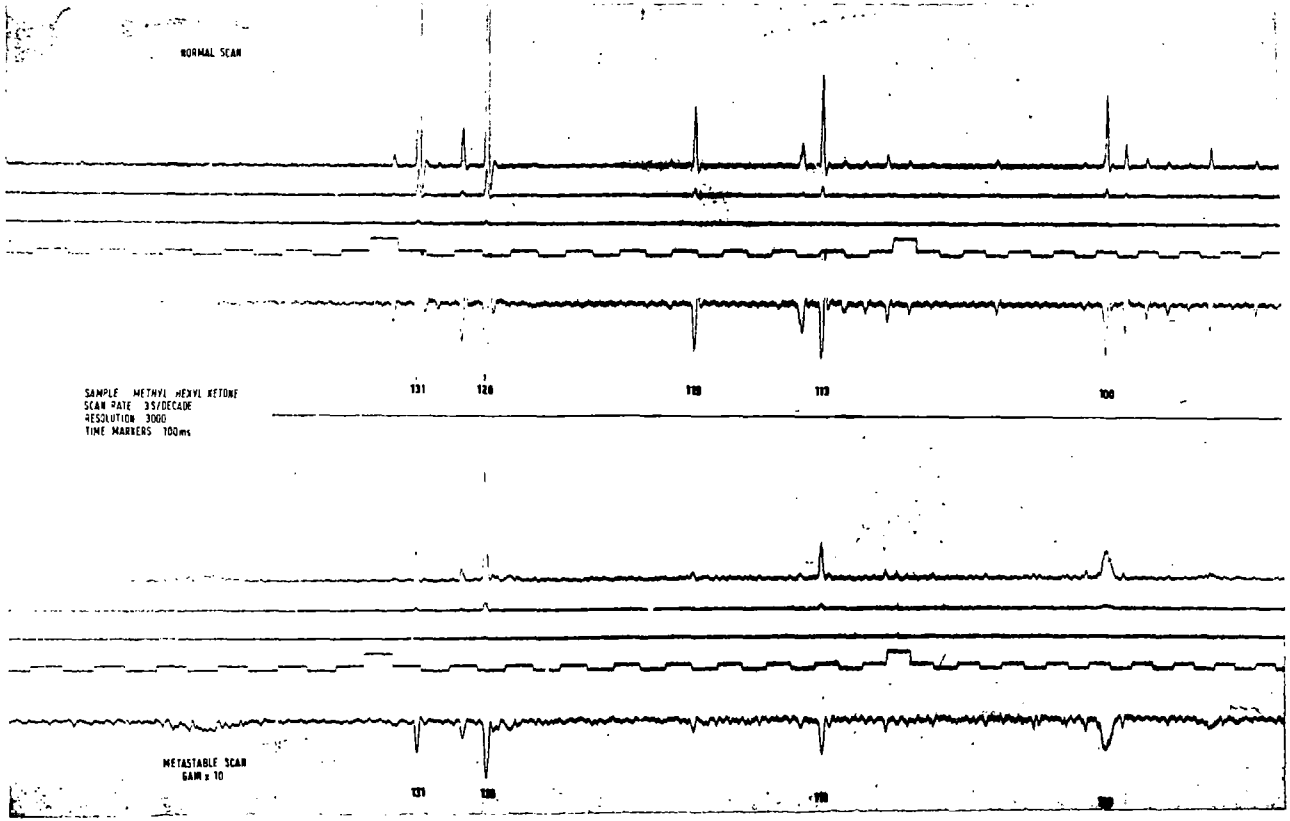

Fig. 3. Normal and Metastable Scans of Methyl Hexyl Ketone.

G.C.-C.I.-M.S.–SOURCE DESIGN

W. Kruger, N. Kuypers, J. Michnowicz

Hewlett-Packard
Scientific Instr. Div., Palo Alto, Ca. 94304

Since the introduction of chemical ionization mass spectrometry (CIMS) by Professors Field and Munson in 1965, chemical ionization (CI) has proven itself to be a valuable analytical technique to the mass spectroscopist. CI produces very simple spectra which are easier to interpret in most cases than electron ionization spectra. Chemical ionization is also as sensitive, if not more sensitive, than electron ionization. The spectra produced are complimentary in nature to electron ionization and often supply information not found in electron ionization spectra. There also is a relatively large M + H ion intensity in most CI spectra which aids the mass spectroscopist in identification of the molecular ion, often the most sought after piece of information from a mass spectrum.

CI, however, is not without some disadvantages. In its initial stages chemical ionization was thought to produce spectra that were too simple and therefore, produced very little information for structural elucidation. This drawback, however, has been allieviated in recent times by the use of other reactant gases than the traditional methane or isobutane. Such gases as hydrogen, which is a stronger proton donating agent than methane, or charge exchange gases like helium, argon, or nitrogen can produce spectra with extensive fragmentation.

Two other disadvantages claimed for chemical ionization result from the necessary changes in source design to perform chemical ionization. These changes usually result in a CI source which is very insensitive if used for electron ionization or one in which tight source effects are very pronounced.

The insensitivity is easily explained by considering the total number of electrons entering and ions leaving the CI source when used in the electron impact mode. In comparison to a standard electron ionization source, the electron entrance and ion exit slits are greatly reduced. It is, therefore, quite reasonable to expect the total number of ions in a CI source to be much less than those produced in an EI source.

In the past, the usual way to correct this problem has been to increase the sample concentration, produce a larger sample pressure in the ion source and therefore, get an effective larger number of ions being produced from the CI source. This, however, has led to the other disadvantage of a CI source when used in the electron impact configuration, that is, the tight source effect. If the sample concentration in a CI source used for electron impact is increased in an effort to get a stronger signal, the pressure can become so large that chemical ionization reactions can occur between the sample molecules. This becomes a serious problem if computer interpretation of EI spectra produced in a CI source is desired. Anamalous peaks which can occur may cause serious difficulties with computer interpretation or computer searches.

A CI–EI source for the HP 5930 mass spectrometer which solves these difficulties of chemical ionzation has been constructed. The source consists of two separate, distinct sources; one which is designed especially for chemical ionization and one which is designed especially for electron ionization. Changing from one configuration to the other configuration takes less than one minute. The top of Figure 1 shows the chemical ionization configuration. It consists of a selector level, bellows, filament, sample inlets, and all other normal components found in a CI source. The electron entrance and ion exit slits are designed especially for CI operation. To change from the chemical ionization to electron impact configuration, all that is necessary is to change the selector level from the CI to the EI position. This moves the sliding bellows which contains the

CI source to the left, and replaces the CI source with one designed especially for electron impact work. All necessary electrical contacts are also changed when this is done. Thus, in less than a minute, the optimum CI source has been switched to an optimum EI source without breaking vacuum.

In evaluating this source and vacuum system design two criteria were used: resolution and sensitivity. If the system is adequately pumped, there should be no dependence of resolution with pressure. Figure 2 shows several scans of the 575 ion produced in perfluorotributylamine. The first scan was produced in the electron impact confirguration at low pressure, approximately 1×10^{-6} Torr. There is almost baseline resolution between the 575 and 576 peaks. The next two scans represent CI spectra taken at the indicated ion source pressure, 0.55 Torr and 1.40 Torr. As is seen, the resolution has remained constant and indicates that the pumping system is more than adequate.

Typical CI sensitivites are shown in Figure 3. 10 ng of barbital were injected on a gc column and a full spectrum was scanned at 100 amu/sec. The signal to noise ratio of the M + H ion (185) is approximately 400:1. The peaks above 200 amu are primarily column bleed, plus the $M + C_2H_5^+$ and $M + C_3H_5^+$ addition ions.

One of the goals in producing this mass spectrometer was to maintain the same EI sensitivity as the standard HP 5930A mass spectrometer. The sensitivity specifications for this standard electron impact mass spectrometer include a 100:1 signal to noise ratio at the parent ion peak for a 10 ng sample of methyl stearate introduced by the direct insertion probe. Figure 4 shows a probe sample of methyl stearate with our dual CI-EI source used in the EI configuration. The signal to noise ratio of the 298 ion is approximately 200:1. Thus, the goal of producing a dual CI-EI source with excellent CI performance and EI sensitivity as good as a standard electron impact mass spectrometer has been accomplished.

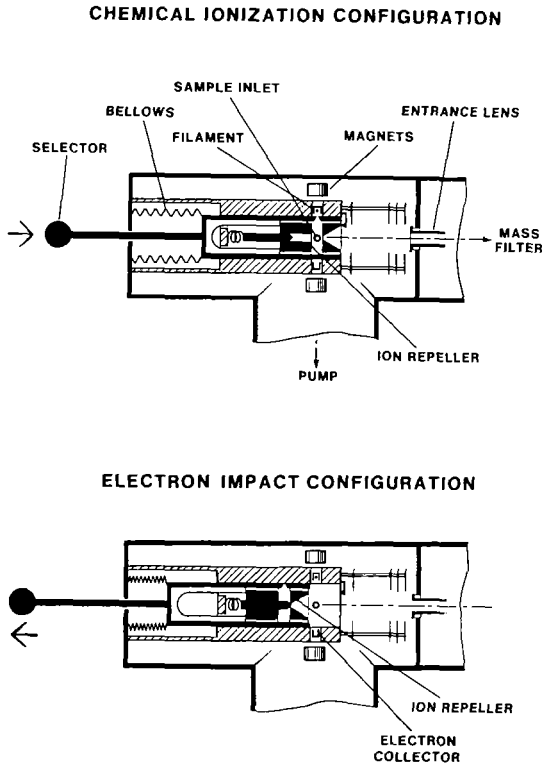

Figure 1

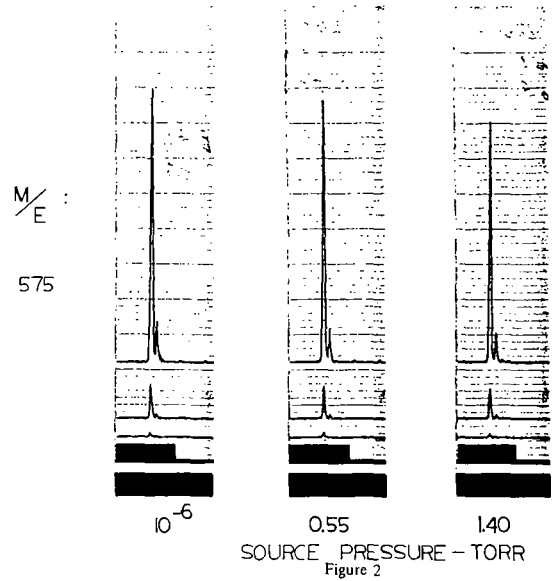

Figure 2

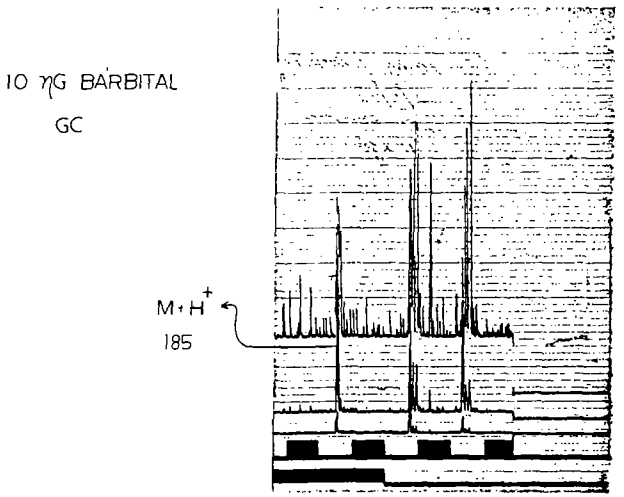

Figure 3

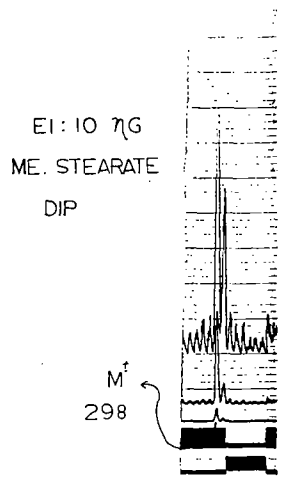

Figure 4

A NEW MASS SPECTROMETER FOR ISOTOPIC ANALYSIS

N. C. Fenner, M. C. Jackson, R. E. Powell, W. A. P. Young

A.W.R.E., Aldermaston, Berkshire, England

The instrument (which is designated the MSF at Aldermaston*) is a single stage machine with 30 cms radius and 90° magnetic deflection. It has been built to replace the ageing spectrometers at A.W.R.E. that have been in use for about 15 years. The design brings together several items that have been used in other A.W.R.E. instruments and they combine to produce a spectrometer with greatly improved performance.

Ion Source

A batch loading system of sample handling is employed which avoids the vacuum problems of a sliding seal. Six filaments are loaded into a turret that is removed completely each time and replaced by a freshly loaded batch. The 1st drawing out plate (DOP) is part of the turret and is electrolytically cleaned each time, and the hemisphere in which the turret sits is wiped clean. The connections are made through silver alloy contacts on wiping arms backed by phosphor bronze leaf springs. The accelerating-focussing system is a conventional Nier type with two DOPs, D plates and two collimating slits.

The collector is a conventional scintillation detector and a Faraday bucket is available for direct ion collection. The layout enables direct collection to be made by simply earthing the electrode of the detector. In front of the collection system is a pair of grids (one earthed, the other near EHT volts) which reject ions that have lost energy in the flight path from the source. This improves the abundance sensitivity by up to a factor of 10. It also has the property of spreading the slit image after passing through the grids, so giving a lower level of bombardment to larger areas of the electrode and scintillator. This increases the life of the scintillator, and removes the effect of any inhomogeneities in the electrode or the scintillator and so improves the flatness of the peak tops.

The collector slit is adjustable, by a proving ring system, from zero to 1.5 mm which may be set to within ± 5 μm by a calibrated control. A small degree of rotation is provided by a simple system of adjustment using two screws which rotates the whole detector body ± 0.5° and slightly flexes the flight tube. (Large adjustments of ± 5° are made by reboltîng the body to the flight tube flange). This method avoids interaction with the slit width mechanism and does not change the position that the ions strike the detector electrode. It is also cheap and fully bakeable.

Electronics

The units used in the spectrometer have for the most part been designed and built at A.W.R.E. The details of their design will not be described here but the performance of each unit is specified.

The magnet unit can be varied to cover masses 2 to 300 with an HT of 8 kV. This is a variation of 100 mA to 5 A into a magnet load of 10 H and 8 Ω. The stability is 2 parts in 10^5 over a period of 30 minutes. The output can be adjusted manually or controlled by an external programming voltage of 0 to 2.5 V. This external voltage is supplied by a sweep unit that provides a double ramp. The unit will scan 1 mass width in 1 minute at its minimum and can scan up to 10% of the maximum field. The total scan time can vary from 15 seconds to 25 minutes.

The filament unit provides up to 7 A stabilised directly on the filament current and floats at the source potential. The drift has been measured at less than 2 parts in 10^5 over 30 minutes.

The accelerating volts are provided by a FLUKE model 410 B. The output is fed to a resistor chain from which are taken variable potentials for the filament, the DOPs, the D plates and the retardation filter.

The output from the photomultiplier is fed to a solid state electrometer amplifier type Philbrick No. 1702 to provide a virtual earth at the photomultiplier output. A wide dynamic range of voltages is produced and so an auto ranging dvm is required as the next step. The model chosen was the Dana Electronics 4800. As the field is scanned the dvm is set to take readings at the rate of 2 per second. This output is punched

* A spectrometer of similar design is manufactured by V.G. Micromass Ltd., Winsford, Lancs. with the name 'Aldermaston Micromass 30'.

onto paper tape using a Tally 120 and the tape is then processed by the IBM 370 computer at A.W.R.E. An output is also fed to a chart recorder to provide a permanent record of the run and an alternative method of measurement when required. A Cary Model 31 vibrating reed electrometer is used to measure the current from the Faraday bucket.

Performance Figures

The ultimate resolution of the spectrometer depends on the spread of the ion beam; the following figures were obtained:- at 10% intensity, 0.02 mm; at 1% intensity, 0.10 mm, and at 0.1% intensity 0.15 mm spread.

The abundance sensitivity was measured using the U 235 peak of an enriched uranium sample having peaks at masses 234 and 236. This means that the tails of the 235 peak have to be interpolated but using this method it was not necessary to record the top of the 235 peak and the changes in ion beam during the measurement were overcome. The measurements (9×10^{-7} on the high mass side and 3×10^{-6} on the low mass side) were made with a collector slit of 0.55 mm, a resolution of 450, which gives a good flat topped peak. When the slit was reduced to 0.20 mm the values were reduced to 6×10^{-7} and 9×10^{-7} for the high and low mass side respectively, but under these conditions the flat peak top is very small. The overall sensitivity using 5×10^{-9} gm of uranium was 9×10^{-5} ions per atom for a triple filament, and 1.5×10^{-4} ions per atom for a benzene treated sample in a rhenium boat filament. The electronic noise including the data handling system is about one ion in two seconds (10^{-19} Amps).

The degree of contamination of one sample by others loaded in the same turret was measured in an experiment in which two uranium samples and three blanks were loaded together. The blanks were in fact loaded with a small quantity of plutonium for focusing purposes. The results can be summarised by saying that the contamination is less than 10^{-6} for an adjacent sample and less than 10^{-9} for an 'opposite' sample. The results for a lithium sample, which is notoriously easy to contaminate, were 10^{-3} and 10^{-8} respectively. The influence of one sample on the sample following it in the same position was measured as 1.3×10^{-9} using natural uranium. The peak shape produced by the spectrometer has a top that is flat to $\pm$ 0.5% of the peak height when using a collector slit of 0.5 mm.

Routine samples produce a beam of 10^{-13} A and therefore provide 5×10^{5} ions of a 1% abundant isotope from a 20 peak run. The smallest error possible ($1/\sqrt{n}$) is therefore 0.15% and when 12 standard samples were run, 3 approached this error. The between run standard deviation (68% confidence limit on one measurement) of this set was 0.36% and while well outside the theoretical limit is about the same as that on many instruments using larger samples. A standard sample having a ratio of 2 to 1 and a theoretical error of 0.11% gave a standard deviation of 0.13% from a set of 8 measurements. The machine bias for both these standards was 0.06% per mass.

To be published in Int. Jnl. of Mass Spectrometry and Ion Physics.

PERFORMANCE OF A NEW MASS SPECTROMETER FOR ISOTOPE RATIO DETERMINATIONS

L. F. Herzog
Nuclide Corporation
642 East College Avenue
State College, Pa. 16801

In 1940, Alfred Nier described a gas-analysis mass spectrometer with a "double collector" with which one could detect two ionic species simultaneously on separate collectors and thereby measure the ratio of their currents instantaneously. Since variations in beam intensity affect each isotopic species proportionately to its abundance, use of a double collector made it possible to achieve a substantial increase in the precision with which isotope ratios could be measured.

During World War II, development of this type of instrument continued in the Manhattan Project's heavy water and uranium hexafluoride production programs.

Just after the war, Harold Urey, who had participated in this wartime work, set up, at the University of Chicago, a research group to apply this technique to geochemical studies.

The analysis system was improved by the addition of a dual inlet system, which made it possible to switchover rapidly from the analysis of a standard to the analysis of an unknown, meanwhile keeping conditions in the ionization chamber, source, and analyzer scrupulously constant - except for any difference in pressure that might arise due to a difference in the relative abundance of the less abundant isotope of the element being studied.

The first slide shows the approximate ranges in nature of certain isotope ratios for the elements hydrogen, carbon, nitrogen, oxygen, and sulfur - the elements that have received the most study. These range from 6% for nitrogen 14/15 to over 50% for deuterium/protium.

While stable isotope geochemistry has developed rapidly, the study of similar variations in living organisms - plant and animal - has until now developed much more slowly. However, one important application, the use of isotopes of low natural abundance as tracers to study metabolic processes - did develop primarily in the life sciences, where it was initially applied (for example by David Rittenberg and colleagues) to studies of human metabolism where the use of radioactive tracers was contraindicated due to dosage considerations.

The classical isotope ratio-difference measurement instruments all used 6-inch radius, 60 degree deflection, direction-focusing magnetic analyzers. The 6-60-RMS, introduced by Nuclide Corporation in 1956, is the lineal descendant of these pioneering instruments, utilizing the same types of analyzer, double collector, dual inlet, and gas handling system.

Numerous improvements in circuitry and in vacuum technology have been made in the 6-60-RMS over the years. However, about two years ago we concluded that there was need for an instrument embodying all of the same basic principles, but having a smaller ion analyzer and somewhat relaxed performance capabilities, for use especially for the isotopic tracer studies, and also for studies of natural variations in hydrogen isotope abundances. Last year at this meeting Dr. D. J. Marshall described our new 3-60 "Sectorr" MS system, which has a 7.5 centimeter (3"), 60° ion analyzer, and in which we have combined the ion acceleration supply, source lens voltage supply, electron emission regulator, and two electrometers into a single component, termed the Master Electronic Control (MEC). Both the mass spectrometer tube and the "waste" line of the dual inlet are ion pumped; the dual gas handling system may be pumped either by ion pumps or diffusion pumps.

Today, I wish to describe the results of some performance tests of the variant of this new system that is intended to be used for ratio-difference studies, which we designate as Model 3-60-RMS/HD.

First, it may be useful to review certain features of these isotope ratio mass spectrometers, for the benefit of those in attendance who are not familiar with them. Slide 2 (not reproduced herein*) is a photograph of the dual gas-handling system used in both our 3-60 and 6-60 ratio instruments. It is made of pyrex glass. (We, and others, have also built metal systems, but we believe that for most laboratories, glass is the better choice, due to the availability of glassblowers.)

Slide 3, a sketch, shows how the dual gas handling system interfaces with the dual inlet system and how this interfaces with the mass spectrometer. The gases to be compared are stored in the two mercury "piston" equipped reservoirs. In practice one adjusts the intensities of the ion beams of the major isotopes of sample and standard to strict equality by raising and lowering the mercury. The samples flow from the mercury-piston reservoirs through fine capillary tubes of 0.004 to 0.007 inch I.D. and approx. 1 foot length into a pair of magnetically-operated glass valves. Flow through these tubes is viscous when the pressures in the reservoirs are in the normal range - 1 to 10 cm. The positions of the valves are switched simultaneously so that while one gas is flowing into the ion source, the other is flowing into a so-called "waste" line. At the next switching, their destinations are reversed. Each line also includes a constriction, which is used at the outset to adjust the flows through them to strict equality for equal reservoir pressures.

Slide 4 (not reproduced) shows the glass valves and the line leading into the ion source. There is an iron box around the valves to contain the magnetic fields of the solenoid valve actuators. The "waste" line 11 liter ion pump is partially hidden behind the valve enclosure; there is a valve ahead of it whose purpose is to adjust the flow through the waste line to equal that into the MS, so as to avoid pressure surges when switching. The photo also shows the 3-60 analyzer with its 25 lusec ion pump. The small magnet on the source is used for two purposes - to lengthen the paths of the ionizing electrons (to provide more collisions per electron), and to collimate the electron beam. Note also the small size of the 3-60 analyzer magnet. The paired EAH-300 preamplifiers are mounted on either side of the collector.

The dual inlet system and the ion analyzer are mounted on the top of the electronics console, as is shown in Slide 4 (not reproduced). The MEC-3 master electronic control is shown at the top left. The unique feature of the traditional dual collector mass spectrometers, the beam "balancing panel" with its precision decade resistances, is to the right of the recorder.

The type of double collector used for measuring hydrogen isotope ratios (designated "HD") is shown schematically in Slide 5. Because the mass of HD is a 50% greater than the mass of HH, separate Faraday cup collectors can be used for each mass. The mass 2 collector sits considerably ahead of the mass 3 collector in the tube, because the radius of the orbit described by ions of mass 2 in the magnet is 2.7 inches compared to 3.3 inches for mass 3. For studying N, S, C and O as the molecules N_2, SO_2 and CO_2, a different dual collector (type RMS) is used. In this, one of the collectors is a topless box that has an adjustable slit in its bottom plate, the other is a Faraday cup behind that slit. Almost always, the less-abundant species is focussed onto the slit and collected in the Faraday cup, while the other isotopic species are collected in the box, or multi-collector.

The ratio of the ion currents to the two collectors is measured by a classical "null" technique. A voltage proportional to the multi-collector current is developed by one electrometer. A fraction of this voltage, selected by switching resistors in the balance panel's precision voltage divider, is converted into a negative current, which is combined with the positive current reaching the single-species detector. The sum of these currents is converted to a voltage by a second electrometer, and this voltage is displayed on a recorder which has been set up so that the zero current "null" condition corresponds to the mid point of the chart. Slide 6 shows a typical trace for the case

*This and the other photographs referred to can be obtained if desired by writing to the author.

when the carbon 13/carbon 12 ratio is being determined using carbon dioxide, with mass 45 ($C^{13}O^{16}O^{16}$) in focus on the slit. The 100 millivolt full scale range was being used and the voltage divider was set at 0.2307 for the standard gas and at 0.2309 for the unknown - which in this case has a ratio so close to that of the standard that an offset was purposely introduced to make it easier to determine on the record when a valve switching occurred. The sensitivity of the measurement system is determined by changing the voltage divider setting by a known amount - in this case by 2 divisions, from 0.2307 to 0.2305 - about 0.1%; this shifted the trace about 5 divisions, that is, by 5 millivolts, downscale. This is equivalent to a minor-isotope intensity shift of 2.5×10^{-14} amperes. The trace separation could have been increased by shifting to a different range - for example 30 mv full scale - but the "noise" would have been increased proportionately. (In this example noise was about ± 0.4 mv, or 2×10^{-15} amps, RMS.) In practice, different operators select a range to use on the basis of personal preference; the choice has no apparent effect on precision. It should be mentioned that the indicated ratio is near 0.2 because the resistor that converts the mass 44 etc., signal into a voltage has a nominal value of 1×10^{10} ohms while the mass-45 current passes through a 2×10^{11} ohm resistor; hence the actual ratio is about 1/20th of the indicated ratio, or 0.01. This checks, since carbon-13 is a 1% isotope. The mass-44 beam intensity when this run was made was approx. 3×10^{-9} amperes, and the 45 beam intensity was about 3×10^{-11}A.

Since the essence of the dual-inlet dual-collector technique is that one measures differences in ratio, not absolute ratios, determining the absolute values of these high meg resistors is unnecessary - however one must be sure that their resistances do not change as a function of ion current or ambient temperature, during an analysis.

Slide 7 shows a ratio trace for oxygen, measured with mass 46, ($C^{12}O^{16}O^{18}$), in focus on the slit. Since the relative abundance of this molecule is smaller (the indicated ratio is about 0.08 with the same resistors), the 30 mv scale was used to record the traces. Slide 8 shows a sensitivity-calibration trace for this run. To calibrate the chart, the voltage divider setting was shifted by 4 parts in 819, or about 0.5%; this shifted the trace by 34 divisions. The sensitivity was therefore about 36 millivolts for a 1% ratio difference; this compares to 74 millivolts for a 1% difference for the mass 45 molecule. The noise is about the same ($\lesssim 0.5$ mv) although it looks larger here because it is being observed on the 30 mv scale.

Differences in isotope ratios are, of course, obtained by adding to the difference between the decade settings, the difference represented by the average distance between the recorder traces, after converting this into a per mil or percent value using the calibration data. But ratio differences can also be measured digitally, for example, by using an integrating digital ratiometer such as Nuclide's IR2A. The IR2A includes a pair of precision magnetic voltage-to-frequency converters which are linear to $\pm 0.01\%$ and are so mounted that their temperature coefficients tend to cancel. The digitizer samples and integrates the residual signals representing the less significant digits of the ratio for a preset time of up to two minutes (much longer than is possible with usual IDVMS) and then commands the glass valves to switch. The residual voltages are displayed on a 7-digit LED display. They can also be printed-out on a paper tape or punched tape suitable for entry into a computer.

Slide 9 shows the ratio residuals for the oxygen run just shown that were obtained digitally while they were simultaneously being recorded on the potentiometric recorder. Three readings were made on each sample before switching.

The actual oxygen 18/16 ratio difference between these samples was 0.245%. The operator obtained $0.2445\% \pm 0.0046\%$ by measuring average trace separations on the chart, while the integrating digital ratiometer gave $0.2480\% \pm 0.0035\%$ (the precision measure given is the standard deviation of the mean for a single determination). The precision obtained with the digital ratiometer was slightly better than that obtained by the classical technique of chart measurement in this instance.

Slide 10 shows a ratio difference run for nitrogen 29/28. Since the samples are atmospheric and tank nitrogen, the ratio difference is rather large - about 1.6 percent,

Still, however, the standard deviation of the difference measurement was $\pm 0.003\%$.

Slide 11 shows the appearance of a typical deuterium/hydrogen ratio difference measurement chart. Since the abundance of HD is only about 300 parts per million of that of HH, a larger resistor - 10^{12} ohms - is used to convert the mass 3 current to a voltage. As will be seen, even in this unfavorable situation the ratio difference was measured to ± 0.01 percent. (This is the standard deviation of the run; the value 0.03% shown on the slide is the S.D. of a single switching.)

A special problem in the analysis of hydrogen is the formation of HHH^+ in the ion source due to the second order reaction

$$H_2 + H_2^+ \longrightarrow H_3^+ + H$$

Slide 12 shows the effect of this reaction in a classical 6 inch 60° mass spec. Since, for a given repeller voltage, H_2 current is proportional to the pressure in the source, and is easier to measure accurately, H_2 current has been plotted vs the observed mass 3/mass 2 ratio. The ionization chamber contains a "repeller" plate. With this set at 5 volts, when the H_2 current is 20 volts, the ratio is about 3 times as large as it is at zero pressure - in other words, at 20V H_2^+ there is twice as much HHH^+ as HD^+. If the repeller voltage is increased to 40 volts, however, the ratio of HHH^+ to HD^+ decreases substantially - but so does the total ion current.

We have been working to reduce the magnitude of HHH^+ as much as possible while retaining high sensitivity, and have made considerable progress on the problem. For example, Slide 13 shows a much improved situation - a 6-60 calibration run made using two NBS standards, Potomac river water and Yellowstone snow, in which, with the repeller set at 51 volts, at 20 volts of H_2, HHH^+ is only about 20% of HH^+. Under these conditions the HHH^+ correction can be made with excellent accuracy.

Even better performance has now been achieved with the 3-inch M.S. Slide 14 shows a run in which HHH^+ is only about 10% of HD, at 20V HH^+, for a sample which is depleted in HD^+ by nearly 50% compared to "standard" hydrogen. Since HHH^+ can only be formed from protium, this corresponds to a 5% HHH^+ "contribution" to the mass-3 ion current for "normal" samples such as standard mean ocean water (indicated on this chart as SMOW). The contribution will be even less for D-enriched samples.

In summary: it has been determined that when gas flow and ion source conditions are adjusted such that the major isotope produces an ion current to the detector of the 3-60-RMS/HD of the order of 2×10^{-9} amperes, ratio differences as small as 2 parts in 10^5 can be detected in carbon as CO_2, in a run of a few minutes duration. The detection limits for other elements are: for nitrogen, 3 parts in 10^5 or better; for oxygen, 5 in 10^5; and for hydrogen, 10 in 10^5. The precision of measurement (standard deviation) achievable in the measurement of differences of a few percent or less is comparable to this. Still better precision can be obtained by taking additional sets of data and/or by using the IR2A integrating digital ratiometer. The actual capabilities of the instrument in fact exceed our design objectives for precision by about a factor of ten.

Pubs. 1346-0573

SOME ISOTOPE RATIO VARIATION RANGES IN NATURE

ISOTOPES	APPROX. RANGE OF RATIO	% RANGE
$^{1}H/^{2}H$	5900 - 8900	51%
$^{12}C/^{13}C$	83 - 99	19%
$^{14}N/^{15}N$	265 - 280	6%
$^{16}O/^{18}O$	480 - 525	10%
$^{32}S/^{34}S$	21.0 - 23.2	11%

Slide 1

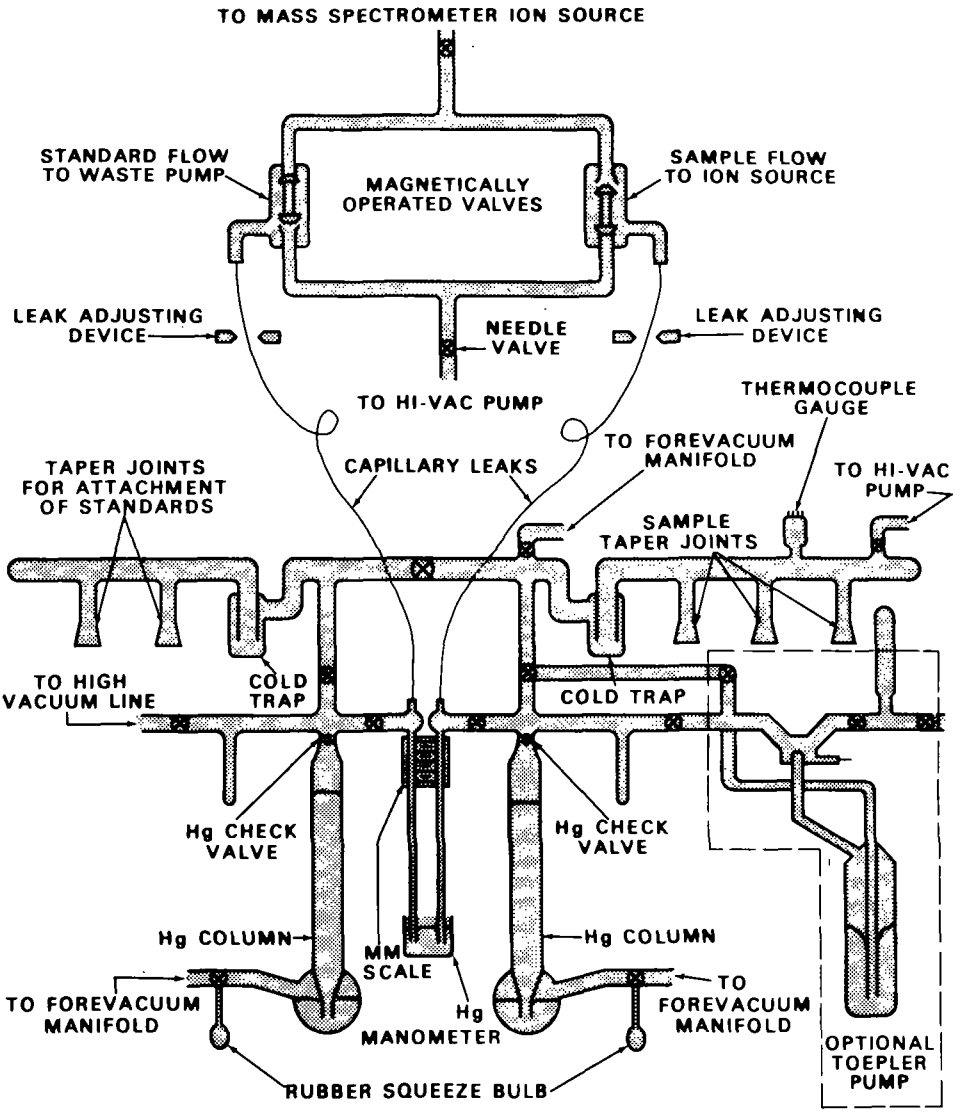
TO MASS SPECTROMETER ION SOURCE
STANDARD FLOW TO WASTE PUMP
MAGNETICALLY OPERATED VALVES
SAMPLE FLOW TO ION SOURCE
LEAK ADJUSTING DEVICE
NEEDLE VALVE
LEAK ADJUSTING DEVICE
TO HI-VAC PUMP
THERMOCOUPLE GAUGE
TO FOREVACUUM MANIFOLD
TO HI-VAC PUMP
TAPER JOINTS FOR ATTACHMENT OF STANDARDS
CAPILLARY LEAKS
SAMPLE TAPER JOINTS
TO HIGH VACUUM LINE
COLD TRAP
COLD TRAP
Hg CHECK VALVE
Hg CHECK VALVE
Hg COLUMN
Hg COLUMN
MM SCALE
TO FOREVACUUM MANIFOLD
Hg MANOMETER
TO FOREVACUUM MANIFOLD
OPTIONAL TOEPLER PUMP
RUBBER SQUEEZE BULB

Slide 3

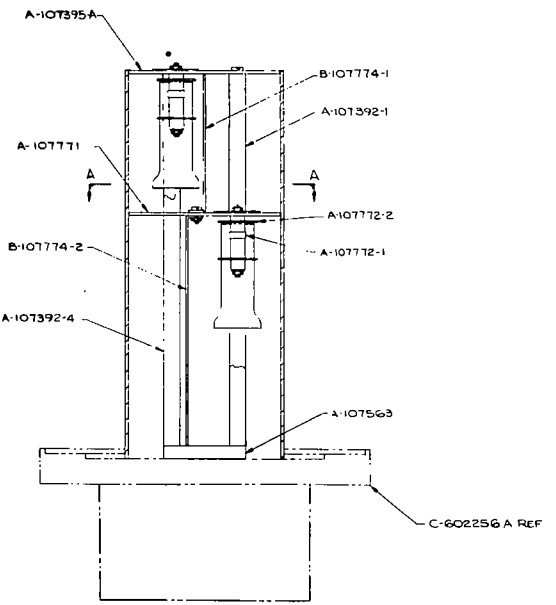
A-107395-A
B-107774-1
A-107392-1
A-107771
A
A
A-107772-2
A-107772-1
B-107774-2
A-107392-4
A-107563
C-602256 A REF

Slide 5

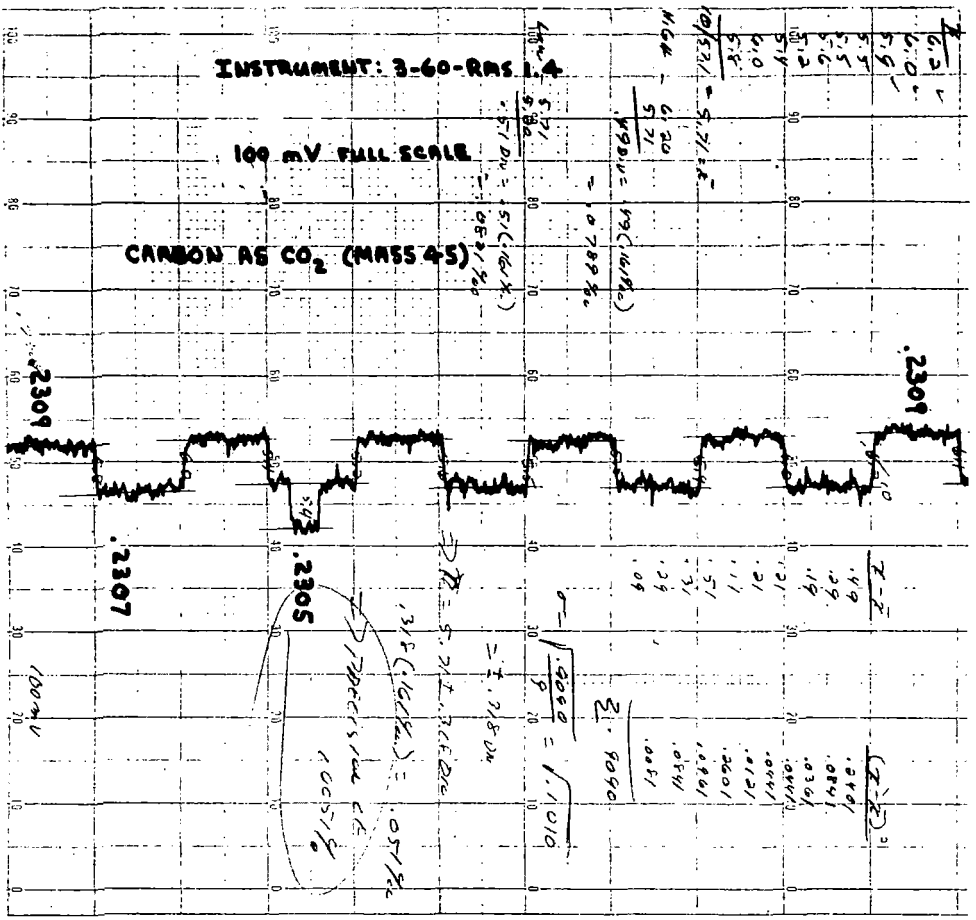
INSTRUMENT: 3-60-RMS 1.4
100 mV FULL SCALE
CARBON AS CO_2 (MASS 45)
.2309
.2307
.2305
.2301

Slide 6

INSTRUMENT: 3-60-RMS 1.4
C-6
OXYGEN AS CO_2 (MASS 46)
30 mV FULL SCALE
L180°
L180°
L180°

Slide 7

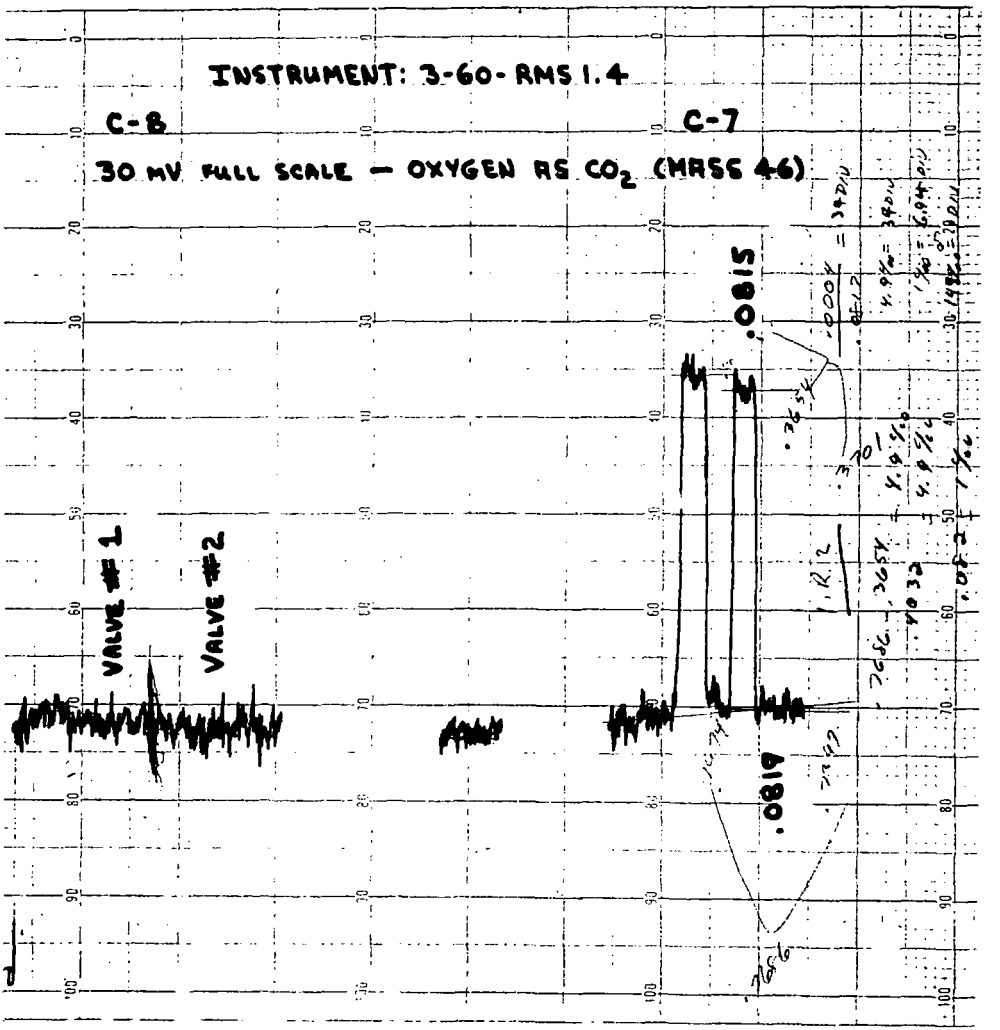
INSTRUMENT: 3-60- RMS 1.4
C-8
C-7
30 MV FULL SCALE — OXYGEN RS CO_2 (MASS 46)
VALVE #1
VALVE #2
.0815
.0819

Slide 8

OXYGEN RATIO DIFFERENCE TEST USING
INTEGRATING DIGITAL VOLTMETER (IR-2)
3-60-RMS1.4 - 4 JAN. 73

1	0	(1-6)	0	3	5	7	0	6	9
1	1	✓	0	3	6	7	9	1	4
1	2		0	3	6	3	1	9	6
2	0		0	5	5	6	7	3	3
2	1	✓	0	5	5	9	0	2	3
2	2		0	5	4	8	2	4	5
1	0		0	3	4	2	6	0	6
1	1	✓	0	3	3	8	7	9	4
1	2		0	3	4	1	0	6	1
2	0		0	5	4	6	5	5	6
2	1	✓	0	5	5	5	9	7	2
2	2		0	5	4	9	3	8	7
1	0		0	3	4	7	9	6	5
1	1	✓	0	3	5	2	7	6	9
1	2		0	3	4	3	0	1	5
2	0		0	5	7	0	6	3	2
2	1	✓	0	5	7	8	8	3	5
2	2		0	5	7	8	9	6	1
1	0		0	3	6	8	7	2	1
1	1	✓	0	3	5	4	3	9	4
1	2		0	3	5	7	6	4	3
2	0		0	5	5	9	5	9	9
2	1	✓	0	5	5	4	7	1	9
2	2		0	5	4	1	9	3	4
1	0		0	3	4	0	2	4	0
1	1		0	3	4	2	0	9	3
1	2		0	3	4	4	9	0	5
2	0		0	5	5	8	1	1	5
2	1	✓	0	5	6	1	1	6	9
2	2		0	5	6	6	7	1	5
1	0		0	3	5	0	2	2	3
1	1	✓	0	3	3	6	2	6	1
1	2		0	3	5	5	7	6	4
2	0		0	5	8	0	4	4	7
2	1	✓	0	5	7	5	6	5	7
2	2		0	5	8	5	2	0	2
1	0		0	3	5	7	8	6	1
1	1	✓	0	3	5	6	2	6	5
1	2		0	3	4	4	1	3	3

Denominator = 320 volt/seconds (req. approx. 37 sec)

Delay = 16 sec; Rest, 2 x 4 sec (two replications)

Sensivitity determined (per c7) as 1 per mil = 0.082

Avg.	Diff.	$(x-\bar{x})$	$(x-x)^2 \times 10^8$
.3627			
.5546	.1919	.0213	45369
.3408	.2138	.0006	36
.5506	.2098	.0034	1156
.3479	.2027	.0105	11025
.5761	.2282	.0150	22500
.3602	.2159	.0027	729
.5520	.1918	.0214	45796
.3424	.2096	.0036	1296
.5620	.2196	.0064	4096
.3474	.2146	.0014	196
.5804	.2330	.0198	39204
.3527	.2277	.0145	21025

$\bar{x} = 2.5586/12 = 0.2132$;
$(x-\bar{x})^2 = 0.0019$
$\sigma = \sqrt{0.0019/11} = \pm 0.0131$
$\sigma = 0.0131/0.086 = 0.152$ ‰ (0.015%)
$\bar{\sigma}_{12} = 0.035$‰ (0.0035%)
$\bar{x} = 0.2132/0.086 = 2.48$‰ (0.248%)

COMPARISON WITH DATA FROM RECORDER TRACE

$\bar{x}$ = 16.98 div (1 div = 0.144‰)
σ = 1.09 div = 0.156‰; $\bar{\sigma} = 0.046$‰
δ = 2.445‰
Actual δ = 2.450‰

Slide 9

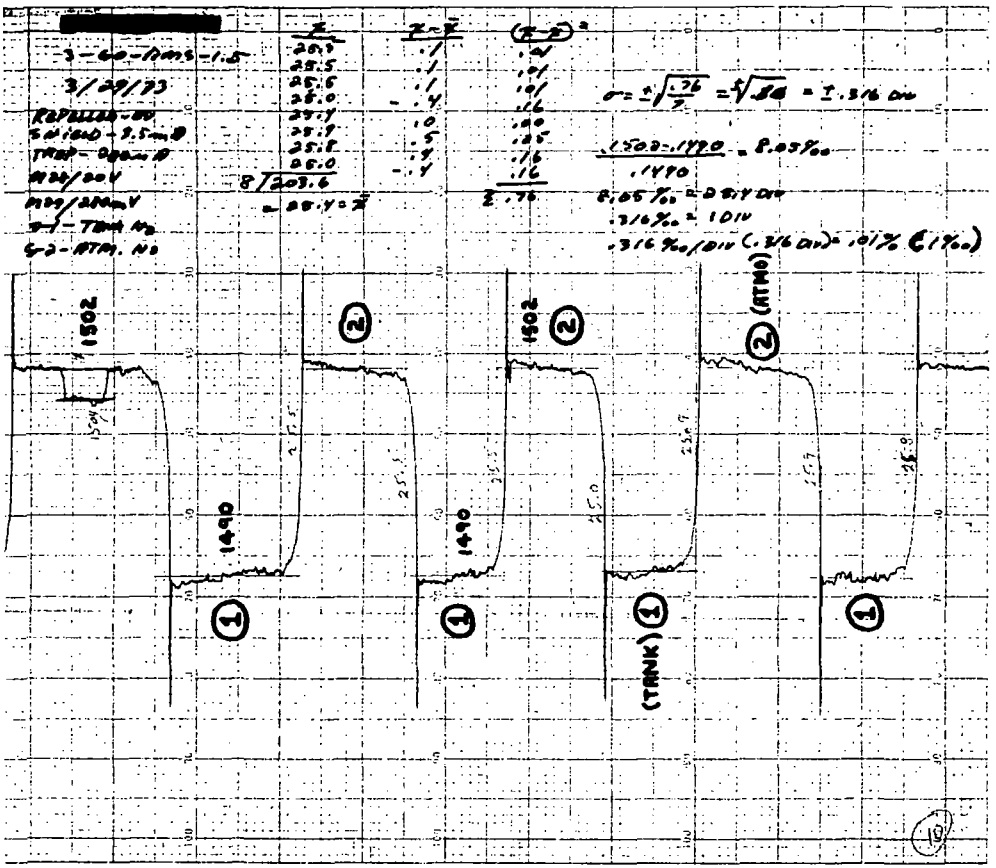

Slide 10

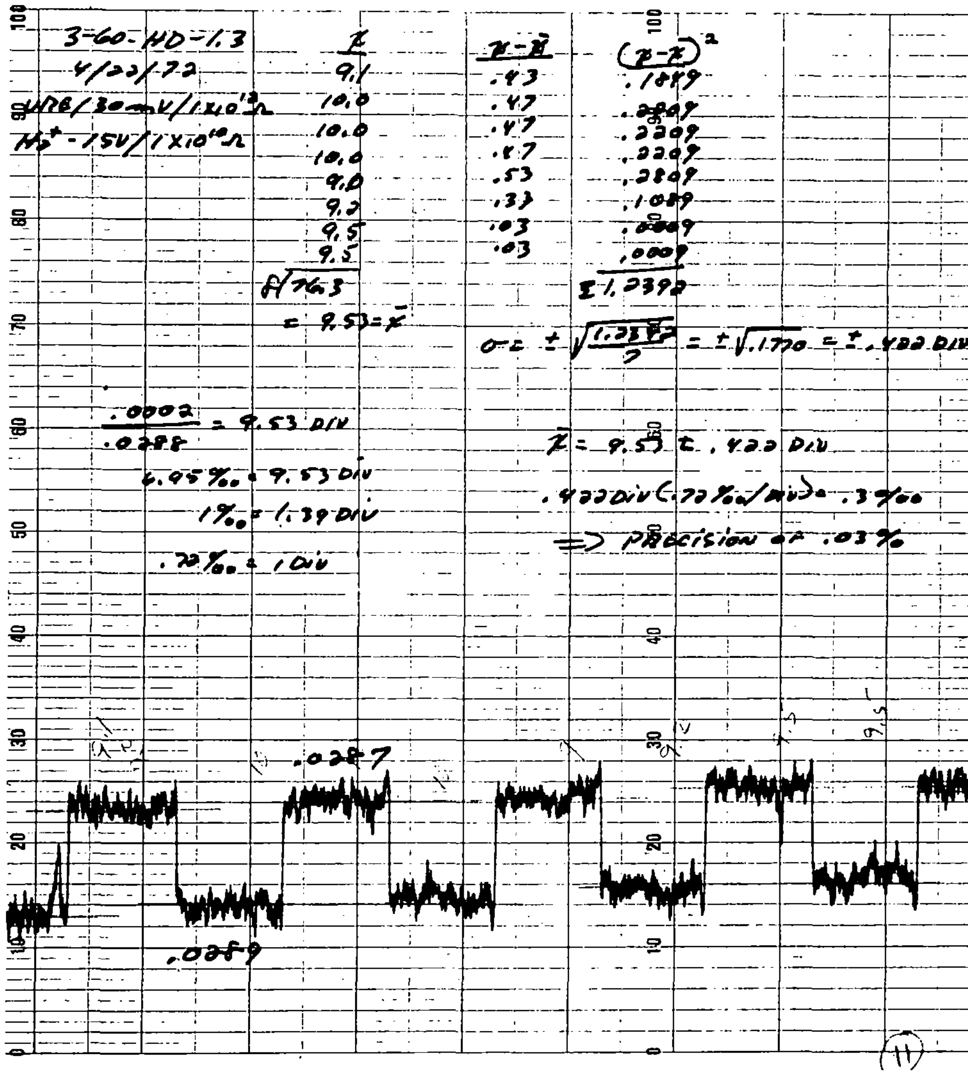
3-60-HD-1.3
4/22/72
x̄
9.1
10.0
10.0
10.0
9.0
9.2
9.5
9.5
8/76.3
= 9.53 = x̄
x-x̄
.43
.47
.47
.47
.53
.33
.03
.03
(x-x̄)²
.1849
.2209
.2209
.2209
.2809
.1089
.0009
.0009
Σ1.2392
.0002
.0288
= 9.53 DIV
6.95‰ = 9.53 DIV
1‰ = 1.39 DIV
.72‰ = 1 DIV
x̄ = 9.53 ± .422 DIV
=> PRECISION OF .03%
.0287
.0289
(11)

Slide 11

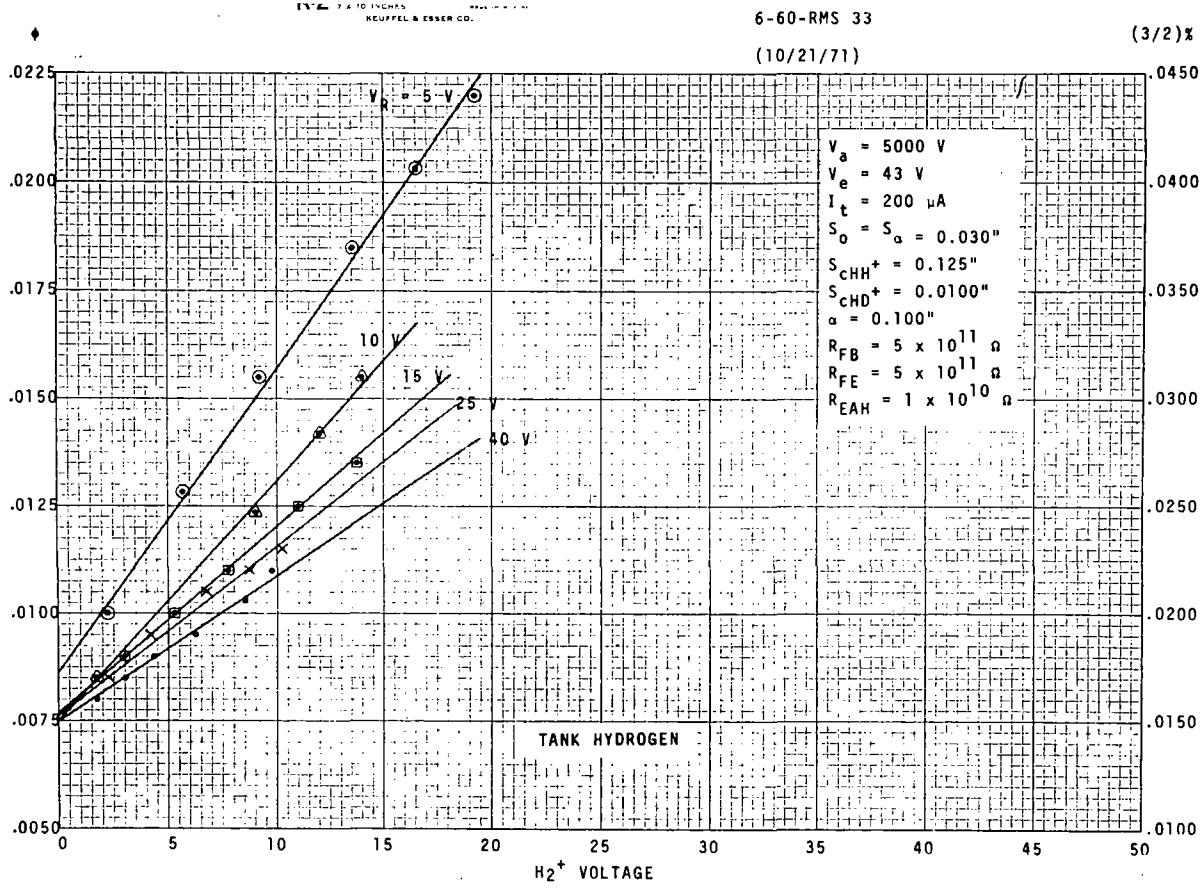
KEUFFEL & ESSER CO.
6-60-RMS 33
(10/21/71)
(3/2)%
V_R = 5 V
10 V
15 V
25 V
40 V
V_a = 5000 V
V_e = 43 V
I_t = 200 μA
$S_o = S_\alpha$ = 0.030"
S_{cHH^+} = 0.125"
S_{cHD^+} = 0.0100"
α = 0.100"
$R_{FB} = 5 \times 10^{11}$ Ω
$R_{FE} = 5 \times 10^{11}$ Ω
$R_{EAH} = 1 \times 10^{10}$ Ω
TANK HYDROGEN
.0225
.0200
.0175
.0150
.0125
.0100
.0075
.0050
.0450
.0400
.0350
.0300
.0250
.0200
.0150
.0100
0
5
10
15
20
25
30
35
40
45
50
H_2^+ VOLTAGE

Slide 12

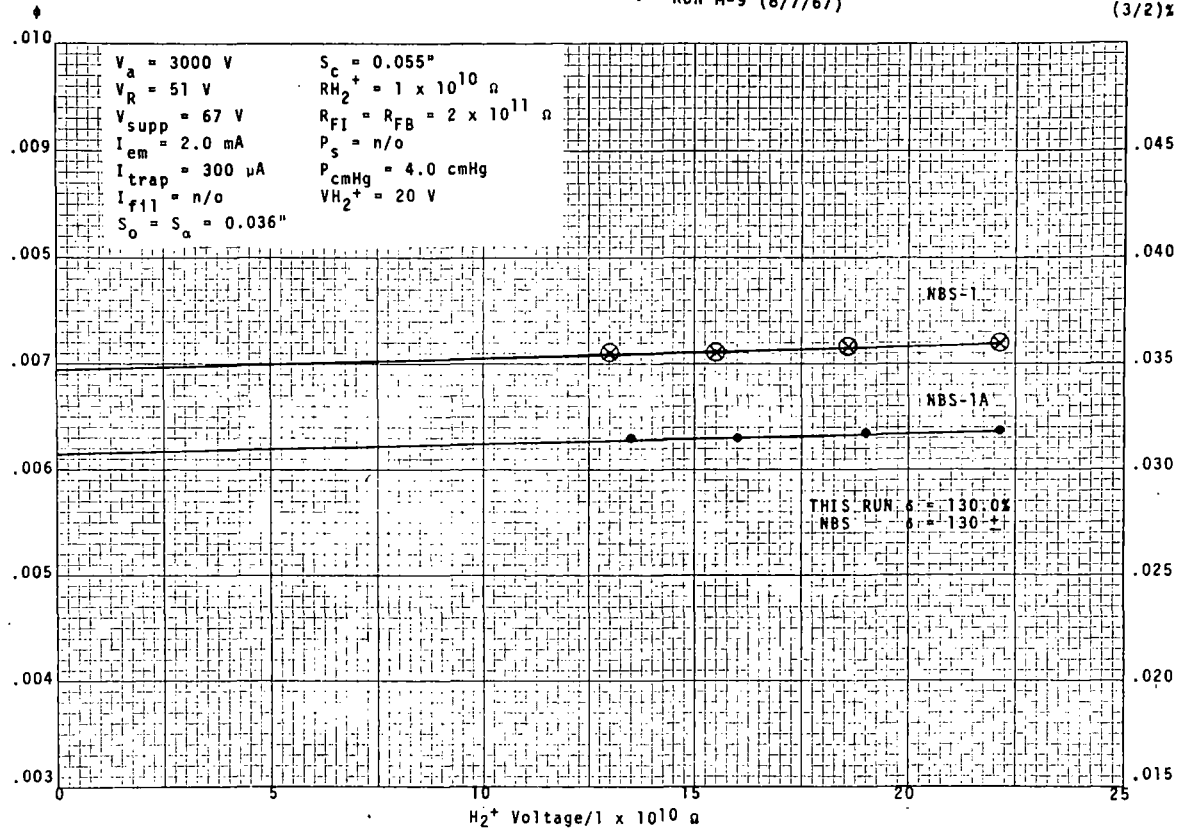
6-60-RMS 22
NBS-1 vs NBS-1A
RUN M-9 (8/7/67)
(3/2)%
V_a = 3000 V
V_R = 51 V
V_{supp} = 67 V
I_{em} = 2.0 mA
I_{trap} = 300 µA
I_{fil} = n/o
$S_o = S_a$ = 0.036"
S_c = 0.055"
RH_2^+ = 1 x 10^{10} Ω
$R_{FI} = R_{FB}$ = 2 x 10^{11} Ω
P_s = n/o
P_{cmHg} = 4.0 cmHg
VH_2^+ = 20 V
NBS-1
NBS-1A
THIS RUN δ = 130.0%
NBS δ = 130 ±
.010
.009
.007
.006
.005
.004
.003
.045
.040
.035
.030
.025
.020
.015
0
5
10
15
20
25
H_2^+ Voltage/1 x 10^{10} Ω

Slide 13

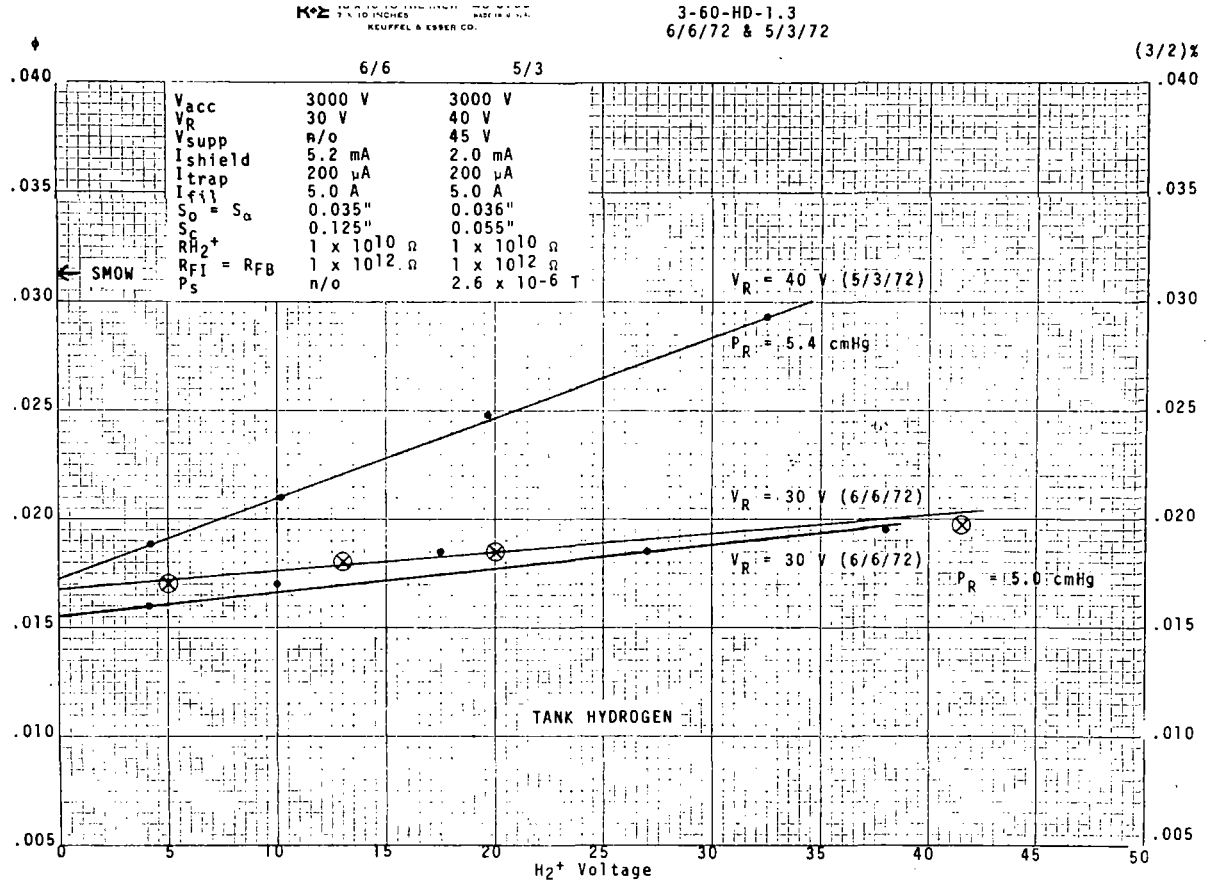
KEUFFEL & ESSER CO.
3-60-HD-1.3
6/6/72 & 5/3/72
(3/2)‰
6/6
5/3
V_{acc} 3000 V 3000 V
V_R 30 V 40 V
V_{supp} n/o 45 V
I_{shield} 5.2 mA 2.0 mA
I_{trap} 200 μA 200 μA
I_{fil} 5.0 A 5.0 A
$S_o = S_\alpha$ 0.035" 0.036"
S_c 0.125" 0.055"
RH_2^+ 1 x 10^{10} Ω 1 x 10^{10} Ω
$R_{FI} = R_{FB}$ 1 x 10^{12} Ω 1 x 10^{12} Ω
P_s n/o 2.6 x 10-6 T
← SMOW
V_R = 40 V (5/3/72)
P_R = 5.4 cmHg
V_R = 30 V (6/6/72)
V_R = 30 V (6/6/72)
P_R = 5.0 cmHg
TANK HYDROGEN
.040
.035
.030
.025
.020
.015
.010
.005
0
5
10
15
20
25
30
35
40
45
50
H_2^+ Voltage

Slide 14

A MASS SPECTROMETER SENSOR SYSTEM FOR METABOLIC ANALYSIS AND ATMOSPHERIC MONITORING ON SKYLAB AND FUTURE MANNED SPACECRAFT

Ralph B. Lehotsky

The Perkin-Elmer Corporation, Aerospace Division
Pomona, California 91767

On extended manned space flight missions, such as Skylab, Space Shuttle, and future space bases, multiple component gas mixtures are utilized, requiring the usage of partial pressure sensors for monitoring and controlling the atmospheric constituents. A distinct advantage in using a mass spectrometer for such partial pressure sensing is that it can perform separation and analyses of all atmospheric constituents as a single system, as opposed to multiple sensors using varying analytical techniques.

To meet the partial pressure sensing requirements, a Mass Spectrometer Sensor System was developed following an optimization and feasibility study which showed:

1. Usage of a magnetic sector spectrograph approach can provide simultaneous and continuous monitoring, which is more preferable and simplified than peak scanning or stepping approaches.

2. A small single focusing system can achieve the system requirements using relatively conservative design techniques.

The mission specifications to which the system was designed are shown in Figure 1, which shows the partial pressure range, output sensitivity and accuracy requirements for the gas species monitored. The system has six channels for monitoring nitrogen, oxygen, water vapor, carbon dioxide, hydrogen, and total contaminants (TC). The accuracies specified are those required over 1440 hours of operating time without recalibration.

The mass spectrometer design specifications created to achieve these mission requirements are shown in Figure 2.

The molecular inlet leak was developed using the compression of sintered stainless steel powder to achieve the desired conductance value. This design is capable of being set at any value between 10^{-3} and 10^{-7} cc/s of nitrogen prior to installation, depending upon the sample pressure range of the application. The molecular inlet leak is very reliable, and has been stability tested in a life study exceeding 9000 hours without any degradation, using unfiltered laboratory air.

The ion pump was developed to obtain the required pumping speed, while keeping its weight and volume minimized. This pumping speed is maintained from 10^{-8} to 10^{-5} torr, while the total operating pressure range is from less than 10^{-9} to 10^{-2} torr. Pulsing characteristics have never been observed and one pump has been life tested for more than 9000 hours at 10^{-6} torr. The pump life at 10^{-6} torr is estimated in excess of 25,000 hours.

The ion source is a nonmagnetic design in which the two filaments are located in redundant orthogonally mounted electron guns from which electrons are focused into a common ionizing region. This basic design has been incorporated into over 50 space flight systems and has proven very stable and reliable on five unmanned satellites and many ground base test programs. The ion source is heated and controlled at 110°C, requiring a maximum of three watts heater power over the spacecraft environmental temperature range. Beryllia ceramic insulators are used to minimize thermal response time. The ionizing region is differentially pumped and operates at about 100 times the pressure in the mass spectrometer, reducing errors due to background signals. The filaments are located in the low pressure region, extending their life spans and reducing errors due to sample distortion by filament interactions.

The 90 degree magnetic sector has a three centimeter nominal radius at m/e 32, and uses normal ion entry and exit. A flux level of about four kilogauss is provided by a small permanent magnet weighing approximately one pound. The collector slit positions for each m/e were located using a computer ion trajectory analysis program with a completely stored mapped magnetic field of a final design magnet. However, all collector slits are not located at optimum focal points. Rather, they are placed at

positions which minimize the size of the mass analyzer, yet maintaining the resolving power requirements. A typical scan of mass peaks obtained at each collector is shown in Figure 3. One hundred percent of the ions exiting the ion source are transmitted to the collectors in order to maintain stable output signals over a defined range of ion accelerating voltage. The resultant flat topped peaks simplify alignment criteria of the collector slits and also negate signal variations due to thermal effects on the power supplies and permanent magnet over the operating temperature range. A cutaway view of the mass spectrometer is shown in Figure 4.

A block diagram of the complete sensor system is shown in Figure 5. Of unique significance is the closed loop electronics system which maintains stable operation over long term operating periods. Summation of proportionately scaled ion currents, corresponding to partial pressures, is compared against a total pressure signal measured by a transducer attached to the sampling gas line, the ionizing electron current being regulated to balance these signals. This mode compensates the mass spectrometer for any gain changes which are common to all channels, e.g., leak conductance or source sensitivity changes.

Manual selection of an open loop mode sets the system to the conventional ionizing electron current regulation mode. This mode is used during operation prior to sample introduction and for applications where percentage outputs are desired instead of partial pressures. It is also a backup mode in the event of a channel failure when operating in the closed loop mode.

Self contained protective circuitry and status indicator outputs are provided. When the pressure within the vacuum envelope is greater than 10^{-3} torr, both the ion pump and system electronics operation are inhibited. When the ion pump is operating at pressures between 10^{-3} and 10^{-5} torr, the system electronics are disabled.

An open loop indicator displays manual selection of the open loop mode, or when closed loop mode is disabled due to exceeding the dynamic range of the closed loop system. (The latter event occurs infrequently, if the astronauts forget to open the sample inlet valve).

The filament switching circuitry permits selection of an automatic filament change mode, in case of a failure when the sensor is incorporated in an atmospheric control system. A manual switching mode is also provided for sensor applications as a monitor only.

The systems produced have shown that stable operation is achieved for periods greater than one year in either continuous or cyclic testing, without any recalibration requirements. The short term stability of the channels over a five hour continuous test period are nominally less than 0.1 percent of the full scale partial pressure. This is significant since there are no potentiometric or other adjustments. The complete electronics system uses only fixed value components.

The system control requirements were to achieve simplicity in the design in order to maintain minimum astronaut operational procedures and training requirements. The sensor system control requirements consist of five switches, in conjunction with three status indicator lamps.

In addition to these controls, two manually actuated valves are utilized.

The first valve is used to admit the sample gas to the mass spectrometer. The second valve is used only in a contingency procedure, which provides for roughing down the vacuum envelope to space vacuum, in case of accidental venting of the mass spectrometer.

In addition to the mass spectrometer and ion pump, the sensor package contains about 1400 individual electronic components, which are located in 26 welded wire modules and on 21 printed wiring boards, in addition to the required interconnect cabling and structural mounting frame. The sensor cylinder size is 7.2 inches in diameter by 12.5 inches long and requires a nominal 16 watts of power, with a worst case limit of 28 watts. The aluminum enclosure is electron beam welded to provide a hermetically sealed flangeless package which is capable of withstanding external overpressures of 38 lb_f/in^2 abs (psia). Following all final assembly, but prior to the final enclosure weld, the system is completely filled with isocyanate foam for structural support. The resultant system has been flight qualified for all spacecraft environmental stress requirements.

Aboard the Skylab space station, the sensor system was incorporated with spirometers and additional electronics for both atmospheric monitoring and in-flight metabolic activity experiments in conjunction with an ergometer. The sensor was identical to the system described, except that only four channels were outputed with rescaled channel ranges, as is shown in Figure 6. In addition, the sintered stainless steel inlet leak

conductance was rescaled and its design slightly modified to provide faster time response.

The efforts required for the development of these systems were supported by NASA, Johnson Space Center, under Contract NAS9-9799, monitored by A.C. Copeland and John Lem.

SAMPLE CONSTITUENT	PARTIAL PRESSURE RANGE‡ (TORR)	OUTPUT SENSITIVITY (TORR/VOLT)	ACCURACY		OUTPUT VOLTAGE RANGE (VOLTS)
			% FS	TORR	
N_2	0-660	132.0	±2	±13.2	0 TO 5
O_2	0-330	66.0	±2	±6.6	0 TO 5
H_2O	0-33	6.6	±5	±1.65	0 TO 5
CO_2	0-23.1	4.62	±3	±0.7	0 TO 5
H_2	0-3.3	0.66	±20	±0.66	0 TO 5
TC*	0-0.33**	N/A†	N/A†	N/A†	0 TO 5

* MONITORED BY MEASURING ALL CONSTITUENTS HAVING M/E RATIOS BETWEEN 50 AND 120.

** BASED UPON 500 PPM FULL SCALE ASSUMING COMPOUNDS HAVING AN EQUIVALENT SENSITIVITY TO N_2 AT M/E 28.

† CALIBRATION REQUIRED FOR MIXTURES OF CONTAMINANTS EXPECTED IN SPECIFIC APPLICATION.

‡ TOTAL PRESSURE RANGE LIMITED AT 0 TO 800 TORR

FIGURE 1. Mission Specifications

MASS SPECTROMETER:	1. SINGLE FOCUSING 90° MAGNETIC SECTOR 2. COLLECTORS: M/E: 2, 18, 28, 32, 44, 50-120 SAMPLE SPECIES: H_2, H_2O, N_2, O_2, CO_2, TC 3. RESOLUTION: @M/E: 2, 18, 28, 32, 44, 50-120 M/ΔM: 3, 18, 10, 10, 12, N/A RESOLUTION FROM M/E: $1(H^+)$, $4(He^+)$; $17(OH^+)$; $32(O_2^+)$; $28(N_2^+)$; $40(A^+)$; N/A
ION SOURCE (DUAL FILAMENT, NONMAGNETIC)	1. SENSITIVITY (N_2): 1.5×10^{-6} A (N_2^+)/TORR (N_2) 2. OPERATING PRESSURE (MAX): 2×10^{-4} TORR 3. HEATED TO 110°C (LIMITED TO 3 WATT HEATING POWER) 4. IONIZING ELECTRON CURRENT (NOMINAL): 7.5 μA AT 100 EV 5. DIFFERENTIAL PUMPING RATIO: 100/1 WITH 4 LITER/SEC ION PUMP
MOLECULAR INLET LEAK	1. COMPRESSED SINTERED STAINLESS STEEL 2. GAS CONDUCTANCE (N_2): 6.25×10^{-6} CC/SEC
ION PUMP	1. Ta - Ti CATHODES (FOR INCREASED NOBLE GAS PUMPING) 2. PUMPING SPEED (AT 10^{-6} TORR, N_2): 4 LITER/SEC 3. OPERATING PRESSURE RANGE: 10^{-9} TO 10^{-2} TORR

FIGURE 2. Mass Spectrometer Design Specifications

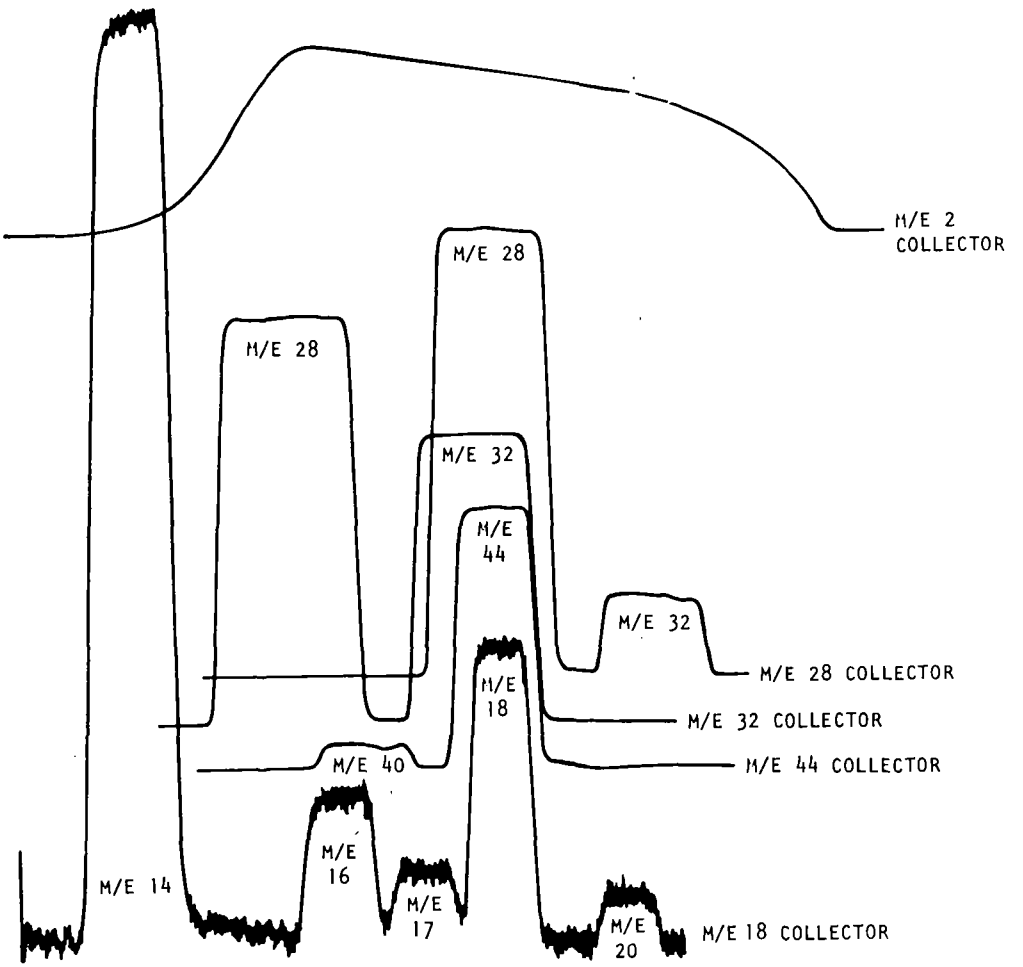

FIGURE 3. Typical Mass Peaks and Collector Alignment

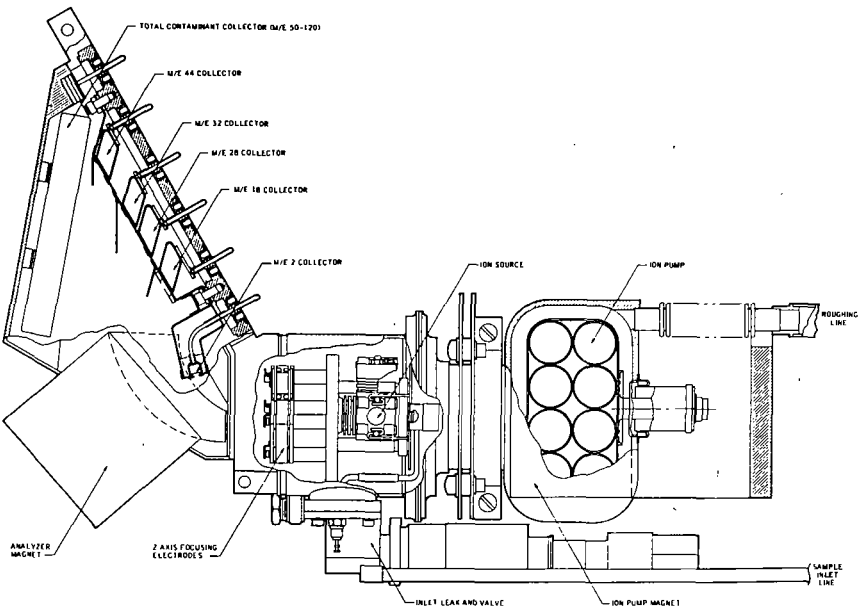

FIGURE 4. Mass Spectrometer Configuration

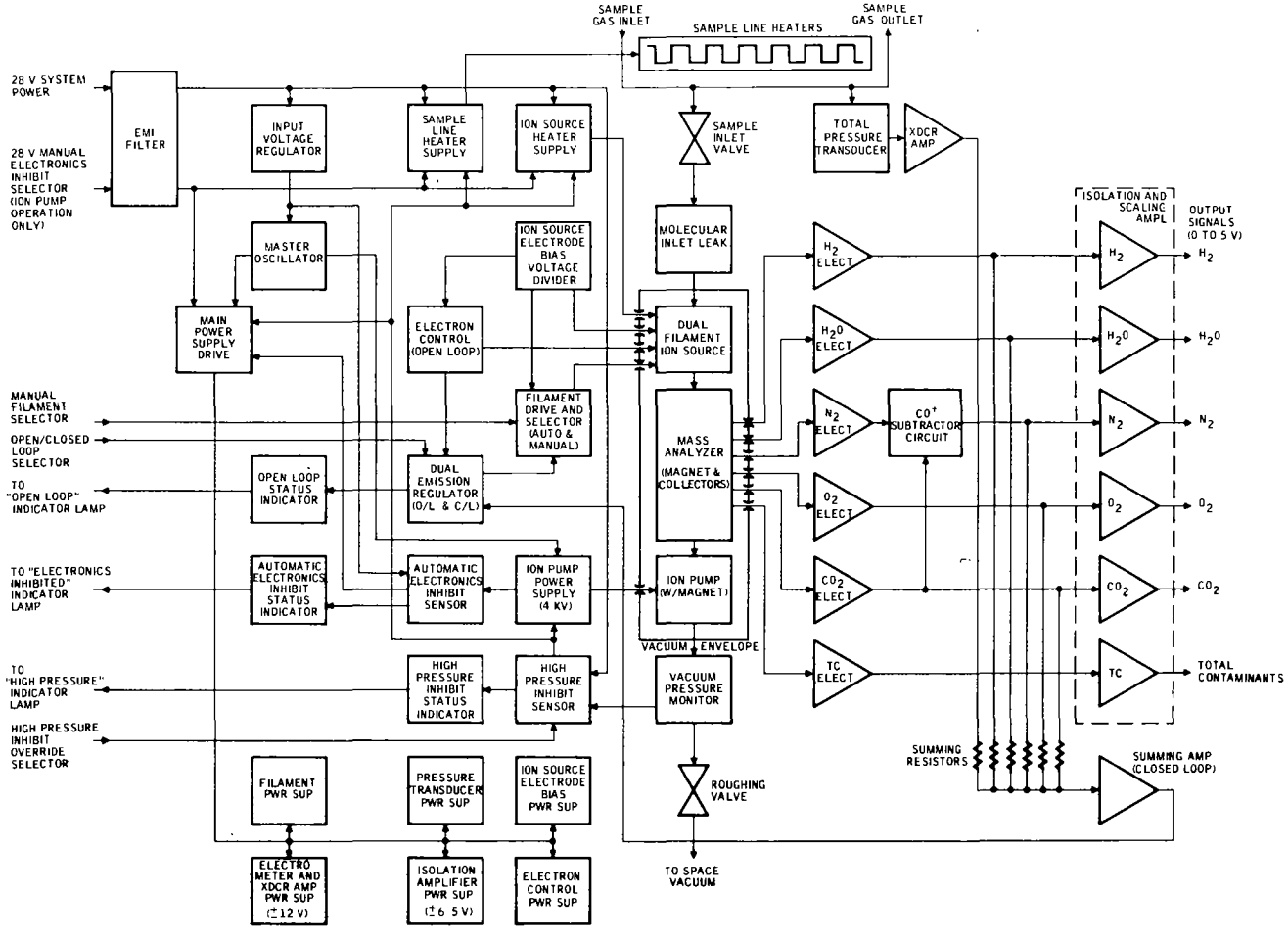

FIGURE 5. Block Diagram - Mass Spectrometer Sensor System

SAMPLE CONSTITUENT	PARTIAL PRESSURE RANGE (TORR)†		OUTPUT SENSITIVITY(TORR/VOLT)		ACCURACY		OUTPUT VOLTAGE RANGE (VOLTS)
	FLIGHT UNITS	ASTRONAUT* TRAINING UNITS	FLIGHT UNITS	ASTRONAUT* TRAINING UNITS	%	TORR	
N_2	0-220	0-220	44.0	44.0	±2	±4.4	0 TO 5
O_2	0-250	0-65	55.0	13.0	±2	±5.0	0 TO 5
H_2O	0-66	0-66	13.2	13.2	±5	±3.3	0 TO 5
CO_2	0-66	0-25	13.2	5.0	±3	±2.0	0 TO 5

* FOR TRAINING PURPOSES AT NORMAL SEA LEVEL ATMOSPHERIC COMPOSITION, WITH PRESSURE DIVIDER INSTALLED IN SAMPLE INLET LINE.

† TOTAL PRESSURE RANGE LIMITED AT 0 TO 330 TORR.

FIGURE 6. Skylab Specifications

A QUADRUPOLE MASS SPECTROMETER FOR THE IDENTIFICATION AND CHARACTERIZATION OF NEUTRAL FRAGMENTS FORMED BY THE INTERACTION OF ELECTRONS WITH GASEOUS MOLECULES

J. R. Reeher and H. J. Svec

Ames Laboratory-USAEC and Department of Chemistry
Iowa State University, Ames, Iowa 50010

In a conventional mass spectrometer ion source, gaseous molecules interact with electrons in various ways to form many species, including positive ions, negative ions, and neutral radicals and molecules, all of which may be formed in ground or excited states. In order to completely characterize the behavior of gaseous molecules under electron impact, all of these species must be identified and the energetics of their formation and ionization determined. The application of mass spectrometric methods to the detection of positive and negative ions and the determination of their energetics of formation are well documented. However, the neutral fragments formed during decomposition processes and the energetics of their formation and ionization are not so well known. Although indirect methods, such as metastable ion transitions, isotopic labelling, and deconvolution of ionization efficiency curves, are available for deducing the makeup of neutral fragments, methods for direct detection have had limited success. However, a quadrupole mass spectrometer with a modified ion source and ion detection system for characterizing the neutral fragments formed in a mass spectrometer ion source has been developed recently in our laboratory. This instrument has several advantages over developments described previously for this purpose, including those by Beck, Osberghaus, and Niehaus,[1-6] Melton,[7-11] Saunders, Larkins, and Saalfeld,[12] and Preston, Tsuchiya, and Svec.[13] These advantages include:

1) Greatly improved sensitivity for detecting neutral fragments.

2) Convenient scanning of neutral fragment mass spectra.

3) Convenient measurement of neutral fragment appearance potentials and vertical ionization potentials.

The ion source (Figure 1) has a primary (1Y) reaction chamber with a pulsed electron beam for producing the neutral fragments and a secondary (2Y) ionization chamber with a DC electron beam for ionizing the neutral fragments formed in the first. The two chambers are separated by three tungsten mesh grids, each of which is 92% transparent and which preserve the integrity of the electric fields in the ion source. The distance between the centers of the two chambers is less than 8 mm.

Sample gases enter the primary reaction chamber through a nozzle perpendicular to the primary electron beam and are condensed on a liquid nitrogen-cooled surface immediately after traversing the primary ionization region.

The electron guns are pentodes with two grids between the filament and the shield or ionization chamber. The pulsed electron beam in the primary chamber is produced by pulsing the second grid of the primary electron gun. The grid closest to the filament collects the electrons emitted during the "off" cycle of the pulsed electron beam, eliminating the problem of space charge building up in the vicinity of the filament. In the second chamber, the two grids act as a lens to focus the electron beam.

Grounded plates between the components of the two electron guns reduce pickup of the AC pulse by the components of the secondary electron gun. Opposing the electron guns also helps to eliminate this problem.

In general, maximum trap currents of 50μA are utilized in the secondary electron beam to minimize ion trapping. However, in the primary reaction chamber, higher trap currents (up to 200 μA) may be utilized to produce neutral fragments, since they are not trapped by the electron beam.

The processes which occur in the primary reaction chamber to produce positive ions and neutral fragments are shown in Fig. 2. The positive ions and neutral fragments are produced at the frequency of the pulsed electron beam. The positive ions are attracted to the primary drawout plate, while the neutral fragments are allowed to diffuse through the tungsten mesh grids to the secondary ionization chamber.

The processes which may occur in the secondary ionization chamber are shown in Fig. 3. Those gas molecules which enter this chamber and interact with the secondary electron beam without having first interacted with the primary electron beam produce a DC ion current, which after mass analysis yields the normal mass spectrum of the sample gas. The particles which interact with the secondary electron beam after having interacted with the pulsed primary electron beam produce an AC ion current, which after mass analysis yields the neutral mass spectrum of the sample gas.

Let us trace the path of the total ion current produced in the secondary ionization chamber through the instrument as shown in Fig. 4. The ion beam is focussed into the quadrupole mass filter where it is mass analyzed. The ions which pass through the mass filter are deflected to the first dynode of a 17-stage Cu-Be electron multiplier. The function of the deflector is to eliminate any direct optical path between the ion source and the electron multiplier. A platinum black surface situated opposite the exit hole from the mass filter serves to absorb any photons which originate in the source region and traverse the mass filter to the deflector region. After amplification by the electron multiplier, the output signal (Fig. 5) is fed into a preamplifier which separates the signal into its AC and DC components and amplifies them. The DC component, with a gain of 10^8 V/A, is recorded directly as the normal mass spectrum of the sample. The AC component, with a gain of 10^9 V/A is processed by a Princeton Applied Research lock-in amplifier whose output is recorded as the neutral mass spectrum of the sample.

The neutral mass spectrum of mesitylene is shown as recorded from the instrument in Fig. 6. In order to relate these raw data to the relative abundances of the neutral fragments present, two major corrections must be made. First, the spectrum must be corrected to compensate for the mass discriminations inherent in the quadrupole mass filter. Second, since each neutral fragment has a different cross-section for ionization, the neutral mass spectrum must be corrected by dividing each peak intensity by its corresponding cross-section. After making these two corrections, a spectrum is obtained as shown in Fig. 7. Here, the neutral mass spectrum is plotted with ascending mass while the normal mass spectrum is plotted above it with descending mass, so that correlations between neutral fragments and complimentary positive ions can be observed more readily. Although exact correlation is not made, it should be noted that the shape of the envelope of the two spectra plotted in this manner have the same general appearance.

The neutral mass spectra of several methylsubstituted aromatic compounds are compared in Fig. 8. Note the increase in methyl radical abundance as more methyl groups are substituted on the ring, and the increase in abundance of higher mass neutrals in the heavier molecules. Note also that many of the same neutral fragments are observed from all of these compounds. This observation indicates that these compounds are randomizing to a great extent after interacting with an electron and before dissociating in the primary reaction chamber.

Some uncorrected ionization efficiency curves of toluene neutral fragments being ionized in the secondary chamber are shown in Fig. 9. The energy scale was calibrated with the parent ion from benzene. The data obtained from these curves is tabulated in numerical form on Fig. 10. The values determined are reproducible to about ±0.06 volt, with good agreement between the linear extrapolation and extrapolated voltage difference methods of treating the data. A literature value for the vertical ionization potential C_4H_3 was not available. Measurement of neutral fragment ionization potentials such as these is essential to the determination of bond energies from mass spectrometric data. Appearance potentials of neutral fragments can be determined similarly by scanning the energy of the primary electron beam.

In conclusion, we hope that this instrument development will open a new area of mass spectrometry which will lead to a better understanding of the processes which occur in a conventional mass spectrometer ion source.

References

1. D. Beck and O. Osberghaus, Z. für Physik, 160, (1960), 406.
2. D. Beck and A. Niehaus, J. Chem. Phys., 37, (1962), 2705.
3. D. Beck, Disc. Faraday Soc., 36, (1964), 56.
4. H. Genzel and O. Osberghaus, Z. Naturf., 22a, (1967), 331.
5. A. Niehaus, Z. Naturf., 22a, (1967), 690.
6. F. W. Lampe and A. Niehaus, J. Chem. Phys., 49, (1968), 2949.
7. C. E. Melton, J. Chem. Phys., 45, (1966), 4414.
8. C. E. Melton, J. Sci. Instr., 43, (1966), 927.
9. C. E. Melton and P. S. Rudolph, J. Chem. Phys., 47, (1967), 1771.
10. C. E. Melton, Int. J. Mass Spec. Ion Phys., 1, (1968), 353.
11. C. E. Melton, J. Chem. Phys., 74, (1970), 582.
12. R. A. Saunders, J. T. Larkins, and F. E. Saalfeld, Int. J. Mass Spec. Ion Phys., 3, (1969), 203.
13. F. J. Preston, M. Tsuchiya, and H. J. Svec, Int. J. Mass Spec. Ion Phys., 3, (1969), 323.

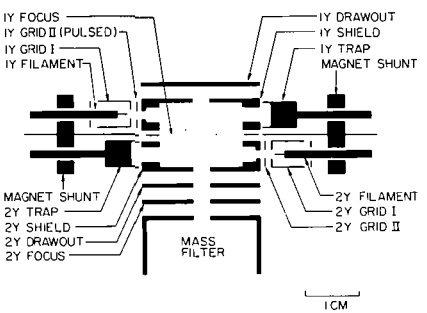

Figure 1

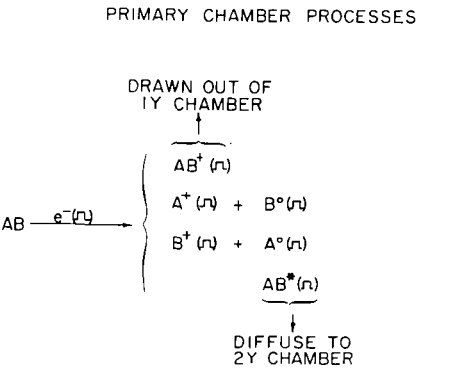

Figure 2

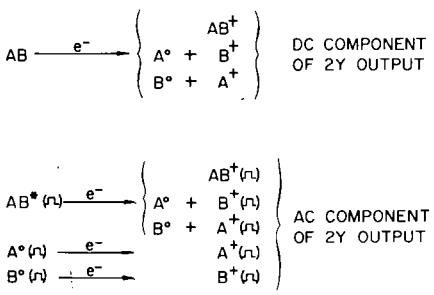

Figure 3

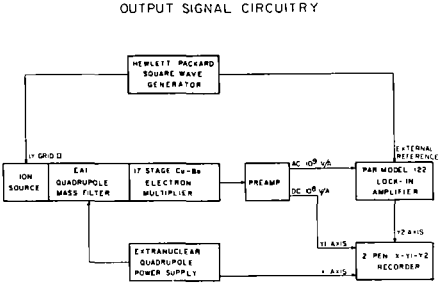

Figure 5

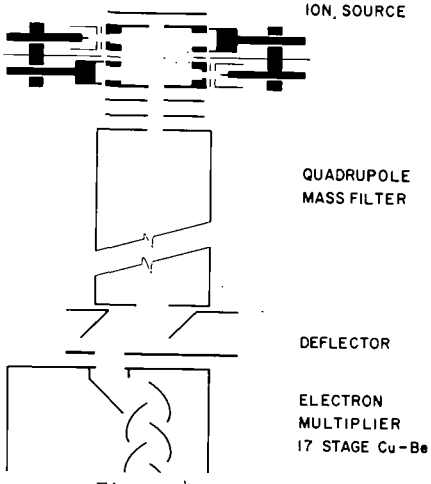

Figure 4

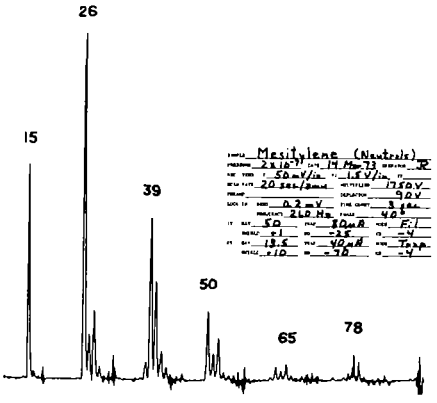

Figure 6

NEUTRAL MASS SPECTRA

1Y 50 eV 80μA

2Y 15 eV 40μA

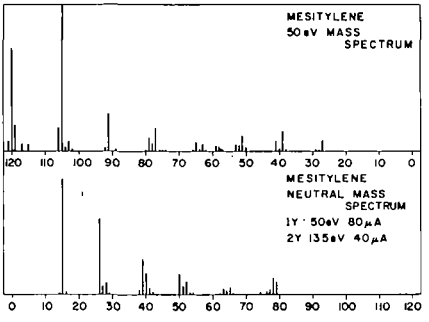

Figure 7

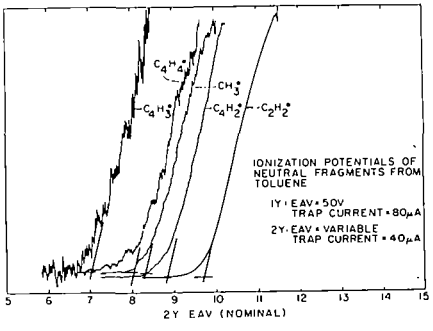

Figure 9

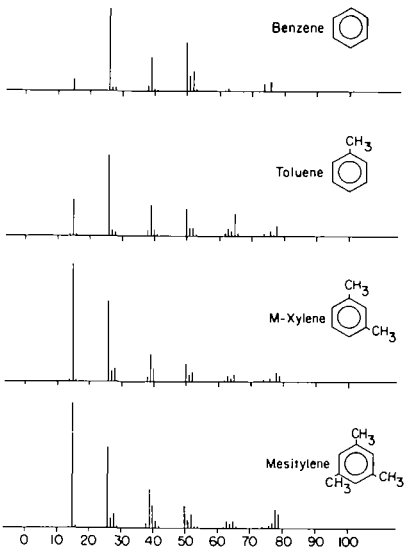

Figure 8

IP'S OF NEUTRAL FRAGMENTS FROM TOLUENE

M/e	MOLECULAR FORMULA	LITERATURE	LE	EVD
15	CH_3	9.91	9.93	9.94
26	C_2H_2	11.40	11.38	11.37
39	C_3H_3	———	9.43	9.37
50	C_4H_2	10.20	10.47	10.37
51	C_4H_3	———	8.67	8.61
52	C_4H_4	9.87	9.68	9.70

Figure 10

A Crossed-Beam Apparatus for Investigation of Ion-Molecule Reactions*

M.L. Vestal, C.R. Blakley, P. Ryan, and J.H. Futrell

Department of Chemistry
University of Utah
Salt Lake City, Utah 84112

INTRODUCTION

The crossed-beam machine is a new instrument that will permit detailed analysis of ion-molecule reactions. Basically, the instrument, which is shown schematically in Fig. 1, consists of several differentially pumped high vacuum chambers in which an ion gun produces a low energy, monoenergetic beam of the desired ion which is then crossed at right angles with a beam of neutral molecules. Resulting ionic reaction products are then energy and mass analyzed in a detector assembly. Movement of this detector about the collision region permits construction of intensity contour plots (Newton diagrams) from which mechanistic information can be obtained. While superficially not unlike other crossed-beam instruments, this particular machine incorporates several design features which greatly enhance its information obtaining capability.

The first of these features is the use of a chemical ionization source. The large number of collisions ($\sim 10^6$) that are required of an ion before exiting virtually ensures that the ion beam will have a thermal energy distribution and, additionally, that the ions will be in the ground state. This "state selection" of the ion beam will provide information about the role of excited states in reactions.

The second feature is the decelerating lens. Whereas most decelerating lenses do not function well at low energies (<1 eV), this particular lens was designed to yield a truly exponentially retarding field. Calculations predicted that thermal energies should be readily attainable, hence allowing the study of reactions at these low energies.

A third important feature of the apparatus is that the detector assembly--consisting of a retarding filter lens energy analyzer, quadrupole mass filter, and secondary electron multiplier--can be rotated through a full octant of a sphere. A ramp generator is used to provide the retarding voltage, and the output data is fed through a preamplifier to a multichannel analyzer for time-averaging of the energy spectrum of mass-resolved product ions.

These features make the instrument unique. Other features will become apparent as the instrument is described more fully below.

SOURCE/ION GUN

The CI source and initial optics are essentially identical to others used in our laboratory and have been reported elsewhere.[1] Cylindrical geometry is used throughout, in contrast to the rectangular optics used in commercial mass spectrometers. Located in the analyzer tube, ~1 inch from the object aperture, is a strong focusing quadrupole pair lens. This lens is used to refocus the beam in the vertical plane--that is, the non-focusing plane of the magnet--in order to maintain cylindrical geometry through the analyzer tube and thus increase the beam intensity through the image aperture.

PRIMARY MASS ANALYZER

Mass analysis of the ion beam is done with a 5-inch, 60° sector magnet. This particular analyzer was salvaged from a Hitachi Perkin-Elmer Model RMS-4 mass spectrometer. Only the magnet, flight tube, and some of the power supplies are used. Its resolution is approximately 200.

The ion beam energy is determined by the potential of the source chamber above ground. This was done so that the collision region may be left at earth ground, but required that the flight tube of the primary mass analyzer be floated below ground. Consequently, the flight tube was insulated from ground with glass-to-metal seals and nylon flanges. Floating of the tube may be compared to normal mass spectrometric practice in which the source is at high potential and the tube is at ground.

DECELERATING LENS

Ions emerge from the analyzer tube through a 0.020-inch diameter circular hole into the retarding lens. This consists of a stack of 42 elements connected together by resistors so as to produce an exponential field between the analyzer (-750 V) and the collision region at ground potential. The lens is 8 inches long and is cylindrically symmetrical with a 0.5 inch diameter aperture. To compensate for fringing fields and other imperfections, potentials of the initial and final few stages can be independently adjusted. Additionally, it was found necessary to add vertical and horizontal steering plates and an einzel lens near the entrance of the lens to correct for misalignment and to further compensate for fringing fields.

Testing the lens showed that it works almost exactly as calculated. Transmission remains very nearly 100% down to ~ 1.0 eV before falling off, of which ~90% is focused into a 1/8"-diameter aperture located at the collision center. Because of the relatively large angular

magnification the beam does have a fairly large angular spread of $\sim 5^{\circ}$ (FWHM) as measured by the detector.

NEUTRAL BEAM

The neutral beam is produced by a conventional supersonic nozzle source. After passing through the skimmer, the beam is chopped by a rotating slotted disk and emerges through a 3-mm diameter hole into the main vacuum chamber, where it intersects the ion beam. The beam traverses the main chamber and passes through a 1-inch diameter aperture into the neutral beam collection chamber. The beam detector is a flow-through ion gauge mounted in line with the beam whose output, when synchronized with the beam chopper, permits measurement of the neutral beam's time-of-flight distribution and hence its velocity distribution.

COLLISION REGION/DETECTOR

The ion and neutral beams cross in the main chamber, an 18-inch diameter glass bell jar that is differentially pumped by a baffled 6-inch diffusion pump. Scattered reaction products enter the detector (acceptance angle = 5°) which contains the energy analyzer, mass filter, and electron multiplier. The detector assembly can be moved through a full octant of a sphere about the collision region, permitting measurements both in and out of the plane of the crossed beams. Upon entering the detector, the ions are energy analyzed with a retarding filter lens from which an integral energy distribution is obtained. The resolution of this analyzer is about 0.1 eV. After leaving the energy analyzer, the ions are reaccelerated into a Finnigan quadrupole mass filter (0.250-inch diameter rods, 5.5-inches long), whose mass resolution is approximately 50. Transmitted ions enter a Bendix Spiraltron electron multiplier whose output is fed through a preamplifier to a multi-channel analyzer.

A digital ramp generator (see Fig. 2) is used to provide the retarding voltage for the energy anaylyzer so that the energy spectrum can be time averaged to improve the signal to noise ratio for low intensity beams. Additionally, in order to eliminate spurious signals from background scattering, phase sensitive detection is used by gating the multi-channel analyzer input with a beam chopper in the path of the neutral beam. During alternate half cycles, the signal obtained with the beam off is subtracted from the signal with the beam on, hence only those product ions resulting from direct interaction of the ion and neutral beams are counted. The integral energy distributions thus obtained are then punched onto paper tape and off-line processed on a PDP 11/20 computer.

APPLICATIONS

This apparatus is currently being used for studies on reactive scattering. Preliminary results have been obtained for the reactions

$$D_3^+ + H_2 \rightarrow H_2D^+ + D_2$$

$$\rightarrow HD_2^+ + HD$$

and on the reaction

$$t\text{-}C_4H_9^+ + C_3H_6 \rightarrow C_3H_7^+ + C_4H_8$$

These reactions all appear to occur by a long-lived complex at low initial kinetic energies.

---

* To be submitted to Reviews of Scientific Instruments.

[1] M.L. Vestal, T.A. Elwood, L.H. Wojcik, and J.H. Futrell, 20th Annual Conference on Mass Spectrometry and Allied Topics, Dallas, Texas, June 4-9, 1972, paper P10.

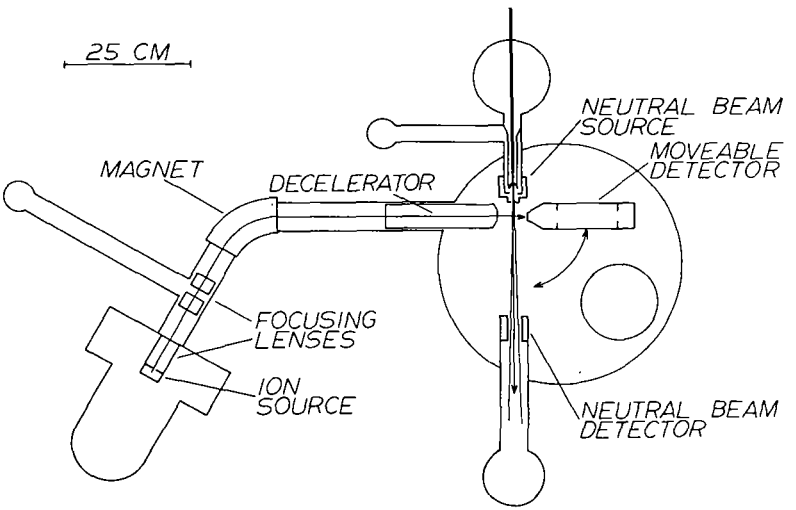

Fig. 1 Schematic of crossed-beam machine

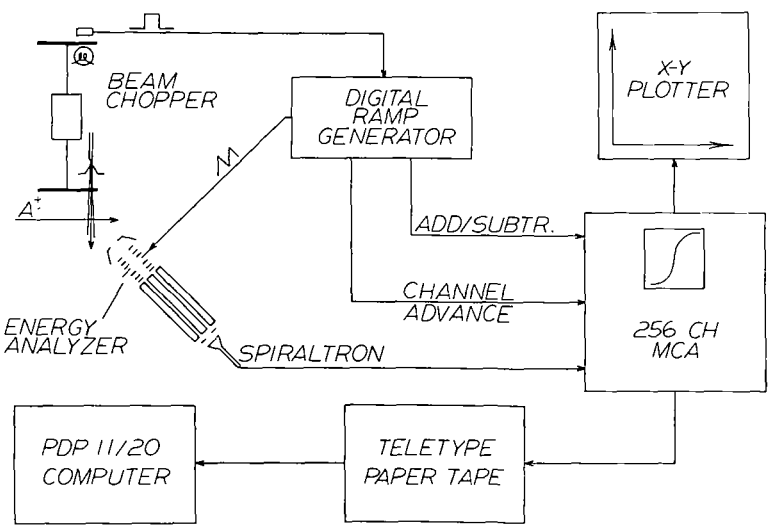

Fig. 2 Block Diagram of data system

AN RPD SYSTEM WITH DIGITAL SCANNING AND PHASE-SENSITIVE DETECTION

T. J. Eskew
Nuclide Corporation
642 East College Avenue
State College, PA 16801

The retarding-potential-difference method in the original form described by Fox et al (1) required the operator to switch a retarding voltage on one grid of the electron gun between two slightly different values, and to measure the resulting change in the ion current. It was necessary to repeat this procedure at each setting of the electron accelerating voltage for which a data point was desired on the ionization efficiency curve.

Those who have used this technique will be aware of several difficulties, however:

a. The fluctuations or "noise" on the ion current limit one's ability to measure small changes, as required by the method;

b. It is tedious to plot the difference in ion current as a function of electron accelerating potential, particularly for the large number of data points that are usually desired;

c. The adjustments of the electron gun and source magnet are critical, since certain combinations of the adjustments can impart fictitious features to the curve; moreover, the consequences of a small change in the adjustments usually cannot be seen until after the data is plotted.

Now the RPD method can be regarded as an example of a modulation technique, in which the desired information is the change, or a-c component, of an output signal that results from a change, or a-c modulation, in an input parameter. The input parameter is, of course, the retarding potential in the electron gun, and the output is the mass-resolved ion current. An elegant electronic technique, phase-sensitive detection, was developed long ago for application in just this sort of problem. When used in an RPD experiment, the phase-sensitive detector responds only to that portion of the a-c component of the ion current that is precisely in step with the modulating signal, and discriminates strongly against random noise and other extraneous fluctuations.

In spite of the fact that the phase-sensitive detection method has been well known since the fifties, it has not been widely used in RPD measurements. An engineering problem that may inhibit the use of this method lies in the necessity of coupling a synchronizing signal across the high potential difference that exists between the ion source and the collector. Some of the earliest reports of RPD experiments with phase-sensitive detection (2,3) were of work with a total-ionization tube rather than a mass spectrometer, so that the high-voltage isolation problem did not arise.

The synchronizing signal can be coupled through a capacitor, a transformer, or by means of a lamp and photocell. A high-voltage capacitor, for example, was used by Hudson (4).

Recently, inexpensive couplers have become available which incorporate a light-emitting diode and a phototransistor, with insulation suitable for 25 kV; very little engineering is required to interface them with standard transistor circuits.

We have lately built an RPD system incorporating these couplers and have taken advantage of the inexpensive integrated circuits and digital components which have become available in recent years. The system is outlined in Figure 1.

The mass spectrometer is the Nuclide model 12-90-G, in which the ion source may be operated at 12,000 volts above ground. The lock-in amplifier, a Princeton Applied Research model 120, is tuned to a fixed frequency of 94 Hz. This amplifier generates the synchronizing signal which is coupled to the RPD supply across the 12,000-volt potential difference as shown. The modulated ion current is amplified by an electrometer having a bandwidth limited to about five times the modulation frequency. In addition, a bandpass filter (20 to 500 Hz) is added at the input of the lock-in amplifier.

The synchronously detected output, which is proportional to the ion current differences required by the RPD method, is displayed on one pen of a two-pen recorder. The electron voltage scan circuit in the RPD supply generates a coded signal, which is coupled through two additional isolators to the second pen of the recorder.

Figure 2 is a diagram of the RPD ion source and the power supply. The electron gun incorporates four narrow apertures followed by a wide one, the dimensions being similar to those given by Gordon et al (5). The fifth aperture is the entrance to the ionization chamber, and is about twice as wide as the first four.

The four plates and the ionization chamber or shield are driven by the circuits E1 through E5, as shown. These voltages are all referred to the midpoint of the filament. The repeller and trap-voltage circuits are referred to the shield. Each of these circuits incorporates operational amplifiers or transistors to develop a low output impedance.

E1, the drawing-out voltage, is positive with respect to the filament and adjustable over the range 0 to 10 volts; 1 volt is a typical setting. E3 is the usual retarding voltage which is switched between two negative levels by means of a mechanical chopper. A second pole of the chopper also switches E2. This is the scheme of Gordon, Haarhoff and Krige (5), who found that it is easier to obtain a good adjustment of an RPD gun if two voltages are switched together in this manner.

E4 and the repeller voltage are driven from switching circuits, controlled by a 50-kHz pulse generator. E4 is held at 0 volts for several microseconds and then switched to -10 volts. After a delay of about 0.2 μsec, the repeller is switched on. The cycle repeats at a 50-kHz rate.

E5 is the electron accelerating voltage; it can be set at any value from 0 to 100 volts to a precision of 1 millivolt, by means of two decade switches and a ten-turn potentiometer. The scan circuit covers any 40-volt portion of the range.

The trap voltage is adjustable from about -1 to +100 volts, but is normally set at 1 to 5 volts for RPD work. The trap current is measured by an electrometer circuit, 10^{-8} to 10^{-3} A full scale in 6 ranges. A special vacuum feed-through is used for the trap lead, with a guard ring attached directly to the trap voltage supply. In this way, leakage currents flowing across the high voltage portion of the insulator are intercepted, and do not interfere with the trap current measurement.

A trap-current-regulating feedback loop can be switched in if the ion source is used for ordinary analytical work, but for RPD work, the filament current is regulated independently of the trap current.

Figure 3 shows some details of the E3 circuit. The circuit is arranged so that the output impedance is the same for either position of the chopper contact; this is the function of the upper or "dummy" section of the two-gang potentiometer used to set ΔE3. The other capacitors and the resistors in the chopper leads serve to damp any pulses that could otherwise be reflected on the cable, because of pickup from the 50-kHz switching pulse on E4.

The switching rate for the retarding potential has been as high as 1 kHz (3) or as low as 22 Hz (4). 94 Hz was used here because it seemed high enough to permit rapid scanning, and because it is often recommended as having no simple relation to the 60-Hz mains frequency. In retrospect, it appears that Hudson's 22 Hz may have been a better choice, since it may have allowed a wider dynamic range of the lock-in amplifier.

The E2 circuit is identical to the one shown here, except for the range of the controls.

The operational amplifiers are integrated circuit types (Motorola MC1456) with temperature coefficients of a fraction of a millivolt per °C.

Figure 4 shows the switching circuit which drives the repeller. This circuit includes the innovation of an adjustable negative voltage on the repeller during the time that ions are being formed; hopefully, this voltage can be adjusted to compensate for the field leaking into the ionization chamber from the ion gun, so that the ions are formed in a region of zero potential gradient. The positive voltage, which pushes the ions out about 200 nsec after the electron beam is switched off, can be independently set for best operation. The field effect transistor switches permit these features with a simple circuit configuration, and are quite fast enough for RPD work: the rise and fall times, with 30 feet of 93-ohm cable, are about 75 nanoseconds.

The E4 drive circuit is similar, except that the two voltages are 0 and -10 (with respect to the filament), and are not adjustable.

Figure 5 shows the circuit which scans E5. One bit on the D-to-A converter produces a 10 millivolt shift in the filament-to-shield potential; the full 12-bit range is therefore +40.95 volts. The slowest scan rate, 1 mV/sec,requires one pulse every ten seconds at the input to the 12-bit counter; the required pulse rates are divided down from the clock, as shown. The binary-to-BCD decoder drives the 4-digit LED display, and also the optical isolators. This is the arrangement used to indicate the electron voltage on the recorder. During the scan, the second pen makes a small step for every 100 millivolts and a larger step for every volt. The converter is accurate within $\pm$ 1/2 bit, so that the marks made by this pen are accurate within $\pm$ 5 millivolts.

Figure 6 is an ionization efficiency curve for the mass 16 peak of methane, plotted automatically by this system. The main trace is the lock-in amplifier output, and the trace at the left-hand margin shows the steps for each 1/10 volt, and the displacement of the trace for every volt, as the electron energy is scanned upwards from 12 volts.

This is the kind of result that has led many mass spectrometrists to be suspicious of the RPD method. The features of this cure are artifacts; they can be completely changed by a small adjustment of E2 or by a small motion of the source magnet.

Note the time scale: the scan rate was 10 mV/sec; thus, the steps on the left-hand trace were at 10-second intervals, and it took only four minutes to record the entire curve.

Gordon *et al* mention "several months of experimenting with various instrument settings" using the original scheme in which only one voltage is switched. With their new technique in which two voltages, E2 and E3, are switched simultaneously, they were able to readily find an adjustment which caused the tail of the ionization efficiency curve to fall below the baseline, but by an amount just equal to the experimental uncertainty. With this technique, they could obtain good results after only "a day or two."

Figure 7 shows a curve obtained with a retuning of the gun giving a pronounced negative dip. This tuning can be found in only a few minutes, and the curve was plotted in only 4 minutes.

Figure 8 shows the result of a slight increase in E3, and a reduction of ΔE3 to 50 millivolts. The negative dip is, of course, still larger than the experimental uncertainty, but has been reduced.

Figure 9 shows a smooth curve in which the negative dip has completely disappeared. The optimum adjustment, according to Gordon, would be intermediate between this curve and the previous one.

I do not wish to make any assertions about the shape of these curves, or the correct break points for CH_4. I wish only to show that one can check a number of adjustments in a few minutes, rather than the hours or days required by the original method.

To conclude: the apparatus described here permits one to explore the effects of various tunings of the electron gun in a relatively short time, to take full advantage of the method of Gordon et al, and to avoid the sort of tuning that can sometimes give spurious results.

I would like to thank Dr. Timothy Thomas of the Department of Chemistry, University of Missouri at Kansas City, in whose laboratory these experiments were done.

References

1. R.E. Fox, W. M. Hickan, T. Kjeldaas, Jr. and D. J. Grove, Phys. Rev. 84, 859 (1951).

2. G. J. Schulz, J. Chem. Phys. 33, 1661 (1960).

3. V. E. Grob, Jr., J. Chem. Phys. 39, 972 (1963).

4. J. E. Hudson, Ph. D. Thesis, Dept. of Chemistry, Penna. State Univ. (1969).

5. S. M. Gordon, P. C. Haarhoff and G. J. Krige, Int. J. Mass Spectrom. Ion Phys. 3, 13 (1969).

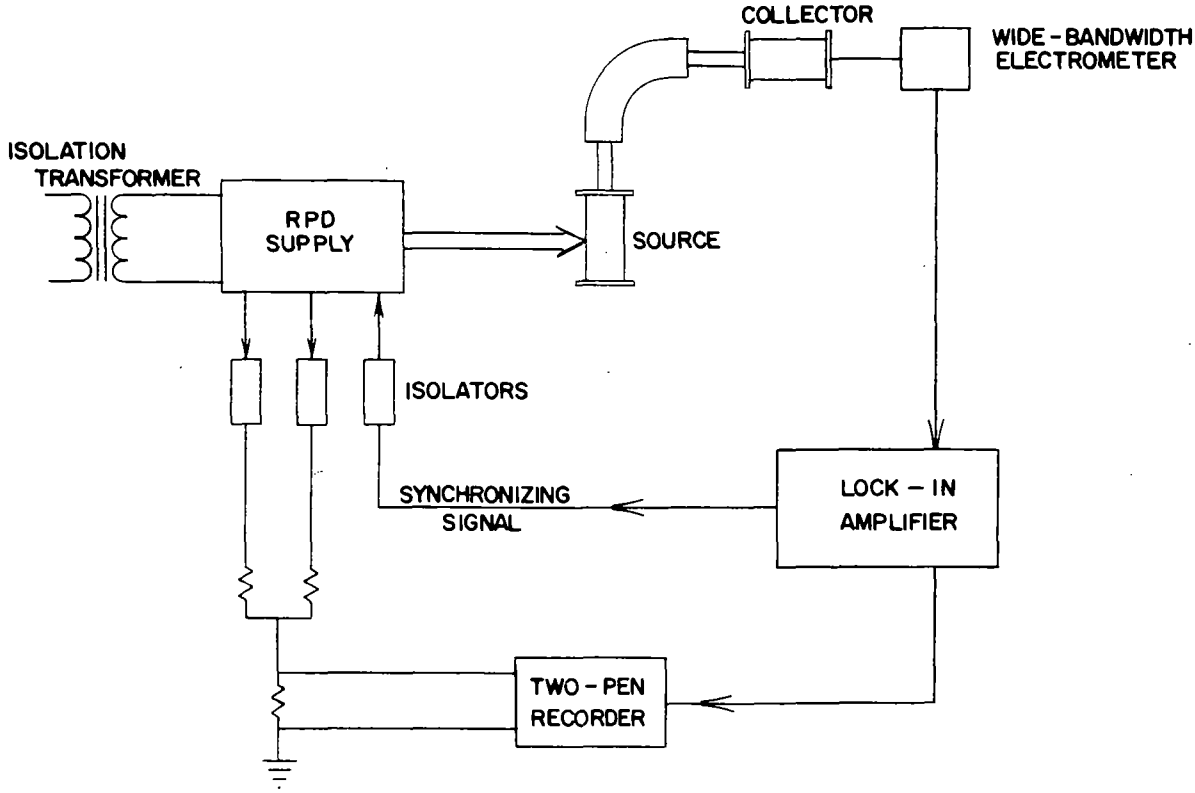

SYSTEM DIAGRAM

Figure 1

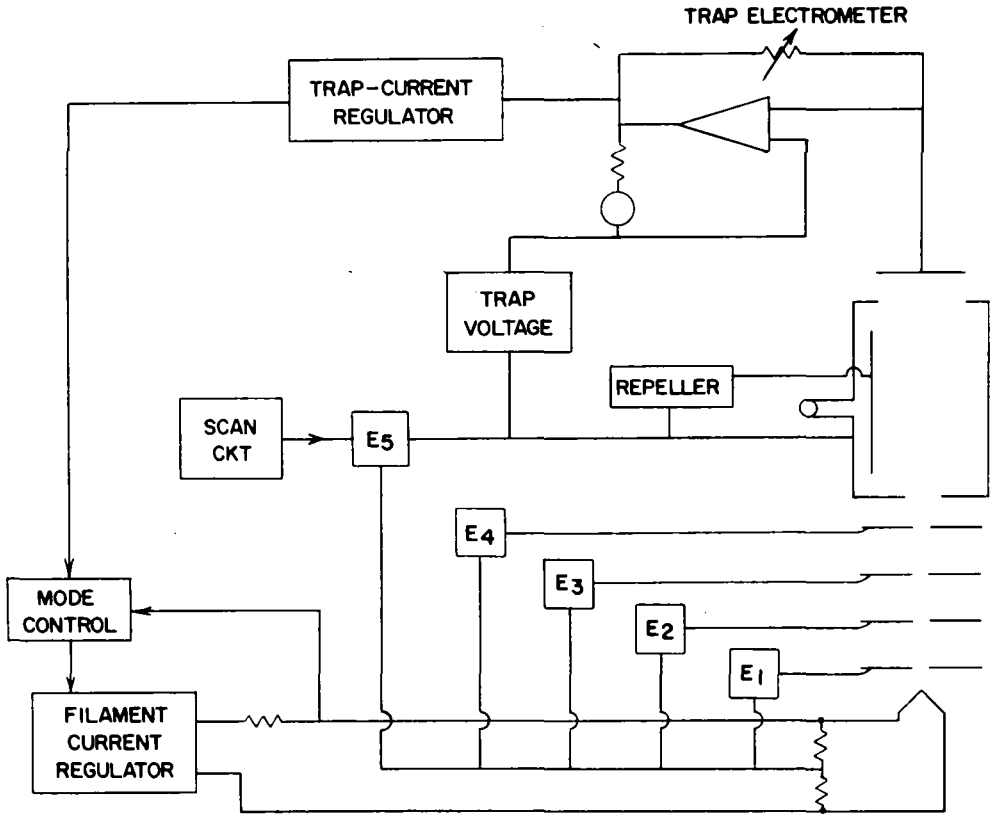

RPD SUPPLY

Figure 2

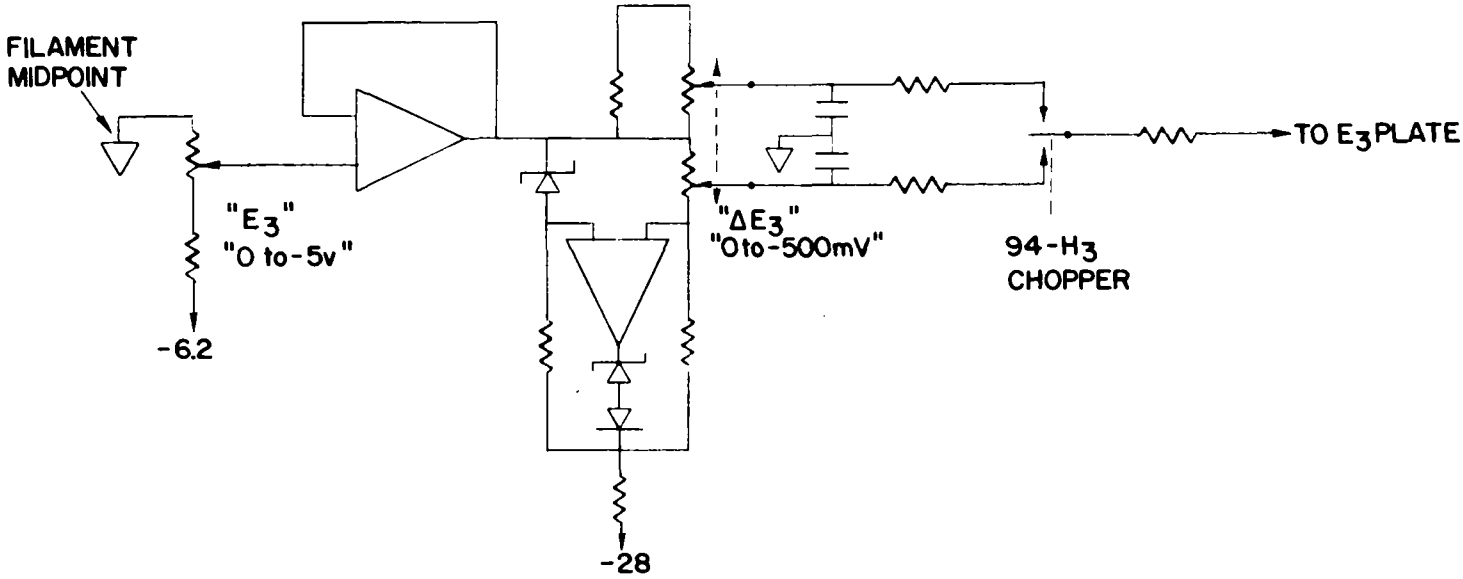

E_3 CONTROLS

Figure 3

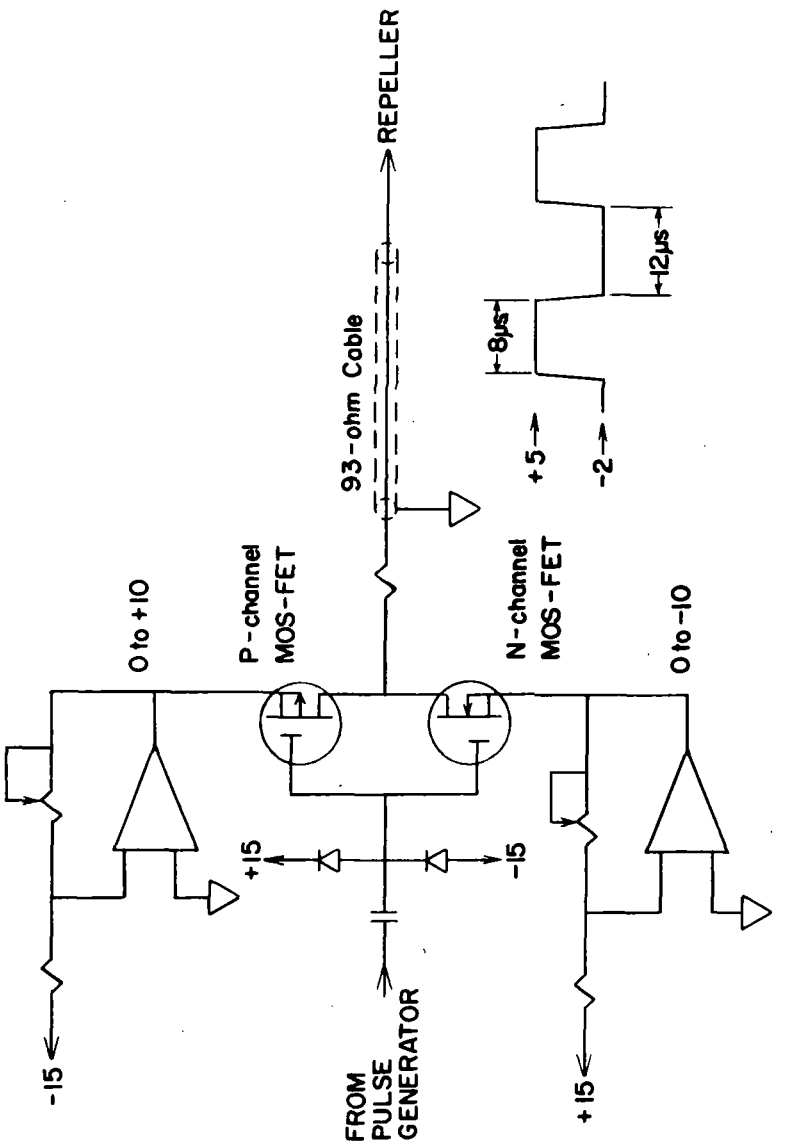

REPELLER DRIVE CIRCUIT

Figure 4

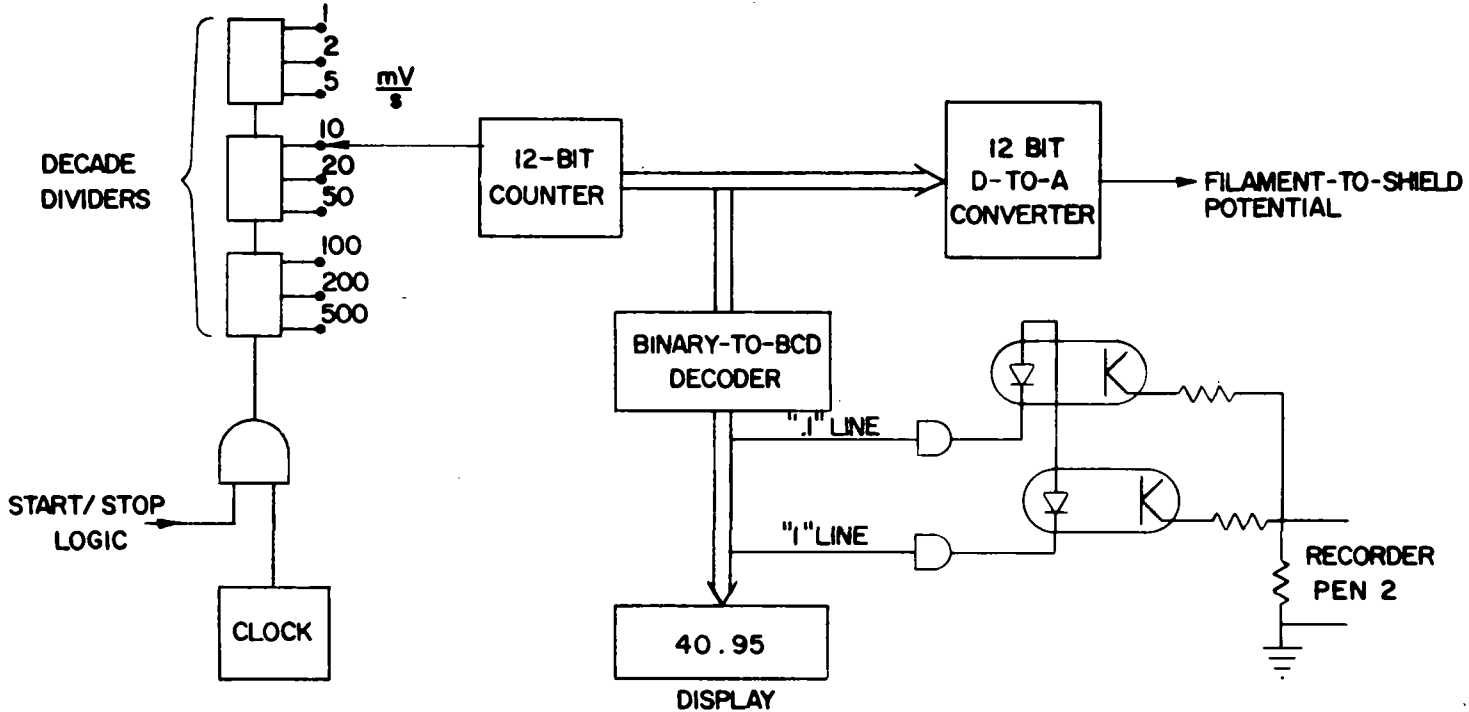

DIGITAL SCAN CIRCUIT

Figure 5

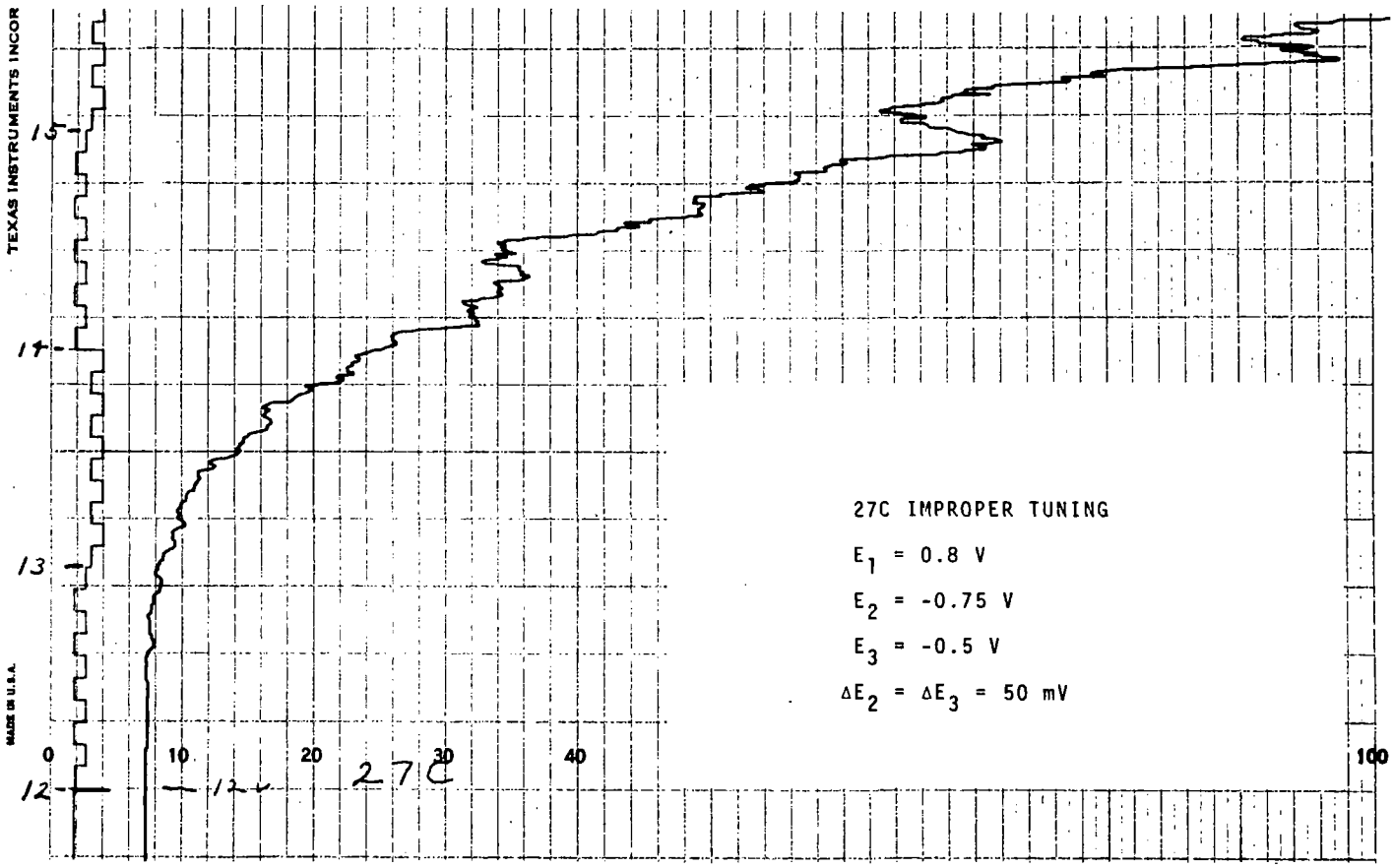
TEXAS INSTRUMENTS INCOR
MADE IN U.S.A.
15
14
13
12
0
10
20
30
40
100
12 V
27C
27C IMPROPER TUNING
E_1 = 0.8 V
E_2 = -0.75 V
E_3 = -0.5 V
$\Delta E_2 = \Delta E_3$ = 50 mV

Figure 6

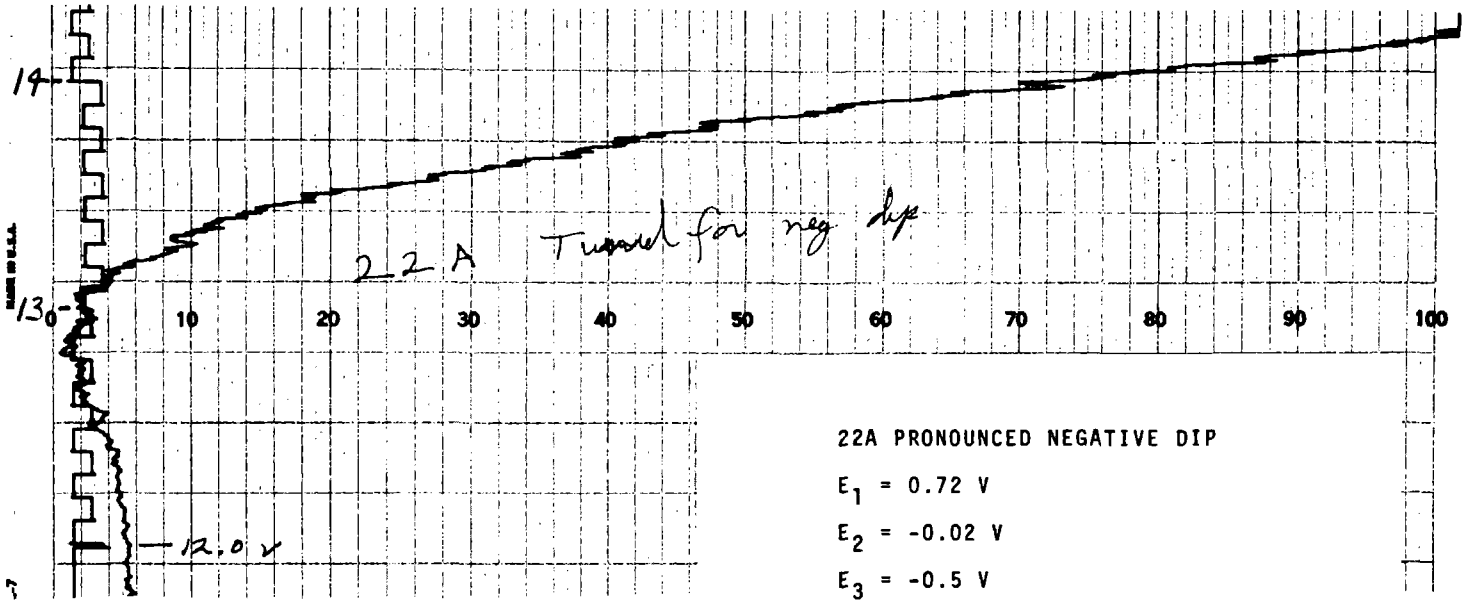
14
13
10
20
30
40
50
60
70
80
90
100
22A Tuned for neg dip
12.0 V
22A PRONOUNCED NEGATIVE DIP
E_1 = 0.72 V
E_2 = -0.02 V
E_3 = -0.5 V
ΔE_2 = -0.05 V
ΔE_3 = -0.1 V

Figure 7

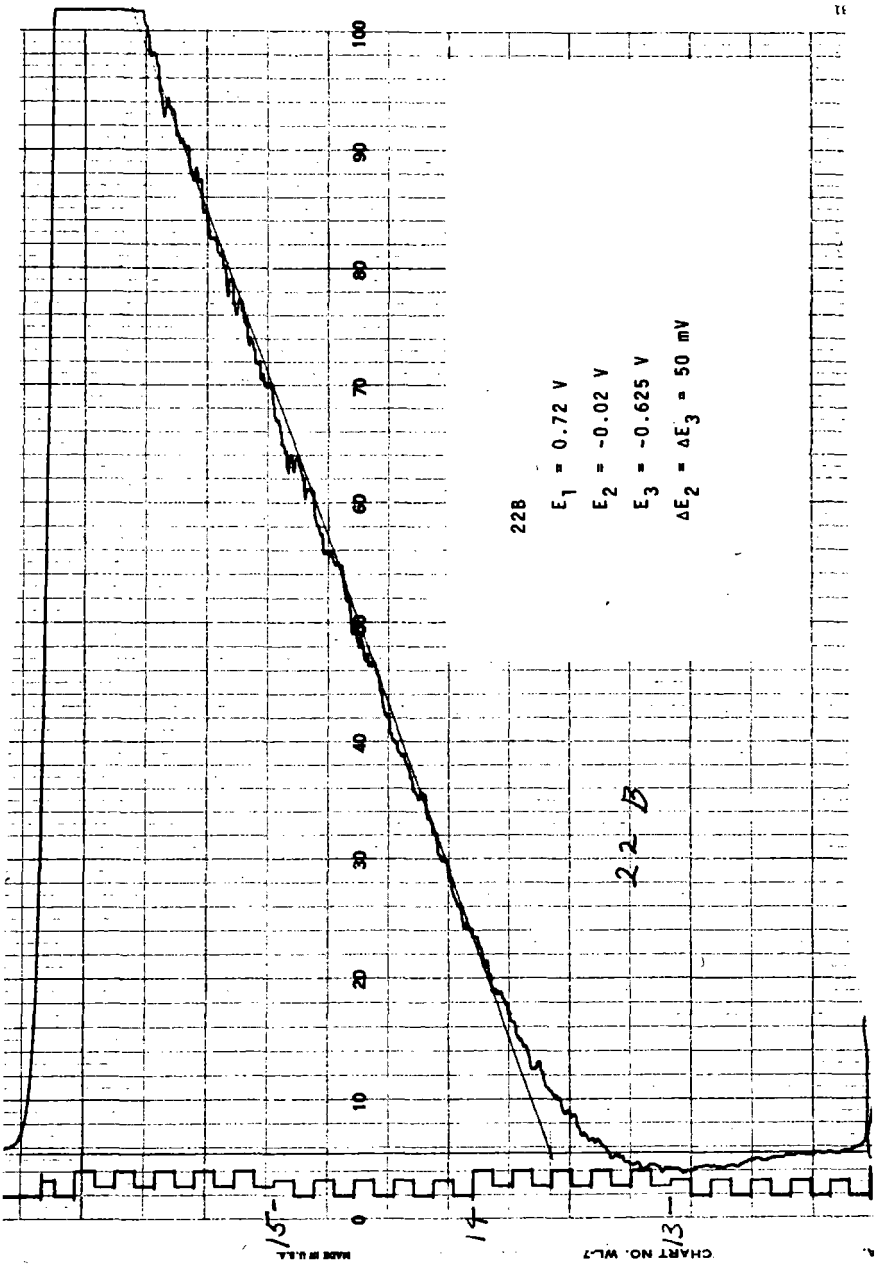
228
E_1 = 0.72 V
E_2 = -0.02 V
E_3 = -0.625 V
$\Delta E_2 = \Delta E_3$ = 50 mV
2.2 B
CHART NO. WL-7

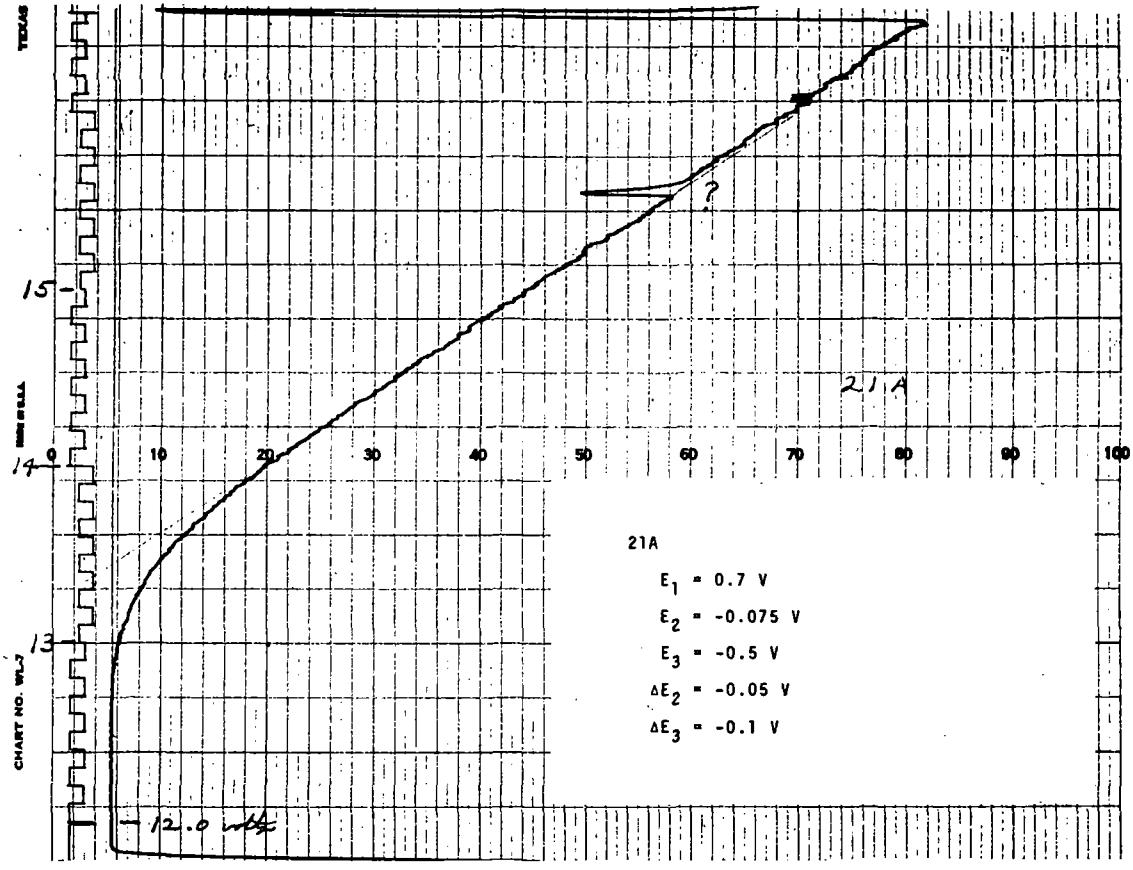
15
14
13
0
10
20
30
40
50
60
70
80
90
100
?
21A
21A
E_1 = 0.7 V
E_2 = -0.075 V
E_3 = -0.5 V
ΔE_2 = -0.05 V
ΔE_3 = -0.1 V
12.0 mA

Figure 9

GC/MS SYSTEM FOR PICOGRAM SAMPLES

D. Damoth, P. McGinnis, G. DeLaney

The Bendix Corporation, Scientific Instruments Plant, Rochester, N. Y. 14603

Analytical instruments today are becoming more sensitive. The GC/MS has progressed from micrograms to nanograms and is now moving into the picogram range. This trend has developed because the GC/MS is being used in areas such as pesticide residues, toxicological analyses, and others. In many of these cases, only very small samples are available, and in other cases, the requirement is to approximate non-destructive testing.

In an effort to meet these sensitivity requirements in a GC/MS, it seemed obvious that, ideally, all of the sample passing through the gas chromatograph should be analyzed by the mass spectrometer. This has been done with capillary columns, but not with packed columns in the 25 standard cc/minute range. The gas flow of 25 std. cc/min. is roughly equivalent to 40,000 liters/second at 10^{-5} Torr. It was clear that to achieve that kind of pumping speed it would be necessary to put the mass spectrometer inside a 48-inch diffusion pump. While these pumps are available, they are a bit expensive for a GC/MS system. Obviously, a large but practical vacuum system was needed. The best choice seemed to be a PBA-100A six-inch unit. This was developed into the MA-015 ion source differential pump. This pumping system has a four-inch gate valve on top of a Freon-cooled baffle, a 6" Convalex-10 charged BlueLine pump, and a 5 cfm mechanical pump. The system is rated at 950 liters/second for air; therefore, it will take over 2,000 liters/second of helium.

To make use of such a pumping speed, the volumetric conductance out of the ion source must be very good. The ion source housing on the MA-2 mass spectrometer is made with 3-1/2" diameter tubing which is adequate, provided the length is kept very short. Both the differential pumping system on the source and the analyzer pump in the MA-2 TOF have a sliding gate valve for rapid access to the vacuum system. Each vacuum system is protected by a GIC-300A Bayard-Alpert gauge. The analyzer pumping system on the MA-2 uses a four-inch PAS-4IC stack with a net speed of 250 liters/second. Figure 1 shows a diagram of the system.

The sample does not see metal from the time it leaves the syringe until after it passes through the ion source. The separate pump on the analyzer maintains a lower pressure in the analyzer because of the baffle between the source and analyzer. Typical pressure readings in the source and analyzer with a 25 cc/minute flow are 2×10^{-5} Torr and 3×10^{-6} Torr.

In a typical procedure the end of the sample delivery tube is aimed directly into the ionization region, and the sample plus carrier gas stream goes through the source into the throat of the MA-015 pumping system. It is this effect, plus a high localized pressure in the source, that allows pumping "40,000 liters/second" with a 2,000 liters/second pump.

An additional benefit of this big pump is that if you want to do high pressure ionization, such as ion-molecule studies, or chemical ionization, the pumping equipment is already in place, and only the source needs to be changed.

The all-glass system, plus the beaming of the total GC effluent into the ion source, are vital points of this high sensitivity technique. Our developmental work on glass jet separators shows that the efficiency of the glass jet is about 1/3 of that of the direct coupled system. Also, the jets seem to have difficulty passing compounds higher than C_{27}, while the direct coupled system does not appear to have an upper limit.

Another reason for the high sensitivity of the GC/MS is the use of multiple ion detection or mass fragmentography. The TOF transmits all of the spectrum to the detector on each repetitive cycle, so some of the advantage of the simultaneous collection efficiency of the Mattauch-Herzog type geometry is obtained. Ultimately, all of the ions on each cycle will be collected when computer technology can provide the necessary 100 megahertz sampling rate.

One of the tests used to determine the sensitivity of this system involves analyzing a mixture of three pesticides by single ion monitoring. Figure 2 shows a part of the results. A sample was prepared that contained one nanogram each of dieldrin, heptachlor and P,P' DDT per microliter. One microliter of this was injected into the GC and a scanner gate was put on mass 99 for heptachlor, mass 79 for dieldrin, and mass 286 for DDT. The result is that the detection limit is well down into the picogram range. Similar or better sensitivity is being obtained on methyl stearate injected on-column.

In summary, a system has been developed which permits picogram range analysis of samples which would otherwise be lost on metal surfaces, and which might have difficulty passing through a separator.

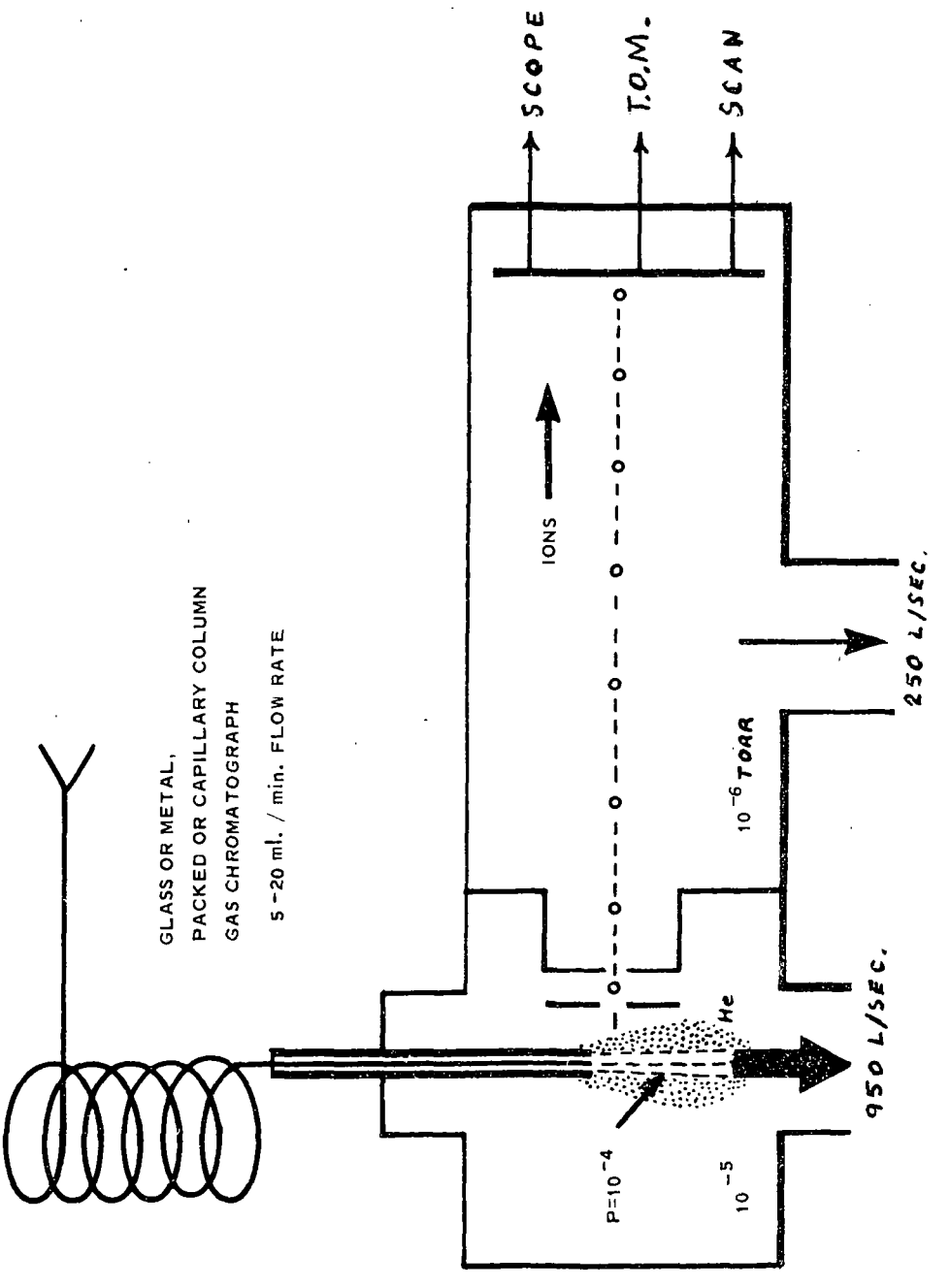

Figure 1 DIRECT COUPLED GC / MS SYSTEM

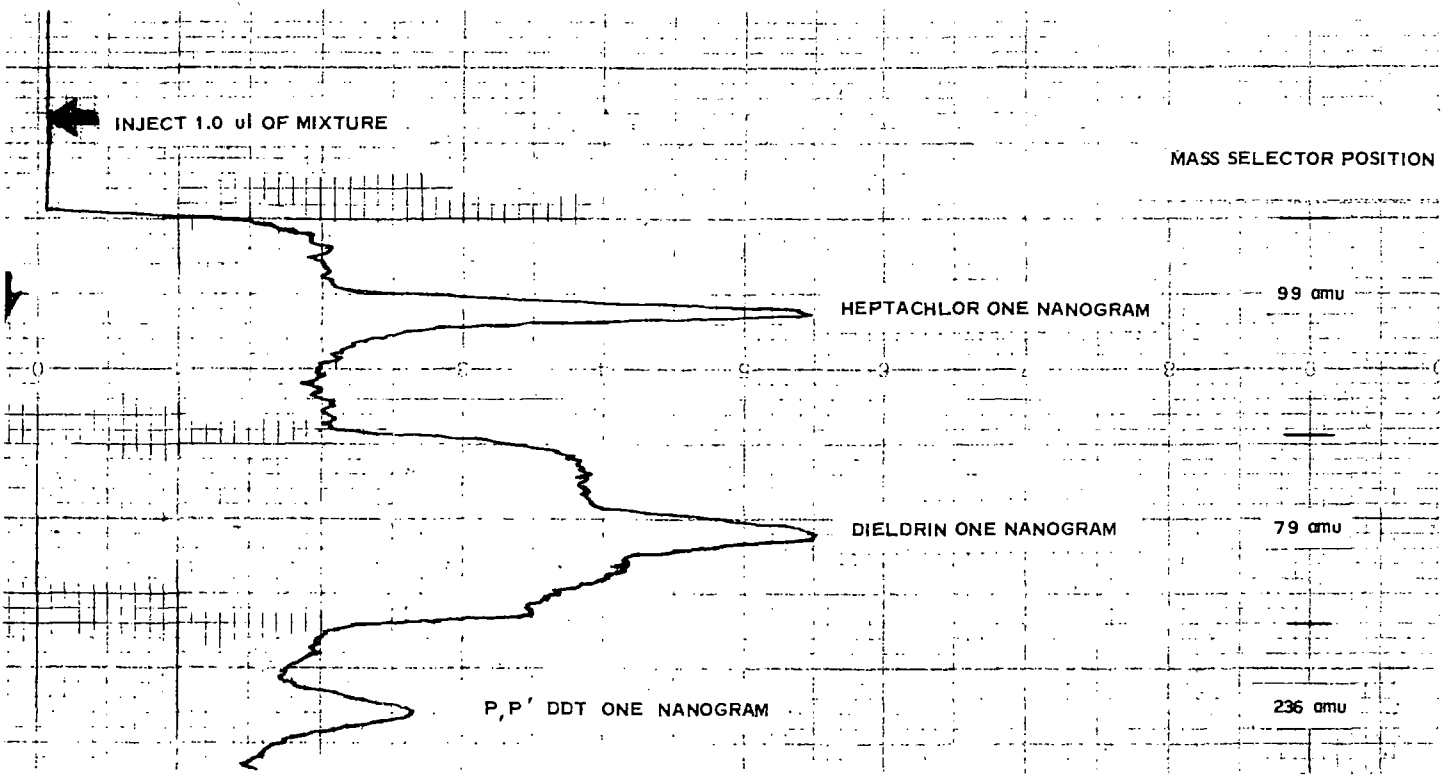

FIGURE 2

Picogram Range Sensitivity on Pesticides

SOLAR: SPECTROMETER FOR ON-LINE ANALYSIS OF RADIONUCLIDES

J. J. Stoffels

Battelle
Pacific Northwest Laboratory
Richland, Washington 99352

A mass spectrometer has been built for on-line analysis of fission product nuclides. The spectrometer ion source is located inside the thermal column of a TRIGA reactor and consists of a high temperature oven containing fissile target material. Fission product nuclides born in the target are thermally ionized and accelerated out of the reactor through a 2.3-meter long flight tube. The flight tube includes two einzel lenses for focusing the beam. Outside the reactor the ion beam is deflected 90 degrees by an electrostatic mirror. The collateral neutron and gamma radiation continue on into a beam stop. Mass analysis of the ions takes place in a 12-inch radius, 60-degree deflection magnetic field. 7.5 degrees of non-normal entry and exit provide some Z-focusing and place the electron multiplier detectors at a greater distance from the neutron and gamma radiation. To reduce the background noise due to buildup of decaying fission products on the first dynode, two multipliers are used and the ion beam is switched between them electrostatically.

A paper describing the SOLAR System in detail will be submitted for publication in Nuclear Instruments and Methods. This work was supported by the DOD Advanced Research Projects Agency.

A New Multiple Specific Ion Detection System, EDWARD M. CHAIT, ROBERT G.BEIMER, CHARLES HULL, Instrument Products Division, E.I. Du Pont de Nemours & Co.(Inc.), Monrovia, California 91016.

The technique of multiple specific ion detection or mass fragmentography has become well established as a method in biomedical research. Under these conditions the sensitivity of a conventional mass spectrometer is increased as much as a thousand fold allowing picogram detection of materials such as catecolamines, prostiglandins and drug metabolites. An apparatus has been developed for a 4" radius 90° sector double focusing mass spectrometer (Du Pont 21-491) which allows switching among four different masses at selectable rates of 4 or 40 peaks a second for the purpose of multiple specific ion detection. Detection sensitivities are well within the picogram range with quantities as small as 10 picograms routinely detected. The instrument produces a 4 channel recorder output which is a smooth curve record of the fragment ion chromatograms. Other applications of such an apparatus include the accurate determination of isotope ratio for materials injected into a gas chromatograph interfaced with the mass spectrometer and the resolution of partially resolved gas chromatographic peaks by removing the effect of interfering peak tails with the specific ion detection ability.

ELECTRO-OPTICAL MULTI-CHANNEL ION DETECTOR FOR A MASS SPECTROMETER

Heinz G. Boettger
Jet Propulsion Laboratory
California Institute of Technology
Pasadena, CA. 91103

ASMS 21st Annual Conference on Mass Spectrometry
and Allied Topics
Paper #T-5
May 25, 1973

For some time we have heard discussions about the relative merits of single ion monitoring vs multiple ion monitoring vs a complete spectrum. We have heard various rationalizations for or against each of these techniques. But, only a complete mass spectrum makes proper use of the full information content which is produced during mass spectrometric analysis of a sample. Then, why are we bothering with single or multiple ion monitoring at all? As we all know, when scanning a mass spectrum, the sensitivity of a given instrument is directly related to the duty cycle. For example, if we scan a spectrum at medium resolution over a range from 12-1000 in 50 sec, each peak is observed for a period of about 1-5 millisec. Thus, the duty cycle is at best

$$E_H = \frac{\text{Peak width}}{\text{Scan Time}} < \frac{5}{50} \times 10^{-3} < 1 \times 10^{-4}$$

In other words, we use less than 100 picograms of a 1 microgram sample. As we decrease the width of the scan and, therefore, increase the duty cycle, we regain this lost sensitivity until we arrive at full sensitivity by monitoring a single peak.

However, in doing this we lose more and more specificity until, in the case of single ion monitoring, we are hoping that the ion that we observe is really part of compound "A" and not all, or at least in part, from some unknown compound "X".

The answer to the problem obviously lies in a mass spectrometer that focuses all the ions of a mass spectrum simultaneously on an integrating detector.

I am not going to revive the old photoplate vs electrical recording controversy. We all know that it takes in the order of 10^3 ions to make a measurable trace as well as all the other pros and cons of both techniques.

I am proposing to take another lesson from our friends in astronomy. More than 50 years ago they gave Lord Aston his first emulsions from which todays ion sensitive plates evolved. During the last few years researchers at Caltech and elsewhere have developed "Vidicon Astronomical Photometers" to replace photographic plates. These "vidicons" are nothing else but television cameras. The same cameras which have just finished taking those spectacular pictures of Mars. It is obvious that, if we can record these pictures on Mars, transmit them to earth, and faithfully reproduce them here, we must be able to record and reproduce the ion image in the focal plane of a mass spectrograph.

Now let us discuss how this task can be accomplished.

Figure 1 shows the well-known configuration of a Mattauch Herzog type mass spectrometer to which a camera system has been added. The latter consists of:

1. an ion-to-electron converter
2. an electron-to-photon converter
3. an image dissector
4. the vidicon camera tube

The ion converter can take one of several forms:

a. It can take the form proposed by May and Wagener which consists of a single electron emitter electrode. Typically, such a device will have a gain factor in the neighborhood of 5 (Fig. 2).

b. One can use a microchannel multiplier array which has a nominal gain of 10^3 in the single stage version and 10^8 in the "Chevron" version (Fig. 3). The generated electrons are accelerated upon a metalized phosphor screen which is coated upon the polished fact plate of the "Image Dissector" (Fig. 4). This device is an assembly of specially formed fiber optics ribbons which converts the long and narrow image format at the focal plane to a nearly square image at the target of the vidicon.

The image is integrated and stored on the target until a sufficient charge has been collected or the sample is exhausted, at which time the signal is read out and processed in conventional fashion. Integration times can be as long as several hours as has been demonstrated in certain astronomical applications while the readout time for a picture frame is in the order of a few seconds or less.

Figure 5 shows a plot of typical peak separation in a Mattauch Herzog type mass spectrometer over the range of m/e 30 to 1000. It shows a minimum separation of ~200 µm at the high mass end of the spectrum. Current state of art channel elements have a geometric resolution in the order of 10-20 micron. Thus our primary goal of unit resolution at an m/e somewhat in excess of 1000 appears guaranteed. Eventually, we hope to achieve enough resolving power for precise mass measurement and resolution of at least 1/5000 which appears quite feasible with todays technology. With satisfactory resolution within our reach, let us turn to the question of sensitivity.

The overall efficiency of the instrument depends on a number of parameters which must be optimized in the design of such a system. These parameters are summarized in Fig. 6. The most important parameters are:

1. Ion-to-Electron Conversion

2. Electron-to-Photon Conversion

3. Attenuation in Fiber Optics to Vidicon Interface

In order to study the effect of the efficiency parameters, we have combined them into the efficiency equation which is presented in Fig. 6.

As mentioned above, we have two primary choices of system configuration. These are an electron multiplier array-ion to electron converter and lense optics to vidicon interface vs single stage converter and direct coupled interface. Both systems have their advantages and disadvantages. Obviously, the multiplier array is capable of much greater gain while it is limited in resolution by the channel size. Similarly, the lense optics interface is capable of higher resolution than a direct coupled fiber interface, but it suffers from high transmission losses. Another factor in favor of a lense optic interface is the ability of operating in combination with mechanical shutter and diaphragm systems for exposure control. This type of system may have advantages over ion-optical exposure control. If we assign the numerical values which are shown in Fig. 7 to the efficiency parameters, we calculate efficiencies of 1.3×10^5 and 1.75×10^6, respectively. The detection limit of state-of-the-art vidicons is 20 m-volt for S/N = 2. Thus, the minimum detectable sample (MDS) becomes

$$MDS = \frac{20}{S}$$

If we substitute the appropriate values for S, the minimum detectable sample becomes 0.1 and 0.01 picogram, respectively.

The above considerations lead to the conclusion that the electro optical multichannel detector system permits the design of a mass spectrometer that combines advantages of electrical detection with the benefits of simultaneous collection and integration of all ions in a focal plane. This will permit us to utilize the entire information content of the sample at a sensitivity which brings us closer to the solution of most of todays mass spectrometric problems.

MASS SPECTROMETER ION OPTICS
AND DETECTOR CONFIGURATION

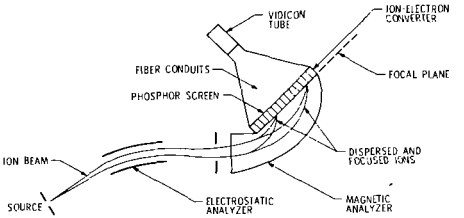

Fig. 1

MULTI CHANNEL ION DETECTOR
OPTION 2

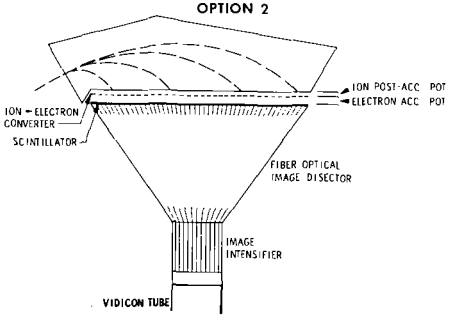

Fig. 2

MULTI CHANNEL ION DETECTOR
OPTION 1

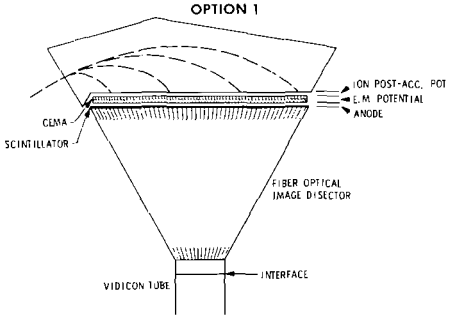

Fig. 3

MASS SPECTROMETER DETECTOR AND SIGNAL CONVERSION SYSTEM

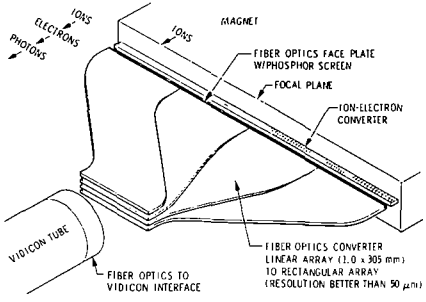

Fig. 4

TYPICAL ION SEPARATION PERFORMANCE

MATTAUCH-HERZOG-ROBINSON GEOMETRY FOCAL PLANE MASS SPECTROMETER

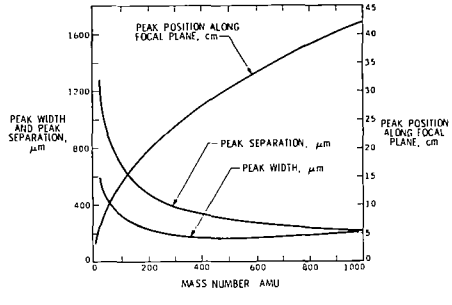

Fig. 5

THRESHOLD SENSITIVITY (S_0)

$$S = \left\{\left[\frac{S_{IS}\, f_{BP}\, T_A}{1.6 \times 10^{-19}}\right] f_{CPA}\right\}\left\{G_{EMT}\, Y_P\, E_{FO}\, E_{LO}\, S_{VID}\right\}$$

WHERE,

- S_{IS} = ION SOURCE SENSITIVITY
- f_{BP} = FRACTION OF ION CURRENT IN BASE PEAK
- T_A = MS ANALYZER TRANSMISSION EFFICIENCY
- f_{CPA} = FRACTIONAL ACTIVE AREA OF ION-ELECTRON CONVERTER
- G_{EMT} = ION TO ELECTRON GAIN OF ION-ELECTRON CONVERTER
- Y_P = ELECTRON TO PHOTON CONVERSION EFFICIENCY AT PHOSPHOR
- E_{FO} = FIBER OPTICS EFFICIENCY
- E_{FVC} = FIBER OPTICS TO VIDICON CONV EFF
- S_{VID} = SENSITIVITY OF VIDICON

Fig. 6

ESTIMATED VALUES OF EFFICIENCY FACTORS

	(CEMA)	SINGLE-STAGE CONVERTER
$S_{IS} \times T_A$	5×10^{-14} coulombs / nanogram	5×10^{-14} coulombs / nanogram
f_{BP}	0.7	0.7
f_{CPA}	0.6	1.0
G_{EMT}	1×10^{4}	5
Y_P	20 photons / electron	20 photons / electron
E_{FO}	0.9	0.9
E_{FVC}	0.05	0.9
S_{VID}	1×10^{-4} millivolts / photon	1×10^{-4} millivolts / photon
	$S_0 = 1.3 \times 10^{5}$ millivolts / nanogram	$S_0 = 1.75 \times 10^{5}$ millivolts / nanogram

Fig. 7

A COMPUTER CONTROLLED MULTIPLE ION DETECTOR

W. H. Holland, B. L. Shore, and W. F. Holmes

Department of Biochemistry and the
Biomedical Computer Laboratory
Washington University School of Medicine
St. Louis, Missouri 63110

A computer controlled variable accelerating voltage source has been designed and constructed using a D-A converter and a high voltage amplifier interfaced to a PDP-12/30 computer. The D-A converter and high voltage amplifier are commercial units complete with internal power supply. The variable voltage source has been attached to an LKB-9000 mass spectrometer, and a program written to acquire data as a multiple ion detector.

The computer interface is constructed from two standard modules sold by the computer manufacturer (Digital Equipment Corp., Maynard, Mass.), and is usable with any PDP-8I or PDP-12 computer. The interface consists of a buffer register with twenty-four output lines along with several trigger pulses for control. This is sufficient for any likely D-A converter, leaving extra lines for potential control of other devices. Twelve input lines are also available. A Fluke 4216A D-A converter with fifteen bit resolution is used so that the entire variable portion of the accelerating voltage can be specified with sufficient precision such that the mass spectrometer can accurately focus on any fragment ion within range. A Kepco NTC-2000 high voltage amplifier is attached to the output of the D-A converter and provides a potential accelerating voltage range of two thousand volts. The range is adjustable by the choice of input resistors. The high voltage amplifier is placed in series with the standard accelerating voltage, which is floated. We have chosen to operate the circuit so that it varies the accelerating voltage between 3-4000 volts, a mass range of about 30%. The standard accelerating voltage for the LKB-9000 is 3500 volts. A low voltage switch can remove the computer and D-A converter from the amplifier input. The rest of the circuit then acts like a fixed accelerating voltage source.

A computer program has been written to make the circuit operate as an eight channel multiple ion detector, with special provision for monitoring drift. A computer display allows the user to type in up to eight exact masses, which are converted to the D-A converter values corresponding to the appropriate accelerating voltages for focussing each mass. Every second all eight of the mass channels are sampled, alloting one hundred milliseconds to each channel. The accelerating voltage is allowed to settle for sixteen milliseconds at each channel. Then the fragment ion intensity signal is sampled over three hundred twenty times, averaged, and stored. During the remaining two hundred milliseconds of each second, any one of the eight mass channels can be scanned by a small computer generated ramp voltage centered around the mass specified. The fragment ion intensity signal is sampled and stored temporarily for display as an aid in monitoring mass spectrometer drift.

The data acquisition described above operates on an interrupt basis, with approximately 50% of the time devoted to acquisition; and 50% to display. The first display shows the result of the voltage scan displayed as a fragment ion peak, intensity versus mass. The slits are adjusted using this display to produce a wide flat-topped peak to minimize the effects of mass spectrometer drift. It has been possible to work routinely above mass 500 with only occasional adjustments of the magnet focus knob on the mass spectrometer, generally between GC runs. The system has been used almost exclusively for GC analysis.

The second display shows the intensity signal versus time of any three of the masses for the past five minutes. The mass channels that are displayed can be changed at any time during or after data acquisition. Two movable pointers on the display allow selection of GC peaks for a printout of mass, time, peak height, peak area and the background. The latter is selected by a movable line on the display. The clock time since the beginning of the experiment is visible on both displays and stored with the data. A revision of the program nearly completed allows for storage on magnetic tape, and output on an incremental or electrostatic plotter.

A full description of this work along with experimental results has been submitted to Analytical Chemistry.

ION COUNTING WITH PEAK SWITCHING

BY CHARLES M. JUDSON

SSR INSTRUMENTS CO.
Santa Monica, California

The subject of this paper is the use of ion counting with a mass spectrometer operated in the peak switching mode, that is with the mass spectrometer repetitively stepping from one to another of some small number of mass peaks.

The common uses of peak switching are the following:

1. Isotope ratio measurement;
2. Component ratio measurement;
3. Multiple ion detection;
4. Integrated multiple ion detection;
5. Precise mass measurement.

Precise mass measurement involves determining the center of a mass peak rather than its intensity, and is essentially different from the first four applications. It is listed only to note that peak switching controls provided for precise mass measurement may be useful for other applications of peak switching. For other applications where peak intensities are measured, however, there is a common advantage in the use of ion counting to optimize precision of measurement.

I am going to consider primarily isotope ratio measurement, where precision of the ratio is the primary consideration of the measurement, and multiple ion detection in gas chromatography applications, where detection of small fluctuations in background also requires optimum precision.

Component ratio measurement is listed to note that ratios are of interest for quantitative analysis of components as well as for isotopes, and that ratio measurements are used in spark and secondary ion analysis as well as with instruments using electron bombardment sources

Integrated multiple ion detection is a method which has been described by Majer for trace detection in a sample evaporated from a direct introduction probe, the ion current for a few masses being integrated over the entire evaporation time. This method also could be used for other methods of introduction, the advantage of integration over the entire sample period not being limited to systems with direct introduction probes.

The system of hardware used is shown in Figure 1. The mass spectrometer was a UTI model 100C quadrupole, fitted with a channeltron multiplier. The ion counting equipment was equipment manufactured by SSR Instruments Co., a model 1120 amplifier-discriminator, and a model 1108 or 1110 scaler. The model 1110 permits time averaging of two peaks, but is limited to a 3 decimal floating point readout. The model 1108 has an 8 decimal fixed point readout, but does not have internal capacity for time averaging. The peak switching and control of the scaler were performed manually, but the object was to show the performance which would be obtained with an automatic switching control. The data were recorded in digital form with a printer, but for practical use in multiple ion detection, the scaler would presumably also be equipped with a D/A converter for analog recording.

There are two reasons for using ion counting in a peak switching system. The first is that ion counting measurements can provide precision limited only by statistical limitations of the random nature of the ion arrivals, which is the best precision which can be obtained by any method when a small current must be measured in a short time. The second is that ratios can be conveniently time averaged in an ion counting system, integrating each peak over several switching cycles, which is required for precise measurement of ratios of quantities which are changing during the measurement. Time averaging does not require ion counting, but ion counting offers a convenient method for obtaining time averaged measurements.

Figure 2 shows data obtained for the precision of ten successive measurements of an argon or carbon dioxide mass peak. The probable error from the observed deviations from the average is compared with the probable error from theory. These experiments were made with counts per measurement time varying from 10 counts to 10^7 counts, and for measurement times of 10 seconds or less. The results fit the theoretical line which predicts a probable error of 0.67 / N where N is the number of counts, except in the region between 0.1% and 0.01% where the errors are larger than theoretical. This tells us that we do not have any sources of drift or noise other than the statistical noise until we get to precisions of a few hundredths of a percent.

These are measurements of a single peak. Precision for ratio measurements was only slightly better. The limitation was apparently due to drift of the mass scale. The mass scale control used did not have a fine adjustment so that the peaks were not precisely centered. Further, no special adjustment of the quadrupole was made to attempt to obtain flat top peaks.

Under these conditions the two peaks were found to drift at different rates. The control voltage, however, was very stable, even on the sides of the peaks, accounting for the remarkably good precision obtained in spite of the fact that the peaks were not precisely centered.

With better peak centering or flatter peaks, or with integration across the peaks or across the tops of the peaks, it seems reasonable to expect that 0.01% precision in ratios could be obtained.

There is nothing novel in measuring isotope ratios by time averaged ion counting, and I have in fact not made any measurements comparing ratios with standard ratios. It is, however, apparently novel to use a quadrupole for precision measurement of isotope ratios. The only reference I find in the literature to measurement of isotope ratios in quadrupoles is a paper by Yinon and Klein at the Weizman Institute in which 0.5% precision was obtained using sample and hold amplifiers, although there is probably other unpublished work involving isotope ratios with quadrupoles.

I do have a proposal which I believe is novel, but which has not been tested experimentally, for obtaining high precision with ion counting when the values of the ratio are large. Because count rates for the large peak is limited by the coincidence error, while the precision of the ratio is limited by the total number of counts for the small peak, counting times may become prohibitively long for high precision when the ratios are large. My experiments were done with the 45/46 ratio which is a small number, but one commonly needs to measure much larger ratios.

The proposal is to switch sensitivities at the same time we switch masses. To show the advantage of such sensitivity switching, assume an isotope ratio of 100. If we wish to obtain a precision of 0.01%, we must limit the number of coincidences to 1% of the count at most. With a short dead time of 10 nanoseconds, this means a maximum count rate of 10^6 counts/second for the large peak and 10^4 counts/second for the small peak. Since 0.01% precision requires of the order of 10^8 counts, the measurement will take 10^4 seconds which is an unreasonably long time.

However, if we switch sensitivities as we switch masses, so that both peaks have approximately the same count rates, we can reduce the measurement time by a factor of 100 to 100 seconds which is a quite reasonable time. Whether the maximum allowed count rate is 10^6 counts/second or more or less, sensitivity switching reduces the time by the value of the isotope ratio. The required control of sensitivity can probably be most easily made by control of source voltages, adjusting the accelerating, repeller or focus voltage.

I will now turn to the application of ion counting to multiple ion detection. The point of multiple ion detection is to measure only a few pre-selected peaks so as to get maximum precision for detecting small changes in peak intensity, and the requirement of optimum precision is just as important as in isotope ratios.

Figures 3 and 4 show simulated analog records of small signals, calculated from measured digital values. Figure 3 shows, at the bottom, a background of 400 counts/time interval, with a simulated square GC peak causing a 20% increase in the background level. I have shown the record as it would appear with an undamped recorder connected to the A/D output of the scaler. This is clearly a detectable peak, several times the minimum detectable peak.

In the upper plot in Figure 3, we see what happens if we increase the measurement time from 1/10 of a GC peak width to 1/2 of a GC peak width. With longer measurement times we have more counts and a higher precision, but when the measurement time approaches a peak width we distort the information about the time the peak occurred. This effect would be similar with a damped recorder giving a smoothed curve, or with a real GC peak which of course is not square.

In Figure 4 we see in the upper portion two equal GC peaks being recorded, with peak B displaced by 1/5 of a peak width from peak A. With 10 sample intervals per peak width, we can clearly see that peaks A and B are displaced and can estimate the displacement. The lower two records show the same data with 5 times longer sample intervals. In this case there is again increased sensitivity, but we see that there is some doubt about the relative times at which these peaks occurred.

The conclusion drawn from these simulated multiple ion detection plots is that the response time of a multiple ion detection system, whether determined by a counting integration time or a recorder response time, can approach the GC peak width if peak detection is the sole criterion, but if detection of unresolved GC peaks is an objective, the response time must be shorter than the peak resolution time sought.

It may be interesting to obtain simultaneously mass chromatograms for both short and long response times, with the idea of using the short time measurements for detecting unresolved GC peaks, and the long time for detecting the smallest peaks, accepting that we cannot detect small position shifts in the smallest peaks. This could be done with two recorders per peak, or by storing digital data in a computer and playing it back with variable integration times.

In summary, evaluation of the precision of successive measurements using a quadrupole in the peak switching mode with ion counting showed that the theoretical limiting precision was obtained over a wide range of count rates. Approaches to further improvement in the precision were identified. Where ion current and measurement time are both limited, ion counting measurements will generally be as precise as any measurements can be, and measurements using current measurement rather than ion counting should be tested to show to what extent the precision of current measurements is lowered by additional noise sources.

Applications to isotope ratio and multiple ion detection measurements have been considered. Novel suggestions involving sensitivity switching for isotope ratio measurements and use of parallel measurements for short and long detection times in multiple ion detection have been made.

The author thanks the SSR Instruments Co. for support of this work which was carried out under a consulting contract with that company, and UTI and Jim Burden of that company for providing a mass spectrometer and assisting with the measurements.

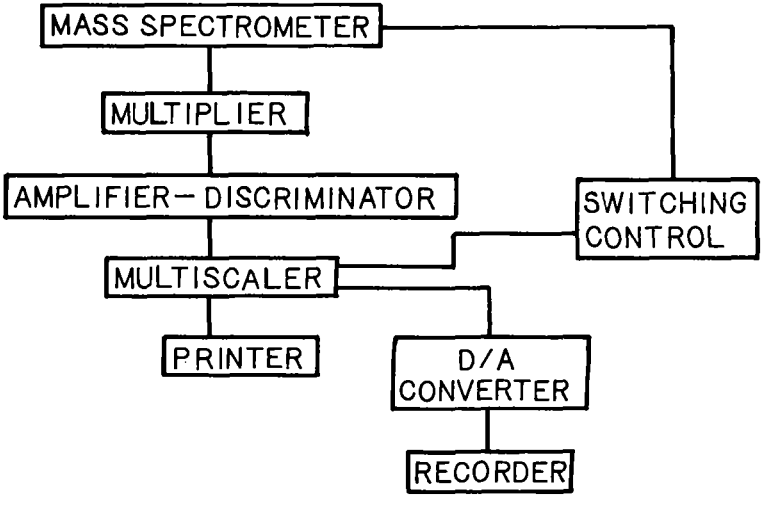

FIGURE 1

System Block Diagram

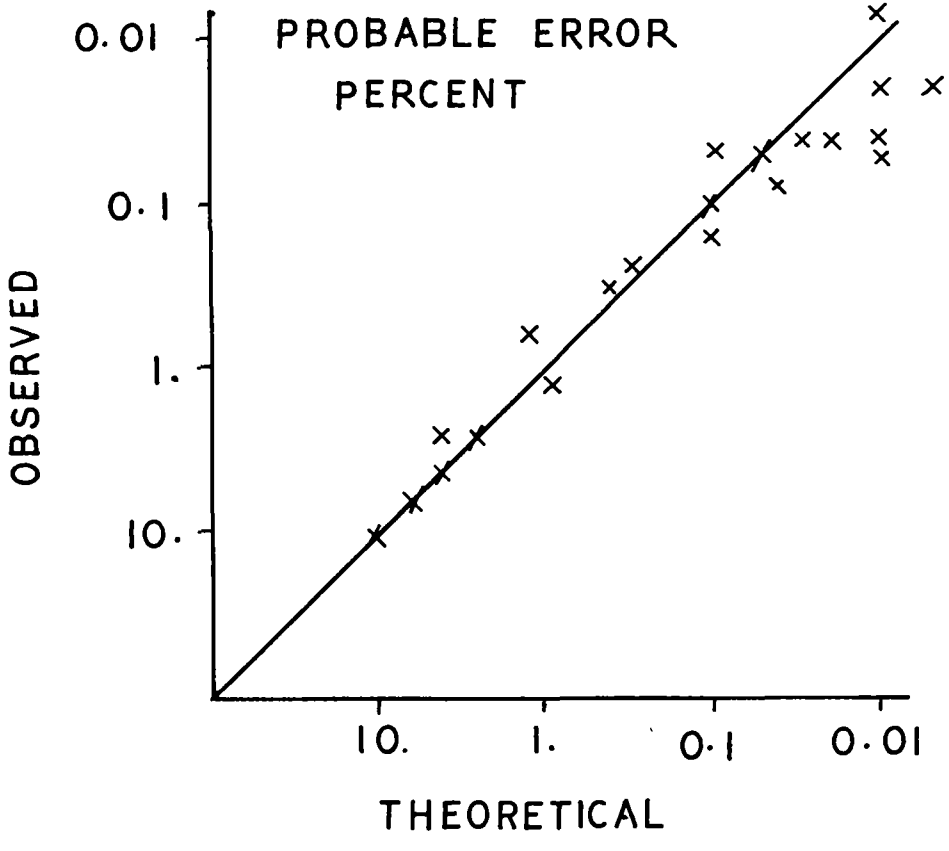

FIGURE 2

Percent probable error for measurements of a single mass peak.

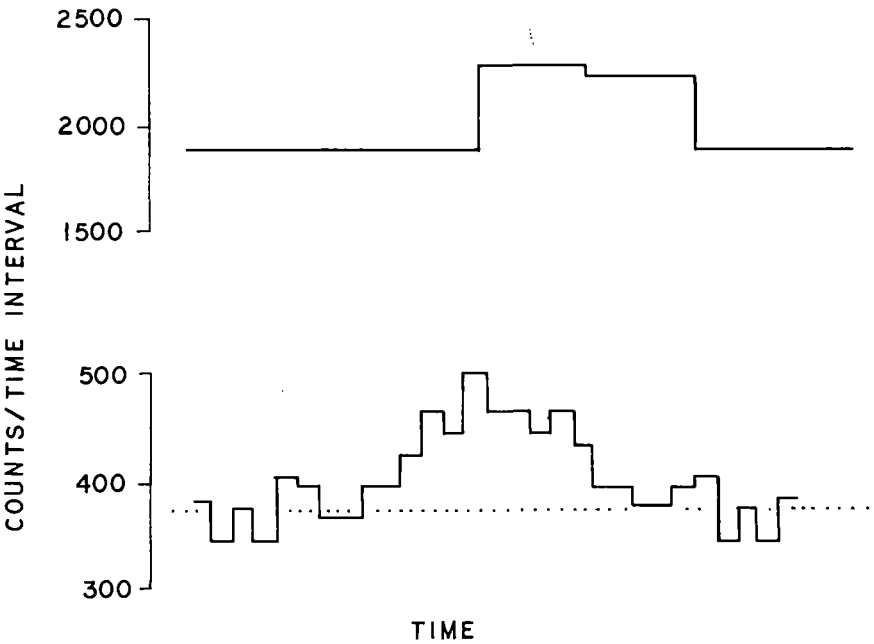

FIGURE 3

Small signal analog recordings for measurement times of 1/2 (upper) and 1/10 of a GC peak width.

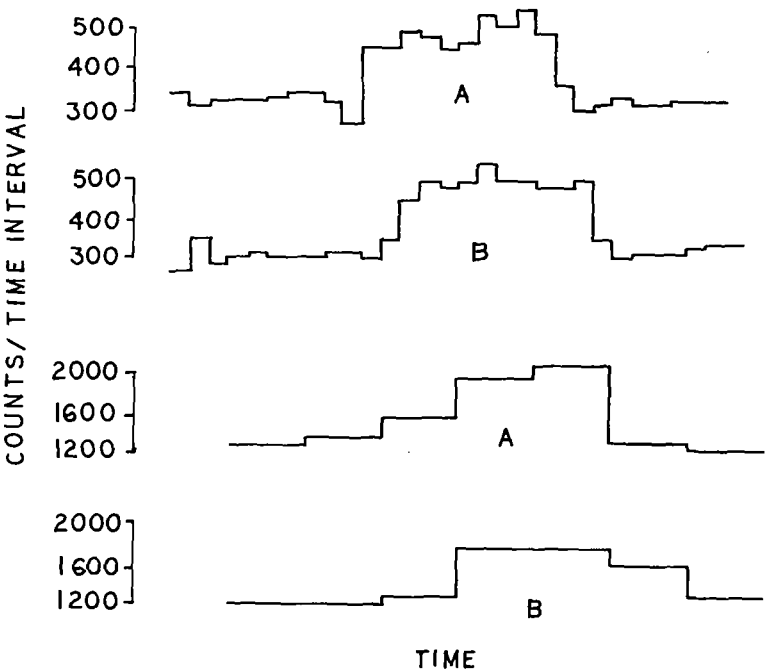

FIGURE 4

Equal GC peaks (A,B) with small time separation (upper) which vanishes at five times longer sample time (lower).

MULTIPOINT FIELD IONIZATION SOURCE DEVELOPMENTS*

W. Aberth, C. A. Spindt, and R. R. Sperry

Stanford Research Institute
Menlo Park, California 94025

More detailed evaluations and a number of improvements have been performed on the multipoint field ionization source since it was last reported.[1] These improvements, involving both the fabrication of the multipoint structure and the techniques for sample handling, have improved performance reliability and have broadened the range of applications for field ionization.

Briefly, the multipoint structure consists of a uniform array of points about 40 microns high and spaced 25 microns apart. They are formed on a porous substrate over an area of about 1 mm^2. Initially, a 65% dense sintered tungsten wafer about 250 microns thick was used for the porous substrate. This was brazed on the end of a 1/8" diameter molybdenum tube prior to forming the multipoint array. Although this type of porous substrate field ionization source[1] yielded usable ion beams, a number of drawbacks were encountered with the substrate structure. The structure itself requires special machining and brazing capabilities and is expensive to produce. Its porosity is often highly non-uniform with the major sample gas passage occurring through a few channels and the perimeter seam thus preventing uniform ionization by the points; the rough surface consistant with the porous structure caused the loss of a number of points and prevented uniformity in point heights. Figure 1 is a scanning electron micrograph of such a structure after about 1,000 hours of operation with a large variety of both organic and inorganic samples. Note the presence of micro needles on some of the points. These needles were grown by a toluene activation procedure described by Beckey.[2] The uneven distribution of micro needles on the points is caused by the nonuniform distribution of sample gas leak and the unevenness in point heights.

An improvement on the porous tungsten substrate utilizes a 400 line/cm grid for the multipoint support. In this structure the grid is supported on a hollow molybdenum tube by a press fitted ring. The field ionizing points are then formed on the intersecting portions of the grid wires. Figure 2 shows a scanning micrograph of a grid supported point structure. These points, spaced 25 microns apart, are 40 microns high and cover an area of about 1 mm^2.

In order to handle samples of both high and low volatility, a source structure was designed capable of rapidly switching different solid samples and converting to the gas sampling mode. Figure 3 is a cross section of the source. A solid sample contained in a sample holder (shown at the bottom of Figure 3) can be inserted from the outside through a vacuum lock into the back of the ion source. Heating of the

*Sponsored in part by the National Cancer Institute, National Institutes of Health, Grant # 1 RO1 CA 12213-01 RAD.

sample is accomplished with two heating cartridges inserted into the base of the source structure. A temperature of 400°C can be reached in about 20 minutes. Replacing the solid sample holder with a ceramic tube which communicates with an externally located gas sample allows the source to handle volatile gases. Thus conversion can be completed in a few minutes while maintaining the source at a high vacuum.

A major difficulty in obtaining high mass resolution with the present source arises from the relatively large size of the field ionizing region. Masking this region, which is about 750 microns in diameter, with a slit aperture potentially increases the mass spectrometric resolving capability of the source but results in a corresponding loss of beam intensity. A new source has been constructed and is currently under test, which may overcome these difficulties. This source (see Figure 4) contains two grids which are parallel and registered with respect to each other and the multipoint array. Figure 5a illustrates the diverging nature of the ion stream produced from each point as it leaves the grid, when only a single grid is used. In the new source, Figure 5b, the grid closest to the points has its potential adjusted to produce the necessary field ionization. The potential of the second grid produces a decelerating ion focusing field in the region between the grids. Thus ions emerging from the second grid are focused by the lens action of the grid holes to leave perpendicular to the grid surface. These ions can then be focused to a sharp point by a simple aperture lens. This new cross-over point can be used as the effective ion source of the mass spectrometer and should produce increased resolution and sensitivity.

REFERENCES:

[1] W. Aberth, C. A. Spindt, and R. R. Sperry, 20th Annual Conference on Mass Spectrometry and Allied Topics, Dallas, Texas (1972) p. 249.

[2] H. D. Beckey, S. Blöching, M. D. Migahed, E. Ochterbeck, and H. R. Schulten, Int. J. Mass Spectrom. Ion Phys. 8, 169 (1972).

SA-1977-26

FIGURE 1 SCANNING ELECTRON MICROGRAPH OF A MULTIPOINT FIELD IONIZATION SOURCE AFTER ABOUT 1000 HOURS OF OPERATION

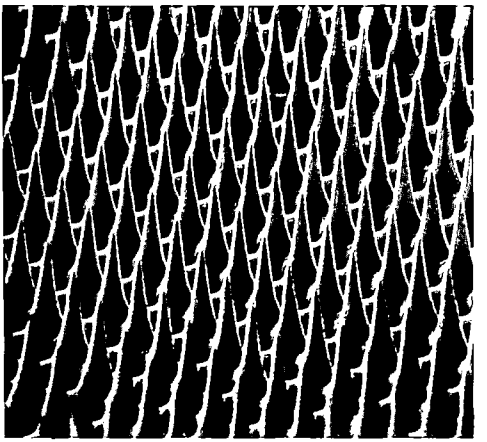

SA-1977-25

FIGURE 2 SCANNING ELECTRON MICROGRAPH OF NEW MULTIPOINT STRUCTURE

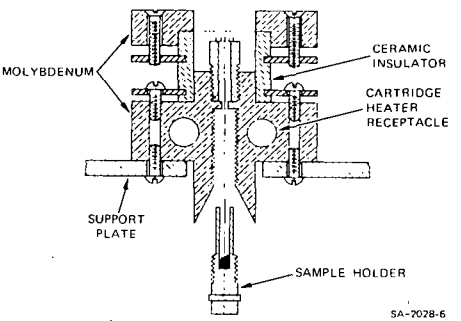

FIGURE 3 SCHEMATIC CROSS SECTION OF A MULTIPOINT SOURCE SHOWING METHOD OF INTRODUCING A SOLID SAMPLE AND HEATING TECHNIQUE

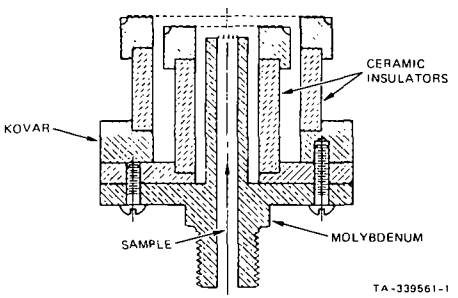

FIGURE 4 SCHEMATIC CROSS SECTION OF NEW TYPE OF SOURCE UNDER DEVELOPMENT.

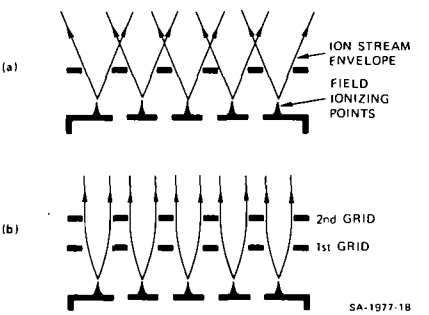

FIGURE 5 ILLUSTRATION OF FOCUSING EFFECT OF DOUBLE GRID. (a) Highly diverging ion streams that result from a single grid source. (b) The effect of the second grid acting as multiple decelerating lens focuses the diverging ion stream. A large lens (not shown) can then form the parallel moving ions into a sharp object for the mass spectrometer.

INTERFACING MULTIPOINT FIELD IONIZERS WITH QUADRUPOLE MASS FILTERS

H. L. Brown, W. H. Aberth and M. Anbar
Mass Spectrometry Development Group
Stanford Research Institute
Menlo Park, California 94025

Within the framework of our research program on multipoint field ionization sources, we have tried to interface such a source with a quadrupole mass analyzer. The quadrupole is one of the most popular analyzers, and its rapid sweep rate make it highly desirable as a fragmentation-free analytic instrument. The results were not encouraging at first because of a persistent fast increase in the background at the lower end of the mass spectrum. This feature was observed with different multipoint field ionization sources and with two different types of quadrupole analyzers when the apparatus was arranged as in Figure 1. The quadrupole shown is an Extranuclear Laboratories Model 270-9 mass filter (16.00 mm rods, 22 cm long) with a SRI multipoint field ionizer mounted in lieu of the electron impact ionizer and with a paraxial particle multiplier. The instrument can be operated in a manual or programmed mass sweep mode. In the latter case a TMC CAT 1000 is utilized in the multiscaling mode to accumulate data from many passes through the portion of the mass spectrum to be studied. The accumulated data is then plotted by a X-Y recorder. The multipoint field ionizers used had copper points deposited on a sintered tungsten substrate and an alumina backed nickel grid. The ionizers were activated with toluene and were observed to function normally in other mass spectrometers. Likewise the mass filter was known to operate normally with an electron impact ionizer. When the field ionization source was interfaced with the quadrupole, however, we found the unusual feature visible at low masses in Figures 2 and 3, where the gas introduced into the ionizer was iso-octane and toluene respectively. Features of this type were observed in varying degrees in any sample. (To date only hydrocarbons have been studied.) It was of interest, therefore, to understand this phenomenon and to eliminate it from the spectrum.

As shown in Figure 3 this clutter increases with increasing ionization voltage (3.0 kV, 3.5 kV, and 4.0 kV). This dependence was shown to result from total ion production (as opposed to an instrumental effect related to the applied potential) by also varying the ionizer gas pressure at a fixed voltage. The feature was thus found to be approximately linearly dependent on total ion production.

Next we made the particle multiplier's high voltage much more negative than the field ionization grid voltage to eliminate the possibility that the feature is due to scattered electrons. This procedure confirmed that only positive ions entered the multiplier. At the same time we grounded the points and put a positive D.C. bias on the quadrupole rods which completely removed the parent ion from the spectrum but the base line feature still remained. By throttling the pump while in this configuration, the background pressure was varied over two orders of magnitude, but no noticeable change was noted in the spectrum. From this we concluded that this effect could only be due

to species which leave the field ionization source as neutrals and are converted to ions by a unimolecular process within the quadrupole itself.

To check this hypothesis, the apparatus was modified as shown in Figure 4. In this configuration ions produced by the source are deflected from the axis of the ionizer and onto the axis of the quadrupole, but neutrals leaving the source cannot enter the quadrupole except by multiple scattering events.

The results of this modification can be seen in Figures 5 and 6. The ion at mass 92 is from toluene. At masses 57, 100, and 114 are the fragment and parent ions of isooctane. From the data shown in Figure 5, it is apparent that the absence of the low mass clutter is actually due to the elimination of the neutral beam component and not due to mass discrimination as a result of tuning the system at the parent ion mass. This was also confirmed by additional experiments where artificial markers were introduced to the spectrum at low masses.

The effect is believed to arise from high velocity grazing collisions of the parent ion with the screen. When the ion strikes the surface it breaks up into fast neutral fragments some of which are highly excited. In a linear arrangement, these fragments can enter the quadrupole where they are subjected to a high field. Some of these neutral fragments are sufficiently excited for the field to induce autoionization in the field, leaving a high velocity ion which has too short a residence time in the quadrupole to be fully resolved, but which is subsequently detected by the particle multiplier. The result is a very broad feature (or features) as masses lower than the parent ion.

A similar effect has been observed in H_2 by Chupka and Berkowitz[1] for high Rydberg states which are near the ionization threshold. They found that one of these states, which has a long lifetime against spontaneous autoionization, can be induced to autoionize by relatively weak electric fields (on the order of 15 V/cm) and that still another state requires higher fields. Autoionization can have efficiencies approaching unity, but in our case even an efficiency of a few percent is sufficient to produce the low mass feature due to the substantial fraction of initial ions which collide with the grid structure. Normal autoionization or metastable decay is probably not the cause of the phenomenon we observed since these states usually have very short lifetimes and decay within the source or very close to the grid, resulting in fragment ions which would be resolved by the quadrupole. Another possible mode for this conversion of the neutrals to ions is that the neutral may be in a superexcited state above the ionization threshold and that the transition to the ionic state is induced by eigenstate mixing in the electric field. Analogous to the situation pointed out by Falick[2] for the case of normal metastable ion decomposition, observation of these phenomena are critically dependent on the particular potential arrangement of the mass spectrometer and, therefore, may not be observed by magnetic sector instruments unless an effort is made to do so.

Our production hypothesis was checked in two ways. First, the results of using a screen of higher transparency are shown in Figures 7 and 8. To obtain these data, the ion source, deflector system and quadrupole were made coaxial. The transmission of the 1000-mesh screen was 48% and that of the 250-mesh screen was 70%. One observes a decrease of neutral fragmentation with the increased transmission as expected. Secondly, while monitoring the low mass clutter with the deflectors, field ionization source, and quadrupole coaxial, we put 4.6 kV/cm field between deflector plates and observed the disappearance of the clutter as shown in Figure 9. Here the upper spectrum is the usual spectrum and the lower occurs because the excited neutral is induced to ionize in field between the deflectors just as the same excited neutrals could be induced to ionize inside the quadrupole. Since the field between the deflector plates also sweeps out the ions formed, the low mass clutter disappears as shown on the lower trace in Figure 9.

An additional benefit of the offset method of eliminating the neutral beam was an apparent increase in resolution, Figure 10 shows the toluene isotopes 92^{-+} and 93^{-+} for the directly mounted source and Figure 11 shows the same ions with the neutral beam eliminated. This improvement is probably due to both the improved signal-to-noise ratio and also to better energy definition due to the energy selection properties of the deflector plate set.

In conclusion, we have succeeded in interfacing a field ionization source with a quadrupole mass filter by the elimination of the undesirable low mass clutter while preserving the ion spectrum produced by the field ionization source and have simultaneously improved the resolution of the instrument.

REFERENCES:

[1] W. A. Chupka and J. Berkowitz, J. Chem Phys. 51, 4244 (1969).

[2] A. M. Falick, P. J. Derrick, and A. L. Burlingame, 21st Annual Conference on Mass Spectrometry and Allied Topics, San Francisco (May, 1973) p. _____.

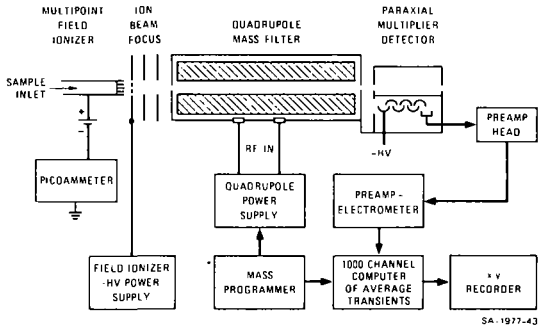

FIGURE 1 FIELD IONIZATION SOURCE—QUADRUPOLE SYSTEM

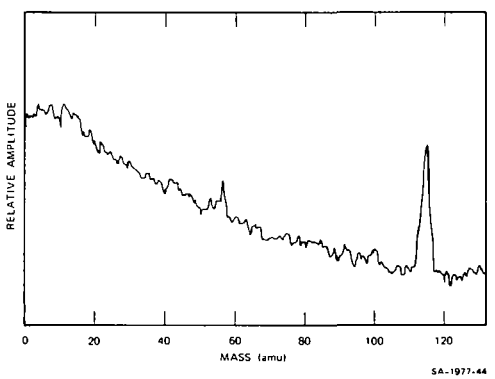

FIGURE 2 ISO-OCTANE SPECTRUM FOR DIRECTLY MOUNTED SOURCE

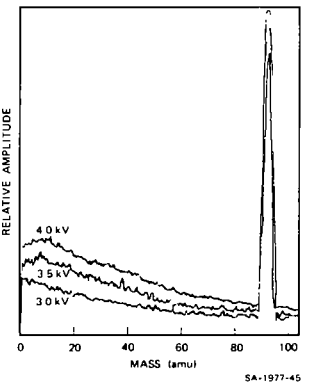

FIGURE 3 TOLUENE SPECTRUM FOR DIRECTLY MOUNTED SOURCE

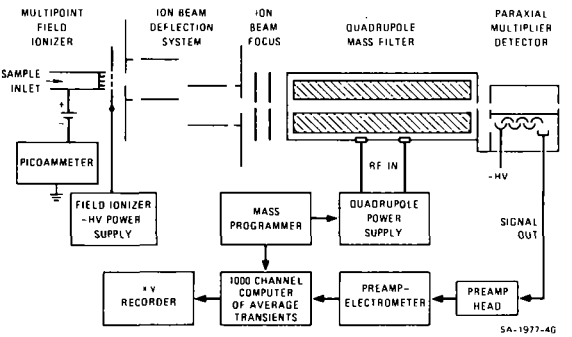

FIGURE 4 FIELD IONIZATION SOURCE—DEFLECTOR PLATE—QUADRUPOLE SYSTEM

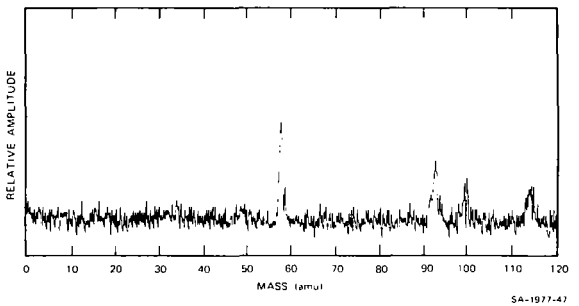

FIGURE 5 ISO-OCTANE WITH OFFSET SOURCE

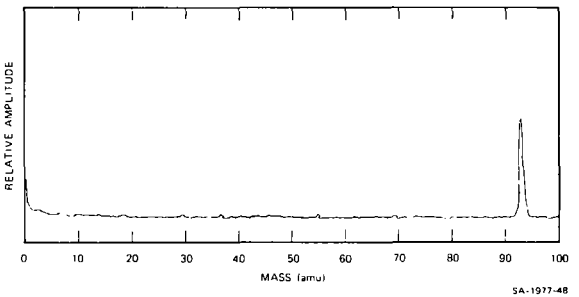

FIGURE 6 TOLUENE WITH OFFSET SOURCE

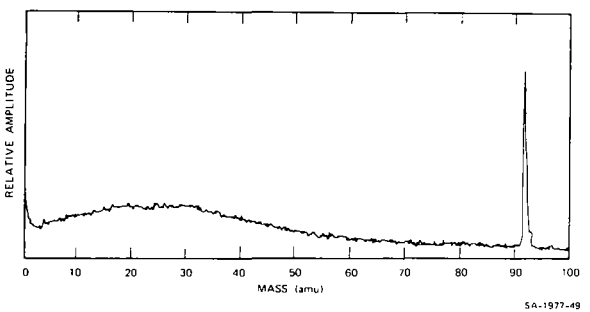

FIGURE 7 UNDEFLECTED TOLUENE FROM 1000-MESH SCREEN

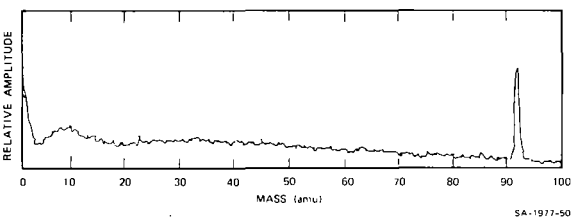

FIGURE 8 UNDEFLECTED TOLUENE FROM 250-MESH SCREEN

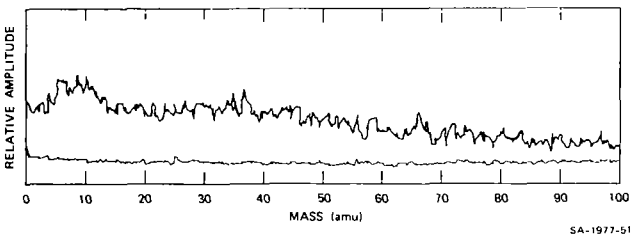

FIGURE 9 UNDEFLECTED TOLUENE WITH AND WITHOUT PLATE VOLTAGE

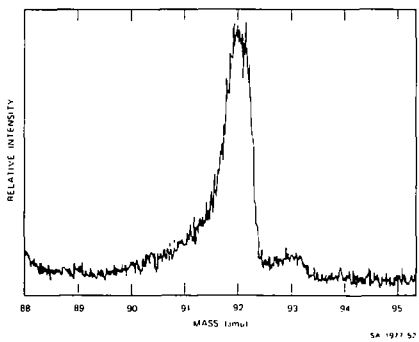

FIGURE 10 TOLUENE RESOLUTION WITH DIRECTLY MOUNTED SOURCE

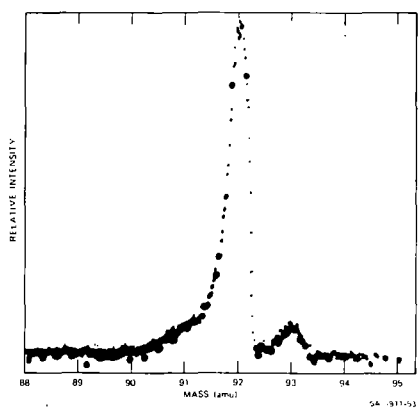

FIGURE 11 TOLUENE RESOLUTION WITH OFFSET SOURCE

Space and Energy Focusing in Time-of-Flight Mass Spectrometers of Various Geometries

Ronald P. Stein

Department of Physics, The Pennsylvania State University
University Park, Pennsylvania 16802

It is generally known that the main factor preventing an increase in the resolution of the conventional two-field time of flight mass spectrometer is the spread in the initial ion energies[1-5]. In fact, an instrument 4.4 cm long could have a resolving power of about 1500 if there were no spread in the initial energy of the ions[6,7]. Using cylindrical and spherical geometries with radial ion paths does not significantly alter the situation. In order to improve the resolution it becomes necessary to find a way of time focusing the ions of differing initial energies. A general equation describing space and velocity focusing with respect to time is presented. This equation is used to develop resolution and resolving power equations for two classes of linear time of flight mass spectrometers.

Space and Velocity Focusing

When particles with zero initial kinetic energy start at different positions in a force field and arrive at the same time, all at the same time, the particles are said to be perfectly space focused. Mathematically this can be expressed as $\partial T/\partial x_0 = 0$, where T is the total flight time and x_0 is the starting position. When particles start at the same point with different initial velocities in a force field and arrive at the same point all at the same time, the particles are said to be perfectly velocity focused. Similarly, this can be expressed as $\partial T/\partial v_0 = 0$ where v_0 is the initial velocity. Numerical analysis shows that it is possible in theory to have velocity focusing in the normal two field time-of-flight mass spectrometer. In order to do this, it is necessary to have the ions' initial velocities away from the collector and to have the source electric field increased considerably. In addition, numerical analysis tends to indicate that it is not possible to have space and velocity focusing simultaneously in a linear instrument. In the next section, it will be shown that this simultaneous focusing is impossible.

Focusing Equation

A particle starts at an arbitrary point, x_0, with an initial velocity v_0, as shown in Figure 1. If the forces acting on the particle are conservative, and if we consider the one dimensional case, then the time of flight, T, of the particle is given by:

$$T = \pm (m/2)^{1/2} \int_{x_0}^{x'} \frac{dx}{\left(1/2\ mv_0^2 + V(x_0) - V(x)\right)^{1/2}} \qquad \text{(Time of Flight Equation)}$$

where:

m = particle mass.
F_0 = force on the particle at x_0.
x' = final particle position (fixed collector).
V(x) = particle potential at x.

It can tnen be shown, by taking derivatives under the integral sign, and by careful analysis where the argument of the integral goes to infinity, that:

$$v_0 \frac{\partial T}{\partial x_0} + \frac{F_0}{m} \frac{\partial T}{\partial v_0} + 1 = 0 \qquad \text{(Focusing Equation)}$$

This equation is very powerful because it describes a relationship between the space and velocity focusing independent of the forces the particle experiences after the flight has started! Notice that the equation contains only the force the particle experiences at the starting point. Forces at later times do not enter. We said nothing about the form of the potential V(x) in our time of flight equation, so the focusing equation applies to any one-dimensional conservative system.

At first glance, the focusing equation is rather unbelievable. Both $\partial T/\partial x_0$ and $\partial T/\partial v_0$ are obviously a function of the force the particle experiences as it moves to the collector. However, when $\partial T/\partial x_0$ and $\partial T/\partial v_0$ are combined, this functional dependence disappears.

If either $\partial T/\partial x_0$ or $\partial T/\partial v_0$ is zero, the other cannot be zero. Hence space focusing and velocity focusing together are impossible in one dimension.

There is nothing special about the starting position that was chosen. It could have been any location. This means that the focusing equation holds for any position and any velocity throughout the particle's flight. So what we have here is a partial differential equation describing the motion of a particle in a conservative force field in one dimension. The solution to this differential equation is given by the above integral for the time of flight. So, the partial differential equation in itself does not appear to be useful in solving for the time of flight of particles.

In this partial differential equation, the normal roles of position and velocity versus time are reversed. We normally think of position and velocity as depending on time. In the focusing equation we have the time of flight depending on position and velocity. Using this inverted system is a bit difficult since this is contrary to the way we normally think.

Resolution Equation

We now apply the Focusing Equation to find a Resolution Equation. Using the focusing equation as a constraint, and assuming that the ions have a gaussian number distribution in space and velocity, it can be shown that the minimum differential time of arrival, ΔT, of the ions is given by

$$\Delta T = \frac{m\Delta v_0 \Delta x_0}{\left((mv_0\Delta v_0)^2 + (F_0\Delta x_0)^2\right)^{1/2}} \qquad \text{(Resolution Equation)}$$

where

Δx_0 = root mean square spread in the initial starting position.
Δv_0 = root mean square spread in the initial starting velocity.

To minimize ΔT we demand that:

$$\frac{\partial T}{\partial x_0} = -\frac{m^2 v_0 \Delta v_0^2}{(mv_0\Delta v_0)^2 + (F_0\Delta x_0)^2}$$

Applications

We now apply the Resolution Equation to several specific types of mass spectrometers. In the first type, (see Figure 2) we have the initial force equal to zero. If we also assume that the ions make two passes through the drift region of length D, and spend most of their time in this drift region, it can be shown that the maximum resolving power, R, is:

$$R = \frac{T}{2\Delta T} = \frac{D}{\Delta x_0}$$

Note that this equation for resolving power is independent of the spread in the ion's initial energy. By using beam switching techniques it is possible to produce ion bunches with a thickness of a fraction of a millimeter[4,8,9,10]. Therefore the resolving power of this type of instrument can be greater than one thousand with a flight tube one meter long. An experimental device of this nature has been made with a resolving power in excess of 3000[8]. The maximum resolving power was calculated without knowing the details of how the mass spectrometer was operated.

It is considerably more difficult to analyze the conventional two-field time of flight mass spectrometer. (See Figure 3) Using the fact that at a zero average initial velocity $2v_0 = \Delta v_0$, (see Figure 4) and redefining some terms we find the maximum resolving power is:

$$R = \frac{T}{2\Delta T} = \frac{D\left((4U_0)^2 + U_p^2\right)^{1/2}}{4(U_a U_0)^{1/2}\,\Delta x_0}$$

where we have assumed that the ions spend most of their time in the drift region, and where:

D = length of drift region.
T = total time of flight.
U_0 = $1/2\ mv_0^2$ = spread in the ion initial energy.

U_p = $F_0 \Delta x_0$ = potential drop across the effective source region times the ion charge.
U_a = accelerating potential times ion charge.
Δx_0 = width of source region where ions are initially found.

If time lag focusing is included, the maximum resolving power goes up linearly with the increase in the time lag.

In the derivation of the above resolving power equation, it was not necessary to assume planar geometry. Therefore, the result applies to cylindrical and spherical geometries with radial ion paths as well as the planar geometry.

Discussion and Conclusions

A focusing equation for the linear case was presented. This equation shows that it is impossible to have simultaneous space and velocity focusing in a linear time of flight mass spectrometer.

The focusing equation was used to develop an equation which describes the best time resolution possible as a function only of the source conditions. This resolution equation allows the calculation of the maximum resolving power of a large class of mass spectrometers. The results of two different calculations were presented. In the first, the initial force the ions experience was zero. In the second, the ions' initial velocity spread was centered at zero.

The results of this work allows one to clearly see just what parameters are important in improving the resolving power of the linear time of flight mass spectrometer. In comparing the two types of instruments analyzed, it appears that the one with zero initial force gives considerably better resolving power.

Since there are clear limitations on the linear time of flight instruments with constant electric fields, it seems reasonable to develop other types of time of flight mass spectrometers. This has already been done in a number of devices[11-14]. The next paper, presented by George Sanzone, presents yet another possible way to get around the above limitations by using a large impulsive initial force.

A more complete treatment of the development of the focusing equation, and a more detailed analysis of the application of this equation is being prepared for publication. The material on applications will be submitted to the International Journal of Mass Spectrometry and Ion Physics. I would like to thank Professor B. R. F. Kendall and Professor Peter Shaw for their helpful discussions and suggestions.

The work was supported by the NASA Grant NGL 39-009-032.

References

1. Ionov, N. I. and B. A. Mamyrin, Zh. Tekh. Fiz., 23, 2101, 1953.
2. Wiley, W. C. and I. H. McLaren, Rev. Sci. Instr., 26, 1150, 1959.
3. Agishev, E. I. and N. I. Ionov, Zh. Tekh. Fiz., 26, 203, 1956.
4. Mamyrin, B. A., Doctoral Dissertation, FTI AH USSR, Leningrad, 1966. (Not personally seen by the author.)
5. Sanzone, G., Rev. Sci. Instr., 41, 741, 1970.
6. Zabielski, M. F., H. T. Diem, and B. R. F. Kendall, Int. J. Mass Spectrom. Ion Physics, 5, 349, 1970.
7. Zabielski, M. F., R. Stein, and B. R. F. Kendall, Int. J. Mass Spectrom. Ion Physics, 10, 109, 1972-73.
8. Karataev, V. I., B. A. Mamyrin, and D. V. Shmikk, Sov. Phys.-Tech. Phys., 16, 1177, 1972.
9. Fowler, T. K. and W. M. Good, Nucl. Instr. and Meth., 7, 245, 1960.
10. Bakker, J. M. B., Doctoral Dissertation, U. of Warwick, England, 1969.
11. Carrico, J. P., Dynamic Mass Spectrometry, edited by D. Price, 2, 161, Hedjdon and Son, Ltd., London, 1971.
12. Bakker, J. M. B., Int. J. Mass Spectrom. Ion Physics, 6, 291, 1971.
13. Poschenrieder, W. P., Int. J. Mass Spectrom. Ion Physics, 6, 413, 1971.
14. Poschenrieder, W. P., Int. J. Mass Spectrom. Ion Physics, 9, 357, 1972.

Figure 1. A particle starts at an arbitrary point in a one dimensional conservative force field.

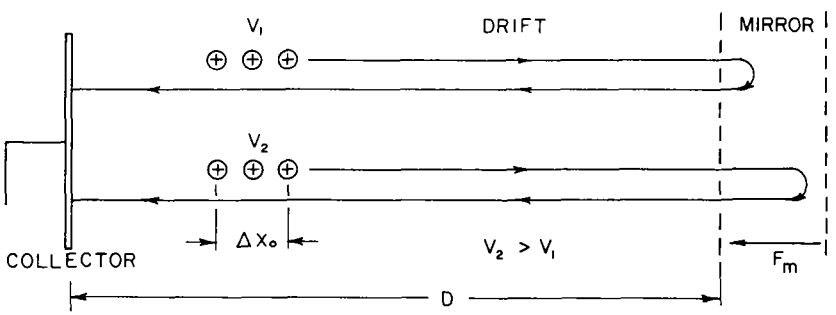

Figure 2. A time of flight mass spectrometer with velocity focusing and zero initial force on the ions.

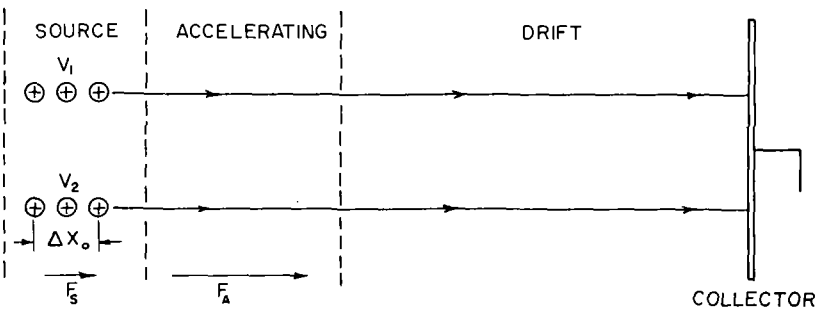

Figure 3. The conventional time of flight mass spectrometer with space focusing and an average initial velocity equal to zero.

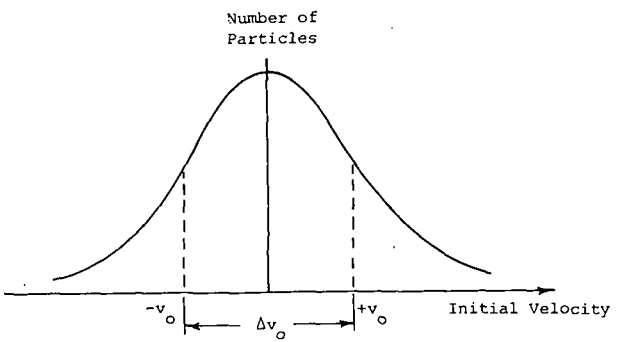

Figure 4. The spread in initial velocity is equal to twice the root mean square initial velocity. ($\Delta v_o \approx 2v_o$)

THE IMPULSE-FOCUSSED T.O.F. MASS SPECTROMETER*

by

Nina L. Marable and George Sanzone**

Dept. of Chemistry, Virginia Polytechnic Institute and State University

Blacksburg, Virginia 24061

ABSTRACT

The conventional Time-of-Flight mass spectrometer is limited in its mass resolution by the initial energy distribution of the ions to be analyzed. A new method of focussing has been devised which employs time-dependent ion drawn-out fields. The technique should provide mass resolution to greater than M/q of 2600; it is applicable to T.O.F. instruments of any drift length. The theory of the method is presented together with calculations of expected performance of two commercial instrumental configurations equipped with Impulse Focussing. Mass resolution to as high as 4000 can be obtained but resolution to greater than 2600 is obtained only with a degradation in the focus of the low-mass part of the spectrum. The new technique of focussing should allow direct measurement of the kinetic energy of primary and fragment ions.

THE TIME-OF-FLIGHT PRINCIPLE

Ions which have the same total kinetic energy but which have different masses must have different velocities. If they are injected into a drift tube the ions will separate according to their mass; lighter ions will arrive at the end of the drift length before heavier ions. This is the operating principle of the conventional time-of-flight (TOF) mass spectrometer. The remainder of the theory deals with the effects of finite initial formation or injection volume and of nonzero initial kinetic energy; these effects perturb the equality of the kinetic energy and the simultaneity of the injection process. The ability of the TOF to compensate for initial volume is called space resolution while compensation for nonzero initial velocity is called energy resolution. Wiley and McLaren[1] have shown how to minimize the effects of initial volume. In this paper, we consider how to improve energy resolution.

* This research was supported by a grant from the Petroleum Research Fund Administered by the American Chemical Society.

** To whom correspondence on this paper should be addressed.

ENERGY RESOLUTION

In a recent publication[2] a theorem was proved which demonstrates that the Wiley-McLaren two-step ion source provides the theoretical limit for energy resolution of a large class of TOF spectrometers and provides the practical limit for all other conventional TOF's which employ time-independent fields. In this work, we report the results of model calculations on the resolution of TOF's which employ two-step ion sources with time-dependent ion draw-out. The criterion for resolution is the vanishing of the time-of-flight difference between the slowest ion of a packet of mass M and the fastest ion of a packet of mass M + 1. (See Figure 1).

An ion, at draw-out, experiences an electric field E_τ for a duration of τ nanoseconds, after which the draw-out field switches to a field strength E_s; the field E_s has the value necessary for conventional Wiley-McLaren space focussing. For the calculation, two parameters were required: duration τ of the Impulse Focussing Field (IFF) and the amplitude E_τ. For convenience, the latter quantity was scaled in terms of the field strength E_s by the parameter N.

$$E_\tau = E_s \{1 + \frac{N}{2}\}$$

The calculations were performed for two conventional TOF configurations which are defined in Figure 2. Configuration I will be recognized as a 100 cm TOF with a nominal ion energy of 3000 eV; Configuration II as a 167 cm TOF with a nominal ion energy of 5000 eV. Some results of the calculations are given in Tables 1 and 2. Notice that for pulse widths greather than 100 nsec, the low-mass sector of the spectrum goes out of focus. This effect is due mainly to the fact that duration τ exceeds the time which the defocussed ions spend in the ionization region.

The marked improvement of the resolution of the TOF mass spectrometer derives from the fact that IFF technique reduces the so-called ion "turn-around time."[3] The IFF technique need not be mass dependent as is the method of Time-Lag[1] focussing; it does not discard the time-resolution capability of the TOF by continuous ion sampling as does Studier Focussing[4]; it promises a significant improvement in the mass resolution in time-of-flight mass spectrometry. A TOF instrument is currently being equipped with IFF focussing.

A more detailed discussion of this work has been submitted to Analytical Chemistry.

ACKNOWLEDGEMENTS

We wish to acknowledge the helpful discussions of Dr's. R. Rover, J.C. Schug, and J.W. Viers and to thank Gary L. Campbell and Thomas A. Ligon for their assistance with the computing.

REFERENCES

1. W. C. Wiley and I. H. McLaren, Rev. Sci. Instr. 26, 1150 (1955).

2. G. Sanzone, Rev. Sci. Instr. 41, 741 (1970).

3. D. B. Harrington, "Encyclopedia of Spectroscopy" (Reinhold Publishing Corp., N. Y., 1960), p. 628.

4. M. H. Studier, Rev. Sci. Instr. 34, 1367 (1963).

Table 1. CASE I MASS RANGE

τ (nsec)	N = 1		N = 2		N = 3		N = 4	
	M/q		M/q		M/q		M/q	
	min	max	min	max	min	max	min	max
0	–	220	–	220	–	220	–	220
10	–	225	–	230	–	275	–	350
20	–	350	–	450	–	530	–	600
30	–	500	–	600	–	680	–	750
40	–	600	–	700	–	800	–	900
50	–	675	–	800	–	900	–	1050
60	–	750	–	900	–	1050	–	1125
70	–	825	–	975	–	1125	–	1225
80	–	900	–	1075	–	1200	–	1300
90	–	950	–	1150	–	1275	–	1350
100	(10)	1000	(10)	1200	(10)	1325	(25)	1500
200	70	1500	75	1650	80	1650	125	1800
300	130	1775	175	1850	210	1925	250	1900
400	240	1900	300	1900	375	1950	440	2000
500	375	2025	475	1900	575	1950	675	1900
600	540	2075	690	2050	840	1925	980	2000
700	725	2125	925	1950	1125	1800	1325	1650
800	950	2075	1225	2050	1475	1875	>1625	1625
900	1225	2125	1540	1900	>1650	1650		
1000	1500	2250	1900	2025				

Table 2. CASE II MASS RANGE

τ (nsec)	N = 1		N = 2		N = 3		N = 4	
	M/q		M/q		M/q		M/q	
	min	max	min	max	min	max	min	max
0	–	320	–	320	–	320	–	320
10	–	340	–	360	–	355	–	500
20	–	500	–	675	–	800	–	900
30	–	740	–	900	–	1050	–	1175
40	–	910	–	1100	–	1250	–	1400
50	–	1050	–	1250	–	1440	–	1550
60	–	1175	–	1400	–	1600	–	1775
70	–	1300	–	1530	–	1750	–	1925
80	–	1400	–	1650	–	1875	–	2100
90	–	1500	–	1775	–	2000	–	2250
100	(10)	1600	(10)	1900	(10)	2175	(10)	2375
200	60	2350	80	2700	110	3050	125	3200
300	120	2950	200	3250	250	3500	275	3550
400	270	3300	350	3475	440	3850	520	3825
500	420	3650	560	3725	675	3750	800	3700
600	640	3650	800	3950	975	3875	1150	3550
700	880	3875	1100	3925	1350	3650	1575	3300
800	1040	4200	1450	3900	1750	3525	2050	2850
900	1425	4100	1840	3800	2240	3225	2600	2625
1000	1775	4300	2250	3700	2750	3040	>2350	2350

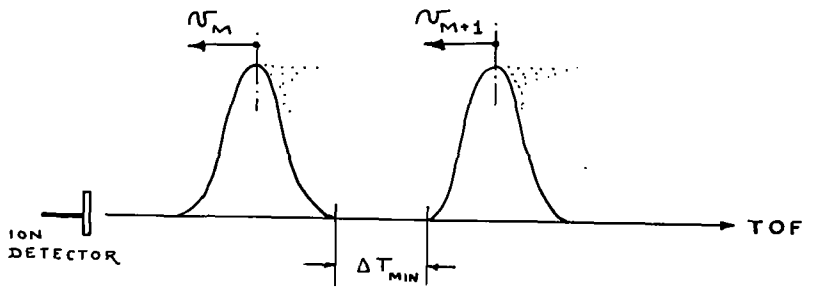

Figure 1.
Peaks M and M + 1 are resolved if $\Delta T_{min} > 0$.

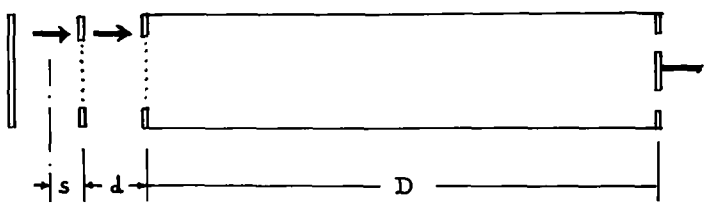

	Case I	Case II	
s	0.480	0.480	cm
Δ^s	0.009	0.009	cm
d	0.700	0.700	cm
D	98.0	167	cm
U	2689	4678	eV
U_o	0.09	0.09	eV
E^o_s	275	325	V/cm

Figure 2.
TOF Mass Spectrometer Configurations.
Arrows indicate the directions of the electric fields E_s and E_d in the s and d regions, respectively.

Techniques and Applications of Double Beam Mass Spectrometry.

BY : M.L. Aspinal, J.R. Chapman, K.R. Compson, D. Hazelby, A. Riddoch.

AEI Scientific Apparatus Ltd, Manchester, England.

The A.E.I. MS30, which was the first double beam mass spectrometer, has been described at a previous meeting of the American Society of Mass Spectrometry and is now in use in many laboratories throughout the world. The instrument may be described in very simple terms as having two sources with independent supplies and vacuum systems. The two ion beams pass through a common analyser system before being separated to independent collectors.

A number of advantages follow from the use of this technique. The best established of these is chemical mass marking, in this one beam is used to provide a reference spectrum such as that of perfluorokerosene whilst the other is used for the sample. Figure 1 shows an example of chemical mass marking in which perfluorokerisene is used to mass mark the parent region of the cholesterol spectrum. The peaks in the sample can be easily identified from the m/e 367, 381 and 303 peaks of the reference compound.

This method of mass marking is unambiguous, remains accurate at high mass, is unaffected by changes of scan speed and does not require calibration.

A unique application of double beam mass spectrometry is mass measurement at low resolving power. With a single beam instrument the sample and reference compound are admitted to the same source and high resolving power is necessary to separate the sample peaks from those of the reference compound. In many cases a resolving power of 4,000 to 5,000 is adequate but with mass deficient compounds, for example many pesticides, the resolving power has to be in the region of 10,000.

It can be shown from a consideration of the number of ions in a peak that the accuracy of mass measurement should be unaffected by resolving power. A double beam mass spectrometer is able to use one beam for the sample and the other for the reference compound and so obtain accurate mass measurements whilst working at low resolving power. The high sensitivity associated with low resolving power operation means that the smallest peaks are recorded, metastable peaks can be observed and there is optimum detection of gas chromatograph peaks on the total ion monitor. In addition, when using a data system, it is possible to take scans in a routine manner at low resolving power, and at a later time, take the decision to process the data in order to obtain accurate mass measurements.

The technique is clearly ideal for obtaining accurate mass measurements when working with chemical ionization, field ionization and field desorption sources, as the problem of providing accurately known reference peaks is overcome by using the reference spectrum in the second beam.

We are currently using double beam mass measurement at a resolving power of 1,600. Two compounds have been chosen to illustrate the accuracy and dynamic range of the technique; these are the drug phenobarbitone and the pesticide DDT. All the spectra were taken at a scan speed of 10 seconds per decade and processed by an A.E.I. DS30 data system.

Table I shows the mass measurement accuracy obtained for the m/e 232 and 204 peaks of phenobarbitone when one microgram of material was injected onto the G.C. column. Results are given for four successive injections. The average error of 2 millimass units for the eight mass measurements shown is equivalent to 8 parts per million.

Table II is similar to table I but shows the results obtained from three successive injections of 100 nanograms onto the G.C. column. The average error of 2.7 millimass units for the six mass measurements shown is equivalent to 12 parts per million.

Table III shows the mass measurement accuracy obtained on the m/e 354, 319, 284 and 235 peaks of DDT. This compound is a severe test of a mass spectrometer data system because of the low intensity of the m/e 354 and 319 peaks. The average error for the eight measurements on these two peaks, obtained from four successive injections of one microgram, was 3.3 millimass units, equivalent to 10 parts per million. Table IV shows the mass measurement accuracy obtained on the m/e 284 and 235 peaks of DDT for three successive injections of 100 nanograms onto the G.C. column. The average error of 1.9 millimass units for the six mass measurements was 7 parts per million.

TABLE I

1 microgram of phenobarbitone on column

Composition	Nominal Mass	% Base Peak	Error (mMU)
$C_{12}H_{12}O_3N_2$	232	16	2.7 4.5 3.8 2.0
$C_{10}H_8O_3N_2$	204	100	0.5 0.5 1.0 0.5

TABLE II

100 nanograms phenobarbitone on column

Composition	Nominal Mass	% Base Intensity	Error (mMU)
$C_{12}H_{12}O_3N_2$	232	16	3.1 5.7 1.9
$C_{10}H_8O_3N_2$	204	100	1.1 1.9 2.7

TABLE III

1 microgram of D.D.T. on column

Composition	Nominal Mass	% Base Peak	Error (mMU)
$C_{14}H_g{}^{35}Cl_4{}^{37}Cl$	354	1	2.3 6.3 2.5 5.6
$C_{14}H_g{}^{35}Cl_3{}^{37}Cl$	319	1.2	2.0 1.5 3.5 2.5
$C_{14}H_g{}^{35}Cl_2{}^{37}Cl$	284	9	1.7 1.0 2.7 6.2
$C_{13}H_g{}^{35}Cl_2$	235	100	0.3 4.0 1.8 2.5

TABLE IV

100 nanograms of D.D.T. on column

Composition	Nominal Mass	% Base Peak	Error (mMU)
$C_{14}H_g{}^{35}Cl_2{}^{37}Cl$	284	9	2.4 2.1 1.0
$C_{13}H_g{}^{35}Cl_2$	235	100	2.3 2.3 1.3

The results presented in tables I, II,III and IV together with additional data are shown in figure 2. The chemically most significant masses in the two compounds were selected and the errors in parts per million were plotted against the intensity of the peak. It is found that for peaks above 2% of the base peak on a 1 microgram injection or 20% of the base peak on a 100 nanogram injection 70% of the peaks were measured with an accuracy of better than 10 ppm and 96% of the measurements were

better than 15 ppm. Taking the results as a whole 61% of the mass measurements were better than 10 ppm and 82% better than 15 ppm.

The figure shows that for an injection of one microgram of compound onto a G.C. column the dynamic range of the mass measurements approached three orders of magnitude.

Table V shows mass measurement results obtained by the double beam method when 50 nanograms of dichlorobenzene was injected onto the G.C. column. Results of measurements obtained at 10,000 resolving power with 250 nanograms injected are shown for comparison and it can be seen that the limit of detection for the smaller peaks has been reached at a much higher sample level.

TABLE V

(A) 50 nanograms on the G.C. column, 1,500 resolution, double beam.

(b) 250 nanograms on the G.C. column, 10,000 resolution, single beam.

Atomic Composition	Calculated Mass	Relative Intensity	(A) Error mMU	(B) Error mMU
$^{12}C_6H_4\ ^{37}Cl_2$	149.9630	8.4	-0.5	Not observed
$^{12}C_6H_4\ ^{35}Cl\ ^{37}Cl$	147.9660	57.2	0.8	1.4
$^{13}C\ ^{12}C_5H_4\ ^{35}Cl_2$	146.9723	8.0	-1.2	3.1
$^{12}C_6H_4\ ^{35}Cl_2$	145.9689	100.0	-1.2	2.4

As a final illustration of double beam mass measurement at low resolving power, fig. 3 shows the chromatogram obtained from the total ion monitor trace of a steroid mixture from the urine of a new born baby. The identity of the steroid represented by the major peak was required. Table VI shows a summary of the atomic composition report that was obtained, from which it was possible to determine the molecular formula of the steroid unambiguously.

TABLE VI

Steroid from New Born Baby

Composition	Nominal Mass	% Base Peak	Error (mmU)
$C_{24}\ H_{40}\ O_2\ Si$	388	21	3.6
$C_{23}\ H_{37}\ O_2\ Si$	373	21	4.0
$C_{22}\ H_{37}\ O\ Si$	345	17	7.3
$C_{21}\ H_{30}\ O$	298	37	3.9
$C_{20}\ H_{27}\ O$	283	60	0.9
$C_{19}\ H_{27}$	255	70	2.5

Conclusions.

Double beam mass spectrometry provides mass measurements at low resolving power over a wide dynamic range. These mass measurements are obtained simultaneously with conventional low resolution data such as metastable peaks and detection and mass marking of very small peaks.

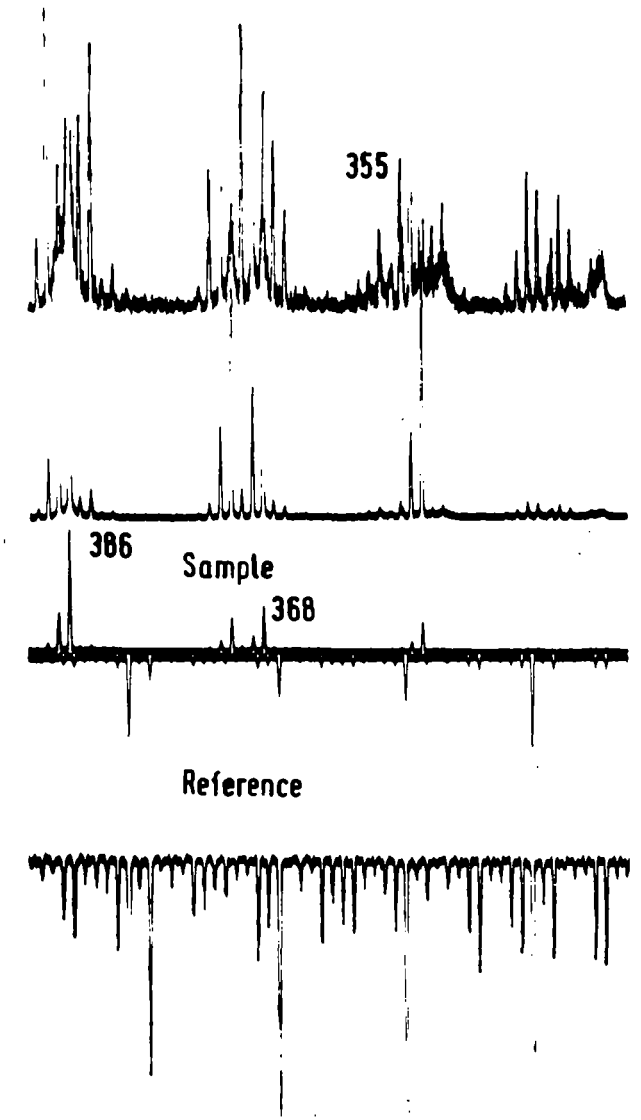

Fig. 1 Parent region of cholesterol spectrum.

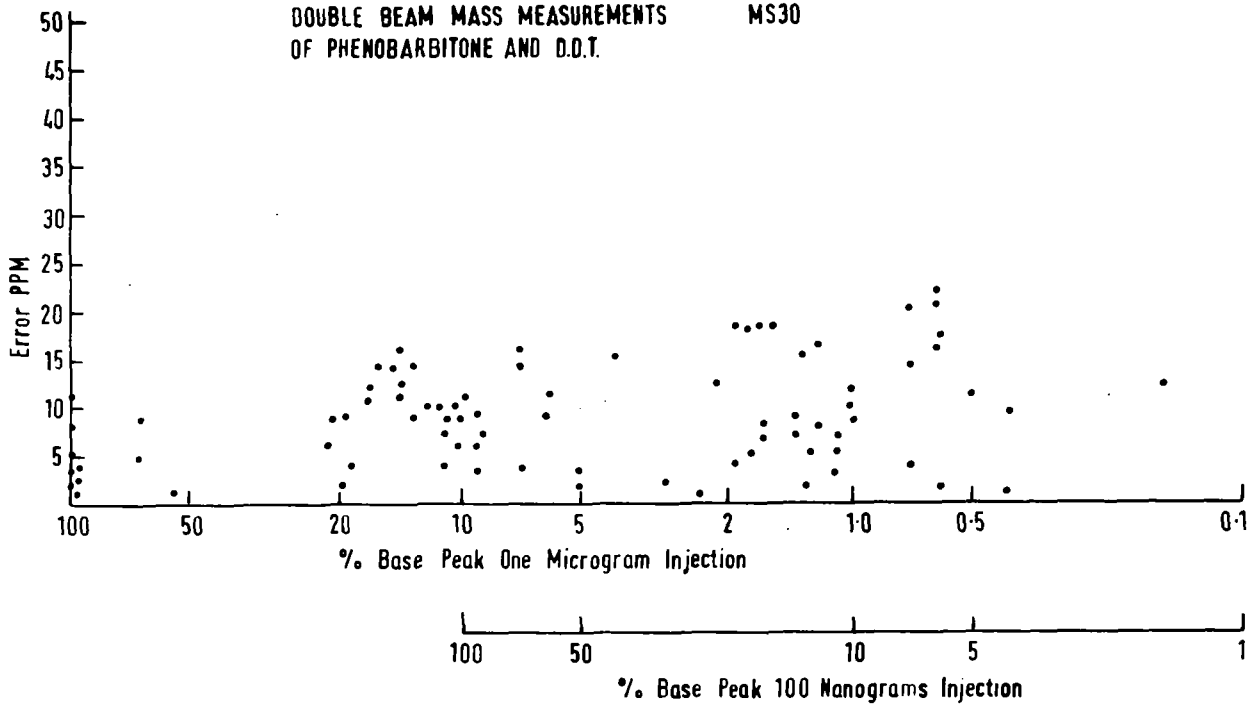

Fig. 2 Graphic presentation of accuracy of mass measurement.

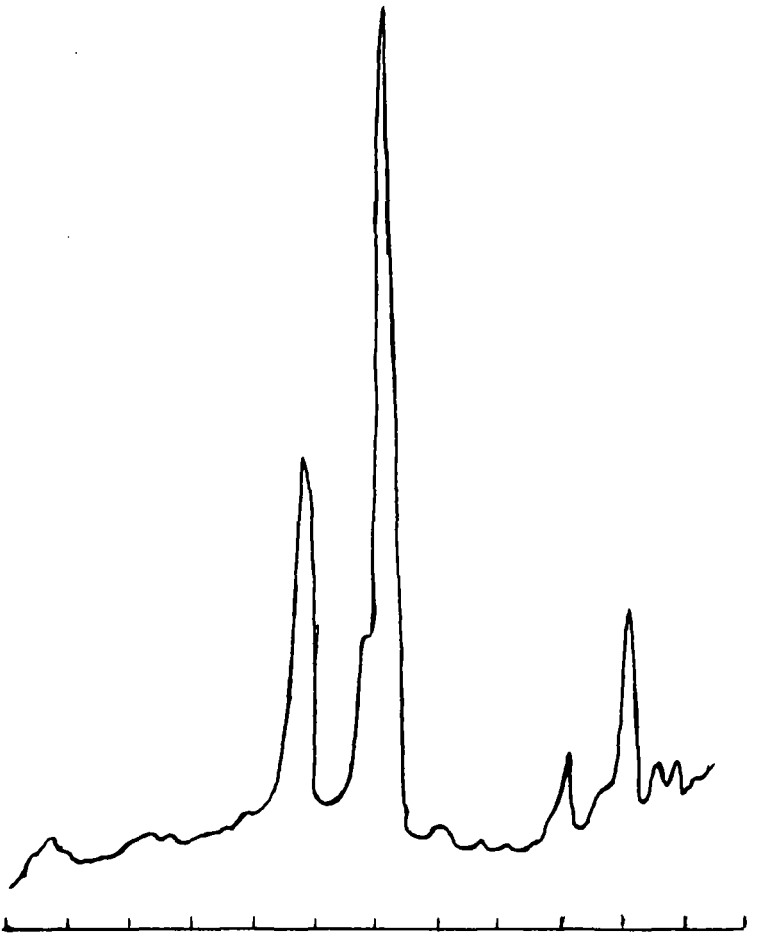

Fig. 3. Chromatogram of steriod extract from new born baby.

Electrohydrodynamic Ionization Mass Spectrometry*

Bruce N. Colby and Charles A. Evans, Jr.

Materials Research Laboratory

Urbana, Illinois 61801

Electrohydrodynamic (EH) Ionization is a type of field ion emission which results from the interaction of a strong electrostatic field and a liquid meniscus. The basic ionization process and preliminary information on the ionic species produced have been previously discussed. This paper will discuss two aspects of EH ionization mass spectrometry. The first of these is the instrumentation required for reliable operation of an EH ion source and the application of this instrumentation to several liquid metals. The liquid metals studied are Ga-In-Sn, Cerrolow 117 and impurity doped Ga-In-Sn.

A more complete discussion of this research has been accepted for publication in the September, 1973 issue of Analytical Chemistry.

* This research was supported in part by the National Science Foundation Grant GH-33634.

A NEW TECHNIQUE FOR RELIABLY INITIATING THE ACTIVATION OF FI/FD EMITTERS*

D. F. Barofsky and E. Barofsky
Department of Environmental Technology
Oregon Graduate Center
Beaverton, Oregon 97005

Successful field ionization (FI)/field desorption (FD) mass spectrometry requires a reliable means for producing field anodes. The benzonitrile activated wire emitters developed by Beckey, et al.[1] and Migahed and Beckey[2] are apparently the most successful field anodes. In attempting the various published activation techniques,[1,3] we have had difficulty in initiating needle growth; in fact, in many instances, we were unsuccessful in getting the activation to proceed at all. We have overcome this problem by developing a simple process for controlled pre-roughing of the emitter surface prior to the organic activation.

Study of the emitters on which we were able to produce some needles revealed that they begin growing on existing protrusions on the tungsten emitter wire. After investigating different means of producing a roughened wire, we found the most successful to be a process of oxidizing and then reducing the tungsten surface. The idea for this process is borrowed from the theory of crystal whisker growth.[4] During oxidation at elevated temperatures the mobile oxide migrates to lattice imperfection sites on the surface effecting a growth of needles and ridges at these sites. Subsequent reduction of the oxide transforms these oxide growths into the desired whiskers or ridges.

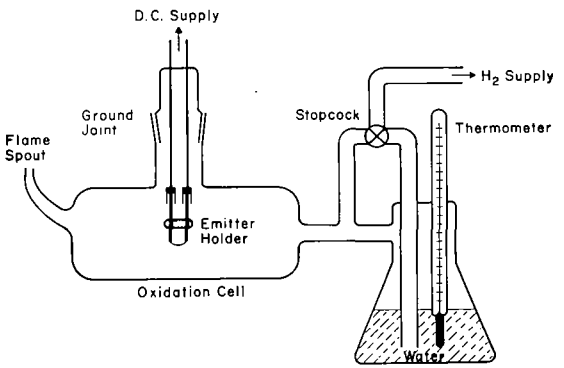

Fig. 1. Emitter Oxidation-Reduction Apparatus

Fig. 1 is a drawing of the oxidation-reduction cell we use.** Our emitters are made of 8 μm wire. An emitter is introduced into the cell and the whole system is flushed with hydrogen. The stopcock is set so that the hydrogen bypasses the water, and in this atmosphere the emitter is heated to about 1300°C (~200 ma) for 1-2 minutes. After this cleaning process the emitter temperature is reduced to about 750°C (165-175 ma; this temperature is just below the limit of visible red heat). The stopcock is slowly rotated to allow the hydrogen to flow through the water bath (maintained at 85°C) and then immediately rotated back (~4-5 seconds for the whole process). This oxidation step leaves the middle portion of the wire with a characteristic

blue-black oxide layer. This layer is reduced by raising the emitter temperature back to 1300°C in a pure hydrogen flow for 1-2 minutes. The resulting surface is uniformly roughened with metal protrusions and ridges.

The organic activation process initiates and proceeds readily on these roughened surfaces. We employ an activation cell like that described in Ref. 1. The procedure for activation is essentially that of Schulten and Beckey.[3] 1-10 μm of benzonitrile are admitted into the activation chamber, the emitter temperature is raised to about 1200°C (~28 ma) and the high voltage is set to 10 kV. The activation initiates and proceeds rapidly. In order to compensate for the cooling of the needle tips as they increase in length as well as to extend the growth more toward the support electrodes, the emitter temperature is raised gradually during the activation time. If extremely dense growth is desired, the high voltage is left at 10 kV for the entire activation time. Less dense growths are achieved by reducing the high voltage over a period of time to about 5 kV after about one hour initiation time at the higher voltage. The needle density is inversely proportional to the rate of this voltage decrease. Very sparse growths can be obtained by initiating and continuing the process at voltages less than 10 kV. In all instances, a quick growth to a quite uniform needle length of about 13 μm occurs within a period of 3 to 4 hours. Attempts to increase the needle length of the dense to medium dense growths by increasing the activation time beyond this period result only in sparse, spindly, dendritic whiskers grown on top of the more dense underbrush. Very long needles can be grown from the less dense growths by allowing the activation to proceed for 12-24 hours.

References

1. H. D. Beckey, A. Heindrichs, E. Hilt, M. D. Migahed, H. R. Schulten, and H. U. Winkler, Messtechnik 79, 196 (1971).

2. M. D. Migahed and H. D. Beckey, Int. J. Mass Spectrom. Ion Phys. 7, 1 (1971).

3. H. R. Schulten and H. D. Beckey, Org. Mass Spectrom. 6, 885 (1972).

4. F. R. N. Nabarro and P. J. Jackson, in "Growth and Perfection of Crystals," R. H. Doremus, ed. New York, Wiley, pp. 13-101 (1958).

* A more detailed description of this technique is being submitted for formal publication in the Int. J. Mass Spectrom. Ion Phys.

** The authors would like to acknowledge Prof. Erwin Rudy of our Department of Metallurgy and Materials Science for contributing a number of suggestions on the process described here.

SIMULTANEOUS MEASUREMENTS OF MASS-EFFUSION AND MASS-SPECTROMETRIC INTENSITIES OF EFFUSATE*

J. R. McCreary and R. J. Thorn

Chemistry Division, Argonne National Laboratory
Argonne, Illinois 60439

Equipment has been assembled and tested for the simultaneous determination of mass-effusion and mass-spectrometric analysis of the effusate from a Knudsen cell. The cell, suspended on a vacuum balance (semi-micro, recording) and surrounded by a current concentrator, is weighted continuously while being heated by rf current of an induction heater. The water-cooled surfaces surrounding the cell condense excess effusate so that only the molecular beam from the orifice in the bottom of the cell enters the mass spectrometer. A quadrupole mass spectrometer mounted within an ion pump, is located directly below the cell. A small grate valve permits the spectrometer to remain evacuated at 10^{-8} torr at all times. The temperature of the cell is controlled and measured with an automatic recording pyrometer. All measurements are automatically recorded for rapid data reduction by computer. Three uses of the equipment are discussed with data obtained from the sublimation of lanthanide trifluorides: (1) Determination of mass-spectrometric sensitivity and absolute cross-sections for ionization and fragmentation, (2) Determination of thermochemical quantities, and (3) Use of equipment for complete analyses of solids.

*Work performed under the auspices of the U.S. Atomic Energy Commission.

Fig. 1. Schematic diagram of equipment for simultaneous measurements of mass-effusion and mass-spectrometric intensities of effusate. A-semimicro vacuum balance; B-quadrupole mass spectrometer; C-ion pump, 100 l/s; D-ion pump, 400 l/s; E-effusion cell (see Fig. 2); F-current concentrator; G-rf coil for induction heater; V_1-vacuum gate valve; V_2-vacuum gate valve. The temperature of the cell is measured with an automatic optical pyrometer through prisms indicated. A shutter located immediately above valve V_2 is operated magnetically to intercept the molecular beam.

Fig. 2. Sketch of effusion cell consisting of outer cylinder, ends, and inserted cylinder. The solid (C) is secured in cell either with cylinder (A) made of wire mesh for powders or with notch (B) for melted sample cast in cavity.

Fig. 3. Plot of logarithm of ion intensities (i.e., TI^+) vs logarithm of rate of effusion (i.e., $\sqrt{T}\ dw/dt$) for three separate experiments with gadolinium trifluoride. Line represents least-squares' values for all three experiments combined. $\log TI = -(5.0646 \pm 0.0031) + (0.9985 \pm 0.0166) \log(\sqrt{T}\ dw/dt)$.

Fig. 4. Summary of thermochemical quantities derived from sets of determinations of 8 to 10 values for each ℓnp vs. T^{-1}. In each case, half are derived from mass effusion and half from mass spectrometer accomplished simultaneously. In the first columns are listed the fluorides, followed in parentheses by the number of sets of simultaneous determinations. In the second and third columns are listed the averaged values for the enthalpies and entropies, weighted according to standard deviations derived from sets of ℓnp vs. T^{-1}. In column 4 are listed their pressures in atmospheres at 1400 K.

CaF_2 is given only as reference in that the only other laboratories we have to compare our values for the trifluorides with are Searcy and co-workers [J. Phys. Chem. 67, 103 (1963)], and Margrave and co-workers [J. Phys. Chem. 67, 877 (1963)], both of whom have measured the heat and entropy of CaF_2. In most cases for the trifluorides, our measured values are as much as 10 kcal/mole higher than Margrave and co-workers and agree quite well with Searcy and co-workers.

Our measured pressure for CaF_2 at 1475 K compares to Searcy and co-workers to be within 14% of a 6 degree translation in temperature scale, and is consequently reconcilable. The difference between our value for CaF_2 and Margrave and co-workers is equivalent to 28° in the temperature scale and seems not readily reconcilable.

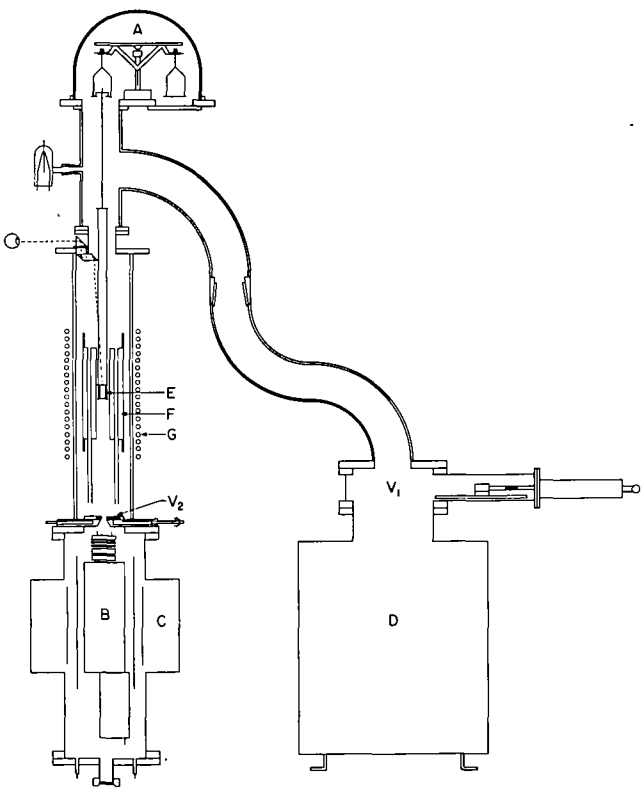

McCreary, U-4
Figure 1

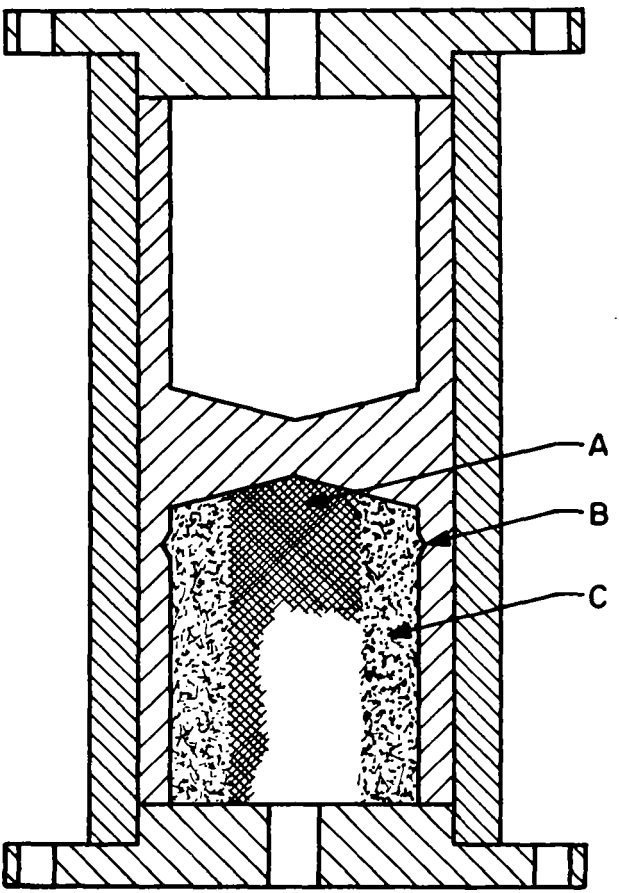

McCreary, U-4
Figure 2

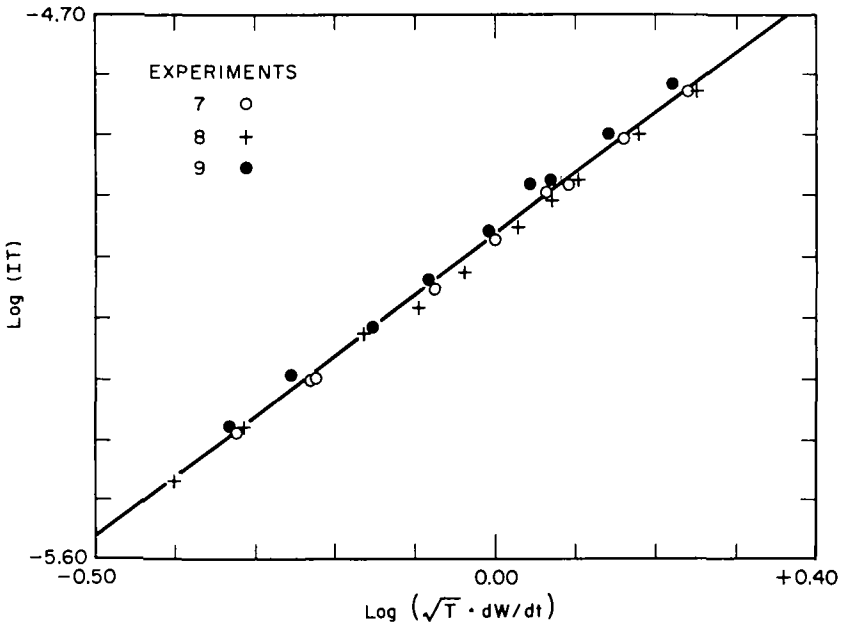
-4.70
-5.60
-0.50
0.00
+0.40
Log (IT)
Log (√T · dW/dt)
EXPERIMENTS
7 o
8 +
9 ●

Summary of Thermochemical Quantities for Sublimation of Some Lanthanide Trifluorides

Fluoride	ΔH°(kcal/mole)	ΔS°(e. u.)	$p \times 10^{-7}$ at 1400 K
CeF_3(14)	96. 67± 0. 48	42. 37± 0. 34	14. 8
NdF_3(6)	99. 07± 0. 14	43. 84± 0. 07	13. 1
GdF_3(11)	100. 55± 0. 19	43. 34± 0. 09	5. 97
TbF_3(6)	100. 77± 0. 06	44. 46± 0. 03	9. 69
HoF_3(4)	104. 25± 0. 05	46. 27± 0. 03	6. 90
ErF_3(6)	106. 16± 0. 43	47. 88± 0. 23	7. 82
TmF_3(6)	94. 99± 0. 36	40. 02± 0. 19	8. 28
CaF_2(7)	93. 29± 0. 23	37. 00± 0. 16	3. 34

McCreary U-4
Figure 4

THE USE OF HIGH RESOLUTION PHOTOPLATE TECHNIQUES IN THE IDENTIFICATION OF ORGANOCHLORINE COMPOUNDS AND THEIR METABOLITES IN BIOLOGICAL SAMPLES*

W. D. Jamieson, O. Hutzinger, S. Safe
Atlantic Regional Laboratory, National Research Council of Canada, Halifax, Nova Scotia

J. F. S. Crocker
Killam Hospital for Children, Halifax, Nova Scotia

V. Zitko
Environment Canada, Fisheries Service, St. Andrews, New Brunswick

The relatively large mass deficiencies of both chlorine isotopes (for ^{35}Cl, -31.2 mmu; ^{37}Cl, -34.1 mmu) cause the exact masses of ions which contain chlorine to be usually less than other ions of the same nominal m/e value which contain only isotopes of C, H, N or O, the elements most commonly occurring in samples of biological origin. The differences in mass between such C, H, N or O ions and organochlorine ions are usually large enough that spectrometers of only moderately high resolution ($\geq$10,000) can be used to distinguish between them. This allows organochlorine compounds to be identified in the presence of large amounts of coextracted natural products if suitable high resolution spectra have been recorded for the total mixture sample. Since xenobiotic compounds often contain one or more atoms of a mass deficient isotope, this same principle aids in the identification of other types of xenobiotic compounds (e.g., containing metals, S, P, etc.) by reducing or eliminating the need for extensive mixture separation procedures prior to mass spectrometric analysis. This method is particularly useful for the identification of polar metabolites partially separated from coextracted products by thin-layer chromatography since gas chromatography/mass spectrometry is often unsuitable for such compounds.

The photographic plate, an integrating detector for ions, is well suited to record the high-resolution spectrum of a complete sample of a mixture since exposure times of up to one hour or more are feasible. This aids in the additive recording of the mass spectra of mixture components which may differ greatly in volatility and also in the identification of specific compounds even when these may only be present

*Issued as NRCC 13256.

in trace amounts (<1 ppm). In our laboratory, experience with this technique (1-4) has shown that organochlorine and organometallic residues down to 10 ppb could be identified using 10-20 µg samples of crude extracts of biological material from which the solvent (e.g., hexane, benzene) had been removed.

This approach is not as suitable for quantitative analyses, particularly in routine uses, as many alternative methods requiring less costly instrumentation. We believe the method very effective, however, as a semi-quantitative way to 'screen' efficiently small quantities of sample for a very wide range of compounds which may be of interest. It seems well suited, too, to aid in the development of suitable separation methods for complex mixtures of biological origin and in the selection or development of methods for routine quantitative analysis, particularly where compounds of interest occur at trace or residual levels. The advantages of the method are high sensitivity, versatility and relative freedom from such effects as selective sample losses, side reactions and introduction of artifacts (or new impurities) often associated with separation procedures needed to yield 'clean' samples for analysis.

Experimental

Mass Spectrometer and Operating Conditions. A Dupont/CEC 21-110B instrument was used, fitted with an electron impact ionization source and equipped for ion detection by either photographic plate or electrode/electron-multiplier. Stability of the instrument performance was improved by the use of two high-stability power supplies (Power Designs, Inc., Model 2K-10) to maintain potentials for the field plates of the electrostatic analyzer and to provide a voltage reference to the ion accelerator power supply. With careful attention to maintenance of the magnet and other power supplies, the resolution evident in spectra recorded photographically with the modified instrument did not deteriorate even when exposures of between one and two hours were used. The object slit was usually adjusted to yield a resolution of about 15000. Typically, the total ion current passed by the electrostatic analyzer was kept at about 10^{-12} amp while the mass spectrum of a mixture sample was recorded photographically over a period of about 30 minutes. During this time, the temperature of the subliming, directly-introduced sample was gradually increased using a probe (5) which allowed the sample temperature to be controlled at values within the range -80 to 180° while

the temperature of the ionization chamber remained constant at about 200°.

Photographic Plates. Although we have used Ilford Q2 plates successfully to determine organochlorine residues at levels of 10 ppb (1), Ionomet vacuum-deposited silver bromide plates are preferred for this technique because of the higher 'gamma' and lower 'background' (greater clarity) of these plates. The higher effective sensitivity of these plates reduces the exposure time required to detect trace levels of compounds or can yield more information about those less abundant ions in the spectrum of a compound sometimes useful in confirming an identification.

Photoplate Measurements. A Gaertner Model M-1205-PC was used. Manually measured data (perfluorokerosene as internal standard) yielded experimental m/e values usually well within 10 ppm of 'true' values. The data was processed using programs written in 'BASIC' to operate with a Hewlett-Packard 2000C time-shared system (Maritime Computers, Ltd.). The program used a least-squares polynomial curve-fitting routine to 'smooth' calibration data and determine the best dispersion relationship.

An automatic data acquisition/reduction system using a dedicated minicomputer is under development.

Examples of Results

This technique has recently been applied further to identify submicrogram levels of organochlorine pesticides (e.g., DDT, DDD, DDE) and pollutants (e.g., PCB, PCT) in biological samples such as marine wildlife, human tissue, human breast milk and polar bear tissue and has also been used to identify chlorohydroxybiphenyl and chlorohydroxy-methoxybiphenyl metabolites in the urine of rabbits dosed with chlorobiphenyls.

The detection of tetrachlorobiphenyl residues in a crude hexane extract of human brain tissue is demonstrated by Figure 1. The detection of hexachlorohydroxybiphenyl and pentachlorohydroxymethoxybiphenyl in a crude ether extract of the urine of a rabbit dosed with hexachlorobiphenyl is demonstrated by Figure 2.

REFERENCES

1. O. Hutzinger and W. D. Jamieson. Bull. Environ. Contam. Toxicol. 5, 587 (1971).
2. O. Hutzinger and W. D. Jamieson. Pesticide Chemistry, Proc. 2nd International IUPAC Congress, ed. A. S. Tahori. 4, 7 (1971).

3. O. Hutzinger, W. D. Jamieson and S. Safe. Int. J. Environ. Anal. Chem. 1, 85 (1971).
4. W. D. Jamieson. Proc. Intern. Sym. Ident. Meas. Environ. Pollutants, Ottawa, 1971. p. 232, Discussion. Publ. 1972, NRCC, Ottawa.
5. W. D. Jamieson and F. G. Mason. Rev. Sci. Instrum. 41, 778 (1970).

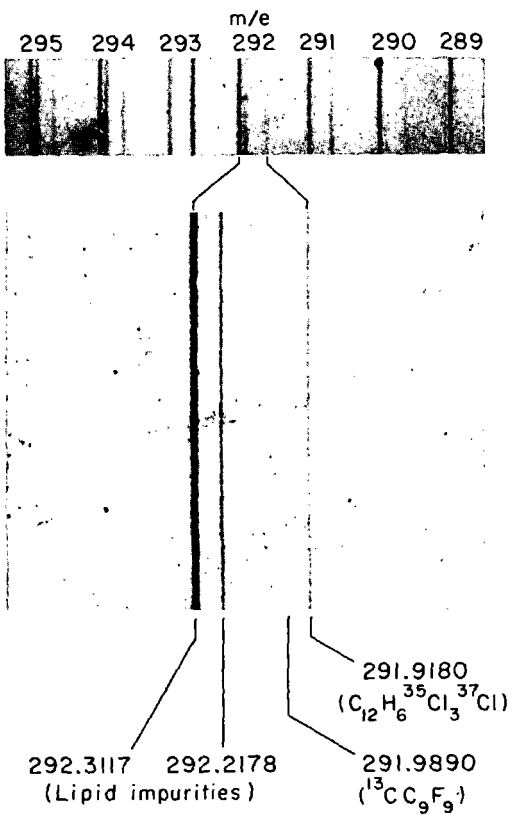

Figure 1. Partial Mass Spectrum of Crude Hexane Extract of Human Brain Tissue.

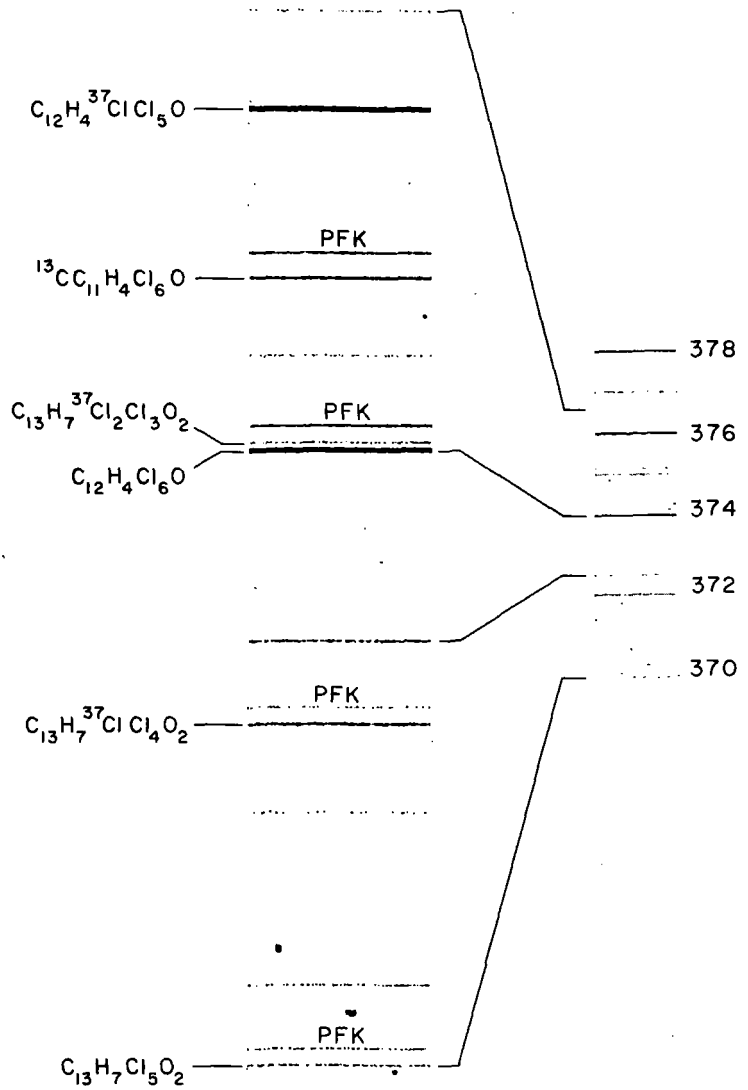

Figure 2. Partial Mass Spectrum of Crude Ether Extract of Rabbit Urine.

ANALYSIS OF PETROLEUM STREAMS USING HIGH RESOLUTION MASS SPECTROMETRY

I. P. Fisher and H. P. Fischer
Gulf Oil Canada Limited
Research & Development Department
Sheridan Park, Ontario, Canada

ABSTRACT

A method has been developed to analyse selected petroleum streams using a high resolution mass spectrometer. Separation of the sample into saturates and aromatics is not required. The calibration matrix was derived from the high resolution spectra of pure compounds and of narrow cuts separated from petroleum.

INTRODUCTION

For many years mass spectrometry has been used in the oil industry to analyse for the hydrocarbon types present in petroleum. The only method reported to date[1] which involved the use of high resolution mass spectrometry used low resolution matrices modified for use with a high resolution instrument. We did not obtain satisfactory results from the published matrix. The work reported here is a continuation of earlier work[2] directed towards obtaining quantitative information from a high resolution mass spectrometer.

EXPERIMENTAL

An A.E.I. Ltd. MS902 high resolution mass spectrometer was used. All the instrumental parameters were set up in accordance with the procedures described earlier[2]. In summary, the dynamic resolution was 10,000, scan speed 4.6 min/decade and the ion source temperature set to give, for the standard paraffin blend[2], $\Sigma 71/TI = 0.56 \pm 0.02$ and $71/TI = 0.30 \pm 0.02$.

The MSDS-30 data system, supplied with the instrument, automatically calculates the atomic compositions of all the ions in the sample spectrum and records their intensities. These data are stored on the 256K disk for subsequent processing. Error limits of 4.0 m.m.u. on the accuracy of mass measurement were routinely used enabling identification of ≈90% of all the peaks.

CALIBRATION

Pure chemicals and blends of these were run as calibrants under standard high resolution scan conditions. Numerous blends of all the group type mixtures were also run to establish weight sensitivity factors. The method routinely calculates the weight percentages of paraffins, mono + noncondensed cycloparaffins, condensed cycloparaffins, all the aromatic group types from Z=-6 to Z=-30, five aromatic sulphur types (-10S, -16S, -18S, -20S and -22S) and one aromatic oxygenated type (-16O).

All pattern coefficients were expressed as fractions of the total ionization and the intensities of the characteristic ions were measured for the ions identified not by their integral masses but by their atomic compositions. Paraffins were characterized by the sum of intensities for the series of atomic compositions C_5H_{11}, C_6H_{13}, C_7H_{15} and C_8H_{17}. The characteristic ion intensities for the non paraffinic saturates corresponded to the integral masses selected by Clerc et al[3]. For the remainder of the group types the intensities were summed over the whole spectrum for the compositions corresponding to $C_nH_{2n-Z} + C_nH_{2n-(Z+1)}$.

The results for unknown samples were calculated by the usual techniques associated with group type analyses[4].

RESULTS

The first criterion for acceptability was the determination of saturate and aromatic percentages in agreement with values obtained from a liquid chromatographic technique (e.g. A.S.T.M. D.2007). Figure 1 shows a comparison between the weight percentages of saturates and aromatics determined by this method and by A.S.T.M. D.2007.

An aromatic oil was analysed over a period of two months to assess the repeatability of the method. Figure 2 shows these results. The weight percentages of each group type is shown with its associated precision at the 95% confidence level (L_{95}). The standard deviation is also shown. Repeatability for duplicate analyses may be defined as $2L_{95}$.

Figure 3 shows the results of analysing the same oil after having added 46.3% by weight of its aromatic fraction. The calculated and observed weight percentages may be compared to assess the additivity of the procedure.

DISCUSSION

The method was developed to analyse mainly straight run streams. However the data in Figure 1 shows reasonable results are also obtainable with catalytically cracked stocks and lubricating oil basestocks. The method did not give satisfactory results for aromatic oils extracted from distillates during lubricating oil production. The method may be used to cover the boiling range of about 500 to 1000 deg F. Providing the criteria established earlier[2] are observed it seems likely that the method may be used with the output from other Nier-Johnson type mass spectrometers.

Anyone requiring a copy of the 22X22 calibration matrix should contact I. P. Fisher.

REFERENCES

1. E. J. Gallegos, J. W. Green, L. P. Lindeman, R. L. LeTourneau and R. M. Teeter, Anal. Chem., 39, 1833 (1967).
2. W. F. Brown and I. P. Fisher, Talanta, 19, 798 (1972)
3. R. J. Clerc, Archie Hood and M. J. O'Neal, Jr., Anal Chem. 27, 868 (1955).
4. M. J. O'Neal, A. Hood, R. J. Clerc, M. L. Andre and C. K. Hines, 4th World Petroleum Congress, Proceedings Section v/c Paper 3.

STREAM TYPE	HRMS	LIQ. CHROM.	
LIGHT DIST.	76.8 23.2	80.8 19.2	
HVY DIST.	74.8 25.2	76.1 23.9	
'AA' DIST.	67.2 32.8	69.4 30.6	
FCCU FEED	68.3 31.7	68.5 31.5	
'B' DIST.	61.3 38.7	59.5 40.5	
'B' BASESTOCK	81.4 18.6	78.9 21.1	
N-1000	47.6 52.4	45.7 54.3	
DECANT OIL	7.9 92.1	9.7 90.3	
LIGHT CYCLE OIL	20.0 79.8	21.7 78.3	(INCLUDES ≈5% OLEFINS)

FIGURE 1. SATURATE AND AROMATIC PERCENTAGES BY HRMS AND ASTM D2007

GROUP TYPE	Z. NO.	WT % AVGE OF 18 ANALYSES	S, STANDARD DEVIATION	L_{95}
PARAFFINS	+2	12.5	0.95	0.48
CYCLOPARAFFINS	< 0	19.1	0.75	0.38
COND. CYCLOPARAFFINS	<-2	30.4	1.80	0.92
BENZENES	-6	5.5	0.81	0.41
INDANES	-8	4.9	0.33	0.17
DINAPHTHENE BENZENES	-10	5.2	0.34	0.16
NAPHTHALENES	-12	4.4	0.16	0.08
ACENAPHTHENES	-14	3.7	0.33	0.17
FLUORENES	-16	3.6	0.35	0.18
PHENANTHRENES	-18	3.4	0.51	0.26
NAPHTHENEPHENANTHRENES	-20	1.1	0.62	
DINAPHTHENEPHENANTHRENES	-22	0.6	0.25	
CHRYSENES	-24	0.3		
DINAPHTHENEPYRENES	-26	0.1		
DIBENZOFLUORENES	-28	-		
DIBENZANTHRACENES	-30	-		
BENZOTHIOPHENES	-10S	1.6	0.31	
DIBENZOTHIOPHENES	-16S	2.7	0.36	
NAPHTHODIBENZOTHIOPHENES	-18S	0.2		
DINAPHTHODIBENZOTHIOPHENES	-20S	0.2		
	-22S	-		
DIBENZOFURANS	-16O	0.5		

FIGURE 2. STATISTICAL ANALYSIS OF A LUBE OIL BASESTOCK

GROUP TYPE	Z. NO	CALCULATED WT %	OBSERVED WT %
PARAFFINS	+2	7.2	8.4
CYCLOPARAFFINS	< 0	10.3	11.9
COND. CYCLOPARAFFINS	<-2	19.1	19.1
BENZENES	-6	6.7	6.6
INDANES	-8	6.6	6.9
DINAPHTHENE BENZENES	-10	8.1	7.4
NAPHTHALENES	-12	6.8	6.7
ACENAPHTHENES	-14	6.6	5.9
FLUORENES	-16	6.1	6.2
PHENANTHRENES	-18	6.8	6.3
NAPHTHENEPHENANTHRENES	-20	3.1	2.7
DINAPHTHENEPHENANTHRENES	-22	1.7	1.7
CHRYSENES	-24	0.6	0.9
DINAPHTHENEPYRENES	-26	0.9	0.4
DIBENZOFLUORENES	-28	-	-
DIBENZANTHRACENES	-30	-	-
BENZOTHIOPHENES	-10S	2.0	2.3
DIBENZOTHIOPHENES	-16S	4.5	4.6
NAPHTHODIBENZOTHIOPHENES	-18S	0.9	0.7
DINAPHTHODIBENZOTHIOPHENES	-20S	0.7	0.4
	-22S	-	-
DIBENZOFURANS	-16O	1.1	0.9

FIGURE 3. ANALYSIS OF OIL + 46.3% OF ITS AROMATIC CUT

USING A QUADRUPOLE MASS SPECTROMETER AS A QUANTITATIVE ANALYTICAL INSTRUMENT

Donald E. Meyer
TEXAS INSTRUMENTS INCORPORATED, SEMICONDUCTOR GROUP
MANUFACTURING PROCESS LABORATORY - DALLAS, TEXAS 75222

INTRODUCTION

Although the quadrupole mass spectrometer (QMS) cannot provide the high resolution attainable from certain other mass spectrometers, in every other respect a properly designed, constructed and operated QMS can function as well if not better than other mass spectrometers as a quantitative tool. In general a QMS suitable for quantitative analysis of gaseous species to levels below 1 ppm is less expensive, smaller, easier to operate (manually or computerized), and potentially more sensitive and precise at lower mass range (e.g., 1 to 200 amu). Of these, sensitivity and precision are of concern in this communication, but the other factors are of no little importance. Also, quantitative analysis of more complex species are not considered, but it is obvious from reviewing the literature that a QMS combined with gas chromatograph is indeed a powerful analytical tool.

All mass spectrometers must be calibrated in some manner to qualify as quantitative instruments. The QMS is no exception and is more dependent upon good calibration to take advantage of its high sensitivity and precision. For certain gases it is possible to calibrate by comparison to standard mixtures. Such gases must have one or more unique spectral peaks. A suitable example would be SO_2 at 64 and 48 amu. An unsuitable example would be CO at 28 amu. Calibration curves of ion current vs concentration for species with unique peaks can be made as illustrated in Fig. 1. This is work by Bunyard and Raby.[1] Note that NO at mass 30 could not be uniquely measured with any accuracy below 200 ppm for the example presented because of isotopes of mass 28.

An alternate method for calibration consists of a combination of calibration by standard mixtures and of utilizing measured fragmentation and isotope patterns. For instance, in the case of NO in auto exhaust, the 30 amu peak would be used with corrections for contributions from isotopes of N_2 and CO, and of hydrocarbon fragmentation peaks. Contributions from NO_2 and N_2O to mass 30 would be determined from their respective fragmentation patterns. The ion current for mass 30 would then be corrected appropriately, and the signal due to NO would be converted to concentration by using a calibration curve such as in Fig. 1. Accurate fragmentation patterns and isotope corrections themselves would allow continuation of the calibration curve in Fig. 1.

Such an exercise looks good on paper but is largely dependent upon the sensitivity of the QMS and on its ability to accurately reproduce fragmentation patterns. Instrument stability is of prime importance, but it is also necessary to sample both calibration and unknown mixtures equivalently. Gases for calibration and fragmentation pattern generation must be pure. Recording and reduction of data is important. For the accuracy and precision of a good QMS to be realized, it is necessary to digitize the spectral data as well as the system's pressure and functioning parameters such as emission current and electron multiplier gain.

System Construction and Operation

A workable configuration for a QMS gas analyzer is shown in Fig. 2, although there are other suitable ways for sampling and other types of pumping equipment available. An ion pump was chosen because of its low background contributions and base pressure. The system as described is capable of 1×10^{-9} Torr or lower with extended high temperature baking; however, such a practice is not always advisable for achieving reproducible results for reactive gases. The mechanical sampling pump can be a source of contamination, particularly hydrocarbons and water vapor, and care must be taken to assure the traps are efficient and pressures are maintained high enough to inhibit backstreaming. With the system described, it was necessary to lower the pressure at the leak valve to around 100 to 300

microns. This reduced pressure was held constant and was necessary to minimize discrimination by the leak and keep pressures in the ion pump low enough that variation in pumping speeds would not affect fragmentation patterns.

The system described in Fig. 2 is a modification of the Q-30 Precision Gas Sampler manufactured by UTI of Sunnyvale, California. The QMS incorporated in the system is a UTI MA-10, the earliest precurser of the UTI 100-C QMS. Analysis conditions were as follows: ionizer pressure = 5 x 10^{-6} Torr, emission current = 2mA, ion energy = 15v, electron energy = 70v, focus voltage = -20v, and electron multiplier gain was held at a nominal 2 x 10^{4}. The plumbing and valving were heated from 80° to 120°C, and the QMS probe and housing were kept at 135° to 140°C.

Two types of filaments were used, tungsten and thoriated tungsten. (Filaments for the MA-10 are approximately four times larger than those presently used by UTI on more recent models.) Emission current was held constant by the instrument for both types of filaments, but there was a difference in filament temperatures. The thoriated tungsten filaments behaved quite differently as will be discussed later.

Peak intensities were read in a digital mode significant to 4 figures using an autoranging DVM. When intensities varied more than two orders of magnitude, the pico-amp meter on the QMS was manually ranged to obtain adequate signal out. When the pico-amp meter was properly zeroed, there was error of less than 0.1% from ranging. Total system pressure was read by the QMS filter in total pressure mode. Pressure at the ionizer was controlled manually by adjusting the inlet pressure at the leak valve (see Fig. 2) and by adjusting the leak valve itself. The orifice between the QMS probe and ion pump limited regurgitation and provided a constant pumping speed for all gases. Maintaining ionizer pressure at 5 x 10^{-6} Torr (arbitrarily set as the standard pressure to carry out work) was the most difficult part of the work. Pressure could vary ± 10% over a period of two minutes. It was possible to make correction for pressure fluctuations but this still remained the major source of error. System background for most mass numbers was very low, but in any case background was always subtracted out.

Experimental Results

A considerable list of gases and mixtures were sampled and fragmentation patterns obtained. Specific ones will be reported here to show how fragmentation patterns and calibration curves can be used together to yield quantitative data. There are some problems involved and the accompanying data should serve to help those who might follow the same route, particularly with a QMS.

Fragmentation patterns of linear hydrocarbons are of particular value because they can often be a source of error for analysis of gases below 100 ppm. With the QMS used, variations in peak intensities from one run to the next on a short term varied less than 0.1% unless pressure fluctuation occurred. However, when fragmentation data were made weeks or months apart, variations of as much as 5% were common. Fragmentation patterns for CH_4, C_2H_2, and C_2H_6 are given in Tables 1, 2 and 3. These data were obtained over a period of several months and are the averages of numerous runs. The range for each mass number is expressed as a per cent of each average peak intensity of the various runs. The patterns for C_2H_4 and C_2H_6 were more similar than one would note in the literature. The presence of 16 and 29 for C_2H_4 could have been due to impurities such as CH_4 or C_2H_6 or the formation of CH_4 and C_2H_5 in the ionizer. If these data were used to correct calibration curve data, an indication of the error involved is given.

The above data was taken with dual thoriated tungsten (not thoria coated) filaments. Fragmentation was different when just tungsten filaments were used. The data in Table 4 compares fragmentation patterns of N_2 for the

two types of filaments. In either case the ionizer emission current was identical, kept at 2.0 mA for this work. A variety of data suggest that there may be some filament/gas interaction taking place. When only one of the dual filaments was powered, less fragmentation was noted as indicated in Table 5, although the emission current was still 2.0 mA. There was little or no difference when only a single tungsten filament was used.

The object of using thoriated tungsten filaments was that the lower work function would allow cooler operation and therefore less "filament pumping" of oxygen as described by Dabiri and Stickney.[2] When a new set of filaments were used, correction factors for oxygen were usually about a factor of 3 to 4. As the filaments were used, this could increase to as high as 20 to 25. Data for a specific set of thoriated tungsten filaments is given in Table 6. Oxygen pumping as indicated by larger CO and CO_2 levels increased with filament age. It should also be noted that fracturing of O_2 at 32 to 16 decreased with filament age. This was generally the case as can be seen in Fig. 7 for CO and CO_2. Fracturing is decreased with the older thoriated tungsten filament.

Another problem to be recognized when using fragmentation patterns for quantitative work with or without calibration curves is that the cracking pattern for a gas such as CO or CO_2 is different for the pure gas and for a mixture. This is demonstrated in Table 8. The presence of 98% N_2 has a marked influence on the fragmentation of CO and CO_2. The same thing has been noted with high levels of O_2, although data such as in Table 8 is more ambiguous for O_2 than with N_2. Of particular importance is the effect of oxygen partial pressure on SO_2 fragmentation patterns. As a result it is necessary to construct a calibration curve for SO_2 as in Fig. 1 using a diluent mixture for the standard similar in composition to the mixture anticipated during actual analysis.

There are a variety of other factors to watch such as temperatures, pressures at the ionizer, system warm-up time, noise from power lines and other sources, air leaks in plumbing, improper materials used in construction of a system, and exact duplication of operating parameters such as electron multiplier gain and emission current. The effect of emission current on fragmentation of O_2 and N_2 is shown in Table 9. Slight variations in emission current can also have a significant effect on peak heights, particularly for H_2O and O_2 at low concentrations. It is desirable to have digital readout of emission current to keep it at a set level. For instance, when analyzing water vapor content in semiconductor packages it was noted that a ± .1 mA change in emission current could cause a ± 20% change in water vapor percentage around the 500 ppm level.

Discussion of Results

It should be noted that the above data was obtained with a quadrupole mass spectrometer using dual filaments larger in size than normally found in mass spectrometer analyzers. Also, most of the work reported was done using thoriated-tungsten filaments and not thoria coated filaments. As a result, it is undeterminable how appropriate this data is to other mass spectrometers, particularly if they are not quadrupoles. With the increased use of QMS instruments, it is beneficial to get as much information as possible into the literature on QMS performance.

The following observations can be made as a result of this work.

1. It is practical to use a combination of calibration curves and fragmentation and isotope spectra to obtain quantitative data on gases down to the ppm range.
2. Fragmentation patterns obtained by the equipment used varied 5% or less in range over several months.
3. The reproducibility of fragmentation spectra depended to a large extent on constant operating conditions including electron multiplier gain, emission current, pressure in the ionizer, type of filaments, accuracy of data readout, and general long-term stability of the QMS used.

4. Thoriated-tungsten filaments tended to increase degree of fragmentation but would age. An older set of filaments caused less fragmentation but still more than a tungsten filament.

5. Thoriated-tungsten filaments exhibited less tendency to "pump" active gases, but this ability decreased with age.

6. The fragmentation patterns of gases studied varied depending upon whether data was taken with pure gas or with a mixture. There was an indication that reactions were taking place at the filaments.

7. Calibration curves need to be made using mixtures of gases as similar as possible to mixtures anticipated during actual analysis.

The combination of a good QMS and a well-designed sampling and pumping system can produce an acceptable quantitative instrument with some accuracy, precision, and sensitivity. If certain precautions and efforts are taken, it is possible to make considerable improvements in all of these.

1. G.B. Bunyard and B.A. Raby, "The Quadrupole as an Ubiquitous Sensor," 8th Annual Symp. of New Mexico Cptr. of AVS, Albuquerque, N.M., March 23, 1972.

2. A.E. Dabiri and R.E. Stickney, "Analysis of the "Oxygen Pumping Effect" of Tungsten Cathodes in Ionization Gauges and Mass Spectrometers," J. Vac. Sci. Technol. 9, 1032 (1972).

TABLE 1

FRAGMENTATION PATTERN FOR C_2H_4

Emission Current = 2.0 ma
Pressure = 5×10^{-6} Torr

MASS NO.	INTENSITY	RANGE IN % OF INTENSITY
1	7.560	5.26
2	27.123	1.02
12	2.766	.72
13	4.851	2.37
14	10.878	.78
15	1.343	3.05
16	(.637)	5.02
24	3.253	.03
25	13.382	.69
26	65.934	.87
27	65.391	.53
28	100.000	--
29	(.541)	2.11

T A B L E 2

FRAGMENTATION PATTERN FOR C_2H_6

Emission Current = 2.0 ma
Pressure = 5×10^{-6} Torr

MASS NO.	INTENSITY	RANGE IN % OF INTENSITY
1	7.588	4.92
2	24.716	1.21
12	2.627	2.21
13	4.602	2.65
14	11.358	.98
15	1.266	4.11
16	.643	5.60
24	3.074	3.64
25	12.588	1.53
26	63.011	3.93
27	61.788	5.71
28	100.000	--
29	2.468	3.52

T A B L E 3

FRAGMENTATION PATTERN FOR CH_4

Emission Current = 2.0 ma
Pressure = 5×10^{-6} Torr

MASS NO.	INTENSITY	RANGE OF % OF INTENSITY
1	8.853	5.23
2	8.601	1.69
12	3.025	2.15
13	10.522	2.40
14	21.275	1.99
15	88.143	.25
16	100.000	--

TABLE 4

FRAGMENTATION PATTERN FOR N_2 USING THORIATED-TUNGSTEN AND TUNGSTEN FILAMENTS

Emission Current = 2.0 ma
Pressure = 5×10^{-6} Torr

Mass No.	Spectral Percentage Thoriated-Tungsten	Tungsten
14	12.44	4.691
15	.04	.014
28	100.00	100.000
29	.836	.762
30	.022	.014

TABLE 5

EFFECT ON FRAGMENTATION OF NUMBER OF FILAMENTS (THORIATED-TUNGSTEN)

Emission Current = 2.0 ma
Pressure = 5×10^{-6} Torr

MASS NO.	BOTH FILAMENTS	ONE FILAMENT
14	12.44	10.65
15	.04	.04
28	100.00	100.00
29	.826	.760
30	.022	.015

TABLE 6

EFFECT OF FILAMENT AGE ON OXYGEN SPECTRA WITH THORIATED-TUNGSTEN FILAMENTS

Emission Current = 2.0 ma
Pressure = 5×10^{-6} Torr

MASS NO.	NEW FILAMENT	OLD FILAMENT
16	21.81	16.42
28	4.65	7.38
32	100.00	100.00
44	7.40	10.97

TABLE 7

EFFECT OF FILAMENT AGE ON CO AND CO_2 SPECTRA WITH THORIATED-TUNGSTEN FILAMENTS

MASS NO.	NEW FILAMENTS	OLD FILAMENTS
CO-12	10.92	8.50
CO-16	3.27	2.81
CO_2-12	13.85	7.82
CO_2-28	51.95	34.04
CO_2-16	19.69	12.40

TABLE 8

EFFECT OF ANOTHER GAS ON SPECTRA OF CO AND CO_2 WITH THORIATED-TUNGSTEN FILAMENTS

Emission Current = 2.0 ma
Pressure = 5×10^{-6} Torr

MASS NO.	100% CO	98% N_2-2% CO
CO-12	10.92	16.47
CO-16	3.27	10.10
	100% CO_2	98% N_2-2% CO_2
CO_2-12	13.85	39.15
CO_2-28	51.95	---
CO_2-16	19.69	53.29

TABLE 9

EFFECT OF EMISSION CURRENT ON SPECTRA OF O_2 AND N_2

EMISSION CURRENT	MASS 16/MASS 32	MASS 14/MASS 28
0.6 ma	39.29	--
1.2 ma	41.63	20.65
1.8 ma	25.85	12.08
2.4 ma	19.55	9.25

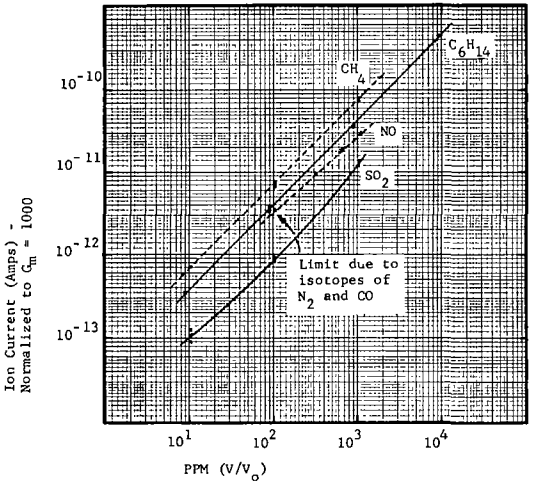

Figure 1. Calibration Curves for CH_4, C_6H_{14}, NO and SO_2. From work by Bunyard and Raby.[12]

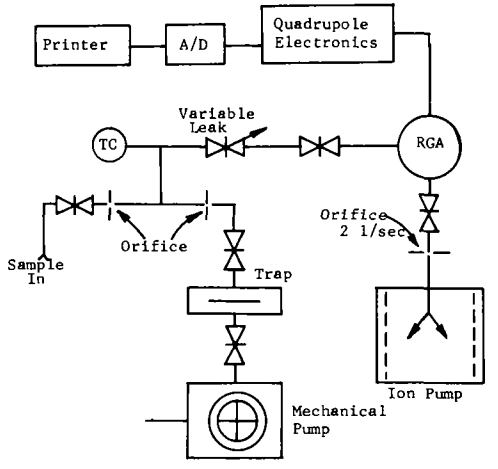

Figure 2. Functional Layout of Quadrupole Gas Analyzer System

COMPUTERIZED DENSITOMETRY USING ION DENSITY AREAS FOR PHOTOGRAPHIC QUANTITATION IN SPARK SOURCE MASS SPECTROGRAPHY

R. A. Burdo,* G. H. Morrison, and J. R. Roth
Department of Chemistry, Cornell University, Ithaca, N.Y. 14850

* Present address: Dept. of Chemistry, Univ. of Rhode Island, Kingston, R. I. 02882

Photographic detection is still the most used method of data acquisition and analysis in spark source mass spectrometry. However, precision and accuracy can be degraded by failure to account for variations in spectral line-width and shape. Compensation for such variations is complicated by the fact that it is not the area under the experimentally recorded transmittance profile which is proportional to the number of ions striking that portion of the emulsion, but rather the area under the corresponding ion density profile. The density profile is derived by a point-to-point conversion of transmittance into ion density according to a calibration curve or photographic response function.

A routine aerial density system has been constructed for the acquisition and storage of digital transmittance profiles obtained from the densiometric output of ion-sensitive photoplates in SSMS using a scanning densitometer interfaced to a PDP-11 computer. A comprehensive profile determination routine based on modified point replacement precisely and accurately defines background and threshold levels. The stored digital profiles are made available in a structured manner to extensive calibration programs which accommodate peak-height, aerial, and approximate aerial densities for response plots. The method of unit slope for calibration has proven effective and can be applied to calibration using beam monitor exposure values or relative isotopic abundances as the abscissa of the response plot.

Automatic concentration programs compute concentrations both within and between exposures so that analyses are available even when analyte and standard lines do not appear on the same exposure. Up to ten standard isotopes of the same element can be handled simultaneously. Output can be extended to a full description of every profile.

The complete system is entirely documented and its aerial quantitative capabilities are shown to equal and surpass the best case for peak-height densities. An isotope ratio can be determined to within 2% error for ten measurements with a precision of 7-8% RSD. The application of aerial density to external standard analysis yields large improvements in precision and accuracy. For internal standard analysis, precision improvements occur when low-mass analyte lines are referred to high-mass standard lines. The use of half-densities is shown to be valid. In no general case does aerial density prove inferior to peak-height density.

The complete paper based on this study has been submitted for publication in ANALYTICAL CHEMISTRY.

Ion Detection in Mass Spectrometry. A Consideration of Ion-Sensitive Plate Response as a Function of Plate Type

T. J. Odiorne, D. M. Desiderio and Paul Vouros

Institute for Lipid Research

Baylor College of Medicine

Houston, Texas 77025

For several years investigators have recognized that the blackening (response) of a photoplate by a given number of impinging ions is dependent on both the energy (1) and mass (2) of the ions. More recently this laboratory and others have shown that the response is also dependent upon the ion's structure and have been involved in describing this dependency (3).

A model (4) has been developed from these data to correlate not only energy and mass effects but also that of ion structure. This model has been applied to the data from both emulsion (Ilford Q2) plates and thin film (Ionomet) plates (5). The results are shown in Table I, where N refers to the number of fragments formed upon impact according to this interpretation.

Table I

Ion (8 KV)	Plate			
	Ilford Q2		Ionomet	
	Rel. response	N	Rel. response	N
Xenon $(Xe)^+$	3.0	1	1.0	1
Perfluorokerosene $(C_3F_5^+)$	2.0	1-1/2	1.1	1-1/2
Naphthalene $(C_{10}H_8^+)$	1.1	3	1.3	3
n-Nonane $(C_9H_{20}^+)$	1.0	3-1/2	1.8	3-1/2

In an attempt to further test the validity of the model, a series of experiments were performed to measure the relative response (Xe vs. n-Nonane) as a function of energy. This has been done for both emulsion and evaporated film plates. The response ratios are shown in Table II.

Table II

Plate type	Ratio	Energy		
		8KeV	6KeV	4KeV
Ilford Q2	$\frac{Xe}{C_9}$	3.0	3.8	5.1
Ionomet	C_9/Xe	1.8	1.5	1.1

These results at different energies yield fragmentation numbers in good agreement with those shown previously.

Preliminary results indicate that the ratios of these fragmentation numbers are very similar to the entropy ratios of the same neutral species.

References

1. J. R. Woolston, R. E. Honig, and E. M. Botnick, Rev. Sci. Instrum., 38, 1708 (1967).
2. J. M. Hayes, Anal. Chem., 41, 1966 (1969).
3. Paul Vouros, D. M. Desiderio, J. G. Leferink and J. A. McCloskey, Anal. Chem., 42, 1275 (1970).
4. R. E. Honig, Trace Analysis by Mass Spectrometry, A. J. Ahearn, Ed., Academic Press, (1972).
5. Paul Vouros, D. M. Desiderio, J. G. Leferink, T. J Odiorne and J. A. McCloskey, Int. J. Mass Spectrom. Ion Phys., 10, 133 (1972).

Electrical Detection System in a Spark Source Mass Spectrometer

M. Arai, M. Naito, T. Takagi and M. Takeuchi,

Analitical Instrument Division, JEOL Ltd.,
Akishima, Tokyo, Japan.

Introduction

Spark source mass spectrometry has been used for qualitative and quantitative analysis of all elements in solid materials with such well known features as relatively non-selective sensitivity for different elements, small matrix effect, simplicity of spectrum pattern, high sensitivity in impurity analysis and so on.

In most cases, the sample is ionized by a high voltage RF spark, and the resultant ion has a rather wide fluctuation over a period of time. This is one of the reasons why the photo plate is used as the detection system of the spark source mass spectrometer. Because photo plate detection constitutes the integral simultaneous detection of all ions.

However, one has to develop the plate and convert the spectrum density into the amount of ions for quantitative analysis. These procedures may be time consuming in a sense.

In recent applications of the spark source mass spectrometer, it has become necessary to quickly see what elements are included in the sample and to show very accurate quantitative results from particular elements. This requirement can be met by electrical detection instead of photo plate detection. This advanced instrument reflects the development of the electrical detection system for spark source mass spectrometry.

Description and result

The unique features of the advanced electrical detection system may be summarized as follows:

a) Automatic spark gap control by spark voltage monitoring.
b) Automatic ion beam control by synchroneous passer.
c) Multi-channel linear ratio amplifier with multi-channel recorder.
d) Hall-probe-controlled magnetic-field switching through same B-H hysterisis curve.
e) On-line data processing of peak switching with mini computer or programable electronic calculator.

Fig. 1 shows a block diagram of the entire E/D system, which mainly consists of three control loops so as to obtain a continuous stable ion beam and accurate analytical results.

Part I refers to the automatic spark gap controller, which keeps the spark gap between the sample electrodes at a constant setting value by monitoring the spark voltage or spark current.

Part II shows the automatic ion beam controller. Total ion beam intensity is picked up by a monitor at the exit of the electrostatic analyzer. The output of the ion beam is fed back to the synchroneous passer, so as to keep the total ion current at a preset value by modulating the frequency of the passer.

Part III consists of a total ion current & charge meter, an individual ion current & charge meter, a linear ratio amplifier, a scanning controller, a peak switching unit, and a beam display unit.

The spark voltage (or current) is picked up by a probe located under the source housing. The signal picked up by the probe is amplified and detected, then compared to the reference voltage which is presettable. The error signal is fed back to a servo-motor, which controls the position of the sample electrode, mechanically.

The sparking voltage (or sparking current) between the sample electrodes has a characteristic relationship with the gap between the two electrodes.

An example of such a relationship is shown in Fig. 2.

This is a recording of spark voltage monitored by an automatic spark gap controller, by changing the reference level at several stages, step by step. Fairly good control of the spark voltage (which is nearly proportional to the sample gap) is attained over a wide range of the gap, from the narrowest gap (close to contacting) to the widest gap (completely open).

When continuous sparking is attained by the automatic spark gap controller, the next important matter-in obtaining stable and accurate analytical result is to minimize ion current fluctuation. Fig. 3 shows an example of mass spectrum reproducibility with and without the automatic ion beam controller mentioned previously. Partial repetitive scanning was made in the ion (Fe) isotope region without the ratio amplifier.

It is observed that there is a big difference between total ion current that is controlled and that not controlled. This automatic ion beam control is not so important when a ratio detection system is provided, but is still valuable for improving measuring accuracy.

For recording the ratio of total ion current and mass peak current, we used multi-channel linear output ratio amplifiers as the detection system in the scanning mode.

This system permits easy analytical surveys of the wide mass range at a fairly high speed, and it covers a large dynamic range of intensity in the linear scale in one scanning.

Fig. 4 shows a block diagram of the 4-channel linear ratio amplifier.

Fig. 5 shows an Al peak scanned (slowly) three times at a scanning speed of 60 min per 3 decades (or full range) when manually changing the total ion current by a factor of 2. Each average value of the Al peak height before and after changing of the total ion current is 24.25 ± 1.05% and 23.5 ± 2.1% respectively. Thus, a peak height variation of ±1.6% or less is observed when the total ion current variation factor is 2.

In Fig. 6, the resolution of this system is demonstrated by showing a Pb spectrum obtained at a scanning speed of 60 min per 3 decades (or full range). $^{206}Pb^+$ and the peak width (W) at 5% of the peak height from the base line of $^{206}Pb^+$ and the peak distance (L) between $^{206}Pb^+$ and $^{207}Pb^+$ are measured; that is, W = 4.5mm, L = 15.0mm, respectively, on the chart.

The resolution (R) calculated by the equation $R = M \times \frac{L}{W}$ (shown here) becomes R = 680 (10% valley).

In Fig. 7, sensitivity in scanning operation is demonstrated by showing a spectrum of 0.03ppm a ^{204}Pb in a Cu-standard sample (A-6 Johnson-mauc), using a scanning speed of 40 min /3 decades (or full range).

The peak setting stability and reproducibility in peak switching operations are shown in Fig. 8. In this case, a spectrum of ^{55}Mn in Fe sample was picked up at switching channel No. 1 and displayed on the CRT screen. This display was attained by moving the ion beam with the coil located at the entrance of the main magnetic field.

The photographs shown here were taken under the following conditions:

1) This photo was taken under the original setting.
2) Taken after 12 different magnetic field switchings.
3) Taken after 12 channel switchings.
4) After sample exchange.
5) Taken after 12 channel switchings.
6) Repeated after 12 channel switchings.

These show that the peak setting stability and resettability was within the 0.02 mass unit during all of the above measurements (approx. 4 hrs). This stability can be obtained by switching the magnetic field through the same B-H hysterisis curve. Every time the magnetic field is switched, the magnetic field is once set at maximum about 10 sec.

Table I shows the measurement reproducibility of peak switching detection. A standard sample of Iron #661 (NBS), which includes 5ppm of ^{119}Sn, was used for this measurement. A 5ppm a spectrum of ^{119}Sn was picked up at peak switching channel No. 2 with a range of 3×10^{-10} coulombs full scale of the charge meter, while a matrix spectrum of ^{56}Fe was picked up at channel No. 1 with a range of 1×10^{-9} C.F.S. of the detector charge meter. Switching measurements were repeated 8 times successively in both cases.

Measurement reproducibility is estimated as standard deviation in per cent.

2.37% for ^{119}Sn; 5ppm impurity peak

0.69% for ^{56}Fe; matrix peak

Table 2 shows an example of an isotope ratio measurement of $^{194}pt/^{195}pt$ and $^{117}Sn/^{119}Sn$.

A fairly good agreement between the natural abundance ratio and observed values can be seen from these data. The data of Table 1 and 2 were obtained by an on-line automatic data acquisition system, using a Wang 600 mini computer. This system is operated in the peak switching mode. The output data from this system include normalized peak intensity, channel nos., the amp. gain used in the measurements, normalized mean values, and standard deviation.

In conclusion, we would like to express our thanks to Dr. Paulsen of N.B.S. for his timely suggestions on the linear amp system and for other useful comments.

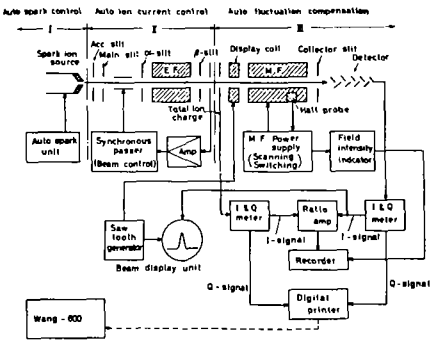

Block diagram of electrical detection system

Fig. 1

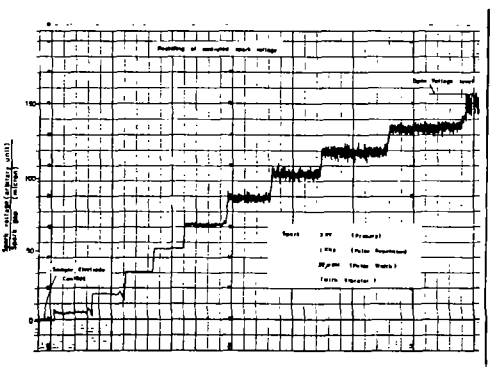

Fig. 2

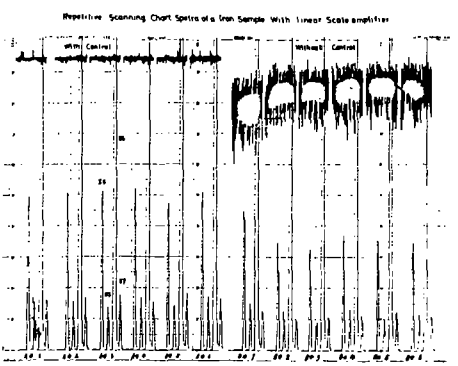

Fig. 3

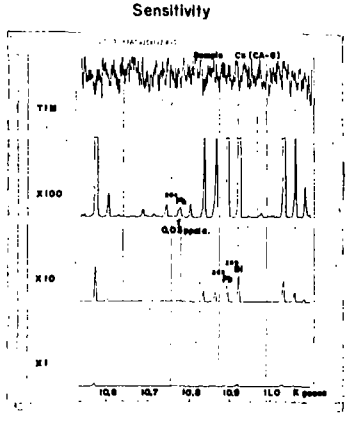

Fig. 7 The measuring conditions.
Main slit: 0.1mm; collector slit: 0.2mm;
Vacc: 25kV; multi voltage: 3kV;
detector current meter range:
1 x 10^{-10}A/full scale;
chart speed: 2.0mm/sec.

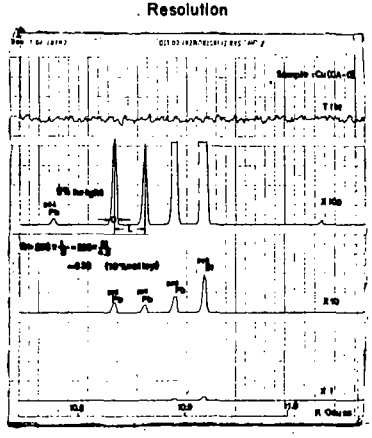

Fig. 6 The measurement conditions.
Main slit: 0.1mm; collector slit: 1.0mm;
-slit: 1.0mm; collector slit: 0.2mm;
ion source: Vacc = 25kV; spark voltage: 3kV
primary side; pulse repetition: 1kHz;
pulse width: 40 μsec.

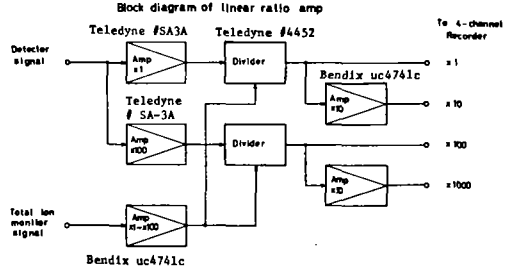

Fig. 4

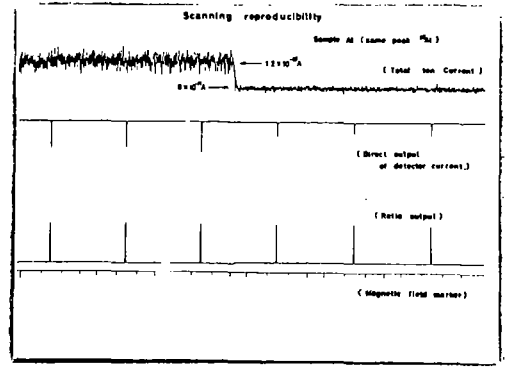

Fig. 5

Reproducibility of measurment

	$^{56}Fe^{+}/_{Fe}$ (Matrix)			$^{119}Sn^{+}/_{Fe}$ (5PPma Imp)		
	1st	2nd	3rd	1st	2nd	3rd
1	0.5858	0.5726	0.5845	0.0219	0.0232	0.0219
2	0.5909	0.5765	0.5857	0.0216	0.0224	0.0216
3	0.5846	0.5783	0.5907	0.0216	0.0221	0.0216
4	0.5843	0.5737	0.5897	0.0222	0.0221	0.0231
5	0.5762	0.5806	0.5848	0.0219	0.0223	0.0214
6	0.5889	0.5795	0.5872	0.0233	0.0216	0.0216
7	0.5812	0.5721	0.5916	0.0225	0.0231	0.0212
8	0.5693	0.5789	0.5821	0.0217	0.0222	0.0223
Average	0.5854	0.5785	0.5870	0.0221	0.0224	0.0218
Std. deviation	0.0040	0.0032	0.0031	0.00052	0.00080	0.00058
Std. dev. / Aver	0.687%	0.566%	0.538%	2.36%	2.28%	2.65%

Table I

Isotope ratio measurement of Pt and Sn

	Pt (Matrix)		Sn (5 PPMA Imp)	
	$^{194}Pt^{+}$	$^{195}Pt^{+}$	$^{117}Sn^{+}$	$^{119}Sn^{+}$
1	0.2191	0.2205	0.1198	0.1275
2	0.2169	0.2174	0.1217	0.1355
3	0.2140	0.2171	0.1216	0.1356
4	0.2180	0.2181	0.1208	0.1316
5	0.2132	0.2224	0.1231	0.1308
6	0.2152	0.2190	0.1235	0.1383
7	0.2140	0.2202	0.1250	0.1349
8	0.2121	0.2189	0.1243	0.1368
Average	0.2145	0.2192	0.1225	0.1338
Std. deviation	0.0036	0.0017	0.0017	0.0033
Normalize	32.97% ←	33.7%	7.61% →	8.31%
Isotope ratio	32.8 %	33.7%	7.61%	8.58%

Table II

The measuring conditions.

Main slit: 0.1mm; collector slit: 0.2mm;

Vacc: 25kV; multi: 2kV for ^{119}Sn

and 0.5kV for ^{56}Fe.

Sample: Sn in Fe

Main slit: 0.1mm; collector slit: 0.2mm; TIM: 1×10^{-9}

IM: 1×10^{-9} C.F.S.

Multi: 2kV; Vacc: 25kV;
anode V: 3kV; 3kHz repetition;
20μsec. pulse width

The measuring conditions.

Sample: 0.2 t pt sheet, NBS 681

Channel: No. 7, ^{194}pt

" : No. 8, ^{195}pt

TIM: 1×10^{-9} coulombs

IM: 1×10^{-9} C.F.S.

Spark conditions: pulse:
Vacc: 25kV 1kHz repetition;
20μsec. width
multi: 500V; anode: 1kV

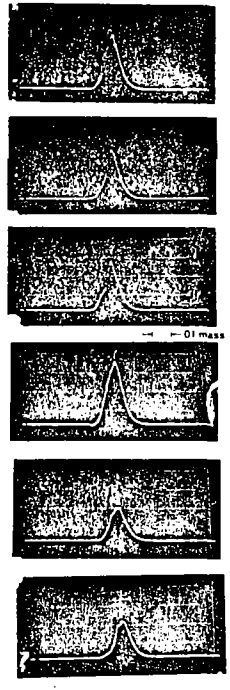

Field setting stability

① 8:05
Original setting ($^{55}Mn^{+}/_{Fe}$)
at CH-1

② 8 25
Same peak after
full channel switching

③ 8 45
Same peak again after
full channel switching

④ 10 00
Same peak after
sample re-set

⑤ 10 15
Same peak after
full channel switching

⑥ 10 35
Same peak again after
full channel switching.

Fig. 8

RADIO FREQUENCY SPARK SOURCE MASS SPECTRA OF GROUP I AND GROUP II CARBOXYLATE SALTS

R. P. Buck and J. R. Hass*
William R. Kenan, Jr., Laboratory of Chemistry
University of North Carolina
Chapel Hill, N. C. 27514

Abstract

The rf spark source mass spectra of a series of C_1-C_{10} carboxylate salts have been obtained. Characteristic of the class of compounds is appearance of the ions $M(I)_2A^+$ and $M(II)A^+$ which suggests the possible application of spark source spectra to qualitative anion identification in salt samples. Our interpretation of the fragmentation patterns is consistent with very rapid decomposition of polymeric (possibly dimer) radical ions with the same composition as the salt. The latter may originate from salt vaporization as neutral species due to local electrode heating. Thermal decomposition of the sample material within the electrode has been shown to be unimportant as a process leading to the observed molecular ions but may, in fact, decrease the useful molecular ion intensities by generation of increased amounts of small ion fragments such as Na^+, Na^{2+}, CO^+, etc. Recombination reactions, charge exchange and solid-solid reactions in the electrode have minimal effects on the observed species in the spectra.

This paper has been accepted for publication by Analytical Chemistry.

---

*PRESENT ADDRESS: Department of Molecular Science, University of Warwick, Coventry, England

MAGNETIC PEAK SWITCHING IN SPARK SOURCE MASS SPECTROMETRY

C. W. Magee and W. W. Harrison

Department of Chemistry
University of Virginia
Charlottesville, Virginia 22901

A magnetic peak selector has been constructed for an MS-702 spark source mass spectrometer, allowing the operator to use magnetic peak switching (MPS), with its attendant advantages over electrostatic peak switching (EPS). In the present model, up to 10 peaks may be preset and switched onto the collector slit to within $\pm$ 0.1 amu. A slight fine tuning of the accelerating voltage is then used to maximize the collector-to-monitor ratio. The magnetic sensing element for the unit is a Hall Probe, mounted beside the analyzer. MPS has several advantages over EPS. The full mass range can be covered while using a fixed accelerating voltage, thus maintaining constant transmission efficiency. Also, elemental sensitivity differences attributable to changes in accelerating voltage (multiplier sensitivity effects) are avoided. The ability to locate peaks rapidly with the Hall Probe enables MPS to be used for RSF determination and peak switch integration in total elemental analysis.

A paper detailing this study will be submitted to Analytical Chemistry

The Structure of an Interactive Program for Spark-Source Photoplate Data Processing

by

J. Rogers Woolston
RCA Laboratories
Princeton, N.J. 08540

A unique highly interactive data processing system for spark-source mass spectrographic data has evolved over the past five years. The system consists of a hardware part and a software part. The hardware part, described in its initial form at the 17th Annual ASTM E14 Conference in Dallas in 1969, has since been enhanced by the addition of an electro-optical linear position encoder and is diagrammed in Fig.1. While the emphasis of this paper will be placed on the software aspects of the system, a brief description of the hardware is necessary to an understanding of the whole system.

SPARK-SOURCE MASS SPECTROGRAPHIC PHOTOPLATE DATA COLLECTION HARDWARE

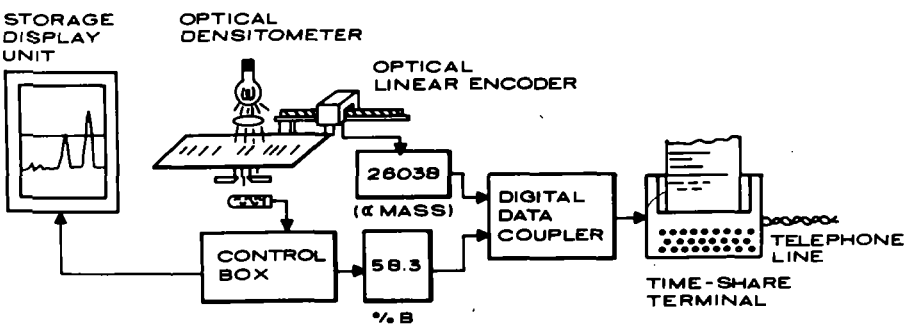

Fig. 1

As shown in Fig. 1, the hardware part of the system is built around a JACo 23-100 optical densitometer on which the 2 in. x 10 in. photoplates are positioned for observation and measurement of percent blackening. As a small portion of the photoplate is mechanically scanned past the measurement slit and photomultiplier, the blackening profile is drawn and stored on the face of the storage display unit (Tektronix 611). The control box then provides a horizontal, non storing cursor whose vertical location can be aligned with any portion of the stored blackening profile. Simultaneously, a digital voltmeter displays the corresponding value of percent blackening. The digital output of this voltmeter is fed into a specially designed digital data coupler which, on command via a pushbutton, causes the percent blackening value to be both printed at the time-share terminal and transmitted to the computer to which the terminal is connected by phone lines. The optical linear encoder provides a digital indication of the instantaneous absolute location of the stage of the densitometer. This in turn, via software, is converted to an exact mass value, accurate to within about 10 millimass units.

The complete system is based on the assumption that the mass spectral plate "reading" will be done by experienced personnel who can recognize, identify, and select the pertinent mass spectral lines on sight. The overall objective, therefore, is to provide all possible aid to the analyst in making "difficult" identifications, in carrying out any and all needed calculations, and in the report writing of results. In other words, the system provides the analyst with a set of "tools" that extends his own sensory and mental capabilities; it does not attempt to do his job for him. Except for a few cases of simple, straightforward spectra, most attempts at performing the entire

plate interpretation automatically have been disappointing. This is due in part to the extreme variety and unpredictability of the spectra of many materials and to the difficulty of programming the requisite chemical and physical intelligence. Furthermore, considerable sophistication is needed to distinguish between spectral lines on the photoplate and dirt and scratches. The human eye and mind represents an extremely efficient "pattern-recognition computer".

The basic organization of the software is illustrated by Fig. 2. A central point in the program issues a blanket "read" to the terminal (indicated at the terminal by a colon) and then analyzes the input entered by the analyst. If the input is valid,

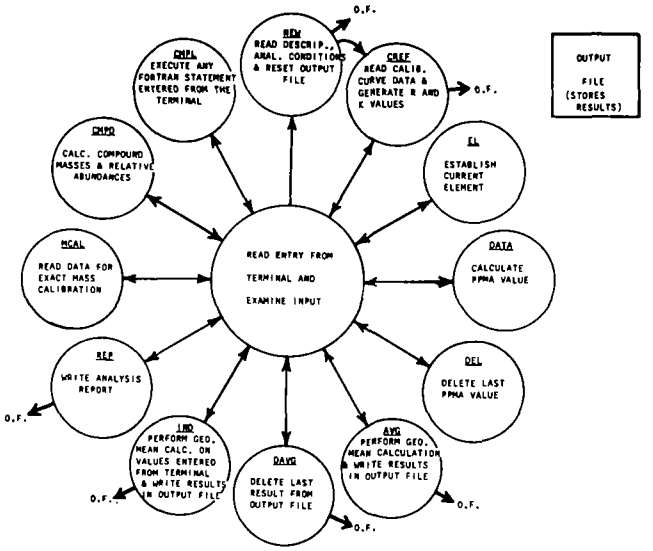

Fig.2

control is transferred to the appropriate section of the program. Several of the satellite functions in Fig. 2 are shown with an arrow labelled "O.F." to indicate that these functions affect the "output file". The output file is a temporary storage area where the calculated results for each processed impurity are stored for later report printing. The program may be halted or interrupted deliberately or unintentionally (computer failure) but these results are not lost. Hence, an analysis may be processed in several stages or sessions. All numerical constants and values pertinent to the current analysis are also automatically stored and retrieved from this file.

The input recognition mentioned earlier represents "data context entry", which means that the program is able to understand what is to be done merely by examining the "format" or context of the entry. For example, the following represent valid entries and will cause the appropriate action:

:FE	element symbol - 1 or 2 alphabetic chars. - establish current element
:56,62.3,5.5,.01,1	data string (ISO,PEAK,BKG,EXP,RSF) - 5 numeric values - cause calculation of a ppma value for the current element
:AVG	program code - 3 or 4 alphabetic chars. - perform function
:MgAl3S 02	compound formula - element symbols with optional digits - list compound isotopic masses and relative abundances
:MgAl3S 02/3	compound formula/multiply charged state - as above suffixed with a slash and an integer - list masses and abundances
:26038	exact mass encoder reading - 5 digits - print out exact mass
:*PRINT RAVG	FORTRAN statement prefixed by an asterisk - execute immediately

While this program is actually written largely in machine code (akin to Assembly Language), it could be written in any of several common programming languages, perhaps with somewhat less efficiency. For example, in FORTRAN the basic structure could be achieved as follows:

```
                .
                .
  1 CALL INPUT (N)
    GO TO (10, 20, 30, 40, etc.), N
 10 CALL NEW
 20 CALL CREF
    GO TO 1
 30 CALL EL
    GO TO 1
 40 CALL DATA
    GO TO 1
                .
                .
```

where subroutine INPUT performs the data context entry diagnosis. This can, of course, be greatly simplified by prefixing every entry with a numeric or alphabetic code, but it is preferable to limit the amount of typing done by the analyst to the essentials. A portion of a typical session showing the entries required for processing three lines for one impurity is given below:

```
:FE

:56,62,3,5,5,.01,1
   FE      3854.995

:54,41,6,,,
   FE      3930.724

:56,34,5,,,.004,
   FE      3377.266

   GEO. MEAN =     3710.000       3 VALUES
   ERROR FACTOR =     1.08

COMMENTS = STEEL VIAL

:
```

where the underlined characters were entered by the analyst (always followed by a carriage return). As evident above, data which remain the same from one entry to the next, e.g., ISO,BKG,EXP, or RSF, need not be re-entered. This is a great convenience to the analyst. A further convenience that not only saves time but greatly reduces errors is the pushbutton entry of the peak and background blackening values. Along the same line, but not illustrated in Fig. 1, are a set of pushbuttons, each of which causes a frequently used code or character string to be entered at the time-share terminal. These hard-wired, fixed data are a part of the digital data coupler. The repertoire is easily expanded at will by the addition of more circuit cards to the custom-built coupler.

A software feature of particular value to the analyst facing a spectrum containing many "unknown" masses and interferences from compound and multiply charged ion species is accessed as follows: An arbitrary string of valid element symbols, optionally followed by digits, is entered. This causes the immediate printing of a list of the compound isotopic masses and relative abundances as illustrated below:

```
:Gd0
 168      0.80
 169      0.00
 170      8.63
 171     59.12
 172     82.19
 173     63.08
 174    100.00
 175      0.17
 176     88.09
 177      0.03
 178      0.18
```

The analyst might wonder, for example, about the degree of interference of this compound with the isotopes of, say, Yb. He may obtain an immediate listing of the Yb isotopes and abundances by entering Yb1 (which distinguishes it from merely establishing the

current element or from a program code) as follows:

```
:Yb1
 168       0.42

 170       9.52
 171      44.94
 172      68.53
 173      50.66
 174     100.00

 176      39.98
```

By suffixing a slash (/) and a numerical value (integer) to an element symbol or compound, the appropriate multiply charged masses and relative abundances will be listed. Below are several examples:

```
:Pb/4
  51.00       2.83

  51.50      45.12
  51.75      43.21
  52.00     100.00


:S103/2
  52.00     100.00
  52.50      10.31
  53.00       7.59
  53.50       0.41
  54.00       0.16


:F7P8As5Au13Bi2Nb4CoAl/15
 147.33     100.00
```

Not apparent from any of the examples given is the fact that the software part of the system performs extensive error checking on the input entered by the analyst. Appropriate messages are immediately printed together with the sounding of the alarm bell in the terminal to alert the analyst to the nature of the error. The isotope, for example, must be a valid isotope of the current element; the background blackening must be less than peak blackening; element symbols in compounds must be valid; all characters in a data string must be numeric, commas, or decimals; codes must be valid; etc.. Such error checking with immediate correction is, of course, the forte of any time-sharing system, but it is not always realized that error checks must be explicitly programmed: they are not inherent.

The final aspect of this system is the printing of analytical reports. This obviates the need to have a secretary prepare the reports and means further that when the analyst is finished reading a photoplate he has his report ready to go to his customer within minutes. The system provides several report formats including a library of "canned" explanatory texts which the analyst includes by appending a string of one-character commands to the program code "REP". The analyst himself may easily expand the library whenever he wishes to cover new analytical situations.

Over 3000 analyses have been processed with this system and its precursors in the past five years or so. A typical plate requires about an hour, involving up to a hundred spectral lines for 20 to 30 impurity elements. Further enhancements presently planned include the ability to measure ion-density areas to achieve a further increase in precision. Such improved precision is only warranted, however, for analyses referenced to good standards, which is not the majority case.

ANALYSIS OF TRACE ELEMENTS IN COAL DUST BY SPARK SOURCE MASS SPECTROMETRY

By

A. G. Sharkey, Jr., T. Kessler, and R. A. Friedel

Pittsburgh Energy Research Center, Bureau of Mines
U. S. Department of the Interior, Pittsburgh, Pa. 15213

As part of the respirable mine dust research program at the U. S. Bureau of Mines, spark-source mass spectrometry has been used to determine trace elements in respirable range mine dusts and coal dusts. The object of the research is to obtain information for correlating the incidence of coal workers' pneumoconiosis with the composition of mine dusts. Ten pairs of respirable dusts collected in mines and respirable size coal (prepared samples) were analyzed. Samples were obtained from one medium volatile bituminous (mvb), five high volatile A bituminous (hvAb), and four low volatile bituminous (lvb), mines representing eight coal seams in Pennsylvania, West Virginia, Virginia and Utah.

Very little data have been reported on the analysis of elements in whole coal and mine dusts in particular. Kessler, Sharkey and Friedel reported the analyses of trace elements in coals from mines in ten coal seams located in Pennsylvania, West Virginia, Virginia, Colorado and Utah.[1] Sixty-four elements ranging in concentration from 0.01 to 41,000 ppm[a] wt were determined. Several surveys published previously have provided data on the concentration of minor elements in ashes from coals rather than a direct determination on the whole coals or mine dusts. The early investigations include studies by Headlee and Hunter,[2] Nunn, Lovell and Wright,[3] and Abernethy, Peterson and Gibson.[4]

Because the atmosphere in the mine can contain in addition to coal dust other materials such as rock dust ($CaCO_3$), slate and organic contaminants, there is the possibility that respirable dust can have a different composition than coal of a similar size from the same mine. The purpose of this phase of the investigation is to determine if extraneous materials not present in prepared samples of 3-5 micron size coal dust can be detected in mine dusts collected during actual mining operations.

The instrument used in this investigation was a commercial Mattauch-Herzog[b] mass spectrometer equipped with photographic and electrical detection systems and an RF spark source. The resolution of the instrument was 1 part in 5,000. All trace elements were determined from mass spectra recorded on Ilford Q-2 photographic plates. Major elements were determined using the electrical detection system. Electrodes were prepared by mixing the samples with equal parts of pure graphite. To insure homogeneity of mixing and to determine the plate sensitivity, 50 ppm of indium was added as an internal standard to the sample-graphite mixture.

To obtain a representative sample for the analysis of the elements present in the coal, 400 pounds of raw coal were obtained from each of the seams investigated. The raw coal sample was first crushed to 3/8 by 0 inch. The crushed coal was divided by successive riffling to obtain a final 25-pound sample. The 25-pound sample was air dried and then divided twice to obtain a 6.25-pound sample. The 6.25-pound sample (3/8 by 0 inch) was reduced to - 200 mesh by grinding on a micro mill equipped with Stellite blades. Using a wind tunnel - Andersen Sampler system, the - 200 mesh coal was separated into the following particle sizes: >9.2, 5.5-9.2, 3.3-5.5, 2.0-3.3, 1.0-2.0, and <1.0 microns. Previous work has shown that the 3.5-5.5 micron coal fraction has a particle size distribution similar to respirable mine dust. This fraction was used for the spark-source analyses.

The elemental compositions of the respirable dust and 3.3-5.5 micron coal fraction from the ten mines are similar. The elements showing a difference in concentration greater than a factor of 2 are Ag, Cd, Cu, Zr, Rb, Ca, Cl, P, and Br. The majority of samples show higher concentrations of the above elements in the respirable dust than in the corresponding 3.3-5.5 micron coal fraction. The average

a/ In this paper, parts per million are given in terms of weight.
b/ Reference to specific equipment is made for identification only and does not imply endorsement by the Bureau of Mines.

ratios of the concentration of the various elements in the dust compared to the coal are as follows: Ag 27, Cd 36, Cu 9, Zr 16, Rb 4, Ca 6, Cl 200, P 71, and Br 72. The increased concentrations are considerably more than the factor of two differences normally expected in duplicate runs in spark source survey analyses. There are many different materials carried into mines from mining operations. The source of these high concentrations of the above elements is not known.

Differences observed in the organic material in mine dust and coal from the same mine are illustrated in figure 1. High-resolution mass spectral data for the carbon-hydrogen (C-H) distributions in <74 micron and 3.3- 5.5 micron coal, and mine dust are shown. Formulas were detected for compounds with C-H values included in the lines. For this particular coal many of the C-H ratios approach 1 indicating the highly aromatic character of the organic material. Of particular interest is the additional series of highly saturated material detected in the mine dust. While it is not within the scope of this investigation to determine the adverse health effects of higher concentration of particular elements, certain of these elements could be hazardous and further investigation is warranted.

REFERENCES

1. Kessler, T., A. G. Sharkey, Jr., and R. A. Friedel. Analysis of Trace Elements in Coal by Spark-Source Mass Spectrometry. BuMines Rept. of Inv. 7714, 1973, 8 pp.

2. Headlee, A. J. W., and R. G. Hunter. Characteristics of Minable Coals of West Virginia. Part 5. The Inorganic Elements in the Coals. W. Va. Geol. Survey, 13A, 1955, pp. 36-122.

3. Nunn, R. C., H. L. Lovell, and C. C. Wright. Spectrographic Analyses of Trace Elements in Anthracite. Trans. Ann. Anthracite Conf. Lehigh Univ., Bethlehem, Pa., v. 11, 1953, pp. 51-65.

4. Abernethy, R. F., M. J. Peterson, and F. H. Gibson. Spectrochemical Analyses of Coal Ash for Trace Elements. BuMines Rept. of Inv. 7281, 1969, 20 pp.

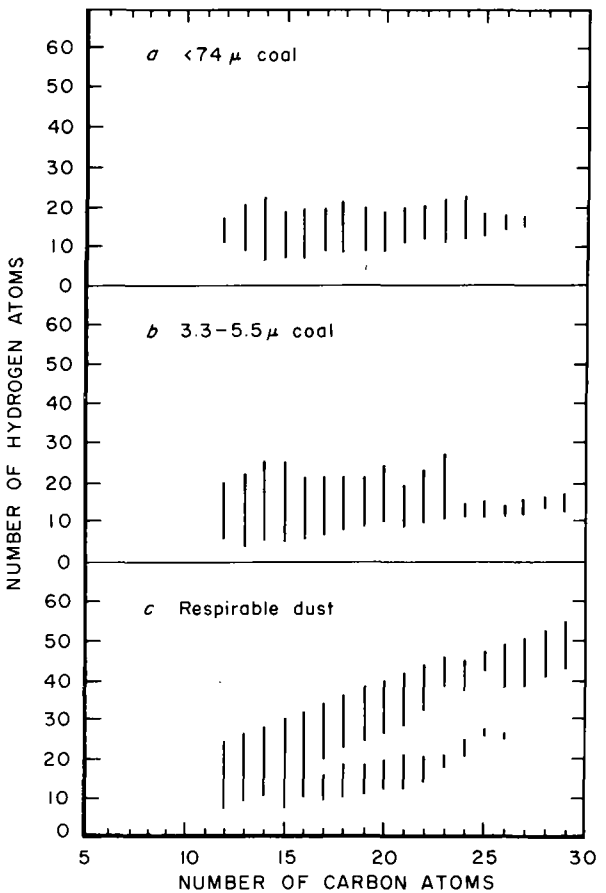

Fig. 1 Carbon-hydrogen distribution in coal and mine dust.

L-12475

The Determination of Trace Elements in Fly Ash by Spark Source Mass Spectrography

Charles A. Evans, Jr.
Materials Research Laboratory
and
David F. S. Natusch and John R. Wallace
Department of Chemistry,
University of Illinois, Urbana, Illinois 61801

Spark source mass spectrography has been used in conjunction with X-ray fluorescence spectroscopy, atomic absorption and flame emission spectroscopy, D.C. arc emission spectroscopy and differential pulsed anodic stripping voltammetry to determine trace elements in fly ashes from coal-fired power plants. The advantages of spark source mass spectrography for this application and the agreement between its results and those of other methods are discussed. The analyses showed that many toxic trace metals, notably Pb, As, Sb, Tl, Cd and Se, increase markedly in concentration in very small particles (<5μ) with the lowest values being found in particles readily retained by control equipment. Concentrations of Thallium in excess of 70 μg/gm were found in respirable fly ash particles emitted from a number of sources. The environmental significance of these findings is discussed.

A complete description of this work is in preparation and will be submitted to Environmental Science and Technology.

Acknowledgments

This work was supported by National Science Foundation Grants No. GI-31605 and GH-33634.

IN-DEPTH ANALYSIS BY ION MICROANALYZER

H. Tamura and T. Kondo
Naka-Branch, Central Research Laboratory, Hitachi Limited;
T. Hirano, K. Nakamura and T. Noda
Naka works, Hitachi Limited;
882 Ichige, Katsuta, Ibaraki, Japan

Introduction

In-depth analysis is one of the most important application fields of ion microanalyzer. Various attempts have been made already and some of them have been used in practical applications[1]. Conventional in-depth analysis, however, includes the following problems.

1) In-depth analysis of a selected micro area
2) In-depth analysis of thin surface layers

The above 1) is important for analysis of any small area of semiconductor devices and crystal grain boundary.

The above 2) problem is that secondary ion yield depends on work function of sample surface. In-depth analysis of absorbed layers and oxide layers, therefore, is affected by changes in work functions of these layers and does not reflect true distribution of the concentration. This paper describes some new methods to eliminate these problems and also introduces of the results obtained.

New Method for in-depth analysis

Fig. 1 indicates two new methods for in-depth analysis. One is "Direct ion imaging method" and the other "Scan-stop method". The direct ion imaging method employs a new astigmatic lens and a conventional electrostatic sector. Secondary ion image of sample surface is formed at the position of β-slit. Resolving apetture is mounted in place of the β-slit so that ions in the central portion of the beam can be introduced into the magnetic sector and ions at periphery eliminated. Primary ion beam can either be positioned at any arbitrary point or scanned in an usual manner.

On the other hand, the scan-stop method is such that the primary ion beam is first scanned over sample surface permitting uniform etching. Then, the scan-generater is switched off and a separate X-Y power supply is turned on so that the primary ion beam can be positioned at selected area on sample surface by applying appropriate voltage on the beam deflector. In-depth analysis is performed by positioning the primary beam at any selected area after etching. Repeating this process permits analysis over entire sample surface.

Fig. 2 shows principle of the direct ion imaging method with secondary ions and an example of results obtained. Photograph (a) shows an optical micrograph of the sample and (b) shows a secondary electron image focussed on the fluorescent screen. The secondary ion image is not so sharp as the secondary electron image due to initial energy spread but it is still satisfactry for our purpose.

We have adapted a method described in Fig. 3 in order to eliminate the effects which stems from work function of sample surface. The principle is that the secondary ion yield depends on the work function of sample surface. If we take a ratio of mass-analyzed specific ions to total secondary ions, we can eliminate the changes in work function of sample surface. A part of total ions is collected at β-slit. The ion current monitor is placed bihind the electrostatic sector in order to eliminate reflected ions. These two output signals are fed to a ratio circuit so that the ratio of specific ion current to total ion current can be obtained. The ratio output is then led to a recorder. This method is advantageous for minimizing effect of sample topography.

Experimental Results

Fig. 4 shows an example by the ratio method. The sample is a silicon wafer coated with Al about 2000Å thick. Curve (A) shows total ion current with respect to time and (B) shows Al^+ ion current. The initial peak does not necessarily indicate high concentration at the surface but it may be attributed to change of work function at thin surface layer.

Curve (C) is a ratio of Al^+ ion current to total ion current. Changes in work function at the surface is eliminated and correct in-depth information is obtained. Due to the reason that Al surface is always oxidized, we can see the fact that this curve indicates real distribution qualitatively.

Fig. 5 shows a result of in-depth analysis of Al in Si. The sample was prepared by Al implantation into intrinsic silicon wafer of which impurity concentration was $10^{15}/cm^3$. Surface concentration of Al is $10^{20}/cm^3$. The dotted line is a conventional result and the solid line indicates result obtained by our new method combined with direct imaging and ratio method. It is clearly understood that with conventional method Al concentration does not decrease in long period and resolution in depth analysis is poor. According to results of our new method, Al concentration decreases significantly with depth. It indicates about 10^{-3} concentration of Al at the depth of 7500Å compared to the peak value. It is well known that impurities diffused by ion implantation illustrates Gaussian distribution. It is encouraging to note that our result is close to the Gaussian distribution. Depth was measured by multibeam interferometer after the above analysis. Accuracy of the multibeam interferometer used is better than 50Å.

Fig. 6 shows in-depth distribution of B thermally diffused into a Si single crystal. Primary ion beam scans over an area of 1 mm^2 just like TV raster. Area of analysis is about 1/3 of the entire area scanned. Output signal of the mass spectrometer is fed to multichannel scaler. Etching speed was approx. 1μm/hour. Upper curve was taken at sensitivity 16 times greater than lower curve. With our data we can distingnish concentration difference of B in the order of 3-digits or more and we can get resolution in depth analysis of better than 100Å.

Fig. 7 is a mass-analyzed secondary ion image of Al^+ in semiconductor device using our new method. Photograph (a) is a secondary ion image of Al after slight etching. Circuit pattern of Al is clearly visible. The smallest line width is 10 microns. (b) shows the same Al ion image after ion etching of about a few hundred angstroms. These pictures show reverse contrast. It is obvious that Al circuit has been removed by ion etching. Resolution of better than a few micrometers is demonstrated. (c) shows an ion image of Si^+ ion. (d) shows an ion image of B. B concentration at white spots is approx. $10^{19}/cm^3$. High intensity portion is B glass which has a high concentration of B. Recording time of these pictures was about 6 minites. Longer exposure time increases image contrast.

Conclusion

We have discussed the problem concerned with in-depth analysis which is one of the unique features of ion microanalyzer.

(i) Problems in conventional method
(ii) Two new proposals for in-depth analysis
(iii) Application data based on the new proposals

We have proposed "ratio method" in order to eliminate the effect of work function. However, we would like to make some reservation at this stage. There are many problems still remain to be solved in terms of secondary ion yield and work function despite of aggressive effort by slodzian et al[2]. For in-depth analysis, we have proppsed two new method for the analysis in micro-area as well as in large area. Accuracy of these new methods is dependent on samples but approximately some 10～100 angstroms. Resolution in depth analysis is not just a function of uniformity of ion etching but it also involves problems related to secondary ion generating area. For discussion of resolution better than 100Å order, we think secondary ion generating area is a more serious problem. We would like to keep study of these problems in the future.

Reference

1) H. Tamura, T. Kondo and H. Doi : Triennial Intern. Mass Spectrometry Conf., Brussels (1970) ; Advances in Mass Spectrometry, 5 (1971)
2) G. Slodzian : Pittsburgh Conf. on Anal. Chem. and Appl. Spec., Cleveland, Ohio, (1973)

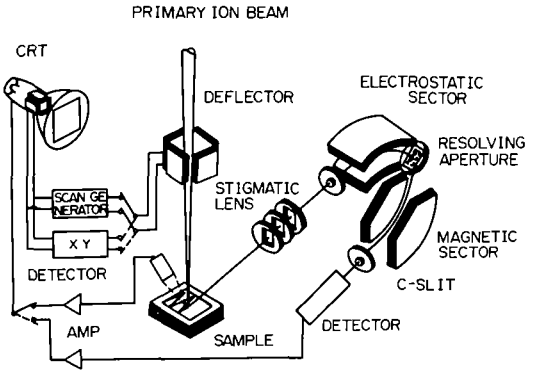

Fig.1 Direct imaging method.

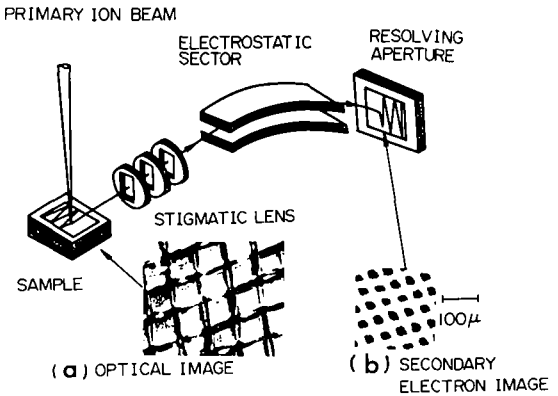

Fig.2 Principle of direct imaging method.

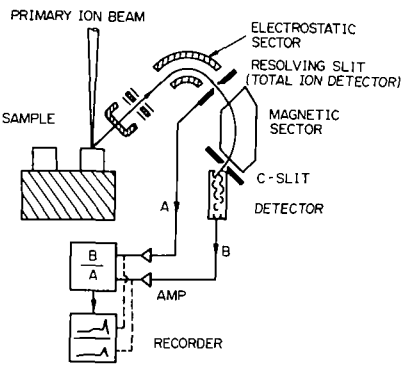

Fig.3 Secondary ions monitoring method.

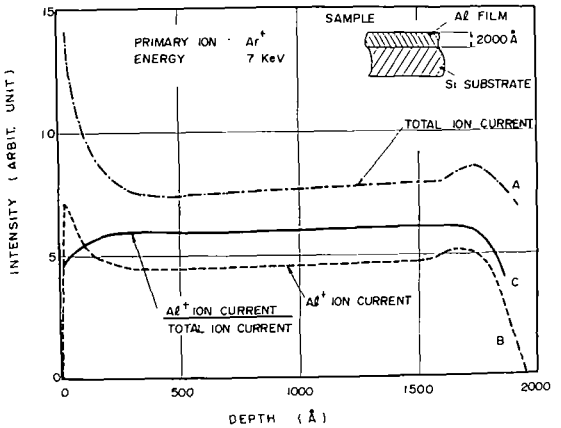

Fig.4 In-depth analysis of evaporated aluminum film.

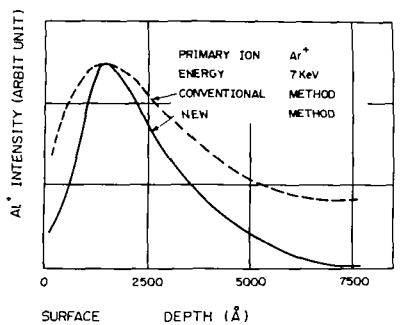

Fig.5 In-depth analysis of aluminum in silicon.

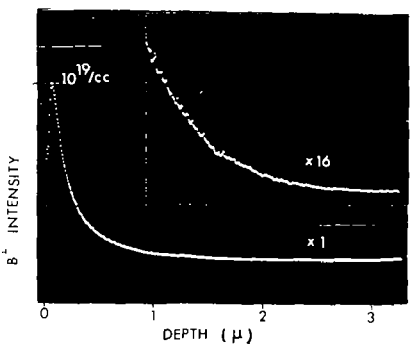

Fig.6 In-depth analysis of boron in silicon.

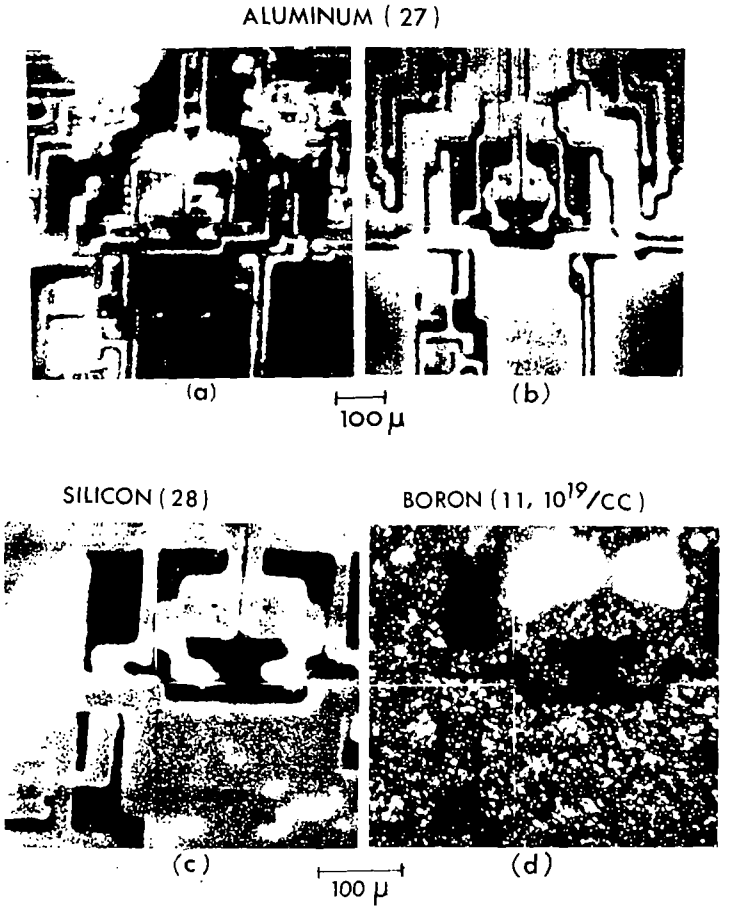

Fig.7 Ion images of a semiconductor device.

MASS SPECTRA OF RARE EARTH TRIIODIDES

C. Hirayama and P. M. Castle
Westinghouse Research Laboratories
Pittsburgh, Pennsylvania 15235

ABSTRACT

The electron impact fragmentation patterns of the stable lanthanide triiodides are characterized by a strong MI_2^+ peak. Depending on whether the metal is in the first or second group of the lanthanide series, the parent ion peak, MI_3^+, is either the weakest or the second strongest in the spectrum. The relationship of the MI_2^+/MI_3^+ relative intensity is best explained by their relative bond dissociation energies.

The triiodides all sublime congruently, and their heats of sublimation are all very similar. Also, the appearance potentials of the corresponding positive ions in the spectra of these triiodides have similar values.

MASS SPECTROMETRIC STUDIES OF THE VAPOR PHASE OVER NaI-CsI MIXTURES

P. M. Castle and C. Hirayama
Westinghouse Research Laboratories
Pittsburgh, Pennsylvania 15235

ABSTRACT

A modified Bendix 12 TOF mass spectrometer equipped with the standard Kundsen cell attachment has been utilized to study the vapor phases of various mixtures of NaI and CsI. These data are compared with those obtained for the pure components using the same instrument. The complex $NaCsI_2$ is one of the principal species observed. Linear extrapolation gives 8.5 eV for the appearance potential of this species. A heat of vaporization for $NaCsI_2$ of 22 kcal/mole was obtained from the 1:1 NaI:CsI mixture.

MASS SPECTRA OF CUPROUS CARBOXYLATES

by

J. B. Westmore and Denis Lin
Department of Chemistry,
University of Manitoba,
Winnipeg, Manitoba, Canada

ABSTRACT

The thermal decomposition of twenty five cupric carboxylates was studied by mass spectrometry. In eleven cases volatile cuprous carboxylates (many of which have not been previously reported) were detected amongst the decomposition products. The cuprous carboxlates from acetic, propionic, n-butyric, isobutyric, difluoroacetic, trifluoroacetic, benzoic, p-fluorobenzoic, p-chlorobenzoic, o-chlorobenzoic and pentafluorobenzoic acids were all found to be dimeric in the vapor phase. Two basically different fragmentation pathways can be proposed depending upon whether the copper salt is formed from an alkyl- or aryl- carboxylic acid. For the former, the spectra are dominated by even-electron fragment ions formed by initial loss of $RCO_2^{\cdot}$ from the molecular ion. For the latter, a parallel fragmentation pathway initiated by loss of CO_2 from the molecular ion and migration of the aryl group to the metal is also present.

A full report of these studies has been accepted by the Canadian Journal of Chemistry.

SOME CHECKS ON THE MASS SPECTROMETRIC METHOD OF MEASURING GASEOUS EQUILIBRIA

D. L. Hildenbrand

Stanford Research Institute
Menlo Park, California 94025

Mass spectrometry is now rather widely used for studies of the thermodynamics of high temperature gaseous reactions, and some of the most reliable thermochemical data for small molecules and other gaseous species stable at high temperatures have been obtained by this technique. In its usual application, the mass spectrometer is used to sample a collision-free molecular beam issuing from a heated effusion oven; thermochemical data are derived from the measured ion abundances and from their temperature dependences. It is the specificity, sensitivity and wide dynamic range of the mass spectrometer which make it essentially unique in this application. A particularly attractive approach involves the study of gaseous isomolecular reactions, since no direct pressure calibration is required. However, in the evaluation of equilibrium constants from ion abundance ratios, it must usually be assumed that ionization cross section and instrumental sensitivity factors will tend to cancel within certain limits, since these and other factors for converting ion current to pressure are unknown or highly uncertain. Based mostly on intuition, it has been customary to assign a factor of two uncertainty to equilibrium constants calculated from the uncorrected ion abundance ratios. Such an uncertainty then leads to uncertainties of 2-3 kcal in third-law enthalpies derived from equilibrium data in the range 1000 to 2500°K.

Over the last few years, it has been possible to examine the validity of this approach for several isomolecular reactions in which the equilibrium constants are known accurately from spectroscopic and/or calorimetric data. All measurements were made with a 12" radius, 60° sector magnetic deflection mass spectrometer equipped with a Nier-Inghram electron impact ion source and an electron multiplier ion detector. Gaseous species were identified from the masses and threshold appearance potentials of the ions, and equilibrium constants were calculated from the parent ion abundances, all measured at the same small (3.5 eV) excess ionizing energy above onset so as to eliminate fragmentation. The effusion cell origin of each signal was ascertained from neutral beam intensity profiles.

The gaseous reactions studied were:

(1)	$SO_2 + S = 2SO$	(1660° to 1970°K)
(2)	$Al + O_2 = AlO + O$	(2210° to 2240°K)
(3)	$Al + SO = AlO + S$	(1960° to 2120°K)
(4)	$HCl + O = Cl + OH$	(1890° to 2030°K)

where 1, 3, and 4 were generated by admitting SO_2 and HCl to an alumina effusion cell, and 2 was generated by the direct vaporization of alumina from a tungsten cell. The thermochemistry of each reaction is now well established, quite independent of any equilibrium measurements, and the equilibrium constants are known with an accuracy of 10% or better.

The ion current analogs, derived directly from the ion abundance ratios as described above, were very consistent and agreed with the known equilibrium constants to within 15%, 35%, 30% and 20% for reactions 1, 2, 3 and 4, respectively. Furthermore, these analogs exhibited the proper temperature dependence. The results suggest that the inclusion of estimated ionization cross section and electron multiplier gain factors is not likely to improve the accuracy of the equilibrium data. Although it is imperative to continue to critically examine the assumptions used in treating the data, the results presented here provide some justification for the method and some evidence of the validity of the equilibrium data obtained from mass spectrometric studies of rather symmetrical isomolecular reactions.

HIGH TEMPERATURE STUDIES ON THE SAMARIUM-SULFUR SYSTEM USING AN AUTOMATED QUADRUPOLE MASS SPECTROMETER

Margaret A. Frisch
Thomas J. Watson Research Center, IBM
Yorktown Heights, New York, 10598

I. Introduction

The preparation of divalent rare earth chalcogenides has been aided substantially by vaporization studies which, for example, have shown that at high temperatures divalent europium compounds behave more like alkaline earths than like lanthanides(1,2). Such information has proven invaluable in developing crystal growth parameters to achieve the desired stoichiometry. Our interest in the relationship between the magnetic and semiconducting properties of samarium sulfide with composition has led to the present investigation. The study was initiated to acquire information on the vapor solid equilibria in the samarium-sulfur system which would be necessary for the development of optimum conditions for crystal growth and thin film deposition and provide some insight into the impurity distribution in the solid and vapor phases.

II. Experimental

The vapor solid equilibria over single crystal SmS, grown in this laboratory, were studied by the Knudsen effusion mass spectrometric technique. The tungsten Knudsen cell, which had a cylindrical orifice 1.1 mm diameter by 5.5 mm length, was employed, using a 25 mg sample size. The cell was heated in a high vacuum resistance furnace and controlled at selected temperatures by a Leeds and Northrup Mark II Automatic Pyrometer. The molecular beam, effusing from the cell, is modulated at 20 cps before entering the ion source of a Finnigan quadrupole mass spectrometer. The spectrometer is in a differentially pumped ultra high vacuum chamber in order to achieve minimum background interference. The essential instrument functions, mass position, ionization energy and the demodulation of the ion signal, are controlled by an IBM 1800 computer. The coherent ion signal, arising from the vapor species in the molecular beam, is derived from the computer demodulation of the ion pulses, obtained from two separate scalers, gated to count in and out of phase, respectively, with the interruption of the beam. This innovation in ion current measurement has considerably enhanced the statistical analysis of the data. Further, the capability to scan rapidly a large number of mass positions (e.g. 250 in 1 minute) has allowed us to make detailed studies of vaporization and diffusion behavior of significant impurity species as a function of temperature.

III. Results and Discussion

During the initial heating of single crystal SmS, commencing at about 1300°K, only the samarium species was observed in the vapor phase. The sample was annealed at 1887°K for 105 minutes, at the end of which time, the ion intensity of the samarium species had decreased to a steady state value and ion signals, corresponding to S, S2, and SmS, were also observed but at intensities less than 1% of the samarium. The thermodynamic studies were made after the vaporization rate of the matrix components had been stabilized. The sample was cycled four times from 1380°to 2014°K in 50°K intervals and ion currents for Sm and SmS were measured. The sample was weighed and the weight loss, combined with the integrated samarium current, yielded the pressure calibration constant for samarium. A Guinier x-ray diffraction pattern on the residue gave a powder pattern which was indexed on the basis of a bcc unit cell with $a_o = 8.544 \pm 0.002$Å, which can be compared to $a_o = 8.556$Å for Sm_3S_4 and $a_o = 8.448$Å for Sm_2S_3(3).

In run 3, the samarium pressure began to deviate from the second law plot at about 1800°K which indicated the disappearance of the SmS phase. The temperature was held at 1989°K until only the Sm_3S_4 phase remained and a new stable equilibrium was achieved. Sm and S were then vaporizing at approximately the same rate. In Table I, the thermodynamic properties for reactions 1 and 2 were derived from measurements obtained from the first 3 temperature cycles for the equilibria of Sm(g) and SmS(g) with SmS and Sm_3S_4 phases. The uncertainties of the enthalpy and entropy of reactions, given in Table I, are the one sigma statistical variation in the data.

Since the residue after run 4 was single phase and had a lattice constant of a composition 11% from that of Sm_3S_4, we assume that a partial conversion of Sm_3S_4 towards the Sm_2S_3 composition occured and that the thermodynamic properties for reactions 3 and 4 in Table I correspond to the equilibria of Sm(g) and SmS(g) in this region of the phase diagram. The dissociation energies of the S_2 and SmS molecules (reactions 5 and 6, Table I) were also measured over this phase.

The complete report on this study will appear in a paper to be submitted to High Temperature Science.

IV. References

1. J. M. Haschke and H. A. Eick, J. of Phys. Chem. 73, 374(1969).

2. A. V. Hariharan and H. A. Eick, High Temp. Sci. 3, 123(1971).

3. M. Picon, L. Domange, J. Flahaut, M. Guittard, and M. Patrie, Bull. de la Soc. Chim. de France, p. 221(1960).

TABLE I.

THERMODYNAMIC PROPERTIES OF THE Sm-S SYSTEM

	Reaction Studied	Temperature Range degree K	ΔH^o_r kcal/mole	ΔS^o_r Gibbs/mole
1.	$4\ SmS(s) = Sm(g) + Sm_3S_4(s)$	1380 - 2014	88.5 ± 0.4	23.6 ± 0.3
2.	$SmS(s) = SmS(g)$	1583 - 1938	115.6 ± 1.3	27.4 ± 0.8
3.	$Sm_{3-x}\ \square_x\ S_4(s) = Sm(g) + Sm_{3-x-1}\ \square_{x+1}\ \square_{x+1}\ S_4(s)$	1583 - 2014	98.6 ± 2.4	23.9 ± 0.5
4.	$Sm_{3-x}\ \square_x\ S_4(s) = SmS(g) + Sm_{3-x-1/4}\ \square_{x+1/4}\ S_4(s)$	1684 - 2014	129.0 ± 1.0	33.5 ± 1.2
5.	$S_2(g) = 2\ S(g)$	1625 - 2000	105.0 ± 0.5	29.3 ± 0.3
6.	$SmS(g) = Sm(g) + S(g)$	1650 - 2000	95.1 ± 0.6	26.1 ± 0.3

QUANTITATIVE ELEMENTAL ANALYSIS OF THIN SOLID LAYERS BY GLOW DISCHARGE MASS SPECTROMETRY

J. W. Coburn, E. Taglauer*, and Eric Kay
IBM Research Laboratory
San Jose, California 95193

The combination of rf glow discharge sputtering and mass spectrometry has been used to determine the elemental composition of solids as a function of depth.[1] The sample is incorporated in the target of a special rf glow discharge sputtering system. An inert gas glow discharge is established by capacitively applying an rf voltage to the target and the sample is sputter-etched by the resulting inert gas ion bombardment of the target. The sputtered species leave the target primarily as neutral particles. Note that sputtered positive ions, which constitute the entire signal in sputtered ion mass spectrometry,[2] are returned to the sample by the prevailing electric field. Negative sputtered ions on the other hand will be accelerated away from the sample into the discharge. No attempt has yet been made to look for negative ions in this work but no indirect evidence has been uncovered which would indicate that negative sputtered ions are significant even during analysis of alkali halides. Therefore it is the sputtered particles which leave the sample as neutrals which constitute the detected signal in this method. A fraction of these sputtered neutral particles is ionized during transit thru the discharge primarily by the Penning ionization process.[3] Some of the ions created in this way pass thru a sampling orifice, located opposite the sample, into a differentially pumped low pressure region containing a quadrupole mass filter with which the ions are mass analysed. The analysis system used has a six-position rotary target structure permitting the analysis of six samples per opening of the vacuum system.

The results of analyses on the following materials were shown to illustrate the capabilities of the method:

1) $MnCrSb_2$ (bulk conducting sample)
2) GaAs (bulk semiconducting sample)
3) Y_2O_3 - Sb_2O_3 (bulk insulating sample)
4) Co (1100Å thin film, $1cm^2$ in area)
5) Ni, V, $Co_{0.8}Ni_{0.2}$ (three layer thin film structure)
6) $Pb_x\ Sn_{1-x}$ (bulk samples x = .1, .3, .5, .7, .9)

The major characteristics of this method as we understand them at this time are:

1) The elemental sensitivity is independent of the matrix in which the element is incorporated.
2) All elements can be detected with approximately the same sensitivity except He and Ne when He is used as the discharge gas.
3) Analysis rates from 1 monolayer per minute to about 200 monolayers per minute can be used.

4) Trace impurities at a concentration of 50 ppm can be detected at high analysis rates. It is anticipated that this figure can be improved upon when a discharge-induced dc background signal is eliminated.

5) The energy of the inert gas ions incident on the sample is typically 100-200eV.

6) Some diatomic species are observed and the intensity relative to the atomic species is determined primarily by the strength of the binary bond involved. Triatomic and more complex species are seen at trace levels only.

7) The entire sample is analysed; that is there is no spatial resolution in the plane of the sample. Samples at least a few mm in linear dimension are required.

8) The sample must be mounted on the sample holder in such a way as to ensure uniform sputter-etching.

It is planned to publish this work in the Journal of Applied Physics.

*Present address: Max-Plank-Institut fur Plasmaphysik Garching, Germany.

1. J. W. Coburn & Eric Kay, Appl. Phys. Lett 19 350 (1971)

2. C. A. Anderson & J. R. Hinthorne, Science 175 853 (1972)

3. J. W. Coburn & Eric Kay, Appl. Phys. Lett. 18 435 (1971)

COMPOSITION AND VELOCITY DISTRIBUTION STUDIES OF CARBON VAPOR SPECIES FROM ALL-GRAPHITE KNUDSEN CELLS**

by

T. A. Milne
J. E. Beachey
S. L. Bennett*
F. T. Greene

Midwest Research Institute
Kansas City, Missouri 64110

INTRODUCTION

To further the understanding and prediction of the ablation behavior of graphite-based nose cones, we have been attempting to extend to higher temperatures, the measurement of vapor composition over graphite. The approach has been the direct determination of the thermodynamics of vaporization of carbon clusters by molecular-beam mass spectrometry of vapor effusing from all-graphite Knudsen cells.

Because so much can be learned by coupling chopped-beam velocity analysis of neutrals with mass spectrometry, implementation of this technique has received a high priority.

This paper briefly reviews the overall design and heating, molecular beam mass spectrometer, the first results of equilibrium species ratio determination and the time-of-flight behavior of neutral beams of carbon vapor, particularly C_3.

CARBON CELLS, HEATING AND MOLECULAR BEAM SAMPLING

A schematic of the entire apparatus is shown in Figure 1. All-graphite Knudsen cells about 1 in. by 1 in. diameter are induction heated with the aid of a copper, water-cooled current concentrator placed inside a section of 4 in. I.D. Pyrex pipe. The Knudsen cells consist of an ATJ graphite cup, with a 1/8 in. diameter orifice, shielded by fully slotted pyrolytic graphite outer sleeves, support and lid. Vapor effusing from the cell is collimated, modulated by a motor-driven chopping wheel and introduced to the ion source of a Nuclide HT-12-90 magnetic mass spectrometer. Alignment of the beam defining slits is such that only vapor issuing from inside the cell can pass by line-of-sight into the ion source. This arrangement permits heating of cells to 3300°K in vacuum (3500°K in one atmosphere inert gas) with alternate monitoring of two ion peaks by rapid electrostatic peak switching.

VAPOR COMPOSITION

Preliminary measurements of carbon species ratios, from the Knudsen cell, as a function of temperature, are shown in Figure 2 (17 ev electrons). The dashed lines are the results of Drowart, et. al. [1] The C_6^+ and C_7^+ signals were quite weak and only give the approximate importance of C_6 and C_7 under equilibrium evaporation conditions. A considerable extension of such measurements is in progress with emphasis on species beyond C_5 and temperatures above 3000°K.

*Department of Chemistry, Rice University

**Work supported by AFML, WPAFB, Contract No. F33615-71-C-1577

NEUTRAL VELOCITY ANALYSIS

A great deal of information about vaporization processes and mass spectral interpretation can be obtained by measuring the neutral velocity distributions of the species of interest. A convenient way to determine the velocities of neutrals is to chop the neutral beam into short pulses by use of a motor driven chopper disc having narrow slots. The time-of-arrival (TOA) of the neutrals at the electron beam can then be determined by synchronizing the detection system with a light pulse from the narrow slot in the chopper disc (see Ref. 2 for details).

In the case of characterizing the vaporization behavior of graphite, such TOA measurements have three chief functions: (1) to determine the neutral precursors of the ion species C_n^+ observed at the ionizing electron energy chosen for mass spectrometry; (2) to deduce an approximate temperature of the source of vapor; and (3) to reveal the onset of continuum-flow expansion conditions during either free or equilibrium evaporation.

A large number of neutral TOA measurements have been made on permanent gases, water, acetone, and hydrocarbons, as well as on carbon vapor species. Normally, a reference light beam was chopped simultaneously (within 10 micro-seconds) with the chopping of the molecular beam. The resulting signal was used to start the sweep of a 1024 channel multichannel analyzer. The selected ion was monitored continuously using ion counting so that its full arrival behavior was mapped out in each of many repetitive sweeps. The stored data, for a particular ion, under given beam, source and ionization conditions, was printed out and/or plotted on an X-Y recorder so that one obtained directly a record of neutral intensity versus arrival time.

A typical record for three species (not normalized, but with true relative time scales) from carbon vapor is shown in Figure 3. At 17 ev the relative times-of-arrival for the neutral species giving rise to C_1^+, C_2^+ and C_3^+ are seen to differ, as would be expected if they were all parent ions. In Figure 4, similar measurements are shown with an ionizing electron energy of 50 ev. Ignoring the second (slow) peak in the C_3^+ curve, the near equality in TOA behavior for the species giving rise to C_1^+, C_2^+ and C_3^+ suggests that at high ionizing electron energies, the C_1^+ and C_2^+ are dominated by fragmentation from C_3 neutral. Such observations are illustrative of the power of neutral TOA analysis in assigning ions to the correct neutral precurser, at least under effusive flow conditions. A further example of the value of TOA analysis is given in Figure 5. Here the actual TOA behavior of the neutral giving rise to C_3^+ is compared with theoretical expectations, assuming that C_3^+ was effusing under molecular flow from the orifice at the measured orifice black-body temperature. The narrower and faster peak of the experimental velocity distribution suggests that continuum flow effects are being encountered under these vaporization conditions.

One must return to the puzzling behavior shown by the C_3^+ peak in Figure 4, (and to a lesser extent in Figure 3). The second (slow) peak in the TOA curve for C_3^+ would require either a very low temperature source of C_3 or that the C_3^+ be a fragment from a rather heavy neutral ($\sim C_{10}$). Numerous tests have been conducted on carbon vapor and on other gases which form clusters, in an attempt to determine if the delayed peak is an artifact of the ion source time response to the chopped beam. However, the most convincing test was one in which the electron beam of the Nuclide ion source was pulsed on for very short intervals, at variably delayed times following neutral beam chopping. Operation in this manner, which should eliminate effects of ion trapping in the ion source, fully confirm the presence of slow neutrals giving rise to the slow peak in the C_3^+ TOA curve. 2/

Summarizing the data from studies of many gases and beam source conditions, it can be stated that under purely effusive conditions or under fully developed supersonic flow, no double-humped TOA curves are seen. Under transition flow conditions, and with gases or vapors where cluster formation can be expected, such delayed peaks are often observed. The relative proportions of the fast and slow TOA peaks are sensitive to both ion source and ionization parameters.

A satisfactory explanation is not at hand for the C_3^+ behavior of Figure 4, but it cannot be ruled out that a heavy parent, either covalently or loosely bound, is contributing substantially to C_3^+ under conditions of our vaporization studies.

ACKNOWLEDGEMENTS

The authors wish to thank Professor Paul W. Gilles for valuable discussions of all aspects of this work.

LITERATURE CITED

1. Drowart, J. R., R. P. Burns, G. DeMaria and M. G. Inghram, J. Chem. Phys. 31, 1131 (1959).

2. Milne, T. A., J. E. Beachey and F. T. Greene. AFML-TR-72-227, Dec. 1972, "Vaporization Kinetics and Thermodynamics of Graphite Using the High Pressure Mass Spectrometer."

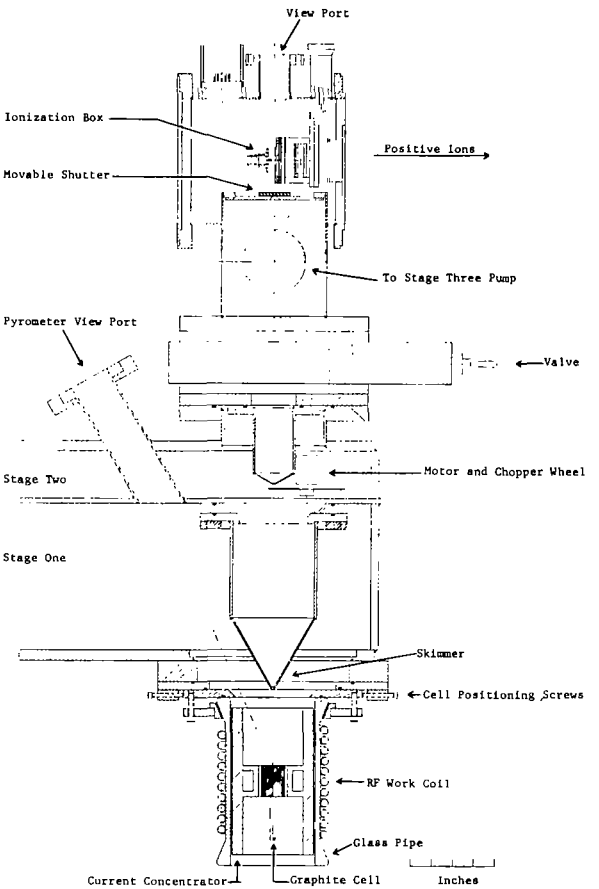

Figure 1 - Scale Drawing of Relevant Ion Source, Beam System and Pyrometer Viewing Geometry. Shutter motion is in and out of plane of paper.

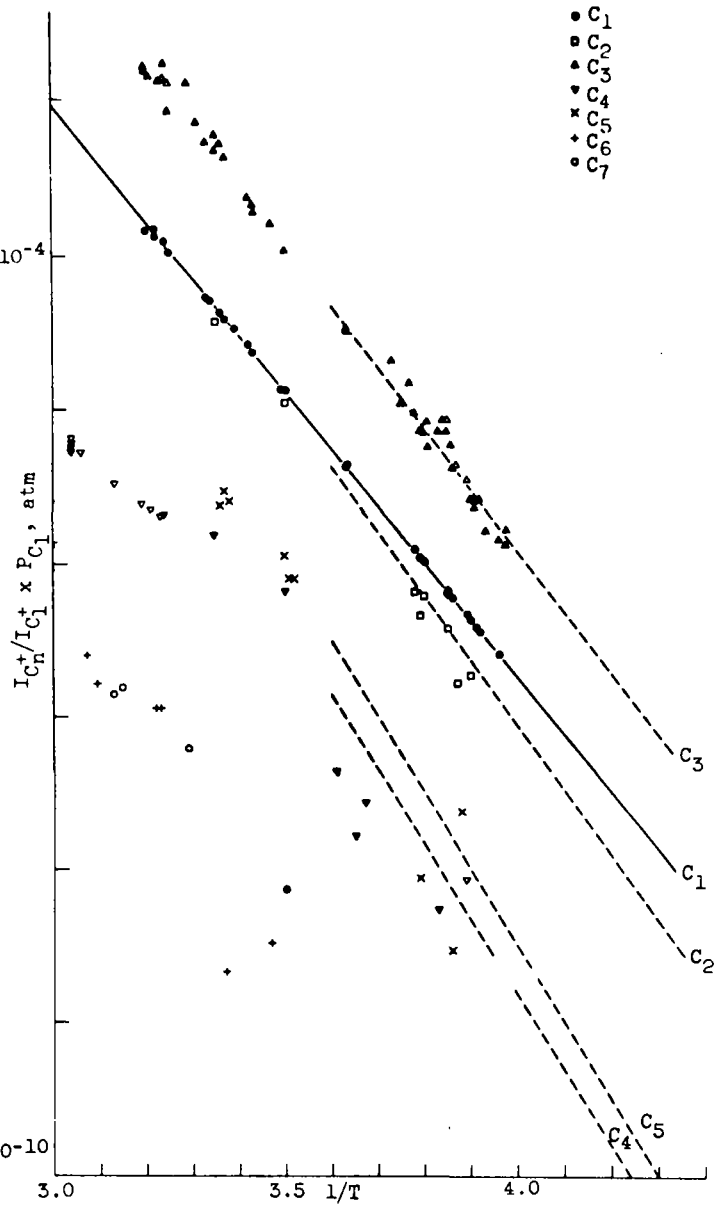

Figure 2 - Ion Intensity Ratios Observed for Carbon Species Issuing from an ATJ Graphite Knudsen Cell with a 1/8-in. Diameter Aperture. Ionizing electron energy 17 ev. Plotted are the observed uncorrected ion ratios normalized to the JANAF values of carbon monomer pressure. The C_2 and C_3 data taken by switching directly with C_1. The higher cluster ratios were determined relative to C_3 and subsequently normalized to C_1.

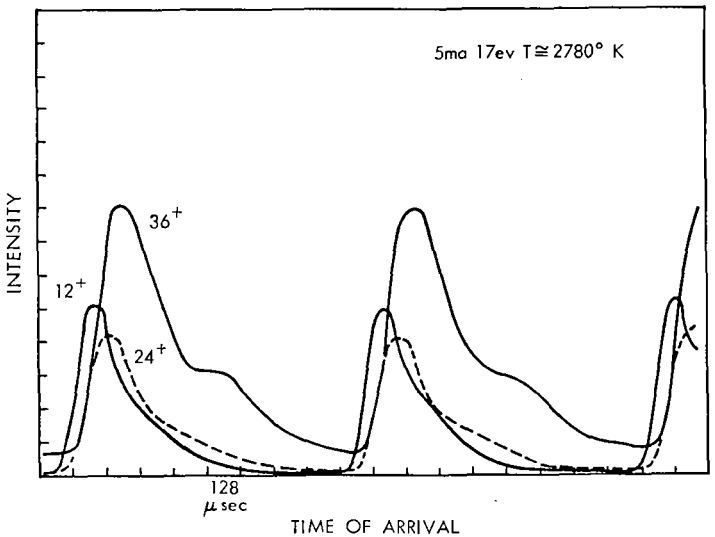

Figure 3 - Superposition of TOA Curves For Carbon Vapor Species at 17 ev Ionizing Electron Energy

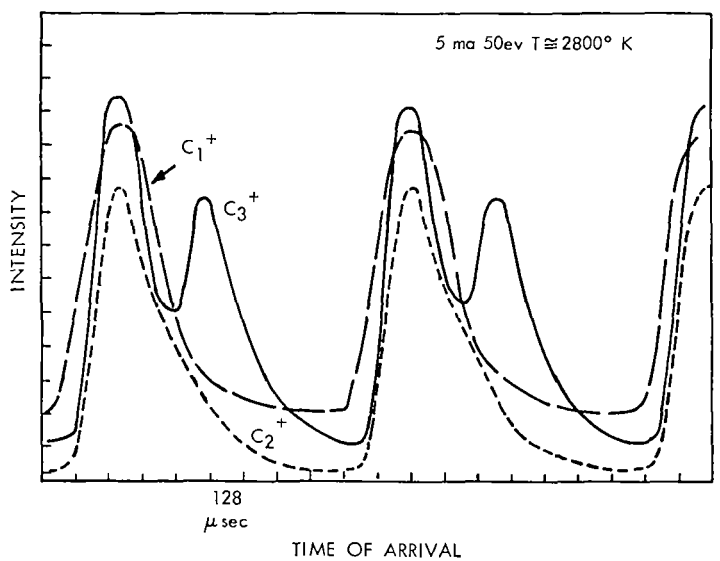

Figure 4 - Superposition of TOA Curves for Carbon Vapor Species at 50 ev Ionizing Electron Energy. Relative Heights of different curves have no significance.

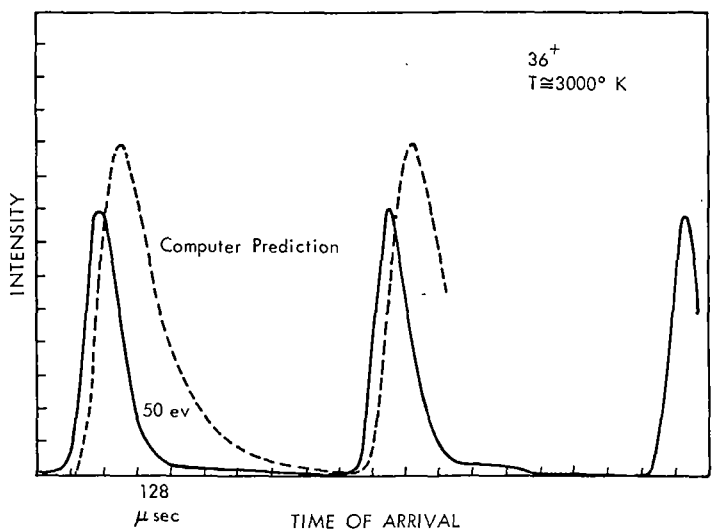

Figure 5 - Comparison of Experimental and Theoretical TOA Curves for 36^+ from Carbon Vapor

PULSED LASER INDUCED VAPORIZATION OF GRAPHITE AND CARBIDES*

Richard T. Meyer, Sandia Laboratories, Albuquerque, New Mexico 87115/U.S.A.

Introduction

The vapor compositions for graphite[1,2] and for metal carbides are being studied by pulsed laser heating and time resolved mass spectrometry for the purposes of: (1) identifying the major elemental and molecular vapor species, with particular interest in the relative abundances of the C_n species; (2) determining whether any correlation exists between the dominant species in the vapor phase and the molecular lattice structure of the solid phase; and (3) comparing the laser induced vaporization kinetics with equilibrium vaporization. In this paper, we report the relative abundances of the vapor species from the following materials, heated both by a normal-mode laser and by a Q-switched laser: graphite, $TiC_{1.2}$, VC, Cr_3C_2, ZrC, NbC, Mo_2C, HfC, TaC, WC, and $UC_{2.2}$.

Laser Mass Spectrometry Techniques

The techniques of pulsed laser heating and time resolved mass spectrometry have been previously described in detail.[1] The samples were located within the ion source of a Bendix model 14-107 time-of-flight mass spectrometer 3.0cm below the ionizing electron beam. The energy of the electron beam was varied from 30eV to 17eV to 0eV (beam off) in order to characterize whether the ion species recorded were ionization fragments, parent neutrals, or thermal ions. The beam from a Korad K1Q neodymium glass laser was focused onto the sample with microscope optics to a spot size of 0.5mm diameter. The incident energy density range was 0.20 to 3750 joules/cm^2 for normal mode (800 μsec duration) and 0.0064 to 6.0 joules/cm^2 for Q-switched (25 nsec duration).

The mass spectrometer was operated at 20 kHz and provided complete mass spectra (1 to 500 amu) every 50 μsec. Raster scope recording of six successive spectra was employed for each laser heating, with the experiment being repeated many times to obtain statistically significant data. For the normal-mode experiments, the raster recording was started at 300 μsec after the start of the laser pulse, whereas for the Q-switched experiments, the first spectrum was recorded at 1 to 50 μsec after the laser pulse.

The metal carbide samples were obtained from three sources as follows: Alfa Inorganics (TaC); Sylvania (VC, Cr_3C_2, ZrC, NbC, Mo_2C, HfC, WC); and E.K. Storms, Los Alamos Scientific Laboratory ($TiC_{1.2}$, $MoC_{0.57}$, $UC_{2.2}$). The graphite was Pfizer Pyroid pyrolytic. All samples were outgassed under vacuum (10^{-7}torr) at 1800 to 2100K for one hour prior to insertion into the spectrometer.

Graphite Vapor Composition

An earlier analysis by us of several investigators' data on the laser induced vaporization of graphite revealed that the relative abundances of the C_n species and the vaporization temperatures were independent of the operational mode of the laser (normal-mode vs Q-switched) and independent of the laser energy density (50 to 8000 joules/cm^2).[2] It appeared that a maximum vaporization temperature in the vicinity of triple point temperature of carbon (4100 to 4600K) was achieved. The averaged values of ion intensities from the laser studies are 1.0, 2.0, 6.0, 0.34, and 0.80 for C_1, C_2, C_3, C_4, and C_5, respectively. Our laser (Q-switched) experiments have yielded the relative values of 1.0, 0.9, 5.1, ~0.25, and ~0.5. Both sets of ion intensities may be compared with the ion intensities reported by Drowart et al.[3] for equilibrium vaporization at 4100K; namely, 1.0, 6.4, 16., 1.7, and 3.2. This comparison shows that the laser heating produces a non-equilibrium distribution of C_n species and that laser vaporization is limited by the kinetics of the dissociation and release of molecules at the graphite surface.

Metal Carbide Vaporization

The results of the laser-induced vaporization experiments on the metal carbides are summarized and are compared with the equilibrium composition data in Table I.

Vaporization by Normal-Mode Heating

The observation of C_3 as the dominant vapor species from several of the carbides indicates that the carbon activity is high, near unity, and that the vapor composition with respect to C_n species is nearly the same as that obtained from pure carbon. This conclusion is confirmed for TiC and VC by the observation that the metal is also a dominant vapor species, which indicates that the metal may be preferentially vaporized and that the remaining condensed phase becomes carbon rich.

The activity of carbon in HfC and TaC appears to be less than unity, since C_1 is the dominant vapor species; the dominance of C_1 is in agreement with the results of Wachi for HfC.[4] The vapor pressures for NbC and Mo_2C are significantly less (10 to 100X) than for the other carbides, based upon the absence of any species as a "major" vapor species.

Principal differences observed between the laser-induced vapor composition and the equilibrium composition are as follows: C_3 rather than C_1 was the major C_n species from ZrC and WC, whereas C_1 rather than C_3 was the major species from TaC. The vapor species UC_3 and UC_6 were newly identified from $UC_{2.2}$ and were present in the vapor along with U, UC_2, and UC_4, the species which have been observed in equilibrium studies.

* This work supported by the U.S. Atomic Energy Commission.

Table I. Comparison of Vapor Species from Laser Induced Vaporization of Metal Carbides with Equilibrium Vaporization Data

Carbide	Normal-Mode		Q-Switched		Equilibrium[b]
	Major Species	Minor Species	Major Species	Minor Species	Composition
$TiC_{1.2}$	Ti^+, C_3		Ti^+, C_3		Ti
VC	C_3, V, V^+	C_6^+ to C_{16}^+	V, C_3	V^+	V
Cr_3C_2	$Cr, Cr_2, CrC, Cr_2C_2, Cr_3C$	C_3, C_6, C_7, C_8	Cr, CrC	C_3	Cr
ZrC	C_3	Zr^+	C_3, Zr	Zr^+	Zr(C_1)
NbC	--	C_3, Nb^+	C_3, Nb^+		(Nb)
$Mo_2C/MoC_{0.57}$[a]	--	Ions	C_3	C_5, C_7	Mo(C_1, C_2, C_3)
HfC	$C_1 > C_3, Hf^+$	$C_3 > C_2$	C_3		Hf(C_1)
TaC	$C_1 > C_3$	$C_3 > C_2$	C_3		(Ta, C_3)
WC	C_3, W^+		C_3		W, C_1
$UC_{2.2}$	C_3, U^+, UC_2^+ UC_3^+, UC_4^+, UC_6^+		C_3, U^+, UC_2^+, UC_3^+, UC_4^+, UC_6^+		U, UC_2, UC_4 (C_1, C_2, C_3)

(a) $MoC_{0.57}$ was used in the Q-switched laser experiments.

(b) Data are taken from Reference 4. Underline designates preferentially vaporized; parentheses indicate assumed vapor species. Absence of a citation for either M or C_n species means that data were not measured for those species.

A high abundance of thermal ions, particularly from TaC and $UC_{2.2}$, has been recorded; this result requires further evaluation with respect to the interaction of the laser beam with the sample surfaces.

Vaporization by Q-Switched Heating

C_3 is the dominant vapor species for all the refractory metal carbides, except for Cr_3C_2 which yields Cr and CrC. C_1^+ and C_2^+ appear in all cases to be due to dissociative ionization of C_3, CO, or CO_2. C_5 and C_7 are observed from $MoC_{0.57}$ but not from any other carbide.

Vaporization of the metal as M and/or as M^+ is observed for TiC, VC, ZrC and NbC but is not observed for $MoC_{0.57}$, HfC, TaC, or WC. This may indicate that the vapor pressures of the metal from the latter carbides are lower by an order of magnitude or more.

The vapor compositions for ZrC, HfC, and WC are different from the equilibrium data, with C_3 being more important in laser vaporization that C_1. In particular, C_1 does not appear to vaporize preferentially from WC during laser vaporization.

Conclusions

Since the present results were obtained for a range of incident laser energy densities and the reflectivities and thermal conductivities varied from material to material, one cannot assume that the data compiled in Table I all apply to the same sample temperature. Nevertheless, the qualitative results do have valid implications with respect to the mechanisms of vaporization and the activity of carbon in the solid phase. This is true because the laser vaporization of graphite can be used as a standard reference and because data is available on the equilibrium vaporization of the carbides and of graphite as a function of temperature. For example, both the laser and the equilibrium vaporization experiments on graphite show that C_3 predominates over C_1 and C_2 for a broad range of laser energies and temperatures. Therefore, it seems reasonable to conclude that a different vaporization mechanism does apply to those metal carbides which show C_1 rather than C_3 as the dominant C_n vapor species. Where C_3 dominates in the vapor, it appears that the laser-heating does cause preferential vaporization from a carbon-rich phase. Where the metal atom and C_3 are both major vapor species, vaporization apparently occurs from separated phases of the metal and carbon. However, where C_1 is the major species, it would appear that a molecular dissociation occurs at the surface as an immediate precursor step to vaporization. In the case of the UC_n vapor species, these molecules probably arise from the vaporization of short-range ordered-structures of the condensed phase.

In general, it appears that normal-mode heating comes closer to producing equilibrium vapor compositions than does Q-switched heating. Our results tend to confirm the hypothesis that Q-switched laser heating produces non-equilibrium effects.

References

1) R. T. Meyer, A. W. Lynch, and J. M. Freese, J. Phys. Chem. 77, 1083 (1973).
2) R. T. Meyer, J. M. Freese, and A. W. Lynch, Paper presented at 20th Annual Conference on Mass Spectrometry and Allied Topics, Dallas, Texas, June 1972.
3) J. Drowart, R. P. Burns, G. De Maria, and M. G. Inghram, J. Chem. Phys. 31, 1131 (1959).
4) E. K. Storms, The Refractory Carbides, Academic Press, New York, 1967.
5) F. M. Wachi and D. E. Gilmartin, High Temp. Sci. 4, 423 (1972).

MASS SPECTROMETRIC DETERMINATION OF MOLECULAR VELOCITIES IN LASER-PRODUCED VAPOR PLUMES*

Kenneth A. Lincoln
Ames Research Center, NASA, Moffett Field, Ca., 94035

Introduction

In recent years high energy lasers have become a common tool for heating refractory materials to the high temperatures required to obtain vaporization data and deduce thermochemical properties. However, under pulsed conditions, the surface temperatures and vaporization mechanisms remain largely unknown. As a means of gaining some insight into these parameters, we have undertaken to measure the velocity of selected molecular species within laser-induced vapor plumes expanding into a vacuum. The high-temperature materials investigated in this work include some common graphites and Al_2O_3.

For measuring these velocities, an earlier technique[1] employing a mass spectrometer as a selective detector for the various species has been refined with improved instrumentation and is utilized in the present work. Each sample is exposed to the laser irradiation under identical conditions at two different distances from the spectrometer which serves to detect the arrival time of the selected mass species at each distance. From this information and the laser pulse itself as a time reference, the individual velocities are calculated. Thus, $v = \Delta d/\Delta t$ for each specie of interest, and factors, such as, time to vaporization, drift time in spectrometer, etc., are cancelled out.

Experimental

The laser/mass spectrometer system has been described previously[2] and includes as a mass detector a Bendix Model MA-2 time-of-flight mass spectrometer with nude ion source configuration. A time-of-flight instrument was chosen for this work for its ability to detect and simultaneously time resolve several mass species produced by single laser bursts. The resultant output of the instrument is an intensity versus time record of the preselected mass peaks. The methods employed here for obtaining time-resolved mass spectra during sub-millisecond time intervals, are delineated in an earlier publication.[3] In the present work the spectrometer was operated at a 40 kHz repetition rate with selected mass peaks gated out of the multiplier into Hewlet-Packard Model 8875A differential amplifiers ahead of the scope; the amplifiers provide some gain and filter out unwanted ringing from the gating pulses.

Figure 1 is a schematic diagram of the system showing the relative positions of the mass spectrometer, the laser beam, the window ports and the corresponding specimen positions approximately 70 cm apart; the farthest position is about 100 cm from the ion source. Not shown is the beam splitter which directs a calibrated fraction of the 1.06 μ laser beam into an EG&G Model 580 laser radiometer; the latter presents a digitized value of the integrated energy for each laser pulse plus an instantaneous value of amplitude which is fed to the scope to record the laser pulse shape along with the time-resolved mass pulses. The laser beam strikes the specimen normal to its surface which is at an angle of 45° to the axis of the vacuum chamber; thus it can be seen that only those vapors leaving the surface at 45° and traveling a line-of-sight path to the ion source are sampled by the mass spectrometer.

Figure 2 is one pair taken from a series of scope photos resulting from identical laser shots on the same specimen; the only difference being that in the lower one the specimen was 69 cm farther from the ion source (also the multiplier gain was set higher for the lower mass 27 pulse to compensate for reduced vapor density at the greater distance). It should be pointed out that the output from the laser operating in the burst mode is actually made up of a train of several hundred one-microsecond spikes, but here the time constant of the detector was adjusted to partially integrate the output to simplify matching the overall pulse shape from shot to shot. The small cyclic component superimposed on the mass 27 pulse corresponds to the repetition rate of the mass spectrometer, i.e., one mass 27 peak occurs in the spectrum every 25 μsec. The easiest way of measuring the time difference between the corresponding mass pulses is one of graphically superimposing one picture upon the other; first the laser pulses are brought into register and then the mass pulses, and the time shift can be read directly from graticule lines.

Important experimental requirements are reproducibility of the laser pulses and the vapor plumes. The former is monitored by the laser radiometer and the latter by the total ion current and the spectra appearing on the scope along with each laser shot. In practice, the laser beam was focused to cover the entire front surface of the graphite specimens and was fired at 10 to 15 sec intervals. It was found that by the fifth or sixth shot in such a sequence the surface was cleaned off and reproducibility attained. An additional consideration is the minimization of multipass transitions of molecules

*Paper will be submitted to Journal of High Temperature Science.

through the ion source of the mass spectrometer so that the spectra will conform to the time resolution of the vapor plumes. This has been enhanced by isolating the ion source with a baffle having a 5 mm diameter aperature and by pumping the mass spectrometer separately. In addition, an ion deflector has been placed ahead of the baffle to prevent any ions produced by the laser from entering the mass spectrometer.

Results and Discussion

By using the above described technique, the velocity of triatomic carbon (mass 36) was measured as it was vaporized from three different types of graphitic materials under identical heating conditions. Similarly, the velocity of monatomic aluminum (mass 27) was measured as vaporized from a 1/2-in disc of Coors Alumina except that a smaller area was heated at higher irradiance. These velocities are listed in Table I. It should be noted that these values represent the velocity of the vapor cloud after it has moved away from the heated surface, and we are faced with the question as to which model should apply. If it is assumed that this represents the "most probable" velocity, i.e., the maximum in the Maxwell-Boltzman curve, where

$$u = \left(\frac{2RT}{M}\right)^{1/2} \quad \text{and} \quad M = \text{molecular weight}$$

then solving for T, yields temperatures much too high as can be seen in column 3 of Table I. On the other hand, if the phenomenon is more akin to a hypersonic free jet expanding adiabaticly into a vacuum, then gas dynamic considerations[4] yield

$$v_{max} = \left(\frac{2}{\gamma - 1}\right)^{1/2} a \quad \text{where} \quad a = \left(\frac{\gamma RT}{M}\right)^{1/2}$$

$$\text{then} \quad v_{max} = \left(\frac{\gamma}{\gamma - 1}\right)^{1/2}\left(\frac{2RT}{M}\right)^{1/2} \quad \text{or} \quad v_{max} = \left(\frac{\gamma}{\gamma - 1}\right)^{1/2} u$$

Using $\gamma = 9/7$ for C_3 and $\gamma = 5/3$ for Al and solving for T yields the temperatures listed in the last column of Table I. These latter temperatures are much closer to the accepted values for graphite ablation, and represent the lower limits, because in each case the measured velocity was equated with the maximum velocity attainable in hypersonic expansion. Consistent with the higher vaporization temperature of the polycrystalline graphite (ATJS), it was found that the quantity of C_3 produced from ATJS was an order of magnitude lower than from the other two types at the same laser irradiance.

At least these results suggest that simple equilibrium kinetic gas theory does not apply throughout the plume, and hypersonic gas dynamic relationships must be considered when vapor measurements are used to deduce prevailing conditions at the solid-gas interface. Future work will include the measurement of velocities under different heating conditions and the measurement of the velocities of several mass species in the same vapor plume. Parallel work will attempt to measure temperature by optical or other means.

Table I. C_3 VELOCITY FROM GRAPHITES 160 kW/cm^2

Material	Velocity	Temperature $u = \left(\frac{2RT}{M}\right)^{1/2}$	Temperature $v_{max} = \left(\frac{\gamma}{\gamma - 1}\right)^{1/2} u$
Pyrolitic	2.7×10^5cm/s	15,800°K	3,500°K
Vitreous	2.7×10^5	15,800	3,500
ATJS	3.4×10^5	25,000	5,500
	Al VELOCITY FROM Al_2O_3 600 kW/cm^2		
Alumina	3.7×10^5cm/s	22,700°K	9,100°K*

*This value stems from the assumption that the entire vapor cloud is monatomic. If the average of the species should be triatomic, then $\gamma = 9/7$ which would yield a temperature of 5,100°K.

References

1. K. A. Lincoln and F. A. Wodley, presented at Seventeenth Annual Conference on Mass Spectrometry and Allied Topics, May 18-23, 1969, Dallas, Texas.
2. K. A. Lincoln, presented at Twentieth Annual Conference on Mass Spectrometry and Allied Topics, Dallas, Texas, June 4-9, 1972, Dallas, Texas.
3. K. A. Lincoln, Int. J. Mass Spectrom. Ion Phys., 2, (1969), 75.
4. A. H. Shapiro, The Dynamics and Thermodynamics of Compressible Fluid Flow, Vol. I, Ronald Press Co., New York, (1953), pg. 79.

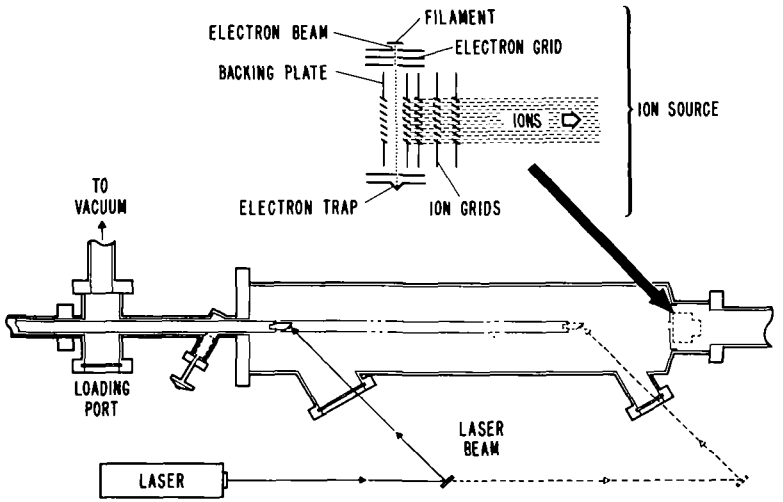

Fig. 1. Mass spectrometer and vaporization chamber.

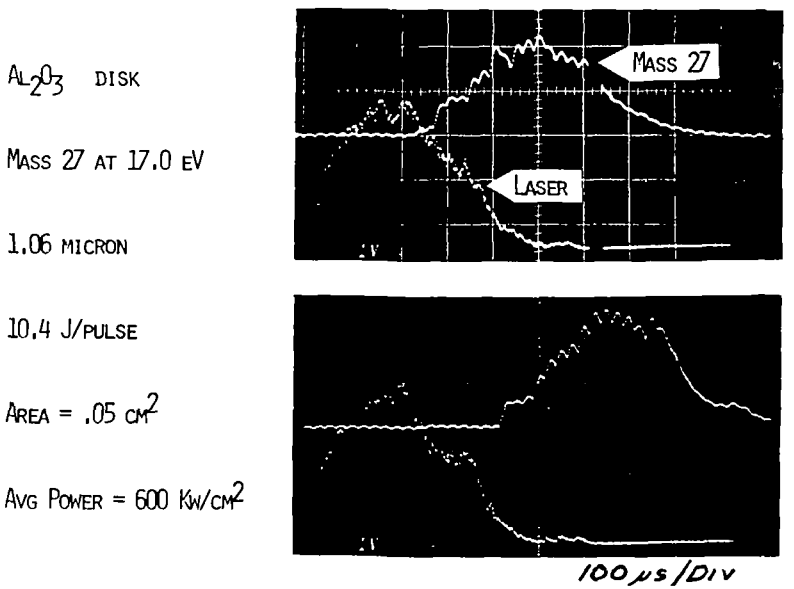

Fig. 2. Laser pulse and resulting aluminum vapor pulse from two laser shots.

Author Index

Author Index

Author Index

Author Index

ASMS COMMITTEES AND ASTM E-14 SUBCOMMITTEES

ASMS Com. II - "Fundamental Aspects", R.S. Berry, Department of Chemistry, University of Chicago, Chicago, Illinois 60637

ASMS Com. III - (formerly Joint Com. III) "Computer and Data Processing", E.M. Emery, Colgate-Palmolive Co., 909 River Road, Piscataway, New Jersey 08854

ASTM E-14 Subcom. IV - "Data and Information Problems", W.B. Askew, Dupont Experimental Station, Wilmington, Delaware 19898

ASMS Com. V - "New Instruments and Techniques", H.J. Svec, Department of Chemistry, Iowa State University, Ames, Iowa 50010

ASMS Com. VI - (formerly Joint Com. IV) "Biological Applications", J.A. McCloskey, Institute for Lipid Research, Baylor College of Medicine, Houston, Texas 77025, and J.R. Roboz, Mt. Sinai School of Medicine, New York, New York

ASMS Com. VII - "Study of Solids", F.D. Leipziger, Kennicott Copper Co., Ledgemont Laboratory, Lexington, Mass. 02173

ASMS Com. VIII - "High Resolution Studies", D.C. DeJongh, Case Postale 6128, l'Universite-de Montreal, Montreal, Quebec, Canada 101

ASMS Com. IX - "Aids to Education", J.G. Dillard, Chemistry Department, Virginia Polytechnic Institute, Blacksburg, Virginia 24061

ASTM E-14 Subcom. X - "Definitions and Terms", G.L. Cook, Laramie Energy Research Center, Box 3395, University Station, Laramie, Wyoming 82070

ASMS Com. XI - (formerly Joint Com. XI) "Environment and Pollution Studies", A.G. Sharkey, Jr., U.S. Bureau of Mines, 4800 Forbes Avenue, Pittsburg, Pennsylvania 15213

ASMS Committee II, Fundemental Aspects

During the past year Committee II has been attempting to assess its responsibilities in view of the expansion of the Society in terms of both total membership and scope of interests. A summary of the results of a questionnaire mailed to the total membership of ASMS last fall is as follows: (1) 112 respondents indicated that they wished to be members of Committee II, while 47 who indicated they did not wish to be committee members nevertheless filled out and returned the questionnaire. (2) By a margin of 3/1 committee members favored retaining responsibility for developing symposia and other programs covering all fundamental types rather than narrowing our interests to gas phase ion chemistry and physics; non-members were about equally divided. (3)(4) Chemical Physics as a name change was voted down by about 2.5/1, while non-members by a small margin considered us to be chemical physicists. (5) Symposia and plenary speakers were about equally favored by both groups. (6) An annual program (rather than alternate years) on Fundamentals was favored by the two groups by margins of 4/1 and 1.3/1, respectively. (7) Workshops were endorsed by 3/1 by both groups. (8) Member respondents were equally split on the question of refereeing papers versus more parallel sessions, while non-members endorsed refereeing papers by 3/1. (9) Both groups nominated ion photodissociation, charge-exchange at low energy, and ion cluster studies as their highest priority symposium topics, while state selection, molecular orbital theory and coincidence measurements were runners-up. Many additional topics were suggested.

At the San Francisco meeting a symposium on ion-photo interactions featured as invited speakers Professor Jean Durup of the University of Paris-Sud, who spoke on "Photo-dissociation of Gaseous Ions"; Professor Carl Lineberger of the University of Colorado spoke on "Laser Photodetachment of Negative Ions"; and Dr. Tom Tiernan of the Aerospace Research Laboratories spoke on "Optical Studies of Internal Excitation in Slow Ion-Neutral Collisions". Plenary lecturers who addressed topics also within the purview of "Fundamentals" were Professors Hans-Dieter Beckey of Bonn, who spoke on "Field Desorption Mass Spectrometry" and George Olah of Case-Western Reserve who spoke on "Carbocations in Gas Phase and Solution Chemistry."

Also at the San Francisco meeting we experimented with workshops dealing with ion source chemistry. Dr. Bill Chupka of Argonne organized a workshop on problems in unimolecular decomposition and ion molecule reactions. An informal format was followed in which Bill summarized briefly the status of various aspects of these problems and called upon active researchers

in each of these areas to give comments from the floor. Active discussion involving these "invited guests" and other participants then ensued.

One tangible product of this workshop was a listing of major references to particular topics as follows:

1) Reviews of Methods for Calculating Energy-Level Densities
   (a) W.Forst, Chemical Reviews 71, 339 (1971)
   (b) H.M. Rosenstock in "Advances in Mass Spectrometry," Vol. 4, p. 523
   (c) P.J. Robinson and K.A. Holbrook, "Unimolecular Reactions," Wiley-Interscience (1972)

2) Conservation of Angular Momentum in Unimolecular Decomposition
   (a) E.V. Waage and B.S. Rabinovitch, Chemical Reviews 70, 377 (1970)--Centrifugal Effects Only
   (b) C.E. Klots, Z. Fur Naturforschung 27a, 553 (1972)
   (c) E.E. Nikitin, Teoreticheskaya i Eksperimental'naya Khimiya, Vol. 1, No p. pp. 144-150 (1965)

3) Radiationless Transitions
   (a) John B. Birks, "Photophysics of Aromatic Molecules," Wiley-Interscience (1970)
   (b) "Transitions Non Radiative dans les Molecules," Journal de Chimie Physique, 1970. Proceedings of 20th Reunion de la Societe de Chimie Physique Paris, 27 au 30 Mai 1969.

Professor Gerry Meisels developed for the committee a workshop on high pressure ion source phenomena which was also held on Thursday afternoon. This consisted of a panel of discussion leaders which included Professors Ralph Doughtery, Frank Field, Paul Kebarle, and Marvin Vestal and Dr. Hank Fales in addition to Professor Meisels. Topics addressed by the panel included the achievment of equilibrium, state of excitation of ions, ion energies and energy distributions, differences in CI spectra between instruments, space charge effects, and other topics. Brief statements by the panelists were followed by a "free-for-all" discussion.

It would appear that both workshops were outstanding successes. Although the formats of the two workshop sessions were somewhat different the fact that about 120 people attended and that many of the participants stayed overtime to discuss one or another aspect of the respective topics suggest to us that this was a very successful endeavor. We anticipate that Committee II will organize workshops at future meetings.

The annual meeting of the Committee took place on Monday afternoon at 4:30 p.m. and was attended by about seventy members. True to past tradition, Committee II rejected the attempts of the chairmen to impose an agenda and a more formal structure--including an Executive Committee--

to struggle with some of the questions raised in the questionnaire reviewed above. Following a general philosophical discussion we then focused on the main purpose of the annual meeting, which was to suggest various symposium and workshop topics. The most popular ones were the following:

1) Molecular obital and other approaches to the structure of small molecular ions.

2) Rigorous tests of the quasi-equilibrium theory.

3) Mechanisms of charge exchange at low energy.

4) Studies of ion equilibrium.

In the report of Committee II activities to the Executive Committee of the Society there developed one item of particular relevance to the broader responsibilities of Committee II. Vice president for Programs, Professor Harry Svec agreed to form an ad hoc committee to consist of the chairmen of the several committees of ASMS with hemself as moderator. This group will serve as a special committee to coordinate overlapping interests of ASMS and ASTM committees. Thus to some extent this committee will share responsibilities with Committee II for insuring equitable coverage of all topics which the title "Fundamental Aspects" implies.

Jean H. Futrell
Chairman

ASMS Committee III, Computer and Data Processing

It is the purpose of this joint committee to promote and provide the means for exchange of computer and data processing techniques in mass spectrometry.

Minutes of the Meeting - 1973: San Francisco

Some 57 persons participated in the transactions of this committee this year. The highlights and conclusions would include:

1. A brief report on the background and current status of ASTM E-31 Committee on Computerized Laboratory Systems was presented by M. E. Fitzgerald. This two year old group has five subcommittees active in Nomenclature, System Definition, System Implementation, Evaluation and Documentation, with significant progress on the horizon. The American Laboratory for Feb. 1973 reflects some of the initial contributions.

2. The objectives for 1972-73 were reviewed. The aims and details of the survey were outlined.

3. Distribution and discussion of the compilation resulting from the survey were carried out. The ability to locate a specific instrument and various supporting computers (and vice versa) was cited as a real benefit to many. There was definite interest shown in knowing of the great variety of applications. The compilation also provided some with the "wedge" to show what they should be doing based on what others have done.

4. It was proposed that all of ASMS and ASTM E-14 be similarly surveyed, so that a full cross-section of our community be taken. This committee tentatively plans inclusion of its survey in the fall mailings of ASMS and ASTM E-14.

5. Persons interested in the aforementioned compilation of the 1972-73 survey may obtain a copy from the committee chairman.

6. It was proposed by the chair that serious consideration be given the proper storage of all our computer efforts. After some discussion, it was decided to utilize the program exchange facilities at Indiana U., if possible. Initial contact with Q.C.P.E. (ref.: C. & E. News, May 21, 1973) has already been made.

7. The closing recommendation was made that an up-to-date listing of materials on hand be appended to the minutes of this meeting.

Respectfully,

Edgar M. Emery
Chairman

At separate business meetings during the week, the joint committee status was abandoned, such that Committee III will now be solely an ASMS committee.

Note should be made of the participation of this committee with that of Committee IV in the "Computer Matching of Observed and Library Mass Spectra", arranged and reported on by Tom Pugh.

1973 - Available Through Committee III

1.	Listing:	Robinson-Cook, Gas Oil Aromatics Method.
2.	Method:	S. Heller, DCRT Retrieval System.
3.	Documentation:	Van der Meulen, Trajectory [K+HBr] publication only.
4.	Documentation:	Crittenden, DEC HIREMS MS-9 PDP-12 extensive hi resol. package, offers LINC tape copies.
5.	Listing:	Rozett, monoisotopic program, MIMS. Sample test data list.
6.	Listing:	Vander Velde, takes abundances for 20 elements, and calc P = 100, P = 1, P + 2, etc.; cards.
7.	Survey:	1968 ASTM E-14 Subcommittee IV Survey of Computer Programs, N. G. Foster, chairman.
8.	Compilation:	Results of 1972-73 Survey, shows instruments, computers, software in many combinations.

COMPUTER MATCHING OF OBSERVED AND LIBRARY MASS SPECTRA

Workshop - Co-sponsored by Joint Committee III - Computer and Data Processing - E. N. Emery, Chmn. and ASTM E-14 Subcomm. IV - Data and Information Problems - W. B. Askew, Chmn.

Arranged by T. L. Pugh, Du Pont Company, Elastomers Dept., Wilm., Del.

Discussion Leaders

S. Grotch - Jet Propulsion Labs
S. Heller - Nat. Inst. of Health
A. McCormick - Mass Spec. Data Centre
J. McGuire - Southeastern Water Lab
F. McLafferty - Cornell Univ.
D. Robertson - U. S. Army Natick Labs

Discussion leaders briefly commented on the search methods in use or under development. Most techniques easily obtained matches with file spectra for a list of 10 unknowns. Prof. McLafferty's group has assembled a very large file and is extending the computer procedure to attempt to identify compounds which are not in the file. They succeeded very well in identifying two of three spectra which were not in the Cornell group's file. The Cornell File will be available for purchase from John Wiley Co. An announcement was made by S. Heller that the NIH search system was being transferred to the Gen. Electric Information Services. The management of the data file will be carried on by the Aldermaston group. J. McGuire also announced that the EPA data search system developed by Battelle's Columbus Laboratories is currently being offered as a service by BCL. (Maynard B. Neher)

A lively discussion followed on the procurement, cost and distribution of mass spectra. The conclusion reached was that everyone wants file spectra, but few people are willing to take the time to contribute their own data to various available libraries.

A bibliography of recent articles concerning computer search methods was distributed. (See attachment). More than 90 persons attended indicating the interest in this topic. A list of the names of the attendees has been sent to the ASMS Sec. by E. Emery of Joint Comm. III.

List of References

Reprinted by courtesy of F. W. McLafferty, et al.
(from paper K-3 of the 21st ASMS Meeting)

(6) P. D. Zemany, Anal. Chem., 22, 920 (1950).
(7) F. W. McLafferty and R. S. Gohlke, Anal. Chem., 31, 1160 (1959).
(8) S. Abrahamsson, S. Ställberg-Stenhagen, and E. Stenhagen, Biochem. J., 92, 2PB (1964); S. Abrahamsson, Science Tools, 14, 129 (1967).
(9) V. L. Talroze, V. V. Raznikof, and G. D. Tantsyrev, Dokl. Akad. Nauk SSR, 159, 182 (1964); 170, 379 (1966).
(10) B. Pettersson and R. Ryhage, Arkiv Kemi, 26, 293 (1967); Anal. Chem., 39, 790 (1967).
(11) L. R. Crawford and J. D. Morrison, ibid., 40, 1464 (1968).
(12) (a) R. A. Hites and K. Biemann, ibid., 40, 1217 (1968); (b) H. S. Hertz, R. A. Hites, and K. Biemann, ibid, 43, 681 (1971).
(13) (a) B. A. Knock, I. C. Smith, D. E. Wright, R. G. Ridley and W. Kelly, ibid., 42, 1516 (1970); (b) R. G. Ridley in "Biochemical Applications of Mass Spectrometry", G. R. Waller, Ed., Wiley-Interscience, New York, N.Y., 1972, p 177.
(14) S. L. Grotch, Anal. Chem., 42, 1214 (1970); 43, 1362 (1971).
(15) P. C. Jurs, B. R. Kowalski, and T. L. Isenhour, ibid., 41 21 (1969); T. L. Isenhour and P. C. Jurs, ibid., 43(10), 21A (1971).
(16) L. R. Crawford and J. D. Morrison, ibid., 40, 1469 (1968); 43, 1790 (1971); D. H. Smith, Anal. Chem., 44, 536 (1972).
(17) M. Senn, R. Venkataraghavan, and F. W. McLafferty, J. Amer. Chem. Soc., 88, 5593 (1966); K. Biemann, C. Cone, B. R. Webster, and G. P. Arsenault, ibid., 88, 5598 (1966):
M. Barber, P. Powers, M. J. Wallington, and W. A. Wolfstenholme, Nature, 212, 784 (1966).
(18) (a) A. Buchs, A. B. Delfino, A. M. Duffield, C. Djerassi, B. G. Buchanan, E. A. Feigenbaum and J. Lederberg, Helv. Chim. Acta., 53, 1394 (1970); (b) D. H. Smith, B. G. Buchanan, R. S. Engelmore, A. M. Duffield, A. Yeo, E. A. Feigenbaum, J. Lederberg, and C. Djerassi, J. Amer. Chem. Soc., 94, 5962 (1972).

Plus recent additions from Anal. Chem.

(1) C. F. Bender, H. D. Sheperd, B. R. Kowalski, 45, 617 (1973)
(2) S. L. Grotch, 45, 2 (1973)
(3) D. H. Smith, 44, 536 (1972)
(4) S. R. Heller, 44, 1951 (1972)

ASTM E-14 SUBCOMMITTEE IV-DATA AND INFORMATION PROBLEMS

Chairman: W. B. Askew (E. I. duPont, Wilmington, Del. 19898)
Secretary: C. J. Dooley (U.S.D.A., Wyndmoor, Pa. 19119)

Subcommittee IV met at 5:00 P.M. on Tuesday, May 22, 1973. The meeting was conducted by W. B. Askew. Approximately 100 persons attended. The activities and progress of the subcommittee were discussed. Letters were sent out in September to all members of ASMS and ASTM E-14 describing the committees activity and decisions reached concerning uncertified mass spectra and that the committee was ready to receive spectra. Although some 2500 to 3000 spectra had been promised from 85 laboratories as a result of letter and questionnaire sent out in March of '72, only 69 spectra were received from 3 laboratories. After citing this spectacular lack of success the chairman asked for opinions of the attendees as to reasons for the small response and the feasibility of continuing the collection of uncertified spectra.

In general the responses can be summarized as follows:

1. There are too many groups requesting spectra with the result that the individual spectroscopists sends his data to none of them.
2. The work of the subcommittee should be continued since this is the only real source of uncertified spectra.
3. It was suggested that there should be better coordination between committees and preferably that the various other committees should submit their spectra to subcommittee IV.
4. A poll was taken to determine how many in attendance would be willing to contribute spectra. Twenty indicated a willingness to contribute.

Subcommittee IV will make every effort to collect uncertified spectra with distribution to be handled by ASTM headquarters, including an index, in sheet form.

Tom Pugh suggested that a group of samples be sent to various laboratories to compare calibration data from various types of instruments when hetero-atoms are present. It was suggested a task group be formed to investigate such data. Since ASTM D-2 task group, chaired by Joe Bendoraitis, has made such a comparison for n-hexadecane and 1-phenylundecane, the chairman will contact Bendoraitis as to his groups future plans. If their only interest is hydrocarbons, a task group will be appointed.

TWENTY-FIRST ANNUAL CONFERENCE ON MASS SPECTROMETRY AND ALLIED TOPICS

REPORT OF ASMS COMMITTEE V MEETING - NEW INSTRUMENTS & TECHNIQUES

Professor F. W. Karasek - Chairman
Dr. B. F. Dudenbostel - Vice Chairman

Almost since the inception of this committee, the procedure has been to hold a very brief business meeting followed by a planned discussion session devoted to some new development within the scope of the committee. This year's program consisted of a workshop discussion session which was held from 3:00p.m. to 5:30p.m. on Thursday, May 24, 1973 in the Rose Room of the Sheraton-Palace Hotel in San Francisco. Our program was presented as follows:

ION SCATTERING SPECTROMETRY

DISCUSSION LEADER	ASPECT PRESENTED
Robert F. Goff ISS Program Leader 3M Company - Research Center St. Paul, Minnesota 55101	Basic Principles and Instrumentation
Ric Honig RCA Laboratories Princeton, N.J. 08540	Applications of ISS to Surface Analysis
David Coulter Department of Anatomy University of Minnesota Minneapolis, Minnesota 55455	Applications of ISS to Bio-Medical Studies

Each speaker made a short presentation of about 20 minutes during which there were questions and discussions with the audience. After all three presentations, a discussion session was held in which all three leaders participated. The entire session was kept as informal as possible. The recorded attendance numbered 52.

Suggestions of suitable topics for next year's ASMS Meeting were solicited by Karasek from the attendees. One suggestion for a topic was to cover the use of special techniques associated with spark source mass spectrometry to detect trace elements in air and water samples.

Submitted by
F. W. Karasek, Chairman

ASMS COMMITTEE VI. BIOLOGICAL APPLICATIONS

Minutes from Meeting, May 21, 1973

The business meeting of Committee VI was called to order by its chairman at 5:05 p.m.; thirty-four individuals were in attendance.

OLD BUSINESS

Sandy Markey presented a status report on the collection of reference mass spectra of compounds of biological interest. A total of 1534 spectra have been obtained from seven laboratories (A. Duffield, M. Horning, E. Jellum, J. Lawless, S. Markey, W. Rainey, C. Williams). It is expected that the number will reach 2000 in the near future. These will be used to supplement the Aldermaston collection, as per our original plan. The cost of reproducing the collection for distribution to ASMS members and other interested parties was then discussed. It was indicated that for 500 copies of the collection in both histogram and tabular form the printing costs would be $4800 or $9.60/copy. All other work involved in putting out the collection is being done gratis. The cost would be reduced to $5.60/copy by putting two spectra on each side of a single sheet (4 spectra/sheet). Tabular presentation only would lower the cost to $3.33/copy. More than four-fifths of the attendees indicated a willingness to pay $10/copy for the collection. Twenty out of thirty-four indicated they would spend $15/copy to obtain a higher quality presentation. It was decided that Sandy Markey with the help of several others would contact a number of the chemical and pharmaceutical companies to ascertain if they would be willing to help underwrite the printing costs.

NEW BUSINESS

James McCloskey suggested that for the 1974 meeting Committee VI might want to change its workshop format from the 1972/73 approach, from more or less formal presentations on a general topic followed by discussion, to having three parallel, less formal, sessions on more specialized topics. It would be hoped that this approach would lead to a greater exchange of information between members active in the specific areas of interest. When put to a vote, two-thirds favored the change to three simultaneous "round table discussions" each with a single leader, whereas one-third were in favor of retaining the more structured approach. A list of possible topics for a workshop at the Philadelphia (1974) meeting was established:

1. sensitivity enhancement (chemical and instrumental)
2. derivatization of peptides and related compounds
3. quantitative measurements with labeled internal standards
   a. choice and availability of isotopes
   b. methods of measurement
4. field desorption and chemical ionization of biological compounds
5. mass spectrometry of phosphates and phosphamides
6. experimental problems relating to GC-MS of high molecular weight (> 1000) compounds.

The chairman indicated that a poll would be taken to finalize the topics sometime later in the year.

Activities at the 1973 ASMS Meeting

Committee VI sponsored a three hour workshop on Measurement and Biological Applications of Carbon-13, attended by 120 persons. Discussion leaders were: J. S. Kirby-Smith, U. S. Atomic Energy Commission; J. M. Hayes, Indiana University; C. C. Sweeley, Michigan State University; P. D. Klein, Argonne National Laboratory.

W. J. A. VandenHeuvel, Secretary

J. A. McCloskey, Chairman

COMMITTEE VII: SOLID STUDIES

Personnel:

F. D. Leipziger, Chairman
R. J. Conzemius, Secretary
W. L. Harrington
G. L. Kearns
J. A. McHugh
E. B. Owens

Committee VII Workshop, November 2 and 3, 1972

A workshop on surface analysis and secondary ion mass analysis sponsored by ASMS was held in Tarrytown, New York. The first workshop session consisted of overviews of ion scattering spectrometry, auger electron spectrometry and secondary ion mass spectrometry and were presented by W. L. Harrington, P. W. Palmberg, and J. M. Morabito respectively.

Depth profiling was the subject of the second workshop session and was highlighted by discussion of results of round robin analyses of phosphorus and O^{18} in Ta_2O_5 films.

The third session dealt with general analytical studies and instrumentation. This workshop was unusually well attended and received, and credit is due to the session chairmen, B. N. Colby, J. M. Morabito, and J. A. McHugh, as well as the Organizing Committee, C. A. Evans, Chairman, and B. N. Colby, G. L. Kearns, and W. Singer.

Committee VII Meeting, San Francisco, May 22, 1973

The committee meeting was attended by approximately twenty-five people and was limited to a discussion on the progress of round robin analyses pertaining to accuracy in spark source mass spectrometry. The first of two samples have been distributed to participating laboratories by E. B. Owens who will report on results at the next meeting.

COMMITTEE VIII: "High Resolution Studies"

Don C. De Jongh, Chairman
Département de Chimie, Université de Montréal
Case Postale 6128, Montréal 101, Québec.

Committee VIII has prepared a set of tests to measure instrument performance at high resolution. Instrument manufacturers and users have contributed ideas and data over the past two years, from which the tests have been proposed and revised when appropriate. At the 1973 Annual Conference, the tests were approved by the ASMS members attending the meeting of Committee VIII, subject to further discussion and possible revision. At the 1974 Annual Conference, a Workshop will be held at which various laboratories will be asked to present the results of their use of these tests and their suggestions for additions or modifications.

The tests cover the following eight aspects of instrument performance at high resolution:

Test 1: RESOLUTION VS. SENSITIVITY

This test gives a quantitative measure of all aberrations existing in the mass spectrometer and expresses a give-and-take relationship between sensitivity and resolution.

A sample compound, e.g. perfluorotributylamine, is introduced into the ion source of the mass spectrometer by means of a constant leak inlet system. The pressure is not important as long as it is not too high. The instrument is tuned to a peak in the middle range, e.g. m/e 219. The mass spectrometer is then tuned and aligned at a resolution in excess of 20 000 or the maximum resolution specified by the manufacturer, 10% valley. This step will take care of any problem in proceeding from low resolution to high resolution. The source and collector slits are then set for a resolution of 1000, 10% valley. The multiplier gain is adjusted to give a large peak amplitude - say 100 V. The value is strictly relative. With the source slit, reduce the amplitude of the peak to 70% of the previous value (in this example, it would now be 70 V). Close the collector slit until the plateau limit is reached. Using the peak match unit, measure the resolution. It should be 1430, 10% valley. Again close the source slit until the amplitude is 70% of the previous value (we are now at 49 V). Repeat the procedure of closing the collector slit to plateau limit and measure the resolution. Continue this process until the peak becomes small. Now the multiplier gain may be increased to make the peak larger and still keep the amplitude relationship, as the only required criterion is to reduce the amplitude for each successive measurement to 70%. The results should be plotted as resolution X sensitivity vs. resolution. This plot should extend to a point where the product R X S has fallen to 10% of its original value.

Test 2: SENSITIVITY

Set the instrument to a static resolving power of 1 000, 70 e.v. ionizing energy, and electron multiplier gain of ca. 10^4 to 10^5 . Source temperature 200°. Introduce a sample of 1 µg diethyl stilbestrol ($C_{18}H_{20}O_2$) (evaporated onto the probe tip from a solution of known concentration). Measure the intensity of the molecular ion (either statically by sitting on the top of the peak, or by repetitively scanning through the peak) on a strip chart recorder until it disappears. Adjust conditions in such a way that this measurement takes 3 minutes or more. Integrate the total signal recorded and report the sensitivity in coulombs/µg. The test values should also be reported at a resolution of 10 000.

Test 3: MULTIPLIER GAIN

There are many straightforward ways to measure ion current from a multiplier. Ions can be counted for a fixed interval on a storage scope or an oscillograph, or an electronic counting apparatus can be used. Another method is based on the impulse response of the recording device.

One method for determining multiplier gain is described below:

a. Introduce a sample but defocus the ion beam so that only a few ions per second strike the multiplier.
b. Turn the sensitivity control to maximum (or close to maximum) and make a record on the oscillograph at 64 in/sec chart speed with a frequency response of 1000 Hz. The record should be long enough to include at least 30 single ion spikes.
c. Throwing out any double ion spikes, determine the average spike height (in chart divisions) for at least 30 spikes.
d. Convert the spike height to current, using recorder sensitivity and amplifier input resistor values. For example, if the oscillograph has a sensitivity of 1.6 mv/division and the amplifier input resistor is 10^7 ohms, an average spike height of 5.8 divisions would convert to: $i = 5.8 \text{ div} \times 1.6 \text{ mv/div} \div 1 \times 10^7 \text{ ohms} = 9.3 \times 10^{-10}$ amps
e. Measure the spike base width in seconds. It will be necessary to make a recorder speed measurement.
f. To determine gain it will be necessary to convert the current obtained in part d. (above) to charge since the charge of 1 on the single ion at the multiplier input must be compared to charge at the multiplier output. The measured spike base width was 6×10^{-4} seconds. Charge = $\frac{1}{2} \times 9.3 \times 10^{-10}$ amperes $\times 6 \times 10^{-4}$ sec $= 2.8 \times 10^{-13}$ coulombs.
g. Gain is now equal to the charge ratio:

$$G = \frac{2.8 \times 10^{-13} \text{ C}}{1.6 \times 10^{-19} \text{ c/ion}} = 1.7 \times 10^6$$

h. Gain at lower sensitivity settings where single ion spikes are not evident, can be determined by ratioing the peak height obtained above to the height of the same peak at the lower setting making sure that the peak remains maximized at the collector with the fine mass adjust.

Test 4: ANALOG DYNAMIC RANGE (SIGNAL-TO-NOISE RATIO)

The bandwidth of the amplifier is set at 1000 Hz. The instrument is set up for 10 000 resolution , and focused on m/e 219 of perfluorotributylamine with the source pressure at $1\text{-}5 \times 10^{-6}$ Torr. The multiplier is set to give the maximum output of the amplifier. The voltage at the top of the peak is noted. The magnet is then moved slightly to tune off the peak and the background peak noise level is measured on an oscilloscope. The effective dynamic range = $\frac{\text{max voltage}}{\text{peak-to-peak noise} \times 2}$
This value can be reported for different amplifier band widths. The test is repeated at a bandwidth of 10 000 Hz.

Test 5: RESOLUTION

a) Dynamic Resolution Using Storage Oscilloscope (for Scanning Instruments):- Set the instrument up at a static resolution of 10 000 (10% valley) at m/e 219 with perfluorotributylamine in the ion source at $1\text{-}5 \times 10^{-6}$ Torr. If necessary, readjust for dynamic scanning and scan exponentially through the spectrum. A storage oscilloscope is set to trigger at 2-5 times the base line noise level and the horizontal sweep is set to record a peak in about $\frac{1}{3}$ of the oscilloscope sweep time. Record the original resolution in static mode as well as the resolution observed for the following peaks in the reference compound: m/e 614, 502, 414, 264, 169, 100, 31.

The resolution is calculated by the formula: $\text{res.} = \frac{t}{w. \ln 10}$

where t = scan time in sec/dec. and w = peak width (at 5% of max) in sec. The results should be plotted as R vs. m/e for several scan speeds, together with a statement of the static resolution.

b) Photoplate Resolution: - The purpose of this test is to see how the resolution varies across the plate. Set up the instrument such that the m/e 605 of high boiling point PFA is located near the top of the high mass end of the plate and adjust the electrical resolution for 30 000, 10% valley or the highest resolution attainable. This should give in excess of 50 000 on the photoplate. Set the peak match unit for 100 ppm and record a double exposure on the plate differing by 100 ppm. Change the peak matcher to successive steps of 80, 60, 40 and 20 ppm and repeat the measurement (on different lines on the photoplate, of course). Care must be taken not to overexpose and it may be necessary to expose more than one line per ppm offset at differing exposure times to prevent this. The resultant data are then examined under a microscope to observe visually the points on the photoplate. These results would then be tabulated for lines <u>not</u> overexposed at other m/e such as 505, 469, 405, 369, 305,

269, 205, 169, 100 and m/e = 70, and a plot of resolution vs. m/e be presented.

Agreed, this is not an exact type of measurement and is subject to "eyeball interpretation", but it is as close as you can come.

Optional Procedure: If there is no objection to testing the combination mass spectrometer/comparator the visual inspection of line separation should be replaced by a recording of the density profile. Lines shall be considered separated if the valley drops to 50% or less.

Test 6: PEAK MATCHING ACCURACY

The instrument is set up for a resolution of 10 000 or higher. PFK is introduced through a heated batch inlet. If necessary, calibrate the peak matching device for m/e 219. Tune the magnet for a standard peak and match to the next higher strong PFK peak and record the ratio. This is repeated for 8 peaks as follows:

Lower Mass	Upper Mass	Ratio	Lower Mass	Upper Mass	Ratio
149.9904	161.9904	1.080005	330.9792	342.9792	1.036256
192.9888	204.9888	1.062180	466.9728	480.9696	1.029973
230.9856	242.9856	1.051951	530.9664	542.9664	1.022600
280.9824	293.9824	1.046266	592.9632	604.9632	1.020237

Report the data as the average of the absolute values of the deviations from true value in ppm.

Test 7: TOTAL INSTRUMENT STABILITY

This test is an overall test of the short term stability of all of the circuits which combine to bring an ion into focus.

The instrument is set up on m/e 219 from heptacosafluorotributylamine with a resolution of 10 000. The magnet current is slightly altered so that the point of focus is on the side of the m/e 219 peak at 50% of total intensity. Allow a stated stabilization time before starting the measurement. The instrument is set for very low band width (1 Hz) and the recorder is started. The drift of the instrument is measured for a 2-minu te period. At 10 000 resolution, a variation of 10% of the peak height from 50% corresponds to a change of ca. 8.5 ppm, a variation of 20% from 50% corresponds to ca. 17.5 ppm. The total period of test is divided into twelve 10-second sections and the average and mean deviation of the 10-second stability test is recorded. If certain environmental conditions (e.g. vibrations) have to be met for this test, these must be stated.

Test 8: DATA SYSTEM TEST - SCANNING INSTRUMENTS

As an overall test of a high resolution mass spectrometer data system, a sample of n-hexatriacontane $C_{36}H_{74}$ is run at a resolution of 10 000.

All of the peaks with a total number of ions greater than 200 should be included in the measurements, made on a single scan at a rate of 30 sec/decade and then on a single scan at a rate of 10 sec/decade. All of the peaks are to be reported in the mass range 69-600.

Error data shall be reported in 2 histograms, one giving the results in ppm and the other in m u.

Anyone wishing a copy of the tests or wishing to make comments on the tests is invited to correspond with the chairman.

It must be emphasized that these tests are designed to measure performance and are not intended to or capable of setting specifications or performance standards for mass spectrometers. The Committee gives no recommendations on how well instruments should perform on these tests. Nevertheless, if instrument manufacturers provide a prospective buyer with data on how well their instruments perform on these tests, he can compare instruments directly in terms of performance. Also, users can evaluate the state of health of their instruments at any time. Again, the function of the tests is one of performance measurement rather than standard setting.

Also included in the 1974 Workshop will be reports on a) data from gc/ms, taken at high resolution, and b) chemical-ionization, field-ionization, and field-desorption mass spectrometry at high resolution. Out of these reports will come the projects with which the Committee will be dealing in the future.

ASMS Committee IX

"Aids to Education"

OBJECTIVES

To disseminate information and aid in providing a better understanding of mass spectrometry and to develop an interest in and enthusiasm for the application of mass spectrometry in all areas of science.

Minutes of Meeting May 21, 1973

San Francisco, California

The committee finalized plans for mailing to the membership a questionnaire which would provide information for establishing a mass spectrometry speaker's bureau and a laboratory visitation program. Some questionnaires were distributed during the 21st meeting (San Francisco), but the response to the request for information was disappointing.

One committee member (Dr. Sanzone) presented the results of a survey of mass spectrometer manufacturers and publishers requesting information on mass spectrometry. An informative booklet containing data on mass spectrometry publications and manufacturers' products and specifications for mass spectrometers has been compiled. Copies of this booklet may be obtained upon request.

The overall goals and purpose of the Committee were discussed. In general, it was felt that the important Committeed efforts should be directed to undergraduate students. In this regard, it was pointed out that students should be made aware of the important role of mass spectrometry in Analytical Chemistry, pollution and drug research, chemistry of the atmosphere, and other areas of science.

The specific goals of the Committee for 1973-74 are to compile the information from the questionnaire, to solicit articles on aspects of mass spectrometry for undergraduates, and to complete the requests for information from manufacturers.

ASTM E-14 Subcommittee X, Definitions and Terms

Annual Report - May 22, 1973

The organic task group, under Chairman Sy Meyerson, has developed preliminary definitions for a set of terms that have been indicated by literature occurrence to be ambiguous or faulty in usage. Similarly, terms related to description of instrument operating conditions have been collected for definition by task group Chairman Jerry McCleary. Each of these sets of terms are ready for distribution to selected spectroscopists for comment. No progress was made in selecting definitions for terms relating specifically to inorganic mass spectrometry.

Dr. James Weber acted as Subcommittee Chairman for the San Francisco meeting. The meeting was poorly attended so that no decisions on publication of definitions were made.

Chairman Glenn Cook resigned, with regret, because of the press of other commitments.

COMMITTEE XI: ENVIRONMENT AND POLLUTION

The major activities of Committee XI are the collection, evaluation and distribution of mass spectral techniques and data relating to environmental problems and pollution.

Eighty-five people attended the committee meeting held in conjunction with the ASMS meeting in San Francisco. The topics discussed were: (1) Activities of the Task Groups on Fire Retardant Chemicals and Spectra of Pollutants, (2) suggestions for a symposium at the 1974 ASMS meeting and (3) the Newsletter. Approximately twenty laboratories have expressed interest in the Task Group on Fire Retardant Chemicals. J. S. Smith, Allied Chemical Corp. will distribute a sample for analysis in attempting to devise a standard technique. John M. McGuire, E.P.A., Southeast Water Laboratory, is Chairman of the task group collecting spectra of pollutants. Distribution of the Newsletter will continue.

A major activity this past year was organization of the symposium titled "Use of Mass Spectrometry in Environmental Studies". Philip L. Levins, Vice Chairman of Committee XI, organized the symposium.

It was announced at the Committee meeting that Committee XI is now an ASMS Committee rather than a Joint ASMS-ASTM Committee.

A. G. Sharkey, Jr.
Chairman

ASTM Committee D-2, R & D DIV, Section M

Dr. Andrew W. Decora, Chairman
U.S. Bureau of Mines
Laramie Energy Research Center
P.O. Box 3395, University Station
Laramie, Wyoming 82070
Phone: (307) 742-2115

Purpose and Scope:

ASTM Committee D-2, R & D DIV, Section M has jurisdiction over six task groups concerned with standardization of mass spectrometer methods of hydrocarbon-type analyses. Task group members participate in suggesting standard methods of analysis and in cooperatively testing the method. Completion of work ends in publication of the method in the Book of ASTM Standards.

Summary of Task Group Meetings, San Francisco, 1973

1. Shale-Oil Naphtha (A. W. Decora, Bureau of Mines, Chairman; J. H. Weber, Bureau of Mines, Acting Chairman). - Analysis of the saturate and aromatic fractions from the shale-oil naphtha is possible with existing mass spectral methods. However, progress continues to suffer from a lack of a suitable method to analyze the olefinic fraction. The chairman reported that some progress has been made at Laramie using a hydrogenation step on an olefinic fraction. But, 25 percent of the olefins still remain after hydrogenation. Further studies are in progress.

2. Shale-Oil Gas Oil (T. Aczel, Exxon Research and Engineering, Chairman; J. H. Weber, Bureau of Mines, Acting Chairman). - Progress in this task group was hampered by lack of samples. The chairman proposed that unseparated samples of the gas oil from shale oil be distributed to those group members who are interested in using Laramie's separation procedure. For those members who are not interested in the separation procedure, saturate, olefin, and polar fractions would be sent to them. All labs will use their own mass spectral procedure to analyze these fractions.

There was no further interest in determining low-voltage sensitivities for aromatic compounds.

3. High-Boiling Aromatic Concentrate (C. J. Robinson, American Oil Co., Chairman). - The task group chairman reported that the manuscript entitled "High Ionizing Voltage, Low Resolution Mass Spectrometric Analyses of Gas Oil Aromatic Fractions" has been completed. It will be published in the ASTM Book of Standards. The work of this task group has been completed.

4. Hydrocarbons from Coal Processing (J. Shultz, Bureau of Mines, Chairman; J. H. Weber, Bureau of Mines, Acting Chairman). - Mass spectral results, using the method of Robinson and Cook, were reported on hydrocarbon fractions from coal processing. Elemental maps were also presented on the fractions. Extensive discussions were held regarding sample preparation and introduction into the mass spectrometer. Separation of samples into fractions more amenable to mass spectral analysis is required.

5. High-Olefinic Gasoline Analysis (J. Grutka, UOP Process Div., Chairman; J. H. Weber, Bureau of Mines, Acting Chairman). - Progress in this group has been delayed because no suitable method for the analysis of high olefin gasolines has been found. Extensive discussions were held on the possible use of low-voltage methods and on the use of trained vectors for this analysis. Separation of the gasoline into defined fractions is desirable.

6. Comparison of Calibration Data from Various Types of Analytical Mass Spectrometers (J. Bendoraitis, Mobil R & D Corp., Chairman; A. W. Peters, Mobil R & D Corp., Acting Chairman). - During the past year, two samples of hydrocarbons were sent out to cooperating laboratories. The hydrocarbon samples were n-hexadecane and 1-phenylundecane. Results were obtained from eight laboratories. From the results on the hydrocarbons, even though many of the instrument parameters were not comparable, it was concluded that to go from a 180° Dempster instrument to a sector instrument one would have to recalibrate.

Some interest was indicated in comparing mass spectral patterns of heteroatom organic compounds. This problem is being considered by Chairman Bendoraitis and Dr. Askew, Chairman of ASMS Committee IV.

THE AMERICAN SOCIETY FOR MASS SPECTROMETRY

CONSTITUTION AND BYLAWS

CONSTITUTION

ARTICLE I. Name

The name of this society shall be "The American Society for Mass Spectrometry".

ARTICLE II. Aims and Purpose

It is the aim and purpose of this society to promote and disseminate knowledge of mass spectrometry and allied subjects.

ARTICLE III. Membership

Membership in the American Society for Mass Spectrometry shall be open to any individual, or with approval of the Board of Directors, any corporate entity with a bona-fide interest in mass spectrometry.

ARTICLE IV. Management

The management of the society shall be vested in the Board of Directors which shall consist of the following voting members: the officers of the society hereafter listed, two elected members at large, and the immediate past President; of the following non-voting members: the duly appointed chairmen of such committees that may be duly appointed within the society.

The Officers of the Society shall be:

President

Vice-President for Programs, whoshall be President Elect of the Society

Vice-President for Arrangements

Vice-President for Standards and Procedures, who shall be the Chairman of ASTM Committee E-14 on Mass Spectrometry and shall serve, ex-officio, as an Officer of the Society.

Secretary

Treasurer

ARTICLE V. Duties of Officers

Section 1. The President shall be the chief executive officer of this society; he shall preside at all meetings of the members and directors; he shall have general and active management of the business of this society; he shall see that all orders and resolutions of the Board of Directors are carried out; he shall execute all bonds, mortgages, and all contracts of this society and cause or direct the affixing of the corporate seal thereto; he shall have general superintendence and direction of all other officers of this society and see that their duties are properly performed; he shall submit a report of the operations of the society for the fiscal year to the Board of Directors and members at their annual meeting, and from time to time shall report to the Board of Directors all matters within his knowledge that may effect this society; he shall be ex-officio a member of all committees and shall have the power and duties and management usually vested in the Office of President in a corporation; he shall appoint all committees except as herein otherwise provided. He may individually send or cause to be sent by the Secretary notices of any meetings of the Board of Directors.

Section 2. The Vice-President for Programs shall be vested with all the powers and shall perform all the duties of the President during the absence of the latter and shall have such other duties as may, from time to time, be determined by the Board of Directors. The same shall be true of the Vice-President for Arrangements who shall be next in the line of succession. In the event that the President shall be absent at any meeting, the Vice-President for Programs shall preside, and if neither is present at a

meeting, then the Vice-President for Arrangements shall preside.

Section 3. The Secretary shall attend all sessions of the Board of Directors and all meetings of members and act as a clerk thereof; and shall record all votes and minutes of all proceedings in a book to be kept for that purpose as directed; he shall send notices of all meetings to the members of the Board of Directors; and shall perform such other duties as may be prescribed by the Board of Directors of the President under whose supervision he shall be; and he shall be the custodian of the corporate seal and all of the books and records of this society, except as may be otherwise provided.

Section 4. The Treasurer, under the direction of the Board of Directors, shall have charge of the funds of this society and shall deposit the same in the name of this society in depositories designated by the Board of Directors; he shall arrange for the payment of all the vouchers or orders properly attested by the President and Secretary from said society funds, and shall make a complete and accurate report of the finances of this society at each annual meeting of the members, or at any other time upon request, to the Board of Directors.

ARTICLE VI. Duties and Powers of the Board of Directors

1. The property and business of this society shall be managed by the Board of Directors.

2. In addition to the general powers of the Board of Directors by virtue of their office, the powers and authority expressly given by law, by terms of the charter of this society, and elsewhere in these by-laws, the following specific powers are expressly conferred on the Board of Directors.

To purchase or otherwise acquire for the society any property, right or privilege which it is authorized to acquire at such price or consideration, and upon such terms as they deem expedient; to appoint, to remove or suspend subordiante agents or servants, to determine their duties and affix their salaries; to confer by resolution upon any officer or agent of this society the power of permanently removing or suspending any subordinate officer or servants; to determine who shall be authorized, on behalf of this society, to sign bills, notices, receipts, acceptances, endorsements, checks, releases, contracts and any other instruments; to delegate any of the powers of the Board to any standing committee, special committee, or to any officer or agent of the society, with such powers as the Board may deem fit and proper to grant; generally to do all such lawful acts and things as are not be law, or by charter, or by these by-laws directed or required to be done by members of the Board of Directors.

3. Any action which may be taken at a meeting of the Directors, may be taken without a meeting by a letter ballot sent by and filed with the Secretary of the Society provided the number of ballots filed represents a quorum of the voting members of the Board of Directors.

4. In the event that the office of any elected officer or member of the Board of Directors shall become vacant, the Board of Directors shall immediately fill the vacancy for the remainder of the unexpired term; however, no member who thus fills a vacancy in the office of Vice-President for Programs shall automatically succeed to the presidency, but the society shall in such event elect its next President. The provision of Article IV which pertains to the immediate past president shall not apply to a president who vacates office.

5. The ballot for the election to membership on the Board of Directors of this society shall be by a closed, written ballot.

6. Any member in good standing shall be eligible to hold office in this society either as an officer or a member of the Board of Directors.

ARTICLE VII. Fidelity Bonds

Section 1. The Board of Directors may require such officers or agents to be bonded as it shall deem necessary; for any amount of amounts as it may deem requisite, at the expense of the Society.

ARTICLE VIII. Location

The principal office of this society shall be located in the City of Pittsburgh, Commonwealth of Pennsylvania.

ARTICLE IX. Dissolution

In the event of either voluntary or involuntary dissolution of the society, the funds or assets of the society, remaining after discharging all just debts of the society or its officers in the name of the society, shall be distributed without encumbrances to a non-profit group, organization or institution of learning engaged in the field of spectroscopy within the contemplation of Section 170 (c) (2) of the Internal Revenue Code (1954). The selection of the recipient or recipients shall be made by the majority vote of the Board of Directors or Governing Board in office at the time of the dissolution but in no event shall the assets be distributed to any member or members of the society.

ARTICLE X. Society Seal

This society shall have a seal, upon which shall be inscribed the name of the society, the year of its creation, and the words "Incorporated Commonwealth of Pennsylvania."

ARTICLE XI. Amendments

Section 1. Proposed amendments to this Constitution and the by-laws of the society, signed by at least three members of the Board of Directors or by twenty members of the society must be submitted to the Secretary at least fifteen weeks before the regular business meeting of the society at which meeting the proposed amendments may be discussed and amended. The Secretary shall send or cause to be sent the proposed amendments to each member within a reasonable time and at least before or with the notice of the next regular meeting thereafter. A two-thirds vote of the members present shall authorize a letter ballot on the proposed amendments (as amended in meeting) and if two-thirds of the votes obtained by letter ballot are in favor of the proposed amendments, they shall be adopted.

Section 2. The Board of Directors shall also have the power to amend the by-laws by a two-thirds vote of the Board of Directors by letter ballot of all the members or a like majority at a meeting where all the Board members are present and voting.

Section 3. The Board of Directors is authorized to renumber articles and sections of the Constitution and Bylaws to correspond with any changes that may be made.

ARTICLE XII. Relations with A.S.T.M.

Section 1. This society shall cooperate with A.S.T.M. and its appropriate committees in matters concerned with standards and procedures relevant to Mass Spectroscopy.

Section 2. This society shall make appropriate arrangements for joint meetings with A.S.T.M. Committee E-14. Other A.S.T.M. groups interested in mqss spectrometry as applied to specific materials are invited to schedule their meetings in conjunction with meetings of the society.

ARTICLE XIII. Constitution and Bylaws

Section 1. The Constitution and Bylaws shall be adopted by a majority vote of the members present and voting at the time of their proposal to the members for the ratification.

Section 2. The Constitution and Bylaws shall be in full force and effect immediately upon their adoption as set forth in Section 1.

BYLAWS

1. Membership

1.1 Application for membership shall be made in writing, on a form to be specified by the Board of Directors. The membership year shall commence October 1 and end September 30.

1.2 Applicants shall be admitted by the action of the Board of Directors and membership thereafter becomes effective upon receipt of dues by the Treasurer.

1.3 Failure to pay dues for six months shall automatically terminate membership. Payment of arrears and current dues shall suffice for reinstatement.

1.4 Membership may be terminated without prejudice by written notice to the Secretary, with the requirement that dues up to and including the year of written notice be paid.

1.5 Every member in good standing shall have the right to vote at the general membership meetings and to hold office.

1.6 Any member not in good standing shall lose the right to vote or hold office.

1.7 The books, accounts and reocres of this society shall be open for inspection to any member of the Board of Directors at any time. Members of this society may upon written request to the Board of Directors, inspect such books, accounts and records of this society at such reasonable times as the Board of Directors may my resolution designate.

2. Collections and Disbursements

2.1 Membership classes and dues within such classes shall be determined by the Board of Directors.

2.2 The Board of Directors is authorized to determine separately a registration fee for each general meeting to cover the expenses of holding the meeting. Payment of this fee is a requirement for attendance.

2.3 Disbursements shall be made in accord with an adopted budget or by approval of a majority of the Board of Directors and the fiscal year of the corporation shall be from October 1 to September 30.

2.4 The Secretary will prepare or cause to be prepared at least one annual membership report to the Board of Directors.

2.5 The Treasurer will prepare or cause to be prepared an annual financial report to the Board of Directors.

2.6 The report of the Secretary of membership and the financial report of the Treasurer shall be made available for inspection for any reasonable purpose by any member of the society of written request to the Secretary or Treasurer.

3. Terms of Office and Election

3.1 The elected officers and directors at large shall hold office for a term of two (2) years, except as otherwise provided in Article IV and VI of the Constitution with their term year commencing on July 1 and ending on June 30.

3.2 The President shall appoint a nominating committee of not less than three members on or before July 1 of his second year in office. He shall not be a member of this committee. The committee shall nominate a slate of candidates and report in writing to the Board of Directors no later than the first day of the following September. The nominating committee's report will recommend one candidate per office and contain each candidate's consent to serve if elected, and a resumé for each candidate. This slate of candidates and the resumés will be distributed to the members by the Secretary before November 1.

3.3 Any ASMS member can nominate another member for any office, except President, by submitting to the Secretary before February 15:

a. signature of at least 50 ASMS members endorsing the nomination;

b. signature of the nominee agreeing to hold office if elected;

c. résumé of the candidate.

3.4 The Secretary shall prepare or cause to be prepared a letter ballot to be mailed to the membership at the time of the final meeting notice and requesting return no later than two weeks preceding the annual meeting. Write in votes shall be accepted.

3.5 The election results shall be made known at the next annual business metting and the new officers shall assume office at the beginning of the next term as specified in paragraph 3.1 of the Bylaws.

4. Committeess

4.1 The President shall appoint such committees as are necessary for the carrying out of the aims and purposes of the society. Membership and chairmanship of such committees shall not exceed the term of office of the President. He may terminate a committee at any time. Members and chairmen may be reappointed by the incoming President.

5. Meetings

5.1 The society shall meet at least once a year in order to present scientific papers and conduct business. Twenty membersh shall constitute a quorum for the transaction of business.

5.2 The time and place of the general meeting shall be determined by the Board of Directors.

5.3 Meetings of the Board of Directors may be called by the President or, in his absence, by the Vice-President for Programs. Alternatively, two-thirds of the Board of Directors may call a meeting by written request to the President. Five directors, including at least three voting members shall constitute a quorum of the Board of Directors.

5.4 A simple majority shall be required to pass any motion at any meeting of the members or Board of Directors, unless otherwise provided. Any member in arrears six months or more shal not have the right to vote or hold office.

5.5 Each Director shall be entitled to two weeks' notice of any meeting of the Board of Directors.

5.6 Notices of all meetings, regular or special, shall be in writing and sent through the United States mails to each member or Director on the Board of Directors as the case may be; at his latest address recorded on the books of this society.

5.7 Each member shall be entitled to thirty days' notice of the annual general meeting.

5.8 The President shall, in response to a petition bearing the signatures of not few than twenty members and requesting that the Board of Directors consider a

specified question, place this item on the agenda of the first meeting of the Board of Directors which is scheduled to convene on a date not preceding the thirtieth day following receipt of the petition. The member whose signature appears first on the petition shall be entitled to two weeks' notice of such meetings, and the same member or a member designated by him shall be entitled to attend such meeting and discuss the specified question with the Board of Directors.

5.9 Unless otherwise provided by law, whenever any notice is required to be given, by the provisions of the Bylaws, a waiver thereof in writing, signed by the person or persons entitled to such notices, whether before or after the time stated herein, shall be equivalent thereto.

6. Compensation

6.1 No voting members of the Board of Directors of the society shall receive salaries or fees for their services.

6.2 Voting members of the Board of Directors of the society shall be reimbursed for all reasonable expenses not otherwise covered, except transportation, incurred in connection with their official duties. Reimbursement for transportation expenses imperative to the business of the society may be authorized by unanimous vote of the Board of Directors.

Benefits of Membership

in

THE AMERICAN SOCIETY FOR MASS SPECTROMETRY

1. The registration fee for ASMS members attending the Annual Conference has been set $10.00 below the nonmember fee.

2. All ASMS members receive the printed collection of Conference papers, regardless of whether or not they attend (in past years, only the attendees were sent the collection).

3. The following publishing houses grant price reduction to ASMS members on journal subscriptions and some technical books:

a. Heyden & Sons, Ltd.
c/o Dr. Gunter Heyden
Spectrum House
Alderton Crescent
London NW 4 3 England

"Organic Mass Spectrometry" - 10% discount on current rates, 20% discount on selected books (ask publisher for recent listing).

b. ElsevoielPublishing Company
c/o Dr. Marc Atkins
Jan van Galenstraat 335
P. O. Box 211
Amsterdam, The Netherlands

"International Journal of Mass Spectrometry and Ion Physics" - 20% discount on regular rate, plus air freight. There is a possibility that the discount may be extended also to some of their books.

c. University Park Press
115 Chamber of Commerce Bldg.
Baltimore, Maryland 21202

20% discount on "Recent Developments in Mass Spectroscopy" (Proceedings of the 1969 Kyoto Conference), K. Ogata and T. Kayakawa, editors - $46.00 instead of regular price of $57.50.

d. Marcel Dekker, Inc.
95 Madison Avenue
New York, N.Y. 10016

25% discount on spectroscopy and spectrometry books.

e. Plenum Publishing Corp.
227 West 17th Street
New York, N.Y. 10011

20% discount on "Ion-Molecule Reactions" edited by J. L. Franklin: list price: volume 1 - $26.00; volume 2 - $26.00.

To obtain these discounts, your order should include the statement "ASMS Member." The subscriptions are for PERSONAL use only.

4. An Emplyment Register for ASMS Members has been established. Contact J. J. DeCorpo, Code 6110, Chemistry Division, Naval Research Laboratory, Washington, D.C. 20375.

F. E. SAALFELD
Secretary

INFORMATION AVAILABLE TO ASMS MEMBERS

In order to keep ASMS members better informed on the activities of their Society, it was decided to publish the following list of items deposited with the Society's Secretary (currently F.E. Saalfeld, Naval Research Laboratory, Washington, D.C. 20375 (U.S.A.):

ASMS Charter
ASMS Seal

"Recent Advances in Mass Spectroscopy," edited by K. Ogata and T. Kayakawa

Vols. 17, 18, 19, 20, and 21 of "Mass Spectroscopy" - the journal of the Mass Spectroscopy Society of Japan

Vol. 6 N 4 Methods Physique d'Analyse GAMS

Abstracts of the 11th, 12th, 15th, 16th, 17th, 18th, 19th, 20th, and 21st meetings of the Annual Conference on Mass Spectrometry and Allied Topics

Bound Volume of the Papers of the 10th ('62), 11th ('63), 12th ('64), 13th ('65), 14th ('66), 15th ('67), 16th ('68), 17th ('69), 18th ('70), 19th ('71), 20th ('72), and 21st ('73) Annual Conference on Mass Spectrometry and Allied Topics (one copy each; not for sale - reference use only).

Any ASMS member having need for the above documents should contact the secretary for details.

F.E. Saalfeld
Secretary

A.S.T.M. Publications on Mass Spectrometry

A. Recommended Practices and Methods of Test*

Title and Citations in 1971 Books of ASTM Standards

D1137-53 (70)	Analysis of Natural Gases and Related Types of Gaseous Mixtures by the Mass Spectrometer, Part 19.
D1658-63 (69)	Carbon Number Distribution of Aromatic Compounds in Naphthas by Mass Spectrometry, Part 17.
D2424-67	Hydrocarbon Types in Propylene Polymer by Mass Spectrometry, Part 18.
D2425-67	Hydrocarbon Types in Middle Distillates by Mass Spectrometry, Part 17.
D2498-68	Isomer Distribution of Straight-Chain Detergent Alkylate by Mass Spectrometry, Part 18.
D2567-68	Molecular Distribution Analysis of Monoalkylbenzenes by Mass Spectrometry, Part 18.
D2601-68	Low Voltage Mass Spectrometric Analysis of Propylene Tetramer, Part 18.
D2650-68	Chemical Composition of Gases by Mass Spectrometry, Part 18.
D2786-71	High Ionizing Voltage Mass Spectrometric Analysis of Gas-Oil Saturate Fractions, Part 17.
D2789-71	Hydrocarbon Types in Low Olefinic Gasoline by Mass Spectrometry, Part 17.
E137-68	Evaluation of Mass Spectrometers for Use in Chemical Analysis, Part 30.
E244-69	Atom Percent Fission in Uranium Fuel, Mass Spectrometric Method, Part 30.
E244-68	Use and Evaluation of Mass Spectrometers for Mass Spectrochemical Analysis of Solids, Part 30.

B. Other ASTM Mass Spectrometric Information

AMD11	Index of Mass Spectral Data, 1969, (Formerly STP 356)
AMD10a	Mass Spectral Data Structure (Punched Card Index - 3200 cards).
AMD10b	Mass Spectral Data - Name (Punched Card Index - 3500 cards)
AMD10c	Mass Spectral Data - Name (Punched Card Index - 3500 cards)
STP No. 149	Chemical Analysis of Inorganic Solids by Means of Mass Spectrometer, 1951 (out of print, available on microfilm.)
STP No. 332a	Manual on Hydrocarbon Analysis, 1968 (Revised manual in preparation).

*Committee jurisdiction for the mass spectrometric practices and methods is as follows:

Committee D3 - D1137
Committee E10 - E244
Committee E14 - E137 and E304
Committee D2 - all others listed

ASMS

In an attempt to inform mass spectroscopists of the existence various organizations concerned with mass spectroscopy throughout the world, the Secretary has collected the following information:

Name of Organization	Benefits of Membership	Dues	Name and address of organization/contact for more information
The American Society for Mass Spectrometry (ASMS)	Yearly Conference; free bound volume of Conference papers; $10.00 lower Conference registration fee; discount rates on several journals and books.	$8.00 (U.S.)/yr.	Dr. F.E. Saalfeld Naval Research Lab., Code 6110, Washington, D.C. 20375, U.S.A,
The Australian Society for Mass Spectrometry	Yearly or bi-yearly Conference; abstract service for all members.	$2.00/yr.	Mr. P.T. Greenhalgh The Australian Soc. for Mass Spectrometry 48 Atchison Street St. Leonards Sydney NSA 2065, Australia
Mass Spectroscopy Society of Japan (MSSJ)	Annual Conferences in May; all members receive the Society's journal "Mass Spectroscopy" - papers are written in Japanese (with English abstract) or in a European language (including English).	$8.00 (U.S.)/yr.	Professor K. Ogata Dept. of Physics, Faculty of Science, Osaka University 1-1 Machikaneyama-cho Toyonaka, Osaka-fu Japan
Mass Spectroscopy Group	Advance Information about the Group's Annual Conference.	None (Conf. Reg. Fee)	Dr. W. Kelly Unilever Research Laboratory Colworth House Sharnbrook, Bedfordshire United Kingdom

(Continued)

Name of Organization	Benefits of Membership	Dues	Name and address of organization/contact for more information
Arbeitegemeinschaft Massenspektroskopie	Lower Conference registration fees.	Membership in the German Physical Society plus $1.25 (U.S.)/yr.	Dr. Grutzmacher, Frachbereich Chemie, University Hamburg, 2 Hamburg, Germany
Groupement pour l'Avancement des Methodes Physiques d'Analyses (G.A.M.S.)	Free participation in GAMS working groups - M.S. group meets every other month; access to documentation, books, reviews and to a large collection of various types of spectra.	$135/yr. (fee is for a firm)	Madame Frere - GAMS 8, 10 rue du Delta 75 Paris 9 e me, France
Time of Flight Symposium	Biennial Conference (1969, 1971 . . .)	Conference Registration Fee	Dr. D. Price, Cockcroft Bldg., Univ. of Salford, Dept. of Chem. and Applied Chem., Salford VII M5 4WT Lancashire, England